TRAKYA UNIVERSITY
JOURNAL OF NATURAL SCIENCES

22 Volume 2 Number October 2021

TRAKYA UNIVERSITY JOURNAL OF NATURAL SCIENCES

TUJNS

Trakya Univ J Nat Sci
ISSN 2147-0294
e-ISSN 2528-9691

Trakya University
Journal of Natural Sciences

Volume: 22 **Number: 2** **October** **2021**

Trakya Univ J Nat Sci

http://dergipark.org.tr/trkjnat
e-mail: tujns@trakya.edu.tr

ISSN 2147-0294
e-ISSN 2528-9691

ISSN 2147-0294
e-ISSN 2528-9691

Trakya University Journal of Natural Sciences
http://dergipark.org.tr/trkjnat
Volume 22, Number 2, October 2021

Correspondence Address
Trakya Üniversitesi Fen Bilimleri Enstitüsü Binası, Balkan Yerleşkesi – 22030 Edirne / TÜRKİYE
e-mail: tujns@trakya.edu.tr
Tel: +90 284 2358230
Fax: +90 284 2358237

This Journal is a peer reviewed journal and is indexed by CAB Abstract, CiteFactor, DOAJ (Directory of Open Access Journal), DRJI (Directory of Research Journal Indexing), ESCI (Emerging Sources Citation Index), ResearchBib, Science Library Index, SIS (Scientific Indexing Services), TUBITAK-ULAKBIM Life Sciences Database (Turkish Journal Index) and Zoological Record.

Publisher
Trakya Üniversitesi Matbaa Tesisleri / Trakya University Publishing Centre

TRAKYA UNIVERSITY JOURNAL OF NATURAL SCIENCES

Volume 22 **Number 2** **October** **2021**

REVIEWER LIST

ISSN 2147-0294
e-ISSN 2528-9691

Trakya University Journal of Natural Sciences
http://dergipark.org.tr/trkjnat
Volume 22, Number 2, October 2021

CONTENTS

Research Article

http://dergipark.org.tr/trkjnat
Trakya University Journal of Natural Sciences, 22(2): 111-129, 2021
ISSN 2147-0294, e-ISSN 2528-9691
DOI: 10.23902/trkjnat.875740

Research Article

NEW RECORDS FOR THE TURKISH FRESHWATER ALGAL FLORA IN TWENTY FIVE RIVER BASINS OF TURKEY, PART VI: CHAROPHYTA

Faruk MARAŞLIOĞLU[1*], Elif Neyran SOYLU[2], Nilsun DEMİR[3], Abuzer ÇELEKLİ[4], Haşim SÖMEK[5], Burak ÖTERLER[6], Tolga ÇETİN[7], Yakup KARAASLAN[7], Tuğba ONGUN SEVİNDİK[8], Tolga COŞKUN[3], Cüneyt Nadir SOLAK[9], Bengü TEMİZEL[2]

[1] Hitit University, Faculty of Arts and Science, Department of Biology, Çorum, TURKEY
[2] Giresun University, Faculty of Arts and Science, Department of Biology, Giresun, TURKEY
[3] Ankara University, Faculty of Agriculture, Department of Fisheries and Aquaculture, Dışkapı, Ankara, TURKEY
[4] Gaziantep University, Faculty of Art and Science, Department of Biology, Gaziantep, TURKEY
[5] İzmir Katip Çelebi University, Faculty of Fisheries, Department of Aquatic Sciences of Fisheries, İzmir, TURKEY
[6] Trakya University, Balkan Campus, Faculty of Science, Department of Biology, Edirne, TURKEY
[7] T.R. Ministry of Agriculture and Forestry, Directorate General of Water Management, Ankara, TURKEY
[8] Sakarya University, Faculty of Arts and Science, Department of Biology, Adapazarı, TURKEY
[9] Dumlupınar University, Faculty of Arts and Science, Department of Biology, Kütahya, TURKEY

Cite this article as:

Maraşlıoğlu F., Soylu E.N., Demir N., Çelekli A., Sömek H., Öterler B., Çetin T., Karaaslan Y., Ongun Sevindik T., Coşkun T., Solak C.N. & Temizel B. 2021. New records for the Turkish freshwater algal flora in twenty five river basins of Turkey, part vi: Charophyta. *Trakya Univ J Nat Sci*, 22(2): 111-129, DOI: 10.23902/trkjnat.875740

Received: 06 February 2021, Accepted: 13 April 2021, Online First: 11 May 2021, Published: 15 October 2021

Edited by:
Naime Arslan

****Corresponding Author:***
Faruk Maraşlıoğlu
farukmaraslioglu@hitit.edu.tr

ORCID iDs of the authors:
FM. orcid.org/0000-0002-7784-9243
ENS. orcid.org/0000-0002-7583-3416
ND. orcid.org/0000-0002-3895-7655
AÇ. orcid.org/0000-0002-2448-4957
HS. orcid.org/0000-0003-4281-9738
BÖ. orcid.org/0000-0002-9064-1666
TÇ. orcid.org/0000-0002-7817-3222
YK. orcid.org/0000-0001-8993-4771
TOS. orcid.org/0000-0001-7682-0142
TC. orcid.org/0000-0001-5732-7424

Key words:
Phytoplankton
Desmidiales
Zygnematales
First record
Lake
River Basin

Abstract: Although planktonic algae are a basic component of freshwater ecosystems, studies on their diversity and species distribution are still not in satisfactory numbers. This study aims to contribute to Turkish freshwater algal flora particularly with the new records reported. A total of 158 Charophyta taxa were determined in the study conducted from 2017 to 2019 in 25 river basins of Turkey. In this study, while the highest Charophyta taxon was found in Sakarya and Batı Akdeniz basins with 50 and 42 taxa, respectively, Burdur basin was the only basin where we did not find the Charophyta species. The highest Charophyta diversity was observed in Girdev Lake (Batı Akdeniz basin) and Işık Dağı Karagöl Lake (Sakarya basin) among the lakes of Turkey's 25 river basins. Thirty-one of these Charophyta taxa represent new records for the freshwater algal flora of Turkey. Of these, 13 species are commonly distributed, while 18 species have rare distribution areas. Morphology, ecology, and distribution of each taxon were also discussed in details.

Özet: Planktonik algler tatlı su ekosistemlerinin temel bir bileşeni olmasına rağmen, onların çeşitliliği ve tür dağılımları konusundaki çalışmalar hala tatmin edici sayılarda değildir. Bu çalışma, özellikle raporlanan yeni kayıtlarla Türkiye tatlı su alg florasına katkıda bulunmayı amaçlamaktadır. 2017-2019 yılları arasında Türkiye'nin 25 nehir havzasında yapılan bu çalışmada toplam 158 Charophyta taksonu tespit edilmiştir. Bu çalışmada, en yüksek Charophyta taksonuna sırasıyla 50 ve 42 takson sayısıyla Sakarya ve Batı Akdeniz havzalarında rastlanırken, Charophyta türüne rastlamadığımız tek havza Burdur olmuştur. Türkiye'nin 25 akarsu havzasındaki göller arasında en fazla Charophyta çeşitliliği Girdev Gölü (Batı Akdeniz havzası) ve Işık Dağı Karagöl (Sakarya havzası)'de görülmüştür. Tespit edilen bu Charophyta taksonlarının 31'i Türkiye'deki tatlısu alg florası için yeni kayıt niteliğindedir. Bunlardan 13 tür yayılış alanı olarak yaygın iken, 18 tür nadir yayılış alanına sahiptir. Her bir taksonun morfolojisi, ekolojisi ve dağılımı da ayrıntılı olarak verilmiştir.

Introduction

In recent years, several projects funded by the Ministry of Agriculture and Forestry, Directorate General of Water Management (DGWM) and General Directorate of State Hydraulic Works (DSİ) have been implemented on biological quality components of aquatic ecosystems. The present study is a part of the "Establishment of Reference Monitoring Network in Turkey" project which is funded by DGWM. In this project, 275 lakes in 25 river basins were studied, and a total of 1363 phytoplankton taxa of which 158 belong to Charophyta were determined.

Among the determined species, new records were reported, in addition to already reported taxa, for Turkish flora. Most of the Charophyta taxa that were identified in our study belong to the order Desmidiales, as seen in many studies.

The most Charophyta taxa identified in the lakes within 25 river basins belong to the order Desmidiales, as seen in many previous similar studies (Shukla *et al*. 2008, Oliveira *et al*. 2010, Hansen *et al*. 2018). Desmids are exclusively found in freshwater habitats (Kouwets 2008) and usually prefer acidic or pH-circumneutral, nutrient-poor, and clear waters (Lenzenweger 1996). According to Şahin and Akar (2019), desmid flora is typical, with a predominance of cosmopolitan species, planktic-benthic forms, acidophilic and pH-indifferent species, and halophobic-to-salinity-indifferent species. It is well known that Desmidiales members, which attracted the attention of scientists due to their forms, exhibit great diversity in their external morphology and show a remarkably complex cell symmetry (Lee 2015). Desmids are also considered excellent bioindicators in terms of the stability of ecosystems (Coesel 1998). In recent years, eutrophication, acidification, desiccation, and cultivation have been identified as processes that could negatively affect desmid habitats (Lenzenweger 1996, Šimek 1997, Coesel *et al.* 1978, Štastný 2009).

Turkish inland waters have quite rich algal diversity with 3690 taxa determined so far (Taşkın *et al.* 2019). However, the number of Charophyta members listed in algaebase (4906 taxa) are more than the total number of algal taxa in Turkey (Guiry & Guiry 2021). The number of Charophyta members identified in Turkish freshwaters is only 385 (Taşkın *et al*. 2019). However, 186 desmid species were detected only in four different localities on the Danish island Bornholm (Hansen *et al*. 2018). Thus, more studies are needed to contribute to completion of the list of algal flora of Turkey. A few checklists containing the algae determined in several studies on freshwater algal flora of Turkey were published by Gönülol *et al.* (1996), Aysel (2005) and Şahin (2005) and new taxa records were given during studies performed in the last couple of decades (Aysel *et al.* 1993, Öztürk *et al.* 1995a, 1995b, Şahin 1998, 2000, 2002, 2007, 2009, Apaydın-Yağcı & Turna 2002, Atıcı 2002, Şahin & Akar 2007, Baykal *et al.* 2009, Sevindik *et al.* 2010, 2011, 2015, 2017; Bekleyen *et al.* 2011, Özer *et al.* 2012, Akar & Şahin 2014, Yüce & Ertan 2014, Varol & Fucikova 2015, Varol & Şen 2016, Maraşlıoğlu & Soylu 2018, Şahin & Akar 2019, Şahin *et al*. 2020).

The studies mentioned above were conducted in different wetlands in Turkey and provided a great contribution to the determination of freshwater algal flora of Turkey and to the checklists published earlier. Reliable descriptive information was also given in these publications about the new records. The aim of the study is to determine the algal flora of Turkish freswater in selected 25 river basins.

Materials and Methods

Study Area

Turkey has 25 river basins (Fig. 1, Table 1), and inland water bodies in these basins consisting of 200 natural lakes, 806 reservoirs and 1000 irrigation ponds. The general directorate of state ydraulic works of Turkey (DSİ) data show that the volume of annual average precipitation is estimated to be 501 billion m^3 water, of which about 55% is lost by evapotranspiration, 31% flows into water bodies (158 billion m^3) and 14% feeds aquifers (69 billion m^3). The Fırat-Dicle Basin provides the largest single volume of available exploitable freshwater resources in Turkey, representing 28.5% of the total (DSİ 2014).

A total of 275 lakes, including reservoirs, were sampled during the study in 25 river basins. The number of studied lakes considering the river basins were given in Table 1. These lakes, located between the longitudes of 26º 19′ and 43º 54′E and the latitudes of 35º 56′ and 42 º 00′N, are grouped in 22 lake typologies based on altitude (R), lake depth (D), lake size (A), and geology (J) (DGWM 2015a). The altitudes of the sampled lakes vary from sea level (Lake Gala) to 2757 m (Lake Çamlu).

Fig. 1. 25 River basins in Turkey.

Table 1. The number and names of sampled lakes in the 25 river basins.

No	Basin	The number of studied lakes	Name of lake
1	Akarçay	10	**(1)** Akşehir Lake, **(2)** Eber Lake, **(3)** Akdeğirmen Reservoir, **(4)** 26 Ağustos TP Lake, **(5)** Karamık Reeds, **(6)** Ağzıkara Pond, **(7)** Tınaztepe Pond, **(8)** Gezler Pond, **(9)** Şehit Uz. Çvş. Nurullah Oymak Pond, **(10)** Tazlar Satı Gelin Pond
2	Antalya	9	**(11)** Eğirdir Lake, **(12)** Kovada Lake, **(13)** Gölcük Lake, **(14)** Cemalalanı Lake, **(15)** Duruca Lake, **(16)** Eğri Lake, **(17)** Küllü Lake, **(18)** Titreyen Lake, **(19)** Düden Lake
3	Aras	3	**(20)** Aktaş Lake, **(21)** Çıldır Lake, **(22)** Aygır Lake
4	Asi	8	**(23)** Reyhanlı (Yenihisar) Lake, **(24)** Yayladağ Reservoir, **(25)** Tahtaköprü Reservoir, **(26)** Karagöl Lake, **(27)** Adsız Lake, **(28)** Yarseli Reservoir, **(29)** Üçpınar Pond, **(30)** Sapkanlı Pond
5	Batı Akdeniz	13	**(31)** Gölhisar Lake, **(32)** Girdev Lake, **(33)** Avlan Lake, **(34)** Dalaman Wetlands, **(35)** Denizcik Lake, **(36)** Kocagöl Lake, **(37)** Kusuru Lake, **(38)** Köycegiz Lake, **(39)** Küçükdalyan Lake, **(40)** Yeşilgöl Lake, **(41)** Yazır Lake, **(42)** Baranda Lake, **(43)** Pozan Lake
6	Batı Karadeniz	14	**(44)** Nazlı Lake, **(45)** Büyük Lake, **(46)** Derin Lake, **(47)** Parçayır Lake, **(48)** Abant Lake, **(49)** Dipsiz Lake, **(50)** Gölcük Lake, **(51)** Keçi Lake, **(52)** Yeniçağa Lake, **(53)** Kuyudüzü Lake, **(54)** Erze Lake, **(55)** Koca Lake, **(56)** Kuru Lake Natural Park, **(57)** Sazlı Lake
7	Burdur	6	**(58)** Acıgöl Lake, **(59)** Burdur Lake, **(60)** Karataş Lake, **(61)** Salda Lake, **(62)** Tefenni Pond, **(63)** Keçiborlu Güneykent Uzundere Pond
8	Büyük Menderes	13	**(64)** Işıklı Lake, **(65)** Bafa Lake, **(66)** Azap Lake, **(67)** Karakuyu Reeds, **(68)** Süleymanlı Lake, **(69)** İkizdere Reservoir, **(70)** Gerenlik Lake, **(71)** Gökgöl Lake, **(72)** Gökpınar Reservoir, **(73)** Karacasu Reservoir, **(74)** Karagöl Lake, **(75)** Saklı Lake, **(76)** Sülüklü Lake
9	Ceyhan	18	**(77)** Gölbaşı Lake, **(78)** Kartalkaya Reservoir, **(79)** Kara Lake, **(80)** B. Yapalak Pond, **(81)** Korkmaz Pond, **(82)** Zorkun Pond, **(83)** Merk Pond, **(84)** Yamaçoba Pond, **(85)** Kızıliniş Pond, **(86)** Arıklıkaş Pond, **(87)** Karacaören Pond, **(88)** Meletmez Pond, **(89)** Postkabasakal Pond, **(90)** Bağtepe Pond, **(91)** Zerdali Pond, **(92)** Kozan Aydın Pond, **(93)** Yumurtalık Zeytinbeli Pond, **(94)** Yumurtalık Ayvalık Pond
10	Çoruh	8	**(95)** Adsız Lake, **(96)** Boğa Lake, **(97)** Balık Lake, **(98)** Şavşat Karagöl Lake, **(99)** Çil Lake, **(100)** Borçka Karagöl Lake, **(101)** Tortum Lake, **(102)** Ürünlü Pond
11	Doğu Akdeniz	12	**(103)** Aygır Lake, **(104)** Uzun Lake, **(105)** Değirmendere Pond, **(106)** Cemilli Çevlik Pond, **(107)** Hacınuhlu Kelce Pond, **(108)** Akın Pond, **(109)** Kızılöz Pond, **(110)** Başyayla Pond, **(111)** Göktepe Pond, **(112)** Bağbaşı Reservoir, **(113)** Yassıbağ Pond, **(114)** Hadım-İnönü Pond
12	Doğu Karadeniz	7	**(115)** Gaga Lake, **(116)** Sera Lake, **(117)** Ulugöl Lake, **(118)** Uzungöl Lake, **(119)** Çamlu Lake, **(120)** Çakır Lake, **(121)** Limni Lake
13	Fırat-Dicle	17	**(122)** Kaz Lake, **(123)** Ahır Lake, **(124)** Haçlı Lake, **(125)** Korlu Lake, **(126)** Hazar Lake, **(127)** Karagöl Lake, **(128)** Yeşildere Pond, **(129)** Palandöken Pond, **(130)** Güroymak Reservoir, **(131)** Kalecik Reservoir, **(132)** Kapıaçmaz Pond, **(133)** Dedeyolu Pond, **(134)** Güzelyurt Sulama Pond, **(135)** Hasancık Pond, **(136)** İncesu Pond, **(137)** Otlukbeli Lake, **(138)** Siverek Yeleken Pond
14	Gediz	6	**(139)** Gölcük Lake, **(140)** Demirköprü Reservoir, **(141)** Marmara Lake, **(142)** Gördes Reservoir, **(143)** Karagöl Lake, **(144)** Küçükler Reservoir
15	Kızılırmak	23	**(145)** Gölbel Lake, **(146)** Ulaş Lake-2, **(147)** Büyük Lota Lake, **(148)** Hafik Lake, **(149)** Küçük Lota Lake, **(150)** Tödürge Lake, **(151)** Arı Lake, **(152)** Aygır Lake, **(153)** Bakkal Lake, **(154)** Dipsiz Lake, **(155)** Elekci Lake, **(156)** Ulaş Lake-1, **(157)** Ulaş Lake-3, **(158)** Deniz Lake, **(159)** Yeşilgöl 1 Lake, **(160)** Bardakçılı Mevki Lake, **(161)** Yenidanişment Mevki Lake, **(162)** Palanga Lake, **(163)** Sugiylan Mevki Lake, **(164)** Kayabaşı Lake, **(165)** Kuru Lake, **(166)** Sıraç Lake, **(167)** Kızılçam Lake
16	Konya	18	**(168)** Sarıot Lake, **(169)** Beyşehir Lake, **(170)** Tuz Lake, **(171)** Süleymanhacı Lake, **(172)** Gök (Kozanlı) Lake, **(173)** Meke Lake (Meke Maarı), **(174)** Gavur Lake, **(175)** Dipsiz Lake, **(176)** Acıgöl Lake 2, **(177)** Bakı Lake, **(178)** Uyuz Lake, **(179)** Acıgöl Lake 1, **(180)** Kayı Lake, **(181)** Düden Lake, **(182)** Kovalı Lake, **(183)** Köpek Lake, **(184)** Küçük Lake, **(185)** Sülüklü Lake

Table 1. Continued.

No	Basin	The number of studied lakes	Name of lake
17	Kuzey Ege	5	**(186)** Boz Lake, **(187)** Güzelhisar Reservoir, **(188)** Karagöl Lake, **(189)** Sevişler Reservoir, **(190)** Tepe Lake
18	Küçük Menderes	6	**(191)** Çatal Lake, **(192)** Tahtalı Reservoir, **(193)** Alaçatı Barajı, **(194)** Belevi Lake, **(195)** Gebekirse Lake, **(196)** Ürkmez Reservoir
19	Marmara	9	**(197)** Habibler Mevki Pond, **(198)** Great Dipsiz Lake, **(199)** İznik Lake, **(200)** Koca Lake, **(201)** Karamaden Lake, **(202)** Danamandıra Lake-1, **(203)** Danamandıra Lake-2, **(204)** Small Dipsiz Lake, **(205)** Sinekli Lake
20	Meriç-Ergene	5	**(206)** Gala Lake, **(207)** Sığırcı Lake, **(208)** Pamuklu Lake, **(209)** Üsküp Sulama Pond, **(210)** Domuz Lake
21	Sakarya	23	**(211)** Taşkısığı Lake, **(212)** Akgöl 2 Lake, **(213)** Çubuk Lake, **(214)** Poyrazlar Lake, **(215)** Sapanca Lake, **(216)** Işık Dağı Karagöl Lake, **(217)** Çavuşcu Lake, **(218)** Mogan Lake, **(219)** Üçlerkayası Pond, **(220)** Çubuk Karagöl Lake, **(221)** Eymir Lake, **(222)** Akgöl 1 Lake, **(223)** Küçük Akgöl Lake, **(224)** Avdan Lake, **(225)** Kayuslu Lake, **(226)** Karamurat Lake, **(227)** Cüneyt Sönmez Pond, **(228)** Çılgınlar Pond, **(229)** Yıldırım Evci Pond, **(230)** Ovacık Lake, **(231)** Sülüklü Lake, **(232)** Çamkoru TP Pond, **(233)** Anagöl Lake
22	Seyhan	12	**(234)** Bahçelik Reservoir, **(235)** Tufanbeyli Demiroluk Pond, **(236)** Adsız Lake, **(237)** Pekmezli-Çatalçam Pond, **(238)** Tufanbeyli Doğanbeyli Pond, **(239)** Gümüşören Reservoir, **(240)** Şıhlı Pond, **(241)** Dölekli Pond, **(242)** Kılıçlı Pond, **(243)** Topacık Pond, **(244)** Hüsniye Pond, **(245)** Çavuşlu Pond
23	Susurluk	9	**(246)** Manyas Lake, **(247)** Uluabat Lake, **(248)** Adsız-1 Lake, **(249)** Gölbaşı Lake, **(250)** Gölcük Lake, **(251)** İkizcetepeler Reservoir, **(252)** Karagöl Lake, **(253)** Kilimli Lake, **(254)** Nilüfer Reservoir
24	Van Gölü	7	**(255)** Akgöl Lake, **(256)** Erçek Lake, **(257)** Bostaniçi Pond, **(258)** Arin Lake, **(259)** Aygır Lake, **(260)** Van Lake, **(261)** Nazik Lake
25	Yeşilırmak	14	**(262)** Akgöl Lake, **(263)** Aşağıtepecik (Gölova) Lake, **(264)** Boraboy Göleti, **(265)** Büyük Lake, **(266)** Düden Lake, **(267)** Kaz Lake, **(268)** Ladik Lake, **(269)** Uyuz Lake, **(270)** Karacaören Mevki Lake, **(271)** Dipsiz Lake 2, **(272)** Sarıçiçek Lake, **(273)** Yenihayat Reservoir **(274)** Dipsiz Lake 1, **(275)** Zinav Lake

Sampling and Identification

Phytoplankton was sampled annually from 2017 to 2019 in three seasons (spring, summer and autumn) at monitoring station(s) in each lake. The number of monitoring points (station) in the lakes varied according to the lake areas determined by the general directorate of water management. According to this, sampling point numbers were determined as 1 for lakes that have a surface area smaller than 50 ha, 2 for lakes that have a surface area between 50 and 500 ha and, 3 for lakes which have a surface area higher than 500 ha (DGWM 2015b). One of the selected stations was determined at the deepest point of the lake. No bathymetric study was carried out in the lakes, and the deepest point of the lake was determined through a depth meter. Three depths (surface, middle, and bottom) of the euphotic depth (Secchi disk depth × 2.5) were sampled with a Ruttner water sampler (Hydro-Bios 2 L, 0.5 m long), then a subsample was taken from mixed water of the three depths. Plankton net with a pore diameter of 50 μm was also used for sampling. Samples were fixed with Lugol's solution. Identification of the algal taxa was performed with compound and inverted microscopes according to the literature (Kolkwitz & Krieger 1971, Lind & Brook 1980, Huber-Pestalozzi 1982, Kadlubowska 1984, Lenzenweger 1996, 1997, 1999, 2003, Compère 2001, John *et al.* 2003, Coesel & Meesters 2007). Identified taxa were checked with the checklist of Aysel (2005), Taşkın *et al.* (2019), and the database of Turkish algae (Maraşlıoğlu & Gönülol 2021). The currently accepted nomenclature and distribution of taxa were given according to Guiry & Guiry (2021). The author names were abbreviated according to Brummit & Powell (1992). Taxa were photographed with a camera attached to the microscopes. List of Charaophyta taxa, the basin and lakes they were obtained are given in Table 2. Species name, synonym, description, ecology, distributional data and obtained basin and lakes information are given only for new taxa in the result section.

Results

A total of 158 Charophyta taxa, of which 31 are new records for the freshwater algal flora of Turkey were determined during the whole study (Table 2). Thity-one taxa from Charophyta were detected as new records for the freshwater algal flora of Turkey in this comprehensive study. 30 of the new records were found to be members of the order Desmidiales and 1 of the order Zygnematales. Morphotaxonomic description, ecology, and distribution of each of these taxa are given below.

Table 2. List of Charophyta taxa (Italic numbers show Basin names in Table 1, bold numbers show lake names in Table 1).

No	Taxa	Localities	
		Basin(s)	Lake(s)
1	*Actinotaenium wollei* (West & G.S.West) Teiling ex Ruzicka & Pouzar 1978*****	*23*	**246**
2	*Closterium acerosum* Ehrenb. ex Ralfs 1848	*2, 16, 18*	**12, 17, 182, 194**
3	*Closterium aciculare* T.West 1860	*16, 17, 18, 19, 23, 25*	**169, 177, 182, 185, 189, 186, 187, 193, 197, 199, 201, 202, 246, 249, 251, 274, 271**
4	*Closterium acutum* Bréb. 1848	*16, 17, 20, 21, 23, 25*	**174, 189, 208, 216, 251, 266, 275**
5	*Closterium acutum* var. *linea* (Perty) West & G.S.West 1900	*21*	**216**
6	*Closterium acutum* var. *variabile* (Lemmerm.) Willi Krieg. 1935	*1, 4, 5, 13, 21*	**8, 10, 28, 31, 42, 122, 124, 129, 211, 219**
7	*Closterium dianae* Ehrenb. ex Ralfs 1848	*2, 5, 8, 11, 21, 25*	**17, 41, 64, 103, 216, 269, 271**
8	*Closterium dianae* var. *rectius* (Nordst.) De Toni 1977*	*1*	**2**
9	*Closterium ehrenbergii* Menegh. ex Ralfs 1848	*18*	**194**
10	*Closterium gracile* Bréb. ex Ralfs 1848	*2, 10*	**12, 99**
11	*Closterium idiosporum* West & G.S.West 1900	*21*	**216**
12	*Closterium jenneri* var. *cynthia* (De Not.) Petlovany 2015	*21*	**216, 219**
13	*Closterium kuetzingii* Bréb. 1856	*15*	**162**
14	*Closterium leibleinii* Kütz. ex Ralfs 1848	*15*	**162**
15	*Closterium limneticum* Lemmerm. 1899	*13, 21*	**129, 131, 138, 232, 225**
16	*Closterium littorale* Gay 1884	*9, 14, 16, 19, 20, 23*	**78, 140, 141, 144, 185, 199, 208, 210, 206, 246**
17	*Closterium lunula* Ehrenb. & Hemprich ex Ralfs 1848	*9,14, 17, 20, 23*	**84, 140, 189, 206, 208, 246, 251**
18	*Closterium moniliferum* Ehrenb. ex Ralfs 1848	*16, 22*	**174, 234**
19	*Closterium navicula* (Bréb.) Lütkem. 1905	*2, 10*	**12, 99**
20	*Closterium parvulum* Nägeli 1849	*8, 16*	**67, 174**
21	*Closterium pronum* Bréb. 1856	*5*	**40, 42**
22	*Closterium pseudolunula* O.Borge 1909	*1*	**2**
23	*Closterium pygmaeum* Gutw. 1890*****	*21*	**224**
24	*Closterium strigosum* Bréb. 1856	*19*	**205**
25	*Cosmarium abbreviatum* Racib. 1885	*4, 21, 25*	**28, 216, 269**
26	*Cosmarium asphaerosporum* Wittr. 1879	*19*	**202**
27	*Cosmarium berryense* Kouwets 1998	*21*	**225**
28	*Cosmarium bioculatum* Bréb. ex Ralfs 1848	*4, 11, 14, 16, 17, 25*	**28, 104, 110, 140, 174, 189, 263**
29	*Cosmarium bioculatum* var. *depressum* (Schaarschm.) Schmidle 1894	*1, 21*	**10, 213, 219, 232**
30	*Cosmarium bireme* G.S.West 1904	*1, 13*	**6, 134**
31	*Cosmarium blyttii* Wille 1880	*24, 25*	**258, 272**
32	*Cosmarium boeckii* Wille 1880	*16*	**175**
33	*Cosmarium botrytis* Menegh. ex Ralfs 1848	*2, 14, 17, 19, 20, 23*	**17, 140, 141, 188, 202, 206, 251**
34	*Cosmarium brebissonii* Menegh. ex Ralfs 1848*****	*5*	**32**
35	*Cosmarium cataractarum* (Racib.) B.Eichler 1895	*4*	**29**
36	*Cosmarium clepsydra* Nordst. 1870	*19, 20*	**199, 210**
37	*Cosmarium contractum* O.Kirchner 1878	*2, 5*	**12, 33**
38	*Cosmarium contractum* var. *rotundatum* Borge 1925*	*15*	**149**
39	*Cosmarium contractum* var. *minutum* (Delponte) Coesel 1989	*13*	**133**
40	*Cosmarium crenatum* Ralfs ex Ralfs 1848	*10*	**97**

Table 2. Continued.

No	Taxa	Localities	
		Basin(s)	Lake(s)
41	*Cosmarium cymatonotophorum* West 1892	*21*	**213, 227, 228**
42	*Cosmarium depressum* var. *planctonicum* Reverdin 1919	*15, 21*	**149, 213**
43	*Cosmarium difficile* Lütkem. 1892	*4, 21*	**28, 216**
44	*Cosmarium distentum* (West) Coesel & Meesters 2015*****	*5, 21*	**32, 214**
45	*Cosmarium formosulum* Hoff 1888	*2*	**12, 15**
46	*Cosmarium galeritum* Nordst. 1870	*15*	**148, 149, 158**
47	*Cosmarium granatum* Bréb. ex Ralfs 1848	*2, 16*	**11, 176, 177**
48	*Cosmarium humile* Nordst. ex De Toni 1889	*5, 10, 15, 19, 21, 25*	**32, 99, 159, 199, 216, 272**
49	*Cosmarium humile* var. *substriatum* (Nordst.) Schmidle 1895*****	*5, 10*	**33, 99**
50	*Cosmarium impressulum* Elfving 1881	*5*	**32**
51	*Cosmarium impressulum* var. *crenulatum* (Nägeli) Willi Krieg. & Gerloff 1965*****	*15*	**162**
52	*Cosmarium laeve* Rabenh. 1868	*2, 4, 5, 6, 11, 13,15, 16, 20, 21*	**11, 16, 27, 32, 35, 48, 104, 105, 106, 107, 132, 133, 147, 149, 176, 185, 206, 224, 225**
53	*Cosmarium mamilliferum* var. *madagascariense* West & G.S.West 1885*	*13*	**126**
54	*Cosmarium meneghinii* Bréb. ex Ralfs 1848	*4, 5, 10, 21, 24*	**26, 32, 99, 216, 261**
55	*Cosmarium moniliforme* Ralfs 1848	*1, 8, 13, 21*	**5, 64, 132, 215, 219**
56	*Cosmarium neodepressum* G.J.P.Ramos & C.W.N. Moura 2020	*3, 5, 6, 15, 22*	**22, 32, 54, 55, 57**
57	*Cosmarium norimbergense* var. *depressum* (West & G.S.West) Willi Krieg. & Gerloff 1969	*5, 21*	**32, 227, 232**
58	*Cosmarium nymannianum* Grunov 1868*****	*2*	**19**
59	*Cosmarium obtusatum* (Schmidle) Schmidle 1898	*5*	**32**
60	*Cosmarium ornatum* Ralfs ex Ralfs 1848	*9*	**86**
61	*Cosmarium phaseolus* Bréb. ex Ralfs 1848	*13, 21*	**132, 229**
62	*Cosmarium phaseolus* var. *subbireme* Racib. 1889	*21*	**216**
63	*Cosmarium polygonatum* Halász 1940	*5, 21*	**33, 214, 216, 219, 224**
64	*Cosmarium pseudowembaerense* Kouwets 1998*	*5, 13*	**33, 131**
65	*Cosmarium punctulatum* Bréb. 1856	*8, 12, 14,20*	**64, 115, 140, 206**
66	*Cosmarium pygmaeum* W.Archer 1864	*5, 10, 16*	**32, 100, 175**
67	*Cosmarium quinarium* Lundell 1871*****	*21*	**224**
68	*Cosmarium regnellii* Wille 1884	*5, 21*	**32, 216, 218, 219, 227, 228**
69	*Cosmarium regnesi* Reinsch 1866	*5, 21*	**32, 216**
70	*Cosmarium reniforme* (Ralfs) W.Archer 1874	*5, 25*	**32, 271, 275**
71	*Cosmarium reniforme* var. *compressum* Nordst. 1887	*8, 21*	**64, 216**
72	*Cosmarium speciosum* Lundell 1871	*2*	**15**
73	*Cosmarium sphagnicola* West & G.S.West 1897*	*5*	**32**
74	*Cosmarium sportella* Bréb. ex Kütz. 1849	*16*	**169**
75	Cosmarium subadoxum Grönblad*	*4, 13, 21*	**28, 29, 132, 135, 214,**
76	*Cosmarium subcostatum* Nordst. 1876	*2, 25*	**19, 269**
77	*Cosmarium subcostatum* var. *minus* (West & G.S.West) Kurt Först.1981	*5*	**33**
78	*Cosmarium subcrenatum* Hantzsch 1868	*10, 17*	**99, 189**
79	*Cosmarium subgranatum* (Nordst.) Lütkem. 1902*****	*21*	**224, 225**

Table 2. Continued.

No	Taxa	Localities	
		Basin(s)	Lake(s)
80	*Cosmarium subprotumidum* Nordst. 1876	*5*	**32**
81	*Cosmarium subquadrans* West & G.S.West 1905*****	*4*	**28, 29**
82	*Cosmarium subquadrans* var. *minus* Nordst. 1873*****	*21*	**215**
83	*Cosmarium subtumidum* Nordst. 1878	*5*	**35**
84	*Cosmarium subtumidum* var. *minutum* (Willi Krieg.) Willi Krieg. & Gerloff 1965	*5, 13*	**33, 133**
85	*Cosmarium subundulatum* Wille 1880	*15*	**148**
86	*Cosmarium tenue* W.Archer 1868	*13*	**132**
87	*Cosmarium tetrachondrum* Lundell 1871*****	*5*	**32**
88	*Cosmarium tinctum* Ralfs 1848	*2, 4, 5, 13, 16, 21*	**12, 30, 37, 133, 136, 138, 176, 185**
89	*Cosmarium venustum* (Bréb.) Archer 1861	*16, 25*	**174, 271**
90	*Cosmarium wembaerense* Schmidle 1898	*1, 21*	**2, 218**
91	*Cylindrocystis brebissonii* (Ralfs) De Bary 1858	*2*	**19**
92	*Desmidium aptogonum* Bréb. ex Kütz. 1849 *****	*8*	**67**
93	*Elakatothrix gelatinosa* Wille 1898	*1, 3, 5, 10, 12, 13, 16, 21, 25*	**3, 9, 22, 32, 35, 42, 95, 115, 117, 129, 131, 130, 134, 135, 175, 211, 214, 227, 231, 232, 213, 216, 225, 264, 265, 275, 274, 271, 273**
94	*Euastrum lacustre* (Messik.) Coesel 1984*****	*15*	**148**
95	*Gonatozygon brebissonii* De Bary 1858	*2, 11*	**11, 104**
96	*Gonatozygon monotaenium* De Bary 1856	*5*	**35**
97	*Groenbladia undulata* (Nordst.) Kurt Först.1973*	*21*	**222**
98	*Heimansia pusilla* (Hilse) Coesel 1993	*1*	**6, 8**
99	*Hormidiopsis crenulata* (Kütz.) Heering 1914	*2*	**15**
100	*Micrasterias furcata* C.Agardh ex Ralfs 1848*****	*21*	**216**
101	*Micrasterias rotata* Ralfs 1848	*10*	**99**
102	*Mougeotia boodlei* (West & West) Collins 1912	*2, 16*	**12, 13, 169, 174, 175, 176, 182**
103	*Mougeotia capucina* C.Agardh 1824	*17, 23*	**187, 249**
104	*Mougeotia nummuloides* (Hassall) De Toni 1889	*2*	**15**
105	*Mougeotia parvula* Hassall 1843	*2*	**11, 19**
106	*Mougeotia quadrangulata* Hassall 1843	*2, 16*	**11, 17, 175, 178, 182**
107	*Mougeotia varians* (Wittr.) Czurda 1932	*5*	**32**
108	*Mougeotia viridis* (Kütz.) Wittr. 1872	*14, 16,17, 19*	**142, 180, 189, 199**
109	*Pleurotaenium trabecula* Nägeli 1849	*2, 4*	**13, 26**
110	*Roya closterioides* Coesel 2007	*21*	**216**
111	*Spirogyra aequinoctialis* West 1907	*22*	**239**
112	*Spirogyra cataeniformis* (Hassall) Kütz. 1849	*2, 16*	**19, 176**
113	*Spirogyra communis* (Hassall) Kütz. 1849	*16*	**176**
114	*Spirogyra dubia* Kütz. 1849	*16*	**176**
115	*Spirogyra decimina* var. *elongata* (Vaucher) Petlovany 2015*****	*2*	**11**
116	*Spirogyra rivularis* (Hassall) Rabenh. 1868	*2*	**19**
117	*Spirogyra weberi* Kütz. 1843	*2*	**11, 13, 15**
118	*Spondylosium panduriforme* (Heimerl) Teiling 1957*****	*13*	**132**
119	*Staurastrum alternans* Bréb. 1848	*20, 23*	**206, 251**

Table 2. Continued.

No	Taxa	Localities	
		Basin(s)	Lake(s)
120	*Staurastrum anatinum* Cooke & Wills 1881	*8*	**73**
121	*Staurastrum avicula* var. *lunatum* (Ralfs) Coesel & Meesters 2013	*5*	**32**
122	*Staurastrum bieneanum* Rabenh. 1862	*5, 21*	**32, 224**
123	*Staurastrum bioculatum* W.R.Taylor 1935	*11*	**110**
124	*Staurastrum chaetoceras* (Schröd.) G.M.Sm. 1924	*9, 13, 14, 17, 18, 19, 20, 23*	**82, 129, 137, 130, 139, 190, 187, 193, 199, 209, 247**
125	*Staurastrum cingulum* (West & G.S.West) G.M.Sm. 1922	*2, 3, 5, 10, 13, 15, 16, 22, 24*	**12, 15, 17, 22, 24, 42, 101, 125, 129, 131, 138, 145, 169, 175, 177, 182, 185, 245, 261**
126	*Staurastrum cingulum* var. *obesum* G.M.Sm. 1922	*15*	**145, 152**
127	*Staurastrum crenulatum* (Nägeli) Delponte 1877	*2, 5, 8, 15*	**17, 35, 64, 151**
128	*Staurastrum denticulatum* (Nägeli) W.Archer 1861	*10*	**99**
129	*Staurastrum furcigerum* (Bréb.) W.Archer 1861	*5, 21*	**32, 216, 224**
130	*Staurastrum gracile* Ralfs ex Ralfs 1848	*8, 14, 15, 16, 17, 19, 20, 23*	**69, 140, 141, 148, 169, 186, 187, 189, 199, 202, 203, 209, 210, 251**
131	*Staurastrum hexacerum* Wittr. 1872	*5*	**32, 33**
132	*Staurastrum lapponicum* (Schmidle) Grönblad 1926	*21*	**218**
133	*Staurastrum manfeldtii* Delponte 1878	*5*	**32**
134	*Staurastrum margaritaceum* Menegh. ex Ralfs 1848	*16*	**174**
135	*Staurastrum muticum* Bréb. ex Ralfs 1848	*10, 11*	**99, 104**
136	*Staurastrum muticum* f. *minus* Rabenh. 1868*****	*13*	**133**
137	*Staurastrum paradoxum* Meyen ex Ralfs 1848	*19, 20, 23*	**201, 209, 254**
138	*Staurastrum pilosum* Bréb. 1856	*23*	**251**
139	*Staurastrum pingue* Teiling 1942	*9, 13, 14, 21, 23*	**77, 127, 140, 219, 251**
140	*Staurastrum pingue* var. *planctonicum* (Teiling) Coesel & Meesters 2013*	*13, 21*	**129, 137, 215, 219**
141	*Staurastrum punctulatum* Bréb. 1848	*12, 25*	**120, 271**
142	*Staurastrum striatum* (West & G.S.West) Ruzicka 1957*****	*5*	**33**
143	*Staurastrum teliferum* Ralfs 1848*****	*10*	**99**
144	*Staurastrum tetracerum* Ralfs ex Ralfs 1848	*4, 5, 6, 10, 12, 13, 16, 21*	**24, 29, 32, 35, 46, 99, 115, 122, 124, 129, 131, 134, 137, 174, 175, 214, 216, 225**
145	*Staurastrum trilobulatum* Dürrschm.*****	*25*	**269**
146	*Staurastrum vestitum* Ralfs 1848	*5*	**32**
147	*Staurodesmus convergens* (Ehrenb. ex Ralfs) S.Lill. 1950	*21*	**216**
148	*Staurodesmus dejectus* (Bréb.) Teiling 1954	*20*	**209**
149	*Staurodesmus dickiei* (Ralfs) S.Lill. 1950	*10, 21*	**99, 216**
150	*Staurodesmus extensus* (O.F.Andersson) Teiling 1948	*21*	**227**
151	*Staurodesmus glaber* (Ralfs) Teiling 1948	*5, 21*	**32, 216, 227**
152	*Staurodesmus lobatus* (Børgesen) Bourr. 1966	*21*	**216**
153	*Staurodesmus triangularis* var. *brevispina* (V.Allorge & P.Allorge) Coesel & Meesters 2013*****	*21*	**216**
154	*Teilingia excavata* (Ralfs ex Ralfs) Bourr. 1964	*21*	**227**
155	*Teilingia granulata* (J.Roy & Bisset) Bourr. 1964	*10, 21*	**99, 216**
156	*Teilingia quadrispinata* f. *evoluta* (A.M.Scott & Grönblad) Pal.-Mordv. 1982*****	*5*	**32**
157	*Xanthidium antilopaeum* Kütz. 1849	*10*	**99**
158	*Zygnema pectinatum* (Vaucher) Agardh 1816	*16*	**174, 180**

* new record for Turkish freshwaters.

Phylum CHAROPHYTA

Classis Zygnematophyceae

Order Desmidiales

Family Desmidiaceae

Genus *Actinotaenium* (Nägeli) Teiling

Actinotaenium wollei (West & G.S. West) Teiling 1978 (Fig. 2a)

Synonym: *Cosmarium globosum* var. *wollei* West & G.S. West 1896

Description: Cells 27.5-47.4 µm long, 20.6-36.7 µm wide, isthmus 19.9-35.2 µm. Cells 1.3-1.5 times longer than broad; cells elliptic to nearly circular, semi cells semi circular; wall finely punctate; chloroplast stellate with a central pyrenoid. The mid-region of the cell is slightly narrowed.

Ecology: This is a freshwater species.

Distribution: *Europe*: Austria, Britain, France, Italy, Netherlands, Spain, Ukraine; *North America*: Arkansas, Québec; *Caribbean Islands*: Cuba; *South America*: Brasil; *South-west Asia*: Bangladesh; *South-east Asia*: Thailand; *Asia*: Russia, Russia (Far East); Australia and *New Zealand*: New Zealand.

Occurrence: It was determined in Susurluk basin (Manyas Lake).

Genus *Cosmarium* Corda

Cosmarium brebissonii Menegh. 1848 (Fig. 2b)

Synonym: -

Description: Cells 45-79 µm wide, 88-110 µm long. Semi cells are about trapeziform with very broadly rounded angles, walls covered with closely and evenly spaced conical granules.

Ecology: This is a freshwater species and characteristic of acidic, oligo-mesotrophic bog sites.

Distribution: *Europe:* Austria, Britain, Czech Republic, France, Georgia, Germany, Hungary, Ireland, Italy, Latvia, Netherlands, Portugal, Russia (Europe), Serbia, Spain, Ukraine; *South America*: Argentina, Brazil; *Asia*: China, Russia; *Australia and New Zealand*: Queensland.

Occurrence: It was determined in Batı Akdeniz basin (Girdev Lake).

Cosmarium contractum var. *rotundatum* Borge 1925 (Fig. 2c)

Synonym: -

Description: Cells 1.5-1.8 times longer than broad, small and globose, 31-52 µm long and 21-33 µm wide; semi cells are globose to subcircular that are connected by an isthmus, lateral margins of the semi cells are convex with smooth and rounded apical margin; isthmus is 3.5-5.5 µm in length. Differs from the nominal variety in that semi cells are virtually circular in outline.

Ecology: This is a freshwater species.

Distribution: *Europe*: Austria, Britain, Czech Republic, Georgia, Germany, Netherlands; *North America*: Arkansas; *South America*: Brazil; *South-east Asia*: Philippines; *Asia*: China; Australia and *New Zealand*: Northern Territory.

Occurrence: It was determined in Kızılırmak basin (Küçük Lota Lake).

Cosmarium distentum (West) Coesel & Meesters 2015 (Fig. 2d)

Synonym: *Cosmarium laeve* var. *distentum* G.S. West

Description: Cells 14-18 µm long, 11-15 µm wide, isthmus 3-4 µm. Cell length to breadth ratio is lower from the described diagnosis of *Cosmarium laeve* Rabenh. Semi cells widely ovate from the broad base, apex rounded or slightly truncate, a prominent tubercle in the center of the semi cell. The cell wall is finely punctate.

Ecology: This is a freshwater species.

Distribution: *Europe*: Netherlands.

Occurrence: It was determined in Batı Akdeniz (Girdev Lake) and Sakarya basins (Poyrazlar Lake).

Cosmarium humile var. *substriatum* (Nordst.) Schmidle 1895 (Fig. 2e)

Synonym: -

Description: Cells 17-28 µm long, 16-26 µm wide. The cell wall is sculptured by both incurvations and granules. Differs from the nominate variety by larger cell dimensions and in that the granules are arranged in two intramarginal series.

Ecology: This is a freshwater species and rather common species in various kinds of circumneutral, meso-eutrophic water bodies.

Distribution: *Europe*: Britain, Germany, Ireland, Italy, Latvia, Netherlands, Serbia, Slovenia, Ukraine; *North America*: Québec; *South America*: Argentina; *South-west Asia*: India; *Asia*: Russia, Tajikistan.

Occurrence: It was determined in Batı Akdeniz basin (Avlan Lake).

Cosmarium impressulum var. *crenulatum* (Nägeli) Willi Krieg. & Gerloff 1965 (Fig. 2f)

Synonym: *Cosmarium crenulatum* Nägeli

Description: Cells 29-33µm long, 20-24 µm wide. Cells longer than broad, in rough outline oval with regularly undulate margin. Half-cells transverse hexagonal. In the apical view elliptical, in the lateral view broadly oval. Cell wall smooth.

Ecology: This is a freshwater species and prefers mesotrophic water.

Distribution: *Europe*: Austria, Britain, Netherlands, Serbia; *South America*: Argentina; *South-west Asia*: India; *South-east Asia*: Thailand.

Occurrence: It was determined in Kızılırmak basin (Palanga Lake).

Cosmarium mamilliferum var. *madagascariense* West & G.S. West 1895 (Fig. 2g)

Synonym: -

Description: Cells 32-43 µm long, 25-36 µm wide, isthmus 7 µm, elliptical apical view, the wall is strongly scrobiculate.

Ecology: No habitat entry has yet been made for this entity.

Distribution: *Africa*: Zimbabwe.

Occurrence: It was determined in Fırat-Dicle basin (Hazar Lake).

Cosmarium nymannianum Grunov 1866 (Fig. 2h)

Synonym: -

Description: Cells 30-54 µm long and 29-42 µm wide; isthmus 12-13 µm wide; subhexagonal, elongate, sinus narrow, linear, semi cells are trapeziform in outline with concave lateral sides and apex**,** truncate-pyramidal with rounded basal and upper angles.

Ecology: This is a freshwater species.

Distribution: *Europe*: Austria, Britain, France, Germany, Ireland, Italy, Latvia, Spain, Ukraine; *North America*: Florida, Newfoundland, Québec; *South America*: Brazil; *South-west Asia:* India, Pakistan; *Asia*: Japan, Russia.

Occurrence: It was determined in Antalya basin (Düden Lake).

Cosmarium pseudowembaerense Kouwets 1998 (Fig. 2i)

Synonym: -

Description: Cells 12-18 µm long, 10-17 µm wide. Cells about as long as broad or a little longer, with a deep, linear sinus, closed for the greater part. Semi cells about hexagonal with broadly rounded angles and straight to slightly concave lateral sides, oval-elliptic in apical view. Apex is distinctly concave. Cell wall is smooth.

Ecology: This is a freshwater species.

Distribution: *Europe*: Czech Republic, France, Germany, Netherlands; *South America*: Brazil.

Occurrence: It was determined in Batı Akdeniz (Avlan Lake) and Fırat-Dicle basins (Kalecik Reservoir).

Cosmarium quinarium Lundell 1871 (Fig. 2j)

Synonym: -

Description: Cells 30-39 µm wide, 36-48 µm long, sinus deep, narrow, linear**.** Trapeziform semi cells with broadly rounded angles and slightly convex sides being marked with distant granules.

Ecology: This is a freshwater species.

Distribution: *Europe*: Austria, Britain, France, Germany, Ireland, Latvia, Netherlands, Scandinavia, Slovakia, Sweden, Ukraine; *North America*: Florida, Québec; *South America*: Brazil; *South-west Asia*: Bangladesh, India, Pakistan; *South-east Asia*: Thailand; *Asia*: Japan, Russia, Russia (Far East), Taiwan.

Occurrence: It was determined in Sakarya basin (Avdan Lake).

Cosmarium sphagnicola West & West 1897 (Fig. 2k)

Synonym: -

Description: Cells 9-13 µm long, 10-14 µm wide. Cells very small, roughly as long as they are wide. Half-cells elongated hexagonal with rounded corners and abroad, flat or slightly concave apex. Apical views elliptical, half-cells in a lateral view broadly oval or almost circular.

Ecology: This is a freshwater species.

Distribution: *Europe*: Austria, Britain, Czech Republic, France, Germany, Hungary, Ireland, Italy, Latvia, Netherlands, Portugal, Romania, Scandinavia, Spain, Ukraine; *North America*: Québec; *South America*: Brazil; *Asia*: Russia, Russia (Far East); *Australia and New Zealand*: New Zealand.

Occurrence: It has been detected in the Batı Akdeniz basin (Girdev Lake).

Cosmarium subadoxum Grönblad 2007 (Fig. 2l)

Synonym: -

Description: Cell 8-11 µm long, 8-11 µm wide. Cells about as long as broad with a deep, linear sinus, closed for the greater part. Semi cells in outline rectangular with convex lateral sides. Semi cells in apical view elliptic with a small, median tubercle on either side.

Ecology: This is a freshwater species.

Distribution: *Europe*: Czech Republic, France, Netherlands; *South America*: Brazil.

Occurrence: It was determined in Sakarya (Poyrazlar Lake), Fırat-Dicle (Kapıaçmaz Pond, Hasancık Pond), and Asi basins (Yarseli Reservoir, Üçpınar Pond).

Cosmarium subgranatum (Nordst.) Lütkem. 1902 (Fig. 2m)

Synonym: -

Description: Cells 20-34 µm long, 15-25 µm wide. Cells longer than broad with a deep, linear sinus, closed for the greater part. Semi cells in rough outline pyramidal with lateral sides and undulations of the magrin are pretty

irregular. Apical view ellipsoid with median inflation. Cell wall smooth.

Ecology: This is a freshwater species and common in meso-eutrophic water bodies, both acidic and alkaline.

Distribution: *Arctic*: Ellesmere Island; *Europe*: Britain, Czech Republic, France, Georgia, Germany, Hungary, Ireland, Italy, Netherlands, Romania, Serbia, Slovakia, Slovenia, Ukraine; *North America*: Northwest Territories, Québec; *Caribbean Islands*: Cuba; *South America*: Brazil; *Middle East*: Iraq; *Asia*: Myanmar; *Asia*: China, Russia (Far East), Taiwan, Tajikistan; *Australia and New Zealand*: New Zealand; *Pacific Islands*: Hawaiian Islands.

Occurrence: It was determined in Sakarya basin (Avdan Lake).

Cosmarium subquadrans West & West 1905 (Fig. 2n)

Synonym: -

Description: Cells small, 11-12.5 µm long, 12-15 µm wide, isthmus 3.5-4 µm wide, semi cells in front view transversely oblong, apex broad, truncate or slightly convex, semi cells in lateral view subcircular; vertical view fusiform-elliptic; cell wall smooth.

Ecology: This is a freshwater species.

Distribution: *Europe*: Austria, Britain, Czech Republic, Germany, Ireland, Italy, Netherlands, Ukraine; *Asia*: China, Japan, Russia, Tajikistan.

Occurrence: It was determined in Asi basin (Yarseli Reservoir, Üçpınar Pond).

Cosmarium subquadrans var. *minus* Symoens 1873 (Fig. 2o)

Synonym: -

Description: Cells 12-13 µm long, 16-18 µm wide. Cells broader than long, in outline oval with a deep, linear sinus, closed for the greater part. Semi cells entire with broadly rounded angles, in apical view fusiform to rhomboid. Cell wall smooth.

Ecology: This is a freshwater species.

Distribution: *Europe*: Czech Republic, Germany, Ireland, Netherlands.

Occurrence: It was determined in Sakarya basin (Sapanca Lake).

Cosmarium tetrachondrum Lundell 1871 (Fig. 2p)

Synonym: -

Description: Cell 20-23 µm long, 23-27 µm wide. Cells broader than long with a deep, linear sinus, closed for the greater part. Semi cells in outline low-trapeziform with broadly rounded angles. Apical view ellipsoid.

Ecology: This is a freshwater species.

Distribution: *Europe*: Britain, Czech Republic, France, Germany, Ireland, Latvia, Netherlands, Ukraine. *Asia:* Japan, Russia.

Occurrence: It was determined in Batı Akdeniz basin (Girdev Lake).

Genus *Desmidium* C. Agardh

Desmidium aptogonum Bréb. 1849 (Fig. 3a)

Synonym: -

Description: Cells 21-31 µm wide, 13-19 µm long, moderately constricted with an acute, open sinus; isthmus 15-24.5 µm wide; semi cells transversely oblong, lateral margins are slightly concave then converging to the apex.

Ecology: This is a freshwater species.

Distribution: *Europe*: Britain, Czech Republic, Finland, France, Georgia, Germany, Ireland, Italy, Netherlands, Portugal, Scandinavia, Slovenia, Spain, Sweden, Ukraine; *North America*: Florida, Maryland, New York, Québec, Wisconsin; *Caribbean Islands*: Cuba; *South America*: Brazil, Uruguay; *Middle East*: Iraq; *South-west Asia*: Bangladesh; India, Pakistan; *South-east Asia*: Myanmar, Thailand; *Asia*: China, Japan, Russia (Far East), Tajikistan; *Australia and New Zealand*: New South Wales, New Zealand, Northern Territory, Queensland, Victoria; *Pacific Islands*: Hawaiian Islands.

Occurrence: It was determined in Büyük Menderes basin (Karakuyu Reeds).

Genus *Euastrum* Ehrenb.

Euastrum lacustre (Messik.) Coesel 1984 (Fig. 3b)

Synonym: -

Description: Cells 28-48 µm long, 26-46 µm wide, isthmus 9-10 µm wide. Cells medium-sized, sinus narrow linear with dilated apex, semi cells nearly quadrangular, cell wall smooth.

Ecology: This is a freshwater species.

Distribution: *Europe*: Britain, France, Netherlands.

Occurrence: It was determined in Kızılırmak basin (Hafik Lake).

Genus *Groenbladia* Teiling

Groenbladia undulata (Nordst.) Kurt Först. 1973 (Fig. 3c)

Synonym: *Hyalotheca undulata* Nordst.

Description: Cells 10-17.5 µm long, 6-9 µm wide, more or less dumbbell-shaped, shallow median indentation; isthmus 4.5-7.5 µm wide, filaments sometimes in a mucilage sheath.

Ecology: This is a freshwater species.

Distribution: *Europe*: Austria, Britain, France, Germany, Ireland, Scandinavia, Spain; *North America*: Arkansas, Maine, Québec; *Caribbean Islands*: Cuba;

South America: Brazil; *South-west Asia*: Bangladesh; *Australia and New Zealand*: Northern Territory.

Occurrence: It was determined in Sakarya basin (Akgöl 1 Lake).

Genus *Micrasterias* Agardh

Micrasterias furcata Agardh 1848 (Fig. 3d)

Synonym: -

Description: Cells 150 µm long, 130 µm wide, isthmus 17-20 µm wide, cells are elliptical in outline with narrowly opened deep sinus. Semi cells with well-developed lateral lobes. The cell wall is smooth.

Ecology: This is a freshwater species.

Distribution: *Europe*: Austria, Britain, Czech Republic, France, Germany, Ireland, Italy, Netherlands, Romania, Spain, Ukraine; *North America*: Arkansas, Maine, Québec, Wisconsin; Caribbean Islands: Cuba; *South America*: Brazil, Uruguay; *Middle East*: Iraq; *Asia*: Russia (Far East); *Australia and New Zealand*: Victoria.

Occurrence: It was determined in Sakarya basin (Işık Dağı Karagöl Lake).

Genus *Spondylosium* Bréb.

Spondylosium panduriforme (Heimerl) Teiling 1957 (Fig. 3e)

Synonym: *Cosmarium moniliforme* var. *panduriforme* (Heimerl) Schmidle

Description: Cells 36-42 µm long, 21-22 µm broad, isthmus 13.2-14 µm. Semi cells circular; apex broadly rounded; cell wall finely punctate. This species is characterized by a copious mucilaginous envelope, enclosing the complete cell body.

Ecology: This is a freshwater species.

Distribution: *Europe*: France, Germany, Ireland, Italy, Netherlands, Ukraine; *South America*: Argentina, Brazil, Uruguay; *South-west Asia:* Bangladesh; *Asia*: Russia (Far East); *Australia and New Zealand*: New South Wales, New Zealand.

Occurence: It was determined in the Fırat-Dicle basin (Kapıaçmaz Pond).

Genus *Staurastrum* Meyen

Staurastrum pingue var. *planctonicum* (Teiling) Coesel & Meersters 2013 (Fig. 3f)

Synonym: *Staurastrum planctonicum* Teiling

Description: Cells 3 radiate, 70-95 µm wide, 57-65 µm long with processes, isthmus 9-13 µm wide; lower part of semi cells elongate, cup-shaped flaring upwards into long, slightly divergent, curved processes, walls smooth.

Ecology: This is a freshwater species.

Distribution: *Europe*: Bulgaria; *Africa*: Democratic Republic of Congo.

Occurrence: It was determined in Sakarya (Sapanca Lake, Üçlerkayası Pond) and Fırat-Dicle basins (Palandöken Pond, Otlukbeli Pond).

Staurastrum muticum f. *minus* Rabenh. 1868 (Fig. 3g)

Synonym: -

Description: Cells 21-22 µm long, 19-21 µm wide, isthmus 7-8 µm. Cells medium-sized, very slightly longer than broad, semi cells narrowly elliptic oval, in vertical view cells triangular, narrowly rounded at the angles, cell wall finely and densely punctate.

Ecology: This is a freshwater species.

Distribution: *Europe*: Ireland, Netherlands; *North America*: Québec; *South America*: Argentina; *South-west Asia*: India; *Australia and New Zealand*: Northern Territory.

Occurrence: It was determined in Fırat-Dicle basin (Dedeyolu Pond).

Staurastrum striatum (West & West) Ruzicka 1957 (Fig. 3h)

Synonym: -

Description: Cells 25-35 µm long, 24-36 µm wide. Cells about as long as broad, deeply constricted. Sinus is widely open, acute-angled. Semi cells (sub) rhomboid with rounded, or rounded-truncate lateral angles**.** Semi cells in apical view 3-angular with slightly concave sides and rounded, or rounded-truncate angles.

Ecology: This is a freshwater species.

Distribution: *Europe*: Czech Republic, France, Germany, Netherlands, Romania, Serbia; *Australia and New Zealand*: New South Wales.

Occurrence: It was determined in Batı Akdeniz basin (Avlan Lake).

Staurastrum teliferum Ralfs 1848 (Fig. 3i)

Synonym: -

Description: Cells 3-radiate, 40-64 µm wide, 32-56 µm long excluding spines, deeply constricted with an open sinus, isthmus 8-10 µm wide; semi cells elliptical with broadly rounded angles.

Ecology: This is a freshwater species.

Distribution: *Europe*: Andorra, Austria, Baltic Sea, Britain, Czech Republic, France, Georgia, Germany, Hungary, Ireland, Italy, Latvia, Netherlands, Portugal, Romania, Scandinavia, Serbia, Slovakia, Slovenia, Spain, Ukraine; *North America*: Northwest Territories, Québec; *South America*: Brazil, Uruguay; *Africa*: Zaire; *Middle East*: Iraq; *South-west Asia*: India; *Asia*: China, Japan, Taiwan.

Occurrence: It was determined in Çoruh basin (Çil Lake).

Staurastrum trilobulatum Dürrschm. (Fig. 3j)

Synonym: -

Description: Cells 1.1-1.4 times longer than wide, 13-26 µm wide, 18-31 µm long, isthmus 5-8 µm; median constriction deep, sinus closed; semi cells subtrapezoidal and 3-lobed, with truncate basal lobes and apex, rectangular basal angles and apical slightly rounded; semi cells elliptic in apical and lateral view, cell wall smooth or finely punctate.

Ecology: This is a freshwater species.

Distribution: No record was found regarding the distribution range of this taxon.

Occurrence: It was determined in Yeşilırmak basin (Uyuz Lake).

Genus *Staurodesmus* Teiling

Staurodesmus triangularis var. *brevispina* (Allorge & Allorge) Coesel & Meesters 2013 (Fig. 3k)

Synonym: -

Description: Cells mostly biradiate, rarely triradiate, 19-25 µm long, 19-25 µm wide (excluding spines). Isthmus short, 5-7 µm wide. This species is characterized by biradiate cells, relatively short spines, and 'elevated' apices. Spinesshorter than 2/3 breadth of the semi cell body. Lateral sides of semi cell body straight to slightly convex.

Ecology: This is a freshwater species.

Distribution: No record was found regarding the distribution range of this taxon.

Occurrence: It was determined in Sakarya basin (Işık Dağı Karagöl Lake).

Genus *Teilingia* Bourr.

Species: *Teilingia quadrispinata* f. *evoluta* (A.M.Scott & Grönblad) Pal.-Mordv. (Fig. 3m)

Synonym: *Sphaerozosma quadrispinatum* f. *evolutum* A.M.Scott & Grönblad

Description: Cells 7.5-10.7 µmlong, 8.7-11.5µm wide, istmus 4.1-5.7 µm.

Ecology: This is a freshwater species.

Distribution: *North America*: Florida, *Asia*: Russia.

Occurrence: It was determined in Batı Akdeniz basin (Girdev Lake).

Family Closteriaceae

Genus *Closterium* Nitzsch

Closterium dianae var. *rectius* (Norst.) De Toni 1977 (Fig. 3n)

Synonym: -

Description: Cells 150-380 µm long, 8-16 µm wide. Cells approximately 8-15 times as long as wide, evenly slightly to strongly curved, cell wall always smooth, without girdles.

Ecology: This is a freshwater species.

Distribution: *Europe*: Czech Republic, Germany, Netherlands.

Occurrence: It was determined in Akarçay basin (Eber Lake).

Closterium pygmaeum Gutw. 1890 (Fig. 3o)

Synonym: -

Description: Cells 57 µm long and 5.3 µm wide, slightly curved, gradually attenuated toward the apex which is rounded; cell wall smooth, cells contain two pyrenoids in half part of the cell.

Ecology: This is a freshwater species.

Distribution: *Europe*: Austria, Britain, France, Germany, Netherlands, Scandinavia, Spain, Ukraine; *South America*: Brazil; *Australia and New Zealand*: New South Wales, Tasmania.

Occurrence: It was determined in Sakarya basin (Avdan Lake).

Order Zygnematales

Family Zygnemataceae

Genus *Spirogyra* Link

Spirogyra decimina var. *elongata* (Vaucher) Petlovany 2015 (Fig. 3l)

Synonym: *Spirogyra elongata* (Vaucher) Dumortier

Description: Cells 45-280 µm long, 26-38 µm wide, chloroplast single, making 2-5 turns of cell; conjugation ladder-like and lateral, conjugation scalariform; median wall smooth, thick with a wavy suture line.

Ecology: This is a freshwater species.

Distribution: *Europe*: Britain, Georgia, Germany, Ireland; Latvia, Netherlands, Romania, Russia (Europe), Slovakia, Slovenia, Spain; *North America*: California, Laurentian Great Lakes, Québec; *South America*: Argentina, Brazil; *Middle East*: Iraq, Turkey; *South-west Asia*: India, *Asia*: China, Japan, Tajikistan; *Australia and New Zealand*: New South Wales, New Zealand, Queensland, South Australia.

Occurrence: It was determined in Antalya basin (Eğirdir Lake).

Discussion

A total of 158 taxa from Charophyta were determined in the study conducted from 2017 to 2019 in 25 river basins of Turkey. Of these 31 taxa represent new records for the freshwater algal flora of Turkey. They belong to genera *Cosmarium* (15), *Staurastrum* (5), *Closterium* (2), *Actinotaenium* (1), *Desmidium* (1), *Eastrum* (1),

Groenbladia (1), *Micrasterias* (1), *Spirogyra* (1), *Spondylosium* (1), *Staurodesmus* (1), and *Teilingia* (1).

Although some of the Charophyta taxa (*Elakatothrix gelatinosa*, *Staurastrum tetracerum*, *Cosmarium laeve*, *Staurastrum cingulum*, *Closterium aciculare*, *Staurastrum gracile*, *Cosmarium neodepressum*, *Staurastrum chaetoceras*, *Closterium acutum* var. *variabile*, *Closterium littorale*) found to have a wide distribution in 25 river basins of Turkey, most of the charophyta taxa (115 taxa) found to have rare distribution and were only observed in 1 or 2 lakes in 25 river basins. Besides, all of 31 new records have a rare distribution range except *Cosmarium subadoxum* and *Staurastrum pingue* var. *Planctonicum*. *Elakatothrix gelatinosa* has the highest distribution rate with its occurrence in 29 lakes, among the member of Charophyta.

There is no direct correlation between the number of lakes sampled in the basins and the number of species found. Despite sampling 23 lakes in Kızılırmak basin, only 15 Charophyta taxa were found in Kızılırmak basin, and only 6 Charophyta taxa were found in Ceyhan basin despite 18 sampling lakes. However, 42 Charophyta taxa were found in Batı Akdeniz where only 13 lakes were studied and 27 Charophyta taxa were found in Antalya basin where only 9 lakes were studied.

Basin-based distributions of Charophyta members identified in this study were as below: 50 taxa in Sakarya, 42 in Batı Akdeniz, 27 in Antalya, 26 in Konya, 21 in Fırat-Dicle, 17 in Çoruh, 15 in Kızılırmak, 13 in Yeşilırmak, Susurluk, Asi, 12 in Meriç Ergene, 10 in Kuzey Ege, 9 in Gediz, Akarçay, Büyük Menderes, 6 in Ceyhan, Doğu Akdeniz, 4 in Seyhan, Küçük Menderes, and 3 in Batı Karadeniz, Doğu Karadeniz, Marmara, Van Gölü, Aras basins. The Burdur basin is the only basin that no Charophyta species were found. The reason for this is that high salinity in Acı Lake, high pH in Salda Lake and higher eutrophic features in Burdur and Karataş Lakes. Thus, Desmids, which are sensitive species, were not found in the lakes of Burdur basin. The highest Charophyta diversity was observed in Girdev Lake (Batı Akdeniz basin) and Işık Dağı Karagöl Lake (Sakarya basin) among the lakes of Turkey's 25 river basins in this study. The moderate ecological status in both lakes proves that desmids are mostly appear in uncontaminated waters.

Charophytes are commonly found in freshwater habitats such as ponds and streams, and few species are found in brackish waters (Adl *et al.* 2005). Most of the species are known from the temperate zone, but they also tolerate polar conditions (Gąbka 2007, Boszke & Bociąg 2008). Desmidales, as an important ordo in Charophyta, are mostly planktonic organisms that very sensitive to environmental changes, and eutrophic conditions do not contain ideal growth conditions for these group members (Davis 1955, Edmondson 1959, Gayathri *et al.* 2011). They occur typically in clean standing waters such as lakes, ponds or shallow pools. The highest diversity is found in mesotrophic, slightly acidic to slightly alkaline water bodies like fen hollows or moorland pools where desmids are among the dominant groups of the phytobenthos, both in terms of species richness and biomass (Coesel & Meesters 2007). Desmids are not merely one of the main freshwater microalgae groups that occur in high mountain lakes biotopes in Turkey, but they also inhabit microhabitats with oligotrophic conditions characterized by relatively acidic to weakly alkaline waters with low conductivity (Şahin & Akar 2019). In this study, only the *Spirogyra decimina* var. *elongata* was identified from the Zygnematales order. *Spirogyra* species were found in freshwater habitats under moderately eutrophic or mesotrophic conditions (Novis 2004, Stancheva *et al.* 2013, Sherwood *et al.* 2018). They mostly occurr in benthos (Volkova et al. 2018) but they can also be found in plankton (Kravtsova *et al*. 2020).

In conclusion, 31 new records were added to the freshwater algal flora of Turkey within this study. 13 of these newly recorded taxa belong to the Charophyta group, which are widely distributed in different parts of the world and 18 taxa are rarely distributed. When the current new records of this study were added to the previous Turkish algae list of Taşkın *et al*. (2019) and the database of Turkish algae (Maraşlıoğlu & Gönülol 2021) which is formed by screening a large number of studies on Turkish algae, it can be concluded that there is nearly around 450 Charophyta species in Turkish freshwaters.

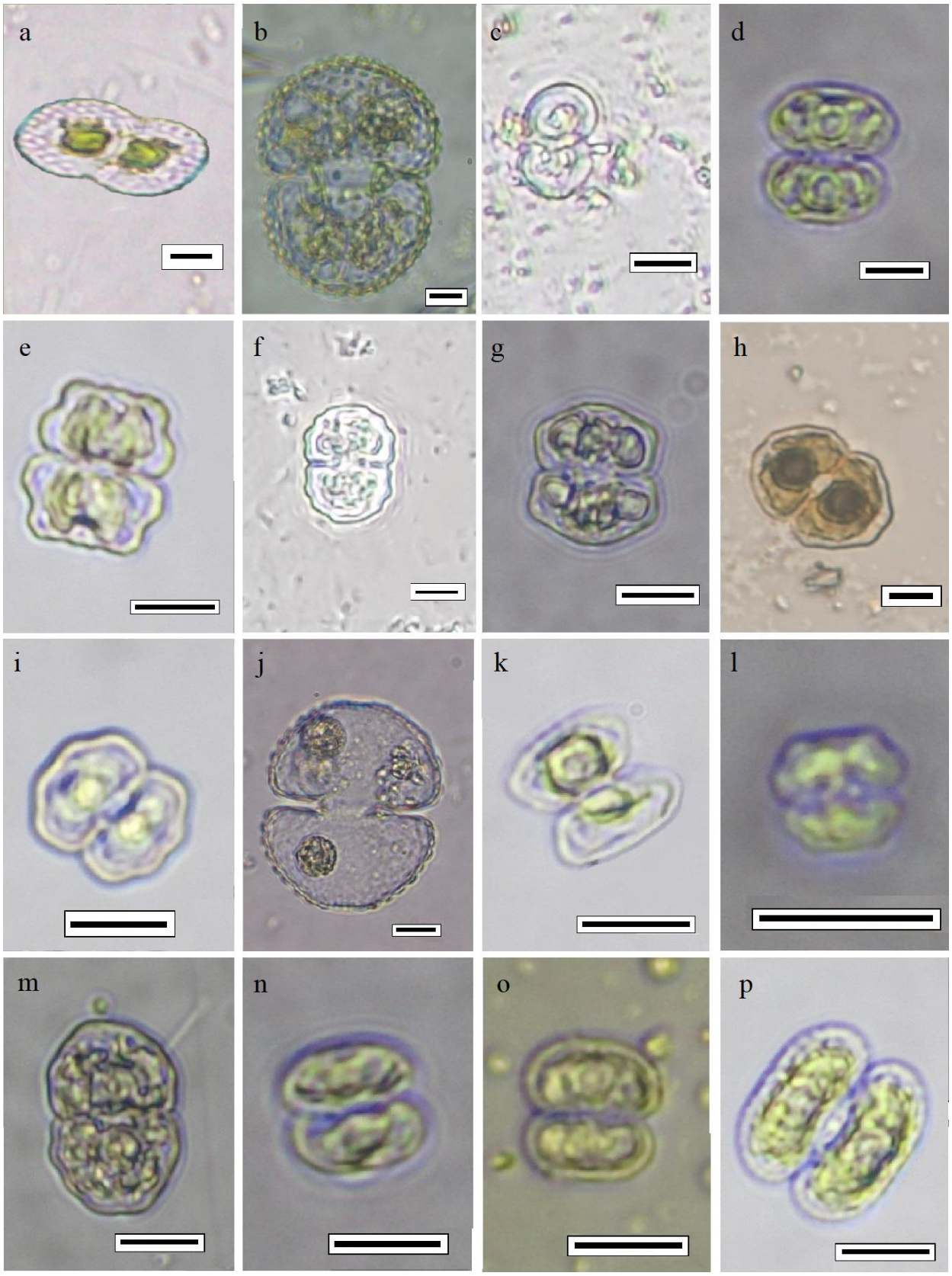

Fig. 2. Microscopic view of determined Desmidiales species; **a)** *Actinotaenium wollei*, **b)** *Cosmarium brebissonii*, **c)** *Cosmarium contractum* var. *rotundatum*, **d)** *Cosmarium distentum*, **e)** *Cosmarium humile* var. *substriatum*, **f)** *Cosmarium impressulum* var. *crenulatum*, **g)** *Cosmarium mamilliferum* var. *madagascariense*, **h)** *Cosmarium nymannianum*, **i)** *Cosmarium pseudowembaerense*, **j)** *Cosmarium quinarium*, **k)** *Cosmarium sphagnicola*, **l)** *Cosmarium subadoxum*, **m)** *Cosmarium subgranatum*, **n)** *Cosmarium subquadrans*, **o)** *Cosmarium subquadrans* var. *minus*, **p)** *Cosmarium tetrachondrum*. Scales 10 µm.

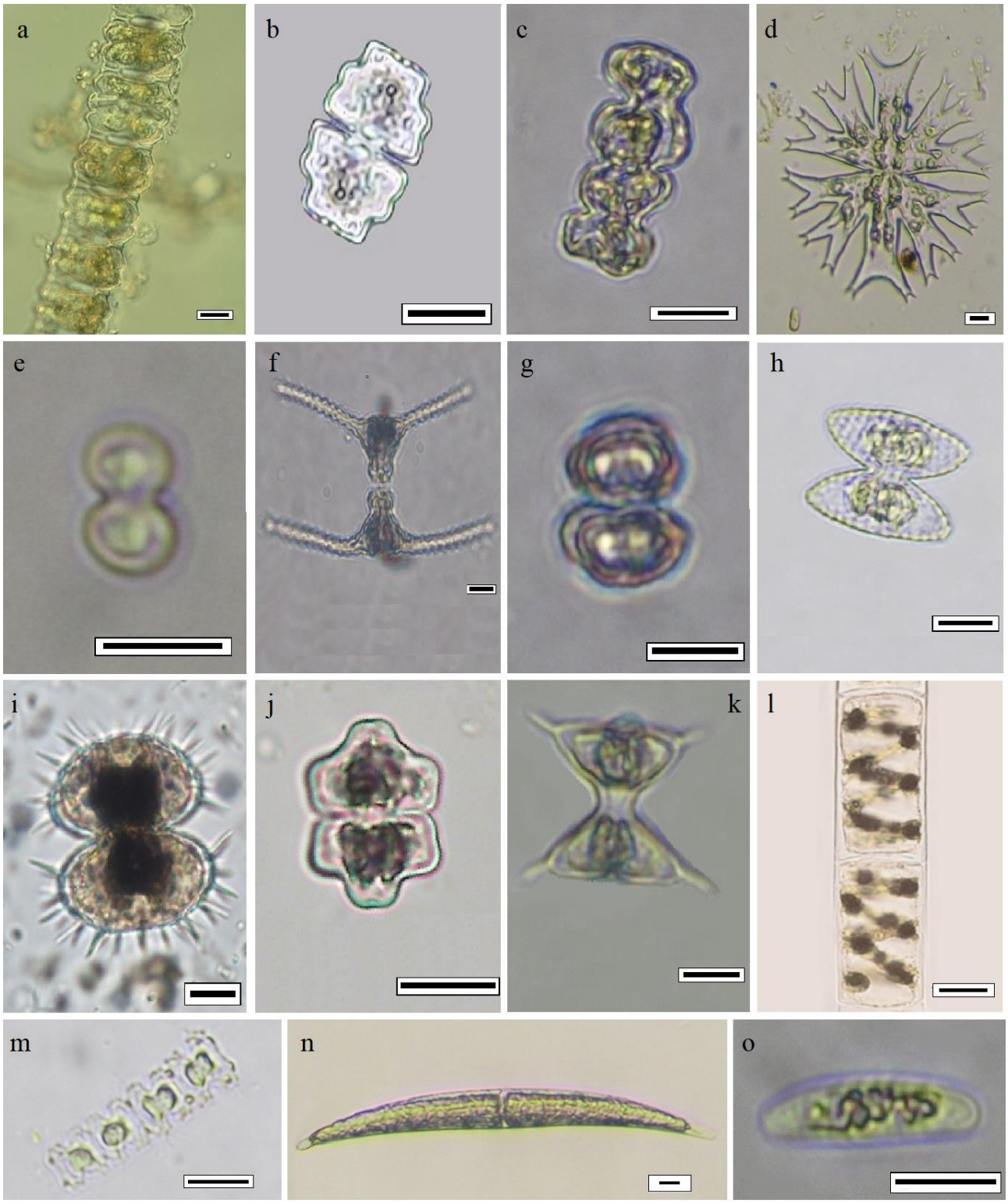

Fig. 3. Microscopic wiew of determined Desmidiales and Zygnematales species; **a)** *Desmidium aptogonum*, **b)** *Euastrum lacustre*, **c)** *Groenbladia undulata*, **d)** *Micrasterias furcata*, **e)** *Spondylosium panduriforme*, **f)** *Staurastrum pingue* var. *planctonicum*, **g)** *Staurastrum muticum* f. *minus*, **h)** *Staurastrum striatum*, **i)** *Staurastrum teliferum*, **j)** *Staurastrum trilobulatum*, **k)** *Staurodesmus triangularis* var. *brevispina*, **l)** *Spirogyra decimina var. elongata* **m)** *Teilingia quadrispinata* f. *evoluta*, **n)** *Closterium dianae* var. *rectius*, **o)** *Closterium pygmaeum*. Scales 10 μm.

Acknowledgement

We would like to thank the executives and the staff of Çınar Engineering Consulting Co. (Turkey) who had executed the Project (Establishment of Reference Monitoring Network in Turkey, 2017-2019).

Ethics Committee Approval: Since the article does not contain any studies with human or animal subject, its approval to the ethics committee was not required.

Author Contributions: Concept: F.M., T.O.S., Desing: F.M., E.N.S., T.O.S., Execution: F.M., E.N.S., N.D., A.Ç., H.S., B.Ö., T.O.S., B.T., Material supplying: F.M., E.N.S., N.D., A.Ç., H.S., B.Ö., T.O.S., T.C., C.N.S., B.T., Data acquisition: F.M., E.N.S., N.D., A.Ç., H.S., B.Ö., T.O.S., T.C., C.N.S., B.T., Data analysis/interpretation: F.M., E.N.S., A.Ç., H.S., B.Ö., T.O.S., B.T., Writing: F.M., E.N.S., T.O.S., Critical review: F.M., T.O.S., T.C., Y.K.

Conflict of Interest: The authors have no conflicts of interest to declare.

Funding: This study was supported by the Ministry of Agriculture and Forestry, Directorate General of Water Management (Project number: 2011K050400).

Editor-in-Chief note: Burak Öterler and Tuğba Ongun Sevindik are members of Trakya University Journal of Natural Sciences Editorial Board. However, they weren't involved in the decision process during manuscript evaluation.

References

1. Adl, S.M., Simpson A.G.B., Farmer, M.A, Andersen, R.A., Anderson, O.R., Barta, J.R., Bowser, S.S., Brugerolle, G., Fensome, R.A., Fredericq, S., James, T.Y., Karpov, S., Kugrens, P., Krug, J., Lane, C.E., Lewis, L.A., Lodge, J., Lynn, D.H., Mann, D.G., McCourt, R.M., Mendoza, L., Moestrup, O., Mozley-Standridge, S.E., Nerad, T.A., Shearer, C.A., Smirnov, A.V., Spiegel, F.W. & Taylor M.F.H.R. 2005. The new higher level classification of eukaryotes with emphasis on the taxonomy of protists. *The Journal of Eukaryotic Microbiology*, 52(5): 399-451. https://doi.org/10.1111/j.1550-7408.2005.00053.x
2. Akar, B. & Şahin, B. 2014. New desmid records of Karagöl Lake in Karagöl-Sahara National Park (Şavşat-Artvin/Turkey). *Turkish Journal of Fisheries and Aquatic Sciences*, 14(1): 269-274. https://doi.org/10.4194/1303-2712-v14_1_29
3. Apaydın-Yağcı, M. & Turna, İ.İ. 2002. A new record for the algal flora of Turkey: *Chaetomorpha crassa* (C.ag.) Kütz. (Cladophoraceae, Chlorophyceae). *Turkish Journal of Botany*, 26: 171-174.
4. Atıcı, T. 2002. Nineteen new records from Sarıyar Dam Reservoir phytoplankton for Turkish Freshwater algae. *Turkish Journal of Botany*, 26(6): 485-490.
5. Aysel, V. 2005. Check-List of the Freshwater Algae of Turkey. *Journal of Black Sea/Mediterranean Environment*, 11: 1-124.
6. Aysel, V., Dural, B., & Gezerler-Şipal, U. 1993. Two new records of Cyanophyceae for the Algal Flora of Turkey. *Turkish Journal of Botany*, 17: 263-266.
7. Baykal, T., Akbulut, T., Açıkgöz, İ., Udoh, A.U., Yıldız, K. & Şen, B. 2009. New Records For the Freshwater Algae of Turkey. *Turkish Journal of Botany*, 33: 141-152.
8. Bekleyen, A., Gokot, B. & Varol, M. 2011. Thirty-four new records and the diversity of the Rotifera in the Turkish part of the Tigris River watershed, with remarks on biogeographically interesting taxa. *Scientific Research and Essays*, 6(30): 6270-6284. https://doi.org/10.5897/SRE11.355
9. Boszke, P. & Bociag, K. 2008. Morphological ¸ variation of oospores in the population of Chara rudis A. Braun in a mesotrophic lake. *Polish Journal of Ecology*, 56(1): 139-147.
10. Brummitt, R.K. & Powell, C.E. 1992. *Authors of Plant Names*. A List of Authors of Scientific Names of Plants, With Recommended Standard Forms of Their Names, Including Abbreviations. Royal Botanic Gardens, Kew, 732 pp.
11. Coesel, P.F.M. & Meesters, K.J. 2007. *Desmids of the lowlands: Mesotaeniaceae and Desmidiaceae of the European lowlands*. Zeist, NLD, KNNV Publishing, 351 pp.
12. Coesel, P.F.M. 1998. *Sieralgen en Natuurwaarden*. 1st ed. Utrecht, the Netherlands: KNNV Publishing, Utrecht, 56 pp.
13. Coesel, P.F.M., Kwakkestein, R. & Verschoor, A. 1978. Oligotrophication and eutrophication tendencies in some Dutch moorland pools, as reflected in their desmid flora. *Hydrobiologia*, 61: 21-31.
14. Compère, P. 2001. *Flore pratique des algues d'eau douce de Belgique.* Tome 5 Desmidiees 1: Mesotaeniaceae, Gonatozygaceae, Peniaceae, Closteriaceae. Meise, BEL, Jardin Botanique National de Belgique, 69 pp.
15. Davis, C.C. 1955. *The marine and freshwater plankton*. Mishigan State University Press, Mishigan, 562 pp.
16. DGWM (Ministry of Agriculture and Forestry, General Directorate of Water Management), 2015a. *Project of Determining Sensitive Area and Water Quality Targets based on River Basin in Turkey*. Final Report, Vol-1.
17. DGWM (Ministry of Agriculture and Forestry, General Directorate of Water Management), 2015b. *The Communique on Sampling and Biological Sampling from Surface Waters, Groundwater and Sediment*. Official Gazette, Number: 29274.
18. DSİ (Turkish Acronym for State Hydraulic Works), 2014. *Water and DSI: 60 Years (1954–2014) Full of Realized Projects*. Booklet by Ministry of Forestry and Water Affairs (English), Ankara.
19. Edmondson, W.T. 1959. *Freshwater Biology*. John Wiley and Sons, New York, 124 pp.
20. Gąbka, M. 2007. Distribution of *Chara tenuispina* A. Braun 1835 (Characeae) in Poland. *Oceanological and Hydrobiological Studies*, 36(1): 241-248.

21. Gayathri, N., Rajashekhar, M., Fatima, K., Vijaykumar, K., Ratandeep & Baburrao, M. 2011. Hydrochemistry and plankton diversity of Tungabhadra reservoir Bellary district, Karnataka. *International Journal of Zoology Research*, 1(1): 01-07.

22. Gönülol, A., Öztürk, M. & Öztürk, M. 1996. A check-list of the freshwater algae of Turkey. *Ondokuz Mayıs University Faculty of Arts and Sciences Journal of Science*, 7(1): 8-46.

23. Guiry, M.D. & Guiry, G.M. 2021. AlgaeBase. World-wide electronic publication, National University of Ireland, Galway. http://www.algaebase.org (Date accessed: 20 January 2021).

24. Hansen, G., Stastny, J., Moestrup, Ø. & Lundholm, N. 2018. Diversity and conservation of desmids in Bornholm, Denmark – revisiting after 130 years. *Nordic Journal of Botany*, 36(10): 1-14. https://doi.org/10.1111/njb.01994

25. Huber-Pestalozzi, G. 1982. *Das phytoplankton des süsswassers systematik und biologie*. Teil 8, 1. Hälfte, Conjugatophyceae Zygnematales und Desmidiales (excl. Zygnemataceae), E. Schweizerbarth'sche Verlagsbuchhandlung (Nagele u. Obermiller), Stuttgart, 543 pp.

26. John, D.M., Whitton, B.A. & Brook, A.J. 2003. *The Freshwater Algal Flora of the British Isles: An Identification Guide to Freshwater and Terrestrial Algae*. The Natural History Museum and The British Phycological Society, Cambridge: Cambridge University Press, 714 pp.

27. Kadlubowska, J.Z. 1984. *Süßwasserflora von Mitteleuropa 16. Chlorophyta VIII: Conjugatophyceae I: Zygnemales*. Jena, DEU, VEB Gustav Fischer Verlag, 531 pp.

28. Kolkwitz, R. & Krieger, H. 1971. *Dr L. Rabenhorst's Kryptogamen-Flora 13*. 2. Abteilung. Zygnemales: Lieferung 1-4, New York, USA, Johnson reprint corporation, 163 pp.

29. Kouwets, F. 2008. The species concept in desmids: the problem of variability, infraspecific taxa and the monothetic species definition. *Biologia*, 63: 881-887.

30. Kravtsova, L.S., Mizandrontsev, I.B., Vorobyova, S.S., Izhboldina, L.A., Mincheva, E.V., Potyomkina, T.G., Golobokova L.P., Sakirko, M.V., Triboy, T.I., Khanaev, I.V., Sherbakov, D.Y. & Fedotov, A.P. (2020). Influence of water motion on the spatial distribution of *Spirogyra* in Lake Baikal. *Journal of Great Lakes Research*, 46(1): 29-40.

31. Lee, O.M. 2015. Additions to the six taxa of the genus *Cosmarium* (Desmidiaceae, Charophyta) in Korea. *Journal of Ecology and Environment*, 38: 629-636.

32. Lenzenweger, R. 1996. *Bibliotheca Phycologica*. band 101. Desmidiaceenflora von Österreich. Teil 1, Berlin, DEU, Cramer, 162 pp.

33. Lenzenweger, R. 1997. *Bibliotheca Phycologica*, band 102. Desmidiaceenflora von Österreich. Teil 2, Berlin, DEU, Cramer, 216 pp.

34. Lenzenweger, R. 1999. *Bibliotheca Phycologica*. band 104. Desmidiaceenflora von Österreich. Teil 3, Berlin, DEU, Cramer, 218 pp.

35. Lenzenweger, R. 2003. *Bibliotheca Phycologica*. band 111. Desmidiaceenflora von Österreich. Teil 4, Berlin, DEU, Cramer, 87 pp.

36. Lind, E.M. & Brook, A.J. 1980. *Desmids of the English Lake District*. Freshwater Biological Association Scientific Publication, No: 42, Ambleside, Cumbria, 123 pp.

37. Maraşlıoğlu, F. & Gönülol, A. 2021. Turkishalgae electronic publication, Çorum, Turkey. http://turkiyealgleri.hitit.edu.tr (Date accessed: 15 January 2021).

38. Maraşlıoğlu, F. & Soylu, E.N. 2018. New Diatom Records for Turkish Freshwater Algal Flora from Lakes Ladik (Samsun, Turkey) and Hazar (Elazığ, Turkey). *Turkish Journal of Fisheries and Aquatic Sciences*, 18(3): 463-474. https://doi.org/10.4194/1303-2712-v18_3_12

39. Novis P.M. 2004. New records of *Spirogyra* and *Zygnema* (Charophyceae, Chlorophyta) in New Zealand. *New Zealand Journal of Botany*, 42: 139-52.

40. Oliveira I., Bicudo C. & Moura C.W.N. 2010. New records of filamentous desmids (Desmidiaceae, Zygnematophyceae) from Bahia state, Brazil. *Acta Botanica Brasilica*, 24(4): 1017-1026. https://doi.org/10.1590/S0102-33062010000400016

41. Özer, T., Erkaya, İ.A., Udoh, A.U., Akbulut, A., Yıldız, K. & Şen, B. 2012. New records for the freshwater algae of Turkey (Tigris Basin). *Turkish Journal of Botany*, 36(6): 747-760.

42. Öztürk, M., Gönülol, A. & Öztürk, M. 1995a. A new record for the algal flora of Turkey: *Pleurotaenium trabecular* (Ehr.) ex Nägeli (Desmidiaceae). *Ondokuz Mayıs University Faculty of Arts and Sciences Journal of Science*, 6(1): 212-218.

43. Öztürk, M., Gezerler-Şipal, U., Güner, H., Gönülol, A. & Aysel, V. 1995b. A new record for the algal flora of Turkey: *Closterium kuetzingii* Bréb. var. *kuetzingii* (Conjugatophyceae, Desmidiales). *Ege Journal of Fisheries and Aquatic Sciences*, 12(1-2): 145-149.

44. Sevindik, T.O., Çelik, K. & Gönülol, A. 2010. Twenty-four new records for the freshwater algae of Turkey. *Turkish Journal of Botany*, 34: 249-259.

45. Sevindik, T.O., Çelik, K. & Gönülol, A. 2011. Twenty New Records for Turkish Freshwater Algal Flora from Çaygören and Ikizcetepeler Reservoirs (Balıkesir, Turkey). *Turkish Journal of Fisheries and Aquatic Sciences*, 11: 399-406. https://doi.org/10.4194/1303-2712-v11_3_09

46. Sevindik, T.O., Gönülol, A., Önem, B., Tunca, H. & Arabacı, S. 2015. Thirty new records for Turkish freshwater algal flora from Danamandıra Ponds (Silivri, İstanbul) and North Mollaköy Lake (Sakarya). *Biological Diversity and Conservation*, 8(2): 4-15.

47. Sevindik, T.O., Gönülol, A., Tunca, H., Gürsoy, N.Y., Küçükkaya, Ş.N. & Durgut Kınalı, Z. 2017. Nineteen new records for Turkish freshwater algal flora from Lake Taşkısığı and Lake Little Akgöl. *Biological Diversity and Conservation*, 10(1): 69-78.

48. Sherwood, A.R., Neumann, J.M., Dittbern-Wang, M. & Conklin, K.Y. 2018. Diversity of the green algal genus *Spirogyra* (Conjugatophyceae) in the Hawaiian Islands. *Phycology*, 57(3): 331-344.

49. Shukla S.K., Shukla C.P. & Misra P.K. 2008. Desmids (Chlorophyceae, Conjugales, Desmidiaceae) from Foothills of Western Himalaya, India. *Algae*, 23(1): 1-14.

50. Šimek, O. 1997. Changes in desmid flora of the nature reserve Řežabinec in South Bohemia after 30 years of intense environmental agriculture. *Algological Studies*, 87: 59-85.

51. Stancheva, R., Hall, J.D., Mccourt, R. & Sheath, R.G. 2013. Identity and phylogenetic placement of *Spirogyra* species (Zygnematophyceae, Charophyta) from California streams and elsewhere. *Journal of Phycology*, 49: 588-607.

52. Štastný, J. 2009. The desmids of the Swamp Nature Reserve (North Bohemia, Czech Republic) and a small neighbouring bog: species composition and ecological condition of both sites. *Fottea*, 9: 135-148.

53. Şahin, B. & Akar, B. 2007. The desmid flora of some high mountain lakes of the Turkish Doğu Karadeniz region. *Pakistan Journal of Botany*, 39: 1817-1832.

54. Şahin, B. & Akar, B. 2019. New desmid records from high mountain lakes in Artabel Lakes Nature Park, Gümüşhane, Turkey. *Turkish Journal of Botany*, 43: 570-583. https://doi.org/10.3906/bot-1810-71

55. Şahin, B. 1998. Some new records of desmids from Turkey. *Pakistan Journal of Botany*, 30: 7-13.

56. Şahin, B. 2000. Some new desmids records for freshwater algal flora of Turkey. *Flora Mediterranea*, 10: 223-226.

57. Şahin, B. 2002. Contribution to the desmid flora of Turkey. *Algological Studies*, 107: 39-48.

58. Şahin, B. 2005. A preliminary checklist of desmids of Turkey. *Cryptogamie, Algologie*, 26(4): 399-415.

59. Şahin, B. 2007. Two new records for he freshwater algae of Turkey. *Turkish Journal of Botany*, 31: 153-156.

60. Şahin, B. 2009. Contribution to the desmid flora of Turkey. *Turkish Journal of Botany*, 33: 457-460. https://doi.org/10.3906/bot-0809-15

61. Şahin, B., Akar, B. & Barinova, S. 2020. Non-diatom algae of the high mountain protected lakes in the Artabel Lakes Nature Park, Gümüşhane, Turkey. *Botanica Pacifica*, 9(2): 47-59. https://doi.org/10.17581/bp.2020.09206

62. Taşkın, E., Akbulut, A., Yıldız, A., Şahin, B., Şen, B., Uzunöz, C., Solak, C., Başdemir, D., Sevik, F., Sönmez, F., Açkgöz, I., Pabuccu, K., Öztürk, M., Alp, M.T., Albay, M., Çakır, M., Özbay, Ö., Can, Ö., Akçaalan, R., Atıcı, T., Koray, T., Özer, T., Karan, T., Aktan, Y. & Zengin, Z.T. 2019. *Türkiye suyosunları listesi (Turkey algae list)*. Ali Nihat Gökyiğit Vakfı Yayını, İstanbul. 804 pp.

63. Varol, M. & Fucikova, K. 2015. Four new records for the freshwater algae of Turkey. *Journal of Limnology and Freshwater Fisheries Research*, 1(2): 83-88.

64. Varol, M. & Şen, B. 2016. New records of Euglenophyceae for Turkish freshwater algae. *Turkish Journal of Fisheries and Aquatic Sciences*, 16(2): 219-225.

65. Volkova, E.A., Bondarenko, N.A. & Timoshkin, O.A.Y. 2018. Morphotaxonomy, distribution and abundance of *Spirogyra* (Zygnematophyceae, Charophyta) in Lake Baikal, East Siberia. *Phycologia*, 57(3): 298-308.

66. Yüce, A.M. & Ertan, Ö.O. 2014. A new record for the freshwater algae of Turkey. *Scientific Research Journal*, 2(4): 21-22.

http://dergipark.org.tr/trkjnat
Trakya University Journal of Natural Sciences, 22(2): 131-138, 2021
ISSN 2147-0294, e-ISSN 2528-9691
DOI: 10.23902/trkjnat.879200

Research Article

QUERCETIN AMELIORATES THE STREPTOZOTOCIN-INDUCED DIABETIC RENAL INJURY BY INHIBITING APOPTOSIS

Emine Ceyda SÖZÜER[1], Yeter TOPÇU TARLADAÇALIŞIR[2*]

[1] Pathology Laboratory Technıques, Vocational School of Health Services, Istanbul Aydın University, Istanbul, TURKEY
[2] Department of Histology and Embryology, Faculty of Medicine, Trakya University, Edirne, TURKEY

Cite this article as:

Sözüer E.C. & Topçu Tarladaçalışır Y. 2021. Quercetin ameliorates the streptozotocin-induced diabetic renal injury by inhibiting apoptosis. *Trakya Univ J Nat Sci*, 22(2): 131-138, DOI: 10.23902/trkjnat.879200

Received: 12 February 2021, Accepted: 11 May 2021, Online First: 01 June 2021, Published: 15 October 2021

Abstract: Diabetes mellitus is an important health problem worldwide due to its frequency and complications. In this study, the protective effect of quercetin on the apoptotic changes of rat kidney in the early stages of diabetes induced by streptozotocin (STZ) was evaluated.
Rats are divided into 3 groups as control, diabetic and diabetic+quercetin groups. STZ was applied as a single dose of 50 mg/kg intraperitoneal (i.p.) to diabetic and diabetic+quercetin groups. Quercetin was given at 30 mg/kg i.p. once a day for 15 days, 48 hours after induction of diabetes. At the end of quercetin treatment, all animals were sacrificed and kidneys were harvested and weighed. The terminal deoxynucleotidyl transferase-mediated dUTP nick end-labeling assay (TUNEL) for apoptosis was performed and evaluated renal histopathology.
The induction of diabetes via STZ caused a significant increase in blood glucose levels, the index of glomerulosclerosis, the histopathologic score, the number of TUNEL positive tubular and glomerular cells. Quercetin treatment lowered blood glucose levels, prevented renal cell apoptotic changes and histopathological alterations in diabetic rat kidney.
The findings of the study suggested that quercetin may be useful in preventing diabetic nephropathy by regulating renal apoptotic changes that occur in the early stages of diabetes.

Özet: Diabetes mellitus, sıklığı ve komplikasyonları nedeniyle dünya çapında önemli bir sağlık sorunudur. Bu çalışmada, streptozotosin (STZ) ile oluşturulan diyabetin erken evrelerinde böbrek dokusunda meydana gelen apoptotik değişiklikler üzerine quercetinin koruyucu etkileri değerlendirildi.
Deneklerden kontrol, diyabetik ve diyabetik + quercetin grupları olarak 3 grup oluşturuldu. Diyabetik ve diyabetik+quercetin gruplarına tek doz 50 mg/kg STZ intraperitoneal (i.p.) olarak uygulandı. Quercetin, diyabet indüksiyonundan 48 saat sonra 15 gün boyunca günde bir kez 30 mg/kg i.p. olarak verildi.
Quercetin tedavisinin sonunda tüm hayvanlar sakrifiye edildi ve böbrekler çıkartılarak, tartıldı. Böbrek dokularında TUNEL (Terminal deoxynucleotidyl transferase-mediated dUTP nick end-labeling) yöntemi ile hücre apoptozu ve ayrıca histopatolojik değişiklikler değerlendirildi.
STZ yoluyla diyabet indüksiyonu, kan glukoz seviyelerinde, glomerülosklerozu indeksinde, histopatolojik skorda, TUNEL pozitif tübüler ve glomerüler hücre sayısında önemli bir artışa neden oldu. Quercetin tedavisi kan glukoz seviyelerini düşürdü, renal hücre apoptozunu ve histopatolojik değişiklikleri azalttı.
Bu çalışmanın bulguları, quercetinin, diyabetin erken evrelerinde meydana gelen böbrekteki apoptotik değişiklikleri düzenleyerek diyabetik nefropati gelişimini önlemede faydalı olabileceğini göstermektedir.

Edited by:
Reşat Ünal

****Corresponding Author:***
Yeter Topçu Tarladaçalışır
yeter_topcu@yahoo.com

ORCID iDs of the authors:
ECS. orcid.org/0000-0003-0352-7361
YTT. orcid.org/0000-0002-1851-7839

Key words:
Streptozotocin
Quercetin
Nephropathy
Apoptosis
Diabetes mellitus
Rat

Introduction

Diabetes mellitus (DM) is a metabolic disease, which affects 8.3% of the world population on average and results from the insufficiency and absence of insulin hormone released from pancreatic beta (β) cells or the unresponsiveness of insulin receptors (Cheisson *et al.* 2018, American Diabetes Association 2019). Retinopathy, nephropathy, neuropathy, and cardiomyopathy are the major complications associated with DM (American Diabetes Association 2019).

Diabetic nephropathy (DN) is a chronic and complex process in which the glomeruli are affected in their early stage and is characterized by thickened glomerular basement membrane (GBM), microalbuminuria, hypertrophy, and subsequent development of

glomerulosclerosis, tubular atrophy, and interstitial fibrosis (Ichinose *et al.* 2007). Hyperglycemia, insulin resistance, inflammation, oxidative stress, apoptosis, and the activation of the renin-angiotensin system (RAS) are very important in the pathogenesis of DN (Mori *et al.* 2014). It has been demonstrated that hyperglycemia induces oxidative stress and facilitates tissue damage by increasing the number of reactive oxygen species (ROS) and reducing the protective antioxidant capacity (Vural *et al.* 2001, Bhathena & Velasquez 2002). It has been reported that high glucose concentration is very important in the development of tubular atrophy and glomerular damage by causing both podocyte and renal tubule cell apoptosis (Gilbert & Cooper 1999, Susztak *et al.* 2006, Chuang *et al.* 2007). However, in the early or late stages of DN, it has been shown that proliferative changes occur in the endothelial, mesangial, and interstitial cells of the kidney and that these affect different fibrotic processes (Li *et al.* 2003).

Quercetin has antioxidant, anti-apoptotic and anti-inflammatory effects. It is a flavonoid that is found in various vegetables and fruits (Anjaneyulu & Chopra 2004, Harwood *et al.* 2007, Al-Rasheed *et al.* 2017). Previous studies have reported that quercetin plays a protective role in experimentally induced-DN by inhibiting oxidative damage (Anjaneyulu & Chopra 2004, Gomes *et al.* 2014, Lin *et al.* 2016). However, there are limited number of studies evaluating the relationship of quercetin with apoptosis, which is an important factor in DN (Zhou *et al.* 2012, Gomes *et al.* 2014, Lin *et al.* 2016, Tunçdemir *et al*. 2018). For this reason, in this study, we evaluated the effect of quercetin on apoptotic changes of rat kidney in the early stages of diabetes induced by streptozotocin (STZ).

Materials and Methods

Ethical approval and animals

The design of the study was approved by the Ethical Committee of Trakya University (TUHADYEK 2017/15). Twenty-four male Wistar albino rats (3-4 months old, weighing 300-370 g) were used in the study. Rats were kept in special conditions (22 ± 1°C temperature, 12 h light:12 h dark cycle, access to free food and water) in Experimental Animal Center of Trakya University. Subjects were divided into three groups as control, diabetic and diabetic+quercetin, each containing 8 rats.

Experimental protocol

Baseline fasting blood glucose (FBG) levels of the subjects were measured after 12 hours of fasting. This measurement was made weekly on blood samples taken from the tail using a glucometer (IME-DC, Hof, Germany). At the beginning of the study, the body weights (Bw) and FBG levels of animals were recorded. For the diabetes induction, the diabetic and diabetic+quercetin groups were given intraperitoneally (i.p.) a single dose of 50 mg/kg STZ (Sigma Aldrich, Taufkirchen, Germany) dissolved in a 0.1 M citrate buffer (Ali *et al.* 2017). Fourthy-eight hours after administration of STZ, diabetes was confirmed by measuring FBG levels > 250 mg/dl (Kushwaha & Jena 2012).

After 48 hours of diabetes induction, 30 mg/kg i.p. quercetin (Alfa Aesar, Ward Hill, Massachusetts, USA) dissolved in dimethylsulfoxide (DMSO) (Merck Millipore, USA) were given to animals of quercetin-treated group daily for 15 days. Control animals were treated with 1 ml/kg DMSO (vehicle of quercetin) in the same way. The doses of quercetin were selected based on previous studies (Yang & Kang 2018). At the termination of the quercetin treatment, after recording final body weights and blood glucose levels, all animals were sacrificed under xylazine/ketamine anesthesia, and their kidneys were harvested and weighed. The right and left kidneys were weighed and the mean kidney weight (Kw) for each rat was calculated. To reveal the profile of renal hypertrophy, the ratio between kidney and body weight (Kw/Bw) was calculated (Liu *et al.* 2003).

Light microscopy

Kidneys fixed in 10% formalin were processed with the standard paraffin embedding method. Sections of 5 μm thickness were stained with hematoxylin-eosin (H&E) and Periodic Acid Schiff (PAS).

Light microscopic analyses were done in randomly selected areas from the medulla and cortex in each kidney section. The evaluations were carried out by blind observers at 200× magnifications. Acute kidney injury including interstitial fibrosis, tubular, and glomerular alterations were semiquantitatively graded (0: normal, 1: mild, 2: moderate and 3: severe). Additionally, 100 glomeruli for each subject were evaluated for sclerosis under 400× magnification on the sections stained with PAS. Glomerulosclerotic injury was graded on a scale of 0 to 4 and the sclerosis index was calculated (Saito et al. 1987).

For 30 glomeruli in PAS-stained section of each rat, the greatest and the smallest diameters of each glomeruli were measured using a micrometric ocular and the average diameters of the glomeruli were calculated.

Terminal deoxynucleotidyl transferase-mediated dUTP nick end labeling (TUNEL) assay

Renal cell apoptosis was evaluated by the TUNEL method using the ApopTag Plus Peroxidase *in situ* Apoptosis Detection Kit (S7101, Merck Millipore, Massachusetts, USA) as described by the manufacturer. To determine the apoptosis, tubular epithelial and glomerular cells on the randomly selected 30 glomeruli were counted in 20 fields/section using a light microscope by blinded observation at 200×. The TUNEL positive tubular and glomerular cells, whose nuclei were stained dark brown, were counted.

Statistical analysis

The results were expressed as means ± SD or median (minimum – maximum). Whether the numerical variables were normally distributed was evaluated using the One-sample Kolmogorov-Smirnov test. For the control, diabetic

and diabetic+quercetin group comparisons, the One-way ANOVA test was used if the numeric variables that were normally distributed and the Kruskal Wallis test if the variable that were not normally distributed. $p<0.05$ was considered statistically significant. Statistical analyses were performed using SPSS 20.0 program (IBM SPSS Statistics for Windows, Version 20.0. Armonk, NY: IBM Corp.).

Results

Blood glucose levels

After 48 h of STZ injection, as indication of diabetes, FBG levels in all animals significantly increased compared with the control animals ($p<0.05$). At the end of the study, FBG levels in the quercetin-treated animals were significantly lowered than the untreated diabetic animals ($p<0.05$) (Fig. 1).

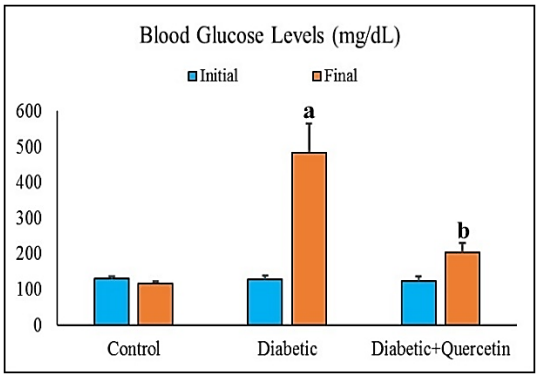

Fig. 1. The mean blood glucose levels (mg/dL) of all groups. [a] $p<0.05$ Compared to the control group, [b] $p<0.05$ Compared to the diabetic group.

Body and kidney weights

The changes in initial and final Bw for all groups are shown in Table 1. Diabetes caused a reduction in body weight. The initial body weights were similar in all groups, whereas, at the end of the experimental period, there was a marked weight loss in the diabetic and diabetic+quercetin groups. Weight loss was more pronounced, especially in the diabetic groups. Although the body weight loss of the quercetin treated group was less compared to the diabetes group, there was no statistically significant difference between the two groups ($p=0.074$).

There was no significant difference in the mean Kw among the groups (Table 1). To determine kidney hypertrophy, we calculated the Kw/Bw ratio (Table 1). All diabetic subjects had significantly higher Kw/Bw ratios compared to control. The highest ratio was determined in the diabetic group (Table 1).

Histopathological findings

The kidney morphologies of the control group were seen as normal (Fig. 2A, D). STZ-mediated diabetes caused severe glomerular and tubular alterations. Hypertrophic glomeruli causing narrowing in Bowman space were observed in the kidney of the untreated diabetic group (Figs 2B, E). The sclerotic injuries including GBM thickening, glomerular capillary collapse and mesangial matrix enlargement were determined in PAS-stained kidney section in this group (Fig. 2E). The tubular dilatation, thickening of the basement membrane, epithelial desquamation, and microvilli loss were observed in the kidney sections of this group (Figs 2B, E and inset). Additionally, the tubular vacuolation characterized by glycogen accumulation (PAS-positive) in the cytoplasm was detected in diabetic rat kidney (Figs 2B, E, and inset). In light of these findings, the kidney damage score, glomerular size, and the sclerosis index of the diabetic group were significantly higher (Table 2). In the quercetin-treated group, STZ-mediated renal structural alterations were reduced (Figs 2C, F), and in parallel, the tissue damage score, sclerosis index and glomerular size in this group was also significantly decreased (Table 2).

TUNEL assay

In the kidneys of the control groups rats, very few apoptotic cells were observed (Figs 3A, B). Diabetes induction with STZ resulted in a significant increase in both tubular epithelial and glomerular cell apoptosis (Table 2). TUNEL positive cells were detected mainly in dilated and damaged tubuli and some glomeruli. Glomerular apoptotic cells were observed to be podocytes due to their localization and size (Figs 3C, D). In the quercetin-treated group, the apoptotic tubular and glomerular cell numbers were significantly decreased compared with the untreated diabetic group (Figs 3E, F, Table 2).

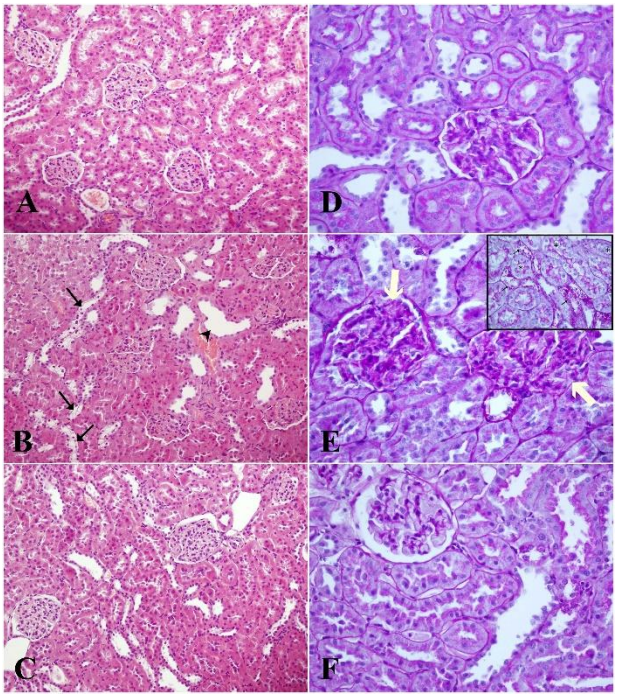

Fig 2. Photomicrographs illustrate morphological changes in rat kidney sections stained with hematoxylin eosin (A, B, C, 200×) and Periodic Acid Schiff (D, E and Inset, F, 400×): Control group (A, D), Diabetic group (B, E), Diabetic+quercetin group (C, F). Arrowheads: tubular dilatation, black arrows: glycogenic vacuolation (glycogen accumulation), asteriks: brush border loss, white arrows: degenere glomeruli enlarged mesangial matrix and narrowed Bowman space.

Table 1. Body weight and kidney weight of the subjects.

	Control	Diabetic Group	Diabetic+Quercetin Group	*p*
Initial Bw	336.17 ± 22.13	330 ± 25.93	327.50 ± 18.91	0.793
Final Bw	352.33 ± 19.98	231.50 ± 38.91 [a]	269.67 ± 25.97 [b]	<0.001
Bw difference	16.50 ± 23.90	-98.50 ± 28.36 [a]	-57.83 ± 35.19[b]	<0.001
Mean Kw	1.35 ± 0.19	1.46 ± 0.18	1.37 ± 0.15	0.552
Kw/Bw (x10^{-3})	3.50 ± 0.84	6.00 ± 0.89 [b]	4.67 ± 0.52[c]	0.002

Data were shown as mean ± S.D. Bw: body weight, Kw: kidney weight. [a] p<0.001 Compared to the control group, [b] p<0.01 Compared to the control group, [c] p<0.05 Compared to the diabetic group.

Table 2. The kidney damage score, sclerosis index, glomerular size and the number of TUNEL positive renal cells of all groups.

	Control	Diabetic Group	Diabetic+Quercetin Group	*p*
Kidney damage score	1 (0-2)	5.5 (4-6) [a]	3.0 (3-4) [ab]	0.001
Sclerosis index	0.2 (0.1-0.3)	1.4 (1.3-1.6) [a]	0.95 (0.9-1.0) [ab]	<0.001
Glomerular size (µm)	115.11 ± 1.25	135.53 ± 1.60[a]	126.00 ± 0.76 [ab]	<0.001
TUNEL positive tubular cells	0.30 (0.1-0.5)	47.5 (42.5-65.0) [a]	8.75 (6.5-17.5) [ab]	<0.001
TUNEL positive glomerular cells	0.5 (0.3-0.5)	2.3 (1.6-2.8) [a]	0.6 (0.6-0.7) [ab]	<0.001

Data were shown as mean ± S.D. or median (minimum – maximum). [a] p<0.05 compared to the control group, [b] p<0.05 compared to the diabetic group.

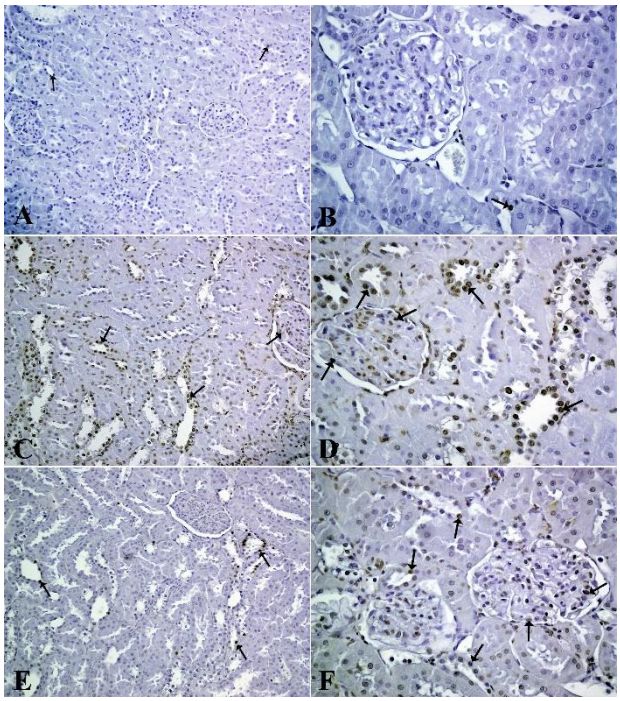

Fig. 3. Detection of apoptotic changes in diabetic rat kidney by TUNEL method. Control group (A, B), Diabetic group (C, D), Diabetic+quercetin group (E, F). Brown staining (arrows) indicates TUNEL positive cells. (A, C, E 200×; B, D, F 400×).

Discussion

In the pathogenesis of DN, hyperglycemia, insulin resistance, inflammation, oxidative stress, apoptosis, and RAS activation play an important role, besides genetic, metabolic, and hemodynamic factors (Ichinose *et al.* 2007, Mori *et al.* 2014).

Our findings show that quercetin treatment decreases blood glucose level and the kidney damage (histopathological score and glomerulosclerosis index) by regulating the renal cell apoptosis accompanying STZ-mediated diabetic nephropathy. Although hyperglycemia was observed in all diabetic animals from the 48th hour following STZ injection until the end of the experiment, quercetin treatment caused a significant decrease in high blood glucose values. This effect of quercetin on blood glucose levels is supported by previous studies (Vessal *et al.* 2003, Gomes *et al.* 2014, Elbe *et al.* 2015, Roslan *et al.* 2017, Tunçdemir *et al.* 2018, Senyigit *et al.* 2019). Vessal *et al.* (2003) reported that quercetin increased insulin release by regenerating β cells of Langerhans islets damaged by STZ in diabetic rats.

It is known that reduction of body weight occurs in diabetic individuals (Andallu & Varadacharyulu 2003). As shown in many studies (Kelly *et al.* 2002, Tunçdemir & Ozturk 2008, Elbe *et al.* 2015), the body weights in diabetic animals decreased significantly in our study. However, literature information on the renal weight in diabetes is controversial. Some studies reported that kidney weights of diabetic animals increased together with a glomerular enlargement (New *et al.* 1996, Tunçdemir & Ozturk 2008). However, it has been shown that diabetes does not alter kidney weight (Kelly *et al.* 2002, Offor *et al.* 2019) or even decreases (Coldiron *et al.* 2002). Despite the increase in glomerular diameters in our study, there was no statistically significant difference between the groups in terms of kidney weights. Renal hypertrophy is considered to be an indicator of structural damage that occurs in diabetic nephropathy (Ziyadeh & Goldfarb 1991). The ratio of "renal weight/body weight" of the diabetic group increased as an indicator of

hypertrophic changes in the kidney. As shown in other DN studies (Vessal *et al.* 2003, Elbe *et al.* 2015), we detected quercetin treatment prevented weight loss due to diabetes, and significantly decreased the kidney weight/body weight ratio and glomerular diameters.

DN is a chronic and complex process in which glomeruli are affected at the early stage and is characterized by tubular atrophy and interstitial fibrosis, leading to a gradual reduction of renal function with the development of glomerulosclerosis (Gilbert & Cooper 1999, Ichinose *et al.* 2007). It is known that hyperglycemia causes oxidative stress and increased oxidative stress in the diabetic kidney promotes apoptosis (Vincent *et al.* 2004, Armagan *et al.* 2006). It has been indicated that genes controlling apoptosis are affected in hyperglycemic conditions and it contributes to the development of diabetic nephropathy (Ortiz *et al.* 1997, Bamri-Ezzine *et al.* 2003). It has been shown the role of podocyte apoptosis in the glomerular injury, which is critical at the beginning of DN, and also, importance of the tubular cell apoptosis the in the tubular atrophy and the progression of the disease (Gilbert & Cooper 1999, Susztak *et al.* 2006, Chuang *et al.* 2007). Additionally, it is known that high levels of ROS under hyperglycemic conditions induce extracellular matrix (ECM) production by activation of the TGF-β Smad signaling pathway in various cells such as tubular epithelial cells, mesaengial cells, vascular endothelial cells (Chen *et al.* 2001, Yasuda *et al.*2001, Li *et al.*2003). The most prominent histological change in diabetic kidneys is the enlargement in mesangium as a result of excessive production and deposition of ECM proteins such as collagen type IV, fibronectin, and laminin (Kolset *et al.* 2012). Similar to other studies (Ichinose *et al.* 2007, Tunçdemir & Ozturk 2008, Offor *et al.* 2019) GBM thickening, mesangial matrix increase, Bowman distance constriction which is mediated by glomerular enlargement with collapsed luminal glomerular capillaries, were also detected in the kidneys of the diabetes group in the present study. An increase in the glomerular size and sclerotic index of the diabetic group were observed as a result of these changes. The histopathological findings obtained were consistent with the results of other studies (Sanai *et al.* 2000, Geoffroy *et al.* 2005, Giribabu *et al.* 2017). Previous studies indicated that glomerulosclerotic changes occurred in the early stages of DN and increased over time (Tucker *et al.* 1991, Sanai *et al.* 2000). Although ECM accumulation and GBM thickening are important mechanisms in the pathogenesis of DN, studies show that podocyte apoptosis caused by hyperglycemia also plays an important role in the development of DN (Susztak *et al.* 2006, Zhou *et al.* 2012). The decrease in the number of podocytes is one of the main reasons for the onset pathogenesis of DN (Wang *et al.* 2018). It has been indicated that renal damage could be prevented by reducing podocyte apoptosis in the early stage of DN (Zhou *et al.* 2012). As a result of oxidative stress in DN, the formation of advanced glycation end products (AGE) is accelerated and apoptosis in podocytes is thought to occur with the accumulation of AGE. The contribution of AGEs and their specific receptors (RAGE) to the development of diabetic nephropathy is known. RAGE is usually localized in podocytes and was shown to increase in diabetes. RAGE activation increases the production of ROS that mediates podocyte apoptosis due to hyperglycemia in early-stage DN (Tan *et al.* 2007, Chuang *et al.* 2007). Chuang *et al.* (2007) reported that AGE and its receptors induce podocyte apoptosis. In our study, the TUNEL analysis revealed an increased podocyte apoptosis. Similarly, recent studies reported increased podocyte apoptosis in the kidney of STZ-induced diabetic rats (Zhou *et al.* 2012, Giribabu *et al.* 2017).

It has been stated that hyperglycemia and AGE accumulated in cells play an important role in the pathogenesis of the changes observed in the tubules in DN (Tan *et al.* 2007). Bleyer *et al.* (1994) showed that tubular cells can be directly damaged by hyperglycemia. The excess glucose in the glomerular filtrate is reabsorbed in the proximal tubules and further increases the effects of hyperglycemia in the proximal tube. Exposure to high glucose stimulates collagen synthesis by increasing TGF-β release in tubular cells, thus leading to thickening of the basement membrane (Nessar 2005). Similar to other studies (New *et al.* 1996, Gilbert & Cooper 1999, Tunçdemir & Ozturk 2008, Offor *et al.* 2019), our study showed that tubular changes associated with diabetes are basal membrane thickening, glycogenic vacuolization in epithelial cells, microvilli loss, and dilatation. We also observed a significant increase in the number of TUNEL-positive tubular cells in diabetic kidneys. It is known that increased oxidative stress in the diabetic kidney due to the formation of free radicals induced by hyperglycemia promotes apoptosis and that apoptosis mediates the development of DN (Allen *et al.* 2003). Bamri-Ezzine *et al.* (2003) reported that glycogen accumulated in tubules triggers apoptosis of epithelial cells which leads to tubular atrophy. Consistent with the findings of the present study, an increase in tubular epithelial cell apoptosis was reported in diabetic kidney by the TUNEL method (Tunçdemir & Ozturk 2008, Ji *et al.* 2019).

The flavonoid quercetin we used in our study is known to exhibit antioxidant, anti-inflammatory, and antiapoptotic properties (Anjaneyulu & Chopra 2004, Harwood *et al*. 2007, Roslan *et al.* 2017, Al-Rasheed *et al.* 2017). Quercetin is also an antidiabetic compound that targets hyperglycemia (Vessal *et al.* 2003). Senyigit *et al.* (2019) reported that quercetin treatment significantly reduces the progression of STZ-induced hyperglycemia and oxidative stress in rats. During the course of diabetes, it is known that excessive formation of AGEs together with ROS increased by hyperglycemia mediates the development of DN and AGE formation decreases as a result of the use of flavonoid-containing antioxidants (Kaur *et al*. 2017). Li *et al.* (2014) stated that quercetin can capture methylglyoxal, a glucose metabolite, thus preventing the formation of AGE.

Previous studies reported that quercetin plays a protective role in experimentally induced-DN by inhibiting oxidative damage (Anjaneyulu & Chopra 2004, Gomes *et al.* 2014, Lin *et al*. 2016). According to our current knowledge, there is a limited number of studies assessing the effect of quercetin on renal apoptotic changes induced by DN (Zhou *et al.* 2012, Gomes *et al.* 2014, Lin *et al.* 2016, Tunçdemir *et al.* 2018). Zhou *et al*. (2012) demonstrated that pretreatment with the total flavone glycosides of Flos Abelmoschus manihot could prevent renal damage and podocyte apoptosis and thus decrease urinary albumin excretion in early-stage DN. Gomes *et al.* (2014) reported that quercetin treatment had beneficial effects on renal function and structural changes and also decreased oxidative stress and apoptosis in the kidney of STZ-induced DN mice. A recent study indicated that antiapoptotic effects of quercetin might be useful in reducing STZ-mediated DN (Tunçdemir *et al.* 2018). Our findings show that quercetin treatment decreases kidney damage (histopathological score and sclerosis index) in STZ-mediated diabetic rats by regulating renal tubular and glomerular cell apoptosis and lowering blood glucose levels. We think that this study may contribute to the literature by emphasizing the effects of quercetin on apoptotic changes and outlines a novel therapeutic strategy for this flavonoid in the treatment of DN.

Conclusion

In conclusion, the results obtained in this study indicated that quercetin of which antioxidant and antidiabetic effects are known was found to be useful in preventing the development of DN by regulating apoptotic changes that occur in the early stages of diabetes.

Ethics Committee Approval: Ethics committee approval was received for this study from the Ethics Committee of Trakya University by the number TUHADYEK 2017/15.

Author Contributions: Concept: E.C.S., Y.T.T, Desing: E.C.S., Y.T.T, Execution: E.C.S., Y.T.T, Material supplying: E.C.S., Y.T.T, Data acquisition: E.C.S., Y.T.T, Data analysis/interpretation: E.C.S., Y.T.T, Writing: E.C.S., Y.T.T, Critical review: E.C.S., Y.T.T.

Conflict of Interest: The authors have no conflicts of interest to declare.

Funding: The study was supported by the Trakya University Scientific Research Committee with project number 2017/15.

References

1. Al-Rasheed, N.M., Fadda, L.M., Attia, H.A., Ali, H.M. & Al-Rasheed, N.M. 2017. Quercetin inhibits sodium nitrite-induced inflammation and apoptosis in different rats organs by suppressing Bax, HIF1-α, TGF-β, Smad-2, and AKT pathways. *Journal of Biochemical and Molecular Toxicology*, 31(5): e21883.
2. Ali, M.A.M., Heeba, G.H. & El-Sheikh, A.A.K. 2017. Modulation of heme oxygenase-1 expression and activity affects streptozotocin-induced diabetic nephropathy in rats. *Fundamental & Clinical Pharmacology*, 31(5): 546-557.
3. Allen, D.A., Harwood, S., Varagunam, M., Raftery, M.J. & Yaqoob, M.M. 2003. High glucose-induced oxidative stress causes apoptosis in proximal tubular epithelial cells and is mediated by multiple caspases. *Federation of American Societies for Experimental Biolog*, 17(8): 908-910.
4. American Diabetes Association: Diagnosis and classification of diabetes mellitus. Diabetes Care. http://care.diabetesjournals.org/content/33/Supplement_1/S62. (2010, accessed 15 May 2019)
5. Andallu, B. & Varadacharyulu, N.C. 2003. Antioxidant role of mulberry (*Morus indica* L. cv. Anantha) leaves in streptozotocin-diabetic rats. *Clinica Chimica Acta*, 338: 3-10.
6. Anjaneyulu, M. & Chopra, K. 2004. Quercetin, an antioxidan bioflavonoid, attenuates diabetic nephropathy in rats. *Clinical and Experimental Pharmacology and Physiology*, 31(4): 244-248.
7. Armagan, A., Uz, E., Yilmaz, H.R., Soyupek, S., Oksay, T. & Ozcelik, N. 2006. Effects of melatonin on lipid peroxidation and antioxidant enzymes in streptozotocin-induced diabetic rat testis. *Asian Journal of Andrology*, 8(5): 595-600.
8. Bamri-Ezzine, S., Ao, Z.J., Londono, I. Gingras, D. & Bendayan, M. 2003. Apoptosis of tubular epithelial cells in glycogen nephrosis during diabetes. *Laboratory Investigation*, 83: 1069-1080.
9. Bhathena, S.J. & Velasquez, M.T. 2002. Beneficial role of dietary phytoestrogens in obesity and diabetes. *American Journal of Clinical Nutrition*, 76(6): 1191-1201.
10. Bleyer, A.J., Fumo, P., Snipes, E.R., Goldfarb, S., Simmons, D.A. & Ziyadeh, F.N. 1994. Polyol pathway mediates high glucose-induced collagen synthesis in proximal tubule. *Kidney International*, 45(3): 659-666.
11. Cheisson, G., Jacqueminet, S., Cosson, E., Ichai, C., Leguerrier, A.M., Nicolescu-Catargi, B., Quattara, A., Valensi, P. & Benhamou, D. 2018. Review of hyperglycaemia: definitions and pathophysiology. *Anaesthesia, Critical Care & Pain*, 37: S5-S8.
12. Chen, S., Hong, S.W., Iglesias-dela Cruz, M.C., Isono, M., Casaretto, A. & Ziyadeh, F.N. 2001. The key role of the transforming growth factor-beta system in the pathogenesis of diabetic nephropathy. *Renal Failure*, 3(3&4): 471-481.
13. Chuang, P.Y., Yu, Q., Fang, W., Uribarri, J. & He, J.C. 2007. Advanced glycation endproducts induce podocyte apoptosis by activation of the FOXO4 transcription factor. *Kidney International*, 72: 965-976.

14. Coldiron, A.D., Sanders, R.A. & Watkins, J.B. 2002. Effects of combined quercetin and coenzyme Q10 treatment on oxidative stress in normal and diabetic rats. *Journal of Biochemical and Molecular Toxicology*, 16: 197-202.

15. Elbe, H., Vardi, N., Esrefoglu, M., Ates, B., Yologlu, S. & Taskapan, C. 2015. Amelioration of streptozotocin-induced diabetic nephropathy by melatonin, quercetin, and resveratrol in rats. *Human and Experimental Toxicology*. 34(1): 100-113.

16. Geoffroy, K., Troncy, L., Wiernsperger, N., Lagarde, M. & Bawab, S.E 2005. Glomerular proliferation during early stages of diabetic nephropathy is associated with local increase of sphingosine-1-phosphate levels. *Federation of European Biochemical Societies*, 579: 1249-1254.

17. Gilbert, R.E. & Cooper, M.E. 1999. The tubulointerstitium in progressive diabetic kidney disease: more than an aftermath of glomerular injury? *Kidney International*, 56: 1627-1637.

18. Giribabu, N., Karim, K., Kilari, E.K. & Salleh, N. 2017. Phyllanthus niruri leaves aqueous extract improves kidney functions, ameliorates kidney oxidative stress, inflammation, fibrosis and apoptosis and enhances kidney cell proliferation in adult male rats with diabetes mellitus. *Journal of Ethnopharmacol*, 205: 123-137.

19. Gomes, I.B., Porto, M.L., Santos, M.C., Campagnaro, B.P., Pereira T.MC., Meyrelles S.S. & Vasquez, E.C. 2014. Renoprotective, anti-oxidative and anti-apoptotic effects of oral low-dose quercetin in the C57BL/6J model of diabetic nephropathy. *Lipids in Health and Disease*, 13: 184.

20. Harwood, M., Danielewska-Nikiel, B., Borzelleca, J.F., Flaam, G.W., Williams, G.M. & Lines, T.C. 2007. A critical review of the data related to the safety of quercetin and lack of evidence of in vivo toxicity, including lack of genotoxic/carcinogenic properties. *Food Chemical Toxicology*, 45(11): 2179-2205.

21. Ichinose, K., Kawasaki, E. & Eguchi, K. 2007. Recent advancement of understanding pathogenesis of type 1 diabetes and potential relevance to diabetic nephropathy. *American Journal of Nephrology*, 27: 554-564.

22. Ji, L., Wang, Q., Huang, F., An, T., Guo, F., Zhao, Y., Liu, Y., He, Y., Song,Yi. & Qin, G. 2019. FOXO1 Overexpression attenuates tubulointerstitial fibrosis and apoptosis in diabetic kidneys by ameliorating oxidative injury via TXNIP-TRX. *Hindawi Oxidative Medicine and Cellular Longevit*,. https://doi.org/10.1155/219/3286928

23. Kaur, N., Kishore, L. & Singh, R. 2017. *Dillenia indica L*. attenuates diabetic nephropathy via inhibition of advanced glycation end products accumulation in STZ-nicotinamide induced diabetic rats. *Journal of Traditional and Complementary Medicine*, 8(1): 226-38.

24. Kelly, D.J., Cox, A.J., Tolcos, M., Cooper, M.E., Wilkinson-Berka, J.L. & Gilbert, R.E. 2002. Attenuation of tubular apoptosis by blockade of the renin-angiotensin system in diabetic Ren-2 rats. Kidney *International*, 61(1): 31-39.

25. Kolset, S.O., Reinholt, F.P. & Jenssen T. 2012. Diabetic nephropathy and extracellular matrix. *Journal of Histochemistry and Cytochemistry*, 60(12): 976-986.

26. Kushwaha, S. & Jena, G.B. 2012. Enalapril reduces germ cell toxicity in streptozotocin-induced diabetic rat: investigation on possible mechanisms. *Naunyn-Schmiedeberg's Archives of Pharmacology*, 385: 111-124.

27. Li, J.H., Huang, X.R., Zhu, H., Johnson, R. & Lan, H.Y. 2003. Role of TGF B signaling in extracellular matrix production under high glucose conditions. *Kidney International*, 63(6): 2010-2019.

28. Li, X., Zheng, T., Sang, S. & Lv, L. 2014. Quercetin ınhibits advanced glycation end product formation by trapping methylglyoxal and glyoxal. *Journal of Agricultural and Food Chemistry*, 62(50): 12152-12158.

29. Lin, C.F., Kuo, Y.T., Chen, T.Y. & Chien, C.T. 2016. Quercetin-Rich Guava (Psidium guajava) juice in combination with trehalose reduces autophagy, apoptosis and pyroptosis formation in the kidney and pancreas of type ıı diabetic rats. *Molecule*, 21(3): 334.

30. Liu, B.C., Chen, Q., Luo, D.D. 2003. Mechanisms of irbesartan in prevention of renal lesion in streptozotocin-induced diabetic rats. *Acta Pharmacologica Sinica*, 24(1): 67-73.

31. Mori, J., Patel, V.B., Ramprasath, T., Alrob, O.A., DesAulniers, J., Scholey, J.W., Lopaschuk, G.D. & Qudit, G.Y. 2014. Angiotensin 1-7 mediates renoprotection against diabetic nephropathy by reducing oxidative stress, inflammation, and lipotoxicity. *American Journal of Physiology-Renal Physiology*, 306(8): F812-F821.

32. Nessar, A. 2005. Advanced glycation endproducts-role in pathology of diabetic complications. *Diabetes Research and Clinical Practice*, 67(1): 3-21.

33. New, J.P., Canavan, J.P., Flyvbjerg, A., Hamon, G. Bilous, R.W. & Marshall, S.M. 1996. Renal enlargement and insulin-like growth factor-1 accumulation in the wistar rat model of experimental diabetes is not prevented by angiotensin converting enzyme inhibition. *Diabetologia*, 39(2): 166-171.

34. Offor, U., Naidu, E.C., Ogedengbe, O.O., Jegede, A.I., Peter, A.I. & Azu, O.O. 2019. Renal histopathological and biochemical changes following adjuvant intervention of *Momordica charantia* and antiretroviral therapy in diabetic rats. *Iranian Journal of Basic Medical Scienc*e, 22(11): 1359-1367.

35. Ortiz, A., Ziyadeh, F.N. & Neilson, E.G. 1997. Expression of apoptosisregulatory genes in renal proximal tubular epithelial cells exposed to high ambient glucose and in diabetic kidneys. *Journal of Investigative Medicine*, 45(2): 50-56.

36. Roslan, J., Giribabu, N., Karim, K. & Salleh, N. 2017. Quercetin ameliorates oxidative stress, inflammation and apoptosis in the heart of streptozotocin-nicotinamide-induced adult male diabetic rats. *Biomed Pharmacother*, 86: 570-582.

37. Saito, T., Sumithran, E., Glasgow, E.F. & Atkins, R.C. 1987. The enhancement of aminonucleoside nephrosis by the co-administration of protamine. *Kidney International*, 32(5): 691-699.

38. Sanai, T., Sobka, T., Johnson, T., El-Essawy, M., Muchaneta-Kubara, E.C., Gharbia, O.B., Oldroyd, S. & El Nahas, A.M. 2000. Expression of cytoskeletal proteins

during the course of experimental diabetic nephropathy. *Diabetologia*, 43(1): 91-100.

39. Senyigit, A., Durmus, S., Mirzatas, E.B., Ozsobacı, N.P., Gelisgen, R., Tuncdemir, M., Ozcelik, D., Simsek, G. & Uzun, H. 2019. Effects of quercetin on lipid and protein damage in the liver of streptozotocin-induced experimental diabetic rats. *Journal of Medicinal Food*, 22(1): 52-56.

40. Susztak, K., Raff, A.C., Schiffer, M. & Böttinger, E.P. 2006. Glucose-induced reactive oxygen species cause apoptosis of podocytes and podocyte depletion at the onset of diabetic nephropathy. *Diabetes*, 55(1): 225-233.

41. Tan, A.L., Forbes, J.M. & Cooper, M.E. 2007. AGE, RAGE, and ROS in diabetic nephropathy. *Seminars in Nephrology*, 27(2): 130-143.

42. Tucker, B.J., Collins, R.C., Ziegler, M.G. & Blantz, R.C. 1991. Disassociation between glomerular hyperfiltration and extracellular volume in diabetic rats. *Kidney International*. 39: 1176-1183.

43. Tunçdemir, M., Mirzataş, E.B. & Uzun, H. 2018. Renoprotective potential of quercetin in experimental diabetic nephropathy: assesing antiapoptotic and antioxidant effects. *Archives of Clinical and Experimental Medicine*, 3(3): 179-185.

44. Tunçdemir, M. & Ozturk, M. 2008. The effects of ACE inhibitor and angiotensin receptor blocker on clusterin and apoptosis in the kidney tissue of streptozotocin-diabetic rats. *Journal of Molecular Histology*, 39(6): 605-616.

45. Vessal, M., Hemmati, M. & Vasei, M. 2003. Antidiabetic effects of quercetin in streptozocin-induced diabetic rats. *Comparative Biochemistry and Physiology*, 135C(3): 357-364.

46. Vincent, A.M., Russell, J.W., Low, P. Feldman, E.L. 2004. Oxidative stress in the pathogenesis of diabetic neuropathy. *Endocrine Reviews*, 25(4): 612-628.

47. Vural, H., Sabuncu, T., Arslan, S.O. & Aksoy, N. 2001. Melatonin inhibits lipid peroxidation and stimulates the antioxidant status of diabetic rats. *Journal of Pineal Research*, 31(3): 193-198.

48. Wang, R.M., Wang, Z.B., Wang, Y., Liu, W.Y., Li, Y. & Tong, L.C. 2018. Swiprosin-1 promotes mitochondria-dependent apoptosis of glomerular podocytes via P38 MAPK pathway in early-stage diabetic nephropathy. *Cellular Physiology and Biochemistry*, 45(3): 899-916.

49. Yang, D.K. & Kang, H.S. 2018. Anti-diabetic effect of cotreatment with quercetin and resveratrol in streptozotocin-ınduced diabetic rats. *Biomolecules & Therapeutics (Seoul)*, 26(2): 130-138.

50. Yasuda, Y., Nakamura, J., Hamada, Y., Nakayama, M., Naruse, K., Nakashima, E., Kato, K., Kamiya, H. & Hotta, N. 2001. Role of PKC and TGF-beta receptor in glucose-induced proliferation of smooth muscle cells. *Biochemical and Biophysical Research Communications*, 281: 71-77.

51. Zhou, L., An, X.F., Teng, S.C., Liu, J.S., Shang, W.B., Zhang, A.H., Yuan, Y.G., & Yu, J.Y. 2012. Pretreatment with the total flavone glycosides of Flos Abelmoschus manihot and hyperoside prevents glomerular podocyte apoptosis in streptozotocin-induced diabetic nephropathy. *Journal of Medicinal Food*, 15: 461-468.

52. Ziyadeh, F.N. & Goldfarb, S. 1991. The renal tubulointerstitium in diabetes mellitus. *Kidney Internationa*, 39: 464-475.

http://dergipark.org.tr/trkjnat
Trakya University Journal of Natural Sciences, 22(2): 139-146, 2021
ISSN 2147-0294, e-ISSN 2528-9691
DOI: 10.23902/trkjnat.873651

Research Article

A NEW TRUFFLE SPECIES ADDITION, *Tuber macrosporum* Vittad., TO TURKISH MYCOTA

Hasan Hüseyin DOĞAN

Selçuk University, Science Faculty, Biology Department, Campus, Konya, TURKEY
hhuseyindogan@yahoo.com ORCID iD: *orcid.org/0000-0001-8859-0188*

Cite this article as:
Doğan H.H. 2021. A new truffle species addition, *Tuber macrosporum* Vittad., to Turkish mycota. *Trakya Univ J Nat Sci*, 22(2): 139-146, DOI: 10.23902/trkjnat.873651

Received: 03 February 2021, Accepted: 15 May 2021, Online First: 02 June 2021, Published: 15 October 2021

Edited by:
Neveen S.İ. Geweely

Key words:
Hypogeous fungi
New record
Truffle
Tuber macrosporum
Turkey

Abstract: *Tuber* P. Micheli ex F.H. Wigg. species have always attracted people's attention, with their high diversity, culinary and economic interest, strong aromas as well as the importance of plant ecosystem and animal nutrition. Interest in truffle species has been increasing in recent years in Turkey. Although some truffle species have been known previously in Turkey, many species are yet to be identified. *Tuber macrosporum* Vittad. samples were collected from Edirne and Tekirdağ regions in 2017 in a field study conducted to find new truffle species. *Tuber macrosporum* samples were firstly identified by macro and microscopic features, and this result was supported as 99% by DNA analyses when compared to GenBank.
A short description of the newly reported species is given along with its macro and microphotographs, and spore images taken by a scanning electron microscope (SEM). Additionally, ITS based evolutionary history of the species is provided with phylogenetic trees.

Özet: *Tuber* P. Micheli ex F.H. Wigg. (trüf) türleri, güçlü aromaları, gastronomik ve ekonomik önemleri, yüksek çeşitlilikleri, bitki ekolojisi ve hayvan beslenmesinde olan önemleri ile her zaman insanların ilgisini çekmiştir. Türkiye'de trüf mantarı türlerine olan ilgi son yıllarda artmaktadır. Türkiye'de daha önce bazı trüf mantarı türleri bilinmesine rağmen, pek çoğu da henüz tanımlanmamıştır. Yeni trüf mantarı türlerinin bulunması amacıyla 2017 yılında Edirne ve Tekirdağ bölgelerinden *Tuber macrosporum* Vittad. örnekleri toplanmıştır. *Tuber macrosporum* örnekleri ilk olarak makro ve mikroskobik özellikleriyle tanımlanmış ve bu sonuç DNA analizleri ile GenBank'a göre % 99 olarak desteklenmiştir.
Yeni rapor edilen türün kısa bir tanımı, makro ve mikro fotoğrafları ve taramalı elektron mikroskobu (SEM) ile alınan spor görüntüleri ile birlikte verilmiştir. Ek olarak, türün ITS'e dayalı evrimsel geçmişi filogenetik ağaçla verilmiştir.

Introduction

Tuber P. Micheli ex F.H. Wigg. species (Ascomycetes) are commonly referred to as ‘‘true truffles’’ and the other hypogeous truffles species in Ascomycetes or Basidiomycetes are known as ‘‘false truffles’. Truffles (*Tuber* spp.) make mycorrhizal associations with trees within gymnosperms and angiosperms. Several *Tuber* species, as in the case of *T. macrosporum* Vittad. (the smooth black truffle), are highly appreciated for their flavours. Due to the high sale price and being a species in demand in the truffle market, *T. macrosporum* is either sold mixed with *T. eastivum* (Wulfen) Spreng. or *T. aestivum* is also sold as *T. macrosporum* to amateur consumers.

Turkey can be characterized by different ecological regions and floral and rich genetic diversity, as an outcome of its particular geographical location and structure. This biological richness is also pronounced for mushrooms, as well as other organisms, and Turkey hosts a large number of mushroom species. After the broad cooperation of Turkish mycologists, A Checklist of the Fungi of Turkey was published in 2020 (Sesli *et al.* 2020). According to this checklist, a total of 5865 fungal taxa including 2782 of Basidiomycota, 2728 of Ascomycota, 282 of Myxomycota, 2 of Chytridiomycota, 33 of Oomycota, and 38 of Zygomycota have been listed in Turkey. Truffle species are among the most preferred mushrooms in Europe that provide economic income with their unique aroma and taste. Some of the exclusive and special restaurants in Europe specialize in truffle dishes and are especially preferred. Aromatic fragrances from truffle species are also evaluated for different purposes as

oil with truffle, cheese with truffle, foods with truffle etc. When considering the importance of truffle species in the world and especially in Europe, to be a commercial potential in Turkey is inevitable. Significant increases in the number of truffle species and their distribution areas in Turkey were revealed by taxonomic studies conducted over the last decade, which led to a significant increase in the number and distribution areas of truffle species. Öztürk *et al.* (1997), reported *Tuber brumale* Vittad. for the first time from the Niğde province in Turkey in the first taxonomic study performed on truffles. More recently, *T. borchii* Vittad. was determined by Kaya (2009) in Kahramanmaraş. *Tuber aestivum*, *T. mesentericum* Vittad. and *T. nitidum* Vittad. were determined by Castellano & Türkoğlu (2012) from Denizli province. In the following years, studies on truffle species in the country increased and more species were reported from various parts of the country [*T. aestivum* from Denizli, Konya (Gezer *et al.* 2014, Türkoğlu *et al.* 2015, Alkan *et al.* 2018); *T. borchii* Vittad. from Aydın, Denizli, Muğla, Samsun, Tekirdağ (Gezer *et al.* 2014, Elliot *et al.* 2016); *T. brumale* from Denizli, Niğde, Osmaniye, Samsun (Türkoğlu & Castellano 2014, Gezer *et al.* 2014, Şen *et al.* 2016); *T. excavatum* Vittad. from Artvin, Denizli, Trabzon (Türkoğlu & Castellano 2014, Şen *et al.* 2016, Uzun & Yakar 2018); *T. fulgens* Quél from Kırklareli (Akata *et al.* 2020); *T. mesentericum* Vittad. from Denizli (Türkoğlu & Castellano 2014); *T. nitidum* Vittad. from Burdur, Kastamonu, Osmaniye (Türkoğlu & Castellano 2014); *T. rufum* Pollini from Antalya, Aydın, Bolu, Burdur, Denizli, Muğla, Kastamonu, Konya, Osmaniye (Gezer *et al.* 2014, Türkoğlu & Castellano 2014, Türkoğlu *et al.* 2015, Şen *et al.* 2016); *T. ferrugineum* Vittad. from Antalya, Aydın, Denizli, Muğla (Elliot *et al.* 2016, Şen *et al.* 2016); *T. puberulum* Berk. & Broome from Denizli (Elliot *et al.* 2016)].

So far studies in Turkey reported the presence of 10 truffle species in the country, and with the present study, *T. macrosporum* is added to the Turkish mycobiota as the 11th species.

Materials and Methods

Macro and microscopic study

Truffle samples were collected in Thrace region of Turkey in 2017 with the help of specially trained dogs. Their colour photographs were taken and brought to the laboratory for microscopic examinations. The photographs of the spores and the tissues were taken with a Leica DM 3000 binocular microscope and calculations were done with the Leica software program. SEM (Scanning electron microscope) photographs were also taken from the asci and ascospores. For spore measurings, an average of 20 different spores was considered. Melzer reagent and 5% KOH were used as the investigation medium. The samples, whose diagnoses were completed and dried, are stored in the Fungarium of Selçuk University Mushroom Application and Research Center in Konya.

For macroscopic and microscopic studies Breitenbach & Kränzlin (1983), Pegler *et al.* (1993), Astier (1998), Medardi (2006, 2012), Montecchi & Sarasini (2000), Gori (2005), Trappe *et al.* (2007, 2009) and Thompson (2013) were followed.

Molecular study

DNA extraction

Total DNA was extracted from dried fruit body tissue by using DNeasy Plant Mini Kit (Qiagen, USA) following the manufacturer's protocol. The quality of the DNA was checked based on electropherogram in 1% TBE-agarose gel. Polymerase chain reaction (PCR) amplification and sequencing amplification of the ITS region of the template DNA was performed using the primers ITS1 and ITS4 (White *et al.* 1990).

The PCR product was purified using A&A Biotechnology (Gdynia). A Clean-up kit was used following the manufacturer's protocol before the sequencing. The sequences of *T. macrosporum* were deposited at GenBank (National Center for Biotechnology Information, NCBI). For the molecular phylogeny, the sanger reads obtained from ITS1/ITS4 were assembled using Bioedit version 7.2 and BLAST analyses were performed with the assembled sequences for the identity rate search. The assembled sequences and the nucleotide sequences of the retrieved in-group and out-group members were aligned using the ClustalW algorithm of MEGAX software (Kumar *et al.* 2018). The phylogenetic trees demonstrating the evolutionary history of HHD18610 and HHD18691 were constructed using the Maximum Likelihood method and K2 nucleotide substitution model with a gamma distribution (Kimura 1980). The bootstrap method was implemented for the accuracy estimation using 1000 bootstrap replicates (Felsenstein 1985).

Results

Taxonomic results

Phylum ASCOMYCOTA

Classis Pezizomycetes

Order Pezizales

Family Tuberaceae

Tuber macrosporum Vittad., 1831 (Figs 1-3)

Genbank No: MW423732, MW432548

Morphological and microscopical features

Fruitbodies 2-5 (6) cm diameter, globose to subglobose, more or less cocooned furrowed, generally irregular in form, lobed, but also regular and subglobose, and reddish-brown to blackish brown, with flat, polygonal warts or a verrucous-areolate (Fig.1a).

Gleba compact, anthracite grey, grey-brown, brown-lilac, finally purple-brown, thick, with thin, numerous interrupted white sterile veins, anastomosed, flaking on the peridium. It has a pleasant garlicky component and delicate perfume of fine white truffle and can be counted among the best edible truffles (Fig. 1b-d).

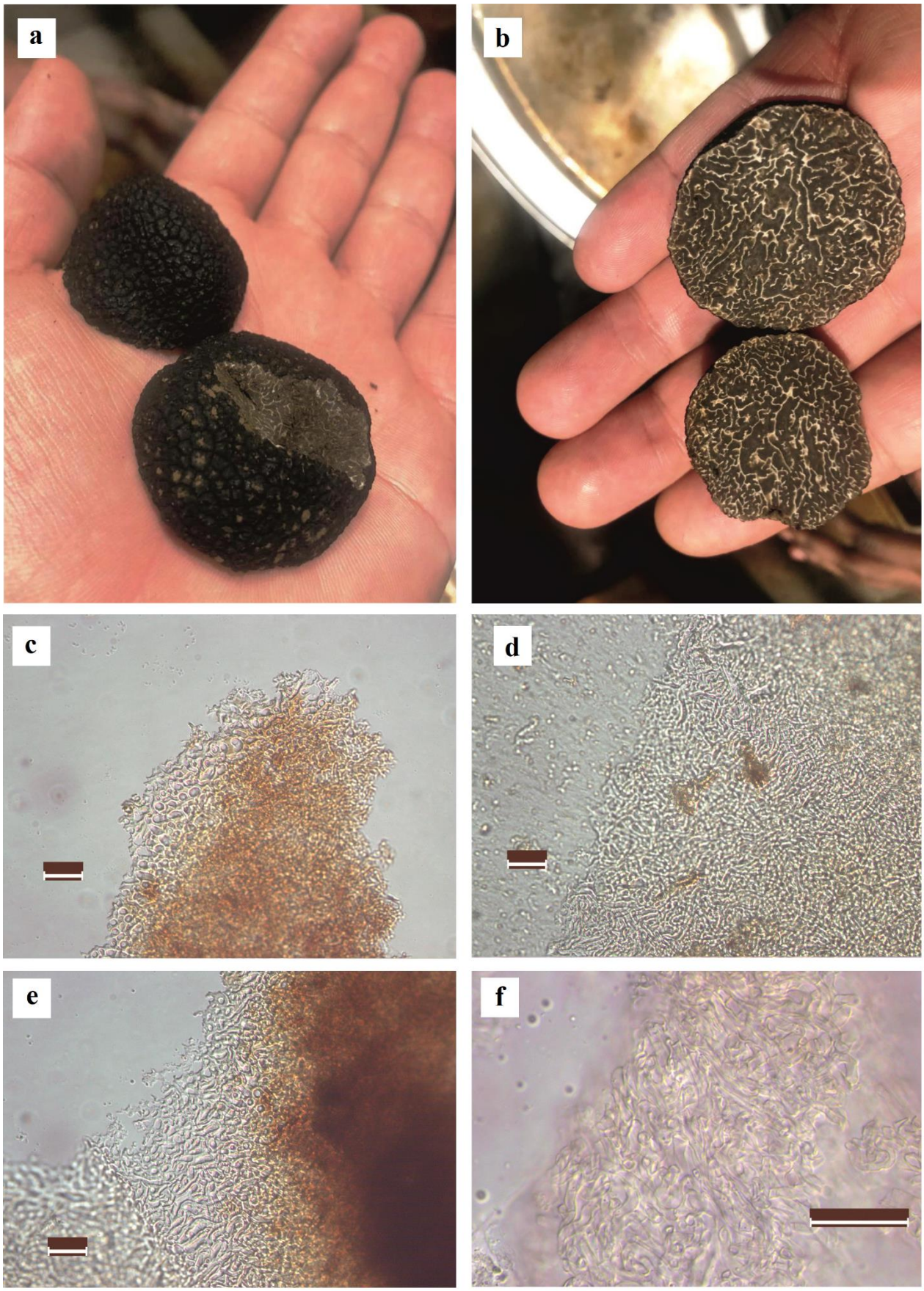

Fig. 1. *T. macrosporm*; a- macro-view of surface, b-macro-view of gleba-cross section, c-general microview of gleba, d-close-up microview of gleba, e- general microview of peridium, f- close-up microview of peridium. Scales 30 µm.

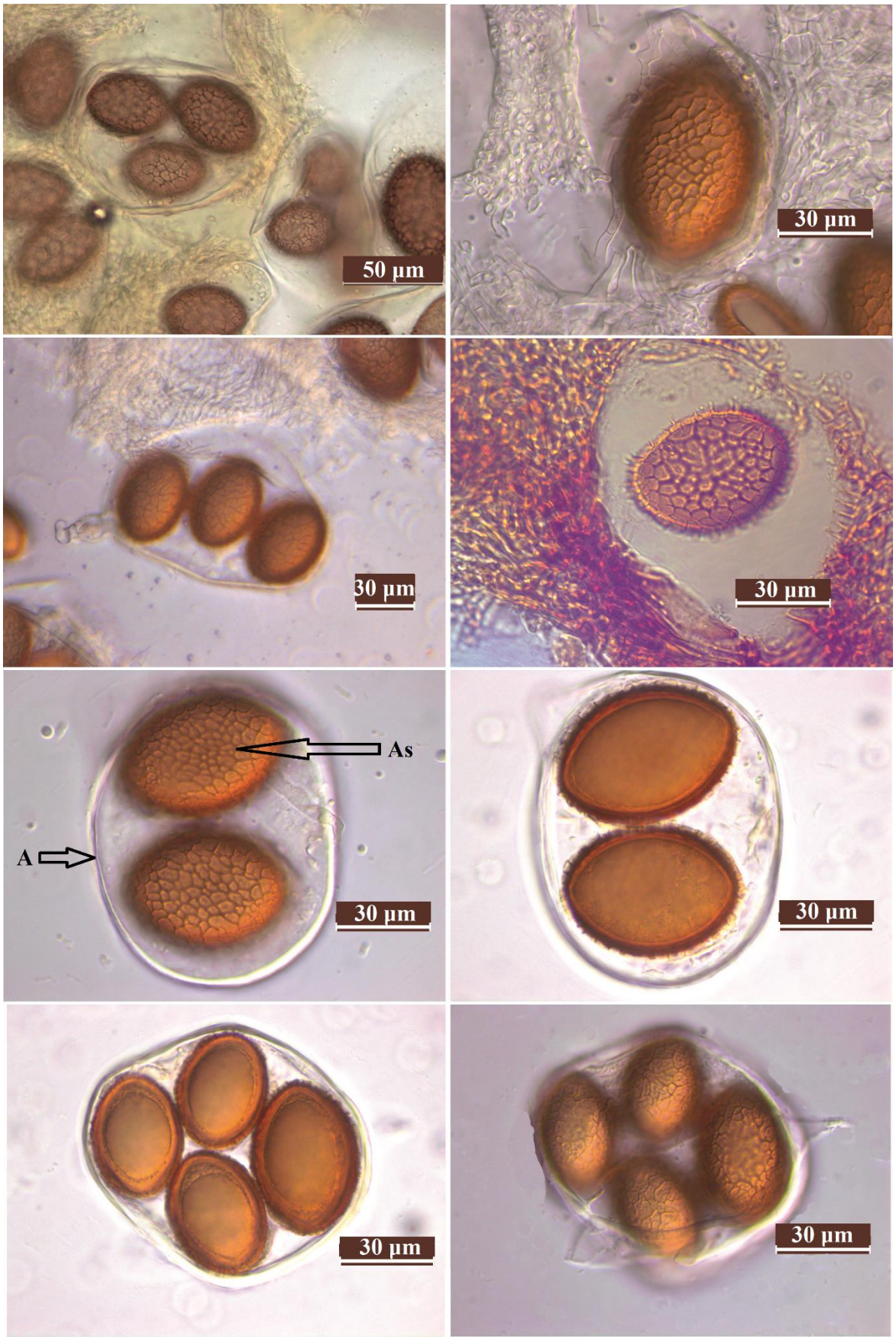

Fig. 2. Different views of Asci (indicated by an arrow, A) and ascospores (indicated by an arrow, As) under a light microscope.

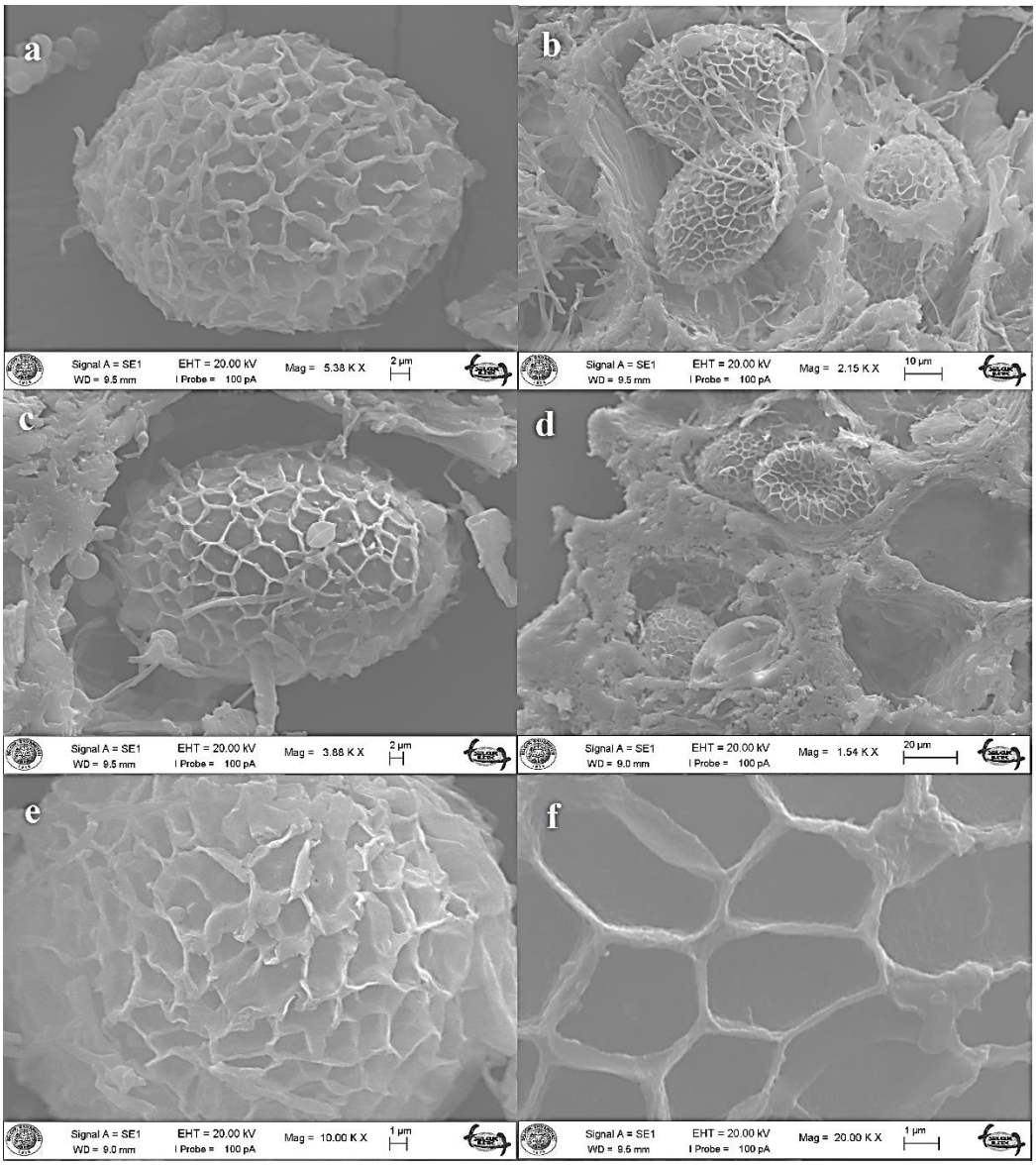

Fig. 3. SEM photograps; a, b-General views of ascospores, c-close-up views of the surface ornaments of ascospores, b-Asci.

Peridium very thin, 0.400-1 mm, hyphal type, not separable. Composed of brown-black, irregularly polygonal, very short verrucous, flattened characteristically and very much variable in dimensions, sometimes absent and with a felty surface (Fig. 1e, f).

Asci subglobose to ellipsoid, with a short peduncle, 1-3 (4)-spored, mainly 3-spored, 90-120 x 60-80 µm (Figs 2, 3b, d).

Ascospores strictly ellipsoidal tapered at the apex, cross-linked-packs, 2-2.5 (5) µm high and 8-12 µm long, brown-yellow, (25-)35-(45-)55 x (40-)45-(70-)85 µm, Q = 1.6-1.7 µm (Figs 2, 3a, b) with reticulate-alveolate irregular, polygonal meshes (Figs 2, 3c, e, f).

Species examined: Tekirdağ-Saray, in oak forest, under *Quercus* sp. 200 m, 14.IX.2017, HHD18610 (GenBank No: MW423732); Edirne-Meriç, Uzunköprü forest management chief area, Kadıdondurma Village, in oak forest, under *Quercus* sp., 150 m, 01.XII.2017, HHD18691 (GenBank No: MW432548).

Molecular results

In phylogenetic analysis of HHD18610 and HHD18691, 19 records of *T. macrosporum* were used to compare specimens similarity and 6 different *Tuber* species were used to show species differences. *Terfezia boudieri* Chatin. from the family *Pezizaceae* was selected for the outgroup (Fig. 4). The results showed that HD18610 and HD18691 showed high similarity in *T. macrosporum* sequences. While HD18610 showed high similarity with ANK Akata 7398 (unpublished data from Turkey), HHD18691 take place in a single line alone in the *macrosporum* group. The closest records to HHD18691 are NW1TMacro1 and ITA 011s. The BLAST analysis implemented with the nuclear ITS rDNA sequence of HHD18610 and HHD18691 revealed identity rates as high as 98-99% between the specimens and different isolates of *T. macrosporum*.

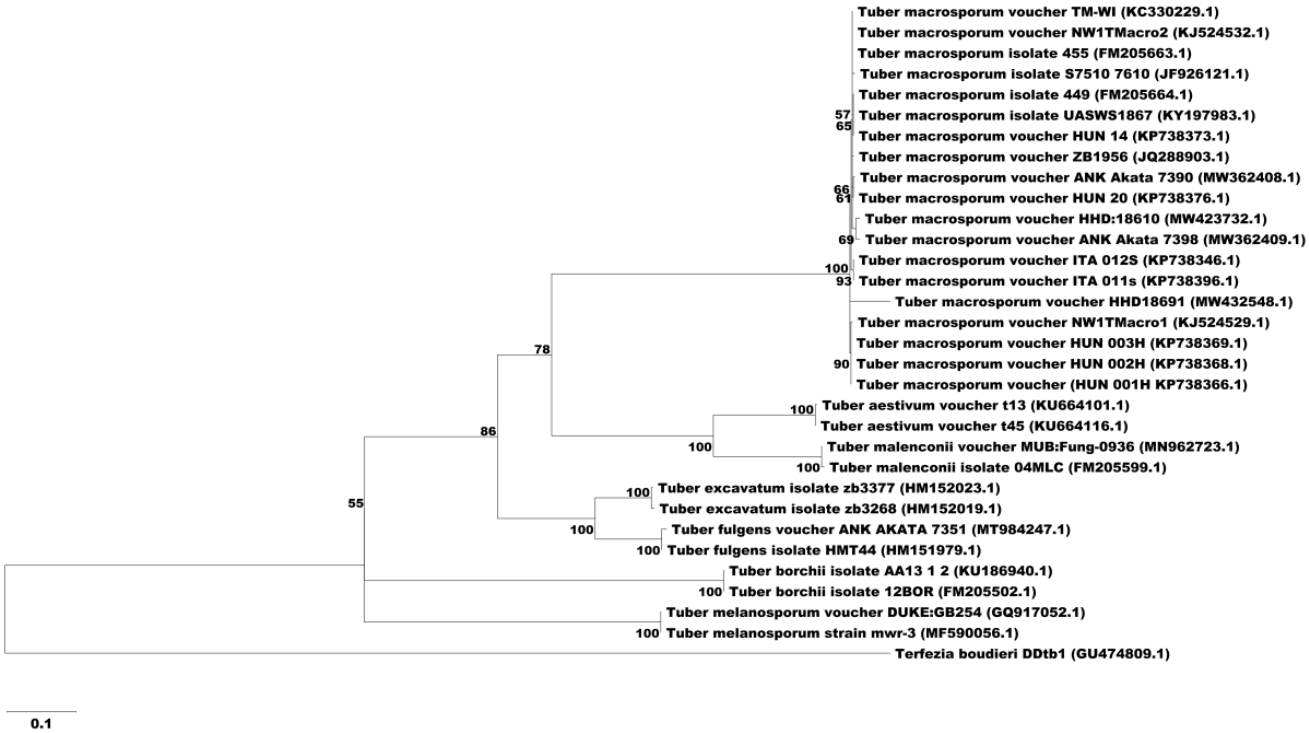

Fig. 4. The Maximum Likelihood tree revealing the phylogenetic relationships of 29 fungal sequences estimated from the nuclear ITS rDNA region. Percentage bootstrap values (≥ 50) were indicated for each branch. *Terfezia boudieri* was included as the outgroup sample in the analysis. The scale bar (lower left) represents a genetic distance of 0.1.

Discussion

Tuber macrosporum is a common species in European countries. So far it has been reported from the Czechia, Bulgaria, France, Hungary, Romania, Serbia, Switzerland, Ukraine, Italy and the United Kingdom where it is considered as rather rare (Hall *et al.* 2007). Recently, the species was found in Germany where it was considered to be extinct (Stobbe *et al.* 2012). *T. macrosporum* grows in an ectomycorrhizal symbiosis with many different tree species such as *Fagus sylvatica* L., *Corylus avellana* L., *Quercus robur* L., *Pinus strobus* L. and *P. sylvestris* L. (Granetti *et al.* 2005, Ławrynowicz *et al.* 2008). According to Bencivenga & Baciarelli Falini (2012), *C. avellana*, *Carpinus betulus* L., *Q. pubescens* Willd. and *Ostrya carpinifolia* Scop. are the usual hosts of *Tuber* species in truffle orchards. The species prefers fresh, wet, occasionally flooded, thick, calcareous soils with variable levels of calcium carbonate, often in lowlands or near rivers (Vezzola 2005, Marjanović *et al.* 2009, Benucci *et al.* 2012). In Italy, fruiting bodies of the fungus are found in the same areas as *Tuber magnatum* Picco (white truffle) and have the same host plants (Hall *et al.* 2007). The time when the species fruits are not clearly defined, yet truffle collectors harvest *T. macrosporum* from August till December (Granetti *et al.* 2005).

The Thrace region creates a very suitable area for *T. macrosporum*. The forest structure generally consists of *F. orientalis* and oak species (*Quercus hungarica* Hubeny, *Q. cerris*, *Q. dschorochensis* K.Koch and *Q. pubescens*) and soil properties are very suitable for the growth of *T. macrosporum*. Due to its very large spores, this species has never given rise to nomenclature or synonymy problems. Amateur collectors can sometimes confuse it with *T. aestivum* (the black truffle). Having bigger spores than in any other similar species, the very short and flat verrucous (similar to crusts) in many cases absent and with a felty surface in exoperidium less than *T. aestivum*, as well as having a pungent garlic smell are the main characters which enable to give it a precise and correct determination. The good and garlicky odour, reminding of *T. magnatum*, makes this species the best of the so-called black truffles, according to many gourmets.

Acknowledgement

I would like to thank Ziyafet Arslan for his valuable effort he made during the field studies.

Ethics Committee Approval: Since the article does not contain any studies with human or animal subject, its approval to the ethics committee was not required.

Conflict of Interest: The authors have no conflicts of interest to declare.

Funding: This study was supported by Selçuk University, Scientific Research Projects Coordinating Office (BAP/20401081).

References

1. Akata, I., Sevindik, M. & Şahin, E. 2020. *Tuber fulgens* Quél. A New record for Turkish truffles. Turkish Journal of Agriculture-Food Science and Technology, 8(11): 2472-2475.
2. Alkan, S., Aktaş, S. & Kaşık, G. 2018. Türkiye'deki *Tuber* türleri ve *Tuber aestivum* için yeni bir lokalite. *Selçuk Üniversitesi Fen Fakültesi Fen Dergisi*, 44(1): 25-29.
3. Astier, J. 1998. *Truffes Blanches et Noires* (*Tuberaceae* & *Terfeziaceae*). Louis-Jean, 127 pp.
4. Bencivenga, M. & Baciarelli Falini, L. 2012. *Manuale di Tartuficoltura*. *Esperienze di Coltivazionedei Tartufi in Umbria*. Assessorato Regionale Agricoltura e Foreste, Regione Umbria, 137 pp.
5. Benucci, G.M.N., Goga Csorbai, A., Di Massimo, G., Baciarelli Falini, L., Bencivenga, M. & Donini, D. 2012. Mycorrhization of *Quercus robur* L. and *Corylus avellana* L. seedlings with *Tuber macrosporum* Vittad. *Mycorrhiza*, 22(8): 639-646.
6. Breitenbach, J. & Kränzlin, F. 1983. *Fungi of Switzerland: Vol.1. Ascomycetes*. Verlag Mykologia, Luzern, 310 pp.
7. Castellano, M.A. & Türkoğlu, A. 2012. New records of truffle taxa in *Tuber* and *Terfezia* from Turkey. *Turkish Journal of Botany*, 36(3): 295-298.
8. Elliott, T.F., Türkoğlu, A., Trappe, J.M. & Yaratanakul, G.M. 2016. Turkish truffles 2: eight new records from Anatolia. *Mycotaxon*, 131: 439-453.
9. Felsenstein, J. 1985. Confidence limits on phylogenies: An approach using the bootstrap. *Evolution*, 39: 783-791.
10. Gezer, K., Kaygusuz, O., Çelik, A. & Işıloğlu, M. 2014. Ecological characteristics of truffles growing in Denizli Province, Turkey. *Journal of Food, Agriculture & Environment*, 12(2): 1105-1109.
11. Gori, L. 2005. *Funghi Ipogei Della Lucchesia di Aitre Province Italiane e dall' Estero*. Pacini Fazzi, 316 pp.
12. Granetti, B., De Angelis, A. & Materozzi, G. 2005. *Umbria, Terra di Tartufi.* Regione Umbria-Gruppo Micologico Ternano, Terni, 303 pp.
13. Hall, I., Brown, G. & Zambonelli, A. 2007. *Taming the Truffle*. *The history, Lore, and Science of the Ultimate Mushroom*. Timber Press, Oregon, 304 pp.
14. Kaya, A. 2009. Macromycetes of Kahramanmaraş province (Turkey). *Mycotaxon*, 108: 31-34.
15. Kimura, M. 1980. A simple method for estimating evolutionary rate of base substitutions through comparative studies of nucleotide sequences. *Journal of Molecular Evolution*, 16: 111-120.
16. Kumar, S., Stecher, G., Li, M., Knyaz, C. & Tamura, K. 2018. MEGA X: molecular evolutionary genetics analysis across computing platforms. *Molecular Biology and Evoluation*, 35: 1547-1549.
17. Ławrynowicz, M., Krzyszczyk, T. & Fałdziński, M. 2008. Occurrence of black truffles in Poland. *Acta Mycologica*, 43(2): 143-151.
18. Marjanović, Ž., Grebenc, T., Marković, M., Glišić, A. & Milenković, M. 2010. Ecological specificities and molecular diversity of truffles (genus *Tuber*) originating from mid-west of the Balkan Peninsula. *Sydowia*, 62(1): 67-87.
19. Medardi, G. 2006. *Ascomiceti d'Italia Atlante Fotografico*. Fondazione Centro Studi Micologici Dell'A.M.B., Vicenza, 678 pp.
20. Medardi, G. 2012. *Atlante Fotografico Degli Ascomiceti d'Italia*. Fondazione Centro Studi Micologici Dell'A.M.B. Vicenza, 454 pp.
21. Montecchi, A. & Sarasini, M. 2000. *Funghi Ipogei d'Europa*. Associazione Micologica Bresadola, Trento, 714 pp.
22. Öztürk, C., Kaşık, G. & Toprak, E. 1997. Ascomycetes makrofunguslarından Türkiye için iki yeni kayıt. *Ot Sistematik Botanik Dergisi*, 4: 53-56.
23. Pegler, D.N., Spooner, B.M. & Young, T.W.K. 1993. *British Truffles*: *A revision of British Hypogeous fungi*. The Royal Botanic Gardens, Kew, 216 pp.
24. Sesli, E., Asan, A., Selçuk, F. (eds.), Abacı Günyar, Ö., Akata, I., Akgül, H., Aktaş, S., Alkan, S., Allı, H., Aydoğdu, H., Berikten, D., Demirel, K., Demirel, R., Doğan, H.H., Erdoğdu, M., Ergül, C.C., Eroğlu, G., Giray, G., Haliki Uztan, A., Kabaktepe, Ş., Kadaifçiler, D., Kalyoncu, F., Karaltı, İ., Kaşık, G., Kaya, A., Keleş, A., Kırbağ, S., Kıvanç, M., Ocak, İ., Ökten, S., Özkale, E., Öztürk, C., Sevindik, M., Şen, B., Şen, İ., Türkekul, İ., Ulukapı, M., Uzun, Ya., Uzun, Yu. & Yoltaş, A. (2020). *Türkiye Mantarları Listesi*. Ali Nihat Gökyiğit Vakfı Yayını. İstanbul, 1192 pp.
25. Şen, I., Allı, H. & Civelek, H.S. 2016. Checklist of Turkish truffles. *Turkish Journal of Life Sciences*, 1(2): 103-109.
26. Stobbe, U., Büntgen, U., Sproll, L., Tegel, W. & Egli, S. 2012. Spatial distribution and ecological variation of re-discovered German truffle habitats. *Fungal Ecology*, 5(5): 591-599.
27. Thompson, P.I. 2013. *Ascomycetes in Colour*: *Found and Photographed in Mainland Britain*. Xlibris, Lexington KY, 408 pp.
28. Trappe, M., Evans, F. & Trappe, J. 2007. *Field Guide to North American Truffles*: *Hunting, Identifying, and Enjoying the World's Most Prized Fungi*. Ten Speed Press, Berkeley, Toronto, 136 pp.
29. Trappe, J.M., Molina, R., Luoma, D.L., Cázares, E., Pilz, D., Smith, J.E., Castellano, M.A., Miller, S.L. & Trappe, M.J. 2009. *Diversity, Ecology and Conservation of Truffle Fungi in Forests of the Pacific Northwest*. United States Department of Agriculture Forest Service Pacific Northwest Research Station General Technical Report PNW-GTR-772, USA, 202 pp.
30. Türkoğlu, A. & Castellano, M.A. 2014. New records of some Ascomycete truffle fungi from Turkey. *Turkish Journal of Botany*, 38: 406-416.
31. Türkoğlu, A., Castellano, M.A., Trappe, J.M. & Yaratanakul, G.M. 2015. Turkish truffles I: 18 new records for Turkey. *Turkish Journal of Botany*, 39: 359-376.

32. Uzun, Y. & Yakar, S. 2018. New locality record for two *Tuber* species in Turkey. *Anatolian Journal of Botany*, 2(2): 88-92.

33. Vezzola, V. 2005. Primi Risultati Produttivi Con Piante Micorrizate da *T. macrosporum* Vittad., 51-55, Paper presented at the Atti Seminario Sullo Stato Attuale Della Artuficoltura Italiana. 21 Febbraio, Spoleto-Italy.

34. White, T.J., Bruns, T., Lee, S. & Taylor, J. 1990. Amplification and direct sequencing of fungal ribosomal RNA genes for phylogenetics. Pp. 315-322. In: Innis M.A., Gefland D.H., Sninsky J.J. & White T.J. (eds). *PCR Protocols: A Guide to Methods and Applications.* Academic Press Inc., New York, 482 pp.

http://dergipark.org.tr/trkjnat
Trakya University Journal of Natural Sciences, 22(2): 147-154, 2021
ISSN 2147-0294, e-ISSN 2528-9691
DOI: 10.23902/trkjnat.925742

Research Article

SYNTHESIS, CHARACTERIZATION AND BIOCOMPATIBILITY OF PLANT-OIL BASED HYDROGELS

Ozlem YALCIN CAPAN[1], Pinar CAKIR HATIR[2*]

[1] Department of Molecular Biology and Genetic, Faculty of Science and Letters, İstanbul Arel University, 34537, Büyükçekmece, Istanbul, TURKEY
[2] Department of Biomedical Engineering, Faculty of Engineering and Architecture, İstanbul Arel University, 34537, Büyükçekmece, Istanbul, TURKEY

Cite this article as:

Yalcin Capan O. & Cakir Hatir P. 2021. Synthesis, characterization and biocompatibility of plant-oil based hydrogels. *Trakya Univ J Nat Sci*, 22(2): 147-154, DOI: 10.23902/trkjnat.925742

Received: 22 April 2021, Accepted: 10 June 2021, Online First: 25 June 2021, Published: 15 October 2021

Abstract: Biocompatible hydrogels are used in a variety of biomedical applications, including tissue scaffolds, drug delivery systems, lab/organ-on-a-chips, biosensors, cell-culture studies and contact lenses. The demand for novel and functional monomers to be used in hydrogel synthesis is increasing as the number of biomedical applications and need for biomaterials increase. The purpose of the study was to develop novel hydrogels from renewable materials. Acrylated methyl ricinoleate, a plant oil-based monomer, was used as the renewable material. The effects of acrylated methyl ricinoleate/N-isopropyl acrylamide molar ratio on hydrogel structural properties, thermal stability and in vitro cytotoxicity were studied. FTIR spectroscopy was used to characterize the structural properties of the hydrogels, while TGA was used to characterize the thermal properties. HEK293 and Cos-7 cell lines were used to test the cytotoxicity of the monomers and hydrogels. IC_{50} values for acrylated methyl ricinoleate and N-isopropyl acrylamide were found to be greater than 25 mg/mL. Cell viability of hydrogels containing 50% or more acrylated methyl ricinoleate was greater than 60%, while hydrogel biocompatibility decreased with decreasing molar ratio of acrylated methyl ricinoleate. Cells showed a minimum viability of 80% when incubated in hydrogel degradation products. An environmentally friendly synthesis method was developed and novel biocompatible hydrogels from renewable materials were produced for biomedical applications.

Özet: Biyouyumlu hidrojeller, doku iskeleleri, ilaç taşıyıcı sitemler ve biyosensörler dahil olmak üzere çeşitli biyomedikal uygulamalarda kullanılmaktadırlar. Biyomedikal uygulamaların sayısı ve biyomalzemelere olan ihtiyaç arttıkça hidrojel sentezinde kullanılacak yeni ve işlevsel monomerlere olan talep artmaktadır. Çalışmanın amacı, yenilenebilir malzemelerden özgün hidrojeller geliştirmektir. Yenilenebilir malzeme olarak bitkisel yağ bazlı bir monomer olan akrillenmiş metil risinoleat kullanılmıştır. Akrillenmiş metil risinoleat / N-izopropil akrilamid mol oranının hidrojellerin yapısal özellikleri, termal dayanıklılıkları ve in vitro sitotoksisiteleri üzerindeki etkileri incelenmiştir. Hidrojellerin yapısal özelliklerini karakterize etmek için FTIR spektroskopisi kullanılırken, termal özellikleri karakterize etmek için TGA kullanılmıştır. HEK293 ve Cos-7 hücre hatları, monomerlerin ve hidrojellerin sitotoksisitesini test etmek için kullanılmıştır. Akrillenmiş metil risinoleat ve N-izopropil akrilamid için IC_{50} değerlerinin 25 mg/mL'den büyük olduğu bulunmuştur. %50 veya daha fazla akrillenmiş metil risinoleat içeren hidrojellerin hücre canlılığı %60'ın üzerinde iken, hidrojellerin biyouyumluluğu, akrillenmiş metil risinoleatın hidrojel içerisindeki mol oranı azaldıkça azalmaktadır. Hücreler, hidrojellerin bozunma ürünlerinde inkübe edildiklerinde minimum %80 canlılık göstermiştir. Sonuç olarak, çevre dostu bir sentez yöntemi geliştirilmiş olup, biyomedikal uygulamalarda kullanılmak üzere yenilenebilir malzemelerden özgün biyouyumlu hidrojeller üretilmiştir.

Edited by:
Reşat Ünal

****Corresponding Author:***
Pinar Cakir Hatir
pinarcakir@arel.edu.tr

ORCID iDs of the authors:
OYC. orcid.org/0000-0002-3806-7118
PCH. orcid.org/0000-0002-7511-3355

Key words:
Hydrogel
Renewable resources
Biocompatibility
Acrylated methyl ricinoleate

Introduction

Hydrogels are crosslinked three-dimensional natural and synthetic polymer networks with hydrophilic properties that can absorb a significant amount of water. Because of their similarity to living tissues, they can be used in a variety of biomedical applications, including drug-delivery systems (Peers *et al.* 2020), scaffolds (Xu *et al.* 2019), lab/organ-on-a-chips (Ding *et al.* 2020), cell-culture studies (Bhattacharya *et al.* 2012) and contact lenses

(Peppas & Hoffman 2020). Hydrogels swell in aqueous media because their network structures contain hydrophilic polymers. Depending on the intended application, the swelling profiles of hydrogels may be altered by using more or less hydrophilic monomers. Hydrogels are frequently designed using acrylic-based monomers such as hydroxyethyl methacrylate and methyl methacrylate (Peppas *et al.* 2000). Furthermore, poly(ethylene oxide) (PEO) and poly(ethylene glycol) (PEG) based hydrogels are gaining popularity due to their biocompatibility and FDA approval. Poly-lactic or glycolic acids are also used in the production of hydrogels, especially for biodegradable systems (Lee & He 2010). Smart hydrogels can also be produced using various monomers such as poly(acrylic acid), poly (methacrylic acid), and poly(vinyl alcohol) (N-isopropyl acrylamide). pH-responsive hydrogel systems are created using acidic and basic monomers (Koetting *et al.* 2015), while thermoresponsive hydrogels are created using N-isopropyl acrylamide (NIPAM) (Dong & Hoffman 1986). Smart hydrogels are stimuli-responsive hydrogels that can respond to external stimuli by changing their structural conformations and swelling-deswelling behaviors. Several monomers are needed to create novel hydrogels with desired hydrophilicity for a variety of applications. Thus, there will always be a need for novel and functional monomers.

One of the top priorities of researchers is to synthesize functional monomers and novel hydrogels while minimizing environmental impact. Therefore, environmentally friendly green raw materials are favored for the production of monomers and polymers. Plant oil-based materials are often used as renewable resources because they contain a large number of functionalizable hydroxyl groups. Furthermore, fatty acids contain double bonds that are easily converted into epoxy groups, resulting in a variety of reactions with ring-opening reagents to synthesize biocompatible polymers (Miao *et al.* 2014). Castor oil, for example, is one of the most popular naturally functionalized plant oil triglycerides as it can be used to create a variety of functional monomers (Dupé *et al.* 2012).

Several studies have been performed on the synthesis of hydrogels from plant-based renewable materials such as lignocelluloses, polysaccharides, and proteins (Mohammadinejad *et al.* 2019) but there are few examples of plant oil-based hydrogel synthesis. Sebacic acid, for example, was used as a fatty acid in the design of hydrogels for biomedical applications (Guo *et al.* 2011). In a recent study, acrylated methyl ricinoleate (AMR), a castor oil monomer, was used to create thermoresponsive hydrogels on glass surface for use in biochips, biosensors, and lab-on-a-chip applications (Cakir Hatir & Cayli 2019). Another recent study demonstrated that bacterial cellulose and castor oil could be successfully combined to create thermoresponsive hydrogels (Isikci Koca *et al.* 2020). In the present study, we aimed to synthesize and characterize novel biocompatible hydrogels derived from renewable resources. We used AMR as the plant-oil based monomer, NIPAM as thermoresponsive monomer and N,N′-Methylenebis (acrylamide) (MBA) as crosslinker. We varied the molar ratio of AMR/NIPAM and evaluated the effects of AMR on structural properties, thermal stability, and in vitro cytotoxicity of hydrogels. We developed a green, environmentally friendly synthesis process in order to create biocompatible hydrogels.

Materials and Methods

Materials

N,N′-Methylenebis(acrylamide) (MBA), 2,2-dimethoxy-2-phenylacetophenone (DMPA) and N-Isopropylacrylamide (NIPAM) were supplied from Sigma Aldrich. Acrylated methyl ricinoleate was synthesized as described before (Cakir Hatir & Cayli 2019). Distilled water was obtained by using Merck Millipore. Solvents were supplied from Sigma Aldrich. PhotoLab Eliza Plate Reader (AMR-100 Microplate) was used to perform cell viability studies. MMM Vacucell vacuum oven was used to dry hydrogels. Photopolymerization reactions were performed under UV light, UVGL-58 230V, 50Hz lamp at 365 nm wavelength. Structural characterizations of polymers were performed by using JASCO FT/IR-6000 Spectrometer. Thermal characterizations were carried out by using HITACHI STA7200 Simultaneous TGA.

Synthesis of hydrogels

Hydrogels were synthesized by using the photopolymerization method with a radical initiator, DMPA, under UV irradiation at 365 nm. MBA (1.25 mg) and NIPAM (Table 1) were weighed in a vial and dissolved in 400 µl of Phosphate Buffered Saline (PBS). AMR and DMPA (1% with respect to the total number of double bonds in the system) were transferred into the solution. All polymerization reactions were performed under UV irradiation at 365 nm for 60 min at 25°C. After the polymerization, the hydrogels were washed with water and methanol to remove unreacted monomers and kept in vacuum oven at 25°C for 24 hours.

Characterization of hydrogels

The hydrogels were characterized by Fourier Transform Infrared Spectroscopy (FTIR) and Simultaneous Thermogravimetric Analyzer (TGA). Structural characterization was performed by using JASCO 6600 spectrophotometer in the range of 400-4000 cm^{-1}. All samples were scanned 32 times and FTIR spectra were obtained with 4 cm^{-1} resolution. Thermal characterization was carried out by HITACHI STA7200 TGA. TGA analyses were carried out under nitrogen atmosphere at a rate of 200 mL/min with a heating rate of 10°C/min from 0°C to 900°C.

Table 1. Hydrogels synthesized by using different ratios of MBA, AMR and NIPAM.

Hydrogels	Molar equivalencies of monomers		
	MBA	AMR	NIPAM
H1	1	100	-
H2	1	80	20
H3	1	50	50
H4	1	20	80
H5	1	-	100

In vitro cytotoxicity assays of monomers and hydrogels

Cytotoxicity assays were performed by using Cos-7 (African green monkey kidney fibroblast-like cell line) and HEK293 cells (Human Embryonic Kidney Cells). The cells were cultured in a complete culture medium consisting of Dulbecco's Modified Eagle Medium (DMEM) supplemented with 2 mM L-Glutamine (Thermo Fisher), 100 IU/mL penicillin-streptomycin (Thermo Fisher) and 10% fetal bovine serum (FBS, Lonza®). Cos-7 and HEK293 cells were seeded in 96-well cell culture plates at $10x10^3$ cells/well and then incubated at 37°C in 5% CO_2. After 24 h of incubation, 100 µL of different concentrations (0.5-1-2-5-10 mg/mL) of monomers in PBS or only PBS as control were added to the wells. For cytotoxicity assay of hydrogels, $14x10^4$ cells/well Cos-7 or HEK293 cells were seeded in 24-well plates which were previously covered with different concentrations of hydrogels. All experiments were carried out in triplicates. After a further incubation for 24 h, cytotoxicity of monomers and hydrogels was measured by the MTT (3-(4,5-Dimethylthiazol-2-yl)-2,5-diphenyltetrazolium bromide) assay.

The MTT cytotoxicity assay is a colorimetric assay that measures the number of living cells which have active enzymes converting yellow tetrazolium salt into insoluble purple formazan. The intensity of the purple color is directly proportional to the metabolically active living cells and assessed by colorimetric analysis.

For MTT assay, 10 µL and 100 µL of sterilized MTT (5 mg/mL) reagent was added to each 96-well and 24-well, respectively. After incubation of plates at 37°C in 5% CO_2 for 4 h, the MTT solution was removed. Purple color formazan products were dissolved in Dimethyl Sulphoxyde (DMSO) by incubating the plates in the dark for 15 min on an orbital shaker. Purple color with an absorbance at 570 nm was measured by using an Eliza Plate Reader. Percentage of cell viability was calculated by taking the ratio of absorbance values for samples and control and multiplied by 100.

In vitro cytotoxicity assays of degradation products

20 mg of hydrogel was weighed and transferred into 1 mL of 0.1 N NaOH solution and incubated at room temperature for 24 h. After the hydrogels were degraded entirely, the pH of the solution was adjusted to 7.4. The solution was filtered to sterilize, afterwards, it was diluted 2, 10 and 100 times with cell culture media. 100 µl of the diluted solutions were transferred to the 96-well plates containing cultured Cos-7 cells and incubated for 24 h at 37°C. Cytotoxicity of the degraded products was evaluated using the MTT assay.

Statistical analysis

For cell viability assays, all experiments were performed as two independent experiments carried out in triplicates. All results are presented as mean ± standard deviation (SD). Statistical significance between different groups were evaluated by using one-way analysis of variance (ANOVA) with Bonferroni correction for post hoc analysis and $p<0.05$ was considered as significant.

Results

Characterization of hydrogels

FTIR spectra of the hydrogels are shown in Fig. 1. Hydrogels, including AMR have a strong peak at 1727 cm^{-1}. Hydrogels synthesized with NIPAM have bands at 1646 cm^{-1} (H3, H4), 1631 cm^{-1} (H5), and 1535 cm^{-1} (H3, H4, H5). H4 and H5 have broad bands at 3292 cm^{-1}. Hydrogels synthesized with AMR have bands at 2923 cm^{-1} and 2854 cm^{-1}, whereas hydrogels without AMR have the same bands at around 2969 cm^{-1} and 2928 cm^{-1}.

TGA curves are shown in Fig. 2. Experiments were carried out under a nitrogen atmosphere at a rate of 200 mL/min with a heating rate of 10°C/min from 0 to 900°C. Hydrogel H1 exhibits a decomposition between 300°C and 500°C and lost 85% of its weight around 320°C. TGA curves of H2 and H4 show roughly 10% weight loss at 274°C and 55% weight loss at 300°C. TGA curve of H3 exhibits three significant segmental losses. H5 lost 12% of its weight between 30°C and 200°C. Two critical parameters, 5% weight loss temperature and 50% weight loss temperature, were also investigated (Table 2). The 5% weight loss temperatures were determined as 240°C, 212°C, 216°C, 268°C and 347°C for H1, H2, H3, H4 and H5, respectively, whereas the 50% weight loss temperatures were determined as 344°C, 339°C, 335°C, 348°C and 403°C for H1, H2, H3, H4 and H5, respectively.

In vitro cytotoxicity assays of monomers and hydrogels

The results of the cytotoxicity assay of AMR, NIPAM and MBA monomer solutions with concentrations ranging from 0.5 mg/mL to 10 mg/mL were shown in Fig. 3. Both Cos-7 and HEK293 cells display at least 70% viability in the presence of a wide range of concentrations (0.5-5 mg/mL) of AMR and NIPAM monomer solutions, whereas a significant reduction in cellular viability (less than 70%) was detected with 10 mg/mL concentrations. The toxicity of MBA monomer solution, on the other hand, is significantly high even with 1 mg/mL concentration, less than 50%. IC_{50} (50% cell growth inhibition) values were also calculated by using the curve constructed by plotting cell viability (%) versus monomer concentration (mg/mL). As shown in Table 3, IC_{50} values of AMR and NIPAM solutions are higher than 25 mg/mL while MBA IC_{50} values are very low, ranging between 1.06 mg/mL and 0.05 mg/mL in Cos-7 and HEK293 cells, respectively.

Table 2. Thermal properties of the hydrogels.

Critical parameters	H1	H2	H3	H4	H5
5% weight loss temperature (°C)	240	212	216	268	347
50% weight loss temperature (°C)	344	339	335	348	403

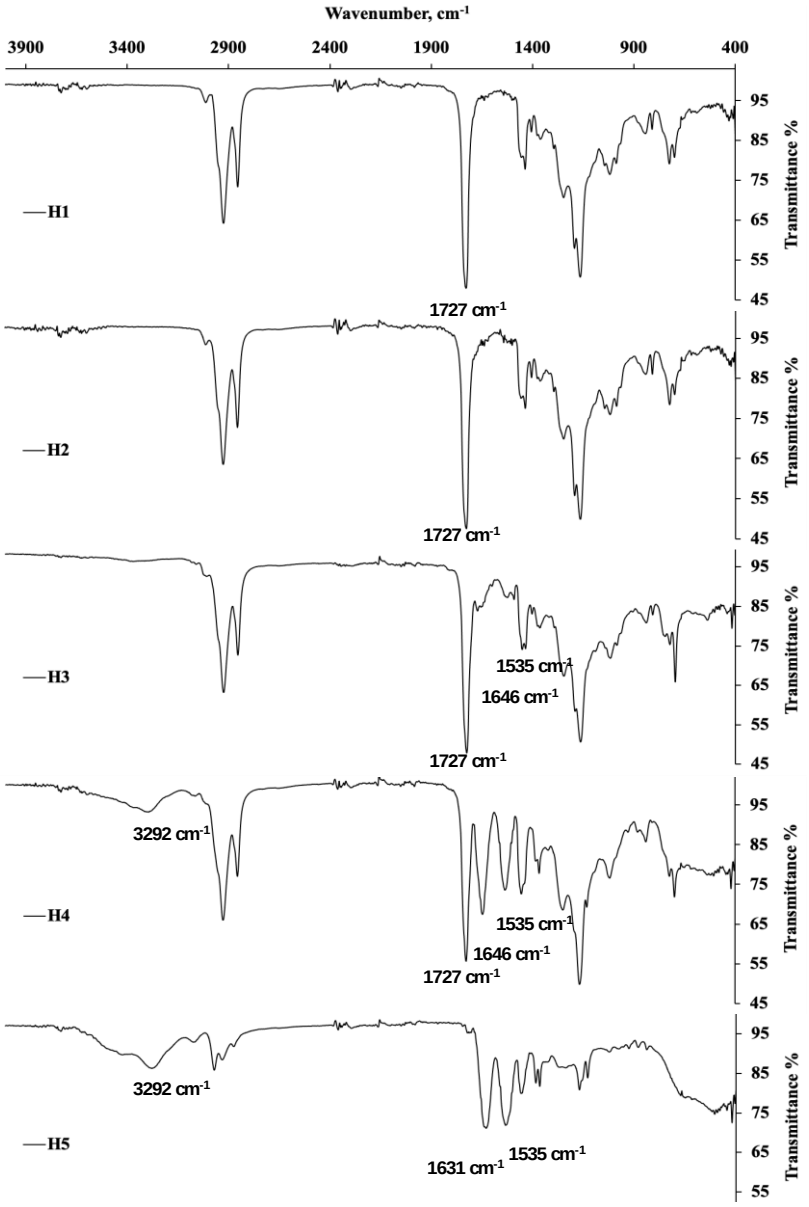

Fig. 1. FTIR spectra of the hydrogels.

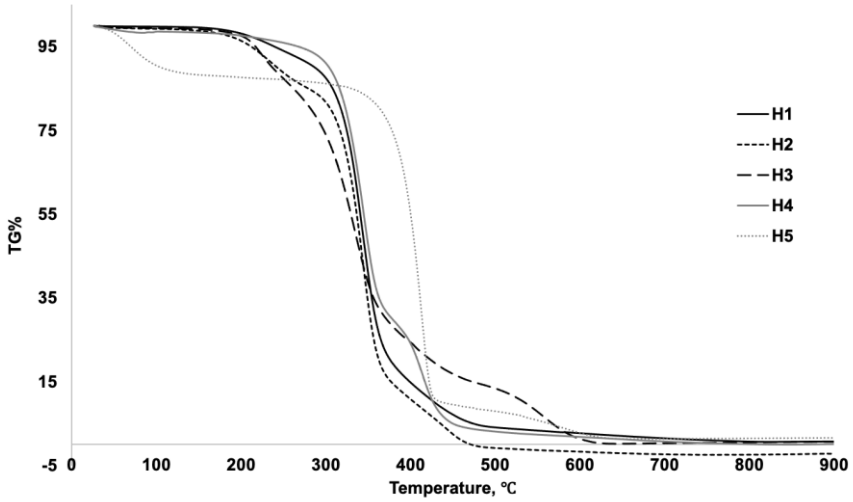

Fig. 2. TGA Curves of the hydrogels.

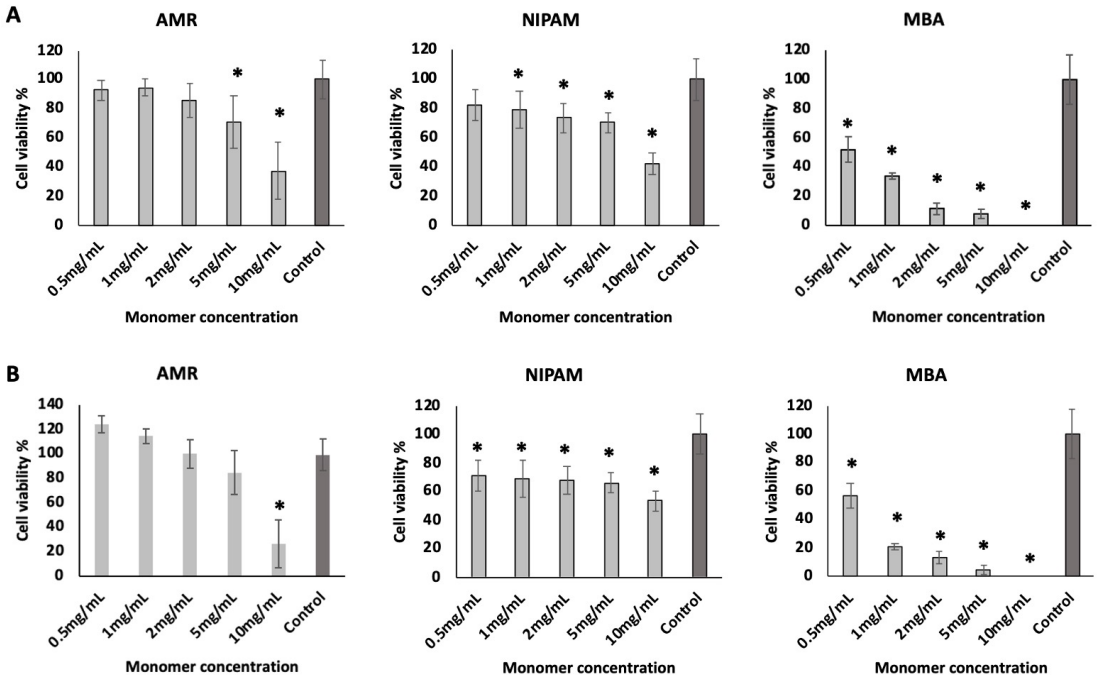

Fig. 3. Cell viability results of two different cell lines (A) Cos-7 and (B) HEK293 with different monomers. Data are presented as mean ± SD of two independent experiments conducted as triplicates. Significant differences between each monomer concentration and the control were evaluated using the one-way analysis of variance (ANOVA) followed by Bonferroni post hoc test. Asterisks (*) indicate a significance difference compared to the control; $p < 0.05$ after Bonferroni correction.

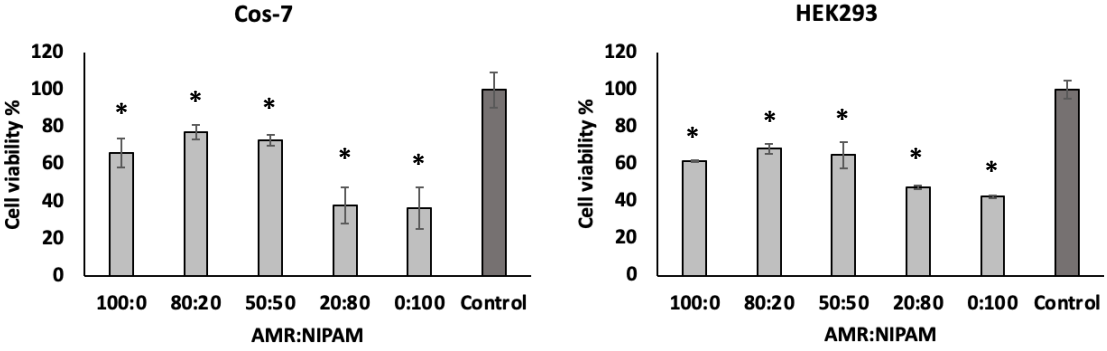

Fig. 4. Cell viability results of two different cell-lines (Cos-7 and HEK293) with different hydrogels. Data are presented as mean ± SD of two independent experiments, conducted as triplicates. Significant differences between each hydrogel and the control were evaluated using the one-way analysis of variance (ANOVA) followed by Bonferroni post hoc test. Asterisks (*) indicate a significance difference compared to the control; $p < 0.05$ after Bonferroni correction.

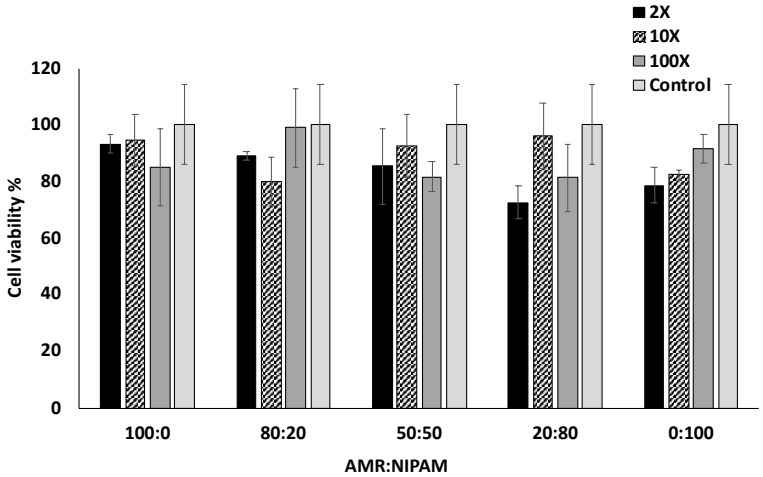

Fig. 5. Cell viability results of the degradation products with different concentrations carried out in Cos-7 cells. Data are presented as mean ± SD of two independent experiments conducted as triplicates.

As shown in Fig. 4, cytotoxicity assay for hydrogels on two different cell lines revealed that the viability of the cells was more than 60% in hydrogels with varied molar ratios of AMR:NIPAM (100:0, 80:20 and 50:50). However, as the amount of NIPAM in hydrogels (AMR:NIPAM, 80:20 and 0:100) increased, a reduction in cell viability was detected. The hydrogels made up of solely NIPAM monomers showed less than 45% cell viability in both cell lines.

In vitro cytotoxicity assays of degradation products

Cytotoxicity of degraded hydrogels with different ratios of AMR:NIPAM was analyzed by MTT assay. Hydrogels were kept in 0.1 N NaOH solution at room temperature for 24 h until they are all degraded. Filtered solutions diluted by 2, 10 and 100 times with cell culture media were applied to Cos-7 cells for 24 h. As shown in Fig. 5, cells showed more than 70% viability when exposed to degraded products in different concentrations supporting the biocompatibility of the hydrogels.

Table 3. IC_{50} values for Cos-7 and HEK293 cells treated with AMR, NIPAM and MBA monomer solution.

Monomers	IC_{50} (mg/mL)	
	Cos-7	HEK293
AMR	30.04	47.71
NIPAM	53.65	25.25
MBA	1.06	0.05

Discussion

Hydrogels generated from natural polymers have attracted significant interest in the field of tissue engineering in recent years due to their low cost of production, biocompatible structure, biodegradability and extracellular matrix mimicking capabilities (Geckil *et al.* 2010, Ko *et al.* 2010, Mantha *et al.* 2019). In this study, novel hydrogels were synthesized using a plant-based monomer (AMR) and a thermoresponsive monomer (NIPAM). The structural and thermal properties of these hydrogels and their effects on cell growth were examined for the first time.

In the first step of the study, FTIR spectra of the hydrogels were evaluated (Fig. 1). AMR has formerly been shown to exhibit two independent ester carbonyl peaks at 1739 cm^{-1} and 1722 cm^{-1} prior to polymerization (Cakir Hatir & Cayli 2019). In the present study, AMR showed two peaks at around 1637 cm^{-1} and 1620 cm^{-1} that indicate acrylate double bonds. The absence of these peaks in hydrogels in the former study suggests that acrylate double bonds were consumed during polymerization. Moreover, hydrogels exhibit a strong peak at 1727 cm^{-1} instead of two separate ester carbonyl peaks, as saturated ester moieties were produced due to polymerization of the acrylate groups. So, the FTIR peaks of the two ester groups shifted to 1727 cm^{-1}, and one ester carbonyl was detected instead of two peaks. These results proved that AMR was involved in the polymerization processes. To establish that NIPAM was also involved in polymerization, the FTIR spectra of NIPAM were analyzed before and after the reactions. The FTIR spectrum of NIPAM revealed a strong peak at around 3280 cm^{-1} caused by N-H stretching of secondary amide, which formed a broad band following monomer polymerization (Ilić-Stojanović *et al.* 2013, Isikci Koca *et al.* 2020). These broad bands are seen in the FTIR spectra of H4 and H5. The broad bands contain both O-H stretching caused by absorbed water, as proven by TGA data and N-H stretching of secondary amide. Furthermore, there is a peak at 1616 cm^{-1} caused by the C=C bond, which should not be seen in polymer spectra (Shah *et al.* 2013). NIPAM hydrogels do not display this peak, instead, they exhibit the bands at 1646 cm^{-1} and 1539 cm^{-1} indicating C=O (amide I) and N-H (amide II) stretching, respectively. H3 and H4 have peaks at 1646 cm^{-1} (H3, H4), H5 has a peak at 1631 cm^{-1} caused by amide I stretching. The bands at around 2950 cm^{-1} represent vibrations of $-CH_3$ and $-CH_2$. The FTIR spectra confirms that H1 has AMR, H5 has NIPAM and H2, H3 and H4 have both NIPAM and AMR. Furthermore, increasing intensity of amide I and amide II bands confirm the increasing molar ratio of NIPAM from H2 to H5. The hydrogels synthesized with AMR have bands at 2923 cm^{-1} and 2854 cm^{-1}, whereas the hydrogels without AMR have the same bands at around 2969 cm^{-1} and 2928 cm^{-1}. Additionally, H4 and H5 have broad bands at around 3292 cm^{-1} which represent NH stretching of NIPAM. In the spectrum of H3, the broad band can barely be seen at around 3300 cm^{-1}. On the other hand, H2 does not have a clear band since the molar ratio of NIPAM is relatively low.

In the next step, the thermal stability properties of the hydrogels were investigated by TGA curves (Fig. 2). Hydrogel H1, synthesized from AMR, exhibited a decomposition between 300°C and 500°C. H1 lost 85% of its weight around 320°C, which might be due to the dissociation of the MR moiety from the main chain (Cakir Hatir & Cayli 2019). TGA curves of H2 and H4 show roughly 10% weight loss at 274°C and 55% weight loss at 300°C, respectively. Decomposed sections of H2 and H4 are proportional to the amount of NIPAM used in the polymerization phase. TGA data of H2 and H4 revealed that when monomers are combined in differing molar ratios, the polymer is produced as a building block. TGA curve of H3 shows three major segmental losses, indicating that the crosslinked polymer network was created in the presence of homogeneously dispersed monomers. H5, produced only using NIPAM, lost 12% of its weight between 30°C and 200°C, indicating evaporation of volatile compounds such as water (Ribeiro *et al.* 2017). H5 is also thermally stable with only a single decomposition step between 340°C and 440°C, as reported in the literature (Ruiz-Rubio *et al.* 2015). Temperatures for 5% and 50% weight loss were investigated (Table 2). The 5% weight loss temperatures were determined as 240°C, 212°C, 216°C, 268°C and 347°C for H1, H2, H3, H4 and H5, respectively, whereas

the 50% weight loss temperatures were determined as 344°C, 339°C, 335°C, 348°C and 403°C for H1, H2, H3, H4 and H5, respectively. Among all hydrogels, H5 showed the highest temperature for both 5% and 50% weight loss. H1, having only AMR has relatively high temperatures for both 5% and 50% weight loss. On the other hand, the combination of AMR and NIPAM caused a slight decrease at the 5% weight loss temperature. From H2 to H5, it was observed that as the molar ratio of NIPAM increases, the temperature for the 5% weight loss increases as well. However, there is no significant change at the 50% weight loss temperatures.

As the hydrogels, which consist of AMR, NIPAM and MBA, can be used for tissue engineering, biocompatibility is crucial for in vivo application. Therefore, we evaluated the cytotoxicity of these monomers and hydrogels with different ratios of AMR and NIPAM. As cytotoxic effects may vary for different cell types with different origins, two different cell lines (Cos-7, kidney fibroblast and HEK293, embryonic kidney cells) were used to evaluate cell viability (Capella *et. al.* 2019). We also calculated the IC_{50} values for each monomer in Cos-7 and HEK293 cell lines (Table 3). IC_{50} values of AMR and NIPAM are higher than 25 mg/mL while MBA IC_{50} values are very low, ranging between 1.06 mg/mL and 0.05 mg/mL in Cos-7 and HEK293 cells, respectively. According to the results, MBA has the lowest IC_{50} value compared to AMR and NIPAM in both cell lines, indicating a high cytotoxic effect for the cells. NIPAM and AMR produced comparable IC_{50} values in which AMR has higher IC_{50} with HEK293 cells, whereas NIPAM has higher IC_{50} with Cos-7 cells.

In addition to the cytotoxicity of monomers, hydrogels were tested as well. The cells grown on hydrogels with increased AMR molar ratio exhibited a higher viability compared to the cells grown on hydrogels with increased NIPAM ratio. Cell viability of hydrogels containing 50% or more AMR was found to be greater than 60%, while biocompatibility of hydrogels reduced with decreasing molar ratio of AMR. The hydrogels made up of only NIPAM showed less than 45% cell viability in both cell lines.

Although building blocks and hydrogels are biocompatible, we also analyzed the cell viability in the presence of degradation products. Cells showed a minimum 80% of viability when they were incubated in degradation products of hydrogels with high molar ratio of AMR (AMR:NIPAM, 100:0, 80:20, 50:50). Therefore, our results indicate that plant oil-based AMR does not lead to cytotoxicity and can be used in tissue engineering applications. However, a longer exposure of hydrogels and degradation products may confirm reliability of the application.

In conclusion, a green, environmentally friendly synthesis method was successfully developed to design biocompatible hydrogels. A plant oil-based monomer, AMR, was used to synthesize novel hydrogels. Molar ratio of AMR to NIPAM was varied and the effects of AMR on structural characteristics, thermal stability, and in vitro cytotoxicity behaviors of the hydrogels were investigated. The findings demonstrated that hydrogels were biocompatible, although their biocompatibility decreased with decreasing molar ratio of plant oil-based monomer. The developed hydrogels can be used in many biomedical applications such as drug-delivery systems, scaffolds, lab/organ-on-a-chip, cell-culture studies and contact lenses.

Acknowledgement

The authors are grateful to Dr. Gokhan Cayli (İstanbul, Turkey), Elif Isikci Koca (İstanbul, Turkey), Seyma Turker (İstanbul, Turkey) and Necla Yucel (İstanbul, Turkey) for their support in hydrogel synthesis and characterization studies.

Ethics Committee Approval: Since the article does not contain any studies with human or animal subject, its approval to the ethics committee was not required.

Author Contributions: Concept: O.Y.C., P.C.H., Desing: O.Y.C., P.C.H., Execution: O.Y.C., P.C.H., Material supplying: O.Y.C., P.C.H., Data acquisition: O.Y.C., P.C.H., Data analysis/interpretation: O.Y.C., P.C.H., Writing: O.Y.C., P.C.H., Critical review: O.Y.C., P.C.H.

Conflict of Interest: The authors have no conflicts of interest to declare.

Funding: The authors declared that this study has received no financial support.

References

1. Bhattacharya, M., Malinen, M.M., Lauren, P., Lou, Y.R., Kuisma, S.W., Kanninen, L., Lille, M., Corlu, A., GuGuen-Guillouzo, C., Ikkala, O., Laukkanen, A., Urtti, A. & Yliperttula, M. 2012. Nanofibrillar cellulose hydrogel promotes three-dimensional liver cell culture. *Journal of controlled release*, 164(3): 291-298.
2. Cakir Hatir, P. & Cayli, G. 2019. Environmentally friendly synthesis and photopolymerization of acrylated methyl ricinoleate for biomedical applications. *Journal of Applied Polymer Science*, 136(38): 47969-47976.
3. Capella, V., Rivero, R.E., Liaudat, A.C., Ibarra, L.E., Roma, D.A., Alustiza, F., Mañas, F., Barbero, C.A., Bosch, P., Rivarola, C.R. & Rodriguez, N. 2019. Cytotoxicity and bioadhesive properties of poly-N-isopropylacrylamide hydrogel. *Heliyon*, 5(4): e01474.
4. Ding, C., Chen, X., Kang, Q. & Yan, X. 2020. Biomedical Application of Functional Materials in Organ-on-a-Chip. *Frontiers in Bioengineering and Biotechnology*, 8: 823-831.
5. Dong, L.C. & Hoffman, A.S. 1986. Thermally reversible hydrogels: III. Immobilization of enzymes for feedback reaction control. *Journal of Controlled Release*, 4(3): 223-227.

6. Dupé, A., Achard, M., Fischmeister, C. & Bruneau, C. 2012. Methyl ricinoleate as platform chemical for simultaneous production of fine chemicals and polymer precursors. *ChemSusChem*, 5(11): 2249-2254.

7. Geckil, H., Xu, F., Zhang, X., Moon, S. & Demirci, U. 2010. Engineering hydrogels as extracellular matrix mimics. *Nanomedicine (London, England)*, 5(3): 469-484.

8. Guo, B., Chen, Y., Lei, Y., Zhang, L., Zhou, W.Y., Rabie, A.B.M. & Zhao, J. 2011. Biobased poly (propylene sebacate) as shape memory polymer with tunable switching temperature for potential biomedical applications. *Biomacromolecules*, 12(4): 1312-1321.

9. Ilić-Stojanović, S.S., Nikolić, L.B., Nikolić, V.D., Milić, J.R., Stamenković, J., Nikolić, G.M. & Petrović, S.D. 2013. Synthesis and characterization of thermosensitive hydrogels and the investigation of modified release of ibuprofen. *Hemijska industrija*, 67(6): 901-912.

10. Isikci Koca, E., Bozdag, G., Cayli, G., Kazan, D. & Cakir Hatir, P. 2020. Thermoresponsive hydrogels based on renewable resources. *Journal of Applied Polymer Science*, 137(28): 48861-48870.

11. Ko, H.F., Sfeir, C. & Kumta, P.N. 2010. Novel synthesis strategies for natural polymer and composite biomaterials as potential scaffolds for tissue engineering. *Philosophical transactions. Series A, Mathematical, physical, and engineering sciences*, 368(1917): 1981-1997.

12. Koetting, M.C., Peters, J.T., Steichen, S.D. & Peppas, N.A. 2015. Stimulus-responsive hydrogels: theory, modern advances and applications. *Materials Science and Engineering: R: Reports*, 93: 1-49.

13. Lee, D.S. & He, C. 2010. In-situ gelling stimuli-sensitive PEG-based amphiphilic copolymer hydrogels. pp. 123-146. In: Ottenbrite, R.M., Park, K. & Okano, T. (eds). *Biomedical Applications of Hydrogels Handbook*. Springer, New York, NY, 432 pp.

14. Mantha, S., Pillai, S., Khayambashi, P., Upadhyay, A., Zhang, Y., Tao, O., Pham, H.M. & Tran, S.D. 2019. Smart Hydrogels in Tissue Engineering and Regenerative Medicine. *Materials (Basel, Switzerland)*, 12(20): 3323-3356.

15. Miao, S., Wang, P., Su, Z. & Zhang, S. 2014. Vegetable-oil-based polymers as future polymeric biomaterials. *Acta biomaterialia*, 10(4): 1692-1704.

16. Mohammadinejad, R., Maleki, H., Larrañeta, E., Fajardo, A.R., Nik, A.B., Shavandi, A., Sheikhi, A., Ghorbanpour, M., Farokhi, M., Govindh, P., Cabane, E., Azizi, S., Aref, A.R., Mozafari, M., Mehrali, M., Thomas, S., Mano, J.F., Mishra, Y.K. & Thakur, V.K. 2019. Status and future scope of plant-based green hydrogels in biomedical engineering. *Applied Materials Today*, 16: 213-246.

17. Peers, S., Montembault, A. & Ladavière, C. 2020. Chitosan hydrogels for sustained drug delivery. *Journal of Controlled Release*, 326: 150-163.

18. Peppas, N.A. & Hoffman, A.S. 2020. Hydrogels. pp. 153-166. In Wagner W.R., Zhang, G, Sakiyama-Elbert, S.E., Yaszemski, M.J., (eds). *Biomaterials science*, Academic Press. 1616 pp.

19. Peppas, N.A., Huang, Y., Torres-Lugo, M., Ward, J.H. & Zhang, J. 2000. Physicochemical foundations and structural design of hydrogels in medicine and biology. *Annual review of biomedical engineering*, 2(1): 9-29.

20. Ribeiro, C.A., Martins, M.V.S., Bressiani, A.H., Bressiani, J.C., Leyva, M.E. & de Queiroz, A.A.A. 2017. Electrochemical preparation and characterization of PNIPAM-HAp scaffolds for bone tissue engineering. *Materials Science and Engineering: C*, 81: 156-166.

21. Ruiz-Rubio, L., Álvarez, V., Lizundia, E., Vilas, J.L., Rodríguez, M. & León, L.M. 2015. Influence of α-methyl substitutions on interpolymer complexes formation between poly (meth) acrylic acids and poly (N-isopropyl (meth) acrylamide) s. *Colloid and Polymer Science*, 293(5): 1447-1455.

22. Shah, L.A., Farooqi, Z.H., Naeem, H., Shah, S.M. & Siddiq, M. 2013. Synthesis and characterization of poly (N-isopropylacrylamide) hybrid microgels with different cross-linker contents. *Journal of the Chemical Society of Pakistan*, 35: 1522-1529.

23. Xu, C., Dai, G. & Hong, Y. 2019. Recent advances in high-strength and elastic hydrogels for 3D printing in biomedical applications. *Acta biomaterialia*, 95: 50-59.

http://dergipark.org.tr/trkjnat
Trakya University Journal of Natural Sciences, 22(2): 155-161, 2021
ISSN 2147-0294, e-ISSN 2528-9691
DOI: 10.23902/trkjnat.896013

Research Article

In vitro REGULATION OF THE EXPRESSION OF THE SARS-CoV-2 RECEPTOR ANGIOTENSIN-CONVERTING ENZYME (*ACE2*) IN LUNG CANCER CELLS BY NATURAL PRODUCTS

Kaan HÜRKAN[1*], Şevki ARSLAN[2], Mehmet Nuri ATALAR[3], Adnan AYDIN[1], İbrahim DEMİRTAŞ[3], Dogukan MUTLU[2], Bahattin TABAR[4], Mehmet Hakkı ALMA[5]

[1] Iğdır University, Department of Agricultural Biotechnology, Faculty of Agriculture, 76000, Iğdır, TURKEY
[2] Pamukkale University, Department of Biology, Faculty of Arts and Sciences, 20000, Denizli, TURKEY
[3] Iğdır University, Department of Biochemistry, Faculty of Arts and Sciences, 76000, Iğdır, TURKEY
[4] Iğdır University, Postgraduate Education Institute, 76000, Iğdır, TURKEY
[5] Iğdır University, Department of Biosystems Engineering, Faculty of Agriculture, 76000, Iğdır, TURKEY

Cite this article as:

Hürkan K., Arslan Ş., Atalar M.N., Aydın A., Demirtaş İ., Mutlu D., Tabar B. & Alma M.H. 2021. *In vitro* regulation of the expression of the SARS-CoV-2 receptor angiotensin-converting enzyme (*ACE2*) in lung cancer cells by natural products. *Trakya Univ J Nat Sci*, 22(2): 155-161, DOI: 10.23902/trkjnat.896013

Received: 12 March 2021, Accepted: 15 June 2021, Online First: 05 July 2021, Published: 15 October 2021

Edited by:
Belgin Süsleyici

***Corresponding Author:**
Kaan Hürkan
kaan.hurkan@igdir.edu.tr

ORCID iDs of the authors:
KH. orcid.org/0000-0001-5330-7442
ŞA. orcid.org/0000-0002-4215-5006
MNA. orcid.org/0000-0003-2993-2605
AA. orcid.org/0000-0003-4126-5374
İD. orcid.org/0000-0001-8946-647X
DM. orcid.org/0000-0003-3259-5822
BT. orcid.org/0000-0001-9632-2060
MHA. orcid.org/0000-0001-7011-3965

Key words:
Oleuropein
Soaproot
Whey
COVID-19
A549 adenocarcinoma cell-line

Abstract: The COVID-19 pandemic continues infecting people causing deaths globally. Although various medicines have been tried to combat with COVID-19, there is no medicine or treatment that has been validated yet. People have been using natural products for centuries against bacterial and viral illnesses. This study aimed to test the effects of the biomolecule oleuropein, whey collected from industrial waste and soaproot extracts obtained from *Gypsophila arrostii* Guss. var. *nebulosa* Boiss. & Heldr. and *Saponaria officinalis* L. on the expression of the human *ACE2* gene as SARS-CoV-2 receptor on the A549 adenocarcinoma cell-line by Real-Time Quantitative Polymerase Chain Reaction (qPCR). According to the cytotoxicity tests, *G. arrostii* var. *nebulosa* and *S. officinalis* extract treatments showed a dose dependent cytotoxic effect on the cells. The EC50 values of *G. arrostii* var. *nebulosa* and *S. officinalis* were found to be 54.3 µg/ml and 17.3 µg/ml, respectively. Oleuropein showed moderate cytotoxic effects with the EC50 value over 250 µg/ml. Whey (fermented and non-fermented) did not show any cytotoxic effect at the applied doses. The qPCR results showed that the *ACE2* mRNA level decreased by 89.8% and 35.2% due to the fermented and non-fermented whey extracts, respectively. Similarly, *G. arrostii* var. *nebulosa* and *S. officinalis* downregulated *ACE2* by 79.8% and 90.1%, respectively. In contrast, oleropein upregulated *ACE2* (102.8%). Our results showed that the natural supporting products produced from soaproot extracts and fermented whey can be used against COVID-19 by both cancer patients and people in potential risk groups.

Özet: COVID-19 pandemisi tüm dünyada küresel çapta insanları enfekte etmeye ve ölümlere neden olmaya devam etmektedir. COVID-19 ile mücadelede birçok ilaç denenmiş olmasına karşın henüz herhangi bir ilaç veya tedavi yöntemi onaylanmamıştır. İnsanlar yüzyıllardan bu yana hastalıklara karşı doğal ürünleri kullanmışlardır. Bu çalışmadaki amacımız bir biyomolekül olan oleuropein, endüstriyel atık olarak bertaraf edilen peynir altı suyu ve *Gypsophila arrostii* Guss. var. *nebulosa* Boiss. & Heldr. ve *Saponaria officinalis* L. bitkilerinden elde edilen ekstraktların A549 kanserli hücre hatlarında ACE2 reseptörünü kodlayan *ACE2* geninin anlatım seviyesi üzerine etkilerini Gerçek Zamanlı Kantitatif Polimeraz Zincir Reaksiyonu (qPCR) ile belirlemektedir. Yaptığımız sitotoksisite testlerine göre *G. arrostii* var. *nebulosa* ve *S. officinalis* ekstraktları sırası ile 54,3 µg/ml ve 17,3 µg/ml EC50 değerleri ile doza bağımlı sitotoksik etki gösterirken, oleuropein 250 µg/ml'nin üzerinde bir değerle orta dereceli sitotoksik etki göstermiştir. Öte yandan peynir altı suyu (ferment eve fermente edilmeyen), çalışmada kullanılan dozlarda sitotoksik etki göstermemiştir. qPCR sonuçlarına göre fermente edilmiş ve edilmemiş peynir altı suyunun *ACE2* genine ait mRNA seviyesini sırası ile %89,8 ve %35,2 oranlarında düşürdüğü belirlenmiştir. Benzer şekilde *G. arrostii* var. *nebulosa* ve *S. officinalis* ekstraktlarının *ACE2* geni mRNA seviyesini sırası ile %79,8 ve %90,1 oranında düşürdüğü belirlenmiştir. Bu sonuçların aksine oleuropein biyomolekülünün *ACE2* mRNA seviyesini %102,8 oranında arttırdığı belirlenmiştir. Çalışma sonuçlarına göre kullanılan bitki ekstraktlarının ve fermente edilmiş peynir altı suyunun COVID-19 ile mücadelede kanser hastalarında ve risk gruplarında kullanılabilecek doğal destek ürünlerinin üretilmesinde kullanılabileceğini göstermektedir.

Introduction

Since December 2019, when the severe, acute respiratory syndrome coronavirus 2 (SARS-CoV-2 or COVID-19) was detected in Wuhan, China, the disease infected more than 173 million people and caused 3.7 million deaths globally. The *ACE2* gene, which encodes receptor of the angiotensin-converting enzyme-2 was proven to be the main gateway for both the SARS-coronavirus (SARS-CoV) and the human coronavirus (HCoV NL63) (Zhou *et al.* 2020). In vitro tests showed that there is a positive correlation between *ACE2* gene expression and COVID-19 infection (Hofmann *et al.* 2004, Li *et al.* 2007). Phylogenetic studies showed that COVID-19 and the SARS-CoV have many similar sequences, and their spike proteins have 76.5% sequence similarity (Xu *et al.* 2020). Therefore, the spike protein of COVID-19 is predicted to have a binding ability to *ACE2*. Studies indicated ACE2 receptor as the potential target to develop therapeutics for COVID-19 (Zhang *et al.* 2020). Despite the great efforts of researchers, there exists no validated therapeutics available for the disease. The COVID-19 pandemic not only affected healthy people, but also people who have major lung diseases. The patients with lung cancer cohort with COVID-19 are at greater risk due to both diseases damaging their lungs (Wang *et al.* 2019, Chen *et al.* 2020, Liang *et al.* 2020, Wang & Zhang 2020). Besides, Feng *et al.* (2011) showed that the overexpression of *ACE2* inhibits angiogenesis on tumor cells both in vitro and *in vivo*.

Plants have been used as medicines for thousands of years because of their healing effects. Plant secondary metabolites have important pharmaceutical effects on many diseases. For instance, the phenolic compounds of olive (*Olea europea* L.), particularly the oleuropein, show high anti-inflammatory and anticancer activities by inhibiting the tumor growth (Carrera-González *et al.* 2013). Oleuropein has also been reported to have anti-viral, anti-cancer, and anti-inflammatory effects (Haris Omar 2010).

Milk and colostrum are health-enhancing natural products due to their protein and peptide contents. Whey is a by-product of the dairy industry during the manufacturing of milk products. Studies showed that the whey proteins lactoferrin and alpha-lactalbumin have antiviral and antitumor activities, and casein has antitumor activity (Almehdar *et al.* 2015, Kanwar *et al.* 2009, Zimecki & Kruzel 2007).

Ribosome-inactivating-proteins (RIPs) are immunotoxins and antiviral reagents and saporins are the basic types of type-1 RIPs. Soaproot is woody roots of some perennial plants. Seven plant species, *Ankyropetalum gypsophiloides* Fenzl., *Gypsophila arrostii* Guss. var. *nebulosa* (Boiss. & Heldr.) Bark., *G. bicolor* (Freyn & Sint.) Grossh., *G. eriocalyx* Boiss., G. *graminifolia* Bark., *G. perfoliata* L. and *G. venusta* Fenzl. are used to obtain soaproot in Turkey (Koyuncu *et al.* 2008). *Saponaria officinalis* L., which is also used to obtain soaproot in Europe, but not in Turkey, contains RIPs on its seeds and leaves (Carzaniga *et al.* 1994). It is also known that soaproot has an antiviral effect (Serkedjieva *et al.* 1990).

In this study, we aimed to test the effects of oleuropein, whey (fermented and non-fermented), and two types of soaproot extracts (*G. arrtosii* var. *nabulosa* and *S. officinalis*) on the expression of *ACE2* gene on the A549 human adenocarcinoma cell-line by qPCR. This is the first study that shows how biomolecules and natural products affect *ACE2* gene expression on the adenocarcinoma cell-line.

Materials and Methods

Obtaining the plant extracts and whey

Oleuropein obtained from BLD Pharmatech Pvt Ltd (India) (Cat. No: BD1777) was used. It was dissolved in dimethyl sulfoxide (DMSO) (final concentration in medium did not exceed 0.5%) before used.

Whey is discarded as an industrial waste in Iğdır province of Turkey. We obtained whey from Has Mandıra Dairy Products Company (Iğdır, Turkey) in Iğdır Organised Industrial Site with its fat and pellet. After discarding the fat, the whey was titrated by 0.1 N NaOH and the pH was adjusted to 6.0. We boiled the mixture and filtered the precipitation. Then, we added yeast extract (0.75%), $MnSO_4$ (20 mg/l) and $CaCO_3$ (1.5%), and sterilised the mixture by autoclaving at 121°C and 1.5 ATM. The sterilised whey was fermented by *Lactobacillus casei* at 37°C for 48 h. Non-fermented and fermented forms of whey were used in the study.

Gypsophila arrostii var. *nebulosa* was collected from Isparta (Turkey – approx. N37.7, E030.5) in May 2020, and the collected specimens were identified by taxonomist Ahmet Zafer Tel from Iğdır University, Department of Agricultural Biotechnology by using the identification key in the Flora of Turkey and the East Aegean Islands (Davis 1970). After cleaning and grinding the roots, we obtained the soaproot extract. We also commercially ordered a second soaproot extract powder, which was made from the roots of *S. officinalis*, from İstanbul Agricultural Products and Food Industry Trade Ltd Company (İstanbul, Turkey) (Cat. No: SAPO-4434) to be tested in the study. It was dissolved in DMSO before the treatment.

Experimental design, cytotoxicity tests and the treatment of the cells with the biomolecules and the natural products

Dulbecco's Modified Eagle Medium (DMEM), fetal bovine serum (FBS), trypsin, penicillin/streptomycin mixture were purchased from Sigma-Aldrich Chemical Company (St Louis, Missouri, USA). The MTT Cell Proliferation Assay Kit was purchased from BioVision, Inc. (USA). All the other chemicals and solvents were obtained from commercial sources at the highest grade of purity available.

A549 cells (European Collection of Cell Cultures. ECACC, UK) were cultured in DMEM containing 10% fetal bovine serum, 100 U ml^{-1} penicillin and 100 μg/ml

streptomycin mixture in a humidified atmosphere with 5% CO_2 under the normal oxygen conditions at 37°C and were passaged every 2-3 days. The cytotoxic effects of isolated molecules and extracts were determined by using the effects of the MTT (3-(4,5-dimethyltiazole-2-yl) -2,5-diphenyltetrazolium bromide) assay as triplicates. For this purpose, we seeded A549 cells in 96-well plates at a density of 5000 cells/well and incubated for 24 h for attachment. The cells were then exposed to different concentrations of isolated molecules and extracts for another 24 h. We incubated the treated and control cells for 24 h at 37°C in humidified 5% CO_2 atmosphere. After 24 h, the medium was removed, and fresh medium was added to each well. After that, 10 µl of the MTT reagent was added to each well and incubated for 4 h in the incubator. After 4 h, the medium was removed carefully and 50 µl of DMSO added to each well. The amount of formazan formed was determined by measuring the absorbance at 590 nm using a microplate reader (Epoch, BioTek). We used three replicated wells for each experimental condition. Viability was expressed as a percentage of the control.

Primer design, RNA extraction, cDNA synthesis and qPCR

We designed the primers targeting the human *ACE2* gene referencing *Homo sapiens* ACE-related carboxypeptidase *ACE2* mRNA, complete CDS (GenBank accession: AF291820.1) as ten alternatives using the National Center for Biotechnology Information (NCBI) Primer-BLAST tool (optimal annealing temperature is 60°C and product size range is 80-110bp). We selected the human glyceraldehyde3phosphate dehydrogenase (*GAPDH*) gene as the reference gene (Goulter *et al.* 2004) (5′-CGGAGTCAACGGATTTGGTC-3′ and 5′-TGAGGTCAATGAAGGGGTCA-3′) for normalisation of the qPCR results. The A549 cells (1×10^7 cells) were seeded to plates and exposed to maximum non-toxic doses dosed of test materials and harvested after a 24 h treatment. Total RNA was extracted by using InnuPREP RNA Mini Kit (Analytic Jena, Germany). Extracted RNA was quantified spectrophotometrically at 260/280 nm, and the integrity was checked using 1% agarose gel electrophoresis. We converted 2.5 µg of RNA to cDNA by EasyScript™ cDNA Synthesis Kit according to the manual provided by the supplier (ABM, Canada) and the cDNA was stored at -80°C for further use. We confirmed the cDNA synthesis by performing end-point PCR using the reference gene *GAPDH*. The qPCR analyses were performed by using SYBR® Green fluorescent dye-containing master mix (KiloGreen 2X qPCR Master Mix, ABM, Canada). qPCR reactions were performed with 10 µl KiloGreen 2X qPCR Master Mix, (ABM, Canada) 0.6 µl (200 nM) of each primer, and 10 ng cDNA template. qPCR was performed on the Applied Biosystems StepOnePlus Real-Time PCR systems (Applied Biosystems, USA). All amplifications were as 95°C for 10 m initial denaturation followed by 45 cycles at 95°C 15 s for denaturation, 60°C 60 s for annealing, and 72°C 60 s for elongation. Melting curve analysis with a ramp rate of 0.5°C/step was added after amplification to confirm specificity of the primers. All the experiments were performed as three biological and three technical replicates. We calculated PCR efficiencies for each primer pairs according to (Ruijter *et al.* 2009), and used the primer only with efficiency value between 90-105% (Forward 5′-TGAAGGCCCTCTGCACAAAT-3′ and 5′-ATGCTAGGGTCCAGGGTTCT-3′). We calculated the gene expression differences according to the comparative Delta Delta Ct method ($2^{-\Delta\Delta C_t}$) (Livak & Schmittgen 2001).

Statistical Analysis

All data presented are mean values of each qPCR treatments. Data were analysed using the statistical program JASP (0.14.1). The analysis of variance (ANOVA) was followed by Fisher's protected LSD test to identify homogenous groups within the means. Significant differences among treatments were considered at the $P\leq0.05$ level.

Results

The cytotoxicity of the pure compounds and extracts on A549 cells was measured by MTT test. *Gypsophila arrostii* var. *nebulosa* and *S. officinalis* extract treatments showed a dose-dependent cytotoxic effect on A549 cells (Fig. 1). The EC50 values of the *G. arrostii* var. *nebulosa* and *S. officinalis* were found to be 54.3 µg ml^{-1} and 17.3 µg ml^{-1}, respectively. Oleuropein showed moderate cytotoxic effects (EC50 value was over 250 µg ml^{-1}), while whey (fermented and non-fermented) did not show any cytotoxic effect at applied doses.

We obtained high quality and sufficient amounts of RNA for the cDNA synthesis. The successful amplification of the *GAPDH* gene by conventional PCR confirmed the cDNA synthesis success.

Preliminary tests were carried out to determine the changes in *ACE2* mRNA levels with respect to extracts and pure compounds. For this purpose, maximum non-toxic doses of the test materials (250 µg ml^{-1} for fermented and non-fermented whey extract, 10 µg ml^{-1} for *S. officinalis* extract, 12.5 µg ml^{-1} for *G. arrostii* var. *nebulosa* extract, and 100 µg ml^{-1} for oleuropein) were selected and applied to the cells for 24 hours. Statistical analysis revealed that there were significant changes in expression levels of *ACE2*. The qPCR results showed that the *ACE2* expression level decreased to 89.8% and 35.2% as a result of the fermented and non-fermented whey extract, respectively (Fig. 2). Similarly, *G. arrtosii* var. *nebulosa* and *S. officinalis* decreased the *ACE2* expression to 79.8% and 90.1%, respectively. On the contrary, oleropein increased the *ACE2* expression level to 102.8%.

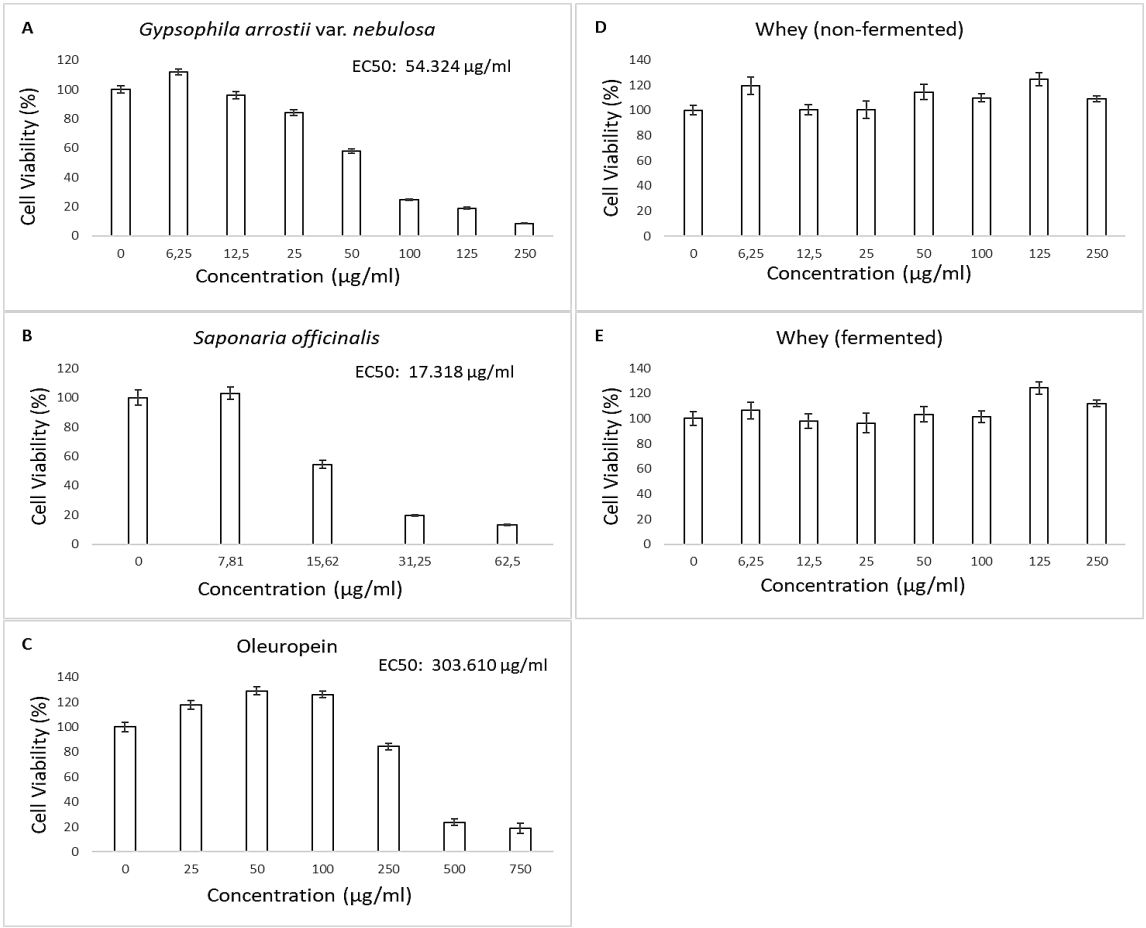

Fig. 1. The cytotoxicity levels of the pure compounds and the extracts measured by MTT test. The EC50 values given on each graph with cytotoxicity effect. *Gypsophila arrostii* var. *nebulosa* and *S. officinalis* (A and B) showed dose-dependent cytotoxicity, oleuropein (C) showed moderate cytotoxicity, and whey (D and E) showed no cytotoxicity. The error bars represent standard deviation values.

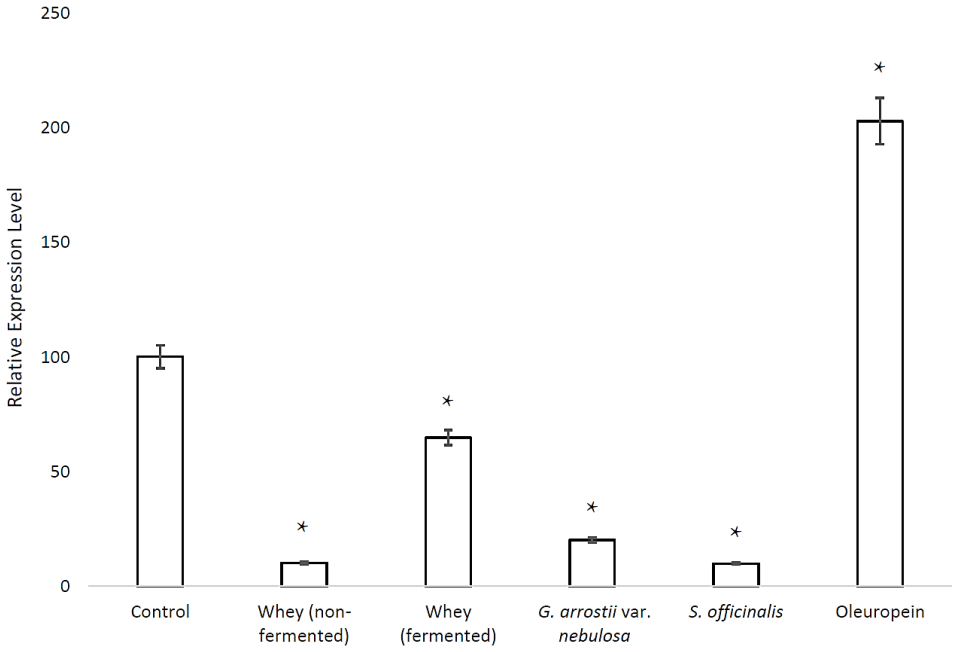

Fig. 2. The qPCR results of the biomolecules and natural products on the expression of the Human *ACE2* gene expression calculated using the Comparative Delta Delta Ct ($2^{-\Delta\Delta C_t}$) method. The values on the Y-axis represent the percentages. The error bars represent standard errors. Statistically significant ($P \leq 0.05$) values were indicated with asterisks.

Discussion

In this study, we investigated the effects of the secondary metabolite oleuropein, industrial waste whey (non-fermented and fermented) and soaproot extracts of the medicinal plants *G. arrostii* var. *nebulosa* and *S. officinalis* on the expression of the Human *ACE2* gene, which has a gateway role for COVID-19, on the A549 adenocarcinoma cell-line. Our cytotoxicity analyses, which helped us to determine the appropriate doses, showed that oleuropein has moderate cytotoxic effects (EC50 value was over 250 μg ml^{-1}), both non-fermented and fermented whey have no cytotoxic effect, and the soaproot extracts have a dose-dependent cytotoxic effect (*G. arrostii* var. *nebulosa* is 54.3 μg ml^{-1}, and *S. officinalis* is 17.3 μg ml^{-1}). The qPCR results showed that oleuropein upregulated the *ACE2* gene by 102.8%, while whey (fermented 89.8% and non-fermented 35.2%) and the two soaproot extracts (*G. arrostii* var. *nebulosa* 79.8% and *S. officinalis* 90.1%) downregulated. These findings make this study the first that shows biomolecules and natural products can regulate the Human *ACE2* expression on adenocarcinoma cells.

Patients with cancer background (both history and active patients) were concluded to be more likely to develop COVID-19 in China (Wang & Zhang 2020, Xia *et al.* 2020). Therefore, COVID-19 patients with cancer cohort are at greater risk. The pathology reports of cancer patients, particularly those with lung cancer, which have adenocarcinoma, cohort with COVID-19 developed oedema, proteinaceous exudate and inflammatory cellular infiltration in their lungs besides the tumours (Tian *et al.* 2020). Researchers concluded that sensitivity to COVID-19 in these patients was related to the excessive expression levels of *ACE2* gene (Jia *et al.* 2020). Therefore, focusing on developing medicines and supporting products for cancer patients is important.

Developing and testing vaccines needs more time than supporting products. Researchers are trying to find therapeutical effects of various biomolecules, active compounds, natural products and easy-to-find plant-derived products on COVID-19. Although most plant-derived products, which have phenolics, secondary metabolites etc., have antiviral effects, no study has been performed so far on Human *ACE2* gene with cancer.

Oleuropein, the only biomolecule that upregulated *ACE2* expression in our study, is the main phenolic component of olive. This is the first study that shows the effects of oleuropein on *ACE2* expression. Previous studies stressed its high anti-inflammatory, anticancer and antiviral effects (Carrera-González *et al.* 2013, Haris Omar 2010). Its inhibitory effect on *ACE1* expression was also reported (Msomi & Simelane 2017). Despite these properties, oleuropein caused a two fold increase of *ACE2* expression on cancer cells we used. The upregulation on *ACE2* might be because of the complex cell differentiation of the cancer cells. *ACE2* expression was reported to depend on the state of cell differentiation (Jia *et al.* 2006). In that study, researchers showed the correlation between cell differentiation and *ACE2* expression on A549 cells. Due to high differentiation rate of cancer cells, oleuropein might induce *ACE2* expression. Researchers indicated the correlation of *ACE2* expression and COVID19 infection (Hofmann *et al.* 2004, Li *et al.* 2007). Therefore, upregulation of *ACE2* by exposing to oleuropein will cause an increment on the ACE2 receptor on the membrane of the adenocarcinoma cells. This case proves that COVID-19 the gateway for the entrance into the cell.

The natural product whey, which is discarded as a waste of manufacturing from various milk products, was tested in this study for the first time on *ACE2* gene and downregulated its expression. We tested two types of whey as non-fermented and fermented. The non-fermented whey drew out the fermented type by almost silencing the *ACE2* with 89.8% downregulation ratio. The fermented whey also had a downregulation effect on *ACE2* by 35.2%. Milk and particularly colostrum are important sources of proteins that have many bioactivities. Whey also has various proteins including a group of milk protein lactoferrin (Teo *et al.* 2016). Lactoferrin was reported as an antiviral, antifungal, antibacterial, antitumor and immune enhancer whey protein (Ng *et al.* 2015). It can bind Heparan Sulfate Proteoglycans (HSPGs) and *ACE2*. Therefore, researchers reported that lactoferrin might have a preventive and therapeutic value for COVID-19 (Kell *et al.* 2020). Alphalactalbumin and lactoglobulin, other proteins included in whey, have an inhibition effect on HIV reverse transcriptase (Ng *et al.* 2015). Due to COVID-19 being a RNA virus, these proteins might affect COVID-19 reverse transcriptase, as well. In another study, fresh buttermilk cultured using paneer whey was reported as ACE enzyme inhibitor (Parekh *et al.* 2017). Supporting our results, having both *ACE2* receptor binding ability and decreasing the *ACE2* gene expression, whey might be a conspicuous natural product against COVID-19 in cancer patients. We think that re-fermentation of whey inhibited its bio-functional properties.

Gypsophila arrostii var. *nebulosa* is being used to obtain soaproot mostly in Anatolia (Koyuncu *et al.* 2008). Since there is no available study about the effects of *Gypsophila* sp. on *ACE2* expression, our result of 79.8% downregulation will open a new avenue for researchers in the field of pharmaceutics. The phytochemical studies on *G. arrostii* var. *nebulosa* showed that triterpene saponins are present in its roots (Arslan *et al.* 2013). Due to their modifying effect on cell membranes, saponins have a potential pharmaceutical value (Mostad & Doehl 1987). Although saponins are commonly found in higher plants, triterpene saponins are very rare in nature (Arslan & Cenzano 2020). A recent review by Arslan & Cenzano (2020) concluded that triterpene saponins have been used in cancer therapies since 1976 (Ebbesen *et al.* 1976). Recent studies showed significant anticancer activities for saponins (Cheng *et al.* 2016). Although it is known that *Panax notoginseng* (Burkill) F.H.Chen saponins have

inhibitor effects on *ACE2* expression (Guo *et al.* 2010), there is no study on the triterpene saponins in the literature. We think that *ACE2* inhibition effect might be related with triterpene saponins in the roots of *G. arrostii* var. *nebulosa*.

According to our results, soaproot extract obtained from *S. officinalis* had the most inhibition effect on *ACE2* expression by 90.1% which may be regarded as silencing of the gene. The main bioactive compound of *S. officinalis* has triterpene saponins, as in *Gypsophila* species. The immune-stimulant effects of triterpene saponins were reported before (Press *et al.* 2000). Koike *et. al.* (1999) discovered new types of saponins in *S. officinalis* such as saponariosides and Saponarioside C. Although there are no studies on the immunological effects of these molecules, they may have immune-stimulant effects similar to triterpene saponins.

Due to the high infection rate, COVID-19 spread throughout the world. The people in the high-risk group, particularly those suffering from cancer, need more attention. In this study, we showed that the natural products whey and soaproot extracts can downregulate the *ACE2* gene, which is the main gateway for COVID-19. Both whey and soaproot extracts have anti-cancer and antitumor effects. Therefore, we conclude that the food-supporting products or medicines made from these natural products would be a good protector against COVID-19 in cancer patients. The results of the study will open an avenue for more clinical studies of natural products.

Acknowledgement

We thank Cathy Seither (Texas, USA) for language proof, anonymous referees and editors who helped to improve the manuscript.

Ethics Committee Approval: Since the article does not contain any studies with human or animal subject, its approval to the ethics committee was not required.

Author Contributions: Concept: K.H., Desing: K.H., Ş.A., M.N.A., A.A., Execution: Ş.A., Data analysis/interpretation: Ş.A., D.M., B.T., Writing: K.H., Ş.A., İ.D., Critical review: İ.D., M.H.A.

Conflict of Interest: The authors have no conflicts of interest to declare.

Funding: The authors declared that this study has received no financial support.

References

1. Almehdar, H.A., El-Fakharany, E.M., Uversky, V.N. & Redwan, E.M. 2015. Disorder in milk proteins: structure, functional disorder, and biocidal potentials of lactoperoxidase. *Current Protein & Peptide Science*, 16(4): 352-365.
2. Arslan, I., Celik, A. & Melzig, M.F. 2013. Nebulosides A-B, novel triterpene saponins from under-ground parts of Gypsophila arrostii Guss. var. nebulosa. *Bioorganic & Medicinal Chemistry*, 21(5): 1279-1283.
3. Arslan, I. & Cenzano, A.M. 2020. N-triterpene saponins in cancer therapy: A review of mode of action. *Revista Brasileira de Farmacognosia*, 30(1): 1-6. https://doi.org/10.1007/s43450-020-00033-5
4. Carrera-González, M.P., Ramírez-Expósito, M.J., Mayas, M.D. & Martínez-Martos, J.M. 2013. Protective role of oleuropein and its metabolite hydroxytyrosol on cancer. *Trends in Food Science & Technology*, 31(2): 92-99.
5. Carzaniga, R., Sinclair, L., Fordham-Skelton, A.P., Harris, N. & Croy, R.R.D. 1994. Cellular and subcellular distribution of saporins, type-1 ribosome-inactivating proteins, in soapwort (*Saponaria officinalis* L.). *Planta*, 194(4): 461-470.
6. Chen, N., Zhou, M., Dong, X., Qu, J., Gong, F., Han, Y., Qiu, Y., Wang, J., Liu, Y., Wei, Y., Xia, J., Yu, T., Zhang, X. & Zhang, L. 2020. Epidemiological and clinical characteristics of 99 cases of 2019 novel coronavirus pneumonia in Wuhan, China: a descriptive study. *Lancet* (London, England), 395(10223): 507-513.
7. Cheng, G., Gao, F., Sun, X., Bi, H. & Zhu, Y. 2016. Paris saponin VII suppresses osteosarcoma cell migration and invasion by inhibiting MMP-2/9 production via the p38 MAPK signaling pathway. *Molecular Medicine Reports*, 14(4): 3199-3205.
8. Davis, P.H. 1970. *Flora of Turkey and the east aegean islands*. Vol. 3. Edinburgh: University Press, 629 p.
9. Ebbesen, P., Dalsgaard, K. & Madsen, M. 1976. Prolonged survival of AKR mice treated with the saponin adjuvant Quil A. *Acta Pathologica et Microbiologica Scandinavica*. Section A, Pathology, 84(4): 358-360.
10. Feng, Y., Ni, L., Wan, H., Fan, L., Fei, X., Ma, Q., Gao, B., Xiang, Y., Che, J. & Li, Q. 2011. Overexpression of ACE2 produces antitumor effects via inhibition of angiogenesis and tumor cell invasion in vivo and in vitro. *Oncology Reports*, 26(5): 1157-1164.
11. Goulter, A. B., Goddard, M. J., Allen, J. C., & Clark, K. L. 2004. ACE2 gene expression is up-regulated in the human failing heart. *BMC Medicine*, 2(1), 1-7. https://doi.org/10.1186/1741-7015-2-19
12. Guo, J.W., Li, L.M., Qiu, G.Q., Deng, Z.J., Fu, Y.H., Yang, M., Pan, J.Q. & Liu, R.X. 2010. Effects of Panax notoginseng saponins on ACE2 and TNF-alpha in rats with post-myocardial infarction-ventricular remodelling. *Journal of Chinese Medicinal Materials*, 33(1): 89-92.
13. Haris Omar, S. 2010. Oleuropein in olive and its pharmacological effects. *Scientia Pharmaceutica*, 78(2): 133-154. http://www.mdpi.com/2218-0532/78/2/133
14. Hofmann, H., Geier, M., Marzi, A., Krumbiegel, M., Peipp, M., Fey, G.H., Gramberg, T. & Pöhlmann, S. 2004. Susceptibility to SARS coronavirus S protein-driven infection correlates with expression of angiotensin converting enzyme 2 and infection can be blocked by soluble receptor. *Biochemical and Biophysical Research Communications*, 319(4): 1216-1221.
15. Jia, H.P., Look, D.C., Hickey, M., Shi, L., Pewe, L., Netland, J., Farzan, M., Wohlford-Lenane, C., Perlman, S. & McCray, P.B.J. 2006. Infection of human airway

epithelia by SARS coronavirus is associated with ACE2 expression and localization. *Advances in Experimental Medicine and Biology*, 581: 479-484.

16. Jia, X., Yin, C., Lu, S., Chen, Y., Liu, Q., Bai, J. & Lu, Y. 2020. Two things about COVID-19 might need attention. https://www.preprints.org/manuscript/202002.0315/v1 (Date accessed 14 July 2020).
17. Kanwar, J.R., Kanwar, R.K., Sun, X., Punj, V., Matta, H., Morley, S.M., Parratt, A., Puri, M. & Sehgal, R. 2009. Molecular and biotechnological advances in milk proteins in relation to human health. *Current Protein & Peptide Science*, 10(4): 308-338.
18. Kell, D.B., Heyden, E.L. & Pretorius, E. 2020. The biology of lactoferrin, an iron-binding protein that can help defend against viruses and bacteria. *Frontiers in Immunology*, 11: 1221.
19. Koike, K., Jia, Z. & Nikaido, T. 1999. New triterpenoid saponins and sapogenins from Saponaria officinalis. *Journal of Natural Products*, 62(12): 1655-1659. https://doi.org/10.1021/np990311r
20. Koyuncu, M., Kiliç, C.S. & Güvenç, A. 2008. Soaproot yielding plants of East Anatolia and their potential in nature | Doğu Anadolu'da Çöven Elde Edilen Bitkiler ve Bunlarin Doğadaki Potansiyeli. *Turkish Journal of Botany*, 32(6): 489-494.
21. Li, W., Sui, J., Huang, I.C., Kuhn, J.H., Radoshitzky, S.R., Marasco, W.A., Choe, H. & Farzan, M. 2007. The S proteins of human coronavirus NL63 and severe acute respiratory syndrome coronavirus bind overlapping regions of ACE2. *Virology*, 367(2): 367-374.
22. Liang, W., Guan, W., Chen, R., Wang, W., Li, J., Xu, K., Li, C., Ai, Q., Lu, W., Liang, H., Li, S. & He, J. 2020. Cancer patients in SARS-CoV-2 infection: a nationwide analysis in China. *The Lancet Oncology*, 21(3): 335-337.
23. Livak, K.J. & Schmittgen, T.D. 2001. Analysis of relative gene expression data using real-time quantitative PCR and the 2-ΔΔCt method. *Methods*, 25. http://dx.doi.org/10.1006/meth.2001.1262
24. Mostad, H.B. & Doehl, J. 1987. Separation and characterization of oleanene-type pentacyclic triterpenes from Gypsophila arrostii by liquid chromatography-mass spectrometry. *Journal of Chromatography A*, 396: 157-168.
25. Msomi, N.Z. & Simelane, M.B.C. 2017. *Olea europaea* subsp. *africana* (Oleaceae). H.A. El-Shemy, ed., active ingredients from aromatic and medicinal plants. Rijeka: IntechOpen. https://doi.org/10.5772/65725
26. Ng, T.B., Cheung, R.C.F., Wong, J.H., Wang, Y., Ip, D.T.M., Wan, D.C.C. & Xia, J. 2015. Antiviral activities of whey proteins. *Applied Microbiology and Biotechnology*, 99(17): 6997-7008.
27. Parekh, S.L., Balakrishnan, S., Hati, S. & Aparnathi, K.D. 2017. Biofunctional properties of cultured buttermilk prepared by incorporation of fermented paneer whey. *International Journal of Current Microbiology and Applied Sciences*, 6(2): 933-945.
28. Press, J.B., Reynolds, R.C., May, R.D. & Marciani, D.J. 2000. Structure/Function relationships of immunostimulating saponins. *Studies in Natural Products Chemistry*, Vol: 24, 131-174.
29. Ruijter, J.M., Ramakers, C., Hoogaars, W.M.H., Karlen, Y., Bakker, O., van den hoff, M.J.B. & Moorman, A.F.M. 2009. Amplification efficiency: Linking baseline and bias in the analysis of quantitative PCR data. *Nucleic Acids Research*, 37(6): e45.
30. Serkedjieva, J., Manolova, N., Zgórniak-Nowosielska, I., Zawilińska, B. & Grzybek, J. 1990. Antiviral activity of the infusion (SHS-174) from flowers of *Sambucus nigra* L., aerial parts of *Hypericum perforatum* L., and roots of *Saponaria officinalis* L. against influenza and herpes simplex viruses. *Phytotherapy Research*, 4(3): 97-100. https://doi.org/10.1002/ptr.2650040305
31. Teo, A., Goh, K.K.T., Wen, J., Oey, I., Ko, S., Kwak, H.-S. & Lee, S.J. 2016. Physicochemical properties of whey protein, lactoferrin and Tween 20 stabilised nanoemulsions: Effect of temperature, pH and salt. *Food Chemistry*, 197(Pt A): 297-306.
32. Tian, S., Hu, W., Niu, L., Liu, H., Xu, H. & Xiao, S.-Y. 2020. Pulmonary pathology of early-phase 2019 novel coronavirus (COVID-19) pneumonia in to patients with lung cancer. *Journal of Thoracic Oncology*, 15(5): 700-704. https://doi.org/10.1016/j.jtho.2020.02.010
33. Wang, H. & Zhang, L. 2020. Risk of COVID-19 for patients with cancer. *The Lancet Oncology*, 21(4): e181. http://dx.doi.org/10.1016/S1470-2045(20)30149-2
34. Wang, Y., Zhou, S., Yang, F., Qi, X., Wang, X., Guan, X., Shen, C., Duma, N., Vera Aguilera, J., Chintakuntlawar, A., Price, K.A., Molina, J.R., Pagliaro, L.C., Halfdanarson, T.R., Grothey, A., Markovic, S.N., Nowakowski, G.S., Ansell, S.M. & Wang, M.L. 2019. Treatment-Related adverse events of PD-1 and PD-L1 inhibitors in clinical trials: A systematic review and meta-analysis. *JAMA Oncology*, 5(7): 1008-1019.
35. Xia, Y., Jin, R., Zhao, J., Li, W. & Shen, H. 2020. Risk of COVID-19 for patients with cancer. *The Lancet Oncology*, 21(4): e180.
36. Xu, X., Chen, P., Wang, J., Feng, J., Zhou, H., Li, X., Zhong, W. & Hao, P. 2020. Evolution of the novel coronavirus from the ongoing Wuhan outbreak and modeling of its spike protein for risk of human transmission. *Science China Life Sciences*, 63(3): 457-460. https://doi.org/10.1007/s11427-020-1637-5
37. Zhang, H., Penninger, J.M., Li, Y., Zhong, N. & Slutsky, A.S. 2020. Angiotensin-converting enzyme 2 (ACE2) as a SARS-CoV-2 receptor: molecular mechanisms and potential therapeutic target. *Intensive Care Medicine*, 46(4): 586-590. https://doi.org/10.1007/s00134-020-05985-9
38. Zhou, P., Yang, X.-L., Wang, X.-G., Hu, B., Zhang, L., Zhang, W., Si, H.-R., Zhu, Y., Li, B., Huang, C.-L., Chen, H.-D., Chen, J., Luo, Y., Guo, H., Jiang, R.-D., Liu, M.-Q., Chen, Y., Shen, X.-R., Wang, X., Zheng, X.-S., Zhao, K., Chen, Q.-J., Deng, F., Liu, L.-L., Yan, B., Zhan, F.-X., Wang, Y.-Y., Xiao, G.-F. & Shi, Z.-L. 2020. A pneumonia outbreak associated with a new coronavirus of probable bat origin. *Nature*, 579(7798): 270-273. https://doi.org/10.1038/s41586-020-2012-7
39. Zimecki, M. & Kruzel, M.L. 2007. Milk-derived proteins and peptides of potential therapeutic and nutritive value. *Journal of Experimental Therapeutics & Oncology*, 6(2): 89-106.

http://dergipark.org.tr/trkjnat
Trakya University Journal of Natural Sciences, 22(2): 163-171, 2021
ISSN 2147-0294, e-ISSN 2528-9691
DOI: 10.23902/trkjnat.884423

Research Article

THE FIRST REPORT OF GEOSMIN AND 2-METHYLISOBORNEOL PRODUCER CYANOBACTERIA FROM TURKISH FRESHWATERS

Zuhal TUNÇ*, Reyhan AKÇAALAN, Latife KÖKER, Meriç ALBAY

Istanbul University Faculty of Aquatic Sciences, Istanbul, TURKEY

Cite this article as:

Tunç Z., Akçaalan R., Köker L. & Albay M. 2021. The first report of geosmin and 2-Methylisoborneol producer Cyanobacteria from Turkish freshwaters. *Trakya Univ J Nat Sci*, 22(2): 163-171, DOI: 10.23902/trkjnat.884423

Received: 23 February 2021, Accepted: 16 June 2021, Online First: 02 August 2021, Published: 15 October 2021

Abstract: Water users consider the safety of water according to its aesthetic properties, primarily taste and odour. Geosmin (GEO) and 2-methylisoborneol (MIB) are the most common taste and odour compounds in freshwaters which cause an earthy and musty odour in water. Since human nose can detect these compounds in concentrations as low as 10 ng/L, it is essential to monitor drinking waters before consumer complaints and to produce a timely solution. Therefore, it is necessary to identify GEO and MIB producers to manage the problem at its source. Cyanobacteria are one of the main producers of these compounds in freshwater ecosystems. In this study, we analyzed 13 samples (9 cyanobacteria cultures from Bafa Lake, Elmalı Dam Lake, İznik Lake, Küçükçekmece Lake, Manyas Lake and Taşkısığı Lake, and 4 environmental water samples from Erfelek and Günpınar Waterfalls and Ömerli Dam Lake) for GEO and MIB production by HS-SPME (Head space-solid phase microextraction) coupled with GC-MS (gas chromatography-mass spectrometry). The presence of Cyanobacteria-specific *GEO* and *MIB synthase* genes were also analyzed by PCR (Polymerase Chain Reaction). Taste and odour production was confirmed in 2 samples by GC-MS while 4 samples yielded positive results by PCR. All positive samples were environmental samples (3 samples from waterfalls from Günpınar and Erfelek Waterfalls, 1 sample from Ömerli Dam Lake -a drinking water reservoir) which were dominated by *Nostoc* Vaucher ex Bornet & Flahault, *Phormidium* Kützing ex Gomont and *Pseudanabaena* Lauterborn. This is the first report of GEO and MIB producing cyanobacteria in Turkish freshwaters by combining microscopy, analytical and molecular techniques.

Özet: Su kullanıcıları, suyun güvenli olup olmadıklarına öncelikle onun tat ve kokusu gibi estetik özelliklerine bakarak karar vermektedir. Geosmin (GEO) ve 2-methylisoborneol (MIB), tatlısularda en yaygın olarak görülen tat ve koku bileşikleridir ve suyun toprak ve küf kokmasına neden olurlar. İnsanlar <10 ng/L gibi düşük konsantrasyonlarda dahi bu kokulara hassas olmalarından dolayı bu bileşiklerin içme sularında tüketici şikayetleri oluşmadan önce izlenmesi ve sorunun çözülmesi oldukça önemlidir. Bu sebeple, problemin kaynağında çözümlenebilmesi için GEO ve MIB üreticilerinin tespit edilmesi gereklidir. Tatlısu ekosistemlerinde bu bileşiklerin başlıca üreticilerinden biri siyanobakterilerdir (Cyanobacteria). Bu çalışmada 13 örnek (9 siyanobakteri kültürü, Bafa Gölü, Elmalı Baraj Gölü, İznik Gölü, Küçükçekmece Gölü, Manyas Gölü, Taşkısığı Gölü'nden ve 4 çevresel su örneği, Günpınar, Erfelek şelaleleri ve Ömerli Baraj Gölü'nden) GEO ve MIB üretiminin tespiti için HS-SPME (Tepe Boşluğu-Katı Faz Mikro Ekstraksiyon) GC-MS (Gaz Kromatografi-Kütle Spektrometresi) yöntemi kullanılarak analiz edilmiştir. Ayrıca siyanobakterilere özgü *GEO* ve *MIB sentaz* genlerinin varlığının tespiti için PZR (Polimeraz Zincir Reaksiyonu) yöntemi kullanılmıştır. İki örnekte GC-MS ile tat ve koku üretimi tespit edilmiş ve 4 örnekte de PZR ile pozitif sonuç alınmıştır. Pozitif sonuç elde edilen örnekler *Nostoc* Vaucher ex Bornet & Flahault, *Phormidium* Kützing ex Gomont ve *Pseudanabaena* Lauterborn cinslerinin baskın olduğu çevresel örneklerdir (3 şelale, 1 içme suyu kaynağı örneği). Bu çalışma Türkiye tatlısularındaki tat ve koku üreticisi siyanobakterilerin mikroskobik, analitik ve moleküler yöntemler birlikte kullanılarak tespit edildiği ilk kayıttır.

Edited by:
Tuğba Ongun Sevindik

Corresponding Author:
Zuhal Tunç
zuhal.t@istanbul.edu.tr

ORCID iDs of the authors:
ZT. orcid.org/0000-0002-6560-6789
RA. orcid.org/0000-0002-0756-8972
LK. orcid.org/0000-0002-9134-2801
MA. orcid.org/0000-0001-9726-945X

Key words:
Geosmin
2-Methylisoborneol
Taste and odour
Cyanobacteria
PCR
GC-MS

Introduction

Geosmin (GEO) and 2-methylisoborneol (MIB) are the most common biogenic taste and odour compounds in freshwaters and considered as indicators of water quality by consumers (Webber *et al.* 2015, Pham *et al.* 2020). Therefore, some countries set a guideline value as 10 ng/L in their drinking waters (Wakayama 2003, NHMRC 2011). The distribution of GEO and MIB in freshwaters varies from lakes, rivers and drinking water reservoirs

with different trophic status (Jüttner &Watson 2007) and their production have been reported so far from several countries such as Australia, China, Finland, Japan and USA (NHMRC 2011, Suurnäkki *et al.* 2015, Otten *et al.* 2016, Zhang *et al.* 2016). GEO and MIB concentration levels in drinking water sources may increase to 100-200 ng/L which are 10-20 times higher than the threshold value (Brown *et al.* 2020).

Cyanobacteria are known to be the main producers of these earthy and musty secondary metabolites in water ecosystems (Watson & Jüttner 2019). GEO and MIB are easily detected by a human in low concentrations (<10 ng/L) (Piriou *et al.* 2009). Although GEO is more common than MIB (Devi *et al.* 2020), intracellular MIB is less bound to cell and consequently can be released into water easier than GEO (Watson & Jüttner 2019). In addition, as a response to environmental factors such as light, temperature etc., MIB production mechanism responds faster in hours while GEO production mechanism response can take days (Watson *et al.* 2016, Watson & Jüttner 2019). The first challenge for monitoring and treatment studies is the estimation of GEO and MIB production time and concentration levels (Fakıoğlu *et al.* 2018). The second challenge is the presence of different producer groups in the same habitat such as Cyanobacteria, Proteobacteria, Actinobacteria and Ascomycota (Mattheis & Roberts 1992, Dickschat *et al.* 2005, Cane *et al.* 2006, Watson *et al.* 2016). To overcome this problem, PCR-based studies have started to be used since 2008, in combination with chemical analytical methods and microscopic techniques, to detect the cyanobacteria-specific *GEO* and *MIB synthase* gene (Giglio *et al.* 2008, Wang *et al.* 2011, Wang *et al.* 2016).

As one of the main producers, Cyanobacteria has a wide range of distribution in different water sources (lakes, reservoirs, rivers and marine environment) in Turkey (Akcaalan *et al.* 2009, Akcaalan *et al.* 2014a, Akcaalan *et al.* 2014b, Koker *et al.* 2017). Studies on their presence and toxin production have increased in recent years, but there is a limited number of studies on cyanobacteria-associated taste and odour problems (Albay *et al.* 2009, Demir *et al.* 2011, Fakıoğlu *et al.* 2018). In addition to this, MIB and GEO have been reporting in drinking water quality reports of İstanbul, especially in summer periods which consequently lead to costly water treatment projects based on granular activated carbon (İSKİ 2020). However, there is no report on producers of GEO and MIB in Turkish freshwaters.

In this study, Cyanobacteria from the culture collection which were isolated from different Turkish freshwaters, and environmental samples were screened for their potential to produce GEO and MIB. To manage the GEO and MIB related taste and odour problems in freshwater ecosystems, it is necessary to detect producer organisms and this is the first study to focus on the detection of taste and odour producing Cyanobacteria using both molecular and analytical methods.

Materials and Methods

Environmental Sample Collection

Environmental samples were collected from Ömerli Dam Lake and Günpınar Waterfall and Erfelek Waterfall in Turkey (Table 1). Ömerli Dam Lake sample was taken by a phytoplankton net with 20 µm pore size from epilimnion and dominant cyanobacterium was identified by microscopy (Komárek & Anagnostidis 2005, Komárek 2013). Waterfall samples were collected manually to a plastic bottle and were transported to the laboratory in cold chain. 15 ml environmental samples were centrifuged at 10,000 x g for 10 minutes and pellets were stored at -20°C until DNA extraction. 5 ml of the samples were used in cyanobacterial strain isolation which was done under the conditions reported by Rippka *et al.* (1979). Under light microscopy, a serial water dilution and trial inoculation process was applied with a sterile Pasteur pipette on the center of an agar plate. All strains were maintained under photoautotrophic growth conditions at 25°C. 1% (w/v) agar including medium BG-11 and its variant BG-11^{minus} (BG-11 with the omission of $NaNO_3$) were used for strain isolation.

Cyanobacterial Culture Conditions

Cyanobacteria cultures (different strains from *Cylindrospermopsis* G.Seenayya & N.Subba Raju, *Dolichospermum* (Ralfs ex Bornet & Flahault) P.Wacklin, L.Hoffmann & J.Komárek, *Microcystis* Lemmermann, *Nodularia* Mertens ex Bornet & Flahault, and *Sphaerospermopsis* Mertens ex Bornet & Flahault genera) were isolated from different freshwater sources and kept in our cyanobacteria culture collection (Table 1). Cultures were maintained according to Rippka *et al.* (1979) in the same conditions with environmental samples at 25°C in 150 ml liquid Medium BG-11. The isolated cyanobacteria species were mainly planktonic and a few of them were benthic species. *Oscillatoria* sp. UHCC 0332, which is a known GEO and MIB producer (in Suurnäkki *et al.* 2015 mentioned as *Planktothrix* sp. 328), was used as a positive control for GEO and MIB PCR reactions. 15 ml culture samples were centrifuged at 10,000 x g for 10 minutes and pellets were stored at -20°C until DNA extraction.

DNA Extraction

DNA extraction was done according to the modified Xanthogenate DNA extraction method (Tillett & Neilan 2000). 1 ml of fresh cell lysis solution was added to the pellets which were obtained after centrifugation of 15 ml samples. The mixture was incubated in 70°C water bath for 2 hours and vortexed every 30 minutes during the incubation process. Then, the tubes were centrifuged 10,000 x g at 4ºC for 10 minutes. Supernatants were transferred into new tubes. Phenol: Chloroform: Isoamyl alcohol solution (25:24:1) was used for nucleic acid extraction. Isopropyl alcohol (≥99%) and 1:10 volume of 3 M Sodium acetate were used for precipitation. DNA quantity and quality were checked on NanoDrop with 2000/2000c software.

Table 1. Collection information for environmental and culture samples.

No	Collection Source	Dominant Cyanobacterium	Location (City-Country)	Coordinates	Collection Date
		Environmental Samples			
1	Erfelek Waterfall	*Nostoc* sp. *Phormidium* sp.	Sinop-Turkey	41° 50′ 10″ N 34° 46′ 44″ E	2016, September
2	Günpınar Waterfall	*Nostoc* sp.	Malatya-Turkey	38° 33' 21″ N 37° 25' 23″ E	2016, April
3	Ömerli Dam Lake	*Pseudanabaena* sp.	Istanbul-Turkey	41° 3' 13" N 29° 22' 50" E	2015, July
		Culture Samples			
1	Bafa Lake	*Nodularia spumigena* IFCC-NS09 *Nodularia spumigena* IFCC-NS18	Aydın-Turkey	37° 30' 12" N 27° 26' 34" E	2011, June
2	Elmalı Dam Lake	*Microcystis aeruginosa* IFCC-MA23	İstanbul-Turkey	41° 04' 39" N 29° 07' 10" E	2010, October
3	Küçükçekmece Lake	*Microcystis aeruginosa* IFCC-MA01	İstanbul-Turkey	41° 00' 16" N 28° 44' 46" E	2005, January
4	İznik Lake	*Dolichospermum mendotae* IFCC-AM02 *Sphaerospermopsis aphanizomenoides* IFCC-AA02	Bursa-Turkey	40° 26' 48" N 29° 32' 02" E	2012, May 2004, August
5	Manyas Lake	*Microcystis aeruginosa* IFCC-MA28 *Cylindrospermopsis raciborskii* IFCC-CR01	Balıkesir-Turkey	40° 12' 08" N 27° 57' 47" E	2010, October 2005, November
6	Taşkısığı Lake	*Microcystis wesenbergii* IFCC-MW01	Sakarya-Turkey	40° 52' 16" N 30° 24' 05" E	2005, February

Table 2. PCR reaction conditions.

PCR Type	**16S**	**GEO**		**MIB**	
Primer Set	27F/ 809R	geo78F/ geo982R	288AF/ 288AR	MIB3324F/ MIB4050R	MIB-Rf/ MIB Rr
Pre-denaturation	94°C, 5 min.	94°C, 2 min.	95°C, 5 min.	94°C, 2 min.	94°C, 3 min.
Denaturation	94°C, 20 sec.	94°C, 30 sec.	95°C, 30 sec.	94°C, 30 sec.	94°C, 30 sec.
Annealing	55°C, 30 sec.	55°C, 30 sec.	55°C, 30 sec.	59°C, 30 sec.	58°C, 30 sec
Elongation **Cycle**	72°C, 60 sec. 30	72°C, 60 sec. 30	72°C, 120 sec. 55	72°C, 60 sec. 30	72°C, 60 sec. 35
Final elongation	72°C, 7 min.	72°C, 5 min.	72°C, 10 min.	72°C, 5 min.	-

PCR

PCR experiments were done according to the published information of the primer sets (Saker *et al.* 2005, Giglio *et al.* 2008, Suurnäkki *et al.* 2015, Wang *et al.* 2016) with minor modifications (Table 2) after optimization experiments. Cyanobacteria phylum specific 16S PCR reactions were done for all samples. Different cyanobacteria-specific GEO and MIB primer pairs were tested and PCR conditions were optimized with the positive control (*Oscillatoria* sp. UHCC 0332) DNA. Sterile water with no template DNA was used as the negative control. GEO and MIB PCR reactions were done under mentioned (Table 3) conditions with 16S positive environmental and culture samples. 20 µl PCR mixture was prepared which includes 2 µl (1-50 ng final) template DNA, 1 U *Taq* polymerase enzyme (Thermo Fisher) and 0.2 µM forward and reverse primers, 0.1 mM – 0.2 mM dNTP mix, 2.5 mM $MgCl_2$, 1x Taq polymerase buffer solution in final concentration with sterile distilled water. PCR products were screened with agarose gel electrophoresis (1.2%) under 60-90 volt for 30-80 min depending on the gel size.

Table 3. Primers used.

Primer	Sequences	Amplicon size	Gene	References
27F	5′-AGAGTTTGATCCTGGCTCAG-3′	782 bp	*16S rRNA*	*Saker et al.* 2005
809R	5′-GCTTCGGCACGGCTCGGGTCGATA-3′			
geo78F	5′-GCATTCCAAAGCCTGGGCTTA-3′	905 bp	*GEO Synthase*	Suurnäkki *et al.* 2015
geo982R	5′-ATCGCATGTGCCACTCGTGAC-3′			
288AF	5′-AACGACCTGTTCTCCTA-3′	288 bp	*GEO Synthase*	Giglio *et al.* 2008
288AR	5′-GCTCGATCTCATGTGCC-3′			
MIB3324F	5′-CATTACCGAGCGATTCAACGAGC-3′	726 bp	*MIB Synthase*	Suurnäkki *et al.* 2015
MIB4050R	5′-CCGCAATCTGTAGCACCATGTTGA-3′			
MIB-Rf	5′-CGACAGCTTCTACAYCYCCATGAC-3′	202 bp	*MIB Synthase*	Wang *et al.* 2016
MIB-Rr	5′-CGCCGCAATCTGTAGCACCAT-3′			

Sequence Analysis

Sequence analysis was performed for positive GEO and MIB PCR products which were sequenced by 2-direction Sanger sequencing technique of MedSanTek (Turkey). Sequences were deposited in GenBank with Accession numbers between MK124613 - MK124616. BLASTn (Basic Local Alignment Search Tool) was used to determine the most similar cyanobacteria-specific GEO and MIB synthase nucleotide sequences to our PCR products (Altschul *et al.* 1990).

HS-SPME Coupled GC-MS

GEO and MIB quantification methods were applied with GEO (Dr. Ehrenstorfer XA14005000ME) and MIB commercial standards (Dr. Ehrenstorfer XA15088400ME). Analysis was done in GC (Perkin Elmer Clarus 680) - MS (Clarus SQ 8T) equipped with a column of Elite-5ms using TurboMass software according to the method published by Kaloudis *et al.* (2017). 10 ml samples were taken from 3rd week old cultures and stored in a freezer (-80°C) until extraction. Günpınar Waterfall and Ömerli Dam Lake water samples were also stored at -80°C. To perform HS-SPME extraction, 10 ml samples were transferred to 20 ml vials which included 3.5 gr NaCl (Merck 1.06404.1000 99) and closed with a crimper. Extraction was done at 500 rpm, 55°C for 30 minutes with SPME fiber (Supelco 57348-U). After the extraction, the manual injection was performed at 250°C for 15 minutes. GC oven temperature initiation was 60°C and it reached 260°C (15°C/min). Helium was used as mobile phase (1 ml/min). Quantification was done in Selected Ion Recording (SIR) mode specific for GEO and MIB.

Results

To screen presence or potential GEO and MIB-based taste and odour problems and also to detect taste and odour producer Cyanobacteria species in different type of samples (monoalgal culture samples, drinking water reservoir sample and waterfall samples) was aimed in the present study. MIB-based taste and odour problem was found in Ömerli Dam Lake while GEO production was found in Günpınar Waterfall together with a potential of Erfelek Waterfall. *Pseudanabaena* sp., *Nostoc* sp. and *Phormidium* sp. were the dominant Cyanobacteria species in environmental samples (Fig. 1). *Oscillatoria* sp. UHCC 0332 (Fig. 1a) is a known GEO and MIB producer cyanobacterium and it was used as the positive control sample in PCR and GC-MS analysis.

Cyanobacteria specific *GEO* and *MIB synthase* genes were selected for PCR analysis to detect the potential GEO and MIB producer cyanobacteria in the samples. Sequence analysis of PCR products was performed to find the closest nucleotide homologs of our products. To reveal whether taste and odour compounds were synthesized or not, GC-MS analysis was performed. The summary of the results is given in Table 4.

PCR Amplification of GEO and MIB Synthase Genes

Primarily, the presence of cyanobacteria in environmental samples were determined. Cyanobacteria specific 16S rRNA PCR was conducted and 16S rRNA positive DNA samples with 782 bp PCR product were used in further GEO and MIB specific PCR analysis (Fig. 2).

MIB and GEO PCR optimization studies were done under different annealing temperatures. Relatively shorter target region-specific primers were also tested in the samples. Target regions were successfully amplified in environmental samples. *GEO synthase* gene was detected in Erfelek and Günpınar Waterfall samples, *MIB synthase* gene was detected in Ömerli Dam Lake sample and culture samples were negative for both GEO and MIB PCR (Table 4)

Sequence Analysis Results

The resulting PCR products were Sanger sequenced and aligned by BLAST. The closest homolog of GEO amplicon from Günpınar Waterfall sample (Sequence ID: MK124615) was *Nostoc* sp. C057 *GEO synthase* (Sequence ID: CP040281) with a good similarity percentage of 91%. Two different GEO amplicons were sequenced from Erfelek Waterfall sample (Sequence ID: MK124614 and Sequence ID: MK124616). The closest homologs of our sequences were *Nostoc* sp. C057 *GEO synthase* (Sequence ID: CP040281) with similarity percentage 85.96% and *Oscillatoria* sp. 372/2 *GEO*

synthase (Sequence ID: KJ658373) with similarity percentage 93.17%. The closest homolog of MIB amplicon from Ömerli Dam Lake (Sequence ID: MK124613) was *Pseudanabaena limnetica* str. Castaic Lake *MIB synthase* (Sequence ID: HQ630883.1) with a perfect similarity percentage of 99%.

Quantification of GEO and MIB by HS-SPME Coupled GC-MS

GEO and MIB commercial standards were prepared and injected in Total Ion Chromatogram (TIC) mode of the mass spectrum to create a specific GC method (Fig. 3). Retention times were found 8.58 for MIB and 11.25 for GEO, qualifier ions m/z values were 95 and 112, respectively. Dilution series of these standards were injected after HS-SPME extraction and quantification of these compounds in the samples were done according to the calibration curves of these standards ($R^2 \geq 0.99$ for each compound).

GEO was detected in Günpınar Waterfall sample while MIB was detected in Ömerli Dam Lake sample (Table 4). GEO production could not be analyzed in Erfelek Waterfall sample because of the unavailability of the strain isolation and limited water sample volume. However, earthy/musty odour was easily confirmed by sensory analysis.

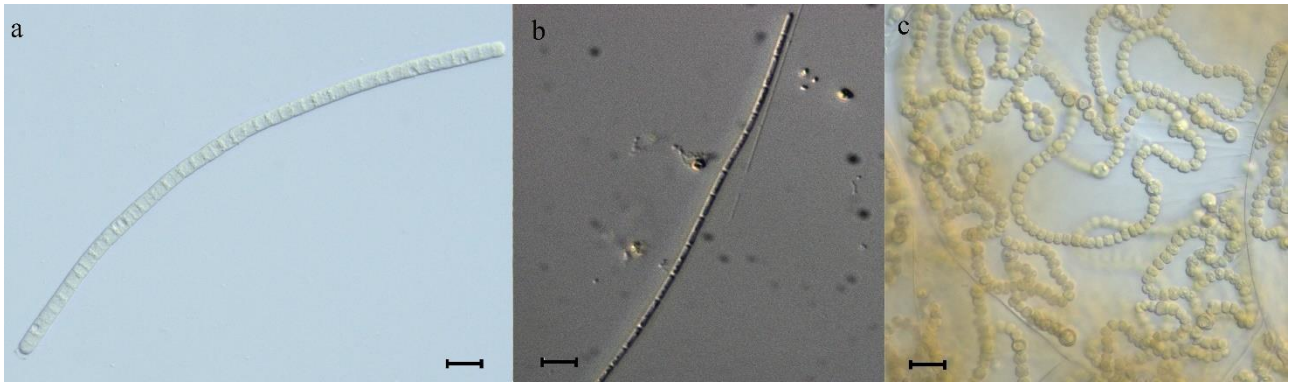

Fig. 1. Microscopy images of potential MIB and GEO producer species detected in the study. **a.** *Oscillatoria* sp. UHCC 0332; **b.** *Pseudanabaena* sp. from Ömerli Dam Lake; **c.** *Nostoc* sp. from Günpınar Waterfall. (Scale bar = 20μm)

Table 4. The species revealed by microscopic observations with their corresponding sources, PCR and GC-MS results and accession numbers from sequencing (nd: not detected, na: not analyzed).

No	Source	Microscopy	PCR		GC-MS		Sequencing
		Cyanobacterium	GEO (+/-)	MIB (+/-)	GEO (ng/L)	MIB (ng/L)	Accession no (GenBank)
1	Erfelek Waterfall	*Nostoc* sp.	+	-	na	na	MK124614
2	Erfelek Waterfall	*Phormidium* sp.	+	-	na	na	MK124616
3	Günpınar Waterfall	*Nostoc* sp.	+	-	323	nd	MK124615
4	Ömerli Dam Lake	*Pseudanabaena* sp.	-	+	nd	21	MK124613
		Culture Samples					
1	Bafa Lake	*Nodularia spumigena* IFCC-NS09	-	-	nd	nd	-
2	Bafa Lake	*Nodularia spumigena* IFCC-NS18	-	-	nd	nd	-
3	Elmalı Dam Lake	*Microcystis aeruginosa* IFCC-MA23	-	-	nd	nd	-
4	Küçükçekmece Lake	*Microcystis aeruginosa* IFCC-MA01	-	-	nd	nd	-
5	İznik Lake	*Dolichospermum mendotae* IFCC-AM02	-	-	nd	nd	-
6	İznik Lake	*Sphaerospermopsis aphanizomenoides* IFCC-AA02	-	-	nd	nd	-
7	Manyas Lake	*Microcystis aeruginosa* IFCC-MA28	-	-	nd	nd	-
8	Manyas Lake	*Cylindrospermopsis raciborskii* IFCC-CR01	-	-	nd	nd	-
9	Taşkısığı Lake	*Microcystis wesenbergii* IFCC-MW01	-	-	nd	nd	-

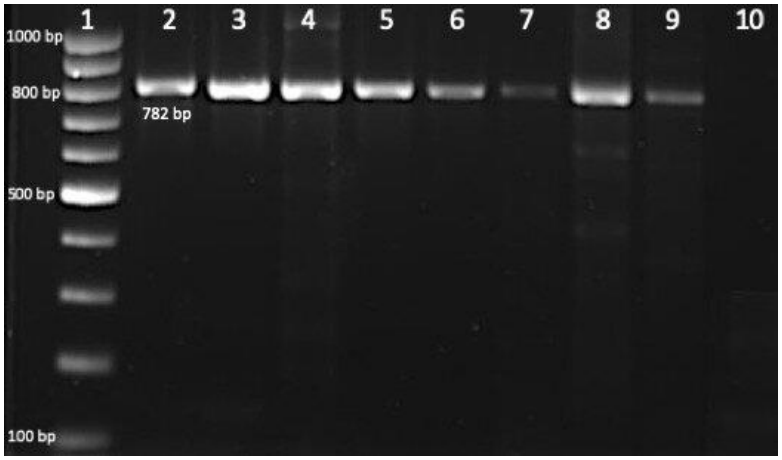

Fig. 2. Cyanobacteria specific 16S rRNA gene amplified from some samples. 1: 100bp size marker (Grisp, Portugal), 2: positive control (UHCC 0332), 3: IFCC-MA01, 4: IFCC-NS18, 5: IFCC-AA02, 6: IFCC-AM02, 7: Günpinar Waterfall, 8-9: Erfelek Waterfall (*Phormidium* sp. and *Nostoc* sp. dominant, respectively), 10: negative control.

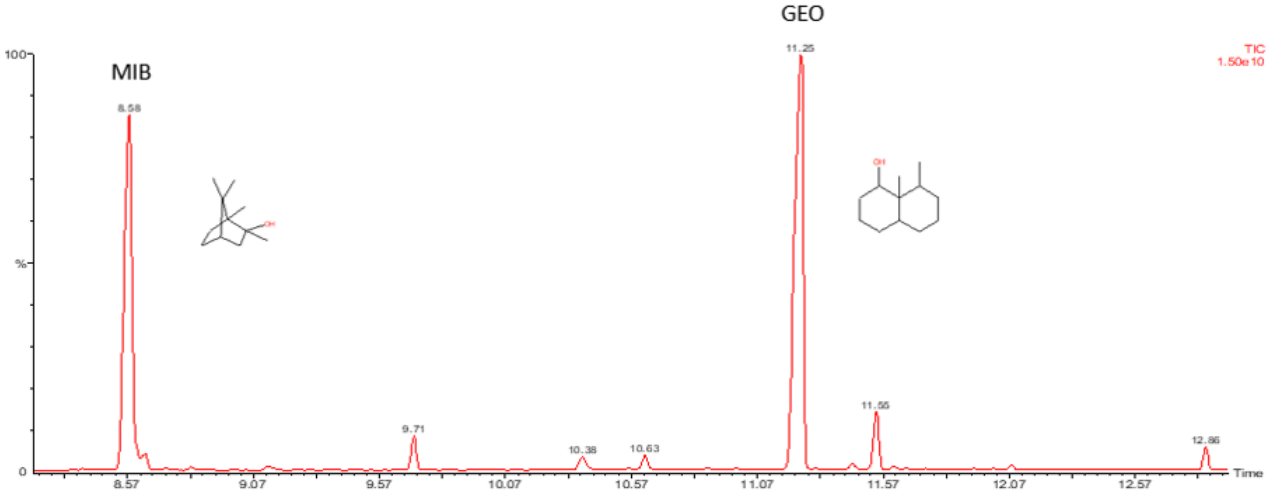

Fig. 3. Total ion chromatogram (TIC) of MIB and GEO mixed standard.

Discussion

Cyanobacteria are the source of many interesting volatile odour compounds (VOCs) in aquatic environments. Some of these VOCs smell "good" like fruit, violet or magnolia while the rest of them smells "bad" like earth, must, septic, garlic, tobacco, fish or cabbage (Lee *et al.* 2017). In addition to their odour causing roles in water, these VOCs could serve to enhance the tolerance of producer in harsh conditions, create allelopathic effects on other algae and aquatic macrophytes, and protect the organism against predators (Zuo 2019). GEO and MIB are two VOCs with earthy and musty odour produced by cyanobacteria. They have no known effects on human health, there are limited studies on the role of these compounds in the aquatic environments and the results are contradictory or the effective concentrations (g/L) are far above common environmental concentrations (Watson 2003). Although their ecological impacts are not yet fully understood, they are the most commonly reported taste and odour compounds in aquatic environments (Devi *et al.* 2020). The genes which encode the key biosynthetic enzymes which are essential for GEO and MIB production in cyanobacteria have recently been reported (Giglio *et al.* 2008, Giglio *et al.* 2011). The nucleotide information is a powerful tool not just to detect GEO and MIB producer Cyanobacteria but also to investigate the effect of environmental parameters on VOCs production at the gene expression level.

In this study, diverse cyanobacteria species in laboratory cultures and environmental samples were screened for the presence of GEO and MIB biosynthetic genes to uncover the responsible producers in aquatic ecosystems. GEO and MIB concentration levels were also quantified to confirm the results of molecular analysis. GEO and MIB biosynthetic genes were successfully amplified in environmental samples. The results were also confirmed with the GC-MS (Table 4). A well-known MIB producer *Pseudanabaena* sp. was found in an important drinking water reservoir, Ömerli Dam Lake sample (Fig. 1b) and sequence analysis of MIB PCR amplicon from this sample has high similarity with the same genus *MIB synthase* sequence (99%). *Pseudanabaena* species are the

main reason for MIB episodes in many countries such as China, Japan, South Korea and USA (Izaguirre & Taylor 1998, Niiyama *et al.* 2016, Zhang *et al.* 2016, Chong *et al.* 2018). However, this is the first MIB producer Cyanobacteria report for Turkey where *Pseudanabaena* species have a wide distribution in freshwaters including lakes, rivers and thermal waters (Fakıoğlu *et al.* 2011, Taşkın *et al.* 2019). MIB production level was found relatively high (21 ng/L) which is above the human odour threshold concentration (<10 ng/L) and also above the drinking water standard limit levels (10 ng/L) according to Australia and Japan guidelines (Wakayama 2003, NHMRC 2011). In the same operational guideline of Australia, it was suggested to increase the sampling period to every 2 days if >10 ng/L GEO/MIB levels are detected at treatment plant inlet and to introduce powdered activated carbon dosing if the same levels are detected at treatment plant outlet. To detect this threshold values is necessary to use appropriate treatment methods in water, and using PCR-based detection tools together with microscopy-based identification would be beneficial to reveal the main sources of the GEO and MIB. MIB producer *Pseudoanabaena* was detected in one sample from Ömerli Dam Lake. Some other toxic Cyanobacteria species (*Aphanizomenon flosaquae* Ralfs ex Bornet & Flahault, *Cuspidothrix issatschenkoi* (Usachev) P.Rajaniemi, Komárek, R.Willame, P. Hrouzek, K.Kastovská, L.Hoffmann & K.Sivonen and *Microcystis aeruginosa* (Kützing) Kützing) were also reported in the lake (Koker *et al.* 2017). Since the lake has a mesotrophic character, the possibility to have cyanobacteria blooms is possible in the following years with a potential of MIB and cyanotoxin production. Although MIB and other VOCs could not demonstrate the presence of toxic cyanobacteria, nevertheless it could be an early warning system about the problems in an aquatic ecosystem.

Other well-known VOC producers, *Nostoc* sp. and *Phormidium* sp., were also identified in Günpınar and Erfelek Waterfall samples (Fig. 1c). *Nostoc* spp. and *Phormidium* spp. are common sources of taste and odour problems which were reported in many countries such as Australia, Canada, Finland, Japan, Serbia and USA (Sugiura *et al.* 1998, Izaguirre & Taylor 2004, Kutovaya & Watson 2014, Milovanović *et al.* 2015, Suurnäkki *et al.* 2015). *Nostoc* and *Phormidium* species were also detected in some important drinking water sources in Turkey (Fakıoğlu *et al.* 2011, Koker *et al.* 2017). Sequence analysis of GEO PCR amplicons from the samples have good similarities with *Nostoc* sp. and *Oscillatoria* sp. *GEO synthase genes* (between 85-93%). Furthermore, GEO level was found much higher than human threshold limits (321 ng/L) in *Nostoc* sp. colonies taken from Günpınar Waterfall sample. Unfortunately, due to its limited amount, GC-MS analysis could not be performed in Erfelek samples. The results from Waterfall samples are the first taste and odour reports for these areas and further detailed studies are important to understand the drivers for the proliferation and odour production of these cyanobacteria.

In waterfall samples, 288AF/288AR primers amplified the targeted region while 78F/982R primers did not. The lack of universal *GEO synthase* primers was considered the main reason for this result. *GEO synthase* gene sequences were found more diverse to design a universal primer in comparison to *MIB synthase* region and challenges for *GEO primer* design has been reported recently (Devi *et al.* 2020). Therefore, limited sequence data to target a more diverse sequence region may have caused the primer-template DNA mismatches as in previous studies (Kutovaya & Watson 2014, Otten *et al.* 2016).

In contrast with the environmental samples, interestingly, isolates of cyanobacteria from Turkish freshwaters are neither capable of producing GEO or MIB nor have a production potential (Table 4). *Dolichospermum, Sphaerospermopsis, Cylindrospermopsis* and *Nodularia* were investigated genera in this study which were already reported as GEO or MIB producer in previous studies (Popin *et al.* 2016, Watson *et al.* 2016, Zhang *et al.* 2017, Pham *et al.* 2020). Also, *Microcystis* strains were investigated with the knowledge of other coccoid cyanobacteria such as *Synechococcus* C.Nägeli or *Coelosphaerium* Nägeli as a producer (Kutovaya & Watson 2014, Godo *et al.* 2017). On the other hand, the results are limited with the investigated strains and VOC production may vary from one strain to another (Watson *et al.* 2016). Further studies should be done also to investigate other VOCs from these genera such as Dimethyl trisulfide (DMTS), β-Cyclocitral, 2,4,7-Decatrienal, 6-Methyl-5-hepten-2-one which cause septic, tobacco, fish or fruit-like odours, respectively, in aquatic environments (Lee 2017).

In this study, GEO positive samples were dominated by benthic filamentous cyanobacteria while MIB positive sample was dominated by planktonic filamentous cyanobacteria. This is the first report of GEO and MIB producing cyanobacteria in Turkish freshwaters which was determined by molecular and analytical methods, identified by microscopy and bioinformatics tools. However, more study should be done for confirmation of gene expression status of these cyanobacteria.

Acknowledgement

The authors are grateful to Ayça Oğuz (Istanbul University, Turkey) for microscopy images. We thank Cüneyt Nadir Solak (Dumlupınar University, Turkey) and Fatma Çevik (Çukurova University, Turkey) for waterfall samples. We thank Suvi Suurnäkki & Kaarina Sivonen (Helsinki University, Finland) for their generous gift *Oscillatoria* sp. UHCC 0332 as a positive control sample for our work. Also, we would like to acknowledge the European Cooperation in Science and Technology, COST Action CA18225 'WaterTOP' for adding value to this study through networking and knowledge sharing with European researchers.

Ethics Committee Approval: Since the article does not contain any studies with human or animal subject, its approval to the ethics committee was not required.

Author Contributions: Concept: Z.T., R.A., Desing: Z.T., R.A., Execution: Z.T, Material supplying: Z.T., R.A., Data acquisition: Z.T., R.A., Data analysis/interpretation: Z.T., R.A., L.K., Writing: Z.T., R.A., L.K., M.A., Critical review: R.A., L.K., M.A.

Conflict of Interest: The authors have no conflicts of interest to declare.

Funding: The study was supported by the Research Fund of Istanbul University (Project Number: FYL-2016-20569).

References

1. Akcaalan, R., Köker, L., Gürevin, C. & Albay, M. 2014a. *Planktothrix rubescens:* a perennial presence and toxicity in Lake Sapanca. *Turkish Journal of Botany*, 38(4): 782-789.
2. Akcaalan, R., Köker, L., Oğuz, A., Spoof, L., Meriluoto, J. & Albay, M. 2014b. First report of cylindrospermopsin production by two cyanobacteria (*Dolichospermum mendotae* and *Chrysosporum ovalisporum*) in Lake Iznik, Turkey. *Toxins (Basel)*, 6(11): 3173-3186.
3. Akcaalan, R., Mazur-Marzec, H., Zalewska, A. & Albay, M. 2009. Phenotypic and toxicological characterization of toxic *Nodularia spumigena* from a freshwater lake in Turkey. *Harmful Algae*, 8(2): 273-278.
4. Albay, M., Yüksel, Ş., Özel, A.H., Gürevin, C., Oğuz, B. & Akçaalan, R. 2009. Environmental factors affecting geosmin and 2-methylisoborneol production in Sapanca Lake, Türkiye. *Phycologia*, 48: 2.
5. Altschul, S.F., Gish, W., Miller, W., Myers, E. & Lipman, D. 1990. Basic local alignment search tool. *Journal of Molecular Biology*, 215(3): 403-410.
6. Brown, J., Nyfennegger, J., Ang, Y., Simpson, M., MacLeod, B., Wolanin, O. & Gilmore, K. 2020. Biological pretreatment: An innovative approach to addressing taste and odor. *AWWA Water Science*, 2(2): e1173.
7. Cane, D.E., He, X., Kobayashi, S., Omura, S. & Ikeda, H. 2006. Geosmin biosynthesis in *Streptomyces avermitilis* molecular cloning, expression and mechanistic study of the germacradienol/geosmin synthase. *The Journal of Antibiotics (Tokyo)*, 59(8): 471-479.
8. Chong, S., Lee, H. & An, K.G. 2018. Predicting taste and odor compounds in a shallow reservoir using a three–dimensional hydrodynamic ecological model. *Water*, 10(10): 1396.
9. Demir, N., Pulatsu, S., Kirkagac, M.U., Topcu, A., Zencir, O. & Fakıoglu, O. 2011. Phytoplankton composition considering the odor occurrence in the Porsuk River (Eskisehir-Turkey). *Asian Journal of Chemistry*, 23(1): 247-250.
10. Devi, A., Chiu, Y.T., Hsueh, H.T. & Lin, T.F. 2020. Quantitative PCR based detection system for cyanobacterial geosmin/2-methylisoborneol (2-MIB) events in drinking water sources: Current status and challenges. *Water Research*, 188: 116478.
11. Dickschat, J.S., Bode, H.B., Mahmud, T., Müller, R. & Schulz, S. 2005. A novel type of geosmin biosynthesis in myxobacteria. *The Journal of Organic Chemistry*, 70(13): 5174-5182.
12. Fakıoğlu, Ö., Atamanalp, M. & Demir, N. 2011. Toxic blue-green algae in dam lakes. *Ankara University Journal of Environmental Sciences*, 3(2): 65-71.
13. Fakıoğlu, M., Karpuzcu, M.E. & Öztürk, İ. 2018. Evaluation of algae related taste and odor problem in drinking water. *Pamukkale University Journal of Engineering Sciences*, 24(6): 1141-1156.
14. Giglio, S., Jiang, J., Saint, C.P., Cane, D. & Monis, P.T. 2008. Isolation and characterization of the gene associated with geosmin production in cyanobacteria. *Environmental* Science & Technology, 42(21): 8027-8032.
15. Giglio, S., Saint, C.P. & Monis, P.T. 2011. Expression of the geosmin synthase gene in the cyanobacterium *Anabaena circinalis* AWQC318. *Journal of Phycology*, 47(6): 1338-1343.
16. Godo, T., Saki, Y., Nojiri, Y., Tsujitani, M., Sugahara, S., Hayashi, S., Kamiya, H., Ohtani, S. & Seike, Y. 2017. Geosmin-producing species of *Coelosphaerium* (Synechococcales, Cyanobacteria) in Lake Shinji, Japan. *Scientific Reports*, 7(1): 1-10.
17. İSKİ (İstanbul Water and Sewerage Administration) 2020. Istanbul Water Quality Reports http://www.iski.gov.tr/ (Date accessed: 10.08.2020).
18. Izaguirre, G. & Taylor, W.D. 1998. A *Pseudanabaena* species from Castaic Lake, California, that produces 2-methylisoborneol. *Water Research*, 32(5): 1673-1677.
19. Izaguirre, G. & Taylor W.D. 2004. A guide to geosmin- and mib-producing cyanobacteria in the United States. *Water Science & Technology*, 49(9): 19-24.
20. Jüttner, F. & Watson, S.B. 2007. Biochemical and ecological control of geosmin and 2-methylisoborneol in source waters. *Applied and Environmental Microbiology*, 73(14): 4395-4406.
21. Kaloudis, T., Triantis, T.M. & Hiskia, A. 2017. Determination of geosmin and 2-methylisoborneol in water by HS-SPME-GC/MS, 469-474. In: Meriluoto, J., Spoof, L & Codd, G.A. (eds). *Handbook of Cyanobacterial Monitoring and Cyanotoxin Analysis*. John Wiley & Sons, Chichester, 576 pp.
22. Koker, L., Akcaalan, R., Oguz, A., Gaygusuz, O., Gurevin, C., Akat Kose, C., Gucver, S., Karaaslan, Y., Erturk, A., Albay, M. & Kinaci, C. 2017. Distribution of toxic cyanobacteria and cyanotoxins in Turkish waterbodies. *Journal of Environmental Protection and Ecology*, 18(2): 425-432.
23. Komárek, J. 2013. *Cyanoprokaryota: 3rd Part Heterocytous Genera*. Springer-Verlag, Berlin/Heidelberg, 1130 pp.
24. Komárek, J. & Anagnostidis, K. 2005. *Cyanoprokaryota: 2nd Part Oscillatoriales*. Elsevier Spektrum Akademischer Verlag, München, 759 pp.

25. Kutovaya, O.A. & Watson, S.B. 2014. Development and application of a molecular assay to detect and monitor geosmin-producing cyanobacteria and actinomycetes in the Great Lakes. *Journal of Great Lakes Research*, 40(2): 404-414.

26. Lee, J., Rai, P.K., Jeon, Y.J., Kim, K.H. & Kwon, E.E. 2017. The role of algae and cyanobacteria in the production and release of odorants in water. *Environmental Pollution*, 227: 252-262.

27. Mattheis, J.P. & Roberts, R.G. 1992. Identification of geosmin as a volatile metabolite of *Penicillium expansum*. *Applied and Environmental Microbiology*, 58(9): 3170-3172.

28. Milovanović, I., Mišan, A., Simeunović, J., Kovač, D., Jambrec, D. & Mandić, A. 2015. Determination of volatile organic compounds in selected strains of cyanobacteria. *Journal of Chemistry*, 2015. http://dx.doi.org/10.1155/2015/969542

29. NHMRC, NRMMC 2011. Australian Drinking Water Guidelines. National Water Quality Management Strategy. National Health and Medical Research Council, National Resource Management Ministerial Council, Commonwealth of Australia, Canberra. https://www.nhmrc.gov.au/file/16934/download?token=gAKh3uQk (Date accessed: 12.12.2020).

30. Niiyama, Y., Tuji, A., Takemoto, K. & Ichise, S. 2016. *Pseudanabaena foetida* sp. nov. and *P. subfoetida* sp. nov. (Cyanophyta/Cyanobacteria) producing 2-methylisoborneol from Japan. *Fottea Olomouc*, 16(1):1-11.

31. Otten, T.G., Graham, J.L., Harris, T.D. & Dreher, T.W. 2016. Elucidation of taste-and odor-producing bacteria and toxigenic cyanobacteria in a midwestern drinking water supply reservoir by shotgun metagenomic analysis. *Applied and Environmental Microbiology*, 82(17): 5410-5420.

32. Pham, T. L., Bui, M.H., Driscoll, M., Shimizu, K., & Motoo, U. 2020. First report of geosmin and 2-methylisoborneol (2-MIB) in *Dolichospermum* and *Oscillatoria* from Vietnam. *Limnology*, 22(1): 43-56.

33. Piriou, P., Devesa, R., De Lalande, M. & Glucina, K. 2009. European reassessment of MIB and geosmin perception in drinking water. *Journal of Water Supply: Research and Technology—AQUA*, 58(8), 532-538.

34. Popin, R.V., Rigonato,. J, Abreu, V.A.C., Andreote, A.P.D., Silveira, S.B., Odebrecht, C. & Fiore, M.F. 2016. Draft genome assembly of the bloom-forming cyanobacterium *Nodularia spumigena* strain CENA596 in shrimp production ponds. *Genome Announcements*, 4(3): e00466-16.

35. Rippka, R., Deruelles, J., Waterbury, J.B., Herdman, M. & Stanier, R.Y. 1979. Generic assignments, strain histories and properties of pure cultures of cyanobacteria. *The Journal of General Microbiology*, 111(1): 1-61.

36. Saker, M.L., Jungblut, A.-D., Neilan, B.A., Rawn, D.F.K. & Vasconcelos, V.M. 2005. Detection of microcystin synthetase genes in health food supplements containing the freshwater cyanobacterium *Aphanizomenon flos-aquae*. *Toxicon*, 46(5): 555-562.

37. Sugiura, N., Iwami, N. & Inamori, Y. 1998. Significance of attached cyanobacteria relevant to the occurrence of musty odor in Lake Kasumigaura. *Water Research*, 32(12): 3549-3554.

38. Suurnäkki, S., Gomez-Saez, G.V., Rantala-Ylinen, A., Jokela, J., Fewer, D. & Sivonen, K. 2015. Identification of geosmin and 2-methylisoborneol in cyanobacteria and molecular detection methods for the producers of these compounds. *Water Research*, 68: 56-66.

39. Taşkın E., Akbulut A., Yıldız A., Şahin B., Şen B., Uzunöz C., Solak C.N., Başdemir D., Çevik F., Sönmez F., Açikgöz İ., Pabuçcu K., Öztürk M., Alp M.T., Albay M., Çakır M., Özbay Ö., Can Ö., Akçaalan Albay R., Atıcı T., Koray T., Özer T., Karan T., Aktan Turan Y. & Tunç Zengin Z. 2019. *A Checklist Of The Flora Of Turkey (Algae)*. Ali Nihat Gökyiğit Vakfı, İstanbul, 804 pp.

40. Tillett, D. & Neilan, B.A. 2000. Xanthogenate nucleic acid ısolation from cultured and environmental cyanobacteria. *Journal of Phycology*, 36(1): 251-258.

41. Wakayama, H. 2003. Revision of Drinking Water Quality Standards in Japan, Ministry of Health Labour and Welfare, Japan. http://www.nilim.go.jp/lab/bcg/siryou/tnn/tnn0264pdf/ks0264011.pdf (Date accessed: 12.12.2020).

42. Wang, Z., Xu, Y., Shao, J., Wang, J. & Li, R. 2011. Genes associated with 2-methylisoborneol biosynthesis in cyanobacteria: isolation, characterization, and expression in response to light. *PLoS One*, 6(4): e18665.

43. Wang, Z., Song, G., Shao, J., Tan, W., Li, Y. & Li, R. 2016. Establishment and field applications of real-time PCR methods for the quantification of potential mib-producing cyanobacteria in aquatic systems. *Journal of Applied Phycology*, 28: 325-333.

44. Watson, S.B. 2003. Cyanobacterial and eukaryotic algal odour compounds: signals or by-products? A review of their biological activity. *Phycologia*, 42(4): 332-350.

45. Watson, S.B., Monis, P., Baker, P. & Giglio, S. 2016. Biochemistry and genetics of taste- and odor-producing cyanobacteria. *Harmful Algae*, 54: 112-127.

46. Watson, S.B. & Jüttner, F. 2019. Biological production of taste and odour compounds, taste and odour in source and drinking water: causes, controls, and consequences, 63-112. In: Lin, T.F., Watson, S., Dietrich, A.M. & Suffet, I.H. (eds). *Taste and Odour ln Source and Drinking Water: Causes, Controls, and Consequences*. IWA Publishing, London, 322 pp.

47. Webber, M.A., Atherton, P. & Newcombe, G. 2015. Taste and odour and public perceptions: what do our customers really think about their drinking water? *Journal of Water Supply: Research and Technology-Aqua*, 64(7): 802-811.

48. Zhang, T., Zheng, L., Li, L. & Song, L. 2016. 2-methylisoborneol production characteristics of *Pseudanabaena* sp. FACHB 1277 isolated from Xionghe Reservoir, China. *Journal of Applied Phycology*, 28: 3353-3362.

49. Zhang, J., Li, L., Qiu, L., Wang, X., Meng, X., You, Y., Yu, J. & Ma, W. 2017. Effects of climate change on 2-methylisoborneol production in two cyanobacterial species. *Water*, 9(11): 859.

50. Zuo, Z. 2019. Why algae release volatile organic compounds-the emission and roles. *Frontiers in Microbiology*, 10: 491.

http://dergipark.org.tr/trkjnat
Trakya University Journal of Natural Sciences, 22(2): 173-177, 2021
ISSN 2147-0294, e-ISSN 2528-9691
DOI: 10.23902/trkjnat.901480

Research Article

In vitro CYTOTOXIC EFFECTS OF SOME COVID-19 DRUGS ON LUNG CANCER CELLS

Ahmet KARAKUS[1*], Sevgi UNAL KARAKUS[2], Fatma USTA[2], Umit HERDEM[2], Sude AKSU[2], Fatma OZDEMIR[2], Mehri CUKURCAK[2], Ecem CITAKOGLU[2]

[1] Bartın University, Faculty of Science, Department of Biotechnology, 74100, Bartın, TURKEY
[2] Bartın University, Faculty of Science, Department of Molecular Biology and Genetics, 74100, Bartın, TURKEY

Cite this article as:

Karakus A., Karakus S.U., Usta F., Herdem U., Aksu S., Ozdemir F., Cukurcak M. & Citakoglu E. 2021. *In vitro* cytotoxic effects of some Covid-19 drugs on lung cancer cells. *Trakya Univ J Nat Sci*, 22(2): 173-177, DOI: 10.23902/trkjnat.901480

Received: 23 March 2021, Accepted: 05 July 2021, Online First: 02 August 2021, Published: 15 October 2021

Edited by:
Belgin Süsleyici

****Corresponding Author:***
Ahmet Karakuş
akarakus@bartin.edu.tr

ORCID iDs of the authors:
AK. orcid.org/0000-0003-1458-808X
SUK. orcid.org/0000-0002-6409-7783
FU. orcid.org/0000-0002-5583-3785
UH. orcid.org/0000-0002-4059-8284
SA. orcid.org/0000-0001-7958-7737
FO. orcid.org/0000-0002-7978-3700
MC. orcid.org/0000-0001-8224-9392
EC. orcid.org/0000-0001-5145-0560

Key words:
COVID-19 drugs
Lung cancer
Anticancer effect
Cytotoxicity
MTT

Abstract: Cancer, which is the second most common cause of death after cardiovascular diseases, is one of the most important health problems of today. Discovery of effective treatments and drugs are important in cancer treatment. The COVID-19 epidemic, which broke out in Wuhan province of China in December 2019 and is considered as a pandemic worldwide, affected millions of people. The SARS-CoV-2 virus, which causes this epidemic, affects the lungs, heart, brain, kidneys, gastrointestinal system, ovaries and testicles and various drugs are used in the treatment. In this study, we aimed to determine the cytotoxic effect of favipiravir, dornase alfa and ivermectin, which are drugs used in the treatment of COVID-19, on human lung cancer cell line (A549). Favipiravir, dornase alfa and ivermectin concentrations were prepared in doubly increasing doses (0.5-64 µg/mL). The prepared concentrations were tested on human A549 cells. After 24 hours of incubation, the cytotoxic effects of the drugs on cancer cells were detected by the MTT (3-(4,5-dimethylthiazol-2-yl)-diphenyl tetrazolium bromide) method. The results were given as % viability. It was determined that favipiravir, dornase alfa and ivermectin significantly decreased the cell viability in lung cancer cell line with increasing application doses ($p<0.05$).

Özet: Kalp damar hastalıklarından sonra ikinci ölüm nedeni olan kanser, günümüzün en önemli sağlık sorunlarından biridir. Etkili tedavilerin ve yeni ilaçların keşfedilmesi kanser tedavisinde önem arz etmektedir. Aralık 2019'da Çin'in Wuhan eyaletinde patlak veren ve dünya çapında bir salgın olarak kabul edilen COVID-19 salgını milyonlarca insanı etkilemektedir. Bu salgına neden olan SARS-CoV-2 virüsü başta akciğerleri olmak üzere kalbi, beyni, böbrekleri, gastrointestinal sistemi, yumurtalık ve testisleri etkilemekte ve tedavisinde çeşitli ilaçlar kullanılmaktadır. Bu çalışmada, COVID-19 tedavisinde kullanılan ilaçlar olan favipiravir, dornaz alfa ve ivermektinin insan akciğer kanseri hücre hattı (A549) üzerindeki sitotoksik etkisinin belirlenmesi amaçlanmıştır. Çalışmada favipiravir, dornaz alfa ve ivermektin ilaçlarının konsantrasyonları iki kat artan dozlarda (0,5-64 µg/mL) hazırlandı. Hazırlanan konsantrasyonlar, insan A549 hücreleri üzerine uygulandı. 24 saatlik inkübasyondan sonra, ilaçların hücre hatları üzerindeki sitotoksik etkileri, MTT (3-(4,5-dimetiltiyazol-2-il)-difenil tetrazolyum bromür) yöntemi ile tespit edildi. Sonuçlar % canlılık olarak verildi. Artan doza bağlı olarak favipiravir, dornaz alfa ve ivermektinin akciğer kanseri hücre dizisinde hücre canlılığını önemli ölçüde azalttığı belirlendi ($p<0.05$).

Introduction

Cancer is a health problem that forms a group of diseases characterized by uncontrolled division and proliferation of cells in an organ or tissue followed by metastasis to other parts of the body (Jackson & Loeb 2001) and manifested by disruption of molecular pathways (Sivanandam *et al.* 2010, Varkaris *et al.* 2014). The complexity of molecular pathways involved in the process of carcinogenesis is one of the most important factors that makes cancer treatment difficult and slows down the development of molecular targeted therapy. In this context, it is very important to analyze the developmental stages of the cancer process properly and to apply the correct treatment for patients to regain their health.

Unfortunately, there is no definitive treatment method for cancer. In addition to classical treatment methods such as radiotherapy, chemotherapy and surgery in cancer treatment, additional targeted applications (healthy nutrition, regular physical activity, avoidance of stress and targeted therapies) are important for the success of

treatments (Huang *et al*. 2010, Nettore *et al.* 2018, Serda *et al.* 2018). Considering the complex process of cancer and different physiological characteristics of patients, the discovery of more effective drugs in cancer treatment constitute a very important research area.

The COVID-19 epidemic, which appeared in Wuhan province of China in December 2019 and was admited a global pandemic in March 2020, is considered a global threat to public health. COVID-19 patients are either asymptomatic or have the disease with clinical course ranging from mild to severe pneumonia, respiratory failure and sometimes death. In addition to comprehensive public health preventions to deal with this disease, an unprecedented global effort is under way to identify effective drugs for treatment. As a result of understanding the virology of SARS-CoV-2, current and effective pharmacological treatments against COVID-19 are being researched (Potì *et al.* 2020). Favipiravir, dornase alfa and ivermectin are among the potential therapeutic agents used in the treatment of COVID-19.

Favipiravir is an antiviral drug approved in Japan (Joshi *et al.* 2021). Favipiravir triphosphate is a purine analog that is a competitive inhibitor of RNA-dependent RNA polymerase (Coomes & Haghbayan 2020). It has been used in many countries to treat new viral infections, including Ebola and Lassa. As an antiviral drug, Favipravir is authorized for use in the treatment of COVID-19 in many countries, including Japan, Russia and India, under emergency provisions (Nagakrishna & Thawani 2020).

Dornase alfa, known as the recombinant form of the human DNase I enzyme, is a drug that has been used for years to reduce the severity of infections in respiratory diseases and improve lung function in patients with cystic fibrosis. It is well known that pneumonia related with COVID-19 progresses to severe acute respiratory syndrome and even multiple organ failure. The highly viscous mucus structure observed in cystic fibrosis was reported to be very similar to that in COVID-19 (Okur *et al.* 2020). Dornase alfa was found to exert anti-viral effect against coronavirus in Madin-Darbybovine kidney cell line (MDBK) and green monkey kidney cell line (Vero) without cytotoxicity on healthy peripheral blood mononuclear cells (Okur *et al.* 2020).

The potential of ivermectin to reduce transmission of mosquito-induced malaria is being evaluated by various studies worldwide. Ivermectin is reported to inhibit the *in vitro* replication of some positive, single-stranded RNA viruses, such as Zika virus, yellow fever virus, dengue virus (DNV) etc. Recently, ivermectin has been reported to strongly inhibit the replication of SARS-CoV-2 virus *in vitro* (Chaccour *et al.* 2020).

This study was carried out to have a preunderstanding for how can be affected lung cells *in vitro* when a person both COVID-19 and lung cancer if use these drugs, also to determine the cytotoxic effects of favipiravir, dornase alfa and ivermectin on A549 cells. Moreover, since lack of information about cytotoxic effects of COVID-19 drugs on lung cancer cells in literature, this study was performed. However, experimental studies and analyses in this study should be supported with clinical applications and in vivo experiments.

Materials and Methods

Cell lines and culture conditions

The study was carried out at Bartın University Central Research Laboratory, Anticancer Research Laboratory. A549 cell line (ATCC) was used as the cell type in the study. Dulbecco's Modified Eagle Medium (DMEM) (Sigma-Aldrich, USA; prepared by adding 10% Fetal Bovine Serum (FBS), 0.1 mg/mL streptomycin and 100 U/mL penicillin) was used to feed A549 cells. Cells were cultured in 75 cm^2 culture flasks (TPP; Switzerland) and the cultures were incubated in a humidified incubator (37°C, 5% CO_2; N-biotech, Korea). The medium was changed every 3-4 days and the cell passages were made when the cells reached 80-90% confluence.

Test drugs

0.5, 1, 2, 4, 8, 16, 32 and 64 µg/mL concentrations of favipiravir (Santa Cruz Inc.), dornase alfa (Genentech) and ivermectin (Santa Cruz Inc.) were prepared in DMEM (for A549 cells).

MTT assay

The effects of favipiravir, dornase alfa and ivermectin on A549 cell viability were determined by the MTT (3-(4,5-dimethylthiazol-2-yl)-diphenyl tetrazolium bromide) method. Confluent cells were scraped from the bottom of the flasks with Trypsin-EDTA and then counted under the microscope. The cells were seeded in the 96-well plates at a density of 15×10^3 cells per well. The seeded cells were incubated at 37°C in an incubator with CO_2 for 24 h. The media were changed following the incubation, different concentrations of favipiravir, dornase alfa and ivermectin were added to the wells in which the cells were seeded, and the incubation was done for 24 h (Koran *et al.* 2017). Subsequently, the media in the wells were withdrawn, then MTT solution (0.5 mg/mL) prepared in sterile Phosphate-Buffered Saline (PBS) was added to each well, and the plates were incubated for 3 h. Subsequently, the solution in the wells was withdrawn and incubation was stopped by adding 100 µL dimethyl sulfoxide to each well. Optical densities of the cells in microplates were determined by a spectrophotometer (Thermo, Multiscango) at 570 nm wavelength (Mosmann 1983).

The average of the absorbance values of the control wells was calculated and these values were determined as 100% cell viability. Percentages of viability values of cells were determined by proportioning the absorbance values obtained from the wells treated with favipiravir, dornase alfa and ivermectin to the control absorbance value. MTT assays were done 10 times on different days, with double repeats for each plate. According to the MTT assay results, the half maximal inhibitory concentration value (IC_{50}) was calculated using GraphPad Prism 9 (San Diego, CA, USA).

Statistical analysis

GraphPad Prism 9 package program for Windows was used in statistical analyses. One-way ANOVA was used to detect differences among the groups and multiple comparisons were analyzed with Tukey's test. Quantitative data were given as the mean with standard deviation (mean±SD) and $p<0.05$ was indicated as statistically significant.

Results

The cytotoxic effects of favipiravir and dornase alfa drugs on human lung cancer cell line (A549) are shown in Fig. 1 and Fig. 2, respectively. A decrease in cell viability was determined for favipiravir at concentrations of 2 µg/mL and above (2-64 µg/mL) and for dornase alfa at all concentrations (0-64 µg/mL), compared to the control group. These decreases in cell viability were statistically significant ($p<0.05$).

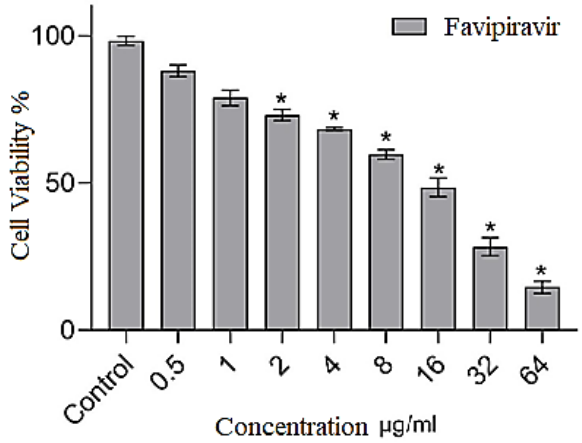

Fig. 1. % Change in viability of A549 human lung cancer cells treated with different concentrations of favipiravir for 24 hours. The data obtained are shown as mean ± SD. *p<0.05 vs control group (There are 15×10^3 cells in each well of 96 microplates).

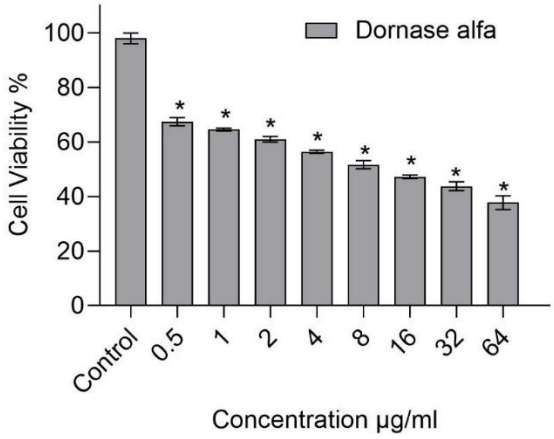

Fig. 2. % Change in viability of A549 human lung cancer cells treated with different concentrations of dornase alfa for 24 hours. The data obtained are shown as mean ± SD. *p<0.05 vs control group (There are 15×10^3 cells in each well of 96 microplates).

The effects of the ivermectin on cell viability of A549 human lung cancer cell line are shown in Fig. 3. Although a significant dose dependent decrease in viability of A549 cells treated with ivermectin was detected at concentrations of 0.5-4 µg/mL compared to control, cell viability remained almost constant between 4-64 µg/mL concentrations.

We also detected the IC_{50} values of the drugs used. While IC_{50} values of favipiravir and dornasa alfa were calculated almost close to each other, IC_{50} value of ivermectin was relatively lower than favipiravir and dornase alfa (Table 1).

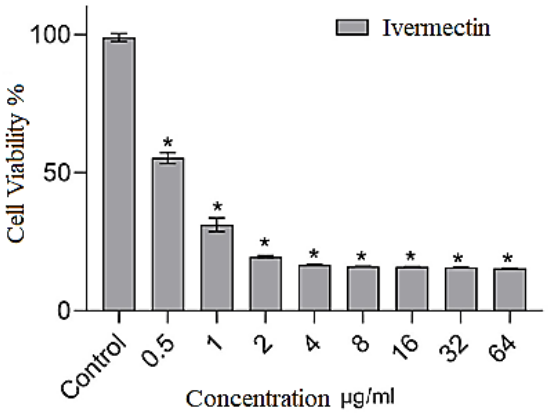

Fig. 3. % Change in viability of A549 human lung cancer cells treated with different concentrations of ivermectin for 24 hours. The data obtained are shown as mean ± SD. *p<0.05 vs control group (There are 15×10^3 cells in each well of 96 microplates).

Table 1. IC_{50} (µg/mL) values of favipiravir, dornase alfa and ivermectin calculated for A549 human lung cancer cells.

	Favipiravir	**Dornase alfa**	**Ivermectin**
Cell	IC_{50} (µg/mL)	IC_{50} (µg/mL)	IC_{50} (µg/mL)
A549	12.55	12.13	0.306

Discussion

Studies reported that various anti-diabetic, antipsychotic, anti-malarial and antiviral drugs have antineoplastic properties against lung, prostate, colorectal, gastric, breast and overian tumors (Kaushik *et al.* 2021). In preclinical studies, it was determined that these non-neoplastic drugs trigger apoptosis by various intracellular signaling mechanisms, stop cell proliferation and exert anti-metastatic effects. Some anti-neoplastic drugs give positive results for cancer in clinical studies (Kaushik *et al.* 2020). Because of these features, it is important to define new therapeutic agents and to determine their biological activities in cancer research.

Ivermectin is a broad-spectrum antiparasitic drug (Khan *et al.* 2020) and has been reported as an anticancer agent in some cancer types due to its potential to inhibit tumor growth (Sharmeen *et al.* 2010, Melotti *et al.* 2014). Ivermectin was reported to have an anti-proliferative effect on esophageal squamous cell carcinoma (ESCC)

cells. Ivermectin also significantly inhibits ESCC cell growth, migration and invasion by blocking PAK1 signaling (Chen *et al.* 2020). We showed that ivermectin decreased A549 cell viability. However, the molecular mechanism of this effect can be elucidated by further studies.

In another study, the cytotoxic effect of ivermectin on human stomach cancer cell lines (MKN1, MKN7, MKN28, MKN45, MKN74, SH-10-TC, NUGC-3, NUGC-4, AGS, GSU and KE-39, RIKEN) was investigated for 48 hours and among the cell lines tested, it was shown that MKN1 cells were the most sensitive to ivermectin and SH-10-TC cells were also drug sensitive. In contrast, MKN7 cells and MKN28 cells were resistant to ivermectin. Therefore, MKN1 and SH-10-TC cells are defined as ivermectin sensitive and MKN7 and MKN28 cells as ivermectin resistant cells (Nambara *et al.* 2017). In our study, A549 cells did not show resistance to the test drugs we used.

Additionally, ivermectin has been reported to induce cell death in human leukemia cells (OCI-AML2, HL60, U937, KG1a) through chloride influx, membrane hyperpolarization, and increased intracellular ROS levels (Sharmeen *et al.* 2010).

As a result, we investigated, for the first time, the cytotoxic effects of favipiravir, ivermectin and dornase alfa, which are drugs used in the treatment of COVID-19, on human lung cancer cells (A549). In our study, we detected for the first time that favipiravir, dornase alfa and ivermectin decreased cell viability by showing cytotoxic effects in human lung cancer cell line. The IC_{50} values on A549 cells were 12.55, 12.13 and 0.306 µg/mL for favipiravir, dornase alfa and ivermectin, respecitevely.

In conclusion, favipiravir, dornase alfa and ivermectin can be considered to be important therapeutic agents due to their potential cytotoxic effects on A549 cells *in vitro*. With further studies, it can be revealed how these drugs affect molecular mechanisms in cancer cells and its use in cancer treatment can be investigated with *in vivo* and clinical studies.

Ethics Committee Approval: Since the article does not contain any studies with human or animal subject, its approval to the ethics committee was not required.

Author Contributions: Concept: S.U.K., A.K., F.U., U.H., S.A., F.O., M.C., E.C., Desing: A.K., Execution: S.U.K., A.K., Material supplying: S.U.K., Data acquisition: F.U., U.H., S.A., F.O., M.C., E.C., Data analysis/interpretation: A.K., Writing: A.K., Critical review: S.U.K.

Conflict of Interest: The authors have no conflicts of interest to declare.

Funding: This study was supported by the Ministry of Industry and Technology, The Scientific and Technological Research Council of Turkey (TÜBİTAK), 2209-A - Research Project Support Programme for Undergraduate Students. Grant Numbers: 1919B012001203, 1919B012001217, 1919B012001262.

References

1. Chaccour, C., Hammann, F., Ramón-García, S. & Rabinovich, N.R. 2020. Ivermectin and COVID-19: keeping rigor in times of urgency. *American Journal of Tropical Medicine and Hygiene*, 102(6): 1156.
2. Chen, L., Bi, S., Wei, Q., Zhao, Z., Wang, C. & Xie, S. 2020. Ivermectin suppresses tumour growth and metastasis through degradation of PAK1 in oesophageal squamous cell carcinoma. *Journal of Cellular and Molecular Medicine*, 24(9): 5387-5401.
3. Coomes, E.A. & Haghbayan, H. 2020. Favipiravir, an antiviral for COVID-19? *Journal of Antimicrobial Chemotherapy*, (75)7: 2013-2014.
4. Huang, W.Y. Cai, Y.Z. & Zhang, Y. 2010. Natural phenolic compounds from medicinal herbs and dietary plants: potential use for cancer prevention. *Nutrition and Cancer*, 62(1): 1-20.
5. Jackson, AL. & Loeb, L.A. 2001. The contribution of endogenous sources of DNA damage to the multiple mutations in cancer. *Mutation Research*, 477: 7-21.
6. Joshi, S., Parkar, J., Ansari, A., Vora, A., Talwar, D., Tiwaskar, M., Patil, S. & Barkate, H. 2021. Role of favipiravir in the treatment of COVID-19. International Journal of Infectious Diseases, 102: 501-508.
7. Kaushik, I., Ramachandran, S., Prasad, S. & Srivastava, S.K. 2020. Drug rechanneling: a novel paradigm for cancer treatment. *Seminars in Cancer Biology*, 68: 279-290.
8. Khan, M.S.I., Khan, M.S.I., Debnath, C.R., Nath, P.N., Al Mahtab, M., Nabeka, H., Matsuda, S. & Akbar, S.M.F. 2020. Ivermectin Treatment May Improve the Prognosis of Patients with COVID-19. *Archivos de Bronconeumologia*, 56(12): 828.
9. Koran, K., Tekin, Ç., Çalışkan, E., Tekin, S., Sandal, S. & Görgülü, A.O. 2017. Synthesis, structural and thermal characterizations and *in vitro* cytotoxic activities of new cyclotriphosphazene derivatives. *Phosphorus, Sulfur, and Silicon and the Related Element*s, 192: 1002-1011.
10. Melotti, A., Mas, C., Kuciak, M., Lorente-Trigos, A., Borges, I. & Ruiz i Altaba, A. 2014. The river blindness drug Ivermectin and related macrocyclic lactones inhibit WNT-TCF pathway responses in human cancer. *EMBO Molecular Medicine*, 6: 1263-1278.
11. Mosmann, T. 1983. Rapid colorimetric assay for cellular growth and survival: application to proliferation and cytotoxicity assays. *Journal of Immunological Methods*, 65: 55-63.
12. Nagakrishna, L. & Thawanı, V. 2020. Favipiravir in COVID-19. *The Antiseptic*, 117: 16-17.
13. Nambara, S., Masuda, T., Nishio, M., Kuramitsu, S., Tobo, T., Ogawa, Y., Hu, Q., Iguchi, T., Kuroda, Y., Ito, S., Eguchi, H., Sugimachi, K., Saeki, H., Oki, E., Maehara, Y. & Suzuki, A. & Mimori, K. 2017. Antitumor effects of the antiparasitic agent ivermectin via inhibition of Yes-

associated protein 1 expression in gastric cancer. *Oncotarget*, 8(64): 107666-107677.

14. Nettore, I.C., Colao, A. & Macchia, P.E. 2018. Nutritional and Environmental Factors in Thyroid Carcinogenesis. *International Journal of Environmental Research and Public Health*, 15(8): 1735.

15. Okur, H.K., Yalcin, K., Tastan, C., Demir, S., Yurtsever, B., Karakus, G.S., Kancagi, D.D., Abanuz, S., Seyis, U., Zengin, R., Hemsinlioglu, C., Kara, M., Yildiz, M.E., Deliceo, E., Birgen, N., Pelit, N.B., Cuhadaroglu, C., Kocagoz, A.S. & Ovali, E. 2020. Preliminary report of *in vitro* and *in vivo* effectiveness of dornase alfa on SARS-CoV-2 infection. *New Microbes and New Infections*, 37: 100756.

16. Potì, F., Pozzoli, C., Adami, M., Poli, E. & Costa, L.G. 2020. Treatments for COVID-19: emerging drugs against the coronavirus. *Acta Bio Medica Atenei Parmensis*, 91(2): 118.

17. Serda, I.F.B.C., van Roekel, E. & Lynch, B.M. 2018. The Role of Physical Activity in Managing Fatigue in Cancer Survivors. *Current Nutrition Reports*, 7(3): 59-69.

18. Sharmeen, S., Skrtic, M., Sukhai, M.A., Hurren, R., Gronda, M. & Wang X. 2010. The antiparasitic agent ivermectin induces chloride-dependent membrane hyperpolarization and cell death in leukemia cells. *Blood*, 116(18): 3593-3603.

19. Sivanandam, A., Murthy, S., Kim, S.H., Barrack, E.R. & Veer Reddy GP. 2010. Role of androgen receptor in prostate cancer cell cycle regulation: interaction with cell cycle regulatory proteins and enzymes of DNA synthesis. *Current Protein & Peptide Science*, 11: 451-458.

20. Varkaris, A., Katsiampoura, A.D., Araujo, J.C., Gallick, G.E. & Corn, P.G. 2014. Src signaling pathways in prostate cancer. *Cancer and Metastasis Reviews*, 33: 595-606.

http://dergipark.org.tr/trkjnat
Trakya University Journal of Natural Sciences, 22(2): 179-185, 2021
ISSN 2147-0294, e-ISSN 2528-9691
DOI: 10.23902/trkjnat.903661

Research Article

A NEW *Suaeda* RECORD FOR FLORA OF TURKEY: *Suaeda aegyptiaca* (Hasselquist) Zohary (CHENOPODIACEAE/AMARANTHACEAE)

İsa BAŞKÖSE*, Ahmet Emre YAPRAK

Ankara University, Faculty of Science, Department of Biology, 06100 Ankara, TURKEY

Cite this article as:

Başköse İ. & Yaprak A.E. 2021. A new *Suaeda* record for flora of Turkey: *Suaeda aegyptiaca* (Hasselquist) Zohary (Chenopodiaceae/Amaranthaceae). *Trakya Univ J Nat Sci*, 22(2): 179-185, DOI: 10.23902/trkjnat.903661

Received: 26 March 2021, Accepted: 09 July 2021, Online First: 07 August 2021, Published: 15 October 2021

Edited by:
Mykyta Peregrym

***Corresponding Author:**
İsa Başköse
isabaskose@gmail.com

ORCID iDs of the authors:
İB. orcid.org/0000-0001-7347-3464
AEY. orcid.org/0000-0001-6464-2641

Key words:
Suaedoideae
Seepweeds and Sea-blites
Şanlıurfa/Akçakale
Turkey

Abstract: In this study, *Suaeda aegyptiaca* (Hasselquist) Zohary is reported as a new record for Turkish flora from Akçakale district in Şanlıurfa province. The species is classified under section *Salsina* Moq. of the genus *Suaeda* Forssk. ex J.F. Gmel. in *Suaedoideae* subfamily. The comprehensive description, distribution maps in Turkey, habitat features, morphological characteristics and digital images of the species are given.

Özet: Bu çalışmada, Şanlıurfa ili Akçakale ilçesinden *Suaeda aegyptiaca* (Hasselquist) Zohary türü Türkiye florası için yeni kayıt olarak verilmektedir. Tür, *Suaedoideae* altfamilyası, *Suaeda* Forssk. ex J.F. Gmel. cinsi *Salsina* Moq. seksiyonu altında sınıflandırılmıştır. Türün kapsamlı betimi, Türkiye'deki dağılış haritası, habitat özellikleri, morfolojik karakterleri ve fotoğrafları verilmiştir.

Introduction

Suaeda Forssk. ex J.F. Gmelin (Chenopodiaceae Vent./Amaranthaceae Juss.; Suaedoideae) is a halophytic genus and is represented by about 100 species worldwide (Ferren & Schenk 2003, Brandt *et al.* 2015). The genus has a cosmopolite distribution and the majority of taxa are spread in saline and alkaline soils.

The genus is taxonomically represented by two subgenera as *Brezia* (Moq.) Freitag & Schütze and *Suaeda* and eight sections are associated with them (Schütze *et al.* 2003). Different researchers conducted systematic (Schütze *et al.* 2003, Kapralov *et al.* 2006, Brandt *et al.* 2015) and taxonomic studies (Schenk & Ferren 2001, Lomonosova & Freitag 2011, Freitag & Lomonosova 2017) at tribus, genus and sectional levels, primarily within the *Suaedoideae* subfamily. Three new species were described in the last two decades (Lomonosova & Freitag 2003, Alonso *et al.* 2004, Noguez-Hernández *et al.* 2013).

In Turkey, the first study on the genus was conducted by Aellen (1967) and a total of seven species were reported in the second volume of "Flora of Turkey". Then, *Suaeda linifolia* Pallas was added in the tenth volume (Davis *et al.* 1988) and *S. splendens* (Pourret) Gren. & Godron was recorded in the eleventh volume by Freitag (2000) making the total number of species nine (Yaprak 2012).

Suaeda aegyptiaca (Hasselquist) Zohary was firstly evaluated under the name of *Chenopodium aegyptiacum* Hasselquist in 1757 and was used with that name until mid-20th century. However, in the study conducted by Zohary in 1957, *Chenopodium aegyptiacum* was transferred from the genus *Chenopodium* L. to the genus *Suaeda* and republished under the name *Suaeda aegyptiaca* (Zohary 1957).

The species is distributed in three continents and in a total of 23 countries, which are in Mediterranean (Cyprus), north Africa (Tunisia, Libya, and Egypt), northeast Africa (Sudan, Eritrea, Ethiopia, Djibouti, and Somalia) central and southwest Asia (Afghanistan, Pakistan, Iran, Iraq, Israel, Lebanon, Syria, and Jordan) and Arabian Peninsula (Saudi Arabia, Yemen, Oman, United Arab Emirates, and Kuwait) (Powo 2021, Wikipedia 2021). The species is also present in South Australia as naturalized. The distribution of *S. aegyptiaca* in Turkey remained unknown until this study.

The aim of this study is to give the record of *S. aegyptiaca*, a new species of the genus, from Şanlıurfa and give some informations about the species.

Materials and Methods

The material of the study comprises the plant samples collected during the fieldwork conducted between the years 2018 and 2019. The samples were pressed and dried, as required by common herbarium rules. The samples were identified using the volumes of "Flora of Turkey" (Aellen 1967, Davis *et al.* 1988, Güner *et al.* 2000) and

the flora of neighboring countries and the relevant literature (Zohary 1966, Tackholm 1974, Meikle 1985, Hedge 1997, Freitag 2013). In addition, digital photographs of the samples associated with the species in international herbaria [BM, BRY, C, E, DES, HGB, P, S, U, WAG (acronyms according to Thiers 2021)] were examined and compared with the specimens. The identified specimens were deposited in the herbarium collection of Ankara University, Faculty of Science, Department of Biology (Herbarium-ANK).

Digital measurements of all morphological characteristics of the specimens were taken using the BAB stereo binocular microscope and the BAB image processing and analysis system (Bs200Pro) using both the dry samples and the samples fixed in 70% Ethanol solution.

Results

Taxonomic Treatment

Suaeda aegyptiaca (Hasselq.) Zohary

≡ *Chenopodium aegyptiacum* Hasselq., Iter Palaest. 460 (1757).

≡ *Schanginia aegyptiaca* (Hasselq.) Aellen in K.H. Rechinger, Fl. Lowland Iraq 195 (1964).

= *Suaeda baccata* Forssk. ex J.F. Gmel., Syst. Nat. ed. 13: 503 (1791).

Type : Alexandria, Fl. Aeg. Arab. p. LXIV N186 p. 69 Cent. III N15 hodie *Suaeda baccata*, September 1761, P. Forsskl 164 (holotype C, photo!).

= *Schanginia baccata* (Forssk. ex J.F. Gmel.) Moq., Chenop. Monogr. Enum. 119 (1840).

= *Suaeda hortensis* Forssk. ex J.F. Gmel., Syst. Nat. ed. 13, 2(1): 503 (1791).

Syntype: Taizz, Fl. Aeg. Arab. p. LXV N188 p. 71 Cent. III N21 hodie *Suaeda hortensis*, 1763, P. Forsskl 145 (C and S, photo!).

= *Schanginia hortensis* (Forssk. ex J.F. Gmel.) Moq. Chenop. Monogr. Enum. 119 (1840).

Plant annual and herbaceous, in early period light green, in late period dark green, glabrous. **Stem** up to 100 cm high, erect, ascending, or rarely decumbent, much and repeatedly branched, branches erect or ascending, the lower often spreading, terete or delicately striate; in young condition pale green throughout, later turning whitish to cream-colored; stem and all branches woody in fruiting time. **Leaves** 7.0-35.0 x 1.5-3.5 mm, succulent, linear or oblong, kidney-shaped in cross section, margin entire, apex obtuse, sessile or at base attenuate into a short petiole, the lower straight, the upper arcuate, ascending to spreading. **Inflorescences** leafy, shorter or longer spike-like, loose or dense, in apical parts often flexuose, axillar and glomerate; **glomerules** 1-30 flowered, 0.5-1.0 cm diameter, alternate arrangement, inserted on very short axillary branchlets, sometimes fused for a very short distance with the petiole of the leaves. Bracts and bracteoles present. **Bracts** 1, 1.0-1.7 x 0.5-1.0 mm, ovate, ovate-deltoid or deltoid, membranous, margin entire or lacerate, apex acute or acuminate, equal or longer than bracteoles. **Bracteoles** 2, 0.6-1.5 x 0.3-0.8 mm, ovate or ovate-deltoid, membranous, united with each other at the base, apex acute or acuminate, margin lacerate. **Flowers** hermaphrodite, 1.8-5.0 x 2.0-5.5 mm, fig-shaped, sessile or rarely with a very short pedicel. **Perianth** segments 5, segments 0.8-2.7 x 0.8-2.2 mm, succulent, united up to 1/2 or 2/3 the length, obovate or oblong, incurved, green with hyaline margin. **Stamens** 5 to numerous, 0.7-2.0 mm, inserted on a disc above the middle of the ovary; **staminode** absent; **anthers** yellow, 4-thecous, 0.45-1.0 x 0.30-0.75 mm, oblong, united to 1/2, open up longitudinally; **filaments** 0.40-1.80 x 0.08-0.30 mm, in the early period short and after anthesis elongating. **Pistil** 1, 2-3 carpellary, 1-lolcular, 2.20-4.50 mm; **stigmas** 2-3, 0.80-1.75 mm long, filiform, with long papillate, light brown; **style** 0.55-1.30 mm long, terete or partly conical, membranous; **ovary** inferior, 0.75-2.0 x 0.5-2.0 mm, obconical, brown. **Fruits** up to 5 mm long, fig-shaped, partly or completely spongy. **Seeds** vertical, 0.8-1.5 x 0.6-1.1 mm, slightly flattened; testa black or reddish, lustrous, with reticulate surface.

Type: [Egypt] "Alexandria rudera prope maris Mediterranei litus" (according to Freitag 1989, it is probably lost).

Material: TURKEY: C7 Şanlıurfa province, Akçakale district**,** Akçakale-Ceylanpınar road, ŞUSKİ waste water treatment facility, on the road of Öncül village, approximately 1-1.5 km, irrigation channel, road and field edges**,** 344 m. a.s.l, 22.09.2018, 28.10.2018, 20.07.2019, N 36° 42′ 52.14″ - E 38° 58′ 48.37″ E, coll. İ. Başköse 4435, 4456, 4746 (ANK!).

Proposed Turkish name: *Suaeda* is called in Turkish **"Cirimotu"**. We propose **"Mısır cirimotu"** as a vernacular name for *S. aegyptiaca*.

Phenology: Flowering period in July; fruiting period September-October.

Habitat: In Turkey, the species is distributed in salty soils, near to irrigation and drainage channels, road or field sides at approximately 350 m. a.s.l. together with species such as *Polygonum equisetiforme* Sibth. & Sm., *Kochia scoparia* (L.) Schrad, *Chenopodium album* L. subsp. *album* L. var. *album*, *Tamarix smyrnensis* Bunge, *Alhagi pseudalhagi* (Bieb.) Desv., *Conyza canadensis* (L.) Cronquist, *Xanthium strumarium* L. subsp. *strumarium* and *Phragmites australis* (Cav.) Trin. ex Steudel.

Additional specimens examined: EGYPT: Alexandria, Fl. Aeg. Arab. p. LXIV N186 p. 69 Cent. III N15 hodie *Suaeda baccata*, September 1761, P. Forsskl 164 (holotype of *Suaeda baccata*, C10003145, photo!); Taizz, Fl. Aeg. Arab. p. LXV N188 p. 71 Cent. III N21 hodie *Suaeda hortensis*, 1763, P. Forsskl 145 (syntype of *Suaeda hortensis*, C-10003147, photo!); Cairo, Fl. Aeg. Arab. p. LXV N188 p. 71 Cent. III N21 hodie *Suaeda hortensis*, 1762, P. Forsskl 165 and 189, (syntype of *Suaeda hortensis*, C-10003148 and C-10003149, photos!); P. Forsskl s.n., (*Suaeda baccata*, BM-000069939, photo!); P. Forsskl s.n., (*Schanginia hortensis*, S-04/1003, photo!); (Sinai) in valle Hebran Arabiae petraeae, 9 July 1835, G.H.W Schimper-438,

(HBG-503718 and HBG-503718, photos!); Aegyptus, pr. Alexandria, Schimper, Georg Heinrich Wilhelm, s.n. (*Suaeda baccata*, COI-00052160, photo!); N. Sinai, El 'Arish, 27 km W of El 'Arish, Sand dunes and wet saline among the dunes, 17 July 1971, A. Danin, (DES-00021272, U-1059959 photos!). **ISRAEL:** North District, Kinneret, Upper Jordan Valley: 1 km. S. of Argaman, 301 m a.s.l, 13 September 1982, M. Zohary, WGS84, (DES-00026372, photo!); Eilath, Eastern outskirts of the town near the Red Sea coast, 2 April 1970, K.U. Kramer-4572, (U-1059960, photo!). **JORDAN:** Judaische Wüste in halophyten-fluren am westl. Nordufer des Toten Meres ca. 300 m a.s.l unter NN., 17 May 1980, B. Nowak, (B-100480074, photo!); Madaba. östl. Totes Meer, Wadi Mujib., 09 April 1989, C. Bayer, (B-100191808 and B-100191815, photos!). **KUWAIT:** Kuwait, As Sulaybiyah, 15 March 2013, 29° 19′ 10″ N, 47° 51′ 40″ E, M. Abdullah MTA346, MTA349 and MTA352 (E-00678509, E-00678529, E00684254, photos!). **SAUDI ARABIA:** Al-Abard, Abha City, Asir. Saudi Arabia Kingdom, 2380 m a.s.l, 11 August 1998, 18° 32′ 38N - 42° 25′ 12E, T. Miyazaki No. 990811AB23 (E-00614671, photo!). **UNITED ARAB EMIRATES:** Prope Dscheddam in littore maris rubri, Schimper 1837 no. 867, (HBG506283, photo!); Ayn al Faidah area, in coastal area and Al Ais area, Salty, sandy soil, s.l. to 200 m a.s.l, December 1989, M. Jongbloed, BYU2 (BRYV-0213632, photo!). **YEMEN:** SE de Yithab, Wadi Najar, Hadramaout, 1000 m, 19 January 1978, T. Monod 17312, (P-00601497, photo!); Sud Yemen: Ju'aimah, NNE de Shiban, Wadi, Hadramaout, 3 January 1978, T. Monod 16905, (P-P00601498, photo!). **SOMALIA:** Cote française des Somalies, Cote mer Rouge, April 1956, E. Chedeville 1633 (P-P04941770, photo!). **ETHIOPIA:** Hararghe prov., Ogaden, Gode, narrow patch of riverine forest along the Webbe Shibeli River, 300 m a.s.l., 1 December 1969, about 6° 00′ N, 43° 30′ E, De Wilde no: 5968, (WAG-1330801, photo!). **ASIA:** *Schanginia baccata*, P-06590542, P-04989863, P-04989864, P-04989866, P-04989868, and P-04989941 photos!); *Suaeda baccata*, (P-04989862, P-04989865, P-04989938, P-04989939, photos!); Suaeda aegyptiaca, (P-04989936 and P-04989937, photos!).

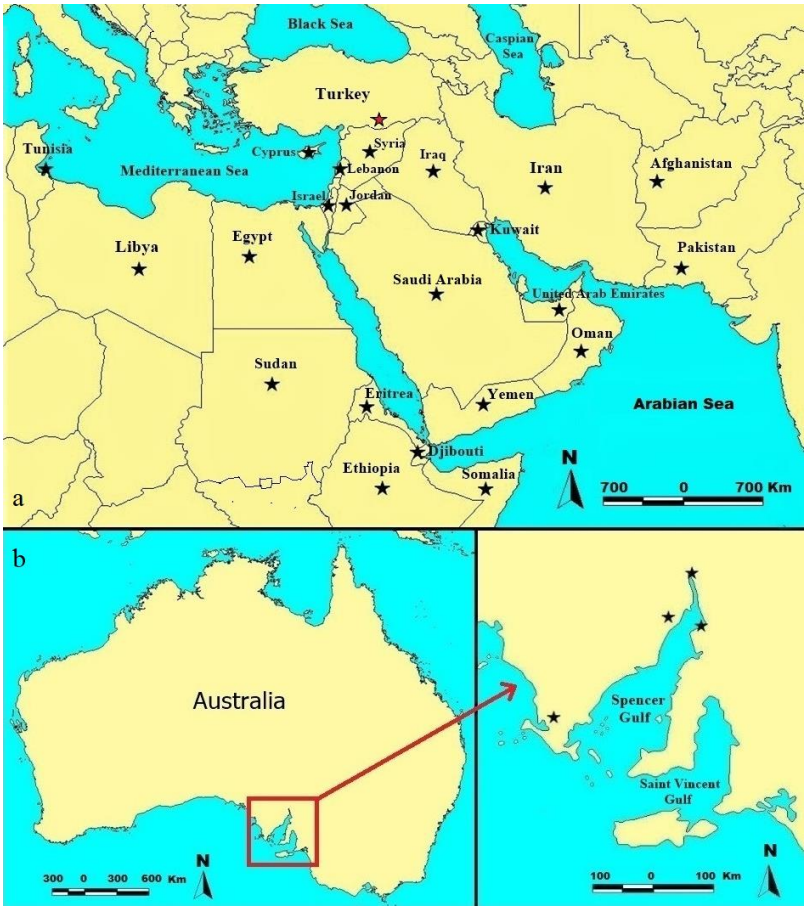

Fig. 1. The distribution map of *Suaeda aegyptiaca* in world with the new record, a. General distribution (Asia, Africa and Arabian Peninsula) Red star indicate the new record, b. It is naturalized in Australia.

Fig. 2. Habitus, leaf, flower, and fruit structures of *Suaeda aegyptiaca*, a. Appearance in flowering time, b. Flower structure, c. Appearance in fruiting time, d. Infructescence, e. Leaf structure, f. Habitat.

Discussion

Suaeda aegyptiaca was classified under different sections by different authors since the 1800s. The study conducted by Moquin-Tandon in 1831 classified the species under the section *Suaeda*. Other studies conducted by Moquin-Tandon in 1840, by Volkens in 1893 and by Ulbrich in 1934 classified the species under the section *Schanginia* (C.A. Mey.) Volk. The study conducted by Schenk and Ferren in 2001 classified the species under the section *Immersa* Townsend. Within the scope of the molecular and morphological study conducted by Schütze *et al.* (2003) on *Suaedoideae* subfamily, the species was classified under the section *Salsina* Moq. Also, in this study, the species classified under the section *Salsina*, based on the study by Schütze *et al.* (2003) and its morphological characteristics.

In the genus *Suaeda*, taxa of the section *Salsina* consists of short trees, shrubs or dwarf-shrubs. Their leaves are either sessile or short petiolate and have the *Suaedoid* C4 anatomy (Schenk & Ferren 2001). Their flower clusters arise from the leaf axil and have a radial symmetry. The number of stigma is three or two and they have a long, thick and papillate structure. Seeds are horizontal or vertical, lenticular, vary in color and size, but not distinctly dimorphic, and they are bright and have a reticulate, punctate or smooth surface (Schenk & Ferren

2001). The type species of the section is *Suaeda vermiculata* Forssk. ex. J.F.Gmel.

In the protologue of *Suaeda aegyptiaca* (≡*Chenopodium aegyptiacum*), morphological definitions of stigma, style and the ovary are provided briefly as "*Germen brevissimum, vix distinguendum. Stylus conicus, crassiusculus, longitudine staminum, integerrimus. stigma bifidum, coronatum laciniis reflexis*" (Hasselquist 1757). However, in the protologue there is no information about bract and bracteole morphologies. After investigating the specimens, we have provided a detailed description of pistil (stigma, style and ovary), bract and bracteole. According to our investigations, Pistil: 1, 2-3 carpellary, 1-lolcular, 2.20-4.50 mm; stigmas 2-3, 0.80-1.75 mm, filiform, with long papillate, light brown; style 0.55-1.30 mm, terete or partly conical, membranous; ovary inferior, 0.75-2.0 x 0.5-2.0 mm, obconical, brown (Figs 3K, K'); Bract: 1, 1.0-1.7 x 0.5-1.0 mm, ovate, ovate-deltoid or deltoid, scarious, either with entire or lacerate margin, apex acute or acuminate and as long as bracteoles (Figs 3B, C); Bracteoles 2, 0.6-1.5 x 0.3-0.8 mm, ovate, scarious, only adnate in basal part, apex acute or acuminate, with lacerate margin (Figs 3B, D, D').

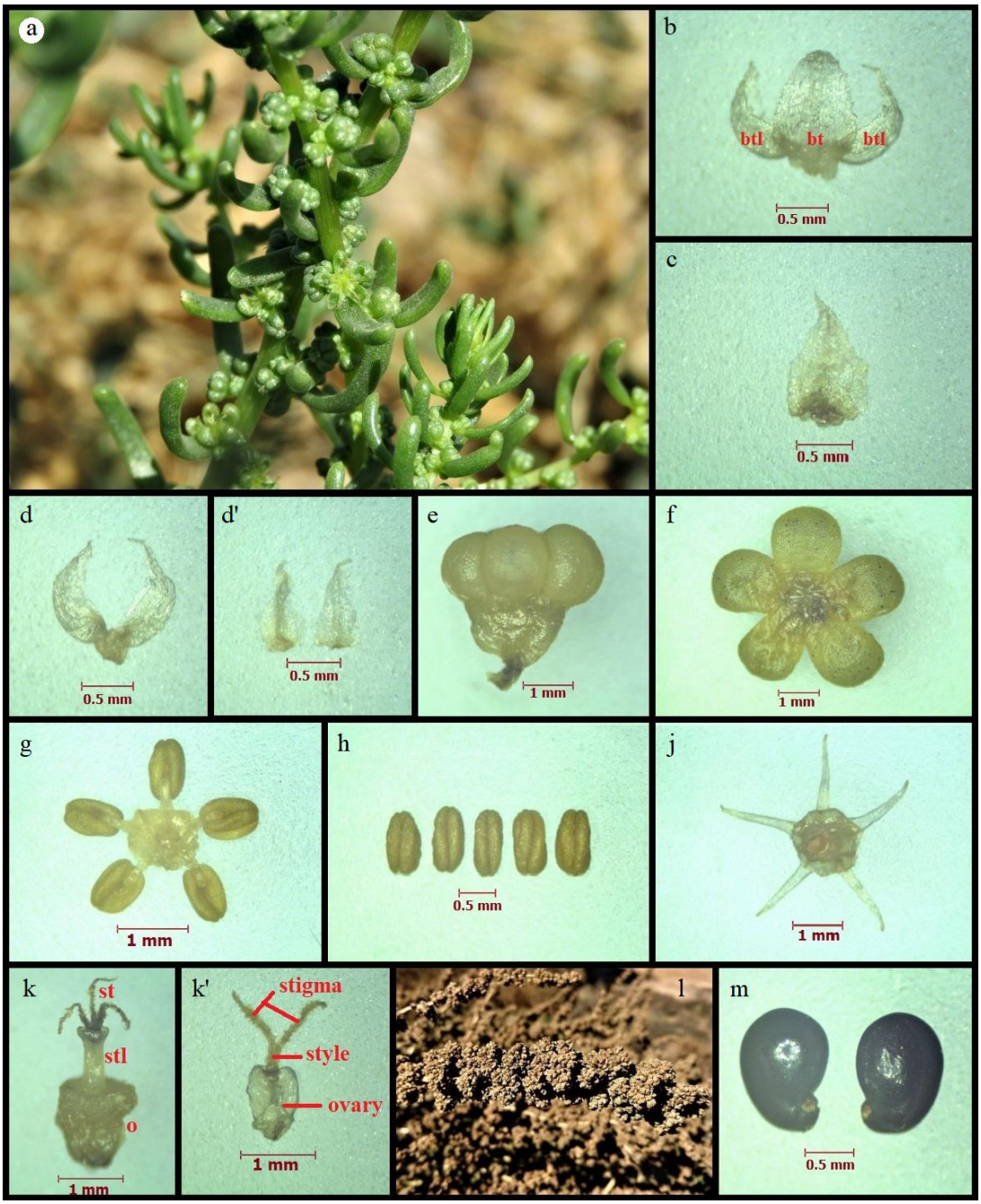

Fig. 3. Morphological characteristics of *S. aegyptiaca*, a. Inflorescence, b. Bract and bracteoles (bt: bract, btl: bracteol), c. Bract, d-d'. Bracteol, e. Flower, f. Perianth segments, g. Stamens, h. Anthers, j. Filaments, k-k'. Pistils (st: stigma, stl: style, o: ovary), l. Fruits, m. Seeds.

In the descriptions of the species in recent literature, morphological features of pistil (stigma, style and ovary), bract and bracteole structures were given incompletely or insufficiently, or were not given at all. Although the study conducted by Meikle (1985) presents the morphological characteristics of the pistil (stigma, style and ovary) structure of the species as "*ovary glabros, pyriform, about 1.5 mm long, 1 mm wide at base; stigmas 3, about 0.4 mm long*", the characteristics of the stylus structure are not explained. Also, it is indicated that the bract structure of the species is "*similar to the leaves, but generally less than 1 cm*" and the bracteoles are "*membranous, erose at apex, broadly ovate, about 0.5 mm long and almost as wide*".

The study conducted by Zohary (1966) provides no information about the morphological characteristics of the pistil (stigma, style and ovary) structure of the species. On the other hand, it is indicated that the bract structure of the species is "*much longer than flowers*", while bracteoles are "*minute and scarious*".

Although the study conducted by Freitag (2001) gives the characteristics of the pistil (stigma, style and ovary) structure of the species as "*Ovary semi-inferior, in its lower, ovule-bearing part fused with the perianth, its upper part forming a ca. 1 mm long column or slender cone; stigmas (2)3(4), 0.7-1.2(1.5) mm long*, with long *papillae, inserted in the center of the collar-like ovary apex*", the characteristics of the style structure are not explained. Also, it is indicated that the bract structure of the species is "*subclavate to clavate, arcuate, spreading, the lower much longer, the upper as long as or even shorter than floral*" and the bracteols are "*0.8-1 mm long, narrow ovate, trullate or triangular, acute or acuminate, the margins lacerate to toothed*".In the fomer studies mentioned above (Zohary (1966, Meikle 1985, Freitag 2001), the structure defined as bract is actually a "leaf" structure which exists in the inflorescence and the structure defined as bracteole is actually "bract" and the characteristics of this structure coincide with the characteristics of the bract structure in our study. From these new findings, it can be understood that the study by Zohary (1966), Meikle (1985), and Freitag (2001) gives no information about the actual bracteole structure of the species.

Finally, the study conducted by Boulos in 1999 only includes the information "*ovary ovoid; stigma 3-4*" regarding the pistil (stigma, style and ovary) structure of the species and does not explain the characteristics of the style structure. Also, it is indicated that the bract of the species is "*bracts 1 mm, deltoid-ovate, with scarious margins*". The study determined that the characteristics of this structure coincide with the characteristics of the bract structure in our study. In addition, the study by Boulos (1999) provides no information about the actual bracteole structure of the species.

We collected some *Suaeda* specimens during the fieldwork conducted in the province of Akçakale district of Şanlıurfa province between the years 2018 and 2019. The identification of the specimens as *Suaeda aegyptiaca* revealed the presence of the species in Turkey, and the number of species of the genus *Suaeda* in Turkey increased to 10.

Conclusion

With this current study, **1)** the presence of the *Suaeda aegyptiaca* in Turkey was revealed for the first time and its extensive description including the distribution area, habitat and morphological characteristics was provided, **2**) the deficiencies concerning the pistil (stigma, stylus and ovary) structure which was not explained properly in most of the recent literature were overcome although clearly specified in the original description, **3)** faulty or inadequate data concerning the bract and bracteole structures which were explained incorrectly or inadequately in most of the literature including the original description was corrected, **4)** and finally it is revealed for the first time that the inflorescence of the species is leafy (Figs 2B, E, 3A).

Acknowledgement

Authors are also grateful to anonymous reviewers for their valuable comments.

Ethics Committee Approval: Since the article does not contain any studies with human or animal subject, its approval to the ethics committee was not required.

Author Contributions: Concept: İ.B., Writing: İ.B., A.E.Y., Critical Review: İ.B., A.E.Y.

Conflict of Interest: The authors have no conflicts of interest to declare.

Funding: We would like to thaks TÜBİTAK (project no. 117Z734) for its financial support.

References

1. Aellen, P. 1967. Suaeda. pp. 324-327. In: Davis, P.H. (ed.) *Flora of Turkey and the East Aegean Islands.* Vol. 2, Edinburgh University Press, Edinburgh, 567 pp.
2. Alonso, M.A., Conticello, L. & Cerazo, M.B. 2004. Suaeda *neuquenensis* (Chenopodiaceae), a new species from Argentina. *Novon*, 14(1): 1-5.
3. Boulos, L. 1999. Chenopodiaceae. pp. 92-129. In: Boulos, L. (ed.) *Flora of Egypt-Azollaceae to Oxalidaceae*. Al Hadara Publishing, Cairo, 419 pp.
4. Brandt, R., Lomonosova, M., Weising, K., Wagner, N. & Freitag, H. 2015. Phylogeny and biogeography of *Suaeda* Subg. *Brezia* (Chenopodiaceae/Amaranthaceae) in the Americas. *Plant Systematics and Evolution*, 301(10): 2351-2375.
5. Davis, P.H., Tan, K. & Mill, R.R. 1988. *Flora of Turkey and the East Aegean Islands*. Vol. 10 (Suppl. I), Edinburgh University Press, Edinburgh, 590 pp.

6. Ferren W.R. & Schenk H.J. 2003. Suaeda. pp. 390-398. In: Morin, N.R. (ed.) *Flora of North America*. Vol. 4, Oxford University Press, 608 pp.
7. Freitag, H. 1989. Contributions to the Chenopod flora of Egypt. *Flora*, 183(1-2): 149-173.
8. Freitag, H. 2000. Chenopodiaceae. pp. 161-163. In: Güner, A., Özhatay, N., Ekim, T. & Başer, K.H.C. (eds.) *Flora of Turkey and the East Aegean Islands*, Vol. 11, (Suppl. 2), Edinburgh University Press, Edinburgh, 656 pp.
9. Freitag, H. 2001. Suaeda. pp.104-178. In: Ali, S.I. & Qaiser, M. (eds.) *Flora of Pakistan*. Missouri Botanical Garden Press, Missouri, 217 pp.
10. Freitag, H. 2013. Chenopodiaceae. pp. 261-275. In: Breckle, S.W., Hedge, I.C. & Rafiqpoor, M.D. (eds.) *Vascular Plants of Afghanistan (VPA)-An Augmented Checklist*. Scientia Bennensis, Bonn-Manama-New York, 598 pp.
11. Freitag, H. & Lomonosova, M. 2017. Restoration of *Suaeda* Sect. *Helicilla* (*Chenopodiaceae*) and typification of its related taxa. *Phytotaxa*, 323(1): 051-060.
12. Güner, A., Özhatay, N., Ekim, T. & Başer, K.H.C. 2000. *Flora of Turkey and the East Aegean Islands*, *Vol. 11 (Suppl. II)*. Edinburgh University Press, Edinburgh, 656 pp.
13. Hasselquist, F. 1757. *Iter Palaestinum Eller Resa Til Heliga Landet, Forratad Ifran ar 1749 Til 1752, Med Beskrifinigar, Ron, Anmarkningar, Ofver De Markvardigstaste Naturalier, På Hennes Kongl*. Utgiven ac Carl Linnaeus, Stockholm, 621 pp.
14. Hedge, I.C. 1997. *Flora Iranica*. Vol. 172, Akademische Druck-u. Verlagsanst. Graz, 371 pp.
15. Kapralov, M.V., Akhani, H., Voznesenskaya, E.V., Edwards, G.E., Franceschi, V.R. & Roalson, E.H. 2006. Phylogenetic relationships in the *Salicornioideae/ Suaedoideae/Salsoloideae* s.l. (*Chenopodiaceae*) clade and a clarification of the phylogenetic position of Bienertia and Alexandra using multiple DNA sequence datasets. *Systematic Botany*, 31: 571-585.
16. Lomonosova, M. & Freitag, H. 2003. A new species of *Suaeda* (*Chenopodiaceae*) from the Altai, Central Asia. *Willdenowia*, 33: 139-147.
17. Lomonosova, M. & Freitag, H. 2011. Typification of plant names in *Suaedoideae* (*Chenopodiaceae*) published by P. Pallas, C. A. Meyer and A. Bunge. *Willdenowia*, 41: 217-229.
18. Meikle, R.D. 1985. Chenopodiaceae. Pp.1370-1383. In: Meikle, R.D. (ed.) *Flora of Cyprus*. Vol. 2, The Bentham-Maxon Trust Royal Botanic Gardens, Kew, 1969 pp.
19. Moquin-Tandon, C.H.B.A. 1831. Premier memoires sur la famille des Chenopods essai monographique sur le genre *Suaeda* et sur les Chénopodées les plus voisines. *Annales des Sciences Naturelles; Botanique*, ser. 1(23): 278-325.
20. Moquin-Tandon, C.H.B.A. 1840. *Chenopodearum Monographica Enumeratio*. Apud P.-J. Loss, Bibliopolam, Via Dicta Haute-Feuille, Paris, 182 pp.
21. Noguez-Hernández, R., Carballo-Carballo, A. & Flores-Olvera, H. 2013. *Suaeda edulis* (*Chenopodiaceae*), una nueva especie de lagos salinos del centro de Mexico. *Botanical Sciences*, 91(1): 19-25.
22. Powo, 2021. Suaeda aegyptiaca. http://www.plantsoftheworldonline.org/taxon/urn:lsid:ipni.org:names:167397-1 (Date accessed: 16.07.2021).
23. Schenk, W. & Ferren, W.R. 2001. On the sectional nomenclature of *Suaeda* (Chenopodiaceae). *Taxon*, 50: 857-873.
24. Schütze, P., Freitag, H. & Weising, K. 2003. An integrated molecular and morphological study of the subfamily *Suaedoideae* Ulbr. (*Chenopodiaceae*). *Plant Systematics and Evolution*, 239: 257-286.
25. Tackholm, V. 1974. *Students' Flora of Egypt, Second Edition*. Published by Cairo University, Beirut, 888 pp.
26. Thiers, B. 2021. Index Herbariorum: a global directory of public herbaria and associated staff. New York Botanical Garden's Virtual Herbarium. Available from: http://sweetgum.nybg.org/ih/ (Data accessed: 08 January 2021).
27. Ulbrich, H. 1934. Chenopodiaceae. pp. 379-587. In: Engler, A. & Prantl, K. (eds.) *Die Natürlichen Pflanzenfamilien*. Vol. 16c, Verlag Von Wilhelm Engelmann, Leipzig, 603 pp.
28. Volkens G. 1893. Chenopodiaceae. pp. 36-91. In: Engler A., Prantl K. (eds.) *Die Natürlichen Pflanzenfamilien*. Vol. 1a, Verlag Von Wilhelm Engelmann, Leipzig, 130 pp.
29. Wikipedia, 2021. *Suaeda aegyptiaca*. https://en.wikipedia.org/wiki/Suaeda_aegyptiaca (Date accessed: 16.07.2021).
30. Yaprak, A.E. 2012. Suaeda. pp. 30. In: Güner, A., Aslan, S., Ekim, T., Vural, M. & Babaç, M.T. (eds.) *Türkiye Bitkileri Listesi (Damarlı Bitkiler)*. Nezahat Gökyiğit Botanik Bahçesi ve Flora Araştırmaları Derneği Yayını, İstanbul, 1290 pp.
31. Zohary, M. 1957. A contribution to the flora of Saudi Arabia. *Botanical Journal of Linnaen Society*, 55: 632-643.
32. Zohary, M. 1966. Chenopodiaceae. pp. 136-18. In: Zohary, M. (ed.) *Flora Palaestina-Equisetaceae to Moringaceae*. The Israel Academy of Sciences and Humanities, Jarusalem, 403 pp.

http://dergipark.org.tr/trkjnat
Trakya University Journal of Natural Sciences, 22(2): 187-197, 2021
ISSN 2147-0294, e-ISSN 2528-9691
DOI: 10.23902/trkjnat.878417

Research Article

SALBUTAMOL AMELIORATES THE PHENOTYPE OF THE SKIN INFLAMMATORY DISEASE PSORIASIS ACCORDING TO SKIN SPHEROID MODELS

Özge Sezin SOMUNCU[1*], Berke DEMİRİZ[2], İrem TÜRKMEN[2], Salih SOMUNCU[3], Berna AKSOY[4]

[1]Stony Brook Medicine, Department of Pathology, New York, USA
[2]Bahçeşehir University School of Medicine, İstanbul, TURKEY
[3]Bezmialem Vakıf University Dragos Hospital, Department of Pediatric Surgery, İstanbul, TURKEY
[4]Bahçeşehir University Faculty of Medicine, Department of Dermatology, İstanbul, TURKEY

Cite this article as:

Somuncu Ö.S., Demiriz B., Türkmen İ., Somuncu S. & Aksoy B. 2021. Salbutamol ameliorates the phenotype of the skin inflammatory disease psoriasis according to skin spheroid models. *Trakya Univ J Nat Sci*, 22(2): 187-197, DOI: 10.23902/trkjnat.878417

Received: 12 February 2021, Accepted: 24 June 2021, Online First: 19 August 2021, Published: 15 October 2021

Edited by:
Enes Taylan

****Corresponding Author:***
Özge Sezgin SOMUNCU
ozge.somuncu@stonybrook.edu

ORCID iDs of the authors:
ÖSS. orcid.org/0000-0002-0841-8263
BD. orcid.org/0000-0002-0419-1786
İT. orcid.org/0000-0003-1692-6417
SS. orcid.org/0000-0002-3154-5527
BA. orcid.org/0000-0003-2346-1865

Key words:
Psoriasis
Skin spheroids
3D models
Salbutamol

Abstract: Psoriasis is a multifactorial chronic inflammatory disorder resulting by the interplay of genetics, the immune system and the environment. It is characterized by the hyperproliferation of epithelial cells, generating red, itchy psoriatic plaques which have no cure but have great negative impact in patients' life. Although corticosteroids or vitamin D analogs might help recovery to some extent, there is yet no total cure for the disease. In this study, we sought to generate three-dimensional (3D) stress-related psoriatic skin spheroids with the screening of the potential efficacy of a β_2-adrenergic receptor agonist, salbutamol. 3D Culture spheroids with human dermal fibroblasts (HDF), human epithelial keratinocytes (HEK) and human monocytic cell line (THP-1) were generated as a representative model of skin and the protocol of stress-related modelling was conducted. The efficacy of the drug salbutamol was evaluated by the changes in mRNA and protein expression levels of selected genes, as well as by several metabolic assays. We developed a method for culturing spherical organoid models of psoriasis *in vitro*. We tested the potential theurapetic effects of salbutamol on psoriasis spheroids. Spheroids treated with salbutamol indicated the effictiveness of the treatment. 3D spheroid system was found partially efficient for mimicking the physiological features of psoriasis *in vitro*. This present work may be a starting point for future investigation as it is the first to generate a stress-related psoriatic model and first to try a β_2 agonist as a potential treatment option. Considering the effects and suitability of topical application of salbutamol, its efficacy should not be underestimated and should be investigated further for translating this knowledge into clinics.

Özet: Sedef hastalığı; genetik, bağışıklık sistemi ve çevrenin karşılıklı etkileşiminden kaynaklanan, çok faktörlü kronik inflamatuar bir hastalıktır. Epitel hücrelerinin hiperproliferasyonu ile karakterizedir ve hastaların yaşamında büyük olumsuz etkileri olan kırmızı, pullu psoriatik plaklar oluşturur. Kortikosteroidler veya D vitamini analogları iyileşmeye bir dereceye kadar yardımcı olabilse de hastalığın henüz tam bir tedavisi yoktur. Bu çalışmada, β_2-adrenerjik reseptör agonisti salbutamol'ün potansiyel etkinliğinin taranması için üç boyutlu (3D) stresle ilişkili psoriatik deri sferoidleri oluşturulması amaçlanmıştır. İnsan dermal fibroblast (HDF), İnsan epidermal keratinosit (HEK) ve İnsan monosit hücreleri (THP-1) ile 3D kültür modelleri oluşturulmuş ve buna göre stres kökenli psoriatik model protokolü uygulanmıştır. İlacın etkinliği, gen ve protein ekspresyon seviyelerindeki değişiklikler ve çeşitli metabolik deneylerle değerlendirilmiştir. Sedef hastalığının sferoid modellerini *in vitro* olarak büyütebilmek için optimize bir yöntem geliştirilmiştir. Salbutamol'ün sedef sferoidleri üzerindeki potansiyel terapatik etkileri test edilmiştir. Salbutamol ile tedavi edilen sferoidler, tedavinin etkinliğini kanıtlayan literatürle paralel sonuçlar göstermiştir. 3D sferoroid sistemimiz, *in vitro* olarak sedef hastalığının fizyolojik özelliklerini taklit etmede kısmen etkili bulunmuştur. Çalışmamız, stresle ilişkili bir psoriatik model oluşturduğu ve potansiyel bir tedavi seçeneği olarak bir β2 agonistini deneyen ilk çalışma olduğu için bir başlangıç noktası olabilir. Salbutamol'ün etkileri ve uygunluğu göz önünde bulundurulduğunda etkinliği küçümsenmemeli ve gelecekte klinikte kullanım potansiyeli göz önünde bulundurulmalıdır.

Introduction

Psoriasis is a chronic inflammatory disease that affects around 125 million people, in other words 2-3% of human population in the world. It is triggered by multifactorial interactions among the immune system, psoriasis-related susceptibility loci (*PSORS1*), auto-antigens, and several environmental triggers (Takeshita *et al.* 2017). The stimulation and upregulation of IL-17 in pre-psoriatic skin creates an inflammatory reaction in keratinocytes that forms the expansion of advanced psoriatic plaques by enhancing epidermal hyperplasia, epidermal cell proliferation, and recruitment of leukocyte branches into the skin (Hawkes *et al.* 2017).

Conventional therapies for psoriasis are typically topical therapies which mostly end up with possible severe side effects. Topical therapies include keratolytics, topical retinoids, topical vitamin analogs, and calcineurin inhibitors. While topical corticosteroids remain first-line treatment that aid alleviating all grades of psoriasis, unwanted side effects including atrophy, striae and/or telangiectases contraindicates their long-term utilization (Torsekar & Gautam 2017). The dual use of corticosteroids and vitamin D analogs display greater efficiency as compared to monotherapy; but side effects like skin irritation, erythema and edema are shown in up to 35% of the patients (Sharma *et al.* 2017). Although more recently developed biological agents such as TNF antagonists, specific monoclonal antibodies, phosphodiesterase 4 or phospholipase A2 inhibitors offer improved anti-psoriatic therapeutic responses, they also pose risk of adverse effects, are expensive, and the potential for development of tolerance or resistance may limit their use (Sharma *et al.* 2017). Hence, there is a need to develop new cost-effective therapies with low side effects.

Commercially accessable psoriasis models are composed of healthy keratinocytes and unhealthy fibroblasts which are isolated from psoriatic lesions of patients. Van den Bogaard *et al.* (2014) were the earliest to complete the generation of three-dimensional (3D) skin counterparts that included diverse T-cell populations. Their study enabled the analysis and relocation of immune cells and discharge of pro-inflammatory cytokines in the context of psoriasis. Nevertheless, hyperproliferation was not detected in 3D skin and cytokine levels were much lower compared to the *in vivo* generated lesion, signifying that in 3D models, critical constituents and pertinent cell types were absent to generate a more accurate psoriasis model (Klicks *et al.* 2017). Up to now, only a few organotypic models emphasize the importance of different cell types in psoriasis, therefore it is important to investigate the inflammatory microenvironment of multi-cellular psoriatic *in vitro* models (Eline Desmet *et al.* 2017). Since animal models cannot reflect the human complexity for the multifactorial etiology of psoriasis, generation of an optimal 3D psoriasis model made by human cells remains crucial (Eline Desmet *et al.* 2017).

Salbutamol is a well-known β_2-adrenergic receptor (β-AR) agonist in the treatment of asthma as well as chronic obstructive pulmonary disease. The inhibitory effects of salbutamol on inflammatory processes is seen for CD4+ cells, monocytes and macrophages and it acts through the inhibition of the ERK pathway (Keränen *et al.* 2017). In addition, anti-inflammatory effects of β-AR on pulmonary inflammation models support the role of receptors in inflammatory conditions (Bosmann *et al.* 2012). There are a couple of studies in literature investigating the effects of salbutamol on psoriasis. Wettey *et al.* (2006) showed the inhibitory effect of salbutamol on CXCR2 (C-X-C Motif Chemokine Ligand 2) which is elevated in psoriatic lesions. A recent study showed the ameliorating effect of salbutamol on psoriasis, correlating with our studies (Liu *et al.* 2020).

Psoriasis has been associated with wound healing and one recent study indicated that in murine skin wound models, stress-induced increase in epinephrine levels were found to delay wound repair (Pullar & Isseroff 2006). Filaggrin 2 is essential for healthy cornification of skin and it functions in skin barrier defense. The expression of Filaggrin 2 was found to be reduced in psoriasis vulgaris in previous studies (T. Makino *et al.* 2014). Matrix metalloproteinase-2 (MMP-2) cleaves native collagen type IV, V, VII, and X, fibronectin, osteonectin, entaxin, laminin, vitronectin, decorin, gelatin, and aggrecan, several chemokines (CCL7 and CXCL12), Tumor Necrosis Factor (TNF) precursors and proTNFβ (Starodubtseva *et al.* 2011). Previous studies showed significant overexpression of MMP-2 in psoriatic skin (Glazewska *et al.* 2016). Interleukin 6 (IL-6) produced from keratinocytes has been shown to be responsible for the inflammation in psoriatic skin lesions (Fujishima *et al.* 2010). Recently, it has been shown that fibroblasts produce IL-8 in cell culture while higher concentrations of IL-8 was detected in psoriatic patients (Glowacka *et al.* 2010). Filaggrin-2, MMP-2, IL-6 and IL-8 were selected as markers in our study depending on their involvememt to psoriasis disease progression. Additionally, an elevated total oxidant status and inadequate antioxidant activity have been defined in psoriatic lesions. The endogenous antioxidant defence mechanism of the body is insufficient to replenish the impairment, and the inadequate skin metabolism deteriorates the state of the skin in psoriasis patients (Asha *et al.* 2017).

In this study, we aimed to generate an optimized 3D stress-related psoriatic skin model along with the investigation of the potential theraupetic effect of salbutamol, a β_2-adrenergic receptor agonist in this psoriatic spheroid model.

Materials and Methods

Cell Culture

Human dermal fibroblasts (HDF) and human epithelial keratinocytes (HEK) were purchased from American Type Culture Collection (ATCC, USA) that was isolated from the newborn foreskin (prepuce) tissue. Briefly, cells were plated in 6-well plates (BIOFIL, TCP,

Switzerland) and grown until 80% confluency in low Dulbecco's Modified Eagle Medium (DMEM) (Gibco/Invitrogen) media supplemented with 10% (v/v) heat-inactivated Fetal Bovine Serum (FBS) and 1% penicillin/streptomycin solution for human dermal fibroblasts according to the reference study (Somuncu *et al.* 2015) and in Defined Keratinocyte -SFM (Serum Free Medium) supplemented with Keratinocyte Growth Supplement (Sigma Aldrich, Germany) and 1% penicillin/streptomycin solution for human epithelial keratinocytes. For passaging, the cells were trypsinized using 0.25% (v/v) trypsin/EDTA (Invitrogen, Gibco, UK) and centrifuged at 1200 rpm for 5 min at room temperature in order to precipitate cells. The pellets were then resuspended in fresh medium accordingly and seeded into T-75 flasks (Zelkultur Flaschen, Switzerland) containing 10 ml media. The cells were preserved at 37°C and 5% CO_2 in a humidified incubator. Cells from passages 3 ~ 4 were used for experiments. THP-1 (Human Monocytic Cell Line) and Human Dermal Microvascular Endothelial Cells (HDMEC) were purchased from American Type Culture Collection (ATCC, USA) and cultures were established following to centrifugation and resuspension at 2×10^4 viable cells/ml. The heterogenous psoriatic cell population (PsorI) induced from keratinocyte cell line by defined protocol (E. Desmet *et al.* 2017) was used as a positive control during the study.

Generation of Skin Spheroids

After removing the media and washing the cells with 1 mL Dulbecco's phosphate-buffered saline (D-PBS) without calcium and magnesium, cells were trypsinized and resuspended in Matrigel as 2×10^5 cells/ml density. Matrigel droplets including HDF, HEK and HDMEC cells were added as 50 µl bubbles into each insert of a Transwell plate (Life Technologies, CA, USA) and incubated for 5-7 days in 1:1 diliution of DMEM and Keratinocyte SFM-1X (ThermoFischer, Turkey) media. Subsequently, 5×10^5 THP-1 monocytes were added to the bottom chamber, cultured for 2 days more and the medium was changed in every three days in top well. Then, the medium was only added to the lower chamber of the insert to generate an air-liquid interface. Spheroid constructs were incubated in Orbital Shaker-Incubator (bioSan, UK) at 37 °C and 5 % CO_2 for 21 days (Vörsmann *et al.* 2013) (Fig. 1a).

Modeling Stress-Related Psoriatic Skin Spheroids

Healthy spheroids were further utilized for disease modeling on 21st day of the procedure. Firstly, UV application was performed for 5 minutes in every two days of one week (Weatherhead *et al.* 2011). At the end of the first week of the protocol, fresh media containing IL-17 was applied and spheroids were incubated for another one week (Chiricozzi *et al.* 2014). At the end of the second week, the media was refreshed and macrophage-activating factor (MAF) administration was performed for 3 days to alert immune cells (Takematsu & Tagami 1990) (Fig. 1a). Samples were incubated at 37°C and 5% CO_2 in Orbital Shaker-Incubator (bioSan, UK). The timeline was established as day 7 (week 1) spheroids, day 14 (week 2 spheroids) and day 40 (cells of spheroids that reseeded in monolayer environment) (Fig. 1b).

Microscopical Analysis of Spheroids

Spheroids were visualized after UV treatment, MAF application, IL-17 application and combination of MAF and IL-17 application with UV treatment in week 1 and week 2 by bright-field microscopy. After optimization of psoriasis modeling, psoriatic skin spheroids were left for incubation and they were visualized in day 7, day 14, day 21 and day 40. Visaualization was accomplished in 40× magnification by ZEISS inverted microscope (Ivascu & Kubbies 2006).

Cell Viability Assay

Salbutamol (S8260-50MG) was purchased from Sigma-Aldrich and used for drug toxicity analysis of heterogenous population of HDF and HEK cells and THP-1 cells. Salbutamol was dissolved in High Glucose DMEM and administered to the cells from 0 to 4.4 µg with 0.2 µg intervals. 3-[4,5-dimethylthiazol-2-yl]-2,5-diphenyltetra-zolium bromide (MTT) cell viability analysis was done after the drug application. Cells were plated in 96 well plates with 5,000 cells per well and incubated for 24 hours. After 24 hours of incubation, salbutamol was applied, and the cell viability was determined for day 1 and day 3. MTT reagent was adminstred as 10 µl to 90 µl of cells and media mix and incubated for 3 hours until purple precipitate was visible. Then, 100 µl Detergent Reagent was added and incubated at room temperature in dark for 2 hours. Absorbance of MTT was recorded at OD 570 nm (Bahuguna *et al.* 2017).

Immunofluorescence Analysis

Cryomolds were organized for Immunofluorescence staining. Optimal Cutting Temperature (OCT) compound was put into plastic cryomolds. Spheroids were positioned on top in correct orientation and OCT was applied by avoiding bubbles until none of the tissue remains uncovered. Mold was placed on top of the aluminium plate on dry ice for rapid freezing. Frozen sections were cut as 8 µm sections and mounted onto slides. Slides were washed with PBS for three times for 5 minutes. Every tissue section was marked with hydrophobic pen (Imedge Pen). Slides were blocked with Blocking Buffer (PBS with 5% horse serum and 0.5% Triton X-100) at room temperature for 1 hour. Slides were then incubated with primary antibodies; Anti-Filaggrin Antibody (ab218395) (1 µg/ml), Anti-Cytokeratin 15 Antibody (ab80522) (5 µg/ml), Anti-IL6 Antibody (ab9324) (1 µg/ml), Anti-IL8 Antibody (ab18672) (1 µg/ml) diluted in blocking buffer at 4°C overnight. Slides were washed with PBS for three times for 5 minutes subsequently. Incubation with secondary antibody Alexa Fluor® 647 Goat Anti-Mouse Antibody (ab150115) (1:200 dilution) was done at room temperature for 1 hour. PBS was used for washing the slides. Slides were stained with DAPI for 1 minute and

fixed with mounting solution. Imaging was performed on Leica DMLB Phase Contrast Fluorescence Microscopy. Fluorescent images were merged with ImageJ software (Ö. S. Somuncu *et al.* 2019).

Quantitative Real Time Analysis for the Detection of Gene Expression

The samples were grouped as healthy skin spheroids, heterogenous PsorI cell population, UV treated spheroids, UV and IL-17 treated psoriasis spheroids, psoriasis spheroids after 10 h salbutamol treatment and psoriasis spheroids after 24 h treatment. According to the instructions, isolation of RNA from each group of samples was done by using High Pure RNA isolation Kit (Roche, Germany). The complementary DNA (cDNA) synthesis from isolated RNA templates was provided with High Fidelity cDNA Synthesis Kit (Roche, Germany). Real time polymerase chain reaction (qPCR) was performed by using Maxima SYBR Green/ROX (Fermentas, US) to determine expression levels of target genes that comprises Keratin 1, Filaggrin 2, IL-6 and MMP-2. The cDNA templates were utilized and mixed with primers and Maxima SYBR Green/ROX qPCR Master Mix (2×). Glyceraldehyde 3-Phosphate Dehydrogenase (GAPDH) was used as house-keeping gene for data normalization (S. Somuncu *et al.* 2019). The results of real-time PCR were obtained via performing normalization with GAPDH. Primer sequences for target genes are shown in Table 1.

Table 1. Primers designed for detection of *MMP-2*, *IL-17*, *Keratin 1*, *Filaggrin 2*, and *IL-6* expression.

Names of the Genes	Primer Sequence (5'-3')
MMP2	Forward Primer: AGCGAGTGGATGCCGCCTTTAA Reverse Primer: CATTCCAGGCATCTGCGATGAG
Filaggrin 2	Forward Primer: CCACACTCACGAGAACACA Reverse Primer: ACCAGAGTGGGAATGTCCAG
Keratin 1	Forward Primer: AGGGTTGTAGGAGCCTTGAC Reverse Primer: CCACTCCAGTGAGGCCAATA
IL-6	Forward Primer: GGGGCTGCCTGCATTAGGAG Reverse Primer: AAGCCCGGGGGACAAAAAGG

All primers were designed by our group. The primers designed with the annealing temperature 60C°.

Total Antioxidant and Oxidant Assay

Total Oxidant Status (TOS) and Total Antioxidant Status (TAS) of each experimental group were measured according to instructions. Sample media was stored at -80°C for the analysis of TAS and TOS. Total Antioxidant Status Assay Kit (Sigma-Aldrich) was used and the kit protocol was followed for TAS determination. 1 mM Trolax standard solution was used for creating a standard curve by setting up different dilutions. 100 µl of Cu^{2+} working solution was added to each well containing standard and samples. Wells were then mixed and incubated at room temperature for 90 minutes. The plate was then transferred to a microplate reader to be analyzed at OD 570 nm (Miller *et al.* 1993). TOS was examined by Erel's TOS method that is about the oxidation of ferrous ion to ferric ion in the existence of diverse oxidative species in the acidic medium. Ferric ion was analyzed by xylenol orange. Briefly, xylenol orange, NaCl and glycerol in a H_2SO_4 solution were incubated with samples for 3 minutes. Ferrous ion and o-dianisidine in H_2SO_4 were applied to the reaction subsequently. The alteration in absorbance was examined, and the results were analyzed by a standard curve of H_2O_2 solution and expressed in µmol/L (Erel 2005).

Statistical Analysis

Complete data sets were presented as means ± standard errors (SEM). Graphics were drawn via GraphPad Prism 8 software (GraphPad Prism, USA). The statistical inquiry of the grades was completed by using one-way ANOVA trailed by multiple-comparison Tukey's Post-Hoc tests with GraphPad Prism 8 software. The stars were stated to flag levels of significance. A p-value less than 0.05 was considered statistically significant (Alabi *et al.* 2019). Heat maps demonstrating gene expression by quantitative real-time PCR were clustered in complete linkage of Heatmapper software presenting both column and row dendogram of hierarchical clustering (Babicki *et al.* 2016). Row Z-scores were demonstrated as green for high values and red for low values, respectively.

Results

UV, IL-17 and GC-MAF sequencial application generated psoriasis-like spheroids

For the optimization of psoriasis modeling, the microscopic phenotypes of the cells after variable UV, IL-17 and MAF treatments were compared with heterogenous psoriatic cell population at the end of week 1 and week 2. With UV treatment to healthy skin spheroids, small sized, dispersed and multiple spheroids were observed in week 1 and at the end of the week 2. The sizes of the spheroids were bigger, total number was increased and they were scattered over the surface instead of generating clusters. After MAF application to skin spheroids, bigger clusters were observed in increased numbers in week 1 and a complete cluster resembling the original lesion was visualized after week 2. When MAF application was combined with UV treatment, these clusters tended to seperate and dissolved completely at the end of week 2. With only IL-17 application, the clusters were bigger in size but more seperate on the surface, resembling seperate spheroidic islands in week 1, and the number of these bigger clusters were decreased with increased number of tiny additional spheroids between them. Combinational UV treatment with IL-17 induced separate clusters to disappear and bigger singular spheroids to appear in week 1, with a dramatic decrement

in quantity while the isolated spheroids were detected in increased size at the end of week 2. The protocol was optimized as UV treatment for 5 minutes in every two days of one week, IL-17 application for one week after UV treatment, and 3 days of GC-MAF application. After optimization of psoriasis modeling protocol, generated psoriasis spheroids were visualized in day 7, day 14 and day 40. Day 7 and day 14 samples indicated the differences in spheroids while day 40 samples were analyzed as monolayer cells of the spheroid content. Spheroids generated clusters, in time resembling a complete psoriatic skin lesion that was established by the monolayer phenotype of cells at the end of day 40 (Fig. 1b).

Cell viability for both THP-1 and HDF cells were established

In order to determine the highest toxic level of salbutamol on HDF, HEK, and THP-1 cells, 22 different concentrations of salbutamol were employed. After dose-dependent drug application, cell viability assay was performed at day 1 and day 3 to establish the optimal dose of drug for further experiments. The highest non-toxic dose for HDF cells was found as 1.6 µg/ml for both day 1 and day 3. For THP-1 cells, despite the peak seen in 2 µg/ml, the optimal dose was determined as 0.8 µg/ml due to the consistency of results in day 1 and day 3 (Fig. 1c).

Salbutamol treatment rescued the psoriasis-like gene expression profile

With the quantitative analysis of PCR (qPCR), relative mRNA expression levels of Keratin 1, Filaggrin 2, IL-6 and MMP-2 were determined before modeling, after modeling and after treatment. Relative Keratin 1 expression was increased with UV application but fell by half with the completion of disease modeling, resembling the levels of psoriatic cells. After salbutamol treatment, no significant change was observed in Keratin 1 expression. Similarly, Filaggrin 2 expression was increased two-fold after UV treatment and decreased three times after completion of modeling, resembling the levels of psoriatic cells. At the end of the treatment with salbutamol, Filaggrin 2 expression levels showed two-fold increase compared with disease model. Likewise, IL-6 expression was increased two-fold with UV application but decreased following the completion of modeling, similar to the levels of psoriatic cells. In the first 10 hours, salbutamol treatment caused a two-fold decreased expression of IL-6 with a subsequent five-fold increment at the end of the treatment. Distinctly, MMP-2 expression was decreased almost three-fold with disease modeling and increased four-fold with 10 hours of salbutamol treatment. At the end of the drug application, expression levels were close to disease models. While Keratin 1, Filaggrin 2 and MMP-2 showed decreased expression after disease modeling, no significant change was observed in IL-6 levels. Salbutamol treatment caused significantly increased expression of Keratin 1, Filaggrin 2, MMP-2 and IL-6 levels when compared between the treatment and psoriasis organoid groups (Fig. 2).

MMP-2 and IL-6 showed similar expression patterns in psoriasis-like spheroids

In order to visualize relative differences in mRNA expression of healthy skin spheroids, Psor1 cells, UV treated spheroids, UV and IL-17 treated complete psoriasis spheroids, psoriasis spheroids after 10 h salbutamol treatment and psoriasis spheroids after salbutamol treatment completed, a heat map was drawn. During modeling, UV treatment caused a decrease in gene expression levels of MMP-2, IL-6 and Filagrin 2 but an increase in the levels of Keratin 1. After modeling, MMP-2, Keratin 1 and Filagrin 2 showed a decreased gene expression, whereas IL-6 levels were increased compared to healthy skin spheroids. Filaggrin 2 and Keratin 1 expressions in psoriasis model showed high resemblance to lesion, whereas MMP-2 and IL-6 expression levels of psoriasis models were the opposite of lesion. After 10 hours of treatment with salbutamol, IL-6, Keratin 1 and Filaggrin 2 expression levels were decreased but MMP-2 levels were increased significantly. At the end of the treatment with salbutamol in psoriasis spheroid model, MMP-2 Filaggrin 2 and IL-6 shared a similar enhanced gene expression pattern and Keratin 1 showed a diminished expression after treatment. Hierarchical clustering of each gene group showed that Keratin 1 and Filaggrin 2 expression indicated the maximum gene expression correlation and the most irrelevant genes were detected as MMP-2 and IL-6 (Fig. 2).

Salbutamol treatment decreased cytokine expression but increased the expression of filament associated protein

Given that Cytokeratin 15, Filaggrin 2, IL-6, IL-8 and IL-17 expression is crucial in the pathophysiology of psoriasis, the expression of each of these was determined with fluorescent IHC in healthy skin model, psoriasis model and after the treatment with salbutamol in psoriasis spheroid model. Cytokeratin 15 expression was increased almost three-fold after disease modeling, then decreased into one fourth of the expression level of disease model after salbutamol treatment, correlating with Keratin 1 mRNA expression. Filaggrin 2 expression was also increased almost three-fold with disease modeling and although less significant, a decrement was seen in the expression after salbutamol treatment. IL-17 expression pattern was observed highest in healthy skin spheroid and decreased both with disease modeling and after treatment, for which expression levels were one fifth of the healthy one. After salbutamol treatment, IL-6 levels decreased into half and IL-8 levels were also decreased, although less significant. Cytokeratin 15, Filaggrin 2, IL-17, IL-6 and IL-8 all shared a similar pattern which was decreased expression after salbutamol treatment. While Cytokeratin 15 and Filaggrin 2 expressions were increased significantly with psoriasis models, IL-17 levels were decreased after modeling in a less significant manner (Fig. 2).

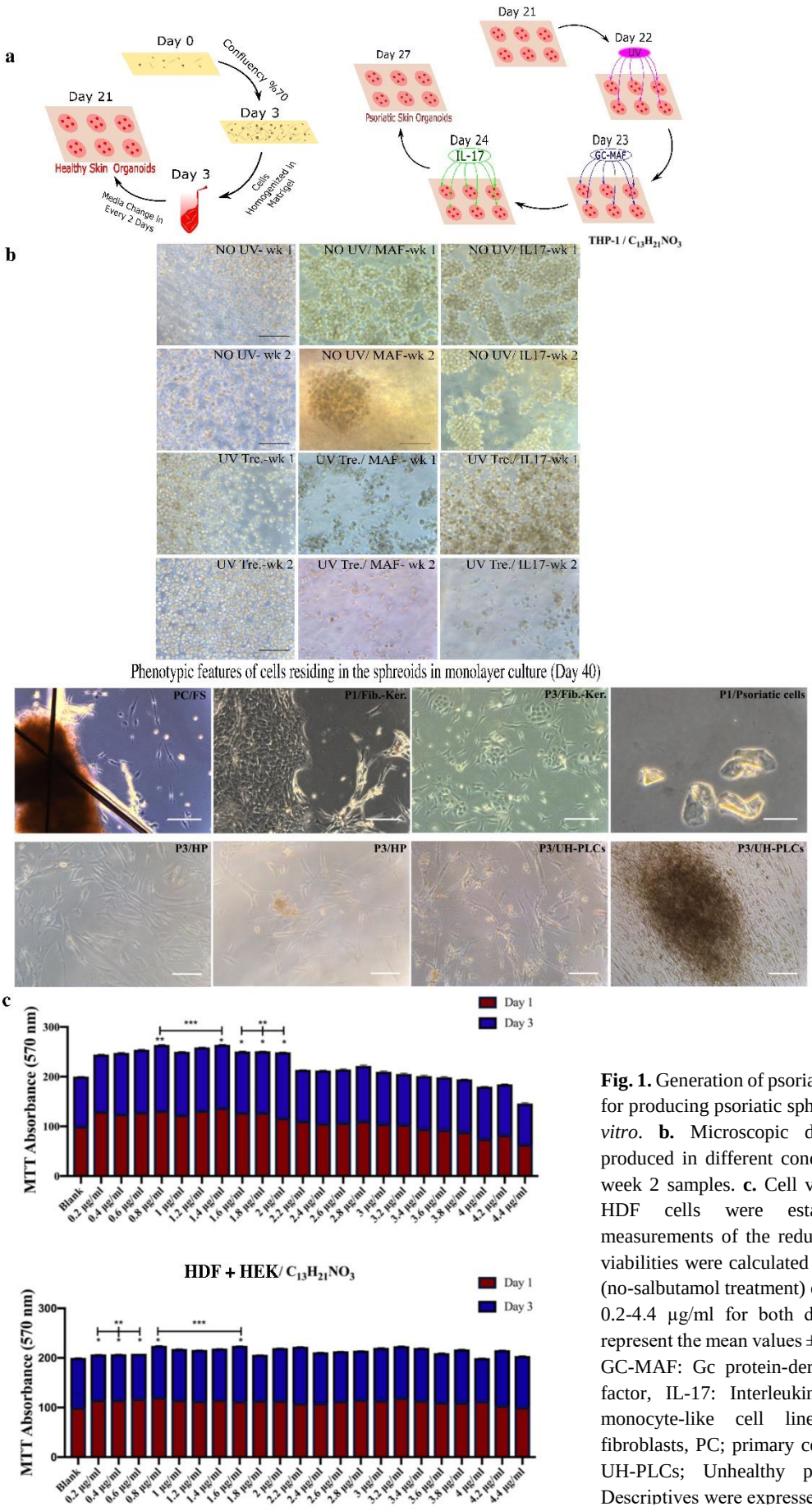

Fig. 1. Generation of psoriatic skin spheroids. **a.** Method for producing psoriatic spheroids in 27 days duration *in vitro*. **b.** Microscopic demonstration of spheroids produced in different conditions for both week 1 and week 2 samples. **c.** Cell viability for both THP-1 and HDF cells were established by colorimetric measurements of the reduction product of MTT. Cell viabilities were calculated as a percentage of the blank (no-salbutamol treatment) over a concentration range of 0.2-4.4 µg/ml for both day 1 and day 3. The data represent the mean values ± SD (n = 3). UV: Ultraviolet, GC-MAF: Gc protein-derived macrophage activating factor, IL-17: Interleukin-17, THP-1; Immortalized monocyte-like cell line, HDF; Human dermal fibroblasts, PC; primary cells, HP; healthy population, UH-PLCs; Unhealthy psoriasis like cells. Note: Descriptives were expressed as mean±standard error.

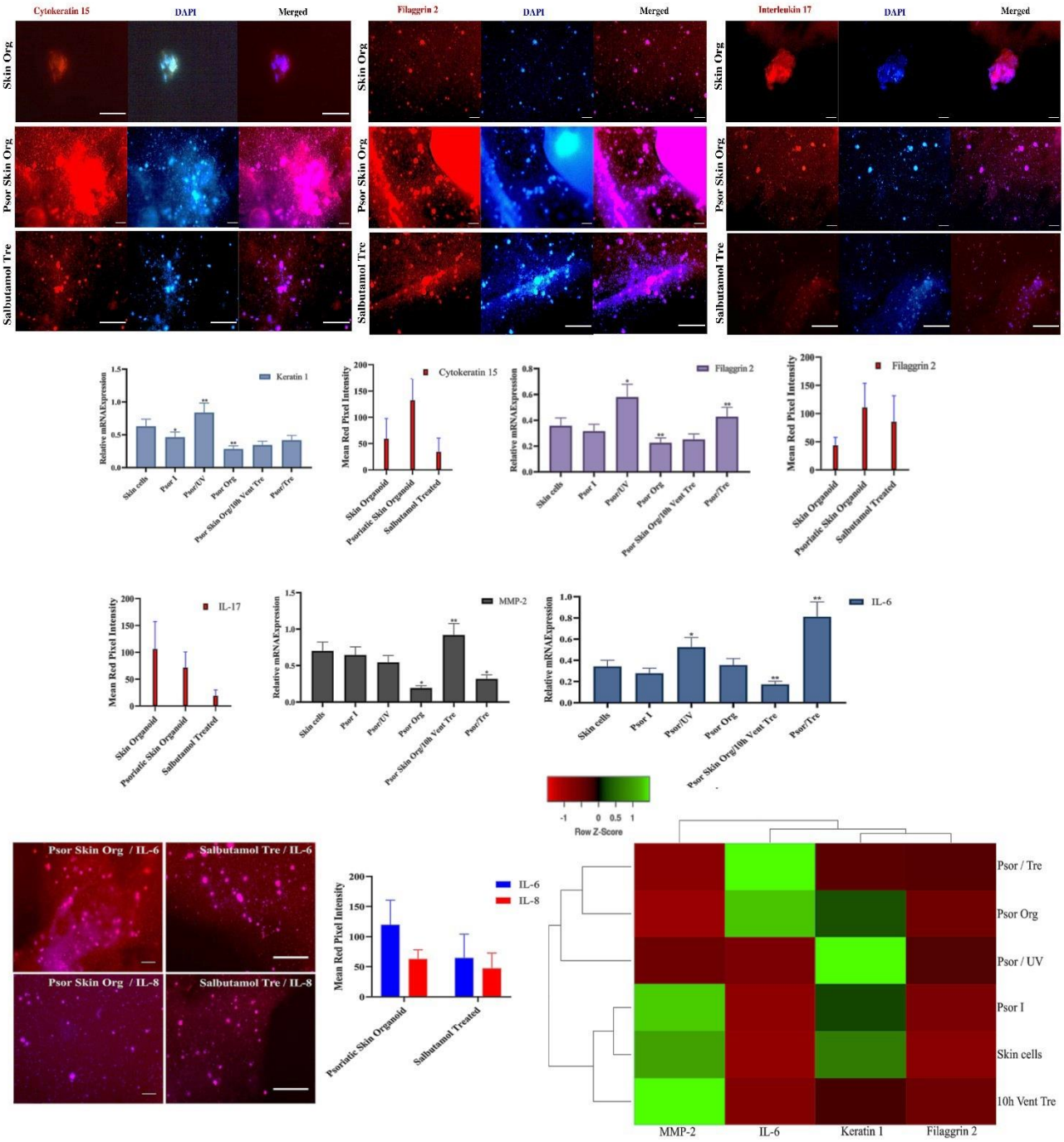

Fig. 2. Gene and protein expression profile of skin and psoriasis spheroids combined with salbutamol treated spheroids in each group. Heat Map presenting the gene expression data for a range of genes analyzed by qPCR. Quantitative representation of genes analyzed by quantitative RT-PCR and proteins analyzed by immunofluorescent staining. Experimental groups are established as following; Psor/Tre: Psoriatic spheroids/organoids treated with salbutamol for 24 hours, Psor Org: Psoriatic organoids, Psor/UV: Psoriatic spheroids induced with UV, Psor I: Psoriatic cells, 10h Vent Tre: Psoriatic spheroids treated with salbutamol for 10 hours. MMP-2: matrix metalloproteinase-2, IL-17: Interleukin-17, IL-6: Interleukin-6, IL-8: Interleukin-8, qPCR: Quantitative real time polymerase chain reaction. Statistically significant at $p<0.05$. Notes: Results were examined by one-way ANOVA and Tukey's Post-Hoc test. Descriptives expressed as mean±standar error.

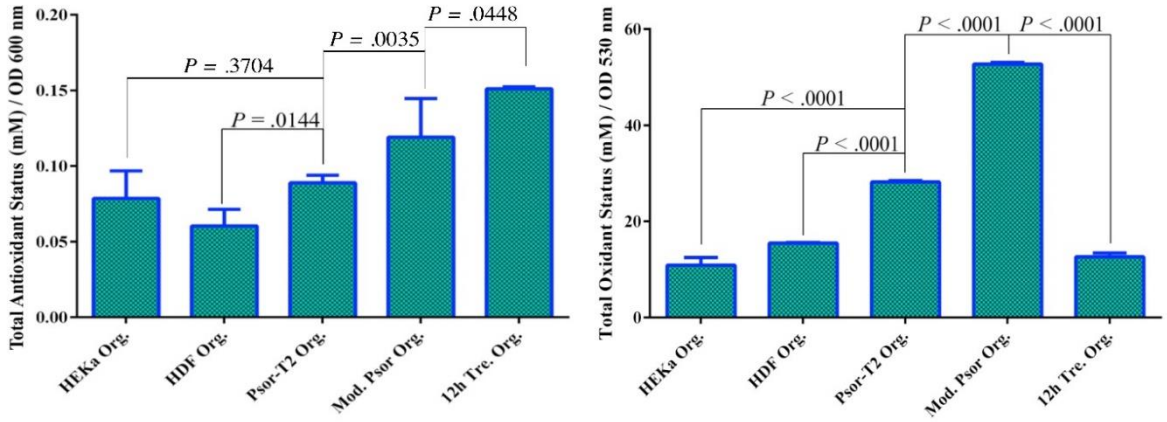

Fig. 3. TAS and TOS levels of the media obtained from treated and untreated spheroid cultures. Experimental groups are established as following; HEKa: Adult normal human epidermal keratinocytes, HDF org: Organoids/spheroids created with human dermal fibroblasts, Psor-T2 Org.: Organoids/spheroids created with Psoriasis type 2 cells, Mod. Psor. Org.: Modelled psoriatic organoids, 12h Tre. Org.: Modelled psoriatic organoids treated with salbutamol for 12 hours. OD: optical density, TAS: total antioxidant status, TOS: total oxidant status. Statistically significant at $p<0.05$. Notes: Results were examined by one-way ANOVA and Tukey's Post-Hoc test. Descriptives expressed as mean±standar error.

Salbutamol treatment significantly decreased oxidant production of psoriatic spheroids

Total oxidant and total antioxidant levels were measured from the cell culture media where the spheroids were grown. After modeling, a five-fold increment ($p<0.0001$) in total oxidant levels were measured and this increment was observed two-fold in psoriatic skin lesion. After 10 hours of treatment, total oxidant levels cut into half ($p<0.0001$) and at the end of the treatment, it was observed one fourth of the levels of psoriasis spheroids ($p<0.0001$). After modeling, the total antioxidant levels were increased significantly ($p=0.0144$). Although not significant, total antioxidant levels were higher in psoriasis model and after 10 hours treatment, two-fold augmentation of total antioxidant levels were observed with still a significant increment after salbutamol treatment (Fig. 3).

Discussion

In this study, we developed a method for culturing spherical organoid models of psoriasis *in vitro*. We tested the potential theurapetic effects of salbutamol, a β-AR agonist, on psoriasis spheroids. Our hypothesis was grounded in the anti-inflammatory effect of salbutamol, which was assumed to act through inhibition of cAMP dependent ERK pathway, thus causing decreased TNF-alpha and MCP-1 production in macrophages. Clinical observations suggested that systemic β-adrenergic blockade may trigger the onset of psoriasis-like skin lesions in some patients (Balak & Hajdarbegovic 2017) (Steinkraus *et al.* 1993). It was reported that the hyperproliferation of keratinocytes in psoriasis was the result of a decreased cAMP production intracellularly, thus current treatment options such as glucocorticoid treatment, UVB irradiation or topical vitamin D treatment have been shown to act through generation of cAMP in response to β-AR in keratinocytes (Sivamani *et al.* 2007). Although a known mechanism was reported before, none of the β_2-agonist drugs were tested for their efficacy in psoriasis patients. Therefore, this study aimed to investigate the efficacy of a β_2-agonist drug in a 3D psoriasis spheroid model for the first time.

Optimization of our psoriasis modeling protocol was determined based on the resemblance of the phenotypes of the spheroids to psoriatic cells upon the application of different stress factors. While UV treatment was observed to cause dysmorphism in the shape of the spheroids, MAF and IL-17 applications resulted in generation of clusters resembling psoriatic skin lesions. Combination of UV treatment with MAF and IL-17 caused dysmorphic clusters and prolongation of this treatment resulted in the loss of colonies. After optimization and incubation of 40 days, psoriatic spheroids generated tight clusters resembling a real psoriatic skin lesion.

Cell viability assays indicated that none of the dosage of salbutamol was toxic. After examination of each dose, 0.8 μg/ml, 1.6 μg/ml and 3.2 μg/ml were selected and evaluated as they were drawn attention for different cell lines. At the end, the optimal dosage was selected as 1.6 μg/ml for application of the drug. As none of the dose was found toxic, this gave the idea of salbutamol being physically processed on skin cells and effective on their cellular behavior.

Psoriatic epidermis is known to have decreased Keratin 1(K1) and K10 levels which are differentiation specific keratins and increased K6 and K16 levels (Thewes *et al.* 1991). In one study, it was suggested that Keratin 15 expression resulting from resident proliferating keratinocytes in the basal layer was uniquely downregulated in hyperproliferative situations such as psoriasis to maintain the activated phenotype of keratinocytes (Waseem *et al.* 1999). Our results showed an increased level of K1 after UV treatment, and a subsequent decrease in these levels were observed at the end of the modeling process suggesting that IL-17 and G-CSF might interfere with Keratin 1 expression in

psoriasis. On the other hand, the protein expression level of Keratin 15 was increased significantly with disease modeling and after treatment, it decreased to even lower levels than the beginning. Since no detailed study was found in the literature suggesting Keratin 15 differences, the mechanism behind this regulation should be further investigated.

Psoriasis is thought to to have a complex autoimmune and inflammatory pathophysiology with a genetic basis. It is thought that IL-17 induced release of keratinocyte-derived inflammatory mediators from TNF pathway form the key mechanisms driving psoriasis pathogenesis and it was seen that those two pathways are affecting each other (Ogawa *et al.* 2018). Supporting this idea, Fujishima et al. (2010) demonstrated that IL-17 stimulates the production of IL-6 from keratinocytes and is responsible for the inflammation in psoriatic skin lesions. Thus, current medical treatments and new small molecules comprising immunotherapies try to decrease the levels of those cytokines. In our study, IL-17 application was used to optimize the psoriasis modeling. Given the result of decrement after salbutamol treatment, it is concluded that psoriasis spheroid model reflects the disease and respond the therapy. IL-6 mRNA and protein expression also increased with disease modeling but decreased significantly after treatment. Despite the decreased protein expression at the end of the therapy, significantly high IL-6 mRNA levels were found, suggesting a different factor interfering with the translation mechanism. IL-17 and IL-6 pathways are known to upregulate IL-8 levels in keratinocytes, which leads to microabscess formation by enhancing neutrophil recruitment in psoriasis (Ogawa *et al.* 2018). Although IL-8 was not significantly changed, IL-6 which is a master regulator of both inflammation and metabolism (Ghanemi & St-Arnand 2018) significantly decreased after treatment.

IL-17 also seemed to be responsible for the reduction of Filaggrin 2 levels in psoriatic lesions and this alters the differentiation of keratinocytes as a part of the pathophysiogical mechanism (Gutowska-Owsiak *et al.* 2012) (Teruhiko Makino *et al.* 2014). Consistently, an increase in Filaggrin 2 protein levels were seen with a decreased IL-17 levels with disease modeling. Although Filaggrin 2 protein expression seemed to increase with disease modeling, mRNA levels first increased with UV treatment but decreased significantly after IL-17 and MAF application, which correlates with the literature (Simonsen *et al.* 2017) (Gutowska-Owsiak *et al.* 2012). After salbutamol treatment, an increased mRNA level of Filaggrin 2 was observed in spite of a decreased level of Filaggrin 2 protein expression. mRNA levels were more consistent with literature data due to decreased levels with disease modeling and increased levels after treatment.

MMP-2 stimulation by IL-6, IL-17 and various other inflammatory cytokines has been reported to be crucial in early progression of psoriasis (Jovanovic *et al.* 2000) (Sun *et al.* 2014). The key role of this molecule is in the modification of ECM and basement membrane, as well as cell migration and tissue remodeling activation. Feliciani *et al.* (1997) was the first to report the significant overexpression of MMP-2 in psoriatic skin. Conversely, our results indicated significantly decreased levels of MMP-2 with disease modeling, and an obvious increase with the salbutamol treatment in the first 10 hours, with a return to the starting levels at the end of the treatment. Application of IL-17 or MAF during disease modeling might be the reason for the MMP-2 expression.

Since psoriasis was a state of oxidative stress, enhanced total oxidant levels and decreased total antioxidant levels were reported in psoriasis patients with several studies (Armstrong *et al.* 2011, Lin & Huang 2016, Peluso *et al.* 2016). After psoriasis modeling, oxidant levels were significantly increased along with a less significant increase in antioxidant levels. This was explained by the effect of formation of the 3D system since the better interaction of cells may create a protective environment through different mechanisms. After treatment, oxidant levels decreased significantly, and antioxidant levels increased two-fold suggesting the efficacy of the drug, although the mechanism should be inquired.

In this study, we created the first stress-related psoriasis spheroid model which exhibited correlation in multiple aspects with the literature and searched for the efficacy of a known drug for the first time in a 3D culture system. One of the main novelties of our study is the investigation of a specific β-agonist for determining its efficacy in psoriasis treatment. Although we proved that salbutamol treatment may be a possible therapy for psoriasis, other β-agonists should also be investigated. In our perspective, considering the known effects and the suitability of topical application of β_2 agonists, the efficacy of salbutamol should not be underestimated and must be evaluated further for translation of this knowledge into clinics.

Limitation of the Study

The main limitation of the study is the lack of demonstration of a specific mechanism underlying the changes in gene expression at mRNA and protein levels. Other limitation is the lack of information on if the spherical psoriatic organoids recapitulate the human disease. Lastly, here there are limited numbers of genes studied. Since psoriasis has a complex background affecting more than one pathway, the change in the expression levels of molecules overriding those pathways with disease modeling must be further analyzed.

Acknowledgement

This project used the Bahçeşehir University Faculty of Medicine research laboratories whereat we thank to the Dean of Faculty Türker KILIÇ (İstanbul, Turkey). We also would like to thank Sam Chiappone from Stony Brook University School of Medicine (New York, USA), Department of Pathology for their efforts in proofreading.

Ethics Committee Approval: Since the article does not contain any studies with human or animal subject, its approval to the ethics committee was not required.

Author Contributions: Concept: Ö.S., B.A. S.S., Desing: Ö.S., B.A. S.S., İ.T., B.D., Execution: Ö.S., İ.T., B.D., Material supplying: Ö.S., B.A. S.S., Data acquisition: Ö.S., B.A. S.S., Data analysis/interpretation: Ö.S., B.A. S.S., Writing: Ö.S., İ.T., B.D., Critical review Ö.S., B.A. S.S.

Conflict of Interest: The authors have no conflicts of interest to declare.

Funding: The authors declared that this study has received no financial support.

References

1. Alabi, B.R., LaRanger, R. & Shay, J.W. 2019. Decellularized mice colons as models to study the contribution of the extracellular matrix to cell behavior and colon cancer progression. *Acta Biomaterialia*, 100: 213-222.
2. Armstrong, A., Armstrong, E., Fuller, E., Sockolov, M. & Voyles, S. 2011. Smoking and pathogenesis of psoriasis: a review of oxidative, inflammatory and genetic mechanisms. *British Journal of Dermatology*, 165(6): 1162-1168.
3. Asha, K., Singal, A., Sharma, S.B., Arora, V.K. & Aggarwal, A. 2017. Dyslipidaemia & oxidative stress in patients of psoriasis: Emerging cardiovascular risk factors. *Indian Journal of Medical Research*, 146: 708-713. https://doi.org/10.4103/ijmr.IJMR_717_16
4. Babicki, S., Arndt, D., Marcu, A., Liang, Y.J., Grant, J.R., Maciejewski, A. & Wishart, D.S. 2016. Heatmapper: web-enabled heat mapping for all. *Nucleic Acids Research*, 44(W1): W147-W153. https://doi.org/10.1093/nar/gkw419
5. Bahuguna, A., Khan, I., Bajpai, V.K. & Kang, S.C. 2017. MTT assay to evaluate the cytotoxic potential of a drug. *Bangladesh Journal of Pharmacology*, 12(2): Online: Apr 8-2017.
6. Balak, D.M. & Hajdarbegovic, E. 2017. Drug-induced psoriasis: clinical perspectives. *Psoriasis (Auckland, NZ)*, 7: 87.
7. Bosmann, M., Grailer, J.J., Zhu, K., Matthay, M.A., Sarma, J.V., Zetoune, F.S. & Ward, P.A. 2012. Anti-inflammatory effects of β2 adrenergic receptor agonists in experimental acute lung injury. *The FASEB Journal*, 26(5): 2137-2144.
8. Chiricozzi, A., Nograles, K.E., Johnson-Huang, L.M., Fuentes-Duculan, J., Cardinale, I., Bonifacio, K.M., Gulati, N., Mitsui, H., Guttman-Yassky, E. & Suárez-Fariñas, M. 2014. IL-17 induces an expanded range of downstream genes in reconstituted human epidermis model. *PloS one*, 9(2): e90284. doi:10.1371/journal.pone.0090284
9. Desmet, E., Ramadhas, A., Lambert, J. & Van Gele, M. 2017. In vitro psoriasis models with focus on reconstructed skin models as promising tools in psoriasis research. *Exp Biol Med (Maywood)*, 242(11): 1158-1169. https://doi.org/10.1177/1535370217710637
10. Desmet, E., Ramadhas, A., Lambert, J. & Van Gele, M. 2017. In vitro psoriasis models with focus on reconstructed skin models as promising tools in psoriasis research. *Experimental biology and medicine*, 242(11): 1158-1169.
11. Erel, O. 2005. A new automated colorimetric method for measuring total oxidant status. *Clinical biochemistry*, 38(12): 1103-1111.
12. Feliciani, C., Vitullo, P., D'Orazi, G., Palmirotta, R., Amerio, P., Pour, S.M., Coscione, G., Amerio, P.L. & Modesti, A. 1997. The 72-kDa and the 92-kDa gelatinases, but not their inhibitors TIMP-1 and TIMP-2, are expressed in early psoriatic lesions. *Exp Dermatol*, 6(6): 321-327. doi: 10.1111/j.1600-0625.1997.tb00180.x
13. Fujishima, S., Watanabe, H., Kawaguchi, M., Suzuki, T., Matsukura, S., Homma, T., Howell, B.G., Hizawa, N., Mitsuya, T., Huang, S.K. & Iijima, M. 2010. Involvement of IL-17F via the induction of IL-6 in psoriasis. *Arch Dermatol Res*, 302(7): 499-505. https://doi.org/10.1007/s00403-010-1033-8
14. Ghanemi, A. & St-Arnand, J. 2018. Interleukin-6 as a "metabolic hormone". *Cytokine*, 112: 132-136. https://doi.org/10.1016/j.cyto.2018.06.034
15. Glazewska, E.K., Niczyporuk, M., Lawicki, S., Szmitkowski, M., Zajkowska, M., Bedkowska, G.E. & Przylipiak, A. 2016. Therapy of psoriasis with narrowband ultraviolet-B light influences plasma concentrations of MMP-2 and TIMP-2 in patients. *Ther Clin Risk Manag*, 12: 1579-1585. https://doi.org/10.2147/TCRM.S113769
16. Glowacka, E., Lewkowicz, P., Rotsztejn, H. & Zalewska, A. 2010. IL-8, IL-12 and IL-10 cytokines generation by neutrophils, fibroblasts and neutrophils- fibroblasts interaction in psoriasis. *Adv Med Sci*, 55(2): 254-260. https://doi.org/10.2478/v10039-010-0037-0
17. Gutowska-Owsiak, D., Schaupp, A.L., Salimi, M., Selvakumar, T.A., McPherson, T., Taylor, S. & Ogg, G.S. 2012. IL-17 downregulates filaggrin and affects keratinocyte expression of genes associated with cellular adhesion. *Experimental dermatology*, 21(2): 104-110.
18. Hawkes, J.E., Chan, T.C. & Krueger, J.G. 2017. Psoriasis pathogenesis and the development of novel targeted immune therapies. *Journal of Allergy and Clinical Immunology*, 140(3): 645-653.
19. Ivascu, A. & Kubbies, M. 2006. Rapid generation of single-tumor spheroids for high-throughput cell function and toxicity analysis. *Journal of biomolecular screening*, 11(8): 922-932.
20. Jovanovic, D.V., Martel-Pelletier, J., Di Battista, J.A., Mineau, F., Jolicoeur, F.C., Benderdour, M. & Pelletier, J.P. 2000. Stimulation of 92-kd gelatinase (matrix metalloproteinase 9) production by interleukin-17 in human monocyte/macrophages: A possible role in rheumatoid arthritis. *Arthritis & Rheumatism: Official Journal of the American College of Rheumatology*, 43(5): 1134-1144.
21. Keränen, T., Hömmö, T., Moilanen, E. & Korhonen, R. 2017. β2-receptor agonists salbutamol and terbutaline attenuated cytokine production by suppressing ERK pathway through cAMP in macrophages. *Cytokine*, 94: 1-7.

22. Klicks, J., von Molitor, E., Ertongur-Fauth, T., Rudolf, R. & Hafner, M. 2017. In vitro skin three-dimensional models and their applications. *Journal of Cellular Biotechnology*, 3(1): 21-39.

23. Lin, X. & Huang, T. 2016. Oxidative stress in psoriasis and potential therapeutic use of antioxidants. *Free radical research*, 50(6): 585-595.

24. Liu, F., Wang, S.P., Liu, B., Wang, Y.K. & Tan, W. 2020. (R)-Salbutamol Improves Imiquimod-Induced Psoriasis-Like Skin Dermatitis by Regulating the Th17/Tregs Balance and Glycerophospholipid Metabolism. *Cells*, 9(2). https://doi.org/10.3390/cells9020511

25. Makino, T., Mizawa, M., Yamakoshi, T., Takaishi, M. & Shimizu, T. 2014. Expression of filaggrin-2 protein in the epidermis of human skin diseases: a comparative analysis with filaggrin. *Biochem Biophys Res Commun*, 449(1): 100-106. https://doi.org/10.1016/j.bbrc.2014.04.165

26. Makino, T., Mizawa, M., Yamakoshi, T., Takaishi, M. & Shimizu, T. 2014. Expression of filaggrin-2 protein in the epidermis of human skin diseases: a comparative analysis with filaggrin. *Biochemical and biophysical research communications*, 449(1): 100-106.

27. Miller, N.J., Rice-Evans, C., Davies, M.J., Gopinathan, V. & Milner, A. 1993. A novel method for measuring antioxidant capacity and its application to monitoring the antioxidant status in premature neonates. *Clinical science*, 84(4): 407-412.

28. Ogawa, E., Sato, Y., Minagawa, A. & Okuyama, R. 2018. Pathogenesis of psoriasis and development of treatment. *The Journal of dermatology*, 45(3): 264-272.

29. Peluso, I., Cavaliere, A. & Palmery, M. 2016. Plasma total antioxidant capacity and peroxidation biomarkers in psoriasis. *Journal of biomedical science*, 23(1): 52.

30. Pullar, C.E. & Isseroff, R.R. 2006. The β2-adrenergic receptor activates pro-migratory and pro-proliferative pathways in dermal fibroblasts via divergent mechanisms. *Journal of cell science*, 119(3): 592-602.

31. Sharma, M., Levenson, C., Clements, I., Castella, P., Gebauer, K. & Cox, M.E. 2017. East Indian sandalwood oil (EISO) alleviates inflammatory and proliferative pathologies of psoriasis. *Frontiers in pharmacology*, 8: 125.

32. Simonsen, S., Thyssen, J.P., Heegaard, S., Kezic, S. & Skov, L. 2017. Expression of filaggrin and its degradation products in human skin following erythemal doses of ultraviolet B irradiation. *Acta dermato-venereologica*, 97(6-7): 797-801.

33. Sivamani, R.K., Lam, S.T. & Isseroff, R.R. 2007. Beta adrenergic receptors in keratinocytes. *Dermatologic clinics*, 25(4): 643-653.

34. Somuncu, Ö.S., Coşkun, Y., Ballica, B., Temiz, A.F. & Somuncu, D. 2019. In vitro artificial skin engineering by decellularized placental scaffold for secondary skin problems of meningomyelocele. Journal *of Clinical Neuroscience*, 59: 291-297.

35. Somuncu, Ö.S., Taşlı, P.N., Şişli, H.B., Somuncu, S. & Şahin, F. 2015. Characterization and differentiation of stem cells isolated from human newborn foreskin tissue. *Applied biochemistry and biotechnology*, 177(5): 1040-1054.

36. Somuncu, S., Somuncu, Ö.S., Ballıca, B. & Tabandeh, B. 2019. Deficiency of Epithelial–Mesenchymal Transition Causes Child Indirect Inguinal Hernia. *Journal of pediatric surgery*, 55(4):665-671. doi: 10.1016/j.jpedsurg.2019.06.020

37. Starodubtseva, N.L., Sobolev, V.V., Soboleva, A.G., Nikolaev, A.A. & Bruskin, S.A. 2011. [Expression of genes for metalloproteinases (MMP-1, MMP-2, MMP-9, and MMP-12) associated with psoriasis]. *Genetika*, 47(9): 1254-1261.

38. Steinkraus, V., Steinfath, M., Stöve, L., Körner, C., Abeck, D. & Mensing, H. 1993. β-adrenergic receptors in psoriasis: evidence for down-regulation in lesional skin. *Archives of dermatological research*, 285(5): 300-304.

39. Sun, W., Liu, D.-B., Li, W.-W., Zhang, L.-L., Long, G.-X., Wang, J.-F., Mei, Q. & Hu, G.-Q. 2014. Interleukin-6 promotes the migration and invasion of nasopharyngeal carcinoma cell lines and upregulates the expression of MMP-2 and MMP-9. *International journal of oncology*, 44(5): 1551-1560.

40. Takematsu, H. & Tagami, H. 1990. Granulocyte-macrophage colony-stimulating factor in psoriasis. *Dermatology*, 181(1): 16-20.

41. Takeshita, J., Grewal, S., Langan, S.M., Mehta, N.N., Ogdie, A., Van Voorhees, A.S. & Gelfand, J.M. 2017. Psoriasis and comorbid diseases: Epidemiology. *J Am Acad Dermatol*, 76(3): 377-390. https://doi.org/10.1016/j.jaad.2016.07.064

42. Thewes, M.s., Stadler, R., Korge, B. & Mischke, D. 1991. Normal psoriatic epidermis expression of hyperproliferation-associated keratins. *Archives of dermatological research*, 283(7): 465-471.

43. Torsekar, R. & Gautam, M.M. 2017. Topical therapies in psoriasis. *Indian dermatology online journal*, 8(4): 235.

44. Vörsmann, H., Groeber, F., Walles, H., Busch, S., Beissert, S., Walczak, H. & Kulms, D. 2013. Development of a human three-dimensional organotypic skin-melanoma spheroid model for in vitro drug testing. *Cell death & disease*, 4(7): e719-e719.

45. Waseem, A., Alam, Y., Lalli, A., Dogan, B., Tidman, N., Purkis, P., Jackson, S., Machesney, M. & Leigh, I.M. 1999. Keratin 15 expression in stratified epithelia: downregulation in activated keratinocytes. *Journal of Investigative Dermatology*, 112(3): 362-369.

46. Weatherhead, S.C., Farr, P.M., Jamieson, D., Hallinan, J.S., Lloyd, J.J., Wipat, A. & Reynolds, N.J. 2011. Keratinocyte apoptosis in epidermal remodeling and clearance of psoriasis induced by UV radiation. *Journal of Investigative Dermatology*, 131(9): 1916-1926.

http://dergipark.org.tr/trkjnat
Trakya University Journal of Natural Sciences, 22(2): 199-205, 2021
ISSN 2147-0294, e-ISSN 2528-9691
DOI: 10.23902/trkjnat.925710

Research Article

DETERMINATION OF FLOW AND VISCOELASTIC PROPERTIES OF THE KYRGYZ ETHNIC FOOD "SÜZMÖ" DEPENDING ON TEMPERATURE AND MOISTURE CONTENT

Janyl ISKAKOVA[1*], Jamila SMANALIEVA[2]

[1]Environmental Engineering Department, Engineering Faculty, Kyrgyz-Turkish Manas University, pr. Aytmatov 56, 720044, Bishkek, KYRGYZSTAN
[2]Department of Food Production Technology, Technology Faculty, Kyrgyz State Technical University after I. Razzakov, pr. Aytmatov 66, 720044 Bishkek, KYRGYZSTAN

Cite this article as:

Iskakova J., Smanalieva J. 2021. Determination of flow and viscoelastic properties of the Kyrgyz ethnic food "Süzmö" depending on temperature and moisture content. *Trakya Univ J Nat Sci*, 22(2): 199-205, DOI: 10.23902/trkjnat.925710

Received: 22 April 2021, Accepted: 31 July 2021, Online First: 22 September 2021, Published: 15 October 2021

Abstract: Consumer interest in concentrated protein-rich food is growing. Kyrgyz traditional food Süzmö, which is a highly viscous dairy product that is produced from fermented milk Ayran, needs to be introduced into the dairy industry. In this study, the rheological parameters of this indigenous food product were investigated in steady and dynamic rheological experiments. The flow behaviours of Süzmö were evaluated at six temperatures (20, 30, 40, 50, 60, and 70°C) and suitable rheological models were found. The flow curves of Süzmö at investigated temperatures have the yield stress (τ_0) values between 32.64 Pa and 285.87 Pa. The flow properties of Süzmö samples at 20 and 30°C correspond to the Bingham model. The Casson model was suitable for describing flow curves at 40, 50, 60, and 70°C with correlation coefficients R=0.9506 – 0.9973. The effective viscosity (η_{eff}) of Süzmö decreased from 15.88 to 0.26 Pa·s with increasing temperature from 20 and 70°C. The effect of temperature on the viscosity corresponds to the Arrhenius relationship. The calculated activation energy was 61.66 kJ/(mol). A linear model was defined taking into account the influence of moisture content ($p>0.05$) on effective viscosity (η_{eff}) and yield stress (τ_0). A temperature-sweep was performed at 20 to 80°C to determine the thermal denaturation of the fermented milk samples. The measured parameters are essential for the industrial production of Süzmö and other concentrated fermented milk products.

Özet: Konsantre protein açısından zengin gıdalara tüketici ilgisi artmaktadır. Kırgız geleneksel fermente sütü "Ayran"dan üretilen yüksek viskoziteli bir süt ürünü olan Süzmö, süt endüstrisine kazandırılmalıdır. Bu çalışmada, bu eşsiz gıda ürününün reolojik parametreleri, kararlı ve dinamik reolojik deneylerde araştırılmıştır. Süzmönün akış davranışı altı sıcaklıkta (20, 30, 40, 50, 60 ve 70°C) değerlendirilmiştir. Akışkan akma gerilimi (τ_0) 32,64 Pa ile 285,87 Pa arasında değişen Newtonian olmayan bir psödoplastik akışkan olarak davranmıştır. 20 ve 30°C'de Süzmö numunelerinin akış eğrisi için en iyi uyum Bingham modeli uygulanarak bulunmuştur. Casson modeli korelasyon katsayıları R=0,9506 – 0,9973 ile 40, 50, 60 ve 70°C'deki akış eğrilerine uyan en uygun model olarak bulunmuştur. Sıcaklık artışıyla birlikte Süzmö'nün efektif viskozitesi 15,88'den 0,26 Pa·s'ye düşmüştür. Viskozitenin sıcaklığa bağımlılığı Arrhenius ilişkisine karşılık gelir ve aktivasyon enerjisi 61,66 kJ/(mol) olarak hesaplanmıştır. Nem içeriğinin ($p>0.05$) etkin viskozite ve akma gerilmesi üzerindeki etkisi dikkate alınarak doğrusal bir model tanımlanmıştır. Fermente süt örneklerinin termal denatürasyonunu belirlemek için 20 ila 80°C'de bir sıcaklık taraması gerçekleştirilmiştir. Ölçülen parametreler Süzmö'nün endüstriyel üretimi için çok önemlidir.

Edited by:
Ayşe Zeynep Hiçşaşmaz Katnaş

****Corresponding Author:***
Jayl Iskakova
janil.iskakova@gmail.com

ORCID iDs of the authors:
JI. orcid.org/0000-0002-1614-3984
JS. orcid.org/0000-0002-3929-4291

Key words:
Fermented food
Paste
Rheological properties
Viscosity
Flow activation energy

Introduction

Dairy products are considered as a main dietary source of minerals like calcium, magnesium, zinc, and B-complex vitamins such as B2, B5, B6, and B12 (Huth *et al.* 2006). Fermentation of food using various starter cultures is one of the oldest and widely used preservation methods (Aryama *et al.* 2016). In Kyrgyz cuisine, fermented milk Ayran is used in concentrated form. Süzmö is also a concentrated product made from fermented milk (yoghurt) using lactic acid bacteria and removing the whey portion. From the perspective of material science, Süzmö is a highly viscous, semisolid, and protein-rich pasty food. Other concentrated milk

products, in addition to Süzmö, are known to be consumed in most places of the world. Süzmö is made from cow, sheep, and goat milk and is well known in Turkey as Torba yoghurt, winter yoghurt, Tulum yoghurt, Pesküten, or Süzme (filtered yoghurt) (Güler & Sanal 2009, Kabak & Dobson 2011). According to Güler & Sanal (2009), the nutritional value of Torba yoghurts made using goat and sheep milks was characterized with 25.3-25.4% total solids, 9.9-10.9% crude protein, 7.5-9.0% fat, and 4.3-6.7% lactose content. The concentration of total solids increases approximately 2.5 times during filtration of yoghurt (Güler & Sanal 2009). In various countries of the Middle East and the Balkans, concentrated fermented milk is also widely used and called Labneh. Labneh, which has 22-26% total solids, is very popular in Europe and the USA as Greek yoghurt. Greek yoghurt has a solid content of about 26-33% (w/w) and contains 10 to 12 g of protein, whereas an identical serving of traditional yoghurt provides only about 5.2 g (Atamian *et al.* 2014, Costa *et al.* 2019). Greek yoghurt contains 5 to 8% carbohydrates, which is approximately half of the carbohydrates compared to traditional yoghurt (Phadungath 2015). As a healthier alternative, homemakers often used Greek and Greek-style yoghurts to replace cream cheese, sour cream, and mayonnaise. It is also possible to find other concentrated dairy products such as Ymer (Denmark), Skyr (Iceland), Tan or Than (Armenia), Shirkland and Chakka (India), and Leben Zeer (Egypt) (Tamime & Robinson 2007).

Süzmö is usually produced in very limited amounts at homes in rural areas of Kyrgyzstan. The production method of Süzmö is similar to the production of Turkish Torba yoghurt and consists of the following steps: milking, filtering, heating until 100°C and cooling down to 40°C. 2% of previous batches of fermented milk called Ayran is used as a sourdough and fermented for 5-6 h at 38-37°C. The obtained fermented milk is ready to consume as fresh Ayran, the rest is transferred to a cloth bag and filtered for several days to remove the whey (Kabak & Dobson 2011, Kamber 2008). Recently, ultrafiltration, centrifugation, and reverse osmosis methods have been recommended for producing concentrated yoghurt (Ozer 2006, Alirezalu *et al.* 2019).

In Kyrgyz cuisine, Süzmö is used as an additive to soups, for preparing a drink called Chalap, and mainly for the production of dried food products called Kurut. It is made in the form of balls or cylinders by hand pressing. Kurut is known in many countries under different names, for instance as Akçakatik, Keş, or Pestigen in Turkey (Kabak & Dobson 2011, Kamber 2008). In Tibet, China, fermented yak milk made by natural fermentation is also known as Kurut (Liu *et al.* 2011, 2012).

In recent years, Kurut has become popular and considered a snack food among most consumers, even among children. Given the growing consumer demand for Kurut production, it is very important to investigate the technological properties of Süzmö in order to obtain a consumer product with high quality. An important technological parameter of pasty foods is rheological properties as viscosity, flow index and elasticity. Consequently, processing parameters and product quality are mainly dependent on rheological properties (Fischer & Windhab 2011). There is sufficient data on chemical composition, microbiological and rheological properties, as well as processing parameters of concentrated yoghurt Labneh (Ozer *et al.* 1998, Abu-Jdayil *et al.* 2000, Abu-Jdayil & Mohameed 2002) and Torba yoghurt, but no information exists about Kyrgyz food Süzmö. Therefore, this research aimed to study the rheological properties of different samples of Süzmö using an absolute rheometer to optimize the domestic technological processes of Kurut.

Materials and Methods

Materials and sample preparation

Seven samples of Süzmö freshly produced from skimmed milk (protein content 8-9%) were purchased from a local market in Bishkek. All samples were kept in plastic bags (500 g) in a refrigerator at 4-6°C until rheological measurements.

Chemical analysis

Titratable acidity, pH, and moisture content of the samples were investigated according to the methods of AACC International (AACC 2019). For measurement of the pH values of the samples, a pH meter SevenCompact S210 (Mettler Toledo, Greifensee, Switzerland) was used. Titratable acidity was measured by potentiometric titration with NaOH (0.1 M) and calculated as the percentage of lactic acid. Dry matter content was calculated by the difference. The measured physicochemical parameters are given in Table 1.

Rheological measurements

The rheological parameters of Süzmö samples were measured on the rheometer MCR 302 (Anton Paar, Graz, Austria) equipped with a concentric cylinder CC27. All measurements were conducted after equilibration of temperature at 20, 30, 40, 50, 60, and 70°C. The steady shear viscosity measurements were carried out in up and down regimes: 1) the shear rate gradually increased linearly from 0.1 to 50 s^{-1}; 2) the shear rate was constant at 50 s^{-1}; 3) the shear rate was decreased from 50 to 0.1 s^{-1}. The area between up and down curves is calculated as the hysteresis area (in Pa/s).

Table 1. Some physicochemical parameters of Süzmö.

Sample	Moisture (%)	Solid content (%)	pH	Titratable acidity (g/100 g)
1	68.18	31.82	3.27	3.48
2	78.90	21.10	3.80	5.27
3	71.50	28.50	3.78	5.76
4	72.00	28.00	3.76	6.57
5	69.20	30.80	3.81	3.48
6	72.00	28.00	3.79	3.47
7	77.50	22.50	4.80	3.72
Average	72.75	27.25	3.86	4.54
SD	3.71	3.71	0.42	1.21

The flow curves obtained in the 3rd interval were modelled using classical equations such as Bingham (1) and Casson (2):

$$\tau = \tau_0 + \eta_{Bp} \cdot \dot{\gamma} \quad (1)$$

where τ_0 is the yield stress, $\dot{\gamma}$ is the shear rate, η_{Bp} Bingham plastic viscosity, n is the flow behaviour index in the Bingham model.

Casson model:

$$\tau^{0.5} = \tau_0^{0.5} + \eta_{Ca} \cdot \dot{\gamma}^{0.5} \quad (2)$$

where η_{Ca} is Casson's coefficient of viscosity or is the infinite shear viscosity.

The activation energy E_a (J/mol) was calculated at maximum shear stress ($\dot{\gamma}$ max = 50 s^{-1}) according to the Arrhenius-type relationship (Eq. 3) at the temperature range 40 - 70°C, as described in Iskakova *et al.* (2019):

$$\eta = Aexp\left(-\frac{E_a}{RT}\right) \quad (3)$$

where A is the constant, R is the ideal gas constant (8.31 J/mol·K), T is the absolute temperature (K) (Steffe 1996).

Viscoelastic behaviour

Curing (denaturation) temperatures of the samples were studied in an oscillatory temperature-sweep experiment in a linear viscoelastic range (LVE) at a strain γ of 10^{-3}% and the angular frequency of 1 Hz as described in Smanalieva & Senge (2009). The temperature of the samples was increased with a heating rate of 0.5°C/min from 20 to 80°C. The measured elastic G′ and loss G″ moduli provide detailed information on the material elasticity (stored energy in the form of deformation) and viscosity (energy dissipation as heat by internal friction). The curing temperatures according to the oscillatory measurements were determined by the loss factor tan δ:

$$\tan \delta = G''/G' \quad (4)$$

Thus, the values of tan δ above 1 indicate more viscous flow behaviour, while any value below 1 is related to the elastic network response (Steffe *et al.* 2013).

Statistical analysis

SPSS software (SPSS Inc., Chicago, IL) was used for regression analysis to model the influence of moisture content on rheological parameters. The RHEOPLUS V 3.61 software (Anton Paar, Ostfildern, Germany) was used for the regression analysis of rheological data to model flow behaviour of Süzmö. All parameters were measured three times.

Results and Discussion

Effect of shear rate on rheological parameters

The viscosity of yoghurt depends on both shear and time effects (Benezech & Maingonnat 1994). The relationship between the dynamic viscosity of Süzmö and the shear rate shows strong shear thinning behaviour (Fig. 1) with high magnitudes of yield stresses (τ_0) at all investigated temperatures (Fig. 2). The flow properties of Labneh with a total solids content of about 23% have previously been described as a shear-thinning fluid (Abu-Jdayil *et al.* 2000). According to Ozer *et al.* (1998), shear-thinning behaviour occurs due to the progressive destruction of aggregates of casein molecules. The shear-thinning flow curves of yoghurt Labneh and other dairy products (e.g., stirred yoghurt and dairy desserts) were described with power-law equation known also as Ostwald - de Waele (Abu-Jdayil *et al.* 2002, Abu-Jdayil *et al.* 2000), and the Herschel-Bulkley model (Karlsson *et al.* 2005). In the current study, the regression analysis of the flow curves for all Süzmö samples was performed according to classical rheological models, such as Herschel-Bulkley, Bingham, and Casson models. The Casson model provided the best fit at 40, 50, 60, and 70°C (R = 0.994-0.997) and the Bingham model provided the best fit at 20 and 30°C (R = 0.9676-0.9890). Therefore, the structure of Süzmö can be classified as semi-solid (Casson) and similar to a plastic fluid (Bingham). The measured and calculated rheological parameters are given in Table 2.

Table 2. Measured and calculated rheological parameters of Süzmö.

T (°C)	Model	τ_0 (Pa)	η_{Bp} or η_{Ca} (Pa·s)	n (-)	R	SD	A_{TH} (Pa/s)	$\eta_{eff\ (50/s)}$ (Pa·s)
20	Bingham	285.87	9.36	1.0	0.9949	6.25	32966.37	15.08
30	Bingham	183.75	4.58	1.0	0.9890	3.30	2655.87	8.25
40	Casson	87.77	1.01	0.5	0.9837	2.38	2274.50	1.90
50	Casson	73.51	0.77	0.5	0.9967	0.76	2562.96	1.58
60	Casson	66.78	0.47	0.5	0.9975	0.42	904.59	1.40
70	Casson	27.51	0.74	0.5	0.9978	0.51	1090.99	0.65
80	Casson	32.64	0.62	0.5	0.90	1.96	225.42	0.74

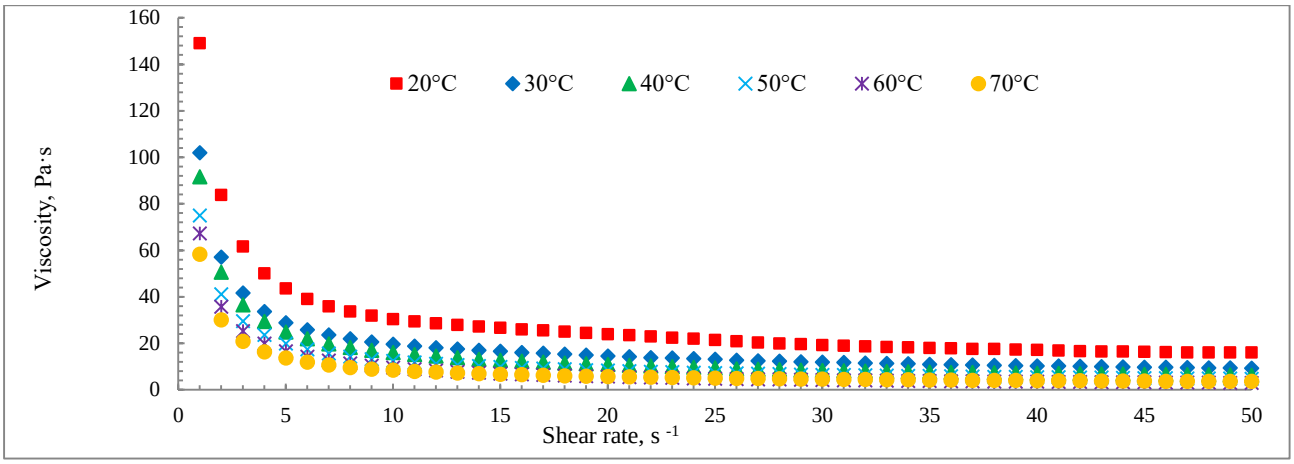

Fig. 1. Dynamic viscosity vs shear rate at 20-70°C.

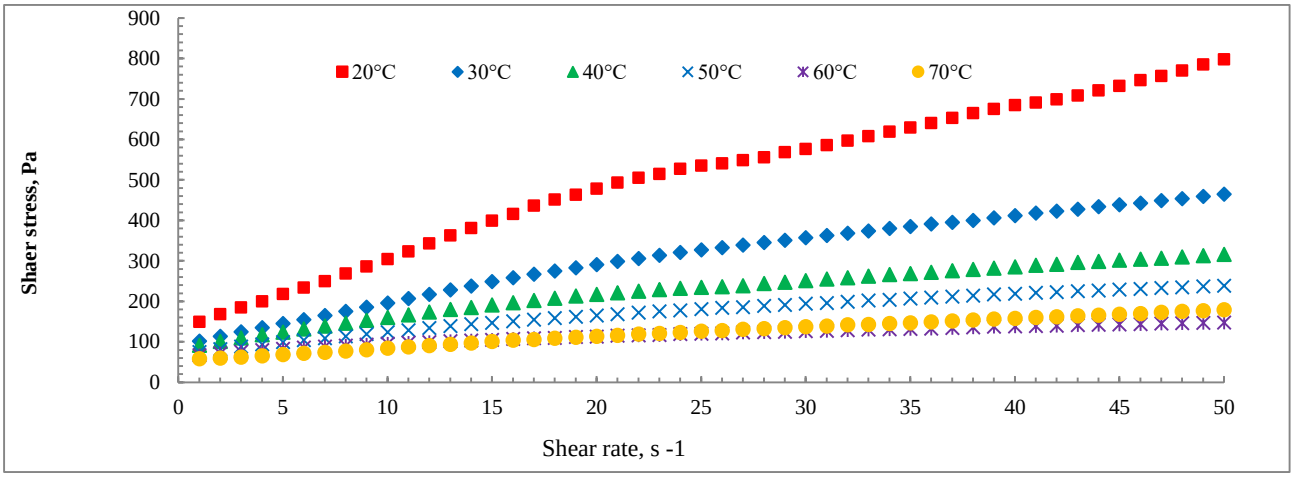

Fig. 2. Shear stress vs shear rate at 20-70°C.

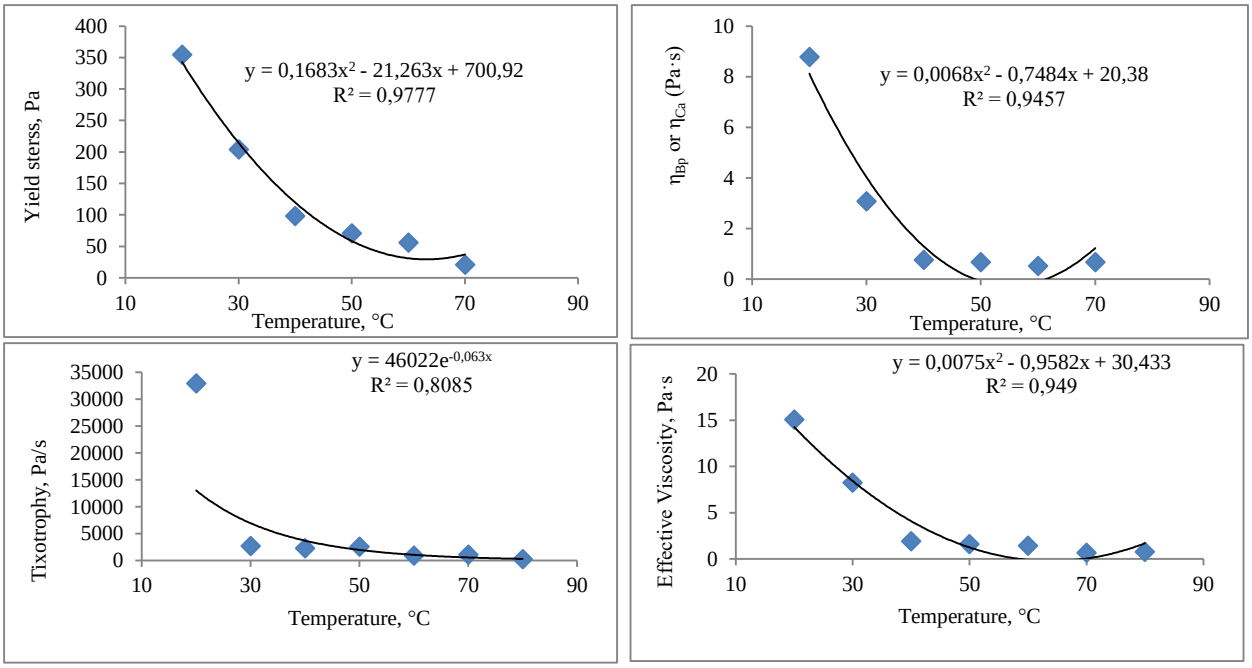

Fig. 3. Temperature effect on yield stress and Bingham η_{Bp} or Casson viscosity η_{Ca} with rheological parameters.

Temperature dependence of rheological parameters

The temperature influence on rheological parameters is shown in Fig. 3. An increase in temperature from 20 to 80°C leads to a change in both rheological parameters: the Bingham (η_{Bp}) or Casson viscosity (η_{Ca}) drop from 8.78 to 0.67 Pa·s and yield stress (τ_0) - from 285.87 to 32.64 Pa. Accordingly, the effective viscosity, calculated at a shear rate of 50 s^{-1}, decreased from 15.88 to 0.26 Pa·s. Abu-Jdayil *et al.* (2002) reported that the viscosity of the Labneh decreases linearly with increasing temperature. Other researchers also reported that the rheological parameters of food materials with the same dry matter content, such as ketchup (Sharoba *et al.* 2005, Juszczak *et al.* 2013), milk concentrates (Sauer *et al.* 2012), or cereal porridges (Iskakova *et al.* 2017) also depend on temperature.

The influence of temperature on the viscosity of food materials, including concentrated dairy products, is usually described using an Arrhenius-type relationship (Sauer *et al.* 2012). To obtain the activation energy of Eq. (3), a linear plot of ln(η_{eff}) versus l/T was plotted (Fig. 4). According to the obtained Eq. from the diagram ln (η_{eff}) = 7417.5·(1/T) - 22.4, the activation energy was calculated as follows: E_a = 61.66 kJ/(mol). On contrary, E_a values for Labneh were lower 2l.26 kJ/mol (Abu-Jdayil *et al.* 2000, Abu-Jdayil *et al.* 2002), for the micellar casein concentrates with reduced 65 and 95% serum protein were in the ranges of 15.1 to 49.9 and 15.8 to 46.2 kJ/mol, respectively (Sauer *et al.* 2012). Krokida *et al.* (2001) revealed that in foods with Newtonian flow behaviour, the activation energy ranges from 14.4 kJ/mol (water) to over 60 kJ/mol (concentrated juices and sugar solutions) (Krokida *et al.* 2001). The value of the pre-exponential parameter A for Süzmö was obtained as 7417.5. This parameter A indicates the internal resistance of the fluid to flow, which is not affected by temperature (Goh 2010). According to Iskakova & Smanalieva (2020), the activation energy (E_a) and coefficient A for high-fat dairy food Sary mai were 26.3-29.9 KJ/mol and 0.0002-0.00004, respectively.

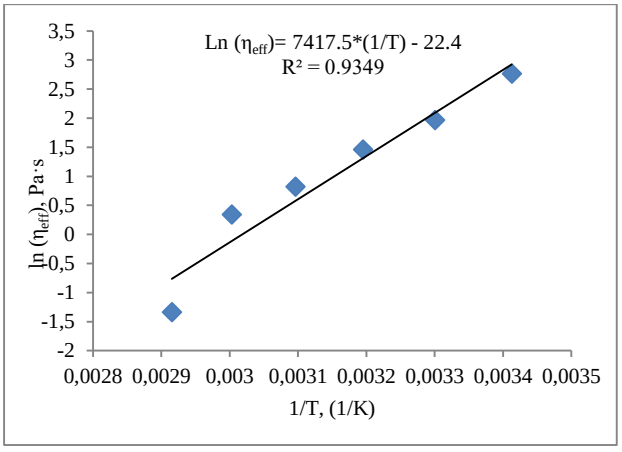

Fig. 4. Arrhenius-type model fit for Süzmö.

Increasing the solids concentration in fermented milk improves the gel formation as a result of the interaction of protein molecules (Mohameed *et al.* 2004). For mathematical modelling, linear (Eq. 5) and exponential equations (Eq. 6-7) were proposed for the dependence of rheological properties of concentrated milk on the solids content (Reddy & Datta 1994, Vélez-Ruiz & Barbosa-Cánovas 2000):

$$n = AX+b \quad (5)$$

$$n = A_n \exp^{bnX} \quad (6)$$

$$K = A_k \exp^{bkX} \quad (7)$$

where n is the flow behaviour index, X is the solid concentration (X w/w), K is the consistency coefficient (Pa·s^n), and A, b are constants (Vélez-Ruiz & Barbosa-Cánovas 2000).

The moisture contents of the investigated Süzmö samples ranged from 68.18 to 77.55%, thus the average moisture content (W) was 73.28% w/w. For mathematical modelling of the dependence of rheological parameters on temperature and moisture content, the linear regression analysis was carried out using the SPSS software. The relationship between moisture content, yield stress, and effective viscosity for all tested Süzmö samples can be expressed by Eq. 8:

$$W=70.28+0.56\tau_0-0.79\eta_{eff} \quad (8)$$

where W is the moisture content (% w/w), τ_0 is the yield stress (Pa), and η_{eff} is the effective viscosity (Pa·s) calculated at a shear rate of 50 s^{-1}. Thus, it can be stated that the rheological parameters of concentrated fermented milk Süzmö also depend on the moisture content.

Determination of curdling/denaturation temperature of Süzmö (Temperature-Sweep)

Fig. 5 shows changes in elastic (G´) and loss (G″) moduli depending on temperature. The G' is greater than the G″, consequently, tan δ is below 1, Süzmö can be classified as a viscoelastic gel system. The G´ and G″ values increase with decreasing temperature to 60°C. Above 60°C, structural compaction or hardening of the gel occurs, with the G´ modulus remaining stable and G″ further decreasing, indicating that Süzmö in the temperature scale becomes stronger and the number of individual protein-protein interactions increase due to heating. Ozer *et al.* (1999) stated that the gel strength of Labneh measured using amplitude- and frequency-sweep modes is mainly dependent on protein content (Ozer *et al.* 1999, Nsabimana *et al.* 2005). According to Lee & Lucey (2004), heating provides energy to increase the entropy of the system, allowing proteins to accept intermediate structures that are important for protein-protein interactions (Lee & Lucey 2004). Thus, the result of the temperature sweep showed that the temperature of Süzmö should be below 60°C to avoid a hard consistency of the final product Kurut.

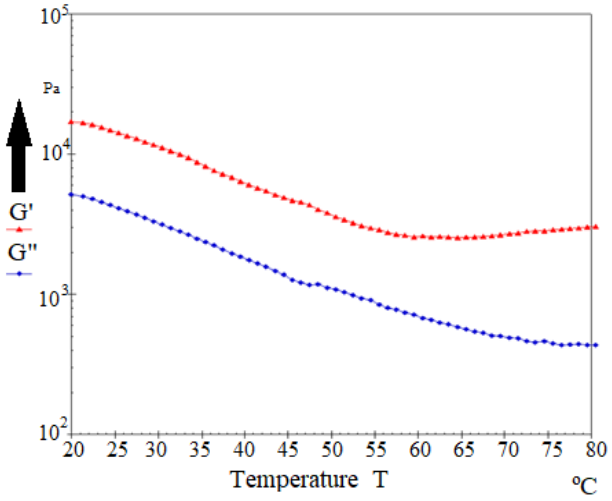

Fig. 5. Temperature-sweeps of Süzmö (heating from 20 to 80°C).

Conclusion

Seven batches of protein-rich food product Süzmö were tested to understand the dependence of rheological parameters on temperature and moisture content. The values of the rheological parameters such as consistency coefficient, yield stress, and apparent viscosity of the tested samples decreased with increasing temperature. Temperature dependence of effective viscosity was calculated using an Arrhenius-type equation. The linear regression analysis was carried for modelling the effect of moisture content ($p>0.05$) on rheological parameters such as effective viscosity and yield stress. The temperature sweep revealed that Süzmö can be classified as a typical viscoelastic gel system. When heated above 60°C, the gel hardens, so the recommended drying temperature should be below 60°C, to avoid a hard consistency of Kurut. The parameters obtained can be used by food manufacturers to control the quality of Süzmö and Kurut.

Ethics Committee Approval: Since the article does not contain any studies with human or animal subject, its approval to the ethics committee was not required.

Author Contributions: Concept: J.I., J.S., Desing: J.I., J.S., Execution: J.I., J.S., Material supplying: J.I., J.S., Data acquisition: J.I., J.S., Data analysis/interpretation: J.I., J.S., Writing: J.I., J.S., Critical review: J.I., J.S.

Conflict of Interest: The authors have no conflicts of interest to declare.

Funding: The authors declared that this study has received no financial support.

References

1. AACC. 2019. *Official Methods of Analysis*, 21st Edition - AOAC International.
2. Abu-Jdayil, B., Jumah, R. & Shaker, R. 2002. Rheological properties of a concentrated fermented product, labneh, produced from bovine milk: Effect of production method. *International Journal of Food Properties*, 5(3): 667-679.
3. Abu-Jdayil, B., Shaker, R. & Jumah, R.2000. Rheological behavior of concentrated yogurt (Labneh). *International Journal of Food Properties*, 3(2): 207-216.
4. Abu-Jdayil, B. & Mohameed, H. 2002. Experimental and modelling studies of the flow properties of concentrated yogurt as affected by the storage time. *Journal of Food Engineering*, 52(4): 359-365.
5. Alirezalu, K., Inácio, R. S., Hesari, J., Remize F., Nematia, Z., Saraiva, J. A., Barba, F.J, Sant'Ana, A. S. & Lorenzo, J.M. 2019. Nutritional, chemical, syneresis, sensory properties and shelf life of Iranian traditional yoghurts during storage. *LWT - Food Science and Technology*, 114: 108417.
6. Aryama, M, Nöbel, S. & Hinrichs, J. 2016. Post-processing of fermented milk to stirred products: Reviewing the effects on gel structure. *Trends in Food Science and Technology*, 54: 26-36.
7. Atamian, S., Olabi, A., Kebbe Baghdadi, O. & Toufeili, I. 2014. The characterization of the physicochemical and sensory properties of full-fat, reduced-fat and low-fat bovine, caprine, and ovine Greek yogurt (Labneh). *Food Science and Nutrition*, 2(2): 164-173.
8. Benezech, T. & Maingonnat, J.F. 1994. Characterization of the rheological properties of yoghurt-A review. *Journal of Food Engineering*, 21(4): 447-472.
9. Costa, M.F., Pimentel, T.C., Guimaraes, J.T., Balthazar, C.F., Rocha, R.S., Cavalcanti, R.N., Esmerino, E.A., Freitas, M.Q., Raices, R.S.L., Silva, M.C. & Cruz, A.G. 2019. Impact of prebiotics on the rheological characteristics and volatile compounds of Greek yogurt. *LWT - Food Science and Technology*, 105: 371-376.
10. Fischer, P. & Windhab, E.J. 2011. Rheology of food materials. *Current Opinion in Colloid & Interface Science*, 16(1): 36-40.
11. Goh, E.G. 2010. The hidden property of Arrhenius-type relationship: viscosity as a function of temperature. *Journal of Physical Science*, 21(1): 29-39.
12. Güler, Z. & Şanal, H. 2009. The essential mineral concentration of Torba yoghurts and their wheys compared with yoghurt made with cows', ewes' and goats' milks. *International Journal of Food Sciences and Nutrition*, 60(2): 153-164.
13. Huth, P.J., DiRienzo, D.B. & Miller, G.D. 2006. Major Scientific Advances with Dairy Foods in Nutrition and Health, *Journal of Dairy Science*, 89(4): 1207-1221.
14. Iskakova, J., Smanalieva, J., Kulmyrzaev, A., Fischer, P. & Methner, F.-J. 2017. Comparison of rheological and colorimetric measurements to determine α-amylase activity for malt used for the beverage Bozo. *International Journal of Food Properties*, 20(9): 2060-2070.
15. Iskakova, J., Smanalieva, J. & Methner, F.-J. 2019. Investigation of changes in rheological properties during processing of fermented cereal beverages. *Journal of Food Science and Technology*, 56(9): 3980-3987.

16. Iskakova, J. & Smanalieva, J. 2020. Investigation of rheological behavior of Kyrgyz traditional food Sary mai. *Manas Journal of Engineering*, 8(2): 84-89.

17. Juszczak, L., Oczadły, Z. & Gałkowska, D. 2013. Effect of modified starches on rheological properties of ketchup. *Food and Bioprocess Technology*, 6(5): 1251-1260.

18. Kabak, B. & Dobson, A.D.W. 2011. An introduction to the traditional fermented foods and beverages of Turkey. *Critical Reviews in Food Science and Nutrition*, 51(3): 248-260.

19. Kamber, U. 2008. The manufacture and some quality characteristics of kurut, a dried dairy product. *International Journal of Dairy Technology*, 61(2): 146-150.

20. Karlsson, A.O., Ipsen, R., Schrader, K. & Ardo, Y. 2005. Relationship between physical properties of casein micelles and rheology of skim milk concentrate. *Journal of Dairy Science*, 88: 3784-3797.

21. Krokida, M. K., Maroulis, Z.B. & Saravacos, G.D. 2001. Rheological properties of fluid fruit and vegetable puree products: compilation of literature data, *International Journal of Food Properties*, 4(2): 179-200.

22. Ozer, B. 2006 Production of concentrated products. Pp. 128-155. In: *Tamime (ed): Fermented milks.* Blackwell Publishing Ltd Oxford, United Kingdom, 250 pp.

23. Lee, W.J. & Lucey, J.A. 2004. Structure and physical properties of yogurt gels: effect of inoculation rate and incubation temperature. *Journal of Dairy Science*, 87(10): 3153-3164.

24. Liu, S., Han, Y. & Zhou, Z. 2011. Lactic acid bacteria in traditional fermented Chinese foods. *Food Research International*, 44(3): 643-651.

25. Liu, W.J., Sun, Z.H., Zhang, Y.B., Zhang, C.L., Menghebilige, Yang, M., Sun, T.S., Bao, Q.H., Chen, W. & Zhang, H.P. 2012. A survey of the bacterial composition of kurut from Tibet using a culture-independent approach. *Journal of Dairy Science*, 95(3): 1064-1072.

26. Mohameed, H.A., Abu-Jdayil, B. & Al-Shawabkeh, A. 2004. Effect of solids concentration on the rheology of labneh (concentrated yogurt) produced from sheep milk. *Journal of Food Engineering*, 61(3): 347-352.

27. Nsabimana, C., Jiang, B. & Kossah, R. 2005. Manufacturing, properties and shelf life of labneh: a review, *International Journal of Dairy Technology*, 8: 129-137.

28. Ozer, B.H., Bell, A.E., Grandison, A.S. & Robinson, R.K. 1998. Rheological properties of concentrated yoghurt (Labneh). *Journal of Texture Studies*, 29(1): 67-79.

29. Ozer, B. 2006. Production of concentrated products. Pp. 128-155. In: *Tamime (ed): Fermented milks.* Blackwell Publishing Ltd Oxford, United Kingdom, 250 pp.

30. Ozer, B.H., Stenning, R.A., Grandison, A.S. & Robinson, R.K. 1999. Rheology and microstructure of Labneh (Concentrated Yogurt). *Journal of Dairy Science*, 82(4): 682-689.

31. Phadungath, C. 2015. Greek-style yogurt and its application in cheesecake. *International Journal of Food Engineering*, 1: 13-17.

32. Reddy, C.S. & Datta, A.K. 1994. Thermophysical properties of concentrated reconstituted milk during processing. *Journal of Food Engineering*, 21(1): 31-40.

33. Sauer, A., Doehner, I. & Moraru, C.I. 2012. Steady shear rheological properties of micellar casein concentrates obtained by membrane filtration as a function of shear rate, concentration, and temperature. *Journal of Dairy Science*, 95(10): 5569-5579.

34. Sharoba, A.M., Senge, B., El-Mansy, H.A., Bahlol, H.E. & Blochwitz, R. 2005. Chemical, sensory and rheological properties of some commercial German and Egyptian tomato ketchups. *European Food Research and Technology*, 220(2): 142-151.

35. Smanalieva, J. & Senge, B. 2009. Analytical and rheological investigations into selected unifloral German honey. *European Food Research and Technology*, 229(1): 107-113.

36. Steffe, J.F. 1996. *Rheological methods in food process engineering*. Second Edition. Freeman Press, East Lansing, 428 pp.

37. Tamime, A.Y. & Robinson, R.K. 2007. Historical background. Pp.1-12. In: Tamime, A.Y. & Robinson, R.K. (eds). *Tamime and Robinson's Yoghurt: Science and Technology.* Woodhead Publishing Limited, Boca Raton, 791 pp.

38. Vélez-Ruiz, J.F. & Barbosa-Cánovas, G.V. 2000. Flow and structural characteristics of concentrated milk. *Journal of Texture Studies*, 31(3): 315-333.

http://dergipark.org.tr/trkjnat
Trakya University Journal of Natural Sciences, 22(2): 207-213, 2021
ISSN 2147-0294, e-ISSN 2528-9691
DOI: 10.23902/trkjnat.974130

Research Article

PHENOLOGICAL BEHAVIOURS OF THE LOCAL ENDEMIC *Paeonia mascula* (L.) Mill. subsp. *bodurii* Özhatay IN ÇANAKKALE, TURKEY

Bahar KÖKÇÜ, Ersin KARABACAK*

Department of Biology, School of Graduate Studies, Çanakkale Onsekiz Mart University, Çanakkale, TURKEY

Cite this article as:

Kökçü B & Karabacak E. 2021. Phenological behaviours of the local endemic *Paeonia mascula* (L.) Mill. subsp. *bodurii* Özhatay in Çanakkale, Turkey. *Trakya Univ J Nat Sci*, 22(2): 207-213, DOI: 10.23902/trkjnat.974130

Received: 25 July 2021, Accepted: 06 September 2021, Online First: 03 October 2021, Published: 15 October 2021

Edited by:
Mykyta Peregrym

Corresponding Author:
Ersin Karabacak
krbersin@comu.edu.tr

ORCID iDs of the authors:
BK. orcid.org/0000- 0002-5349-7263
EK. orcid.org/0000- 0002-5784-6803

Key words:
Conservation biology
Çanakkale
Local endemic
Paeonia mascula subsp. bodurii
Phenology
Turkey

Abstract: This study covers the observation, recording and interpretation of the phenological behaviour of the local endemic *Paeonia mascula* (L.) Mill. subsp. *bodurii* Özhatay in its life cycle. Although phenological observations are mostly applied on cultivated plants, the data obtained from this study on an endemic taxon constitute an important resource for the preparation of a conservation action plan. While the phenological cycle time of the geophyte plant on the ground is determined as 206 days on average, it spends the winter months in dormancy with an average of 159 days underground. It was determined that the populations at lower altitudes in their natural habitats entered the flowering, fruit formation and seed maturation stages relatively earlier than those grown at higher altitudes and remained in these phenophases for longer periods. The total life cycle was more or less the same, although there were differences in phenophases durations and beginnings-ends.

Özet: Bu araştırma, lokal endemik *Paeonia mascula* (L.) Mill. subsp. *bodurii* Özhatay'ın yaşam döngüsü içerisindeki fenolojik davranışlarının gözlemlenmesini, kaydedilmesini ve yorumlanmasını kapsamaktadır. Fenolojik gözlemler çoğunlukla kültür bitkileri üzerinde uygulanmakla birlikte, endemik bir taksonunun üzerinde yapılan bu çalışmadan elde edilen veriler, koruma eylem planı hazırlanmasında önemli bir kaynak oluşturmaktadır. Geofit olan bitkinin toprak üstünde geçirdiği fenolojik döngü süresi ortalama 206 gün olarak tespit edilirken, kış aylarını toprak altında ortalama 159 gün olarak dormanside geçirmektedir. Doğal habitatlarında daha düşük rakımlarda bulunan populasyonların yüksek rakımlarda yetişenlere göre çiçeklenme, meyve oluşturma ve tohum olgunlaşması gibi evrelere nispeten daha erken bir dönemde girdiği ve bu fenofazlarda daha uzun süreli kaldığı belirlenmiştir. Fenofaz sürelerinin, başlangıç-bitişlerinde fark olmasına rağmen toplam yaşam döngüsünün aşağı yukarı aynı olduğu görülmüştür.

Introduction

Climate is the most important complex of ecological factors affecting the main character and distribution areas of plants and plant communities in the world (Daysal 2013). The collective effects of climatic elements such as temperature, humidity, precipitation, wind and light play an important role in both the distributions and life cycles of organisms. Phenology (derived from the Greek word "phainein or Phainestai" meaning 'to show' or 'appear') is a science that studies the repetition times of natural events (Fenner 1998). The duration and time of these natural events vary according to changes in climatic conditions particularly depending on temperature, humidity, precipitation amount and insolation times of plants (Topal 2020).

The results obtained from phenological observations and their long-term averages are very important for a country's agriculture and economy. The averages of phenological observations are the values that should be taken into account in the selection or breeding of crop plants that can best adapt to the climatic conditions of any region (Şimşek *et al.* 2014). Therefore, most of the scientific studies have focused on the phenological observations of agricultural plants. On the other hand, the number of studies revealing the relationship between phenology and the conservation of endemic and rare plants is not too much in number. Endemic and rare plants are species that can be more sensitive and vulnerable to changes in environmental conditions compared to other species. Therefore, the priority of the studies to be carried out should be to determine the phenological characteristics of these sensitive species and to evaluate their results in the preparation of species protection action plans. However, the effects of

phenology on conservation biology and nature management have not yet been adequately studied on a global scale (Morellato *et al.* 2016).

The genus *Paeonia* L. belongs to the *Paeoniaceae* family, and it has 52 taxa under 36 species in the world (The Plant List 2021). *Paeonia* is divided into three sections: sect. *Moutan* DC. (woody or tree peonies, all in China), sect. *Onaepia* Lindl. (the two species restricted to North America) and sect. *Paeonia* (herbaceous peonies, 22 species distributed in Europe, North Africa and Asia) (Hong 2010). All Turkish species belong to the sect. *Paeonia*. In the first volume of "Flora of Turkey and the East Aegean Islands", 6 species were listed from the genus *Paeonia* (Davis & Cullen 1965). In volume 10 published in 1988, *P. wittmanniana* Hartwiss. ex Lindl., and in volume 11 published in 2000 *Paeonia mascula* (L.) Mill. subsp. *bodurii* Özhatay and *P. tenuifolia* L. were published (Davis 1988, Özhatay 2000). There are 6 species and 8 under species taxa reported in the latest available checklist, in Turkey (Körüklü 2012). Among these taxa, only *Paeonia mascula* subsp. *bodurii*, are indicated as endemic (Körüklü 2012).

Paeonia mascula subsp. *bodurii* was described by Özhatay in 1995 as a new subspecies from NW Turkey (Çanakkale province). *Paeonia mascula* is a highly variable species, the leaves are ternately or pinnately compound. This subspecies is very closely related to subsp. *hellenica* Tzanoud., which is distributed in Greece, but it differs from it by its mostly ternate upper cauline leaves, the central and lateral primary segments of the leaves having only 3 (undivided) leaflets, whereas subsp. *hellenica* usually has 9 uppermost leaflets (Özhatay & Özhatay 1995).

When the taxon was first published, it was known from only one locality. The IUCN threatening category of the taxon is given as EN (Ekim *et al.* 2000). However, in later field studies performed by us, it was determined that the taxon was also naturally distributed in different localities within the Çanakkale province (Kökçü & Karabacak 2020). Although the area of the extend of occurrence of the subspecies has expanded with these new localities, the area of occupancy is still rather low. This endemic peony is under high pressure from deforestation, road constructions, wind power plants, mining operations and illegal plant gatherings, and their populations are increasingly negatively affected. Due to lack of information about the phenological behaviour of this highly threatened taxon needed for developing a conservation strategy, the present study was performed with conservation prospective. Phenological observations, together with what can be done on this taxon and other taxa in the future, will both contribute to the conservation of the species and will be an important data source in the monitoring of possible effects of climate changes.

Materials and Methods

The study area

The study was carried out during the vegetation seasons between 2018-2021. During field studies, four localities in Çanakkale province, which is the only natural distribution of *Paeonia mascula* subsp. *bodurii*, were surveyed for assessing the distribution and growth of the taxon (Fig. 1). These are Ağı Mountain (921 m), Kiraztaşı (Üçpınar) (720 m), Beşiktepe (Karamusalar) (454 m) and Aşağıçavuş (440 m).

The climate is warm and of temperate Mediterranean type in Çanakkale. Rainfall in the province is mostly in winter months, while it is relatively less rainy in summer. The annual average temperature is 15.1°C and the amount of precipitation per year is 624 mm (Table 1).

The driest month is August, with 9.4 mm of rainfall. In December, the precipitation reaches its peak, with an average of 105.4 mm. The warmest month of the year is July, with an average temperature of 25.1°C, and January is the coldest month with 6.2°C on average (Table 1).

Phenological Observations

No tools or devices are used during phenology observations (Şimşek *et al.* 2014). Instead, the intensities of phenological events are semi-quantitatively determined and recorded in the field for each phenological stage. Weekly visits were made to the four study areas, and phenological observations on selected plants were recorded in terms of sprouting, bud formation, anthesis, fruiting, seed maturation and senescence.

The phenophase calendars of the taxon at four different altitudes in Çanakkale were determined, and the beginning and ending dates of the phenological periods were recorded. In addition, the phenophase times of the individuals in each population were recorded, so the total phenological cycle times that could occur with altitude and latitude variation were calculated. Fertile plant samples randomly selected for each locality (10-30 individuals selected depending on the population density at the locality) were tagged and monitored throughout the growing season. For the Ağı Mount, where optimum conditions are best, the number of individuals in the population is very high, but the Aşağıçavuş site is the southernmost place where the plant can live, and the number of individuals here is relatively low. For this reason, differences in the number of individuals between locations were used in the selection of the studied sample.

The time between the first date of aerial shoot emergence and the last date of senescence were considered for calculation of the active periods of the taxon.

Coordinates were taken from the Global Positioning System (GPS) device for each locality and the distribution map of the taxon was prepared in ArcView 10.5 software. Photos were taken with Canon 750 D model.

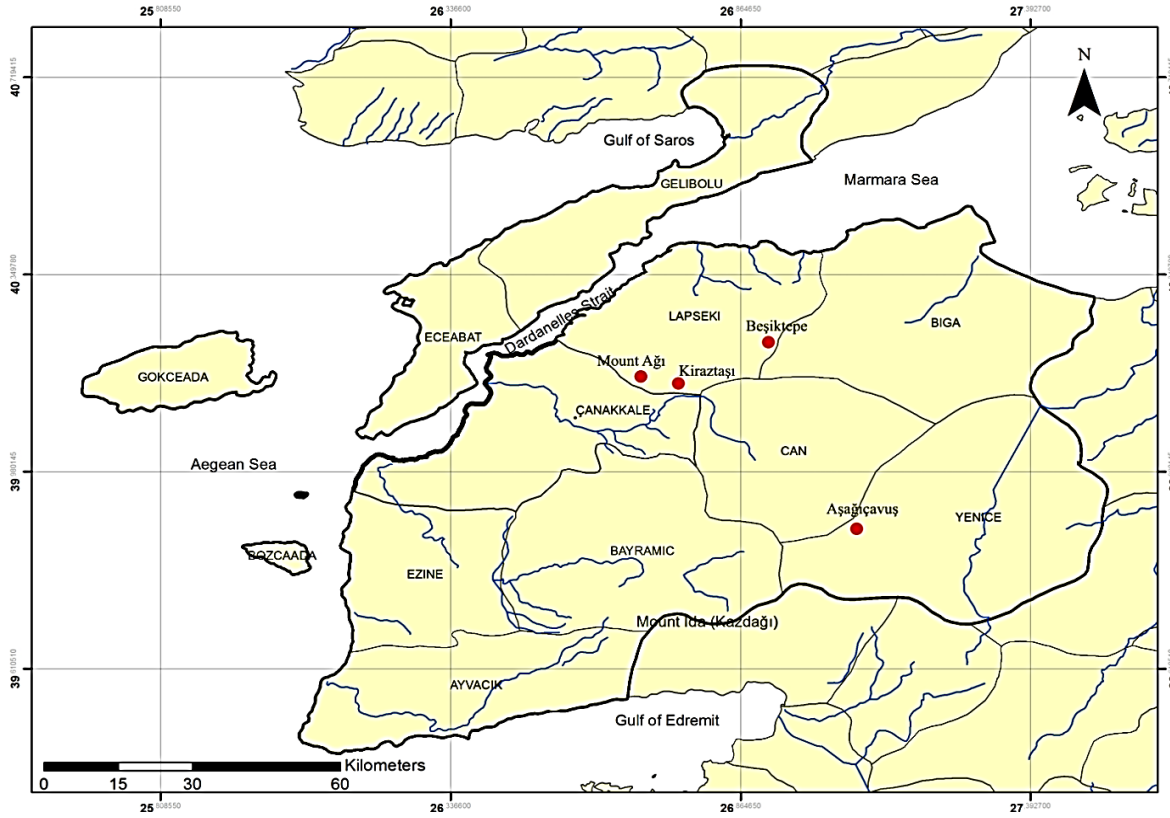

Fig. 1. Distribution map of *Paeonia mascula* subsp. *bodurii* in Çanakkale. Solid red circles denote the localities where the taxon was recorded so far.

Table 1. Long-term climate data table for Çanakkale province between 1929-2020 (Meteorological Service 2021).

	Jan	Feb	Mar	Apr	May	Jun	Jul	Aug	Sep	Oct	Nov	Dec	Annual
Average Temp. (°C)	6.2	6.7	8.4	12.6	17.5	22.2	25.1	25.0	21.1	16.3	12.0	8.4	15.1
Average Max. Temp. (°C)	9.6	10.2	12.5	17.2	22.6	27.7	30.7	30.6	26.4	20.8	15.9	11.7	19.7
Average Min. Temp. (°C)	3.1	3.4	4.7	8.3	12.7	16.6	19.3	19.6	16.0	12.1	8.5	5.3	10.8
Average Precipitation (mm)	91.6	71.7	65.9	45.0	29.8	25.3	14.5	9.4	25.2	55.3	84.9	105.4	624.0

Results

Seven phenological stages including sprouting phase, vegetative phase, bud formation, flowering phase, fruiting phase, seed maturation phase and senescence were observed (Fig. 2). These phenological stages were monitored in all four selected natural populations. This investigation revealed that the plant species entered the vegetative and reproductive stages relatively earlier with the decrease in altitude and the life cycles were longer (Fig. 3).

During the field studies, *Paeonia mascula* subsp. *bodurii* was determined to lived naturally in Ağı Mountain (921 m), Kiraztaşı (Üçpınar) (720 m), Beşiktepe (Karamusalar) (454 m) and Aşağıçavuş (440 m). The plant retreats underground during the fall (by 9 October at the latest) and goes dormant during the winter months (Table 2).

The first plant sprouts in the studied populations started in the 2nd week of March and continued until the end of the 1st week of April. In the mature plants, after the completion of the sprouting stage, the plant started the vegetative phase where flower buds formed. Bud formation began in the last days of March and continued until the last week of April. The anthesis began in the 2nd week of April and continued until the 3rd week of May. The flowers remained active for approximately 6-10 days, depending on the air temperature and precipitation. In the middle of the flowering period, the plant began to bear fruit, and towards the end of the fruiting period, and immature seeds began to appear. Fertile seeds began to mature in the 1st week of June and maturation continued until the 2nd week of August. Senescence and withdrawal of air shoots began in the 3rd week of August and lasted until the 2nd week of October. Thus, the phenological cycle period of the taxon was calculated as 206 days on average. Although the phenophase durations are somewhat prolonged with the lowering of the altitude, the total life cycle is more or less the same in the general perspective (Fig. 4). The geophyte endemic plant spends its winter months underground in dormancy in an average of 159 days.

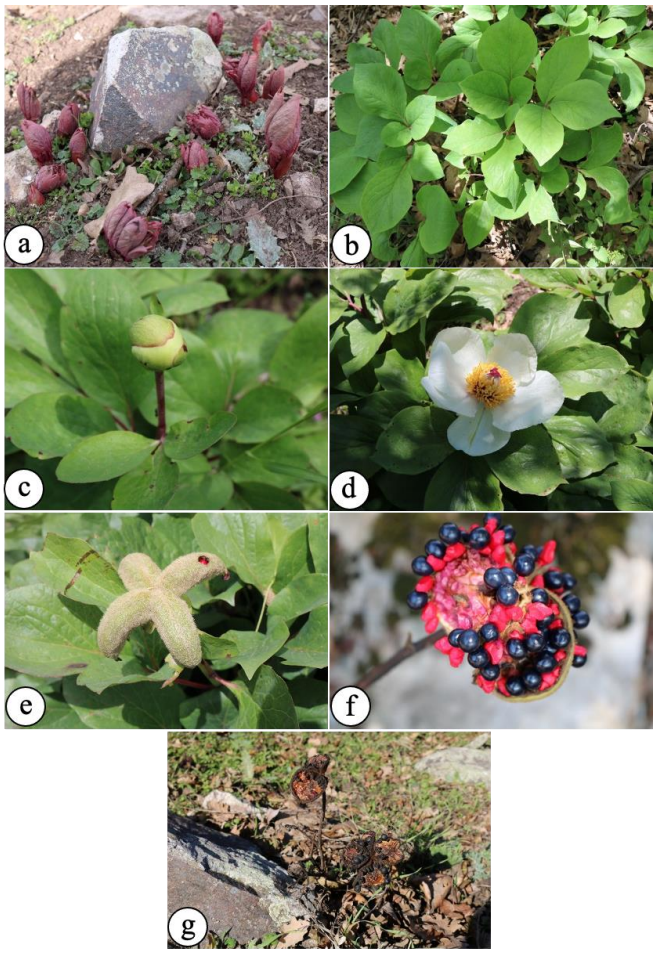

Fig. 2. Phennological stages of *Paeonia mascula* subsp. *bodurii*.a. Sprouting phase, b. vegetative phase, c. bud formation, d. flowering phase, e. fruiting phase, f. seed maturation phase, g. senescence.

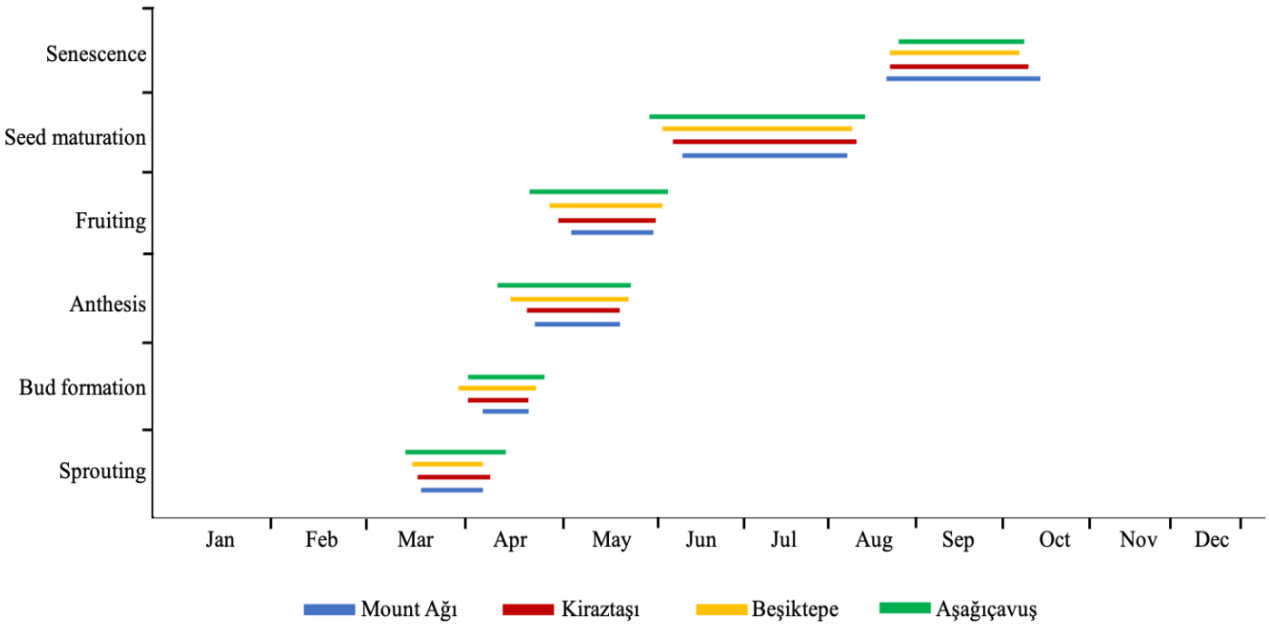

Fig. 3. Phenogram of *Paeonia mascula* subsp. *bodurii* in studied localities.

Table 2. Phenophase dates and durations in four natural populations of the taxon.

Phenophases		Ağı Mountain (921 m)	Kiraztaşı (Üçpınar) (720 m)	Beşiktepe (Karamusalar) (454 m)	Aşağıçavuş (440 m)
Sprouting	Initial	15 Mar	14 Mar	12 Mar	10 Mar
	Completion	5 Apr	6 Apr	5 Apr	11 Apr
	Duration	**22 days**	**24 days**	**25 days**	**33 days**
Bud formation	Initial	4 Apr	1 Apr	30 Mar	1 Apr
	Completion	19 Apr	19 Apr	21 Apr	25 Apr
	Duration	**15 days**	**18 days**	**21 days**	**24 days**
Anthesis	Initial	20 Apr	18 Apr	15 Apr	13 Apr
	Completion	20 May	20 May	22 May	23 May
	Duration	**30 days**	**32 days**	**37 days**	**40 days**
Fruiting	Initial	2 May	29 Apr	27 Apr	22 Apr
	Completion	29 May	30 May	1 Jun	2 Jun
	Duration	**27 days**	**32 days**	**35 days**	**41 days**
Seed maturation	Initial	7 Jun	4 Jun	1 Jun	28 May
	Completion	5 Aug	7 Aug	6 Aug	13 Aug
	Duration	**59 days**	**64 days**	**66 days**	**78 days**
Senescence	Initial	20 Aug	21 Aug	21 Aug	24 Aug
	Completion	9 Oct	5 Oct	2 Oct	4 Oct
	Duration	**50 days**	**46 days**	**43 days**	**42 days**
Duration of phenological cycle		**208 days**	**205 days**	**205 days**	**205 days**

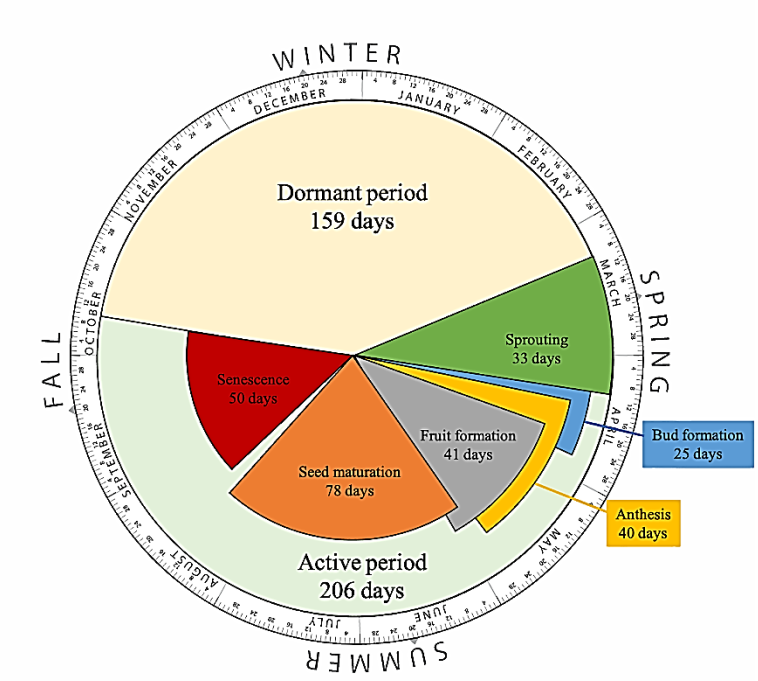

Fig. 4. Phenographic life cycle of *Paeonia mascula* subsp. *bodurii*.

Discussion

Plant phenology includes the timing and duration of repetitive biological events, including reproductive events such as sprouting, flowering, fruiting, and seed dispersal. Therefore, flowering phenology is a very important developmental process to determine the reproductive success of plants. Differences in reproductive cycle times between species and their populations can have important evolutionary consequences (Waser 1978). The information obtained from phenological studies is very important for the planning of successful conservation strategies of endangered plant species and their future ex-situ conservation studies (Gopalakrishnan & Thomas 2014).

The results of this study revealed that there was partial asynchrony in all phenophases of the samples distributed in the studied populations as a result of altitude

differences between the populations and the location differences in the north-south direction. Because the temperature decreases gradually as the altitude increases, the same phenomenon is seen from south to north. Consistent with the present results and that of previous studies (Ziello *et al.* 2009, Nazir *et al.* 2017), as the altitude increases, the plants bloom relatively later than those at lower altitudes. The blooming asynchronization between populations is very useful for increasing the efficiency of pollinators, reducing intraspecific competition and promoting out crossing. In order for a threatened species to be successful in its struggle for survival, it is extremely important that the flowering period is healthy and long, and especially that the pollinators work effectively during that period.

All populations of *Paeonia mascula* subsp. *bodurii* have a life period of 205-208 days from their sprouting to the senescence of the aerial shoots. This knowledge is invaluable in understanding phenological behaviour and developing strategies to effectively conserve wild populations *in-situ* or *ex-situ* in botanical gardens. Although reproductive biology is widely researched in plant conservation biology in Turkey, our present results, which reveal the full life cycle of the local endemic *P. mascula* subsp. *bodurii*, will serve as an exemplary model for further similar studies, since there exists no detailed phenological atlas study as reported here.

Since *Paeonia* species are potentially ornamental plants worldwide, the results of this study will shed light on the evaluation of *P. mascula* subsp. *bodurii* as an ornamental plant natural gene source in terms of agronomical studies in the future.

Acknowledgement

This study was carried out within the scope of the first author's doctoral thesis. We would like to thank Çanakkale Nature Conservation and National Parks Branch Directorate, which is affiliated to the 2nd Regional Directorate of Nature Conservation and National Parks (DKMP), for their assistance during the field studies.

Ethics Committee Approval: Since the article does not contain any studies with human or animal subject, its approval to the ethics committee was not required.

Author Contributions: Concept: B.K., E.K., Desing: B.K., E.K., Execution: B.K., E.K., Material supplying: B.K., E.K., Data acquisition: B.K., E.K., Data analysis/interpretation: B.K., E.K., Writing: B.K., E.K., Critical review: B.K., E.K.

Conflict of Interest: The authors have no conflicts of interest to declare.

Funding: The authors declared that this study has received no financial support.

References

1. Davis, P.H. & Cullen, J. 1965. *Paeonia* L., 204-206. In: Davis, P.H. (ed). *Flora of Turkey and the East Aegean Islands Vol. 1*. Edinburgh University Press, Edinburgh, x + 567 pp.
2. Davis, P.H. 1988. *Paeonia* L., 22-23. In: Davis, P.H., Mill, R.R. & Tan K. (eds). *Flora of Turkey and the East Aegean Islands Vol. 10 (Supplement 1)*. Edinburgh University Press, Edinburgh, xxi + 590 pp.
3. Daysal, N. 2013. Effect of climate on natural plant vegetation in Turkey. *Acta Turcica, Çevrimiçi Tematik Türkoloji Dergisi*, V(1): 1-22 (in Turkish).
4. Ekim, T., Koyuncu, M., Vural, M., Duman, H., Aytaç, Z. & Adıgüzel, N. 2000. *Red Data Book of Turkish Plants (Pteridophyta and Spermatophyta)*. Türkiye Tabiatını Koruma Derneği & Van Yüzüncü Yıl Üniversitesi, Ankara, ix + 246 pp.
5. Fenner, F. 1998. The phenology of growth and reproduction in plants. *Perspectives in Plant Ecology, Evolution and Systematics*, 1(1): 78-91.
6. Gopalakrishnan, K.K. & Thomas, T.D. 2014. Reproductive biology of *Pittosporum dasycaulon* Miq., (Family Pittosporaceae) a rare medicinal tree endemic to Western Ghats. *Botanical Studies*, 55(1): 1-11.
7. Hong, D.Y. 2010. *Paeonies of the World: Taxonomy and Phytogeography*. Royal Botanic Gardens, Kew, London, 302 pp.
8. Kökçü, B. & Karabacak E. 2020. Survival struggle of local endemic *Paeonia mascula* subsp. *bodurii* in Çanakkale, 247, Paper presented at the 2nd International Symposium on Biodiversity Research, 18-20 November, Recep Tayyip Erdoğan University, Rize-Turkey
9. Körüklü, S.T. 2012. Paeoniaceae, 659-660. In: Güner, A., Aslan, S., Ekim, T., Vural, M. & Babaç, M.T. (eds). *Türkiye Bitkileri Listesi-Damarlı Bitkiler*. Nezahat Gökyiğit Botanik Bahçesi Yayınları Flora Dizisi 1, İstanbul, xxi + 1290 pp.
10. Meteorological Service 2021. https://mgm.gov.tr/veridegerlendirme/il-ve-ilceler-istatistik.aspx?k=undefined&m=CANAKKALE (Date accessed: 7 July 2021).
11. Morellato, L.P.C., Alberton, B., Alvarado, S.T., Borges, B., Buisson, E., Camargo, M.G.G., Cancian, L.F., Carstensen, D.W., Escobar, D.F.E., Leite, P.T.P., Mendoza, I., Rocha, N.M.W.B., Sorares, N.C., Silva, T.S.F., Staggemeir, V.G., Streher, A.S., Vargas, B.C. & Peres, C.A. 2016. Linking plant phenology to conservation biology. *Conservation Biology*, 195: 60-72.
12. Nazir, S., Yaqoob, U., Nawchoo, I.A., Wani, A.A. & Wani, S.A. 2017. Phenological behaviour of *Paeonia emodi* Wall. Ex Royle in response to habitat variability and altitude. *Research & Reviews: Journal of Ecology*, 6(1): 1-5.
13. Özhatay, N. & Özhatay, E. 1995. A new white *Paeonia* L. From Northwestern Turkey: *P. mascula* Miller subsp.

bodurii N. Ozhatay. *Karaca Arboretum Magazine* 3(1): 17-26.

14. Özhatay, N. 2000. *Paeonia* L., 15-16. In: Dayser, A., Özhatay, N., Ekim, T. & Başer, K.H.C. (eds). *Flora of Turkey and the East Aegean Islands Vol. 11 (Supplement 2)*. Edinburgh University Press, Edinburgh, xix + 656 pp.
15. Şimşek, O., Nadaroğlu, Y., Yücel, G., Dokuyucu, Ö. & Gökdağ, Ş.A. 2014. *Türkiye Fenoloji Atlası*. Orman ve Su İşleri Bakanlığı, Zirai Meteoroloji Şube Müdürlüğü, Ankara, iii + 104 pp.
16. The Plant List, 2021. http://theplantlist.org/1.1/browse/A/Paeoniaceae/ (Date accessed: 22.06.2021).
17. Topal, H. 2020. *Amasya Ovası Yakın Çevresinde Yetiştirilen Kültür Bitkilerinin Fenolojisi ve Bunların İklim Şartları İle Olan İlişkileri* (Master Thesis), Ondokuz Mayıs Üniversitesi, Samsun, ix + 84 pp.
18. Waser, N.M. 1978. Competition for humming bird pollination and sequential flowering in two Colorado wildflowers. *Ecology*, 59(5): 934-44.
19. Ziello, C., Estrella, N., Kostova, M., Koch, E. & Menzel, A. 2009. Influence of altitude on phenology of selected plant species in the Alpine region (1971–2000). *Climate Research* 39: 227-234.

http://dergipark.org.tr/trkjnat
Trakya University Journal of Natural Sciences, 22(2): 215-243, 2021
ISSN 2147-0294, e-ISSN 2528-9691
DOI: 10.23902/trkjnat.947894

Research Article

THE MYCOBIOTA OF SAMANLI MOUNTAINS IN TURKEY

Hasan Hüseyin DOĞAN[1*], Öyküm ÖZTÜRK[2], Murad Aydın ŞANDA[3]

[1] Selçuk University, Science Faculty, Biology Department, Konya, TURKEY
[2] Hacettepe University, Science Faculty, Biology Department, Ankara, TURKEY
[3] Muş Alparslan University, Science and Letter Faculty, Molecular Biology and Genetic Department, Muş, TURKEY

Cite this article as:
DOĞAN, H.H., ÖZTÜRK, Ö & ŞANDA, M.A. 2021. The mycobiota of Samanlı Mountains in Turkey. *Trakya Univ J Nat Sci*, 22(2): 215-243, DOI: 10.23902/trkjnat.947894

Received: 04 June 2021, Accepted: 31 August 2021, Online First: 04 October 2021, Published: 15 October 2021

Abstract: The Mycobiota of Samanlı Mountains were investigated in this study. Specimens were collected during 3 years between November 2012 and November 2015. 510 macrofungal taxa belonging to 197 genera within 84 families were recorded with field and laboratory studies. Of these, 37 genera and 57 taxa belong to Ascomycota, while 160 genera and 453 taxa belong to Basidiomycota. Nine species were found for the first time in Turkey from *Basidiomycota*. These taxa are *Amanita subnudipes* (Romagn.) Tulloss, *Hebeloma quercetorum* Quadr., *Hygrocybe obrussea* (Fr.) Wunsche, *Lactarius mediterraneensis* Llistosella & Bellù, *Lactifluus glaucescens* (Crossl.) Verbeken, *Russula lilacea* Quél., *R. rubra* (Lam.) Fr., *Stereopsis reidii* Losi & A. Gennari and *Tricholoma roseoacerbum* A. Riva. The *Stereopsidaceae* family and the genus *Stereopsis* D.A. Reid was found for the first time in Turkey.
The richest families in terms of the number of taxa are *Russulacea* with 58 taxa (11.3%), *Agaricaceae* with 46 taxa (8.9%), *Tricholomataceae* with 43 taxa (8.4%), *Boletaceae* with 32 taxa (6.2%), *Polyporaceae* with 23 taxa (4.5%) and the most crowded genera are *Russula* Pers. with 41 taxa (8%), *Tricholoma* (Fr.) Staude with 26 taxa (5%), *Amanita* Dill. ex Boehm. with 19 taxa (3.7%), *Lactarius* Pers. with 16 taxa (3.1%) and *Inocybe* (Fr.) Fr. with 14 taxa (2.7%). The ecological status of the species is as follows; 245 (48%) are saprobe, 226 (45%) are mycorrhizal, 20 (3.7%) are lignicolous, 18 (2.9%) are parasite, and one is entomopathogenic. Habitat distribution in the research area is as follows: 300 species in *Abies nordmanniana* (Stev.) Spach. subsp. *bornmuelleriana* (Mattf.) Coode & Cullen forest, 295 species in *Fagus orientalis* Lipsky forest, 125 species in *Quercus* spp. forest, 88 species in *Pinus nigra* J.F.Arnold forest, 56 species in *Castanea sativa* Mill. forest, 53 species in *Pinus sylvestris* L. forest, 49 species in *Carpinus orientalis* Mill. forest and 24 species in *Pinus maritima* Lam. forest.

Özet: Bu çalışmada Samanlı dağlarının mikobiotası araştırılmıştır. Örnekler Kasım 2012 ve Kasım 2015 arasında 3 yıl boyunca toplanmıştır. 84 familya ve 197 cinse ait 510 makromantar taksonu belirlenmiştir. Bunlardan, 37 cins ve 57 takson Ascomycota'ya aitken 160 cins ve 453 takson ise Basidiomycota'ya aittir. *Basidiomycota*'dan 9 tür Türkiye'de ilk kez bulunmuştur. Bu taksonlar *Amanita subnudipes* (Romagn.) Tulloss, *Hebeloma quercetorum* Quadr., *Hygrocybe obrussea* (Fr.) Wunsche, *Lactarius mediterraneensis* Llistosella & Bellù, *Lactifluus glaucescens* (Crossl.) Verbeken, *Russula lilacea* Quél., *R. rubra* (Lam.) Fr., *Stereopsis reidii* Losi & A. Gennari ve *Tricholoma roseoacerbum* A. Riva.'dur. *Stereopsidaceae* familyası ve *Stereopsis* D.A. Reid cinsi Türkiye'de ilk kez belirlenmiştir.
Tür sayısı bakımından en zengin familyalar *Russulaceae*'den 58 takson (%11,3), *Agaricaceae*'den 46 takson (%8,9), *Tricholomataceae*'den 43 takson (%8,4), *Boletaceae*'den 32 takson (%6,2), *Polyporaceae*'den 23 takson (%4,5) dur. En zengin cinsler ise *Russula* Pers. 41 takson (%8), *Tricholoma* (Fr.) Staude 26 takson (%5), *Amanita* Dill. ex Boehm. 19 takson (%3,7), *Lactarius* Pers. 16 takson (%3,1) ve *Inocybe* (Fr.) Fr. 14 takson (%2,7)'dur. Türlerin ekolojik durumları şu şekildedir; 245 (%48) saprop, 226 (%45) mikorizal, 20 (%3,7) lignikolar, 18 (%2,9) parazit, ve bir tür entomopatojeniktir. Araştırma alanındaki habitat dağılımı aşağıdaki gibidir; 300 takson *Abies nordmanniana* (Stev.) Spach.subsp. *bornmuelleriana* (Mattf.) Coode & Cullen ormanında, 295 takson *Fagus orientalis* Lipsky ormanında, 125 takson *Quercus* spp. ormanında, 88 takson *Pinus nigra* J.F.Arnold ormanında; 56 takson *Castanea sativa* Mill. ormanında; 53 takson *Pinus sylvestris* L. ormanında, 49 takson *Carpinus orientalis* Mill. ormanında ve 24 takson *Pinus maritima* Lam. ormanındadır.

Edited by:
Neeven Geweely

****Corresponding Author:***
Hasan Hüseyin Doğan
hhuseyindogan@yahoo.com

ORCID iDs of the authors:
HHD. orcid.org/0000-0001-8859-0188
ÖÖ. orcid.org/0000-0001- 9846-3668
MAŞ. orcid.org/0000- 0001-8843-4361

Key words:
Fungal distribution
Samanlı Mountains
New records
Turkey

Introduction

Fungal species play important roles in ecosystems. For instance, they decompose organic materials and occupy diverse niches in forest ecosystems. In order to learn their ecological roles, it is necessary to determine their distribution areas, species diversity and the habitat types habitats they occupy. In this way, we can get useful information about common and widely distributed, rare, poisonous or edible species, or species that are important in terms of the ecological cycle. Such a knowledge helps mycologists to understand the macrofungal diversity of an area, region or even a country and allows to make a comparison with the macrofungal data of other studied places. In addition, it is also possible to reveal new or rare species in this way. During field studies, it is important to learn the knowledge of local people about mushrooms and to determine their ways to use them ethnomicologically.

Many studies on macrofungal diversity were carried out and yet many are still ongoing both in Turkey and in world. As a result of these studies, significant contributions have been made to the macrofungal diversity of Turkey. A checklist of the fungi of Turkey was published in 2020 with broad cooperation of Turkish mycologists (Sesli *et al.* 2020). According to this checklist, a total of 5865 fungal taxa, including 2782 Basidiomycota, 2728 Ascomycota 282 Myxomycota, 2 Chytridiomycota, 33 Oomycota and 38 Zygomycota species identified in Turkey have been listed so far. Regarding the ecology and habitat choices of these taxa, the majority are found in coniferous and broadleaved (latifolius) forest ecosystems. Other environments in which fungal species can be found were reported as meadows, waterfronts, humid areas and similar different habitats. When the relevant literature was reviewed, no study was found on fungal diversity of Samanlı Mountains. Samanlı Mountains has different kind of the forest types formed by various trees such as *Abies* sp., *Carpinus* sp., *Fagus* sp., *Pinus* sp. and *Quercus* sp. The climatic conditions of the mountain provide optimum growth of mushrooms. We therefore chose it as the study area to determine the macrofungal diversity present and contribute to the Turkish mycobiota.

Materials and Methods

Description of the area

Samanlı Mountains are located in the southeast of the Marmara Region in Turkey (Fig. 1). The range stretches between Bozburun at the edge of Armutlu Peninsula in the west, and Geyve Strait formed by Sakarya River in the east. A close look at the natural vegetation of the study area highlights kermes oak (*Quercus coccifera* L.), holly oak (*Quercus ilex* L.), and bay laurel (*Laurus nobilis* L.) as the main shrubs and ligneous plants in the maquis formation up to 500-600m. Hawthorn (*Crataegus oxyacantha* L.) and a Black Sea enclave, boxwood (*Buxus sempervirens* L.), are seen in patches among maquis elements. The main ligneous plants in the forest cover of the area are pedunculate oak (*Quercus pedunculata* Ehrh.), oriental beech (*Fagus orientalis* Lipsky), Uludağ fir (*Abies nordmanniana* subsp. *bornmuelleriana* (Mattf.) Coode & Cullen), chestnut (*Castanea sativa* Mill.), black pine (*Pinus nigra* subsp. *caramanica* (Loudon) Businský), stone pine (*Pinus pinea* L.), Turkish pine (*Pinus brutia* Ten.), common hornbeam (*Carpinus betulus* L.) and Scots pine (*Pinus sylvestri*s Lour.). Groups of oriental planes (*Platanus orientalis* L.), maple (*Acer platanoides* L.), and white poplar (*Populus alba* L.) can also be seen in patches. The area is in the Mediterranean climatic zone in terms of macroclimatic type, and the annual rainfall varies between 400 mm and 1200 mm.

Collection and identification of the species

The macrofungi specimens were collected from 148 localities in Bursa, Kocaeli, Sakarya and Yalova provinces during the years 2012-2015 (Fig. 1, Table 1). The localities are listed alphabetically, and coordinates, heights, habitats and collecting time were given in Table 1. Partition numbers refer to the numbers given to forest areas by the forest management directorates in Table 1. Important macroscopical features and ecological information of the specimens were noted in the field and digital images were taken in their habitat. Collected specimens were dried in dehydrators after each study day and the dried materials were put into plastic bags to bring them to the fungarium in good condition for further analysis. Micromorphological characters were examined using a Leica DM3000 light microscope and photographed digitally. Specimen tissues were examined with some chemical reagents (Melzer; KOH in 10%, 5%, 3%, or 2% solutions; cotton blue; IKI; etc.) for macroscopic and microscopic studies. The measurements of at least 20 spores per specimen were taken. The specimens were identified according to Eriksson & Ryvarden (1973,1976), Eriksson *et al.* (1978, 1984), Moser (1983), Breitenbach & Kränzlin (1984, 1986, 1991, 1995, 2000), Hjortstam *et al.* (1987, 1988), Candusso & Lanzoni (1990), Ryvarden & Gilbertson (1993, 1994), Candusso (1997), Basso (1999), Riva (2003a, 2003b), Galli (2003a, 2003b, 2004, 2006, 2007a, 2007b), Neville & Poumarat (2004), Bernicchia (2005), Horak (2005), Muñoz (2005), Kränzlin (2005), Medardi (2006), Robich (2007), Parra (2008), Michael *et. al* (2014), Knudsen & Vesterholt (2008) and Christensen & Heilmann-Clausen (2013). New records were checked according to Sesli *et al.* (2020). Taxa, family, and author citations are quoted according to Cannon & Kirk (2007), Kirk *et al.* (2008), Index Fungorum (http://www.indexfungorum.org/Names/Names.asp) and MycoBank (http://www.mycobank.org). The specimens are kept in the Fungarium of Mushroom Application and Research Centre, Selçuk University, Konya, Turkey.

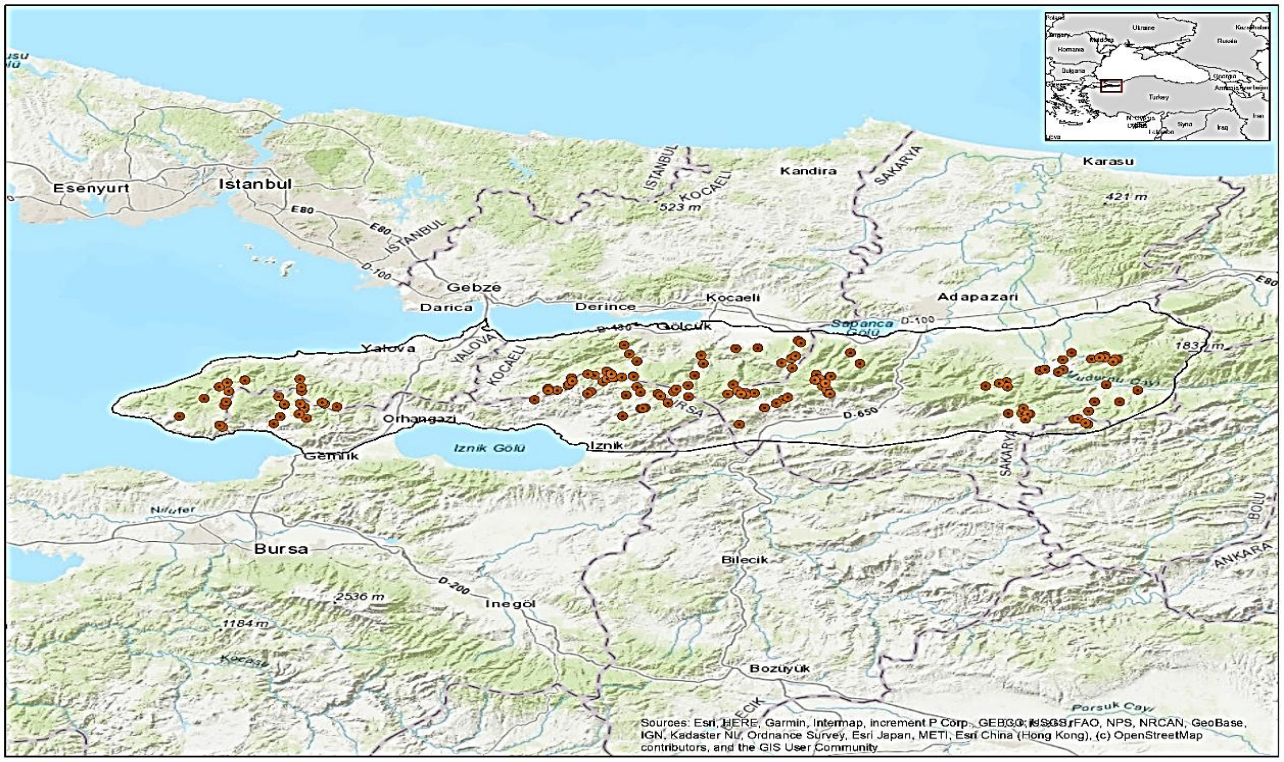

Fig. 1. Map showing the study area. The black line shows the borders of Samanlı Mountains and solid coloured circles correspond the different localities where the specimens were collected.

Locality List

Table 1. The locality names, coordinates, altitudes, habitat types and collection date details.

Loc.No	Localities	Coordinates	Height	Habitats	Date
L1	Bursa, Gemlik, Fevziye Vill., Karagöl district	40°21'04"N, 29°18'26"E	776 m	*F. orientalis, P. nigra, Quercus* sp. forest	10.X.2014
L2	Bursa, Gemlik, Gemlik-Sarıkaya road, Soğanlıtarla district	40°32'25"N, 29°11'50"E	660 m	*Quercus* sp. forest	07.VI.2013
L3	Bursa, Gemlik, Haydariye Vill., Çeşme district	40°30'19"N, 29°07'07"E	420 m	*F. orientalis, C. orientalis* forest	02.VI.2014
L4	Bursa, Gemlik, Haydariye Vill., Dereiçi district	40°32'27"N, 29°08'59"E	470 m	*F. orientalis, C. orientalis*	02.VI.2014
L5	Bursa, Gemlik, Haydariye Vill., Dörtyol cross	40°30'59"N, 29°08'49"E	605 m	*Quercus* sp. forest	23.X.2013
L6	Bursa, Gemlik, Haydariye Vill., Tokat district	40°32'22"N, 29°07'09"E	425 m	*F. orientalis, C. orientalis, Quercus* sp., *R. ponticum forest*	03.VI.2013
L7	Bursa, Gemlik, Haydariye Vill., upper parts of a gezintiyolu district	40°30'37"N, 29°06'37"E	605 m	*P. nigra, A. unedo* forest	23.X.2013
L8	Bursa, Gemlik, Haydariye Vill., Yeşilbaştepe gezintiyolu district	40°30'12"N, 29°06'53"E	405 m	*Quercus* sp. forest	02.VI.2014
L9	Bursa, Gemlik, Küçükkum, upward of Gendarme station	40°27'48"N, 29°07'47"E	300 m	*P. nigra* forest	20.XI.2013
L10	Bursa, Gemlik, Narlı Vill.	40°29'26"N, 28°59'27"E	450 m	*Quercus* sp. forest	02.VI.2014
L11	Bursa, Gemlik, opposite to partition no: 250 of Haydariye Vill.	40°30'27"N, 29°09'44"E	740 m	*F. orientalis, C. orientalis, Quercus* sp., *R. ponticum* forest	03.VI.2013
L12	Bursa, Gemlik, partition no 44,	40°34'14"N, 29°09'10"E	557 m	*F. orientalis* forest	26.X.2013
L13	Bursa, Gemlik, upward of Haydariye Vill.	40°31'02"N, 29°08'51"E	40 m	*F. orientalis, C. orientalis, Quercus* sp., *R. ponticum* forest	03.VI.2013
L14	Bursa, Gemlik, upward of Narlı Vill.	40°29'01"N, 28°59'31"E	480 m	*P. pinea* forest	20.XI.2013

Table 1 Continued.

L15	Bursa, Haydariye Vill., Kolaçandere district	40°31'59"N, 29°09'29"E	544 m	*F. orientalis* forest	23.X.2013
L16	Bursa, İznik, Aybaşı district, forest	40°36'39"N, 29°42'57"E	950 m	*Quercus* sp.	24.X.2013
L17	Bursa, İznik, Çandarlı series, partition no 20	40°34'13"N, 29°53'06"E	955 m	*F. orientalis* forest	05.VI.2013
L18	Bursa, İznik, Çandarlı Vill.	40°31'45"N, 29°49'13"E	858 m	*P. sylvestris, Quercus* sp. *forest*	25.X.2013
L19	Bursa, İznik, Çandarlı, Sarıçam district	40°31'49"N, 29°49'25"E	934 m	*P. sylvestris* forest	05.XI.2015
L20	Bursa, İznik, Çandarlı, Subatım district	40°34'32"N, 29°53'25"E	990 m	*F. orientalis* forest	05.VI.2013
L21	Bursa, İznik, downward of Mecidiye Vill., Boğazdere district	40°34'42"N, 29°44'52"E	623 m	*Quercus* sp. forest	24.X.2013
L22	Bursa, İznik, Elmalı Vill., upward of the Paşa neighbourhood	40°32'34"N, 29°52'25"E	860 m	*F. orientalis* forest	05.VI.2013
L23	Bursa, İznik, Hakkıdüzlüğü district	40°33'41"N, 29°47'31"E	850 m	*P. nigra, Quercus* sp. forest	25.X.2013
L24	Bursa, İznik, İznik-Gölcük border	40°36'23"N, 29°45'26"E	921 m	*F. orientalis* forest	11.X.2014
L25	Bursa, İznik, Kırıntı	40°33'33"N, 29°51'34"E	886 m	*P. sylvestris, Quercus* sp., *C. orientalis* forest	11.X.2014
L26	Bursa, İznik, Merkeztepe district, partition no 27	40°33'29"N, 29°54'50"E	940 m	*F. orientalis* forest	05.VI.2013
L27	Bursa, İznik, next to a mine	40°36'05"N, 29°46'01"E	950 m	*P. nigra, Quercus* sp. forest	25.X.2013
L28	Bursa, İznik, Pilavtepe district	40°35'04"N, 29°40'38"E	730 m	*Quercus* sp. forest	04.VI.2013
L29	Bursa, İznik, Pilavtepe district	40°36'46"N, 29°42'48"E	710 m	*Quercus* forest	24.X.2013
L30	Bursa, İznik, upward of Hacıosman Vill.	40°36'22"N, 29°48'20"E	839 m	*Quercus* sp., *F. orientalis, P. sylvestris* forest	11.X.2014
L31	Bursa, İznik, upward of Kahraman neighbourhood	40°35'59"N, 29°45'14"E	740 m	*P. nigra, Quercus* sp. forest	25.X.2013
L32	Bursa, Mahmudiye, Hacıosman meadow-Kutluca crossroads	40°34'04"N, 29°49'11"E	995 m	*F. orientalis, Quercus* sp. forest	04.VI.2014
L33	Bursa, Mahmudiye, Kutluca Vill.	40°33'51"N, 29°51'13"E	850 m	*F. orientalis, P. sylvestris* forest	04.VI.2014
L34	Bursa, Mahmudiye, Taşlıtarla district	40°36'09"N, 29°46'04"E	947 m	*F. orientalis, C. orientalis forest*	04.VI.2013
L35	Bursa, Mahmudiye, Yapraklıdere district	39°55'07"N, 29°43'41"E	919 m	*F. orientalis, C. orientalis* forest	04.VI.2013
L36	Bursa, Mahmudiye, Yoncalık district	40°34'55"N, 29°48'49"E	1005 m	*F. orientalis, C. orientalis forest*	04.VI.2013
L37	Kocaeli, Gölcük, Başkiraz Plateau	40°36'05"N, 29°41'02"E	780 m	*Quercus* sp. forest	31.V.2014
L38	Kocaeli, Gölcük, downward of Cansuyu district	40°36'22"N, 29°48'20"E	865 m	*F. orientalis* forest	26.X.2014
L39	Kocaeli: Gölcük, İhsaniye Vill., Kurtlarvadisi district	40°38'25"N, 29°48'46"E	250 m	*F. orientalis, Quercus* sp. forest	26.X.2014
L40	Kocaeli, Gölcük, İhsaniye, Ayvazpınarı district, picnic area	40°36'55"N, 29°44'56"E	830 m	*F. orientalis* forest	31.V.2014
L41	Kocaeli, Gölcük, İhsaniye, Ayvazpınarı district, downward of picnic area	40°37'02"N, 29°45'11"E	780 m	*F. orientalis, C. orientalis, C. sativa, C. avellana* forest	26.X.2014
L42	Kocaeli, Gölcük, Mecidiye Vill.	40°35'13"N, 29°44'56"E	760 m	*Quercus* sp. forest	31.V.2014
L43	Kocaeli, Gölcük, Menekşe Plateau	40°35'01"N, 29°54'48"E	890 m	*F. orientalis* forest	05.VI.2013
L44	Kocaeli, Gölcük, next to İnci taşocağı district	40°36'06"N, 29°46'50"E	922 m	*F. orientalis* forest	31.V.2014
L45	Kocaeli, Gölcük, on the way of Ayvazpınarı district	40°36'50"N, 29°45'26"E	840 m	*F. orientalis, C. orientalis, Quercus* sp. forest	01.X.2014
L46	Kocaeli, Gölcük, on the way of Eriklitepe district	40°36'08"N, 29°45'55"E	970 m	*F. orientalis* forest	31.V.2014

Table 1 Continued.

L47	Kocaeli, Gölcük, on the way of İnci taşocağı district to Gölcük, 1. km down of Şelale district	40°36'22"N, 29°48'20"E	850 m	*C. orientalis* forest	01.X.2014
L48	Kocaeli, Gölcük, Pilavtepe crossroad	40°35'38"N, 29°41'08"E	760 m	*P. nigra, Quercus* sp. forest	01.X.2014
L49	Kocaeli, Gölcük, upward of Mecidiye Vill., Kestanelik district	40°39'27"N, 29°47'52"E	560 m	*C. sativa, Quercus* sp. forest	01.X.2014
L50	Kocaeli, Karamürsel, exit of Tahtalı Vill.	40°34'21"N, 29°39'20"E	730 m	*Quercus* sp. forest	01.VI.2014
L51	Kocaeli, Karamürsel, Fulacık crossroad	40°34'37"N, 29°38'16"E	685 m	meadow area	01.X.2014
L52	Kocaeli, Karamürsel, Fulacık, exit from Tahtalı Vill., next to the fountain	40°34'18"N, 29°38'16"E	670 m	*F. orientalis, C. sativa, C. orientalis* forest	01.X.2014
L53	Kocaeli, Karamürsel, Fulacık Vill.,	40°36'06"N, 29°46'50"E	922 m	*Quercus* sp. forest	01.VI.2014
L54	Kocaeli, Karamürsel, Mahmudiye Vill., Tahtalı roadside	40°31'17"N, 29°38'15"E	690 m	*F. orientalis, P. nigra* forest	24.X.2013
L55	Kocaeli, Maşukiye, across Sislivadi district	40°39'14"N, 30°07'45"E	1200 m	*A. nordmanniana* subsp. *bornmuelleriana, F. orientalis forest*	25.X.2014
L56	Kocaeli, Maşukiye, entrance of Kuzuyayla Nature Park	40°38'50"N, 30°06'53"E	1400 m	*A. nordmanniana* subsp. *bornmuelleriana, F. orientalis forest*	25.X.2014
L57	Kocaeli, Maşukiye, Kartepe road, gezintiyolu district	40°41'00"N, 30°08'59"E	460 m	*F. orientalis, P. nigra* forest	28.IX.2014
L58	Kocaeli, Maşukiye, Kartepe, Altıoluk Plateau	40°37'28"N, 30°06'59"E	1310 m	*F. orientalis* forest	25.X.2014
L59	Kocaeli: Suadiye, Altıoluk Plateau, the back of the transmitter	40°38'12"N, 30°05'52"E	1360 m	*F. orientalis* forest	27.V.2014
L60	Kocaeli, Suadiye, Hafızıntarlası district,	40°40'16"N, 30°00'27"E	400 m	*Quercus* sp., *F. orientalis, C. orientalis, C. avelleana* forest	27.XI.2012
L61	Kocaeli, Suadiye, on Kartepe road, left side	40°40'20"N, 30°03'04"E	540 m	*P. sylvestris* forest	27.XI.2012
L62	Kocaeli, Yuvacık, across Servetiye, Dikkulak district	40°39'18"N, 29°56'22"E	460 m	*F. orientalis, C. orientalis, C. sativa* forest	17.IV.2013
L63	Kocaeli, Yuvacık, Aytepe district	40°36'30"N, 29°55'36"E	960 m	*F. orientalis, C. sativa, C. orientalis* forest	28.XI.2012
L64	Kocaeli, Yuvacık, entrance of İnönü Plateau	40°35'09"N, 30°00'06"E	1240 m	*P. sylvestris, A. nordmanniana subsp. bornmuelleriana, F. orientalis* forest	28.XI.2012
L65	Kocaeli, Yuvacık, İnönü Plateau	40°33'52"N, 29°59'30"E	1240 m	*A. nordmanniana* subsp. *bornmuelleriana, P. nigra, F. orientalis, C. orientalis, R. ponticum* forest	29.IV.2014
L66	Kocaeli, Yuvacık, İnönü Plateau, Şehitlik district road	40°33'58"N, 30°01'34"E	1160 m	*F. orientalis, P. sylvestris, forest*	09.VI.2013
L67	Kocaeli, Yuvacık, İnönü Plateau, Şehitlik district	40°33'58"N, 30°02'39"E	1150 m	*F. orientalis* forest	09.VI.2013
L68	Kocaeli, Yuvacık, Servetiye mosque, roadside	40°38'09"N, 29°56'37"E	450 m	*F. orientalis, C. sativa, C. orientalis, R. ponticum* forest	17.IV.2013
L69	Sakarya, Akyazı, Avcıçimeni district	40°31'05"N, 30°34'16"E	1260 m	*A. nordmanniana* subsp. *bornmuelleriana, F. orientalis, Quercus* sp. forest	01.XI.2013
L70	Sakarya, Akyazı, between Avcıçimeni and Yılanlıkaya district	40°31'02"N, 30°34'28"E	1253 m	*A. nordmanniana* subsp. *bornmuelleriana, F. orientalis* forest	30.IX.2014
L71	Sakarya, Akyazı, Çiğdem Plateau,	40°38'56"N, 30°52'13"E	1460 m	*A. nordmanniana* subsp. *bornmuelleriana* forest	24.V.2014
L72	Sakarya, Akyazı, Dokumacı district,	40°33'08"N, 30°34'13"E	1185 m	*A. nordmanniana* subsp. *bornmuelleriana, C. orientalis, Pteridium* sp. forest	02.XI.2012
L73	Sakarya, Akyazı, Dokurcun, down part of Dikmentepe district	40°39'03"N, 30°53'28"E	1350 m	*A. nordmanniana* subsp. *bornmuelleriana* forest	24.V.2014
L74	Sakarya, Akyazı, Dokurcun, Güldürüksu district	40°38'41"N, 30°53'47"E	1390 m	*A. nordmanniana* subsp. *bornmuelleriana* forest	24.V.2014

Table 1 Continued.

L75	Sakarya, Akyazı, Dokurcun, Kındıra Plateau	40°38'01"N, 30°49'12"E	1390 m	*A. nordmanniana* subsp. *bornmuelleriana, F. orientalis* forest	24.V.2014
L76	Sakarya, Akyazı, Dokurcun, upward of Güldürüksu district	40°37'58"N, 30°52'13"E	1510 m	*A. nordmanniana* subsp. *bornmuelleriana* forest	24.V.2014
L77	Sakarya, Akyazı, down part of Hardamalık, Durmuşlar district	40°34'88"N, 30°44'78"E	203 m	*A. nordmanniana* subsp. *bornmuelleriana* forest	22.V.2014
L78	Sakarya, Akyazı, Göktepe, Ahmediye Vill., Kestanedüzü district	40°35'37"N, 30°32'26"E	961 m	*C. orientalis* forest	02.XI.2012
L79	Sakarya, Akyazı, Isırganlık district	40°39'11"N, 30°44'04"E	1200 m	*A. nordmanniana* subsp. *bornmuelleriana* forest	02.XI.2013
L80	Sakarya, Akyazı, Kayabaşı, Kiremitlik district	40°32'43"N, 30°42'51"E	960 m	*A. nordmanniana* subsp. *bornmuelleriana, F. orientalis* forest	29.X.2014
L81	Sakarya, Akyazı, Keremali Pateau	40°38'46"N, 30°45'34"E	1100 m	*A. nordmanniana* subsp. *bornmuelleriana, P. sylvestris, R. ponticum* forest	03.XI.2012
L82	Sakarya, Akyazı, Keremali Plateau, behind the Mosque	40°37'46"N, 30°45'35E	1100 m	*A. nordmanniana* subsp. *bornmuelleriana* forest	22.V.2014
L83	Sakarya, Akyazı, Kuzuluk Nature Park	40°37'19"N, 30°39'10"E	370 m	*F. orientalis, C. orientalis, Quercus* sp. forest	18.IV.2013
L84	Sakarya, Akyazı, Kuzuluk, on the way to Yeniköy from the centre	40°38'55"N, 30°39'12"E	260 m	*Quercus* sp. forest	18.IV.2013
L85	Sakarya, Akyazı, Mansurlar planting area,	40°34'42"N, 30°43'24"E	280 m	*P. nigra* forest	03.XI.2013
L86	Sakarya, Akyazı, Özdemirler Plateau	40°30'12"N, 30°40'49"E	1260 m	*A. nordmanniana* subsp. *bornmuelleriana* forest	04.XI.2012
L87	Sakarya, Akyazı, Pine planting area on the Güzlek road	40°39'42"N, 30°40'07"E	225 m	*P. sylvestris* forest	18.IV.2013
L88	Sakarya, Akyazı, Salihiye	40°37'09"N, 30°36'20"E	160 m	*Quercus* sp. forest	29.X.2014
L89	Sakarya, Akyazı, Soğuksu forest building	40°39'06"N, 30°43'37"E	930 m	*A. nordmanniana* subsp. *bornmuelleriana* forest	02.XI.2013
L90	Sakarya, Akyazı, upper part of Kuruçay Plateau	40°31'25"N, 30°42'07"E	1282 m	*A. nordmanniana* subsp. *bornmuelleriana, F. orientalis* forest	23.V.2014
L91	Sakarya, Akyazı, upper part of Özdemirler P Plateau	40°30'21"N, 30°40'51"E	1300 m	*A. nordmanniana* subsp. *bornmuelleriana* forest	23.V.2014
L92	Sakarya, Akyazı, Yazlık neighbourhood	40°37'12"N, 30°36'21"E	155 m	*Quercus* sp., *C. monogyna, R. caesius* forest	18.IV.2013
L93	Sakarya, Akyazı, Yenikoy, Keremali, side of the forest building	40°38'47"N, 30°42'30"E	942 m	*A. nordmanniana* subsp. *bornmuelleriana, P. sylvestris, F. orientalis, R. ponticum* forest	03.XI.2012
L94	Sakarya, Akyazı, Yeniköy, Keremali, Kestanelik district	40°38'58"N, 30°43'33"E	882 m	*C. orientalis, R. caesius* forest	03.XI.2012
L95	Sakarya, Akyazı, Yeniköy, the side of the Keremali forest building, going to Yeniköy, with 500m remaining	40°39'10"N, 30°43'38"E	972 m	*A. nordmanniana* subsp. *bornmuelleriana, F. orientalis forest*	03.XI.2012
L96	Sakarya, Akyazı, Yılanlıkaya turnoff, towards Avcıçimeni	40°30'59"N, 30°35'12"E,	1260 m	*A. nordmanniana* subsp. *bornmuelleriana, F. orientalis, Quercus* sp. forest	01.XI.2013
L97	Sakarya, Akyazı, Yörükyeri Vill., between Civci and Güney neighbourhood, roadside	40°32'49"N, 30°45'49"E	827 m	*C. orientalis, F. orientalis, Trifolium* sp., *D. laciniatus forest*	04.XI.2012
L98	Sakarya, Akyazı, Yörükyeri Vill.	40°31'09"N, 30°46'17"E	1245 m	*F. orientalis* forest	04.XI.2012
L99	Sakarya, Akyazı, Zincirlibaba tomb road separation	40°34'17"N, 30°37'57"E	941 m	*F. orientalis* forest	30.IX.2014
L100	Sakarya, Akyazı, Zirvedağı	40°38'54"N, 30°43'59"E	1050 m	*A. nordmanniana* subsp. *bornmuelleriana* forest	02.XI.2013
L101	Sakarya, Geyve, Acıelma 2 district	40°35'47"N, 30°09'48"E	1100 m	*A. nordmanniana* subsp. *bornmuelleriana, P. nigra, F. orientalis, C. orientalis, R. ponticum* forest	31.X.2013

Table 1 Continued.

L102	Sakarya, Geyve, Acıelma district, Gümüşdere chiefdom	40°35'56"N, 30°10'23"E	1115 m	*A. nordmanniana* subsp. *Bornmuelleriana, P. nigra, F. orientalis, C. orientalis, R. ponticum* forest	30.X.2013
L103	Sakarya, Geyve, Acıelma district	40°35'49"N, 30°10'60"E	1060 m	*A. nordmanniana* subsp. *bornmuelleriana, F. orientalis* forest	31.X.2013
L104	Sakarya, Geyve, Eskiyayla Vill.	40°32'32"N, 30°05'12"E	935 m	*P. nigra* forest	31.X.2013
L105	Sakarya, Geyve, Gümüşdere, Kazimiye Vill.	40°34'00"N, 30°11'21"E	900 m	*P. nigra, Quercus* sp. forest	30.XI.2012
L106	Sakarya, Geyve, Gümüşdere district	40°33'55"N, 30°11'37"E	917 m	*P. nigra, Quercus* sp. forest	30.XI.2012
L107	Sakarya, Geyve, Kaymakam suyu district	40°35'03"N, 30°10'40"E	970 m	*A. nordmanniana* subsp. *bornmuelleriana, P. nigra, F. orientalis* forest	30.XI.2012
L108	Sakarya, Geyve, Taraklı, Mahdumlar Vill., Karagöl Plateau	40°30'17"N, 30°34'39"E	1150 m	*A. nordmanniana* subsp. *bornmuelleriana, F. orientalis, C. orientalis, B. sempervirens* forest	28.V.2014
L109	Sakarya, Geyve, Taraklı, Şimşirlikboğazı district	40°30'55"N, 30°33'54"E	1250 m	*A. nordmannina* subsp. *bornmuelleriana, B. sempervirens* forest	28.V.2014
L110	Sakarya, Geyve, Taraklı, upper part of Dışdedeler Plateau	40°31'05"N, 30°32'38"E	1315 m	*A. nordmannina* subsp. *bornmuelleriana, B. sempervirens* forest	28.V.2014
L111	Sakarya, Göktepe, the place of Pala district	40°34'53"N, 30°32'34"E	926 m	*C. sativa, F. orientalis, C. orientalis, R. ponticum, R. sanctus* forest	02.XI.2012
L112	Sakarya, Karapürçek district	40°34'55"N, 30°29'56"E	1160 m	*A. nordmanniana* subsp. *bornmuelleriana, F. orientalis forest*	28.X.2014
L113	Sakarya, Karapürçek, Uludere district	40°36'07"N, 30°30'36"E	570 m	*F. orientalis, C. sativa, C. orientalis* forest	28.X.2014
L114	Sakarya, Pamukova, Atalanı district	40°33'08"N, 30°06'04"E	870 m	*A. nordmanniana* subsp. *bornmuelleriana, P. nigra, Quercus* sp. forest	29.XI.2012
L115	Sakarya, Pamukova, Bakacak Vill.	40°33'05"N, 30°06'01"E	910 m	*P. nigra, Quercus* sp. forest	31.X.2013
L116	Sakarya, Pamukova, Katırözü, forest warehouse	40°31'58"N, 30°03'51"E	800 m	*A. nordmanniana* subsp. *bornmuelleriana, P. nigra, F. orientalis* forest	29.XI.2012
L117	Sakarya, Pamukova, Şehitlik district, forest camp	40°31'00"N, 29°59'30"E	1105 m	*A. nordmanniana* subsp. *bornmuelleriana, F. orientalis* forest	29.IX.2014
L118	Sakarya, Pamukova, Soğucak way, under the transmitter	40°33'18"N, 30°11'02"E	1000 m	*F. orientalis, P. nigra, Quercus* sp. forest	27.X.2014
L119	Sakarya, Pamukova, the upper part of Ahiler Vill.	40°29'38"N, 30°00'52"E	631 m	*P. nigra, P. brutia, R. sanctus forest*	29.XI.2012
L120	Sakarya, Pamukova, upper part of Kazımiye Vill.	40°33'53"N, 30°11'33"E	930 m	*P. nigra, Quercus* sp. forest	27.X.2014
L121	Sakarya, Sapanca, Çakılocağı district	40°37'10"N, 30°14'25"E	970 m	*A. nordmanniana* subsp. *bornmuelleriana, Salix* sp., *C. sativa, C. orientalis* forest	26.XI.2012
L122	Sakarya, Sapanca, Geyve entrance from Soğucak Plateau	40°36'20"N, 30°11'34"E	1115 m	*F. orientalis* forest	30.X.2013
L123	Sakarya, Sapanca, Memnuniye Vill.	40°38'10"N, 30°15'09"E	850 m	*A. nordmanniana* subsp. *bornmuelleriana, Salix* sp., *C. sativa, C. orientalis* forest	26.XI.2012
L124	Sakarya, Sapanca, Soğucak Plateau entrance	40°36'55"N, 30°10'52"E	1200 m	*A. nordmanniana* subsp. *bornmuelleriana, P. nigra, P. sylvestris* forest	27.IX.2014
L125	Sakarya, Sapanca, Soğucak Plateau road, Chestnut area	40°39'34"N, 30°13'57"E	477 m	*C. sativa, F. orientalis, C. orientalis, P. nigra* forest	27.IX.2014

Table 1 Continued.

L126	Sakarya, Sapanca, Soğucak Plateau	40°34'35"N, 30°09'59"E	1100 m	*A. nordmanniana* subsp. *bornmuelleriana*, *F. orientalis* forest	14.VI.2012
L127	Sakarya, Sapanca, Soğucak Plateau, on the Geyve dam road	40°36'20"N, 30°11'41"E	1190 m	*C. orientalis* forest	25.V.2014.
L128	Sakarya, Sapanca, upper part of Memnuniye Vill.	40°38'49"N, 30°15'17"E	760 m	*Quercus* sp., *F. orientalis*, *C. orientalis* forest	15.IV.2013
L129	Sakarya, Suadiye, Kuzuyayla district	40°38'52"N, 30°07'02"E	1400 m	*F. orientalis*, *C. sativa*, *C. orientalis* forest	16.IV.2013
L130	Sakarya, Suadiye, Taşkonak villas, upward of Motali	40°41'24"N, 30°08'00"E	280 m	*P. nigra*, *Quercus* sp. forest	16.IV.2013
L131	Yalova, Armutlu, partition no 149	40°32'01"N, 28°59'97"E	760 m	*P. nigra* forest	06.VI.2013
L132	Yalova, Armutlu to Karapinar, partition no 64	40°33'21"N, 28°57'61"E	587 m	*F. orientalis* forest	06.VI.2013
L133	Yalova, Armutlu, Delmece Plateau	40°32'44"N, 29°00'15"E	765 m	*F. orientalis*, *C. orientalis* forest	06.VI.2013
L134	Yalova, Armutlu, Mecidiye Vill.	40°30'42"N, 28°54'42"E	495 m	*P. maritima* forest	10.X.2014
L135	Yalova, Armutlu, partition no 151	40°32'37"N, 29°00'16"E	780 m	*F. orientalis*, *P. nigra* forest	06.VI.2013
L136	Yalova, Beşpınar Plateau	40°32'03"N, 29°13'18"E	720 m	*F. orientalis*, *C. orientalis*, *Tilia* sp. forest	07.VI.2013
L137	Yalova, Çanakpınar Plateau	40°32'40"N, 29°11'34"E	700 m	*F. orientalis* forest	07.VI.2013
L138	Yalova, Çınarcık, Delmece Plateau entrance	40°32'47"N, 29°00'20"E	800 m	*F. orientalis*, *P. sylvestris*, forest	03.VI.2014
L139	Yalova, Çınarcık, Delmece Plateau	40°32'44"N, 29°00'15"E	765 m	*F. orientalis*, *C. orientalis* forest	03.VI.2014
L140	Yalova, Çınarcık, Karlık Plateau, partition no 197, 242	40°34'86"N, 28°59'38"E	840 m	*F. orientalis*, young forest	06.VI.2013
L141	Yalova, Çınarcık, Teşvikiye, Dipsizgöller district	40°37'25"N, 29°05'21"E	595 m	*F. orientalis*, *Quercus* sp. forest	03.VI.2014
L142	Yalova, Çınarcık, Teşvikiye Vill., partition no 15	40°35'25"N, 29°00'21"E	600 m	*P. maritima* forest	11.XI.2014
L143	Yalova, Çınarcık, Teşvikiye Vill., partition no 161	40°36'39"N, 26°05'41"E	500 m	*F. orientalis*, *C. sativa* forest	11.XI.2014
L144	Yalova, Çınarcık, Teşvikiye Vill., partition no 200	40°37'30"N, 29°08'42"E	200 m	*P. maritima* forest	11.XI.2014
L145	Yalova, Çınarcık, Urban forest	40°35'46"N, 29°02'29"E	475 m	*F. orientalis*, *Quercus* sp. forest	03.VI.2014
L146	Yalova, Haydariye Vill., partition no 35	40°33'28"N, 29°06'27"E	550 m	*F. orientalis* forest	26.X.2013
L147	Yalova, Termal, on the way of Haydariye Vill.	40°34'47"N, 29°09'08"E	210 m	*F. orientalis*, *C. sativa* forest	03.VI.2014
L148	Yalova, Termal, Suyolu district	40°34'54"N, 29°10'40"E	200 m	*F. orientalis*, *C. sativa* forest	03.VI.2014

Abbreviations; (E): edible, (F): used as food, (I): inedible, (M): used for medical purposes, (P): poisonous, (U): unknown, (?): suspicious, (L): locality.

Results

Division ASCOMYCOTA

Order Coronophorales

Family *Bertiaceae*

Bertia moriformis (Tode) De Not.: (I), L127, saprobe on herbaceous and woody tissue.

Order Helotiales

Family *Helotiaceae*

Hymenoscyphus calyculus (Fr.) W. Phillips: (I), L70, L86, saprobe.

Hymenoscyphus serotinus (Pers.) W. Phillips: (I), L60, L67, L68, L103, L122, L146, saprobe.

Family *Lachnaceae*

Dasyscyphella nivea (R. Hedw.) Raitv.: (I), L46, saprobe.

Lachnellula calyciformis (Batsch) Dharne: (I), L79, saprobe.

Lachnellula occidentalis (G.G. Hahn & Ayers) Dharne: (I), L95, saprobe.

Lachnellula subtilissima (Cooke) Dennis: (I), L126, saprobe.

Lachnum virgineum (Batsch) P. Karst.: (I), L11, L20, L36, L83, L124, saprobe.

Family *Pezizellaceae*

Calycina citrina (Hedw.) Gray: (I), L24, L41, L588, L63, L65, L70, L78, L95, L102, L119, L122, saprobe.

Calycina parilis (P. Karst.) Kuntze: (I), L63, saprobe.

Family *Rutstroemiaceae*

Rutstroemia firma (Pers.) P. Karst.: (I), L63, saprobe.

Family *Sclerotiniaceae*

Ciboria amentacea (Balb.) Fuckel: (I), L49, saprobe.

Order Hypocreales
Family *Cordycipitaceae*

Ophiocordyceps gracilis (Grev.) G.H. Sung, J.M. Sung, Hywel-Jones & Spatafora: (M), L57, on caterpillar, entomopathogenic.

Family *Nectriaceae*

Nectria cinnabarina (Tode) Fr.: (I), L126, saprobe.

Order Leotiacae
Family *Leotiaceae*

Leotia lubrica (Scop.) Pers.: (I), L3, L65, L126, L146, saprobe.

Order Pezizales
Family *Caloscyphaceae*

Caloscypha fulgens (Pers.) Boud.: (I), L66, parasite on the seeds of conifers.

Family *Helvellaceae*

Dissingia leucomelaena (Pers.) K. Hansen & X.H. Wang: (E, or ?), L75, mycorrhizal.

Helvella acetabulum (L.) Quél.: (E, or ?), L73, mycorrhizal.

Helvella atra J. König: (I), L144, mycorrhizal.

Helvella crispa (Scop.) Fr.: (E, or ?), L93, L112, L125, mycorrhizal.

Helvella elastica Bull.: (E), L3, L41, L112, L147, mycorrhizal.

Helvella fibrosa (Wallr.) Korf: (I), L79, mycorrhizal.

Helvella lacunosa Afzel.: (E, or ?), L5, L58, L71, L83, mycorrhizal.

Helvella leucophaea (Battarra) Pers.: (I), L85, mycorrhizal.

Family *Morchellaceae*

Morchella esculenta (L.) Pers.: (E), L130, mycorrhizal.

Family *Pezizaceae*

Legaliana badia (Pers.) Van Vooren: (I), L3, L133, mycorrhizal.

Pachyella celtica (Boud.) Häffne: (I), L47, L79, saprobe.

Paragalactinia succosa (Berk.) Van Vooren: (I), L49, saprobe.

Peziza arvernensis Roze & Boud.: (I), L70, L75, saprobe.

Peziza depressa Pers.: (I), L112, saprobe.

Peziza micropus Pers.: (I), L83, saprobe.

Sarcosphaera coronaria (Jacq.) J. Schröt.: (E, or ?), L73, L74, saprobe.

Family *Pyronemataceae*

Aleuria aurantia (Pers.) Fuckel: (I), L38, L60, L70, L101, saprobe.

Aleuria splendens (Quél.) Gillet: (I), L64, L111, saprobe.

Geopora sumneriana (Cooke ex W. Phillips) M. Torre: (I), L766, saprobe.

Humaria hemisphaerica (F.H. Wigg.) Fuckel: (I), L52, L70, saprobe.

Otidea alutacea (Pers.) Massee: (I), L103, L10, L126, saprobe.

Tarzetta catinus (Holmsk.) Korf & J.K. Rogers: (I), L58, L68, L70, L71, L73, saprobe.

Tarzetta cupularis (L.) Lambotte: (I), L70, saprobe.

Family *Sarcoscyphaceae*

Sarcoscypha coccinea (Gray) Boud.: (I), L5, L143, saprobe.

Order Xylariales
Family *Diatrypaceae*

Diatrype disciformis (Hoffm.) Fr.: (I), L5, L11, L16, L17, L21, L29, L30, L35, L58, L59, L65, L66, L67, L78, L83, L98, L103, L107, L126, L127, L132, L133, L135, L136, L137, L139, saprobe.

Diatrype stigma (Hoffm.) Fr.: (I), L63, L68, L137, saprobe.

Eutypa acharii Tul. & C. Tul.: (I), L102, saprobe.

Family *Graphostromataceae*

Biscogniauxia nummularia (Bull.) Kuntze: (I), L62, endophytic.

Family *Hypoxylaceae*

Daldinia concentrica (Bolton) Ces. & De Not.: (M), L60, saprobe.

Hypoxylon fragiforme (Pers.) J. Kickx f.: (I), L36, L52, L81, L88, L128, L136, saprobe.

Hypoxylon macrosporum P. Karst.: (I), L78, saprobe.

Hypoxylon rutilum Tul. & C. Tul.: (I), L6, saprobe.

Jackrogersella cohaerens (Pers.) L. Wendt, Kuhnert & M. Stadler: (I), L94, saprobe.

Jackrogersella multiformis (Fr.) L. Wendt, Kuhnert & M. Stadler: (I), L46, L63, L78, L127, L126, L127, L132, L137, saprobe.

Family *Melogrammataceae*

Melogramma campylosporum Fr.: (I), L81, saprobe.

Melogramma spiniferum (Wallr.) De Not.: (I), L58, saprobe.

Family *Xylariaceae*

Kretzschmaria deusta (Hoffm.) P.M.D. Martin: (I), L126, saprobe.

Rosellinia mammiformis (Pers.) Ces. & De Not.: (I), L60, L83, L88, saprobe.

Xylaria hypoxylon (L.) Grev.: (I), L111, saprobe.

Xylaria longipes Nitschke: (I), L125, saprobe.

Xylaria polymorpha (Pers.) Grev.: (M), L46, L56, L57, L63, L70, L86, L126, saprobe.

Division BASIDIOMYCOTA
Order Agaricales
Family *Agaricaceae*

Agaricus arvensis Schaeff.: (E), L108, saprobe.

Agaricus bisporus (J.E. Lange) Imbach: (E), L70, saprobe.

Agaricus bresadolanus Bohus: (P), L90, saprobe.

Agaricus campestris L.: (F), L72, saprobe.

Agaricus comtulus Fr.: (E), L7, saprobe.

Agaricus cupreobrunneus (Jul.Schäff. & Steer) Pilát: (E), L115, saprobe.

Agaricus essettei Bon: (E), L18, L65, saprobe.

Agaricus langei (F.H. Møller) F.H. Møller: (E), L65, saprobe.

Agaricus moelleri Wasser: (P), L52, saprobe.

Agaricus pampeanus Speg.: (E), L18, L126, saprobe.

Agaricus sylvicola (Vittad.) Peck: (E), L30, saprobe.

Agaricus xanthoderma Genev.: (P), L65, L69, L126, saprobe.

Chlorophyllum brunneum (Farl. & Burt) Vellinga: (E, or ?), L78, saprobe.

Chlorophyllum rhacodes (Vittad.) Vellinga: (E), L104, saprobe.

Coprinus comatus (O.F. Müll.) Pers.: (F), L86, L97, saprobe.

Crucibulum laeve (Huds.) Kambly: (I), L41, L70, L79, L93, L119, saprobe.

Cyathus olla (Batsch) Pers.: (I), L99, saprobe.

Cystoderma amianthinum (Scop.) Fayod: (I), L65, L118, saprobe.

Cystoderma carcharias (Pers.) Fayod: (I), L65, saprobe.

Cystodermella granulosa (Batsch) Harmaja: (I), L81, L120, saprobe.

Lepiota clypeolaria (Bull.) P. Kumm.: (P), L09, L108, L120, saprobe.

Lepiota cristata (Bolton) P. Kumm.: (P), L15, L57, saprobe.

Lepiota ignivolvata Bousset & Joss. ex Joss: (P), L18, L30, saprobe.

Lepiota kuehneri Huijsman: (P), L85, saprobe.

Lepiota oreadiformis Velen.: (P), L49, L137, saprobe.

Leucoagaricus leucothites (Vittad.) Wasser: (E), L48, L51, saprobe.

Macrolepiota excoriata (Schaeff.) Wasser: (E), L70, L1012, L126, saprobe.

Macrolepiota heimii (Locq.) Bon: (E), L51, saprobe.

Macrolepiota mastoidea (Fr.) Singer: (E), L10, L18, L60, L65, L66, L86, L103, L116, L126, saprobe.

Macrolepiota procera (Scop.) Singer: (F), L18, L21, L23, L30, L34, L45, L48, L54, L57, L64, L65, L66, L70, L84, L85, L106, L107, L114, L120, L126, L139, saprobe.

Mycenastrum corium (Guers.) Desv.: (E), L15, saprobe.

Family *Amanitaceae*

Amanita battarrae (Boud.) Bon: (U), L39, mycorrhizal.

Amanita caesarea (Scop.) Pers.: (F), L10, L18, L112, mycorrhizal.

Amanita citrina Pers.: (P), L18, L30, L44, L478, L63, L65, L66, L102, L103, L107, L117, L120, L126, L139, mycorrhizal.

Amanita echinocephala (Vittad.) Quél.: (I), L26, L133, mycorrhizal.

Amanita excelsa (Fr.) Bertill.: (E), L17, L20, L34, L64, L100, L124, L137, L141, L146, mycorrhizal.

Amanita franchetii (Boud.) Fayod: (I), L113, L138, mycorrhizal.

Amanita gemmata (Fr.) Bertill.: (P), L3, L8, L33, L35, L43, L44, L46, L58, L62, L65, L66, L69, L77, L81, L82, L108, L124, L126, L127, L132, L136, L138, L139 L140, L141, L143, L145, mycorrhizal.

Amanita mairei Foley: (I), L5, L10, L58, L88, L30, mycorrhizal.

Amanita muscaria (L.) Lam.: (P), L18, L55, L64, L65, L70, L79, L89, L95, L96, L100, L102, L107, L124, L126, mycorrhizal.

Amanita nivalis Grev.: (U), L8, mycorrhizal.

Amanita pantherina (DC.) Krombh.: (P), L8, L10, L52, L60, L63, L93, L95, L118, L139, mycorrhizal.

Amanita phalloides (Vaill. ex Fr.) Link: (P), L17, L34, L38, L81, L125, L135, L139, L140, L141, mycorrhizal.

Amanita rubescens Pers.: (E), L4, L8, L11, L17, L18, L20, L26, L32, L33, L34, L35, L36, L40, L60, L6, L64, L65, L66, L67, L95, L97, L124, L133, L135, L136, L137, L138, L139, L140, L141, L147, L148, mycorrhizal.

Amanita solitaria (Bull.) Mérat: (P), L4, mycorrhizal.

Amanita submembranacea (Bon) Gröger: (U), L4, L9, L11, L36, mycorrhizal.

Amanita subnudipes (Romagn.) Tulloss: (E), (New record for Turkey)

Pileus 30-80 mm wide, conic at first, then convex, mat, with a striate margin, pale pure orange or with a more yellow tint (Fig. 2a). Flesh white, orange-ocherish under the cuticle, thin, almost odourless, taste mild. Lamellae free, subcrowded, and whitish, short lamellae are infrequent. Stipe 110-140 × 12-20 mm, cylindrical, white, or very pale, fragile, exannulate, hollow. The sac-like volva is white, membranous, thin, tall, and persistent. Spores (5-)7.5-10(-13) × (6-)9-12(-18) µm, subglobose to broadly ellipsoid (rarely globose or ellipsoid or narrower) and inamyloid (Fig. 2b). Basidia 10-12 × 50-55 µm, cylindrical to subclavate, 4-spored (Fig. 2c).

Distribution: L11, under *Quercus* sp., mycorrhizal.

Remarks: While this species was previously described as *Amanita crocea* var. *subnudipes* Romagn., it was raised to the species level by Tullos (2000). It is easily separated from *Amanita crocea* with its pure orange or with a more yellow tint pileus, white or very pale and lacking contrasting fibrillose decoration stipe.

Amanita vaginata (Bull.) Lam.: (E), L4, L5, L9, L11, L18, L21, L27, L34, L37, L38, L40, L67, L68, L81, L108, L127, L137, L138, L146, L147, L148, mycorrhizal.

Amanita verna (Bull.) Lam.: (P), L35, L141, L142, mycorrhizal.

Amanita virosa Bertill.: (P), L47, L137, L140, mycorrhizal.

Zhuliangomyces illinitus (Fr.) Redhead: (E), L40, saprobe.

Family *Cortinariaceae*

Cortinarius aureofulvus M.M. Moser: (I), L108, mycorrhizal.

Cortinarius elegantissimus Rob. Henry: (I), L40, mycorrhizal.

Cortinarius humicola (Quél.) Maire: (P), L66, L144, mycorrhizal.

Cortinarius melanotus Kalchbr.: (I), L2, mycorrhizal.

Cortinarius orellanus Fr.: (P), L2, mycorrhizal.

Family *Crepidotaceae*

Crepidotus luteolus Sacc.: (I), L85, L91, mycorrhizal.

Crepidotus variabilis (Pers.) P. Kumm.: (I), L7, L85, saprobe.

Family *Entolomataceae*

Clitopilus prunulus (Scop.) P. Kumm.: (E), L87, L25, saprobe.

Entoloma lividoalbum (Kühner & Romagn.) Kubička: (I), L40, saprobe.

Entoloma rhodopolium (Fr.) P. Kumm.: (P), L6, L108, saprobe.

Entoloma sinuatum (Bull. ex Pers.) P. Kumm.: (P), L11, saprobe.

Family *Fistulinaceae*

Fistulina hepatica (Schaeff.) With.: (E), L50, L84, saprobe, or weakly parasite, causes a brown rot.

Family *Hydnangiaceae*

Laccaria amethystina Cooke: (E), L4, L48, L53, L66, L79, L80, L94, L108, L109, L118, L125, L127, L145, L147, mycorrhizal.

Laccaria laccata (Scop.) Cooke: (E), L4, L42, L47, L48, L53, L62, L64, L66, L94, L96, L109, L108, L112, L127, L22, mycorrhizal.

Laccaria proxima (Boud.) Pat.: (E), L95, mycorrhizal.

Family *Hygrophoraceae*

Ampulloclitocybe clavipes (Pers.) Redhead, Lutzoni, Moncalvo & Vilgalys: (E), L84, L118, saprobe.

Cantharellula umbonata (J.F. Gmel.) Singer: (E), L66, mycorrhizal.

Chrysomphalina chrysophylla (Fr.) Clémençon: (U), L53, L66, saprobe.

Hygrocybe conica (Schaeff.) P. Kumm.: (I), L89, L119, L127, saprobe.

Hygrocybe obrussea (Fr.) Wunsche: (E), (New record for Turkey)

Pileus 15-30(70) mm across, campanulate, obtusely conic at first, later conic-campanulate to plane, often with an obtuse umbo, surface somewhat butyraceous when moist, satiny, dull when dry, orange to yellow-orange or reddish-orange when young, later fading to grey or olive-yellow or olive-brownish, margin acute, somewhat cleft, barely striate (Fig. 3a). Flesh lemon to orange-yellow coloured, thin, odour like *Lactarius quietus*, taste mild, somewhat unpleasant. Lamellae broad, yellow to yellow-orange, broadly adnexed and sometimes decurrent as a tooth, edges yellowish, smooth.

Stipe 4-10 × 25-60 mm, cylindric, somewhat flexuous, at times somewhat compressed, surface smooth, longitudinally fibrillose, dry, with translucent cross-bands, yellow-orange to orange, base sometimes whitish, hollow, elastic. Spores 3.5-5 × 7-9.5 µm, elliptic-cylindric, usually constricted, smooth, hyaline, with drops (Fig. 3b). Basidia 40-50 × 7-8.5 µm, clavate, with 4-sterigmata and basal clamp (Fig. 3b).

Distribution: L40, under *Quercus* sp., saprobe.

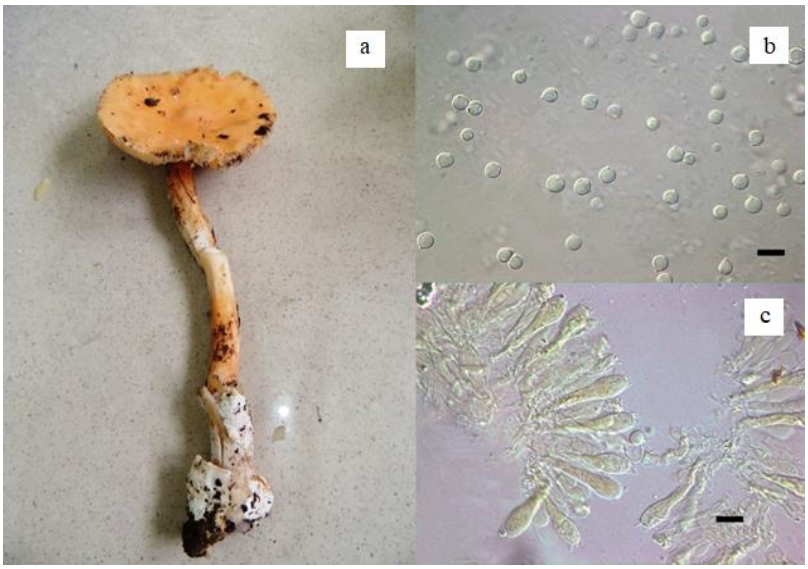

Fig. 2. *Amanita subnudipes*. a) Macroscopic view, b) basidiospores, c) basidia. Scales 15 µm.

Fig. 3. *Hygrocybe obrussea*. a) Macroscopic view, b) basidiospores and basidia, Scale 15 µm.

Remarks: In addition to the dry stipe, the characteristic features of this species are the +/broadly adnexed lamellae (never free), the typical odour like *Lactarius quietus*, and the constricted spores. The epithet *H. obrussea* is interpreted very variously in the lit. Arnolds (1986) clarified this problem and showed that *H. quieta* is a synonym of the Friesian species *Agaricus obrusseus*, and he proposed a neotypification. *Hygrophorus obrusseus* ss. Kuhn. is a different species with free lamellae, without a special odour, with non-constricted spores, and with cheilocystidia. This species was newly described by Arnolds (op.cit.) under the name *Hygrocybe cystidiata* (Breitenbach & Kränzlin, 1991).

Hygrophorus agathosmus (Fr.) Fr.: (E), L101, mycorrhizal.

Hygrophorus chrysodon (Batsch) Fr.: (E), L97, mycorrhizal.

Hygrophorus eburneus (Bull.) Fr.: (E), L2, mycorrhizal.

Hygrophorus hedrychii (Velen.) K. Kult: (U), L144, mycorrhizal.

Hygrophorus penarius Fr.: (E), L4, L31, L121, mycorrhizal.

Hygrophorus poetarum R. Heim: (E), L13, mycorrhizal.

Hygrophorus pudorinus (Fr.) Fr.: (E), L66, L97, L15, L119, mycorrhizal.

Family *Hygrophoropsidaceae*

Hygrophoropsis aurantiaca (Wulfen) Maire: (P), L86, L118, saprobe.

Family *Hymenogastraceae*

Galerina badipes (Pers.) Kühner: (P), L66, saprobe.

Gymnopilus sapineus (Fr.) Murrill: (P), L66, saprobe.

Hebeloma leucosarx P.D. Orton: (U), L2, mycorrhizal.

Hebeloma quercetorum Quadr.: (I), (New record for Turkey)

Fig. 4. *Hebeloma quercetorum*. a) Macroscopic view, b) basidiospores, c) basidia, d) cheilocystidia. Scales 15 µm.

Pileus 20-50 mm, convex at first, expanded with age, margin decurved for a long time, viscid to slimy, somewhat hygrophanous or not, dark pinkish buff to clay-buff or yellowish-brown (Fig. 4a). Flesh elastic and firm, hollow with a hanging string in the stem, white or whitish, with a greyish brown zone over the lamellae. Lamellae deeply emarginate, medium broad to rather broad, fairly crowded, at first pale pinkish buff, then through dark pinkish buff to clay-buff, without droplets. Smell and taste radish-like. Stipe 6-13 × 28-80 mm, cylindrical or with the base widened to 2 mm, whitish, discolouring to brown from the base, finely pruinose, especially in the upper part. Cortina absent, universal veil not observed. Spore deposit umber. Spores 6-8.5 × 10-14 µm, amygdaloid to broadly citriform, ornamentation distinct to rather strong, dextrinoid (Fig. 4b). Basidia 8-12 × 25-32 µm, cylindrical to subclavate, with 4-sterigmata (Fig. 4c). Cheilocystidia 6-8 × 30-55 µm, ventricose with a swollen basal part, less often cylindrical or subclavate (Fig. 4d).

Distribution: L11, under *Quercus* sp., mycorrhizal.

Remarks: *H. quercetorum* has a mixture of differently shaped cheilocystidia. It has ventricose or lageniform cheilocystidia that are mixed with cylindrical below. There are also usually a few intermediates that are clavate-lageniform, i.e. swollen both at the apex and in the basal part. Within Hebeloma. sect. Sinapizantia, and with a large number of ventricose cheilocystidia, can be confused with *H. sinapizans*. However, it is easily separated from *H. sinapizans* macroscopically by the occasional presence of tears, the lower number of lamellae and the less robust appearance, and microscopically by the presence of occasional gently clavate and clavate-lageniform cheilocystidia.

Hebeloma sinapizans (Paulet) Gillet: (P), L90, L120, L121, mycorrhizal.

Family *Inocybaceae*

Inocybe acuta Boud.: (P), L36, mycorrhizal.

Inocybe asterospora Quél.: (P), L9, mycorrhizal.

Inocybe catalaunica Singer: (P), L91, L92, L111, mycorrhizal.

Inocybe fuscidula Velen.: (P), L66, L92, mycorrhizal.

Inocybe godeyi Gillet: (P), L73, mycorrhizal.

Inocybe grammopodia Malençon: (P), L73, mycorrhizal.

Inocybe lacera (Fr.) P. Kumm.: (P), L87, mycorrhizal.

Inocybe phaeodisca Kühner var. *geophylloides*: (P), L66, mycorrhizal.

Inocybe posterula (Britzelm.) Sacc.: (P), L66, L78, L87, L92, L111, mycorrhizal.

Inocybe pseudodestricta Stangl & J. Veselský: (P), L1, L91, mycorrhizal.

Inocybe queletii Konrad: (P), L127, mycorrhizal.

Inocybe sambucina (Fr.) Quél.: (P), L1, mycorrhizal.

Inocybe splendens R. Heim: (P), L74, L104, mycorrhizal.

Inosperma bongardii (Weinm.) Matheny & Esteve-Rav.: (P), L1, mycorrhizal.

Inosperma bongardii (Weinm.) Matheny & Esteve-Rav.: (P), L73, L74, mycorrhizal.

Inosperma erubescens (A. Blytt) Matheny & Esteve-Rav.: (P), L73, mycorrhizal.

Family *Lycoperdaceae*

Bovista plumbea Pers.: (E), L52, L59, L66, L72, L109, L127, saprobe.

Calvatia gigantea (Batsch) Lloyd: (E), L52, L87, saprobe.

Calvatia utriformis (Bull.) Jaap: (E), L66, L72, L95, L118, saprobe.

Lycoperdon atropurpureum Vittad.: (E), L147, saprobe.

Lycoperdon caudatum J. Schröt.: (E), L66, saprobe.

Lycoperdon echinatum Pers.: (E), L19, L31, L50, L53, L66, saprobe.

Lycoperdon excipuliforme (Scop.) Pers.: (E), L96, saprobe.

Lycoperdon lividum Pers.: (E), L82, L87, L135, saprobe.

Lycoperdon mammiforme Pers.: (E), L50, saprobe.

Lycoperdon molle Pers.: (E), L31, L53, L66, L70, L71, L104, L108, L112, L127, saprobe.

Lycoperdon nigrescens Wahlenb.: (E), L74, saprobe.

Lycoperdon perlatum Pers.: (E), L6, L11, L19, L31, L46, L49, L53, L58, L65, L66, L71, L74, L82, L86, L87, L97, L98, L103, L107, L108, L109, L115, L120, L121, L124, L125, L126, L127, saprobe.

Lycoperdon pratense Pers.: (E), L52, L109, saprobe.

Lycoperdon pyriforme Schaeff.: (E), L35, L59, L66, L67, L87, L108, L127, L129, saprobe.

Lycoperdon umbrinum Pers.: (E), L53, saprobe.

Family *Lyophyllaceae*

Lyophyllum fumosum (Pers.) P.D. Orton: (E), L98, saprobe.

Lyophyllum transforme (Sacc.) Singer: (E), L104, saprobe.

Family *Marasmiaceae*

Marasmius bulliardii Quél.: (I), L126, saprobe.

Marasmius cohaerens (Pers.) Cooke & Quél.: (I), L46, saprobe.

Marasmius oreades (Bolton) Fr.: (E), L66, saprobe.

Marasmius torquescens Quél.: (I), L79, L118, saprobe.

Megacollybia platyphylla (Pers.) Kotl. & Pouzar: (I), L12, L18, L21, L27, L34, L36, L44, L45, L51, L59, L65, L66, L82, L84, L104, L108, L125, saprobe.

Family *Mycenaceae*

Mycena crocata (Schrad.) P. Kumm.: (I), L42, L46, L53, L55, L59, L64, L66, L71, L87, L99, L118, L123, L127, L128, saprobe.

Mycena galericulata (Scop.) Gray: (I), L1, saprobe.

Mycena galopus (Pers.) P. Kumm.: (I), L128, saprobe.

Mycena haematopus (Pers.) P. Kumm.: (I), L7, L79, saprobe.

Mycena laevigata (Lasch) Gillet: (I), L127, saprobe.

Mycena latifolia (Peck) A.H. Sm.: (I), L125, saprobe.

Mycena leptocephala (Pers.) Gillet: (I), L60, saprobe.

Mycena pelianthina (Fr.) Quél.: (P), L128, saprobe.

Mycena pura (Pers.) P. Kumm.: (P), L16, L19, L22, L31, L42, L50, L59, L66, L67, L70, L72, L76, L82, L86, L87, L91, L108, L109, L111, L127, saprobe.

Mycena renati Quél.: (I), L60, saprobe.

Mycena rosea Gramberg: (P), L11, L67, L77, L87, L108, L115, L118, L127, L140, saprobe.

Mycena stipata Maas Geest. & Schwöbel: (I), L67, saprobe.

Panellus mitis (Pers.) Singer: (I), L115, saprobe.

Family *Omphalotaceae*

Collybiopsis confluens (Pers.) R.H. Petersen: (I), L71, saprobe.

Gymnopus dryophilus (Bull.) Murrill: (E), L11, L14, L33, L88, L91, L109, L111, L127, L141, saprobe.

Gymnopus foetidus (Sowerby) P.M. Kirk: (I), L40, saprobe.

Gymnopus fusipes (Bull.) Gray: (I), L84, saprobe.

Gymnopus oreadoides (Pass.) Antonín & Noordel.: (I), L84, saprobe.

Mycetinis alliaceus (Jacq.) Earle: (I), L1, L16, L17, L42, L57, L59, L60, L64, L65, L66, L71, L74, L76, L79, L87, L91, L92, L97, L108, L109, L113, L114, L115, L127, L128, saprobe.

Omphalotus olearius (DC.) Singer: (P), L11, L15, saprobe.

Rhodocollybia butyracea (Bull.) Lennox: (E), L4, L66, L71, L96, L120, L147, saprobe.

Family *Physalacriaceae*

Armillaria cepistipes Velen.: (E), L39, parasite, causes rotten root.

Armillaria gallica Marxm. & Romagn.: (E), L55, saprobe or weak pathogen.

Armillaria mellea (Vahl) P. Kumm.: (F), L6, L19, L24, L30, L42, L48, L57, L66, L106, L108, L115, L127, L140, parasite, causes rotten root.

Armillaria solidipes Peck: (U), L22, L66, L145, parasite, causes rotten root.

Hymenopellis radicata (Relhan) R.H. Petersen: (E), L6, L11, L16, L18, L21, L22, L30, L33, L34, L35, L36, L37, L38, L41, L42, L44, L46, L47, L50, L53, L64, L65, L66, L67, L70, L71, L72, L74, L78, L82, L84, L85, L91, L92, L104, L108, L109, L118, L119, L123, L125, L126,

L127, L128, L137, L138, L140, L141, L144, L146, L148, saprobe.

Mucidula mucida (Schrad.) Pat.: (E), L66, L87, L103, L108, L115, L128, L144, saprobe.

Oudemansiella melanotricha (Dörfelt) M.M. Moser: (E), L66, L109, L115, saprobe.

Family *Pleurotaceae*

Pleurotus eryngii (DC.) Quél.var. *eryngii*: (E), L65, mycorrhizal.

Pleurotus ostreatus (Jacq.) P. Kumm.: (F), L87, L90, L147, lignicolous.

Pleurotus pulmonarius (Fr.) Quél.: (E), L32, lignicolous.

Family *Pluteaceae*

Pluteus cervinus (Schaeff.) P. Kumm.: (E), L36, saprobe.

Pluteus petasatus (Fr.) Gillet: (I), L27, L31, L36, L50, L140, L144, saprobe.

Pluteus salicinus (Pers.) P. Kumm.: (I), L46, L82, L127, L138, L141, saprobe.

Volvariella bombycina (Schaeff.) Singer: (E), L137, saprobe.

Family *Psathyrellaceae*

Britzelmayria multipedata (Peck) D. Wächt. & A. Melzer: (I), L70, saprobe.

Coprinellus micaceus (Bull.) Vilgalys, Hopple & Jacq. Johnson: (I), L1, L34, L37, L45, L46, L47, L65, L66, L71, L72, L74, L84, L87, L102, L104, L108, L109, L112, L125, L128, saprobe.

Coprinellus silvaticus (Peck) Gminder: (I), L127, saprobe.

Coprinellus xanthothrix (Romagn.) Vilgalys, Hopple & Jacq. Johnson: (I), L16, L128, saprobe.

Coprinopsis atramentaria (Bull.) Redhead, Vilgalys & Moncalvo: (E, or P), L59, L109, saprobe.

Coprinopsis cinerea (Schaeff.) Redhead, Vilgalys & Moncalvo: (I), L73, saprobe.

Coprinopsis insignis (Peck) Redhead, Vilgalys & Moncalvo: (I), L9, L11, saprobe.

Coprinopsis lagopus (Fr.) Redhead, Vilgalys & Moncalvo: (I), L13, saprobe.

Coprinopsis picacea (Bull.) Redhead, Vilgalys & Moncalvo: (I), L6, L22, L24, L31, L55, L98, L108, L140, saprobe.

Lacrymaria lacrymabunda (Bull.) Pat.: (I), L53, L71, L103, L109, L134, saprobe.

Panaeolus acuminatus (Schaeff.) Quél.: (I), L16, saprobe.

Panaeolus cinctulus (Bolton) Sacc.: (P), : (I), L118, saprobe.

Psathyrella candolleana (Fr.) Maire: (I), L53, saprobe.

Psathyrella cotonea (Quél.) Konrad & Maubl.: (I), L28, saprobe.

Psathyrella murcida (Fr.) Kits van Wav.: (I), L67, saprobe.

Psathyrella phegophila Romagn.: (I), L148, saprobe.

Psathyrella piluliformis (Bull.) P.D. Orton: (I), L31, saprobe.

Psathyrella tephrophylla (Romagn.) Bon: (I), L13, saprobe.

Family *Schizophyllaceae*

Schizophyllum commune Fr.: (M), L34, L60, L69, L82, L87, L95, L112, L113, L138, lignicolous.

Family *Strophariaceae*

Agrocybe dura (Bolton) Singer: (E), L91, L104, saprobe.

Agrocybe paludosa (J.E. Lange) Kühner & Romagn. ex Bon: (I), L104, L109, L134, saprobe.

Agrocybe pediades (Fr.) Fayod: (I), L108, saprobe.

Agrocybe praecox (Pers.) Fayod: (E), L1, L21, L59, L60, L82, saprobe.

Hypholoma capnoides (Fr.) P. Kumm.: (I), L2, saprobe.

Hypholoma fasciculare (Huds.) P. Kumm.: (P), L1, L5, L16, L18, L19, L34, L44, L45, L53, L59, L60, L62, L66, L67, L70, L95, L96, L104, L108, L112, L127, L142, L144, saprobe.

Hypholoma lateritium (Schaeff.) P. Kumm: (P), L67, saprobe.

Leratiomyces squamosus (Pers.) Bridge & Spooner: (I), L53, L66, L87, L118, saprobe.

Pholiota astragalina (Fr.) Singer: (I), L64, saprobe.

Pholiota conissans (Fr.) Kuyper & Tjall.-Beuk.: (I), L77, saprobe.

Pholiota gummosa (Lasch) Singer: (I), L67, saprobe.

Pholiota lenta (Pers.) Singer: (I), L66, saprobe.

Pholiota mixta (Fr.) Kuyper & Tjall.-Beuk.: (I), L112, saprobe.

Protostropharia semiglobata (Batsch) Redhead, Moncalvo & Vilgalys: (E), L109, L118, saprobe.

Stropharia aeruginosa (Curtis) Quél.: (I), L16, L19, L30, saprobe.

Stropharia caerulea Kreisel: (I), L47, L62, L66, L67, L82, L104, L108, L115, L144, saprobe.

Family *Tricholomataceae*

Aspropaxillus candidus (Bres.) M.M. Moser: (E), L2, L66, saprobe.

Atractosporocybe inornata (Sowerby) P. Alvarado, G. Moreno & Vizzini: (I), L66, saprobe.

Clitocybe costata Kühner & Romagn.: (I), L45, L73, saprobe.

Clitocybe nebularis (Batsch) P. Kumm.: (F), L47, L61, L64, L66, L96, L97, L104, saprobe.

Clitocybe odora (Bull.) P. Kumm: (E), L50, L65, L66, L96, L109, saprobe.

Clitocybe phaeophthalma (Pers.) Kuyper: (P), L66, saprobe.

Clitocybe phyllophila (Pers.) P. Kumm.: (P), L118, saprobe.

Infundibulicybe geotropa (Bull.) Harmaja: (F), L86, L87, saprobe.

Infundibulicybe gibba (Pers.) Harmaja: (E), L66, L82, L84, L118, saprobe.

Lepista densifolia (J. Favre) Singer & Clémençon: (E), L73, saprobe.

Lepista nuda (Bull.) Cooke: (E), L19, L66, L67, L78, L123, saprobe.

Melanoleuca exscissa (Fr.) Singer: (E), L145, saprobe.

Paralepista flaccida (Sowerby) Vizzini: (E), L25, L45, saprobe.

Tricholoma acerbum (Bull.) Quél.: (P), L26, mycorrhizal.

Tricholoma albobrunneum (Pers.) P. Kumm.: (P), L19, L62, mycorrhizal.

Tricholoma atrosquamosum var. *squarrulosum* (Bres.) Mort. Chr. & Noordel.: (E), L108, mycorrhizal.

Tricholoma aurantium (Schaeff.) Ricken: (P), L66, L96, L119, mycorrhizal.

Tricholoma basirubens (Bon) A. Riva & Bon: (U), L121, mycorrhizal.

Tricholoma cf. *venenatum* G.F. Atk.: (U), L77, L96, mycorrhizal.

Tricholoma cingulatum (Almfelt ex Fr.) Jacobashch: (U), L122, mycorrhizal.

Tricholoma equestre (L.) P. Kumm.: (E or P), L108, mycorrhizal.

Tricholoma focale (Fr.) Ricken: (I), L124, mycorrhizal.

Tricholoma fulvum (DC.) Bigeard & H. Guill.: (E or ?), L57, L108, L125, mycorrhizal.

Tricholoma imbricatum (Fr.) P. Kumm.: (I), L65, L66, mycorrhizal.

Tricholoma joachimii Bon & A. Riva: (P), L89, mycorrhizal.

Tricholoma populinum J.E. Lange: (E), L20, L61, mycorrhizal.

Tricholoma portentosum (Fr.) Quél.: (E), L39, L62, L121, L124, mycorrhizal.

Tricholoma quercetorum Contu: (U), L40, mycorrhizal.

Tricholoma roseoacerbum A. Riva: (U), (New record for Turkey)

Pileus 50-120 mm, convex with an involute, often ribbed margin, somewhat expanding with age, but margin remaining deflexed or even involute for a very long time, smooth or minutely granulate, slightly viscid in moist weather, almost without radial structure, in the central part pinkish buff to brick or pale vinaceous, somewhat marbled, towards margin whitish to salmon, sometimes with pale yellowish flushes (Fig. 5a). Flesh firm, white to cream; smell weak; taste farinaceous to slightly bitterish. Lamellae emarginate, crowded to very crowded, whitish chrome to cream or straw yellow, often with brown spots when old or damaged. Stipe 15-30 × 20-40 (-60) mm, cylindrical to slightly clavate, often somewhat rooting with attenuated base, white or whitish, often pinkish to ochre flushed in the lower part, smooth or slightly punctate floccose. Spores 3-5 × 4.5-7 μm, average, predominantly ellipsoid (Fig. 5b). Basidia 5.0-7.5 × 20-30 μm, clavate, with 4-sterigmata (Fig. 5c).

Distribution: L66, under *A. nordmanniana* subsp. *bornmuelleriana*, mycorrhizal, L114, L20, under *F. orientalis*, mycorrhizal.

Remarks: *Tricholoma roseoacerbum* is closely related to *T. acerbum*, but differs by the faintly viscid, pinkish buff to the brick cap, and by a less distinctly ribbed cap margin. Another possibility of confusion is *T. stans*, but this species tends to have more well-spaced gills, darker brick cap colours, and a soon expanding cap margin.

Tricholoma saponaceum var. *saponaceum* (Fr.) P. Kumm.: (U), L71, L108, L127, L4, L144, L119, mycorrhizal.

Tricholoma scalpturatum (Fr.) Quél.: (U), L40, mycorrhizal.

Tricholoma sciodes (Pers.) C. Martín: (U), L114, L144, mycorrhizal.

Tricholoma sejunctum (Sowerby) Quél.: (U), L71, L89, mycorrhizal.

Tricholoma stans (Fr.) Sacc.: (U), L96, mycorrhizal.

Tricholoma subannulatum (Peck) Zeller: (I), L117, L121, L135, mycorrhizal.

Tricholoma sulphureum (Bull.) P. Kumm.: (P), L25, mycorrhizal.

Tricholoma terreum (Schaeff.) P. Kumm.: (E), L19, L65, L66, L67, L86, L97, L115, L117, L121, mycorrhizal.

Tricholoma triste (Scop.) Quél.: (E), L40, mycorrhizal.

Tricholoma ustaloides Romagn.: (P), L89, L125, mycorrhizal.

Tricholomopsis rutilans (Schaeff.) Singer: (P), L66, L71, L86, L103, L125, L127, saprobe.

Family *Tubariaceae*

Phaeomarasmius erinaceus (Fr.) Scherff. ex Romagn.: (I), L9, L148, saprobe.

Family *Typhulaceae*

Typhula fistulosa (Holmsk.) Olariaga: (I), L40, saprobe.

Order Auriculariales
Family *Auriculariaceae*

Auricularia auricula-judae (Bull.) Quél.: (E), L63, saprobe.

Family *Exidiaceae*

Exidia truncata Fr.: (E), L9, L54, L93, L63, L84, saprobe.

Pseudohydnum gelatinosum (Scop.) P. Karst.: (I), L66, L71, L109, saprobe.

Order Boletales
Family *Boletaceae*

Boletus aereus Bull.: (F), L11, L19, mycorrhizal.

Boletus aestivalis (Paulet) Fr.: (F), L103, L127, L139, mycorrhizal.

Boletus edulis Bull.: (F), L11, L18, L23, L27, L34, L35, L36, L37, L48, L66, L96, L102, L125, L127, L134, L140, L141, mycorrhizal.

Boletus pinophilus Pilát & Dermek: (F), L11, L65, mycorrhizal.

Boletus reticulatus Schaeff.: (F), L5, L18, L27, L34, L37, L108, L127, mycorrhizal.

Butyriboletus fechtneri (Velen.) D. Arora & J.L. Frank: (E), L27, L35, L109, L127, mycorrhizal.

Butyriboletus pseudoregius (Heinr. Huber) D. Arora & J.L. Frank: (E), L11, L89, mycorrhizal.

Butyriboletus regius (Krombh.) D. Arora & J.L. Frank: (E), L27, mycorrhizal.

Butyriboletus subappendiculatus (Dermek, Lazebn. & J. Veselský) D. Arora & J.L. Frank: (E), L5, L19, L66, L67, mycorrhizal.

Caloboletus calopus (Pers.) Vizzini: (I), L57, L66, L125, mycorrhizal.

Chalciporus piperatus (Bull.) Bataille: (E), L126, mycorrhizal.

Cyanoboletus pulverulentus (Opat.) Gelardi, Vizzini & Simonini: (E), L95, mycorrhizal.

Imperator rhodopurpureus (Smotl.) Assyov, Bellanger, Bertéa, Courtec., Koller,

Loizides, G. Marques, J.A. Muñoz, Oppicelli, D. Puddu, F. Rich. & P.-A. Moreau: (I), L11, mycorrhizal.

Leccinum aurantiacum (Bull.) Gray: (E), L23, mycorrhizal.

Leccinum duriusculum (Schulzer ex Kalchbr.) Singer: (E), L134, L138, mycorrhizal.

Leccinum pseudoscabrum (Kallenb.) Šutara: (E), L138, mycorrhizal.

Leccinum quercinum (Pilát) E.E. Green & Watling: (E), L18, mycorrhizal.

Neoboletus erythropus (Pers.) C. Hahn: (E), L11, L59, L66, L70, L71, L72, L74, L78, L91, L92, L125, L127, L141, mycorrhizal.

Neoboletus luridiformis (Rostk.) Gelardi, Simonini & Vizzini: (E), L125, mycorrhizal.

Neoboletus xanthopus (Klofac & A. Urb.) Klofac & A. Urb.: (I), L118, mycorrhizal.

Rubroboletus dupainii (Boud.) Kuan Zhao & Zhu L. Yang: (P), L65, mycorrhizal.

Rubroboletus rhodoxanthus (Krombh.) Kuan Zhao & Zhu L. Yang: (U), L11, L66, mycorrhizal.

Rubroboletus satanas (Lenz) Kuan Zhao & Zhu L. Yan: (P), L11, L125, mycorrhizal.

Strobilomyces strobilaceus (Scop.) Berk.: (I), L46, L127, mycorrhizal.

Suillellus queletii (Schulzer) Vizzini, Simonini & Gelardi: (E), L11, L70, mycorrhizal.

Suillellus rubrosanguineus (Cheype) Blanco-Dios: (U), L125, mycorrhizal.

Xerocomellus chrysenteron (Bull.) Šutara: (E), L9, L11, L19, L22, L34, L36, L64, L65, L66, L67, L68, L70, L86, L87, L103, L104, L118, L127, L128, L133, L140, L145, mycorrhizal.

Xerocomus depilatus (Redeuilh) Manfr. Binder & Besl: (E), L29, mycorrhizal.

Xerocomus porosporus (Imler ex G. Moreno & Bon) Contu: (U), L66, L75, mycorrhizal.

Xerocomus rubellus (Krombh.) Quél.: (E), L66, mycorrhizal.

Xerocomus subtomentosus (L.) Quél.: (E), L12, mycorrhizal.

Family *Diplocystidiaceae*

Astraeus hygrometricus (Pers.) Morgan: (I), L39, L42, L48, L61, L94, L95, L113, saprobe.

Fig. 5. *Tricholoma roseoacerbum*. a) Macroscopic view, b) basidiospores, c) basidia. Scales 15 µm.

Family *Gomphidiaceae*

Chroogomphus rutilus (Schaeff.) O.K. Mill.: (E), L19, L31, L38, L49, L58, L62, L66, L82, L86, L94, L103, L107, L109, L121, L127, mycorrhizal.

Family *Gyroporaceae*

Gyroporus *castaneus* (Bull.) Quél.: (E), L53, mycorrhizal.

Family *Paxillaceae*

Paxillus involutus (Batsch) Fr.: (P), L4, L5, L17, L47, L62, L96, L109, L112, mycorrhizal.

Family *Rhizopogonaceae*

Rhizopogon abietis A.H. Sm.: (I), L96, mycorrhizal.

Rhizopogon luteolus Kromb.: (E), L17, L107, L140, mycorrhizal.

Rhizopogon roseolus (Corda) Th. Fr.: (E), L19, L94, L124, mycorrhizal.

Family *Sclerodermataceae*

Pisolithus arhizus (Scop.) Rauschert: (M), L145, mycorrhizal.

Scleroderma areolatum Ehrenb.: (I), L95, L144, mycorrhizal.

Scleroderma cepa Pers.: (I), L24, mycorrhizal.

Scleroderma polyrhizum (J.F. Gmel.) Pers.: (I), L144, mycorrhizal.

Scleroderma verrucosum (Bull.) Pers.: (I), L22, L61, mycorrhizal.

Family *Suillaceae*

Suillus bovinus (L.) Roussel: (E), L56, L58, mycorrhizal.

Suillus collinitus (Fr.) Kuntze: (E), L15, L117, mycorrhizal.

Suillus granulatus (L.) Roussel: (E), L31, L82, L107, L108, L124, mycorrhizal.

Suillus luteus (L.) Roussel: (E), L17, L19, L24, L66, L96, L104, L124, L127, mycorrhizal.

Family *Tapinellaceae*

Tapinella atrotomentosa (Batsch) Šutara: (I), L135, saprobe.

Tapinella panuoides (Fr.) E.-J. Gilbert: (I), L82, saprobe.

Order Cantharellales
Family *Hydnaceae*

Cantharellus cibarius Fr.: (F), L4, L5, L34, L43, L50, L58, L66, L118, L135, mycorrhizal.

Clavulina cinerea (Bull.) J. Schröt.: (E), L25, L48, L66, L71, L103, L108, L126, L147, mycorrhizal.

Clavulina coralloides (L.) J. Schröt.: (E), L73, mycorrhizal.

Clavulina cristata (Holmsk.) J. Schröt.: (E), L11, L58, L61, L64, L66, L87, L94, L109, L126, mycorrhizal.

Clavulina rugosa (Bull.) J. Schröt.: (E), L48, L59, L66, L87, L97, L109, L118, L122, L126, L127, mycorrhizal.

Craterellus cornucopioides (L.) Pers.: (F), L4, L42, L47, L48, L50, L59, L66, L71, L89, L104, L108, L109, L114, L118, L126, L144, saprobe.

Craterellus lutescens (Fr.) Fr: (E), L57, L66, L127, mycorrhizal.

Craterellus tubaeformis (Fr.) Quél.: (E), L57, mycorrhizal.

Hydnum repandum L.: (F), L4, L19, L31, L39, L47, L50, L53, L57, L59, L66, L81, L89, L97, L103, L108, L109, L114, L124, L127, L145, mycorrhizal.

Pseudocraterellus undulatus (Pers.) Rauschert: (E), L48, L50, L58, L71, L108, L126, saprobe.

Order Dacrymycetales
Family *Dacrymycetaceae*

Calocera viscosa (Pers.) Fr.: (I), L66, L71, L87, L123, L127, saprobe, causes a white-rot.

Ditiola radicata (Alb. & Schwein.) Fr.: (I), L19, L34, L66, L133, saprobe.

Order Geastrales
Family *Geastraceae*

Geastrum berkeleyi Massee: (I), L115, saprobe.

Geastrum coronatum Pers.: (I), L24, saprobe.

Geastrum fimbriatum Fr.: (I), L58, saprobe.

Geastrum minimum Schwein.: (I), L109, saprobe.

Geastrum triplex Jungh.: (I), L53, under *F. orientalis*, saprobe. L87, saprobe.

Order Gomphales
Family *Clavariadelphaceae*

Clavariadelphus pistillaris (L.) Donk: (E), L40, L55, L118, saprobe.

Clavariadelphus truncatus (Quél.) Donk: (E), L14, L53, L70, L71, L109, saprobe.

Family *Gomphaceae*

Ramaria aurea (Schaeff.) Quél.: (E), L72, L104, L109, L136, mycorrhizal.

Ramaria flava (Schaeff.) Quél.: (E), L66, mycorrhizal.

Ramaria flavescens Schaeff. ex R.H. Petersen: (E), L31, L66, L70, L127, mycorrhizal.

Ramaria flavobrunnescens (G.F. Atk.) Corner: (E), L34, L109, mycorrhizal.

Ramaria formosa (Pers.) Quél.: (P), L71, , mycorrhizal.

Ramaria lutea Schild: (E), L34, L46, L50, L53, L66, L71, L109, mycorrhizal.

Ramaria pallida (Schaeff.) Ricken: (P), L19, L66, L71, L109, mycorrhizal.

Ramaria rubella (Schaeff.) R.H. Petersen: (U), L63, mycorrhizal.

Ramaria stricta (Pers.) Quél.: (E), L46, L140, mycorrhizal.

Family *Lentariaceae*

Lentaria afflata (Lagger) Corner: (I), L104, saprobe.

Order Hymenochaetales
Family *Hymenochaetaceae*

Coltricia perennis (L.) Murrill: (I), L112, mycorrhizal.

Hymenochaete rubiginosa (Dicks.) Lév.: (I), L112, saprobe.

Inonotus nodulosus (Fr.) P. Karst.: (I), L47, saprobe, causes a soft white-rot.

Inonotus radiatus (Sowerby) P. Karst.: (I), L28, saprobe.

Phellinus hartigii (Allesch. & Schnabl) Pat.: (I), L109, L115, parasite.

Phellinus lundellii Niemelä: (I), L131, L141, parasite.

Family *Tubulicrinaceae*

Hyphodontia quercina (Pers.) J. Erikss.: (I), L69, L93, saprobe.

Order Hysterangiales
Family *Phallogastraceae*

Phallogaster saccatus Morgan: (I), L75, saprobe.

Order Phallales
Family *Phallaceae*

Clathrus ruber P. Micheli ex Pers.: (I), L143, saprobe.

Mutinus caninus (Huds.) Fr.: (I), L45, L139, L140, L142, L146, saprobe.

Phallus impudicus L.: (E), L4, L5, L12, L18, L19, L21, L27, L33, L34, L35, L36, L37, L41, L42, L45, L57, L66, L71, L77, L109, L113, L114, L125, L127, L133, L137, L138, L140, L141, L146, saprobe.

Order Polyporales
Family *Fomitopsidaceae*

Antrodia ramentacea (Berk. & Broome) Donk: (I), L129, saprobe.

Daedalea quercina (L.) Pers.: (I), L67, L129, L131, lignicolous.

Fomitopsis pinicola (Sw.) P. Karst.: (M), L1, L5, L67, L70, L71, L74, L75, L97, L104, L108, parasite, causes brown rot.

Neolentiporus squamosellus (Bernicchia & Ryvarden) Bernicchia & Ryvarden: (I), L128, saprobe or weakly parasite, causes a brown rot.

Family *Grifolaceae*

Grifola frondosa (Dicks.) Gray: (E), L13, saprobe or also weakly parasite, causes a white-rot and butt rot of trees.

Family *Irpicaceae*

Ceriporia reticulata (Hoffm.) Domański: (I), L18, L34, L35, saprobe.

Family *Meripilaceae*

Meripilus giganteus (Pers.) P. Karst.: (E), L45, saprobe.

Family *Meruliaceae*

Abortiporus biennis (Bull.) Singer: (I), L10, saprobe.

Bjerkandera adusta (Willd.) P. Karst.: (I), L18, L19, L61, L63, L79, L85, L109, L112, L127, saprobe, causes a white-rot.

Family *Phanerochaetaceae*

Junghuhnia nitida (Pers.) Ryvarden: (I), L63, L69, saprobe.

Phanerochaete caucasica (Parmasto) Burds: (I), L79, saprobe.

Terana coerulea (Lam.) Kuntze: (I), L61, saprobe.

Family *Polyporaceae*

Cerrena unicolor (Bull.) Murrill: (I), L148, parasite, causes canker rot.

Cyanosporus subcaesius (A. David) B.K. Cui, L.L. Shen & Y.C. Dai: (I), L14, lignicolous, causes a brown rot.

Daedaleopsis confragosa (Bolton) J. Schröt.: (I), L6, lignicolous, causes a white-rot.

Faerberia carbonaria (Alb. & Schwein.) Pouzar: (E), L4, L112, saprobe.

Fomes fomentarius (L.) Fr.: (M), L1, L18, L34, L35, L53, L60, L63, L66, L67, L84, L87, L98, L99, L113, L130, L138, saprobe or parasite, causes a white-rot.

Ganoderma australe (Fr.) Pat.: (I), L115, saprobe or parasite, causes a white-rot.

Ganoderma carnosum Pat.: (I), L14, L53, saprobe or parasite, causes a white-rot.

Ganoderma lucidum (Curtis) P. Karst.: (M), L9, L24, L43, L58, L71, L148, saprobe or parasite, causes a white-rot.

Ganoderma resinaceum Boud.: (I), L108, saprobe or parasite, causes a white-rot.

Lenzites betulinus (L.) Fr.: (I), L64, L112, saprobe.

Neofavolus alveolaris (DC.) Sotome & T. Hatt.: (M), L36, L148, L51, saprobe.

Picipes badius (Pers.) Zmitr. & Kovalenko: (E), L1, L16, L18, L21, L34, L37, L45, L59, L66, L68, L76,. L128, L138, L140, saprobe.

Picipes melanopus (Pers.) Zmitr. & Kovalenko: (I), L12, L27, L60, L67, L108, L139, lignicolous.

Polyporus arcularius (Batsch) Fr.: (E), L4, L11, L47, L57, L84, L102, L129, L133, L138, L141, L148, saprobe.

Polyporus brumalis (Pers.) Fr.: (E), L12, L70, L87, L96, L118, L123, saprobe.

Polyporus ciliatus Fr.: (E), L9, L18, L38, L65, L84, L108, L115, L146, saprobe.

Polyporus meridionalis (A. David) H. Jahn: (E), L36, saprobe.

Polyporus squamosus (Huds.) Fr.: (E), L110, lignicolous.

Polyporus tuberaster (Jacq. ex Pers.) Fr.: (M), L1, L37, saprobe.

Polyporus varius (Pers.) Fr.: (E), L5, L18, L21, L34, L37, L59, L66, L79, L96, L102, L104, L127, L133, L146, saprobe.

Pycnoporus cinnabarinus (Jacq.) P. Karst.: (M), L57, lignicolous.

Trametes gibbosa (Pers.) Fr.: (I), L1, L27, L34, L35, L60, L71, L85, L112, L114, L123, L127, lignicolous.

Trametes hirsuta (Wulfen) Lloyd: (I), L1, L12, L16, L17, L34, L42, L53, L59, L60, L61, L69, L82, L84, L87, L92, L93, L94, L99, L108, L129, L133, L137, lignicolous.

Trametes ochracea (Pers.) Gilb. & Ryvarden: (I), L12, L16, L21, L67, L87, L108, L138, lignicolous.

Trametes pubescens (Schumach.) Pilát: (I), L6, L108, lignicolous.

Trametes suaveolens (L.) Fr.: (I), L26, lignicolous.

Trametes versicolor (L.) Lloyd: (M), L14, L35, L36, L45, L47, L55, L59, L64, L82, L84, L85, L88, L94, L95, L96, L108, L112, L114, L118, L119, L126, L128, L137, L133, L141, lignicolous.

Trichaptum abietinum (Pers. ex J.F. Gmel.) Ryvarden: (I), L1, L12, L18, L57, L66, L77, L87, L88, L104, L109, saprobe.

Family *Sparassidaceae*

Sparassis crispa (Wulfen) Fr.: (F), L103, parasite or saprobe on the roots of coniferous trees.

Order Russulales
Family *Albatrellaceae*

Albatrellus cristatus (Schaeff.) Kotl. & Pouzar: (I), L16, L48, L55, L66, L71, L94, L118, L122, mycorrhizal.

Albatrellus pes-caprae (Pers.) Pouzar: (I), L59, L125, mycorrhizal.

Family *Amylostereaceae*

Amylostereum areolatum (Chaillet ex Fr.) Boidin: (I), L65, lignicolous, causes a white-rot.

Amylostereum laevigatum (Fr.) Boidin: (I), L96, lignicolous, causes a white-rot.

Family *Auriscalpiaceae*

Auriscalpium vulgare Gray: (I), L19, L49, L66, L82, L94, L96, L108, L120, L124, saprobe, on the cones of conifers.

Lentinellus cochleatus (Pers.) P. Karst.: (I), L87, saprobe.

Lentinellus micheneri (Berk. & M.A. Curtis) Pegler: (I), L4, L34, L45, L111, saprobe.

Lentinellus ursinus (Fr.) Kühner: (I), L146, saprobe.

Family *Hericiaceae*

Hericium cirrhatum (Pers.) Nikol.: (E), L18, L21, L27, saprobe or/ and parasite.

Hericium coralloides (Scop.) Pers.: (E), L118, saprobe or/ and parasite.

Family *Peniophoraceae*

Peniophora cinerea (Pers.) Cooke: (I), L84, saprobe.

Family *Russulaceae*

Lactarius acerrimus Britzelm.: (I), L125, mycorrhizal.

Lactarius acris (Bolton) Gray: (I), L5, mycorrhizal.

Lactarius blennius (Fr.) Fr.: (I, or P), L118, L139, mycorrhizal.

Lactarius chrysorrheus Fr.: (P), L10, mycorrhizal.

Lactarius deliciosus (L.) Gray: (F), L19, L31, L37, L58, L62, L86, L118, L119, L121, L126, mycorrhizal.

Lactarius evosmus Kühner & Romagn.: (I), L10, L118, mycorrhizal.

Lactarius ilicis Sarnari: (U), L12, mycorrhizal.

Lactarius illyricus Piltaver: (U), L104, mycorrhizal.

Lactarius lacunarum Romagn. ex Hora: (U), L4, L48, mycorrhizal.

Lactarius mediterraneensis Llistosella & Bellù: (U), (New record for Turkey)

Pileus 50-100 mm, fleshy, plano-convex at first, soon depressed in the centre, funnel-shaped at the end, gibbous, lobed, margin thin, at first convoluted, then curved. Cuticle thin, elastic, viscous, from dry to shiny, concentrically scrobiculate-guttulata, creamy colour, yellow-fleshed, cream-yellowish, yellow-ocher, with mostly marginal, irregular and scrobicles concentric, darker, ocher-pink or brown-fleshed (Fig. 6a). Flesh medium, thick and firm, then soft, whitish, yellowish and then cream-pink. Faint fruity odour, acrid and bitter taste. Lamellae little spaced gills, from adnate to sub-decurrent, thin, not very elastic, with lamellule, arcuate, sometimes forked and venous-jointed to the stem, cream, cream-yellowish, cream-pale ocher, brown-ocher in the injuries. Regular, whole and concolour cutting edge. Milk (Latex) little abundant, fluid, white, yellowish either isolated that on flesh and lamellae. Acre and bitter. Macrochemical reaction: flesh + KOH = yellow-orange. Stem 15-30 × 20-40 mm, short and stocky, attenuated cylindrical at the base or truncated cone, even compressed, smooth at the apex, a little guttulated downwards; full, then pithy, fragile and finally hollow, dry, opaque and pruinose, whitish, then cream-whitish, stained with ocher in old age, not scrobiculated. Spores 9-12 × 8-10 µm, subglobose, medium size, crested-reticulated, with ridges not very thick, joined by not very thin connections that form mostly complete lattices (Fig. 6f). Basidia 7-10 × 45-55 µm, clavate, with 4-sterigmata (Fig. 6b). Macrocheilocystidia 5-7 × 30-50 µm, numerous, almost fusiform, attenuated or moniliform at the top. Macropleurocystidia similar to macrocheilocystidia (Fig. 6c).

Distribution: L29, under *Quercus* sp., mycorrhizal.

Remarks: Similar to *L. acerrimus* or *L. zonarius*. It is distinguished by the cap with irregular marginal scrobicles and by the latex which turns yellow both isolated and on flesh and gills.

Lactarius piperatus (L.) Pers.: (E), L9, L148, mycorrhizal.

Lactarius salmonicolor R. Heim & Leclair: (F), L19, L31, L67, L86, L87, L94, L96, L109, L124, L125, L127, mycorrhizal.

Lactarius semisanguifluus R. Heim & Leclair: (E), L115, L118, mycorrhizal.

Lactarius turpis (Weinm.) Fr.: (I), L94, mycorrhizal.

Lactarius volemus (Fr.) Fr.: (E), L64, L122, mycorrhizal.

Lactarius zonarius (Bull.) Fr.: (P), L4, L108, mycorrhizal.

Lactifluus bertillonii (Neuhoff ex Z. Schaef.) Verbeken: (I), L71, L146, L148, mycorrhizal.

Lactifluus glaucescens (Crossl.) Verbeken: (P), (New record for Turkey)

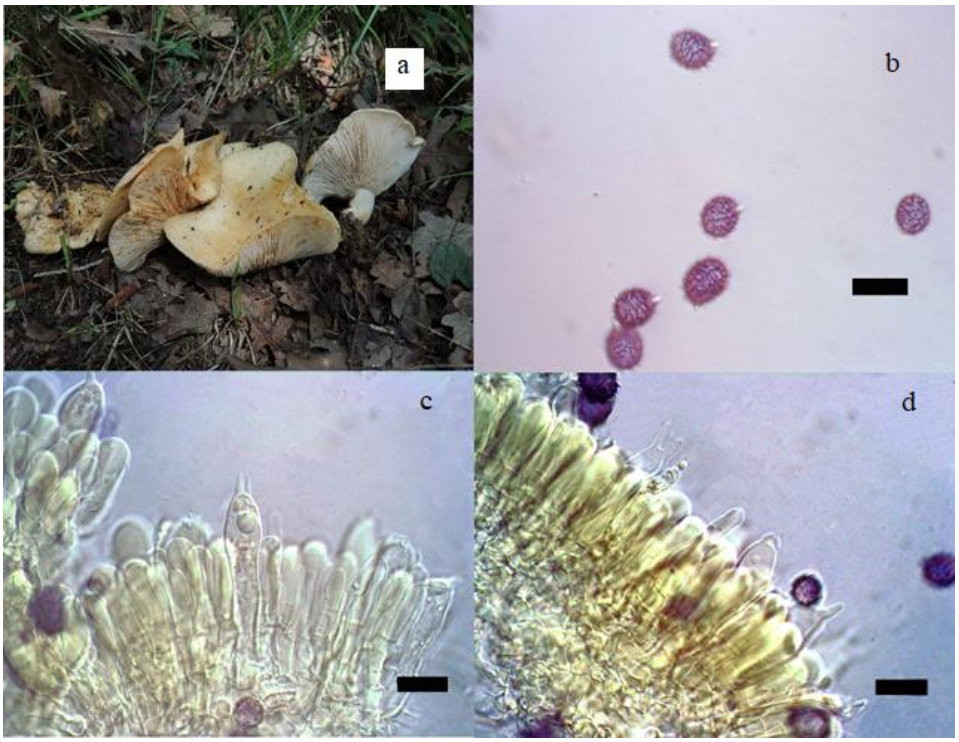

Fig. 6. *Lactarius mediterraneensis*. a) Macroscopic view, b) basidiospores, c) basidia, d) macropleurocystidia. Scales 15 µm.

Pileus 40-120 mm, fleshy, flat-convex, soon flat, flat-depressed in the centre, at the end also funnel-shaped, sometimes wavy-lobed, thick margin, long convoluted, then extended, whole, smooth, lobed. The cuticle is thin, adnate, dry, opaque, velvety, often with cracks (in which the greenish colour change of the flesh is evident). Uneven colour hazelnut cream, cream-ocher when ripe, but always lighter at the edge, from white to cream-whitish (Fig. 7a). Flesh thick and firm, compact, then spongy, white, yellowish-cream in the stem, it becomes green, grey-green and finally dark green in the air. Fruity smell, acrid taste. Lamellae thick, thin and low gills, from adnate to sub-decurrent, finally decurrent, arcuate, forked at the stem, with lamellulae, of a cream-whitish colour, then creamy flesh, grey-greenish in the lesions or when rubbed. Whole cutting edge, concolor. Milk (Latex) not abundant, creamy, white at first, then greenish on the flesh and gills, immutable if isolated. Acre. Macrochemical reactions: pileus, stem and latex flesh + KOH = yellow-orange. Stipe 10-25 × 30-60 mm, robust but not very slender, short, often eccentric or lateral, irregularly cylindrical, sometimes enlarged at the base or compressed, solid and firm, then spongy, dry, opaque, pruinose-velvety, wrinkled, with ocher and finally brown rust in old age or if injured. Spores 5.5-6 × 7-9 µm, elliptic, crested, with thin and dense crests, poorly connected, which do not form complete reticles (Fig. 7b). Basidia 7-8.5 × 35-45 µm, clavate, with 4-sterigmata (Fig. 7c). Macrocheilocystidia 5-7 × 40-60 µm, numerous and subcylindrical, obtuse at the apex. Macropleurocystidia alike to macro cheilocystidia, numerous, but larger, 7-10 × 60-90 µm (Fig. 7d).

Distribution: L9, L143, under *Quercus* sp., mycorrhizal.

Remarks: *Lactifluus glaucescens* is closely similar to *L. piperatus*, which occurs in similar habitats. *L. piperatus* has the white latex, however, does not turn greenish in the air and does not react with KOH.

Russula acrifolia Romagn.: (I), L4, mycorrhizal.

Russula albonigra (Krombh.) Fr.: (U), L4, mycorrhizal.

Russula alutacea (Pers.) Fr.: (U), L29, mycorrhizal.

Russula amethystina Quél.: (E), L37, mycorrhizal.

Russula amoena Quél.: (E), L96, mycorrhizal.

Russula atropurpurea (Krombh.) Britzelm.: (E), L2, mycorrhizal.

Russula aurea Pers.: (E), L18, L118, mycorrhizal.

Russula aurora Krombh.: (U), L94, mycorrhizal.

Russula brunneoviolacea Crawshay: (E), L73, mycorrhizal.

Russula cavipes Britzelm.: (U), L14, L81, mycorrhizal.

Russula chloroides (Krombh.) Bres.: (E), L11, mycorrhizal.

Russula clariana R. Heim ex Kuyper & Vuure: (U), L35, L37, L68, L141, mycorrhizal.

Russula cremeoavellanea Singer: (U), L119, mycorrhizal.

Russula cyanoxantha (Schaeff.) Fr.: (E), L3, L138, mycorrhizal.

Russula delica Fr.: (E), L51, L108, L119, mycorrhizal.

Russula faginea Romagn.: (U), L107, L138, mycorrhizal.

Russula foetens Pers.: (U), L19, mycorrhizal.

Russula fragilis Fr.: (U), L27, L101, mycorrhizal.

Russula gigasperma Romagn.: (U), L19, mycorrhizal.

Russula graveolens Romell: (U), L141, mycorrhizal.

Russula grisea Fr.: (E), L127, L140, mycorrhizal.

Russula insignis Quél.: (U), L12, mycorrhizal.

Russula ionochlora Romagn.: (E), L18, mycorrhizal.

Russula lilacea Quél.: (E, M), (New record for Turkey)

Pileus 30-50 mm across, convex at first, soon flat with a slight central depression, sometimes asymmetrical, obtuse, lobed, the whole then briefly grooved margin, not very fleshy and fragile. Separable cuticle up to and beyond the middle of the radius, dry, pruinose-velvety "opaque" of very variable colour; pink-lilac, reddish-purple, red-vinous, red-carmine, sometimes with brown ocher, cream or pink spots in the centre (Fig. 8a). Lamellae slightly dense, later spaced, free-rounded at the stem, forked to the same, anastomosed with some lamellula, thin, white, dark in old age. Flesh thick but fragile, white, with a slight tendency to grey, odourless and with a sweet taste. Macrochemical reactions flesh + Fe = brown-red rust, flesh + F = brown-red, flesh + SV = carmine red then reddish-brown if dried. Stipe 6-12 × 25-50 mm, initially stiff, soon fragile, cylindrical, sometimes equal at the apex or slightly enlarged towards the base, filled inside, but soon spongy or almost hollow, dry, pruinose then finely wrinkled, white, often tinged with pink or light purple-lilac. Spores 5.5-7 × 6.5-8.5 µm, subglobose-ovoid, warty-echinulate, with both high and sharp and low and obtuse warts, isolated or very rarely joined by some thin tract, amyloid (Fig. 8b). Basidia 10-12 × 40-50 µm, with 4-sterigmata (Fig. 8c). Cheilocystidia 8-10 × 60 µm, not very numerous, cylindrical-fusiform, pointed at the top. Pleurocystidia similar to Cheilocystidia (Fig. 8d).

Distribution: L112, under *C. orientalis*, mycorrhizal.

Remarks: *Russula brunneoviolacea* can occur in the same habitat, and it often has very similar pileal colors and a mild taste. However, it has septate pileocystidia and lacks primordial hyphae. *R. nitida* can also be confused with *R. lilacea*. It likewise has a red-flushed stipe and mild flesh, but it grows with *Betula* and has an ocher spore deposit. *R. turci* also has a pileus with colours very similar to *R. lilacea.* However, it is associated with conifers such as *Picea* and *Abies* and has an ocher-yellow spore deposit.

Russula mairei Singer: (P), L51, mycorrhizal.

Russula nigricans Fr.: (E), L4, L5, L11, L34, L66, mycorrhizal.

Russula odorata Romagn.: (U), L96, mycorrhizal.

Russula olivascens (Fr.) Fr.: (U), L37, mycorrhizal.

Russula pectinatoides Peck: (U), L19, mycorrhizal.

Russula queletii Fr.: (U), L19, mycorrhizal.

Fig. 7. *Lactifluus glaucescens*. a) Macroscopic view, b) basidiospores, c) basidia, d) pleurocystidia. Scales 15 µm.

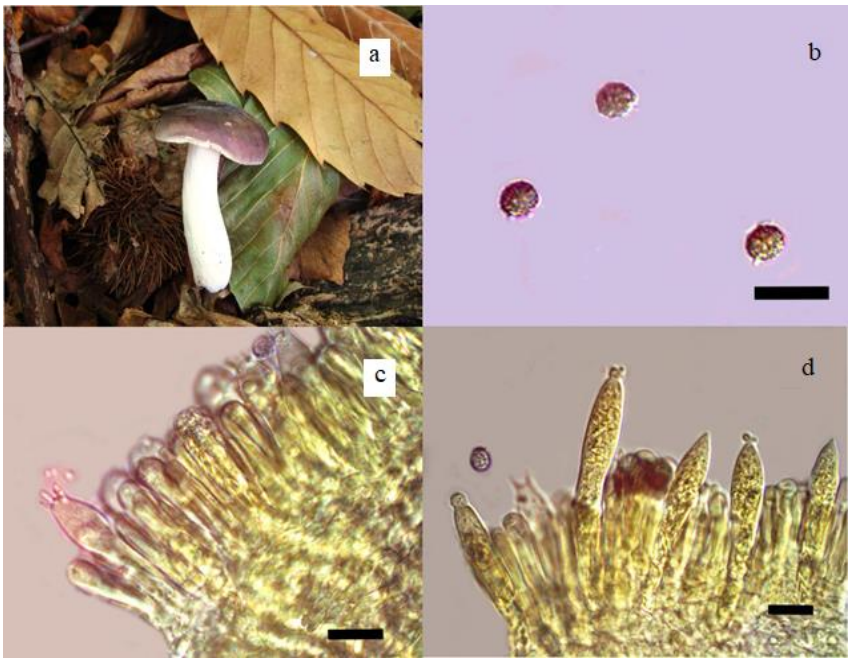

Fig. 8. *Russula lilacea*. a) Macroscopic view, b) basidiospores, c) basidia, d) pleurocystidia. Scales 15 µm.

Russula risigallina (Batsch) Sacc.: (U), L21, mycorrhizal.

Russula rubra (Lam.) Fr.: (E), (New record for Turkey).

Pileus 40-100 mm, firm, hemispherical, then convex, finally flat and slightly depressed in the centre, obtuse and regular margin, whole or slightly grooved only when ripe. Cuticle adnate, separable only at the edge, dry, finely pruinose-velvety, of a beautiful dark pink or pink-red colour, red-vermilion or carmine in the centre (Fig. 9a). Lamellae dense then more spaced, subdecurrent then adnexed and free, forked at the stem and anastomosed on the bottom, wide and thick, cream-whitish then light ocher, with whole and concolored cutting edge. Flesh firm and hard, then more tender and soft especially in the stem, white, with a tendency to grey-yellowish, red under the cuticle, with a fruity-honeyed odour and acrid taste also in the gills. Macrochemical reactions flesh + Fe = yellowish, flesh + G = deep blue-blue, care + F = brownish. Stipe 15-30 × 40-70 mm, firm and robust, cylindrical-clavate or dilated below, attenuated at the base, dry, pruinose then strongly wrinkled especially in old age, full then pithy, white, grey-yellowish at extreme maturity. Spores, 6-8 × 7-9 µm ovoid, warty-subcrested, with obtuse and hemispherical warts, cone, connected by thin short and irregular or incomplete ridges, amyloid (Fig. 9b). Basidia 9-11 × 30-42 µm, clavate to ventricose, with (1, 2) 4 sterigmata (Fig. 9c). Cheilocystidia 8-12 × 60-100 µm, spindle-shaped and slightly bellied, measuring variously appendicular to apex (Fig. 9d). Pleurocystidia are similar to C species of the genus *Cotylidia* heilocystidia (Fig. 9e).

Distribution: L132, under *P. nigra*, mycorrhizal.

Remarks: *Russula rosea* is very similar to *R. rubra*. It occurs in comparable habitats, likewise has a finely pruinose pileus, and has hard flesh. However, its flesh is mild, and it has a paler spore deposit, a generally red-flushed stipe, and reticulate spores. The two similar, mild species, *R. faginea* and *R. pseudointegra* also grow in hardwood forests. *Russula faginea* has a striking herring-like odour and taste, while *R. pseudointegra* has a dark ocher-yellow spore deposit and encrusted primordial hyphae.

Russula sardonia Fr.: (U), L86, mycorrhizal.

Russula sericatula Romagn.: (U), L44, mycorrhizal.

Russula silvestris (Singer) Reumaux: (U), L29, mycorrhizal.

Russula torulosa Bres.: (U), L62, mycorrhizal.

Russula velutipes Velen.: (U), L35, mycorrhizal.

Russula violacea Quél.: (U), L141, mycorrhizal.

Russula violeipes Quél.: (E), L12, L27, mycorrhizal.

Russula virescens (Schaeff.) Fr.: (E), L3, L4, L5, L18, L21, L27, L33, L34, L35, L37, L45, L65, L66, L140, L146, mycorrhizal.

Family *Stereaceae*

Aleurodiscus aurantius (Pers.) J. Schröt.: (I), L131, saprobe.

Stereum gausapatum (Fr.) Fr.: (I), L25, lignicolous, causes a white-rot of the heartwood.

Stereum hirsutum (Willd.) Pers.: (I), L4, L12, L14, L57, L62, L63, L66, L69, L80, L82, L84, L85, L93, L108, L112, L113, L127, L133, L136, L137, L139, lignicolous, causes a white-rot of the heartwood.

Stereum insignitum Quél.: (I), L13, causes a white-rot of the heartwood.

Stereum ochraceoflavum (Schwein.) Sacc.: (I), L84, L85, L93, L108, L131, L148, causes a white-rot of the heartwood.

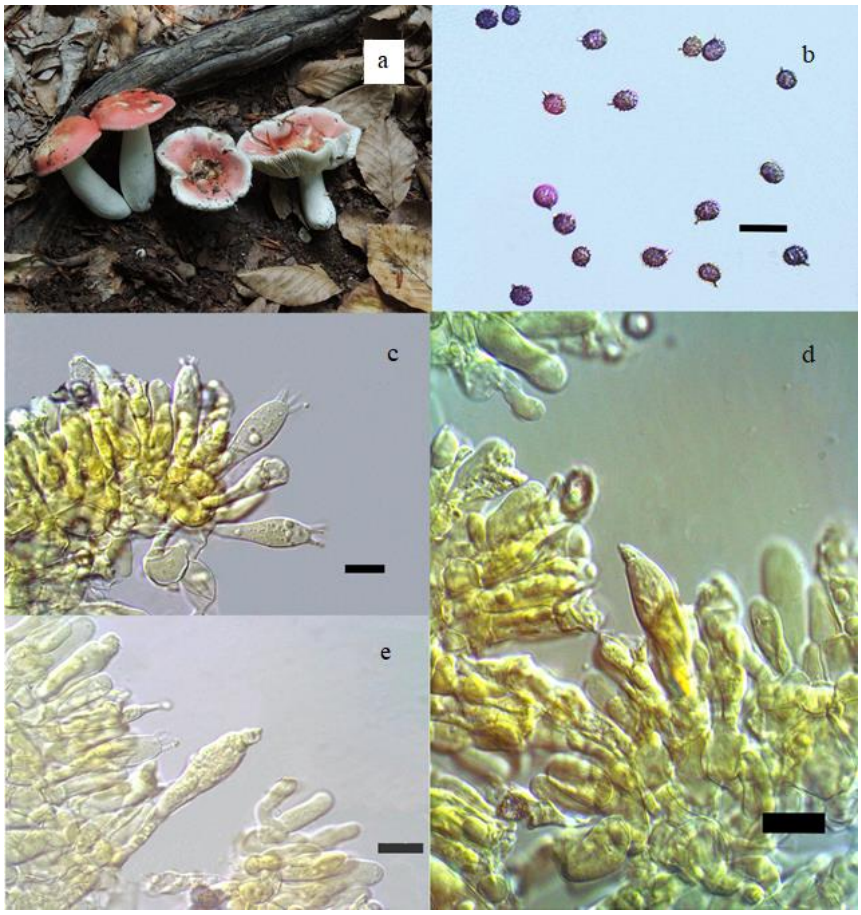

Fig. 9. *Russula rubra*. a) Macroscopic view, b) basidiospores, c) basidia, d) cheilocystidia, e) pleurocystidia. Scales 15 µm.

Fig. 10. *Stereopsis reidii*. a) Macroscopic view, b) basidiospores, c) basidia. Scales 15 µm.

Stereum sanguinolentum (Alb. & Schwein.) Fr.: (I), L56, L126, causes a white-rot of the heartwood.

Stereum subtomentosum Pouzar: (I), L69, L93, L104, causes a white-rot of the heartwood.

Order Stereopsidales
Family *Stereopsidaceae*

Stereopsis reidii Losi & A. Gennari: (I), (New Family and Genus record for Turkey)

Basidioma stipitate, stereoid, infundibuliform to spathulate, upper sterile surface whitish to minutely fibrillose, hymenophore smooth to rugose, whitish, margin undulate, finely fimbriate to laciniate (Fig. 10a). Stipe up to 1 cm long and 1-2 mm in diam, whitish. Basidiospores 3-3.5 × 4-6 µm, ellipsoid to ovoid, with a curved and pronounced apiculus, smooth, thin-walled, hyaline (Fig. 10b). Basidia 4-5 × 25-40 µm, narrowly clavate, with 4-sterigmata, and simple septate at the base (Fig. 10c). Hyphal system 2-6 µm wide, monomitic, hyphae with simple-septa, thin-walled, hyaline. Cystidia not seen.

Distribution: L80, on wood debris of *A. nordmanniana* subsp. *bornmuelleriana*, saprobe.

Remarks: Stereopsidaceae family was first described in 2014 to contain the genera *Stereopsis* by Sjökvist et al. (2014). This genus was classified in the order Polyporales, and *Clavulicium* genus or in the order *Cantharellales* until its taxonomical rank has been changed. After detailed Molecular phylogenetics analysis, it has been shown that this genus belongs to in different order. This order might belong in the subclass Phallomycetidae. The Stereopsidales contain corticoid fungi (*Clavulicium* and *Stereopsis*) and stalked, funnel-shaped fungi (*Stereopsis*). The main characteristic of the species is the shape of basidiocarp, at first narrowly ligulate, spathulate to flabelliform, then becoming confluent and forming complicated fructifications, frequently deeply divided into narrow clavarioid or broad lobes. The stipe is short and rudimental. Macroscopically it can be confused with white species of the genus *Cotylidia* P. Karst, but these have hymenial cystids. A species very similar to the one described is *Cyphellostereum pusiolum* D.A. Reid, that it has fibulae at the base of the terminal hyphae of the pileic lining and larger spores and polymorphic.

Order Thelephorales
Family *Bankeraceae*

Hydnellum caeruleum (Hornem.) P. Karst.: (I), L71, L109, mycorrhizal.

Hydnellum concrescens (Pers.) Banker: (I), L2, mycorrhizal.

Hydnellum glaucopus (Maas Geest. & Nannf.) E. Larss., K.H. Larss. & Kõljalg: (I), L11, mycorrhizal.

Hydnellum scrobiculatum (Fr.) P. Karst.: (I), L71, mycorrhizal.

Hydnellum suaveolens (Scop.) P. Karst.: (I), L120, mycorrhizal.

Phellodon confluens (Pers.) Pouzar: (I), L96, mycorrhizal.

Phellodon niger (Fr.) P. Karst.: (I), L121, L127, L50, mycorrhizal.

Sarcodon imbricatus (L.) P. Karst.: (E), L19, mycorrhizal.

Order Tremellales
Family *Tremellaceae*

Phaeotremella foliacea (Pers.) Wedin, J.C. Zamora & Millanes: (I), L34, saprobe.

Tremella mesenterica Retz.: (E), L5, L9, L11, L12, L22, L14, L34, L41, L45, L143, saprobe.

Discussion

510 macrofungal taxa belonging to 197 genera within 84 families were identified in the research area. Of these, 37 genera and 57 taxa belong to *Ascomycota*, while 160 genera and 453 taxa belong to *Basidiomycota*. Nine taxa from *Basidiomycota* were added to the Turkish Mycobiota as new records. These taxa are *Amanita subnudipes, Hebeloma quercetorum, Hygrocybe obrussea, Lactarius mediterraneensis, Lactifluus glaucescens, Russula lilacea, Russula rubra, Stereopsis reidii* and *Tricholoma roseoacerbum.* As mentioned before, there are different kinds of forest ecosystems in the study area which form mixed or pure forests. These areas are both optimal habitats for macrofungi and provide them with a variety of substrates for their growth. Among these habitats, *F. orientalis* and *A. nordmanniana* subsp. *bornmuelleriana* forests are very suitable for the growth of macrofungi. The distribution of habitat choices of the macrofungal taxa is as follows: *A. nordmanniana* subsp. *bornmuelleriana* 300 species, *F. orientalis* 295 species, *Quercus* spp. 125 species, *P. nigra* 88 species, *C. sativa* 56 species, *P. sylvestris* 53 species, *C. orientalis* 49 species and *P. maritima* 24 species. Tree species mostly form mixed forests in Samanlı Mountains. Therefore, dominant species in the mixed forest were taken into account to prepare the distribution of habitat choices. Species with high distribution in *A. nordmanniana* subsp. *bornmuelleriana* forests are *H. radicata* (32 different localities (DL), *M. alliaceus* (29 DL), *L. perlatum* (27 DL), *A. muscaria* (24 DL), *M. pura* (22 DL), *C. micaceus* (16 DL), and *H. fasciculare* (14 DL). Species with high distribution in *F. orientalis* forests are *A. rubescens* (68 DL), *H. radicata* (62 DL), *P. impudicus* (43 DL), *A. gemmata* (27 DL), *T. versicolor* (22 DL), *A. vaginata* (21 DL), *B. edulis* (21 DL), *M. procera* (20 DL), *D. disciformis* (19DL), *M. platyphila* (19 DL), *P. varius* (17 DL), *A. phalloides* (15 DL) and *F. fomentarius* (14 DL). Macrofungal diversity which was observed in administrative city borders is as follows: 339 taxa in Sakarya, 265 taxa in Bursa, 227 taxa in Kocaeli and 109 taxa in Yalova. Within these cities, the most and least

diverse districts were observed as Akyazı (Sakarya) with 217 taxa and Karapürçek (Sakarya) 24 taxa, respectively.

The forests of Akyazı region consist of pure or mixed beech, hornbeam, oak, pine and fir. These forest areas are also in a very healthy condition, providing more suitable place for the growth of macrofungi species. On the other hand, the forests in the Karapürçek region are not healthy and there are many destroyed areas. We can easily see from the available data that mushrooms develop better in parallel with the healthy forest structure.

The numbers of lignicolous and parasitic species are 20 (3.7%) and 18 (2.9%) on different trees, respectively, such as *D. quercina* on *Quercus* spp.; *S. commune*, *P. squamosus*, and *S. hirsutum* on the stump of *A. nordmanniana* subsp. *bornmuelleriana*; *P. melanopus*, *T. gibbosa* and *T. ochracea* on *F. orientalis*; *C. subcaesius*, *T. hirsuta*, *T. versicolor* on *C. orientalis*; *A. cepistipes* and *A. mellea* on roots of *F. orientalis*; and *F. fomentarius* on the stump of *A. nordmanniana* subsp. *bornmuelleriana*, *F. orientalis*, *Quercus* sp. and *C. orientalis*; *F. pinicola* on trunk of *P. nigra*, *P. sylvestris* and *F. orientalis*. Moreover, 245 (48%) species are saprobe, 226 (45%) are mycorrhizal, and 1 species is entomopathogenic (*Ophiocordyceps gracilis*). Overall graphic about ecological statuses of the species is given in Fig. 11.

According to the reviewed literature data (Boa 2004, Hall *et al.* 2016) 204 (40%) of the 510 taxa are inedible, 7 (1.37%) are edible or suspicious, 12 (12.36%) are used for medical purposes, 153 (30%) are edible, 65 (12.75%) are poisonous, 19 (3.73%) are used as food, 48 (9.4%100) are with unknown status and 2 (0.4%) are edible or poisonous. Among the edible and used as food taxa, 16 are collected and consumed in the region by Vill.rs. Members of the genus *Morchella* are known as "Kuzu göbeği", *M. procera* as "Dedebörü, şemsiye mantarı", *P. ostreatus* as "Kavak mantarı, geyik mantarı", *L. deliciosus* and *L. salmonicolor* as "Kanlıca", *A. caesarea* as "Gelincik mantarı, yumurta mantarı, sarı paça", *A. campestris* as "Çayır mantarı, içi kızıl", *C. comatus* as "Söbelen", *B. edulis* as "Ayı Mantarı, sünger mantarı",

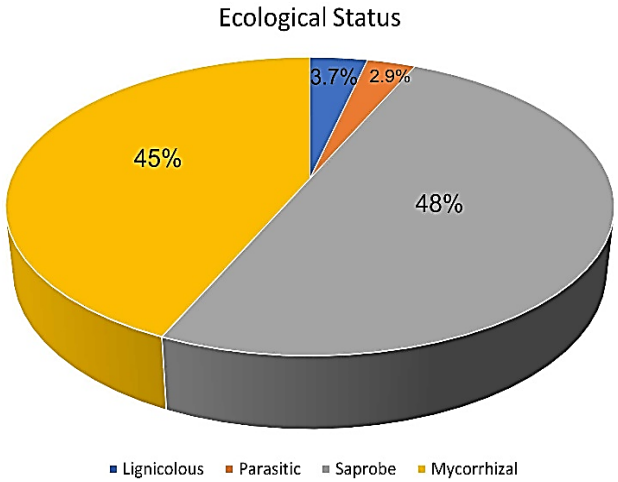

Fig. 11. Ecological status of the species.

Table 2. Similarity percentages of Samanlı Mountains with neighbouring studies in terms of macrofungal species.

Study	Number of identical taxa	Total taxa	Similarity percentage (%)
Kocaeli (Akata *et al.* 2018)	91	131	17.84
Bursa Gücin *et al.* 1995)	56	84	10.98
İznik (Allı *et al.* 2016)	58	91	11.37
Yalova (Allı *et al.* 2017)	42	78	8.23
Samanlı Mountains		510	

A. mellea as "Bal mantarı", *I. geotropa* as "Malkadın", *C. nebularis* as "Cincile", *H. repandum* as "Geyik dili", *S. crispa* as "Kıvırcık", *C. cibarius* as "Kaz ayağı, Sarı kulak", *C. cornucopioides* as "Borazan mantarı, kara borazan". Poisonous species of the area are *E. rhodopolium*, *E. sinuatum*, *A. gemmata*, *A. muscaria*, *A. pantherina*, *A. phalloides*, *A. solitaria*, *A. virosa*, *A. xanthoderma*, *P. cinctulus*, *H. fasciculare*, *I. bongardii* var. *bongardii*, *I. bongardii* var. *pisciodora*, *I. erubescens*, *I. fuscidula*, *I. lacera*, *I. leiocephala*, *I phaeodisca* var. *geophylloides*, *I. posterula*, *I. pseudodestricta*, *I. queletii*, *I. sambucina*, *I. splendens*, *I. acuta*, *I. asterospora*, *C. humicola*, *C. orellanus*, *L. acris*, *L. chrysorrheus*, *R. mairei*, *C. calopus*, *B. satanas*, *H. aurantiaca*, *P. involutus*, *C. phaeophtalma*, *C. phyllophila*, *M. pelianthina*, *M. pura*, *M. rosea*, *T. sulphureum*, *H. lacunosa*, and *H. crispa*.

There exist fungal data on some nearby regions of our study area with former studies in İznik (Allı *et al.* 2016), Yalova (Allı *et al.* 2017), Bursa (Gücin *et al.* 1995) and in Kocaeli (Akata *et al.* 2018). The comparative distribution of the species numbers identified in these studies is given in Table 2. The results of this work showed a few similarities with the findings of the studies carried out in neighbouring regions. The number of identical taxa and similarity percentages of relevant studies are given in Table 2. According to the table, the number of taxa that are common in each study was found as twelve, and these species are *A. pantherina*, *A. mellea*, *C. cibarius*, *F. fomentarius*, *H. fasciculare*, *L. betulinus*, *L. nuda*, *L. pyriforme*, *M. procera*, *P. ostreatus*, *S. commune*, *S. aeruginosa*, *T. versicolor*, and *X. hypoxylon*. The similarity rates of the studies are 17.84% for Kocaeli (Akata *et al.* 2018), 10.98% for Bursa region (Gücin *et al.* 1995), 11.37% for İznik Region (Allı *et al.* 2016), and 8.23% for Yalova region (Allı *et al.* 2017).

Acknowledgement

We appreciate the help of Adapazarı Regional Directorate of Forestry and Zekeriya Beyazlı (Chief of Akyazı Forest Management Department, Turkey), Bursa

Regional Directorate of Forestry, and Turgut Keskin (Manager of Non-Wood Products and Services, Turkey) for the logistic support in collecting of the specimens.

Ethics Committee Approval: Since the article does not contain any studies with human or animal subject, its approval to the ethics committee was not required.

Author Contributions: Material supplying: H.H.D., Ö.Ö., M.A.Ş., Data acquisition: H.H.D., Ö.Ö.

Conflict of Interest: The authors have no conflicts of interest to declare.

Funding: This research is financially supported by The Scientific and Technological Research Council of Turkey (TÜBİTAK, TBAG 112T136) and Selçuk University, Scientific Research Projects Coordinating Office (BAP/13401072).

References

1. Akata, I., Kabaktepe, Ş., Sevindik, M. & Akgül, H. 2018. Macrofungi determined in Yuvacık Basin (Kocaeli) and its close environs. *Kastamonu University Journal of Forestry Faculty*, 18(2): 152-163.
2. Allı, H., Candar, S.S. & Akata, I. 2017. Macrofungal Diversity of Yalova Province. *The Journal of Fungus*, 8(2): 76-84.
3. Allı, H., Şen, İ. & Altuntaş, D. 2016. Macrofungi of İznik Province. *Communications Faculty of Science University of Ankara Series C Biology Geological Engineering and Geophysical Engineering*, 25(1-2): 7-24.
4. Arnolds, E. 1986. Notes on Hygrophoraceae - VI. *Persoonia*, 13: 57-68.
5. Basso, M.T. 1999. *Fungi Europaei*. Vol.7. Mykoflora, Alassio, 767 pp.
6. Bernicchia, A. 2005. *Fungi Europaei*. Vol.10. Edizioni Candusso, Alassio, 808 pp.
7. Boa, E. 2004. *Wild Edible Fungi A global overview of their use and importance to people*. Food and Agriculture Organization of the United Nations, Rome, 147 pp.
8. Breitenbach, J. & Kränzlin, F. 1984. *Fungi of Switzerland*. Ascomycetes Vol.1: Ascomycetes. Verlag Mykologia. Lucerne, 310 pp.
9. Breitenbach, J. & Kränzlin, F. 1986. *Fungi of Switzerland*. Vol.2: Heterobasidiomycetes, Aphyllopharales, Gasteromycetes. Verlag Mykologia. Lucerne, 412 pp.
10. Breitenbach, J. & Kränzlin, F. 1991. *Fungi of Switzerland*. Vol.3: 1st Part, Boletes and Agaricus. Verlag Mykologia. Lucerne, 361 pp.
11. Breitenbach, J. & Kränzlin, F. 1995. *Fungi of Switzerland*, Vol.4: 2nd Part Agaricus. Verlag Mykologia. Lucerne, 368 pp.
12. Breitenbach, J. & Kränzlin, F. 2000. *Fungi of Switzerland*, Vol.5: Agarics part 3, Cortinariaceae. Verlag Mykologia. Lucerne, 338 pp.
13. Candusso, M. & Lanzoni, M. 1990. *Fungi Europaei*. Vol.4. Libreria Editrica Biella Giovanna, Saronno, 743 pp.
14. Candusso, M. 1997. *Fungi Europaei*. Vol.6 Libreria Basso, Alassio, 783 pp.
15. Cannon, P.F. & Kirk, P.M. 2007. *Fungal Families of the World*. CABI Publishing, Wallingford, 456 pp.
16. Christensen, M. & Heilmann-Clausen, J. 2013. *The Genus Tricholoma*. Narayana Press, Gylling, 227 pp.
17. Eriksson, J. & Ryvarden, L. 1973. *The Corticiaceae of North Europe*, Vol.2: Aleurodiscus-Confertobasidium. Fungiflora. Oslo, 231 pp.
18. Eriksson, J. & Ryvarden, L. 1976. *The Corticiaceae of North Europe*, Vol.4: Hyphodermella-Mycoacia. Fungiflora, Oslo, 337 pp.
19. Eriksson, J., Hjortstam, K. & Ryvarden, L. 1978. *The Corticiaceae of North Europe*, Vol.5: Mycoaciella-Phanerochaete. Fungiflora, Oslo, 158 pp.
20. Eriksson, J., Hjortstam, K. & Ryvarden, L. 1984. *The Corticiaceae of North Europe*, Vol.7: Schizopora-Suillosporium. Fungiflora, Oslo, 166 pp.
21. Galli, R. 2003a. *I Tricholomi*. 2a edizione. Edinatura, Milano, 271 pp.
22. Galli, R. 2003b. *Le Russule*. 2a edizione. Roberto Galli, Milano, 480 pp.
23. Galli, R. 2004. *Gli Agaricus*. 1a edizione. Dalla Natura, Milano, 216 pp.
24. Galli, R. 2006. *I Lattari*. 1a edizione. Dalla Natura, Milano, 299 pp.
25. Galli, R. 2007a. *I Boleti*. 3a edizione. Dalla Natura, Milano, 293 pp.
26. Galli, R. 2007b. *Le Amanite*. 2a edizione. Dalla Natura, Milano, 216 pp.
27. Gücin, F., Solak, M.H. & Işıloğlu, M. 1995. Mushrooms of Uludağ (Bursa-Turkey), 402-413. Paper presented at the Plant Life in Southwest and Central Asia Symposium, 21-28 May, İzmir-Turkey.
28. Hall, I.R., Lyon, T., Yun, W. & Buchanan, P. 2016. *Truffles and Mushrooms, A list of putative edible or medicinal ectomycorrhizal mushrooms*. Truffles & Mushrooms (Consulting) Ltd., Dunedin, 45 pp.
29. Hjortstam, K., Larsson, K.-H. & Ryvarden, L. 1987. *The Corticiaceae of North Europe*, Vol.1: Introduction and Keys. Fungiflora, Oslo, 59 pp.
30. Hjortstam, K., Larsson, K.-H. & Ryvarden, L. 1988. *The Corticiaceae of North Europe*, Vol.8: Phlebiella, Thanatephorus-Ypsilonidium. Fungiflora, Oslo, 181 pp.
31. Horak, E. 2005. *Röhrlinge und Blätterpilze in Europa*. Elsevier, Munich, 555 pp.
32. Index Fungorum. www.indexfungorum.org; (Date accessed: 15.09.2021)

33. Kirk, P.F., Cannon, P.F., Minter, D.W. & Stalpers, J.A. 2008. *Dictionary of the Fungi*. CAB International, Wallingford, 445 pp.

34. Knudsen, H. & Vesterholt, J. 2008. *Funga Nordica*: *Agaricoid, Boletoid, Cyphelloid Genera*. Nordsvamp, Copenhagen, 965 pp.

35. Kränzlin F., 2005. *Fungi of Switzerland*, Vol.6: Russulaceae, Lactarius, Russula. Verlag Mycologia, Luzern, 317 pp.

36. Medardi, G. 2006. *Ascomiceti d'Italia*. A.M.B, Venice, 678 pp.

37. Michael, W.B, Alan, E.B. & Arleen, R.B. 2014. *Ascomycete Fungi of North America: a mushroom reference guide.* University of Texas Press, Austin, 488 pp.

38. Moser, M. 1983. *Keys to Agarics and Boleti*. Gustav Fischer Verlag, Stuttgart, 535 pp.

39. Muñoz, J.A. 2005. *Fungi Europaei.* Vol.2. Edizioni Candusso, Alassio, 952 pp.

40. Mycobank. https://www.mycobank.org; (Date accessed: 15.09.2021)

41. Neville, P. & Poumarat, S. 2004. *Fungi Europaei*. Vol.9. Edizioni Candusso, Alassio, 1120 pp.

42. Parra, L.A. 2008. *Fungi Europaei*. Vol.1. Edizioni Candusso, Alassio, 522 pp.

43. Riva, A. 2003a. *Fungi Europaei*. Vol.3. Edizioni Candusso, Alassio, 826 pp.

44. Riva, A. 2003b. *Fungi Europaei*. Vol.3A. Edizioni Candusso, Alassio, 200 pp.

45. Robich, G. 2007. *Mycena D'Europe*. A.M.B, Trento, 728 pp.

46. Ryvarden, L. & Gilbertson, R.L. 1993. *European Polypores*. Vol.1. Fungiflora, Oslo, 387 pp.

47. Ryvarden, L. & Gilbertson, R.L. 1994. *European Polypores*. Part 2: Meripilus-Tyromyces. Fungiflora, Oslo, p: 394-743.

48. Sesli, E., Asan, A., Selçuk, F. (eds.), Abacı Günyar, Ö., Akata, I., Akgül, H., Aktaş, S., Alkan, S., Allı, H., Aydoğdu, H., Berikten, D., Demirel, K., Demirel, R., Doğan, H.H., Erdoğdu, M., Ergül, C.C., Eroğlu, G., Giray, G., Haliki Uztan, A., Kabaktepe, Ş., Kadaifçiler, D., Kalyoncu, F., Karaltı, İ., Kaşık, G., Kaya, A., Keleş, A., Kırbağ, S., Kıvanç, M., Ocak, İ., Ökten, S., Özkale, E., Öztürk, C., Sevindik, M., Şen, B., Şen, İ., Türkekul, İ., Ulukapı, M., Uzun, Ya., Uzun, Yu. &Yoltaş, A. 2020. *Türkiye Mantarları Listesi*. Ali Nihat Gökyiğit Vakfı Yayını, İstanbul, 1177 pp.

49. Sjökvist, E., Pfeil, Bernard E., Larsson, E. & Larsson, K-H 2014. Stereopsidales – A New Order of Mushroom-Forming Fungi. *Plos One*, 9(4): e95227.

50. Tullos, R.E. 2000. Nomenclatural changes in Amanita. *Mycotaxon*, 75: 329-332.

http://dergipark.org.tr/trkjnat
Trakya University Journal of Natural Sciences, 22(2): 245-253, 2021
ISSN 2147-0294, e-ISSN 2528-9691
DOI: 10.23902/trkjnat.960073

Research Article

EXTRACTION OPTIMIZATION OF *Senecio vernalis* Waldst. & Kit AND DETERMINATION OF ANTI-α-AMYLASE/α-GLUCOSIDASE, ANTI-LIPASE AND ANTIOXIDANT ACTIVITIES

Nurcan DOĞAN*, Cemhan DOĞAN

Department of Food Technology, Bogazliyan Vocational High School, Bozok University 66400, Yozgat, TURKEY

Cite this article as:

Doğan N. & Doğan C. 2021. Extraction optimization of *Senecio vernalis* Waldst. & Kit and determination of anti-α-amylase/α-glucosidase, anti-lipase and antioxidant activities. *Trakya Univ J Nat Sci*, 22(2): 245-253, DOI: 10.23902/trkjnat.960073

Received: 30 June 2021, Accepted: 09 September 2021, Online First: 04 October 2021, Published: 15 October 2021

Abstract: The possible side effects of drugs used in type II diabetes are increasing the tendency to herbal resources that have been used for many years. *Senecio vernalis* Waldst. & Kit is one of the annual *Senecio* L. species widely distributed in Turkey and used as a food and folk medicine. In this study, optimization of extraction conditions on the bioactive properties (Total phenolic content (TPC) and antioxidant capacity) of the flowers of *S. vernalis* and the potential of the plant for α-amylase, α-glucosidase, and lipase inhibitory activity were investigated. The optimum extraction conditions were determined at 69.72% water concentration, 59°C for 26.15 min, and the highest experimental values of TPC and 2, 2-diphenyl-1-picryl-hydrazyl-hydrate (DPPH) scavenging activity were observed as 28.14 mg gallic acid equivalent (GAE) g^{-1} and 3165.99 mg trolox equivalent (TE)/100 g sample, respectively. Significant inhibition was observed for α-amylase and α-glucosidase which are the key enzymes in type II diabetes, at a concentration of 100 mg mL^{-1}, with 21.32% and 64.16% respectively. The *S. vernalis* extracts showed no detectable inhibition of lipase. The results showed that *S. vernalis*, which has high antioxidant capacity also has a significant anti-diabetic effect. It can be concluded that *S. vernalis* can be considered a natural resource in many industries such as food and pharmaceuticals.

Özet: Tip II diyabette kullanılan ilaçların olası yan etkileri, uzun yıllardır kullanılan bitkisel kaynaklara olan eğilimi arttırmaktadır. *Senecio vernalis* Waldst. & Kit, Türkiye'de yaygın olarak bulunan, gıda ve halk ilacı olarak kullanılan tek yıllık *Senecio* L. türlerinden biridir. Bu nedenle, bu çalışmada, *S. vernalis* çiçeklerinin biyoaktif özellikleri (Toplam fenolik madde miktarı (TPC) ve antioksidan kapasite) ve α-amilaz, α-glukozidaz ve lipaz inhibitör aktivite potansiyeli üzerinde optimizasyon ekstraksiyon koşulları araştırıldı. Optimum ekstraksiyon koşulları %69.72 su konsantrasyonunda, 59°C'de 26.15 dakika olarak belirlenmiş ve TPC ve 2, 2-diphenyl-1-picryl-hydrazyl-hydrate (DPPH) süpürme aktivitesinin en yüksek deneysel değerleri sırasıyla 28,14 mg gallik asit eşdeğeri (GAE) g^{-1} ve 3165.99 mg troloks eşdeğeri (TE)/100 g numune olarak belirlenmiştir. Tip II diyabette anahtar enzim olan α-amilaz, α-glukozidaz için 100 mg mL^{-1} konsantrasyonunda sırasıyla %21.32 ve %64.16 inhibisyon gözlemlendi. *Senecio vernaris* ekstraktı, saptanabilir bir lipaz inhibisyonu göstermedi. Sonuçlar, yüksek bir antioksidan kapasiteye sahip olan *S. vernalis*'in de önemli bir anti-diyabetik etkiye sahip olduğunu göstermiştir. *Senecio vernalis*'in gıda ve ilaç gibi birçok endüstride doğal bir kaynak olarak değerlendirilebileceği sonucuna varılabilir.

Edited by:
İpek Süntar

****Corresponding Author:***
Nurcan Doğan
nurcan.dogan@bozok.edu.tr

ORCID iDs of the authors:
ND. orcid.org/0000-0001-5414-1819
CD. orcid.org/0000-0002-9043-0949

Key words:
Senecio vernalis
Type II diabetes
Antioxidant activity
Extraction optimization

Introduction

Throughout human history, many diseases have been tried to be treated using herbal cures. Scientific evidence supporting the effects of traditionally used herbs due to their beneficial features has brought these plants into the center of attention again. The World Health Organization (WHO) reports that approximately 80% of the world's population tries to overcome their health problems with herbal resources as the leading treatment agent (Anonymous 2000). Besides, active ingredients of plant origin constitute approximately 25% of prescription drugs in developed countries (Mosihuzzaman & Choudhary 2008). Various plant extracts have vast usage potential in various sectors such as nutraceuticals, pharmaceuticals, food additives and natural pesticides (Anklam *et al.* 1998). The health benefits of plants are mostly related to bioactive compounds, which are their secondary metabolites (Bernhoft 2010). A large number of studies were performed on the rich bioactive components

contained in plants (Azmir *et al.* 2013, Pereira *et al.* 2017). Extraction parameters are vital to benefit from the bioactive components possessed by plants at the highest level (Sasidharan *et al.* 2011). It is crucial to optimize extraction factors such as the solvent type, temperature, and time for the extraction to be effective (Başyiğit *et al.* 2020). Response surface methodology (RSM) successfully combines mathematical and statistical techniques applied with a minimum trial point in optimizing extraction factors (Myers *et al.* 2016).

Diabetes mellitus (DM) is a disease that affects 285 million people worldwide in 2010 and is predicted to affect more than 400 million people by the year 2030. Type II diabetes, which is mainly affected by environmental factors such as diet and lifestyle, has a very high effect on the increase in reported cases (Wild *et al.* 2004). Type II diabetes is a metabolic disorder that affects 90% of diabetes patients and causes an uncontrolled increase in blood sugar (Bhutkar & Bhise 2012). Although this increase in blood glucose level can be regulated by therapeutic drugs, the treatment solution of conscious patients with herbal supplements appears to be an up-to-date approach considering the possible side effects of medical drugs (Cariou *et al.* 2012). During the last couple of decades, *in vitro* and *in vivo* studies on alpha-amylase and alpha-glucosidase inhibition with various food, food components and herbal supplements to reduce glucose absorption have been performed (Matsui *et al.* 1996, Lee *et al.* 2007, Doğan *et al.* 2021).

Senecio L. is a large and diverse genus in the *Asteraceae* family with approximately 1500 described species widely known all over the world (Christov *et al.* 2002). The genus is represented with 39 species in Turkey (Uğur *et al.* 2006). These species are generally called as "Canary grass" and rarely as "Küllüce grass" and "Ekin grass" in Turkey (Baytop 2007). *Senecio* species have long been consumed as food or folk remedies with their antiemetic, anti-inflammatory, and vasodilator properties (Conforti *et al.* 2006a). In addition, some species are known with their antibacterial-antifungal (Kiprono *et al.* 2000), antimicrobial-cytotoxic (Loizzo *et al.* 2006), antioxidant and anti-diabetic activities (Ayoola *et al.* 2019).

The present study was performed to determine the effects of optimized extraction conditions on total phenolic content and antioxidant capacity of *S. vernalis* flowers. Anti-diabetic and anti-lipase activity, which have not been evaluated in previous studies, were also evaluated.

Materials and Methods

Plant material and treatments

Senecio vernalis was collected from Yozgat Bozok University Boğazlıyan Vocational School campus in Turkey (N39°20'25.62", E35°26'07.84"). The collected samples were separated from their flowers and dried at 40°C until they reached constant weight. Before the extraction, flower samples were ground through a laboratory steel blender (Waring 8011, USA) for 1 min. The chemicals used in the analysis were obtained from Merck (Darmstadt, Germany) unless otherwise indicated. α-amylase, α-glucosidase, and lipase were obtained from Sigma-Aldrich (St. Louis, MO, USA).

Creating the experimental design and extraction

The effects of temperature (40-60°C), time (5-60 min) and solvent concentration (water to ethanol: 0-100%) as the extraction conditions (independent variables) on Total phenolic content (TPC) and 2, 2-diphenyl-1-picryl-hydrazyl-hydrate (DPPH) were determined by Design Expert 11.0.0 software (Stat- Ease Inc., Minneapolis, MN) using a face-centered central composite design (FC-CCD). The effects of the extraction conditions on the responses (TPC and DPPH) were expressed by the following quadratic polynomial regression equation (Eq. 1):

$$Y = \beta_0 + \beta_1 X_1 + \beta_2 X_2 + \beta_3 X_3 + \beta_{11} {X_1}^2 + \beta_{22} {X_2}^2 + \beta_{33} {X_3}^2 + \beta_{12} X_1 X_2 + \beta_{13} X_1 X_3 + \beta_{23} X_2 X_3 \ (Eq. 1)$$

where Y is the predicted response (TPC and DPPH), β_0 is the constant, β_1, β_2, β_3 are the linear coefficients, β_{11}, β_{22}, β_{33} are the interaction coefficients, β_{12}, β_{13}, β_{23} are quadratic coefficients, and X_1 (temperature), X_2 (time) and X_3 (solvent concentration) are the independent variables. The whole design was created at 20 experimental points, and the level of independent variables, experimental values, and estimated data was given in Table 1.

For extraction, 0.5 g of sample was mixed with 10 ml of solvent and extracted according to the experimental point. The extracted samples were centrifuged at 5000 rpm for 5 min and the supernatant was collected and stored at -18°C.

Total phenolic content (TPC) assay

0.4 mL sample was mixed with diluted 2 mL Folin-Ciocalteu reagent and 1.6 mL Na_2CO_3 (7.5%) in a test tube. After the mixture was incubated in dark for 60 min, the absorbance was read in the spectrophotometer (Shimadzu UV-1700, Kyoto, Japan) at 765 nm. The absorbance values obtained are expressed in gallic acid equivalent (GAE) (Singleton *et al.* 1999).

Antioxidant activity assay

DPPH method was used to determine the antioxidant capacity of the samples. For this purpose, a 0.1 g sample was mixed with 3.9 mL of DPPH solution (25 mg/L) prepared with methanol in a test tube. After 30 min of incubation in dark, absorbances at 515 nm were recorded using a Shimadzu UV-1700 spectrophotometer (Shimadzu UV-1700, Kyoto, Japan) (Brand-Williams *et al.* 1995). Results are expressed as trolox equivalent (mg TE/100 g sample).

In vitro anti-diabetic activity assays

The anti-diabetic activity of the samples was determined considering the α-amylase and α-glucosidase inhibitory activity. For the α-amylase inhibition test of the samples, after keeping 1 mL of an extract with 1 mL of potato starch and $NaHPO_4$ (20 mM) at 37°C for 5 min, the

reaction was started by adding 1 mL α-amylase. After 30 min of incubation, 0.5 mL of Rochella Salt (5.31 M) and 0.5 mL of 3,5-dinitrosalicylic acid (96 mM) solution were added. The mixture was terminated by standing at 100°C for 15 min. After heat treatment, the absorbance of the mixture was recorded at 540 nm. For the α-glucosidase inhibition test, after mixing 50 µL extract and 1250 µL 67 mM KH_2PO_4 with 50 µL α-glucosidase in a test tube, it was incubated at 37°C for 5 min. Afterward, 125 µL of p-Nitrophenyl-β-D-glucopyranoside (10 mM) solution was added, and the reaction was started and terminated by adding 2 mL of Na_2CO_3 (100 mM) solution after 20 min. The absorbance of the mixture was recorded at 400 nm (McDougall *et al.* 2005a, Cam *et al.* 2020). Absorbances were recorded using the spectrophotometer (Shimadzu UV 1700, Tokyo, Japan) to determine the inhibitory activity of both enzymes.

The α-amylase and α-glucosidase inhibitory activities were expressed as a percentage of inhibition and the following formula was used to determine enzyme inhibitory activity (%) of the samples (Eq. 2).

$$Enzyme\ inhibition\ (\%) = \frac{ABS_{control} - ABS_{sample}}{ABS_{control}} x100\ (Eq.2)$$

where $ABS_{control}$ and ABS_{sample} express the absorbance of the control and samples, respectively.

Lipase inhibition activity

The lipase inhibition activity of the diluted samples was evaluated *in vitro* using the spectrophotometric method. This assay was performed using the method by Gilham & Lehner (2005). Porcine pancreas lipase (10 mg/mL) was prepared as the enzyme solution. 800 µL of 100 mM Tris buffer (pH = 8.2) was mixed in a test tube with 100 µL of diluted extract and 300 µL of the prepared lipase solution. After incubation for 5 min at 37°C, 800 µL of p-nitrophenyl-laurate (300 µg/mL) was added. p-nitrophenyl-laurate is a colored compound and absorbs at 400 nm and through this compound, the enzyme activity is read in the spectrophotometer (Shimadzu UV 1700). The control and blank samples were prepared in the same way by subtracting the extract and both of the extract and enzyme, respectively (Eq. 3).

$$Lipase\ inhibition\ activity\ (\%) = \frac{Abs_{control} - Abs_{extract}}{Abs_{control}} x100\ (Eq.3)$$

where $Abs_{control}$ and $Abs_{extract}$ express the absorbances of the control and extract, respectively.

Statistical analysis

To determine the reliability of the 2nd-order polynomial equations derived from the model, Regression (p-value), coefficient of determination (R^2), adjusted R^2 (R^2_{adj}), predicted R^2 (R^2_{pred}), and lack of fit were demonstrated using Design Expert 11.0.0 software (Stat-Ease Inc., Minneapolis, MN). SPSS 22.0 software (SPSS Inc., Chicago, IL) was used for all data analyses where $p<0.05$ was assumed to be statistically significant. Principle component analysis (PCA) used to determine the correlation between data was performed with Minitab 18 software (Minitab Inc., PA, USA).

Result and Discussion

Checking the model fitting

The experimental value and the predicted data performed at the experimental points created according to the FC-CCD result were given in Table 1.

Table 1. Experimental values and the predicted data according to FC-CCD.

Experimental point	Independent variables			Responses			
	X_1 (°C)	X_2 (min)	X_3 (%)	TPC (mg GAE g^{-1})		DPPH (mg TE/100 g sample)	
				Experimental value	Predicted data	Experimental value	Predicted data
1	40	5	0	2.68	2.70	163.60	166.18
2	50	32.5	50	25.80	25.52	2880.78	2998.21
3	60	60	0	1.86	1.96	114.56	117.13
4	50	32.5	50	25.62	25.52	2949.75	2998.21
5	40	60	100	20.59	20.14	2034.22	1990.33
6	60	5	100	18.19	18.70	1385.79	1404.21
7	60	5	0	2.09	2.02	136.70	134.82
8	60	60	100	19.10	18.09	1553.35	1614.77
9	50	32.5	50	24.24	25.52	2997.25	2998.21
10	40	5	100	24.98	24.93	1783.16	1730.80
11	40	60	0	2.12	2.18	142.49	144.37
12	50	32.5	50	25.05	25.52	2915.26	2998.21
13	50	32.5	0	3.00	2.85	191.42	185.14
14	50	32.5	50	26.28	25.52	2907.98	2998.21
15	60	32.5	50	18.82	19.04	2333.28	2204.81
16	50	60	50	22.36	22.42	2904.52	2766.77
17	40	32.5	50	23.36	23.2	2646.29	2717.60
18	50	32.5	100	24.98	26.38	2211.08	2218.46
19	50	32.5	50	26.22	25.22	3144.74	2998.21
20	50	5	50	25.31	25.36	2717.17	2768.04

Table 2. 2nd-order polynomial equations and statistical parameters for model fitness.

Responses	2nd-order polynomial equations	Regression (p-value)	R^2	R^2_{adj}	R^2_{pred}
TPC	=-3.067+0.178*temperature-0.0045*time+0.065*solvent concentration +0.00016*temperaturetime-0.0019*temperature^2-0.000089*time^2-0.00043*solvent concentration^2	<0.0001	0.999	0.998	0.997
DPPH	=0.643+0.192*temperature+0.0043*time+0.084*solvent concentration +5.09735e-05*time solvent concentration-0.002*temperature^2-0.0001*time^2-0.0006*solvent concentration^2	<0.0001	0.999	0.999	0.998

Table 3. Analysis of variance for responses.

DPPH					TPC				
Source	**Sum of Squares**	**Mean Square**	**F-value**	**p-value**	**Source**	**Sum of Squares**	**Mean Square**	**F-value**	**p-value**
Model	30.43	4.35	2940.88	< 0.0001	**Model**	20.32	2.90	1839.99	< 0.0001
X_1 Temperature	0.1093	0.1093	73.96	< 0.0001	X_1 Temperature	0.0977	0.0977	61.89	< 0.0001
X_2 Time	5.260E-07	5.260E-07	0.0004	0.9853	X_2 Time	0.0381	0.0381	24.13	0.0004
X_3 Solvent concentration	15.42	15.42	10432.69	< 0.0001	X_3 Solvent concentration	12.37	12.37	7836.90	< 0.0001
X_2X_3	0.0393	0.0393	26.59	0.0002	X_1X_2	0.0162	0.0162	10.28	0.0076
X_1^2	0.1131	0.1131	76.54	< 0.0001	X_1^2	0.1036	0.1036	65.69	< 0.0001
X_2^2	0.0176	0.0176	11.94	0.0048	X_2^2	0.0127	0.0127	8.02	0.0151
X_3^2	6.55	6.55	4429.63	< 0.0001	X_3^2	3.20	3.20	2028.31	< 0.0001
Residual	0.0177	0.0015			**Residual**	0.0189	0.0016		
Lack of Fit	0.0126	0.0018	1.77	0.2743	Lack of Fit	0.0142	0.0020	2.16	0.2063
Pure Error	0.0051	0.0010			Pure Error	0.0047	0.0009		
Cor Total	30.44				**Cor Total**	20.34			

The 2nd -order polynomial equations derived from the model and its statistical parameters were given in Table 2. To ensure the reliability of the model, firstly insignificant terms were removed from the polynomial equation. For this purpose, the automatic model selection module of the Design Expert software is used to algorithmically select the terms to be kept in the model. To determine whether there is an unimportant term in the model, the Adjusted R-square selection, which follows one step backwards at a time and removes the least significant term from the model was preferred. This is very important in determining the impact of important factors on responses (Hastie *et al.* 2001). In addition, it is recommended that the difference between R^2_{adj} and R^2_{pred} to be less than 0.2 and R^2 and R^2_{adj} values above 90% in determining the suitability of the model (Myers *et al.* 2004). In addition, the model should not have a lack of fit. P-value of the lack of fit for the TPC and DPPH of the samples was determined as 0.206 and 0.274, respectively, in other words no model lack of fit was detected (Table 3). Additionally, as shown in Table 2, R^2, R^2_{adj}, and R^2_{pred} values are greater than 90%, and the differences between R^2_{adj} and R^2_{pred} values are less than 0.2.

Effects of the extraction conditions on TPC and antioxidant activity

The results of TPC and DPPH are presented in Table 1. When the effects of extraction conditions on TPC and DPPH are examined, while temperature and solvent concentration were significant for both ($p<0.05$), time was significant for TPC ($p<0.05$) but not for DPPH ($p>0.05$). The highest TPC and DPPH values in the extraction at 20 experimental points were detected with 26.28 GAE g-1 and 3144.74 mg TE/100 g sample at the midpoint (50°C, 32.50 min, and 50% ethanol), respectively. The lowest values were obtained with 1.86 GAE g-1 and 114.56 mg

TE/100 g sample in 100% ethanol solvent extraction at the experimental point where the temperature and time values were at maximum. One of the main objective of extraction should be to reduce the use of organic solvents as much as possible. For this purpose, binary solvent mixtures (water-ethanol) were tried rather than single-use of ethanol to extract secondary metabolites, and higher efficiency was obtained in its use. In addition, in studies evaluating the extraction performance, mixed solvents came to the fore (Markom *et al.* 2007). The amount of phenolic compounds in the extract increased up to 50°C but decreased rapidly in parallel with the increase in temperature (Fig. 1). In classical extraction, it is vital to increase the solubility of the tissues by softening the temperature. However, it is a known fact that high temperatures damage phenolics (Dent *et al.* 2013). The increase in time is thought to be insignificant for DPPH since the antioxidants in phenolic compounds pass into the extract until the 32.50th min and are not affected by the increase in time as much as phenolics after that min. By shortening the extraction time, energy wastage is prevented and time is saved in the process (Chew *et al.* 2011). Since the extraction efficiency will vary according to the phenolic compounds of the raw material, the extraction method and conditions, it is crucial to optimize it. In previous studies, some studies determined the TPC and antioxidant capacity of different *Senecio* species (Lone *et al.* 2014, Sharma & Shah 2015, Faraone *et al.* 2018, Ayoola *et al.* 2019). However, studies showing the bioactive properties of *S. vernalis* are extremely limited (Balpinar & Okmen 2019). In addition, the flowers of *S. vernalis* contain high amounts of carotenoids (Mogoşanu *et al.* 2009). The fact that carotenoids have reactive double bonds in conjugated structure gives them antioxidant properties (Suparmi & Prasetya 2012).

Principle component analysis (PCA)

To improve the interpretability of multivariate modelsPCA is a method that has been used frequently in recent years. PCA is a method of finding the projection of data in a multidimensional space onto a lower-dimensional space in a way that maximizes the variance (Alpaydin 2020). The HJ-biplot was constructed with the first (97.6%) and second (2.4%) components, contributing to all of the total variability. On the biplot, the correlation between the variables was expressed by the acute angle at the intersection of the vectors. Moreover, the relationship between 20 experimental points and variables was reflected with the HJ-biplot. Accordingly, the experimental points were divided into 3 groups expressed as a circle, triangle and square. The basis of the grouping was the solvent concentration. The 1st group (circle-shaped) with the lowest phenolic compound and antioxidant capacity was localized farthest away in the absence of water as a solvent. The second group (square-shaped) represents the experimental points where the solvent is 100% water, and since the TPC and DPPH values at these points are higher than the first group, they are closer to the intersection of the vectors. The third group (triangle-shaped), on the other hand, constitutes the large group that includes the midpoints of the test points, as well as the points taken with half the water-ethanol mixture as solvent, and the TPC and DPPH values obtained at these points are the highest. The findings show that the phenolics of the sample are better soluble in the binary solvent system and the aqueous extract is higher than ethanol in the use of a single solvent.

There is an intense relationship between the phenolic content of the plant materials and their antioxidant activities (Aryal *et al.* 2019). As can be seen from PCA, a positive correlation was determined between the phenolic compounds of *S. vernalis* and its antioxidants (Fig. 2).

Optimization and model validation

Optimum extraction conditions and both experimental values and predicted data at this point are presented in Table 3. Optimum extraction conditions were determined as 69.72% water concentration at 57.29°C for 26.15 min. The predicted data according to the model at the optimum point were observed as 28.14 mg GAE g^{-1} and 3165.99 mg TE/100 g sample for TPC and DPPH, respectively. In addition, the experimental values made at this point were determined as 27.94 mg GAE g^{-1} and 3054.77 mg TE/100 g samples for TPC and DPPH, respectively. As it is clear from the results, the predicted data and experimental values are in good agreement. Briefly, there is no statistically significant difference ($p>0.05$).

Anti-diabetic activity and lipase inhibition activity

Dilutions at 1, 2, 5, 10, 20, 50, 75, and 100 mg mL^{-1} were prepared from the extracts taken at the optimization point, and α-amylase, α-glucosidase, and lipase inhibition activities were evaluated. With increasing concentration from 1 to 100 mg mL^{-1}, the inhibition activities of α-amylase and α-glucosidase increased. The results showed that the inhibition activity of α-amylase and α-glucosidase ranged between 4.12%-21.32% and 17.94%-64.16% respectively. α-glucosidase inhibition activity was found to be higher than α-amylase inhibition activity. The reason for this situation is thought to be the bioactive compounds of *S. vernalis*. Wang *et al.* (2010) reported that seven pure flavonoid compounds showed an inhibitory effect on different enzymes. Pancreatic α-glucosidase and α-amylase are needed to convert complex carbohydrates to simple sugars in the gastrointestinal system. Inhibition of these enzymes is one of the methods applied for plasma glucose levels decreased in the blood (Krentz & Bailey 2005). The methods of inhibition of these enzymes and/or restriction of absorption of monosaccharides are utilized in currently used medicinal drugs such as acarbose, miglitol, voglibose, etc. (Dash *et al.* 2018). However, due to the known side effects of these drugs (Su *et al.* 2013), interest in natural agents with strong inhibitory effects and less side effects and/or no side effects has increased in recent years (Kim *et al.* 2004, Ali *et al.* 2006, Bhandari *et al.* 2008, Hung *et al.* 2012).

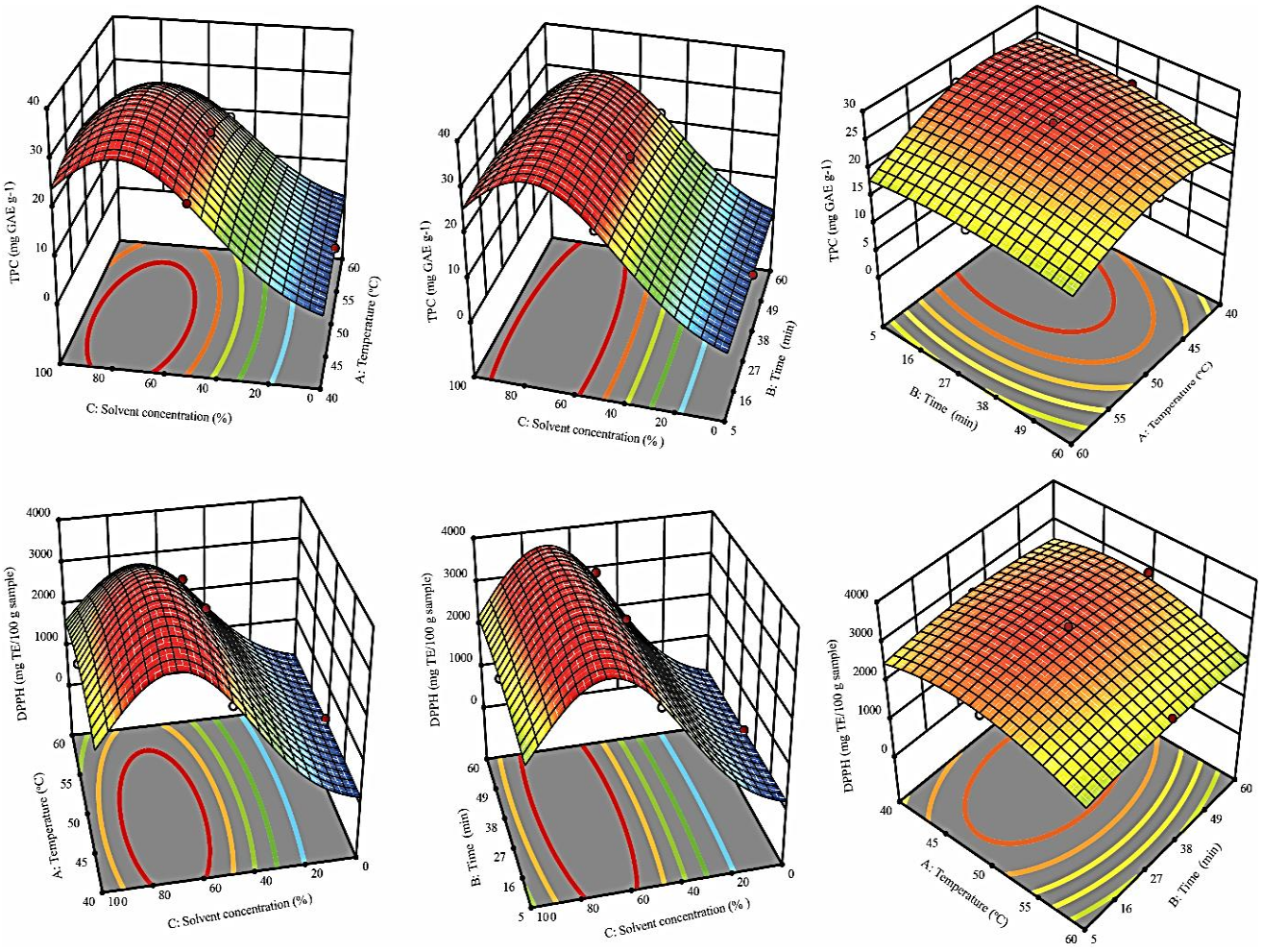

Fig. 1. Representation of the interaction effect of extraction conditions on responses with 3D surface plot.

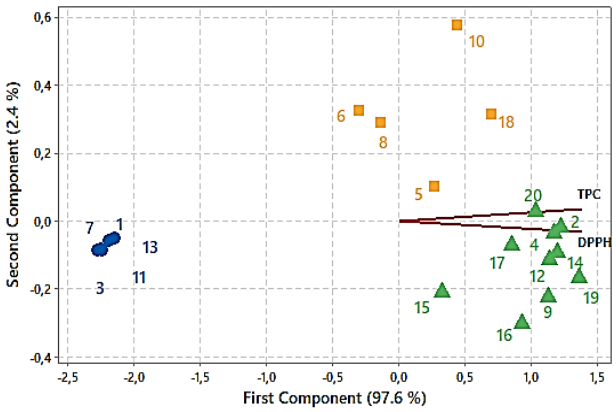

Fig 2. HJ-biplot of the distribution of experimental points over the responses for PCA.

The anti-diabetic activities of different *Senecio* species were determined in previous studies (Conforti *et al.* 2006b, Tundis *et al.* 2012, Ajiboye *et al.* 2018, Ma *et al.* 2018b). However, no study was found to determine the α-amylase and α-glucosidase inhibition capacity of *S. vernalis*. Hyperglycemia is highly correlated with oxidative stress and the activity of key enzymes such as pancreatic α-amylase α-glucosidase (Hung *et al.* 2017). In previous *in vivo* and *in vitro* studies, it was emphasized that oxidative stress causes dysfunction in β-cells responsible for glucose metabolism (Robertson 2004, Tang *et al.* 2012, Chang *et al.* 2013). Therefore, oxidative stress should be reduced as much as possible to prevent or reduce diabetic complications (DeFronzo 1999). Antioxidants play an essential role in avoiding related disorders such as degenerative diseases, diabetes and cancer by controlling oxidative stress (Birben *et al.* 2012). Some studies suggest that the progression of type 2 diabetes can be reduced by consuming diets rich in plant-based antioxidants (Faller & Fialho 2009, Porter 2012). In addition, diabetes is one of the oxidative stress states in which free radicals increase and antioxidant mechanisms are inhibited. Therefore, it is recommended to use anti-diabetics with antioxidant properties to treat diabetes (Memişoğulları 2005). It is also known that plant polyphenols and antioxidants have effective anti-diabetic properties (McDougall *et al.* 2005b, Mai *et al.* 2007). Therefore, in this study, *S. vernalis* was extracted at the point where its antioxidant capacity was at its maximum. Then the inhibition capacities of α-amylase α-glucosidase were investigated. Consequently, it is thought that the high antioxidant activity of *S. vernalis* and its anti-diabetic effect provide dual benefits. None of the extracts showed dose-dependent inhibition of lipase enzymes.

Table 4. Optimum extraction conditions with experimental values and predicted data at these conditions.

Temperature (°C)	Time (min)	Solvent concentration (%)	Desirability score	Responses	Predicted data	Experimental value
57.29	26.15	69.72	1.00	TPC (mg GAE g^{-1})	28.14	27.94
				DPPH (mg TE/100 g sample)	3165.99	3054.77

Conlusion

RSM has been successfully applied to optimise extraction on TPC and antioxidant activity of *S. vernalis* flowers. The most effective extraction conditions were determined as 69.72% water concentration, 59°C for 26.15 min with which the experimental values of TPC and DPPH were observed as 28.14 mg GAE g^{-1} and 3165.99 mg TE/100 g sample, respectively. Extracts at various concentrations exhibited not only antioxidant but also potential α-glucosidase and α-amylase inhibitory activity. Therefore, this extract may be promising for a therapeutic approach in the management of type II diabetes, as it has anti-diabetic potential as well as high antioxidant activity.

Acknowledgement

The plant material was diagnosed by Prof. Ümit BUDAK, who worked in Yozgat Bozok University, Department of Molecular Biology and Genetics. We would like to thank him for his contribution.

Ethics Committee Approval: Since the article does not contain any studies with human or animal subject, its approval to the ethics committee was not required.

Author Contributions: Concept: N.D., C.D., Desing: N.D., C.D., Execution: N.D., C.D., Material supplying: N.D., C.D., Data acquisition: N.D., C.D., Data analysis/interpretation: N.D., C.D., Writing: N.D., C.D., Critical review: N.D., C.D.

Conflict of Interest: The authors have no conflicts of interest to declare.

Funding: The authors declared that this study has received no financial support.

References

1. Anonymous. 2000. General *Guidelines for Methodologies on Research and Evaluation of Traditional Medicine*, World Health Organization, Geneva, 79 pp.
2. Ajiboye, B.O., Ojo, O.A., Okesola, M.A., Akinyemi, A.J., Talabi, J.Y., Idowu, O.T., Fadaka, A.O., Boligon, A.A. & Anraku de Campos, M.M. 2018. In vitro antioxidant activities and inhibitory effects of phenolic extract of *Senecio biafrae* (Oliv and Hiern) against key enzymes linked with type II diabetes mellitus and Alzheimer's disease. *Food Science & Nutrition*, 6(7): 1803-1810.
3. Ali, H., Houghton, P. & Soumyanath, A. 2006. α-Amylase inhibitory activity of some Malaysian plants used to treat diabetes; with particular reference to *Phyllanthus amarus*. *Journal of Ethnopharmacology*, 107(3): 449-455.
4. Alpaydin, E. 2020. *Introduction to Machine Learning*. MIT Press, Massachusetts, 712 pp.
5. Anklam, E., Berg, H., Mathiasson, L., Sharman, M. & Ulberth, F. 1998. Supercritical fluid extraction (SFE) in food analysis: a review. *Food Additives & Contaminants*, 15(6): 729-750.
6. Aryal, S., Baniya, M.K., Danekhu, K., Kunwar, P., Gurung, R. & Koirala, N. 2019. Total phenolic content, flavonoid content and antioxidant potential of wild vegetables from Western Nepal. *Plants*, 8(4): 96.
7. Ayoola, M., Adebajo, A., Zotor, F. & Pinkoane, M. 2019. Justifying antidiabetic ethnomedicinal claim of *Senecio biafrae* through its antihyperglycemic and anti-oxidant activities. *Annals of Complementary and Alternative Medicine*, 1(2): 1006.
8. Azmir, J., Zaidul, I.S.M., Rahman, M., Sharif, K., Mohamed, A., Sahena, F., Jahurul, M., Ghafoor, K., Norulaini, N. & Omar, A. 2013. Techniques for extraction of bioactive compounds from plant materials: A review. *Journal of Food Engineering*, 117(4): 426-436.
9. Balpinar, N. & Okmen, G. 2019. Biological activities and chemical composition of *Senecio vernalis* growing in the lakes region of Turkey. *International Journal of Environmental Science and Technology*, 16(9): 5205-5212.
10. Başyiğit, B., Alaşalvar, H., Doğan, N., Doğan, C., Berktaş, S. & Çam, M. 2020. Wild mustard (*Sinapis arvensis*) parts: compositional analysis, antioxidant capacity and determination of individual phenolic fractions by LC–ESI–MS/MS. *Journal of Food Measurement and Characterization*: 1-11.
11. Baytop, T. 2007. *Türkçe Bitkı Adları Sözlüğü*. Türk Dil Kurumu Yayınları, Ankara, 512 pp.
12. Bernhoft, A. 2010. A brief review on bioactive compounds in plants. *Bioactive Compounds in Plants-Benefits and Risks for Man and Animals*, 50: 11-17.
13. Bhandari, M.R., Jong-Anurakkun, N., Hong, G. & Kawabata, J. 2008. α-Glucosidase and α-amylase inhibitory activities of Nepalese medicinal herb Pakhanbhed (*Bergenia ciliata*, Haw.). *Food Chemistry*, 106(1): 247-252.
14. Bhutkar, M. & Bhise, S. 2012. In vitro assay of alpha amylase inhibitory activity of some indigenous plants. *International Journal of Chemical Sciences*, 10(1): 457-462.
15. Birben, E., Sahiner, U.M., Sackesen, C., Erzurum, S. & Kalayci, O. 2012. Oxidative stress and antioxidant defense. *World Allergy Organization Journal*, 5(1): 9-19.
16. Brand-Williams, W., Cuvelier, M.E. & Berset, C. 1995. Use of a free radical method to evaluate antioxidant activity. *LWT-Food Science and Technology*, 28(1): 25-30.

17. Cam, M., Basyigit, B., Alasalvar, H., Yilmaztekin, M., Ahhmed, A., Sagdic, O., Konca, Y. & Telci, I. 2020. Bioactive properties of powdered peppermint and spearmint extracts: Inhibition of key enzymes linked to hypertension and type 2 diabetes. *Food Bioscience,* 35: 100577.

18. Cariou, B., Charbonnel, B. & Staels, B. 2012. Thiazolidinediones and PPARγ agonists: time for a reassessment. *Trends in Endocrinology & Metabolism,* 23(5): 205-215.

19. Chang, C.L., Lin, Y., Bartolome, A.P., Chen, Y.C., Chiu, S.C. & Yang, W.C. 2013. Herbal therapies for type 2 diabetes mellitus: chemistry, biology, and potential application of selected plants and compounds. *Evidence-Based Complementary and Alternative Medicine,* 2013: 388657.

20. Chew, K., Khoo, M., Ng, S., Thoo, Y.Y., Aida, W.W. & Ho, C.W. 2011. Effect of ethanol concentration, extraction time and extraction temperature on the recovery of phenolic compounds and antioxidant capacity of Orthosiphon stamineus extracts. *International Food Research Journal,* 18(4): 1427.

21. Christov, V., Mikhova, B., Alexandrova, R., Dimitrova, D., Nikolova, E. & Evstatieva, L. 2002. Alkaloids from the roots of *Senecio macedonicus* Griseb. *Zeitschrift für Naturforschung C,* 57(9-10): 780-784.

22. Conforti, F., Loizzo, M.R., Statti, G.A., Houghton, P.J. & Menichini, F. 2006a. Biological properties of different extracts of two *Senecio* species. *International Journal of Food Sciences and Nutrition,* 57(1-2): 1-8.

23. Conforti, F., Marrelli, M., Statti, G. & Menichini, F. 2006b. Antioxidant and cytotoxic activities of methanolic extract and fractions from *Senecio gibbosus* subsp. gibbosus (GUSS) DC. *Natural Product Research,* 20(9): 805-812.

24. Dash, R.P., Babu, R.J. & Srinivas, N.R. 2018. Reappraisal and perspectives of clinical drug–drug interaction potential of α-glucosidase inhibitors such as acarbose, voglibose and miglitol in the treatment of type 2 diabetes mellitus. *Xenobiotica,* 48(1): 89-108.

25. DeFronzo, R.A. 1999. Pharmacologic therapy for type 2 diabetes mellitus. *Annals of Internal Medicine,* 131(4): 281-303.

26. Dent, M., Dragović-Uzelac, V., Penić, M., Bosiljkov, T. & Levaj, B. 2013. The effect of extraction solvents, temperature and time on the composition and mass fraction of polyphenols in Dalmatian wild sage (*Salvia officinalis* L.) extracts. *Food Technology and Biotechnology,* 51(1): 84-91.

27. Doğan, N., Doğan, C. & Atila, F. 2021. Parts from life-cycle of *H. erinaceus*: response surface methodology approach to optimize extraction conditions and determination of its antioxidant, antidiabetic and antimicrobial effect. *Journal of Microbiology, Biotechnology and Food Sciences*, e3703.

28. Faller, A. & Fialho, E. 2009. The antioxidant capacity and polyphenol content of organic and conventional retail vegetables after domestic cooking. *Food Research International,* 42(1): 210-215.

29. Faraone, I., Rai, D.K., Chiummiento, L., Fernandez, E., Choudhary, A., Prinzo, F. & Milella, L. 2018. Antioxidant Activity and Phytochemical Characterization of *Senecio* clivicolus Wedd. *Molecules,* 23(10): 2497.

30. Gilham, D. & Lehner, R. 2005. Techniques to measure lipase and esterase activity in vitro. *Methods,* 36(2): 139-147.

31. Hastie, T., Tibshirani, R. & Friedman, J. 2001. The elements of statistical learning. *Springer series in statistics*, Springer, New York, 764 pp.

32. Hung, H.Y., Qian, K., Morris-Natschke, S.L., Hsu, C.S. & Lee, K.H. 2012. Recent discovery of plant-derived anti-diabetic natural products. *Natural Product Reports,* 29(5): 580-606.

33. Hung, W.C., Ling, X.H., Chang, C.C., Hsu, H.F., Wang, S.W., Lee, Y.C., Luo, C., Lee, Y.T. & Houng, J.Y. 2017. Inhibitory effects of Siegesbeckia orientalis extracts on advanced glycation end product formation and key enzymes related to metabolic syndrome. *Molecules,* 22(10): 1785.

34. Kim, Y.M., Wang, M.H. & Rhee, H.I. 2004. A novel α-glucosidase inhibitor from pine bark. *Carbohydrate Research,* 339(3): 715-717.

35. Kiprono, P.C., Kaberia, F., Keriko, J.M. & Karanja, J.N. 2000. The in vitro anti-fungal and anti-bacterial activities of β-sitosterol from *Senecio lyratus* (Asteraceae). *Zeitschrift für Naturforschung C,* 55(5-6): 485-488.

36. Krentz, A.J. & Bailey, C.J. 2005. Oral antidiabetic agents. *Drugs,* 65(3): 385-411.

37. Lee, S.K., Hwang, J.Y., Song, J.H., Jo, J.R., Kim, M.J., Kim, M.E. & Kim, J.I. 2007. Inhibitory activity of Euonymus alatus against alpha-glucosidase in vitro and in vivo. *Nutrition Research and Practice,* 1(3): 184.

38. Loizzo, M., Tundis, R., Statti, G., Miljkovic-Brake, A., Menichini, F. & Houghton, P. 2006. Bioactive extracts from *Senecio samnitum* Huet. *Natural Product Research,* 20(3): 265-269.

39. Lone, S.H., Bhat, K.A., Bhat, H.M., Majeed, R., Anand, R., Hamid, A. & Khuroo, M.A. 2014. Essential oil composition of *Senecio graciliflorus* DC: Comparative analysis of different parts and evaluation of antioxidant and cytotoxic activities. *Phytomedicine,* 21(6): 919-925.

40. Ma, L., Lin, Q., Lei, D., Liu, S., Wang, X. & Zhao, Y. 2018. Alpha-glucosidase inhibitory activities of essential oils extracted from three chinese herbal medicines. *Chemical Engineering Transactions,* 64: 61-66.

41. Mai, T.T., Thu, N.N., Tien, P.G. & Van Chuyen, N. 2007. Alpha-glucosidase inhibitory and antioxidant activities of Vietnamese edible plants and their relationships with polyphenol contents. *Journal of Nutritional Science and Vitaminology,* 53(3): 267-276.

42. Markom, M., Hasan, M., Daud, W.R.W., Singh, H. & Jahim, J.M. 2007. Extraction of hydrolysable tannins from Phyllanthus niruri Linn.: Effects of solvents and extraction methods. *Separation and Purification Technology,* 52(3): 487-496.

43. Matsui, T., Yoshimoto, C., Osajima, K., Oki, T. & Osajima, Y. 1996. In vitro survey of α-glucosidase inhibitory food

components. *Bioscience, Biotechnology, and Biochemistry,* 60(12): 2019-2022.

44. McDougall, G.J., Dobson, P., Smith, P., Blake, A. & Stewart, D. 2005a. Assessing potential bioavailability of raspberry anthocyanins using an in vitro digestion system. *Journal of Agricultural and Food Chemistry,* 53(15): 5896-5904.

45. McDougall, G.J., Shpiro, F., Dobson, P., Smith, P., Blake, A. & Stewart, D. 2005b. Different polyphenolic components of soft fruits inhibit α-amylase and α-glucosidase. *Journal of Agricultural and Food Chemistry,* 53(7): 2760-2766.

46. Memişoğulları, R. 2005. Diyabette serbest radikallerin rolü ve antioksidanların etkisi. *Düzce Tıp Fakültesi Dergisi,* 7(3): 30-39.

47. Mogoşanu, G., Pintea, A., Bejenaru, L.E., Bejenaru, C., Rau, G. & Popescu, H. 2009. HPLC analysis of carotenoids from *Senecio vernalis* and *S. jacobaea* (Asteraceae). *Farmacia,* 57(6): 780-786.

48. Mosihuzzaman, M. & Choudhary, M.I. 2008. Protocols on safety, efficacy, standardization, and documentation of herbal medicine (IUPAC Technical Report). *Pure and Applied Chemistry,* 80(10): 2195-2230.

49. Myers, R.H., Montgomery, D.C. & Anderson-Cook, C.M. 2016. *Response Surface Methodology: process and product optimization using designed experiments*. John Wiley & Sons, New York, 704 pp.

50. Myers, R.H., Montgomery, D.C., Vining, G.G., Borror, C.M. & Kowalski, S.M. 2004. Response surface methodology: a retrospective and literature survey. *Journal of Quality Technology,* 36(1): 53-77.

51. Pereira, C.G., Barreira, L., da Rosa Neng, N., Nogueira, J.M.F., Marques, C., Santos, T.F., Varela, J. & Custódio, L. 2017. Searching for new sources of innovative products for the food industry within halophyte aromatic plants: In vitro antioxidant activity and phenolic and mineral contents of infusions and decoctions of *Crithmum maritimum* L. *Food and Chemical Toxicology,* 107(1): 581-589.

52. Porter, Y. 2012. Antioxidant properties of green broccoli and purple-sprouting broccoli under different cooking conditions. *Bioscience Horizons: The International Journal of Student Research,* 5:hzs004.

53. Robertson, R.P. 2004. Chronic oxidative stress as a central mechanism for glucose toxicity in pancreatic islet beta cells in diabetes. *Journal of Biological Chemistry,* 279(41): 42351-42354.

54. Sasidharan, S., Chen, Y., Saravanan, D., Sundram, K. & Latha, L.Y. 2011. Extraction, isolation and characterization of bioactive compounds from plants' extracts. *African Journal of Traditional, Complementary and Alternative Medicines,* 8(1): 1-10.

55. Sharma, P. & Shah, G. 2015. Composition and antioxidant activity of *Senecio nudicaulis* Wall. ex DC.(Asteraceae): a medicinal plant growing wild in Himachal Pradesh, India. *Natural Product Research,* 29(9): 883-886.

56. Singleton, V.L., Orthofer, R. & Lamuela-Raventós, R.M. 1999. Analysis of total phenols and other oxidation substrates and antioxidants by means of folin-ciocalteu reagent. *Methods in Enzymology,* 299(1): 152-178.

57. Su, C.H., Lai, M.N. & Ng, L.T. 2013. Inhibitory effects of medicinal mushrooms on α-amylase and α-glucosidase–enzymes related to hyperglycemia. *Food & Function,* 4(4): 644-649.

58. Suparmi, S. & Prasetya, H. 2012. Antioxidant activity of the crude carotenoid pigment extract from yellow ambon banana (*M. parasidiaca sapientum*) peel: its potency as vitamin a supplement. *Sains Medika: Jurnal Kedokteran dan Kesehatan,* 4(1): 78-88.

59. Tang, C., Koulajian, K., Schuiki, I., Zhang, L., Desai, T., Ivovic, A., Wang, P., Robson-Doucette, C., Wheeler, M. & Minassian, B. 2012. Glucose-induced beta cell dysfunction in vivo in rats: link between oxidative stress and endoplasmic reticulum stress. *Diabetologia,* 55(5): 1366-1379.

60. Tundis, R., Menichini, F., Loizzo, M.R., Bonesi, M., Solimene, U. & Menichini, F. 2012. Studies on the potential antioxidant properties of *Senecio stabianus* Lacaita (Asteraceae) and its inhibitory activity against carbohydrate-hydrolysing enzymes. *Natural Product Research,* 26(5): 393-404.

61. Uğur, A., Ertem, H. & Beyatlı, Y. 2006. Antibacterial properties of *Senecio sandrasicus*. on multidrug-resistant *Stenotrophomonas maltophilia*. *Pharmaceutical Biology,* 44(4): 253-257.

62. Wang, H., Du, Y.J. & Song, H.C. 2010. α-Glucosidase and α-amylase inhibitory activities of guava leaves. *Food Chemistry,* 123(1): 6-13.

63. Wild, S., Roglic, G., Green, A., Sicree, R. & King, H. 2004. Global prevalence of diabetes: estimates for the year 2000 and projections for 2030. *Diabetes Care,* 27(5): 1047-1053.

http://dergipark.org.tr/trkjnat
Trakya University Journal of Natural Sciences, 22(2): 255-262, 2021
ISSN 2147-0294, e-ISSN 2528-9691
DOI: 10.23902/trkjnat.947001

Research Article

EVALUATION OF GERMINATION, EMERGENCE AND PHYSIOLOGICAL PROPERTIES OF SUGAR BEET CULTIVARS UNDER SALINITY

Engin Gökhan KULAN[1*], Alper ARPACIOĞLU[1], Nurgül ERGİN[2], Mehmet Demir KAYA[1]

[1] Department of Field Crops, Faculty of Agriculture, Eskişehir Osmangazi University, Eskişehir, TURKEY
[2] Department of Field Crops, Faculty of Agriculture and Natural Sciences, Bilecik Şeyh Edebali University, Bilecik, TURKEY

Cite this article as:

Kulan E.G., Arpacıoğlu A., Ergin N. & Kaya M.D. 2021. Evaluation of germination, emergence and physiological properties of sugar beet cultivars under salinity. *Trakya Univ J Nat Sci*, 22(2): 255-262, DOI: 10.23902/trkjnat.947001

Received: 07 June 2021, Accepted: 01 October 2021, Published: 15 October 2021

Abstract: This study aimed to determine a useful selection criterion for salt tolerance during the early development stage of sugar beet. Four sugar beet cultivars (Orthega, Valentina, FD Shoot, and Mohican) were exposed to NaCl stresses (Control, 5, 10, and 15 dS m^{-1}), and morphological and physiological characteristics were investigated. Germination percentage, mean germination time (MGT), seedling length, and seedling fresh weight (SFW) in germination test; emergence percentage, mean emergence time (MET), root length, shoot length, plant fresh weight, relative chlorophyll content (Chl), relative water content (RWC) and electrolyte leakage of the plants grown in pod experiment were measured. The results showed that the maximum germination at control was recorded in FD Shoot, but it gave the lowest germination at 15 dS m^{-1}. In the pod experiment, the highest emergence rate was detected in Orthega and Mohican at all levels of NaCl. Increased salinity delayed MET and led to reduction in shoot length, root length, and RWC of sugar beet cultivars. Relative Chl content and electrolyte leakage enhanced from 32.7 SPAD and 21.6% in control to 38.5 SPAD and 35.6% in 10 dS m^{-1}, respectively. In general, there were significant differences among sugar beet cultivars, and they could keep the salinity up to 5 dS m^{-1} in terms of the investigated traits. It was concluded that relative Chl content and electrolyte leakage should be used a promising clue for selection of tolerant or sensitive sugar beet cultivars for salinity.

Özet: Bu çalışmada, erken gelişim döneminde şeker pancarının tuza toleransı için faydalı bir seçim kriteri belirlemek amaçlanmıştır. NaCl stresine (Kontrol, 5, 10 ve 15 dS m^{-1}) maruz bırakılan dört şeker pancarı çeşidinde (Orthega, Valentina, FD Shoot ve Mohican) morfolojik ve fizyolojik özellikler incelenmiştir. Çimlenme testinde; çimlenme yüzdesi, ortalama çimlenme süresi, fide uzunluğu ve fide yaş ağırlığı, çıkış testinde; çıkış yüzdesi, ortalama çıkış süresi, kök uzunluğu, sürgün uzunluğu, bitki yaş ağırlığı, bağıl su içeriği, bağıl klorofil içeriği ve elektrolit sızıntısı ölçülmüştür. Sonuçlar, FD Shoot çeşidinde en yüksek çimlenmenin kontrol, en düşük çimlenmenin ise 15 dS m^{-1} seviyesinde kaydedildiğini göstermiştir. Çıkış testindeki tüm NaCl seviyelerinde en yüksek çıkış yüzdesi Orthega ve Mohican çeşitlerinde tespit edilmiştir. Artan NaCl seviyeleri ile şeker pancarı çeşitlerinde ortalama çıkış süresi gecikmiş ve sürgün uzunluğu, kök uzunluğu ve bağıl su içeriği azalmıştır. Bağıl klorofil içeriği ve elektrolit sızıntısı, kontrol ve 10 dS m^{-1} seviyelerinde sırasıyla 32,7 SPAD ve %21,6; 38,5 SPAD ve %35,6 olarak belirlenmiştir. Genel olarak, şeker pancarı çeşitleri arasında önemli farklılıklar bulunmuş ve incelenen özellikler açısından çeşitler 5 dS m^{-1}'e kadar olan tuzluluğa tolerans göstermişlerdir. Bağıl klorofil içeriği ve elektrolit sızıntısının, tuzluluğa toleranslı veya hassas şeker pancarı çeşitlerinin seçiminde umut verici bir ipucu olarak kullanılması gerektiği sonucuna varılmıştır.

Edited by:
Panagiotis Madesis

****Corresponding Author:***
Engin Gökhan Kulan
egkulan@ogu.edu.tr

ORCID iDs of the authors:
EGK. orcid.org/0000-0002-7147-6896
AA. orcid.org/0000-0002-1176-2866
NE. orcid.org/0000-0003-3105-7504
MDK. orcid.org/0000-0002-4681-2464

Key words:
Beta vulgaris L.
NaCl
Relative water content
Chlorophyll content
Electrolyte leakage

Introduction

Soil salinity occurs naturally in arid and semiarid regions where evapotranspiration is greater than precipitation. In irrigated areas, excessive amounts of irrigation water and low quality irrigation water use cause the accumulation of salts in soil. Salt stress is one of the most significant abiotic stresses inhibiting plant growth (Hampson & Simpson 1990, Neumann 1995) and resulting in a wide number of irregularities in morphological, physiological and biochemical processes from germination to harvest (Willenborg *et al*. 2004).

However, seed germination and early seedling growth are the most sensitive phases in many crops to salt stress (Almansouri *et al*. 2001).

Sugar used for human consumption is obtained from sugar beet and sugar cane in the world, while it is produced only from sugar beet in Turkey. Sugar beet is classified as a salt tolerant crop (Katerji *et al*. 2000, Yang *et al*. 2012), although it is sensitive to increased salinity at germination and early seedling stages (Ghoulam & Fares 2001). Routinely, germination and seedling development properties have been tested for salinity tolerance because they are the most sensitive stage in plant life cycle. Jamil & Rha (2004) recorded a significant reduction in germination percentage and a delay in required time to germination, but Jafarzadeh & Aliasgharzad (2007) indicated that there was genotypic variation for germination rate among sugar beet cultivars. Also, Higazy *et al*. (1995) and Mekki & El-Gazzar (1999) reported that salinity stress caused a depressed seedling growth, especially in the seedling fresh and dry weights of sugar beet. Moreover, relative water content, electrolyte leakage and chlorophyll content were recently used for indicators of salinity in barley (Ashraf 2004), in wheat (Farooq & Azam 2006, Jamali *et al*. 2015). In sugar beet, decreased relative water content and chlorophyll content in leaves (Khorshid *et al*. 2018) and increased electrolyte leakage under NaCl were reported by Wang *et al*. (2017) but Skorupa *et al*. (2019) determined no changes in chlorophyll content. Due to the controversial reports and lack of sufficient researches, physiological traits needs to be confirmed by comparing salt stress sensitive and tolerant cultivars in sugar beet. This study aimed to investigate for any potential characteristics to be used for salt-tolerant sugar beet cultivars considering germination, early seedling development traits, relative water content, chlorophyll content and electrolyte.

Materials and Methods

The study was carried out at the Department of Field Crops, Faculty of Agriculture, Eskişehir Osmangazi University, Turkey in 2019. Extensively preferred four sugar beet cultivars (Orthega, Valentina, FD Shoot, and Mohican) from three seed companies and NaCl (Merck) were used in the experiments. Salinity levels were arranged as decreasing in germination and emergence percentage and they were constituted as low (5 dS m^{-1}), medium (10 dS m^{-1}), and high (15 dS m^{-1}) salinity with WTW 3.15 conductivity meter (Germany). Distilled water (0 dS m^{-1}) was used as control.

In the germination experiment, it was aimed to simulate the soil salinity because the seeds were directly placed into salt-contaminated soils. Two hundred seeds as four replicates (4×50) were employed for each cultivar and salinity level. The fifty seeds were counted and inserted into three layers of sterile filter paper with 21 mL of respective salt solutions. As soon as the papers were gently rolled, they were put into sealed plastic bags to prevent water loss. These bags were transferred to the incubator at a constant temperature of 25±1°C in the dark. Germinated seeds with a 2 mm radicle were counted every day for 14 days period. The mean germination time (MGT) was calculated as described in Anonymous (2003). Seedling length and seedling fresh weight were measured at the end of the experiment.

The emergence experiment was designed for simulation of irrigation water salinity under laboratory conditions. It was conducted in peat-filled plastic containers with 100 seeds (4×25) and the seeds of each sugar beet cultivar were sown individually at a depth of 2 cm. The plastic containers were placed in the growth chamber after they were irrigated with respective salt solutions. Emergence percentage, mean emergence time (MET), fresh plant weight, root length, shoot length, relative chlorophyll content (Chl), relative water content (RWC) and electrolyte leakage were measured at 28th day after sowing. Leaf relative Chl was measured at the third leaf from the top of plants by using Konica Minolta SPAD-502 meter. Leaf RWC was assessed on fully enlarged leaves of five plants per replicate. Five leaves were pulled out from each replication and immediately weighed fresh weight (FW). They were immersed in distilled water in a falcon tube for 24 h to regain turgidity, and then turgor weight (TW) was weighted. The samples were dried at 70°C for 48 h in order to determine the dry weight (DW). RWC of the leaves was calculated following the formula (Ghoulam *et al*. 2002) (Eq. 1).

$$RWC\ (\%) = [(FW-DW)/(TW-DW)] \times 100 \quad (Eq.\ 1)$$

After the plants were harvested, the electrical conductivity (EC) values of the growing medium were determined. The saturated paste extract was prepared with a 1:10 medium to water ratio and the EC was measured with the EC meter at 25°C after 24 h with three replicates for each treatment.

Electrolyte leakage was analyzed by using young leaf discs of five plants from each treatment. Leaf samples were washed with deionized water to eliminate electrolytes on the surface of the leaves. Five leaf disks with 10 mm diameter were excised, weighed and placed into glass tubes filled with 20 mL of deionized water. After the incubation period for 24 h at 25°C, the solution's electrical conductivity (L_t) was directly read by the EC meter. They were then autoclaved for 20 min at 121°C, and the electrical conductivity (L_o) was recorded again at 25°C after equilibration (Yadav *et al*. 2012). The electrolyte leakage was calculated by the formula of Ghoulam *et al*. (2002) as follows (Eq. 2).

$$Electrolyte\ leakage\ (\%) = (L_t / L_o) \times 100 \quad (Eq.\ 2)$$

The experimental design was a 2-factor factorial, arranged in a completely randomized design with 4 replications. Analysis of variance was performed by the MSTAT-C software program (Michigan State University, v 2.10). Significant differences among the mean values were compared by Duncan's Multiple Range test ($p<0.05$).

Results

Germination performance and seedling development of sugar beet cultivars in the germination experiment were negatively influenced by increasing NaCl levels (Table 1). Mean values of sugar beet cultivars showed that differences were detected for the investigated traits. Among the cultivars, Mohican gave the highest germination percentage and seedling length, while Ortega produced the heavier fresh weight. At the highest NaCl level of 15 dS m^{-1}, Mohican had the maximum germination percentage, while a dramatic decrease in germination rate of FD Shoot was observed. Considering mean values of NaCl levels, increased NaCl caused a significant reduction in germination, seedling length and seedling fresh weight, but MGT was retarded. Mean values obtained from four cultivars showed higher germination, seedling length and seedling fresh weight; however, the interaction between cultivar and salinity was significant.

Interaction of cultivar × NaCl levels showed that germination percentage of cultivar FD Shoot linearly declined due to an increase in NaCl (Fig. 1a). Under salt stresses, Orthega and Valentina germinated higher than the other cultivars, while the germination rate of Mohican did not change. MGT was clearly delayed by increasing salinity; the most rapid germination was obtained from Valentina (Fig. 1b). The response of seedling length of sugar beet cultivars to salinity levels was different and FD Shoot had the shortest seedling at 15 dS m^{-1} (Fig. 1c).

Table 1. Analysis of variance and mean values of germination and early seedling growth parameters of sugar beet cultivars under salinity conditions in the germination experiment. The means ± SD of four replicates were given. Different letters denote statistically significant differences by Duncan's Multiple Range test ($p<0.05$) among all treatments respectively.

Factors	Germination percentage (%)	Mean germination time (day)	Seedling length (cm)	Seedling fresh weight (mg $plant^{-1}$)
Cultivars				
Orthega	62.7^{b}±9.50	4.61^{b}±1.27	7.06^{b}±0.46	44.4^{a}±5.39
Valentina	61.1^{b}±6.37	3.89^{c}±0.75	7.49^{b}±0.94	33.2^{c}±5.73
FD Shoot	49.3^{c}±28.5	5.50^{a}±1.90	6.95^{b}±2.29	42.5^{ab}±12.9
Mohican	66.3^{a}±3.04	4.07^{c}±1.06	8.62^{a}±1.14	40.8^{b}±5.84
NaCl (dS m^{-1})				
Control	71.8^{a}±6.77	3.30^{d}±0.35	7.24^{b}±0.57	38.6^{c}±6.17
5	63.3^{b}±3.42	3.71^{c}±0.40	8.97^{a}±1.09	49.1^{a}±6.90
10	57.1^{c}±12.1	5.08^{b}±1.02	7.61^{b}±0.60	41.4^{b}±5.04
15	47.2^{d}±23.1	5.97^{a}±1.26	6.30^{c}±1.80	31.8^{d}±6.62
Analysis of Variance				
$D_{Cultivars\ (A)}$	0.000	0.000	0.000	0.000
$D_{NaCl\ (B)}$	0.000	0.000	0.000	0.000
$D_{A\times B}$	0.000	0.000	0.000	0.000

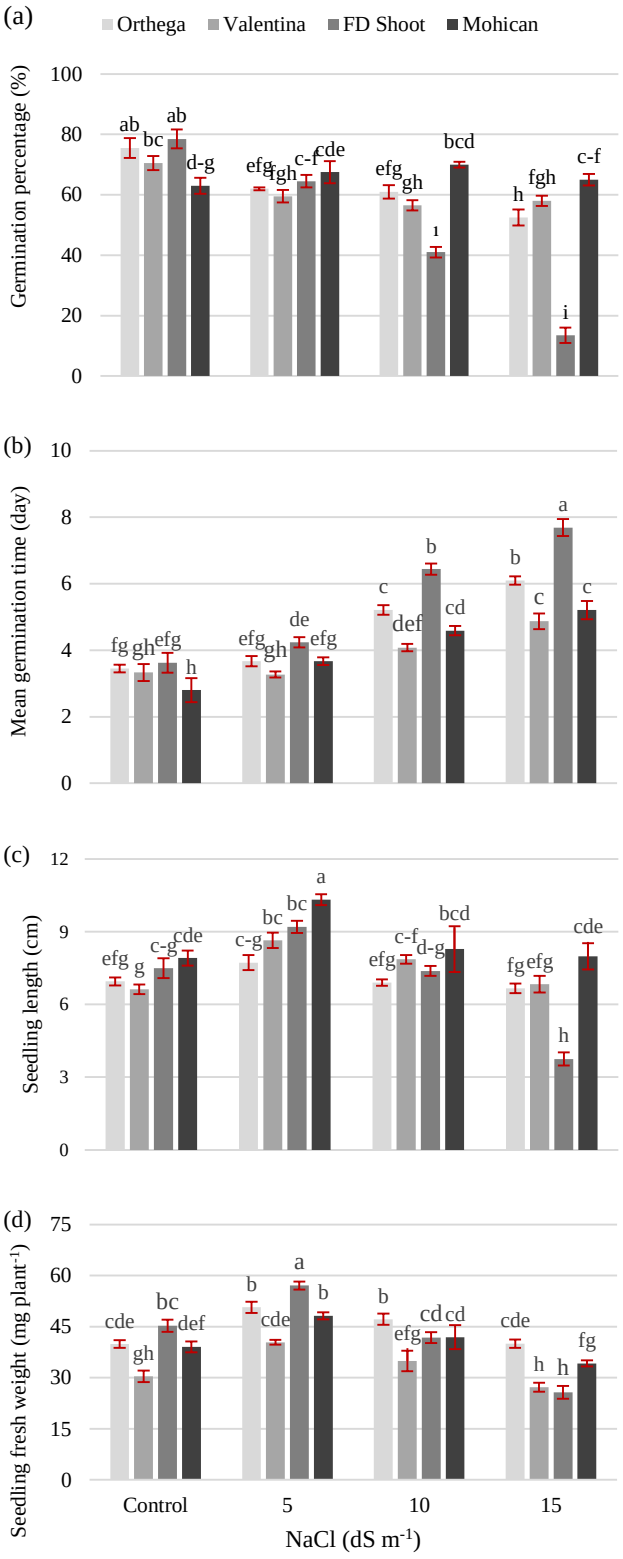

Fig. 1. Interaction of cultivar x NaCl level for a) germination percentage, b) mean germination time, c) seedling length, d) seedling fresh weight of sugar beet cultivars in the germination experiment. The means ± SD of four replicates were given. Different letters denote statistically significant differences by Duncan's Multiple Range test ($p<0.05$) among all treatments respectively.

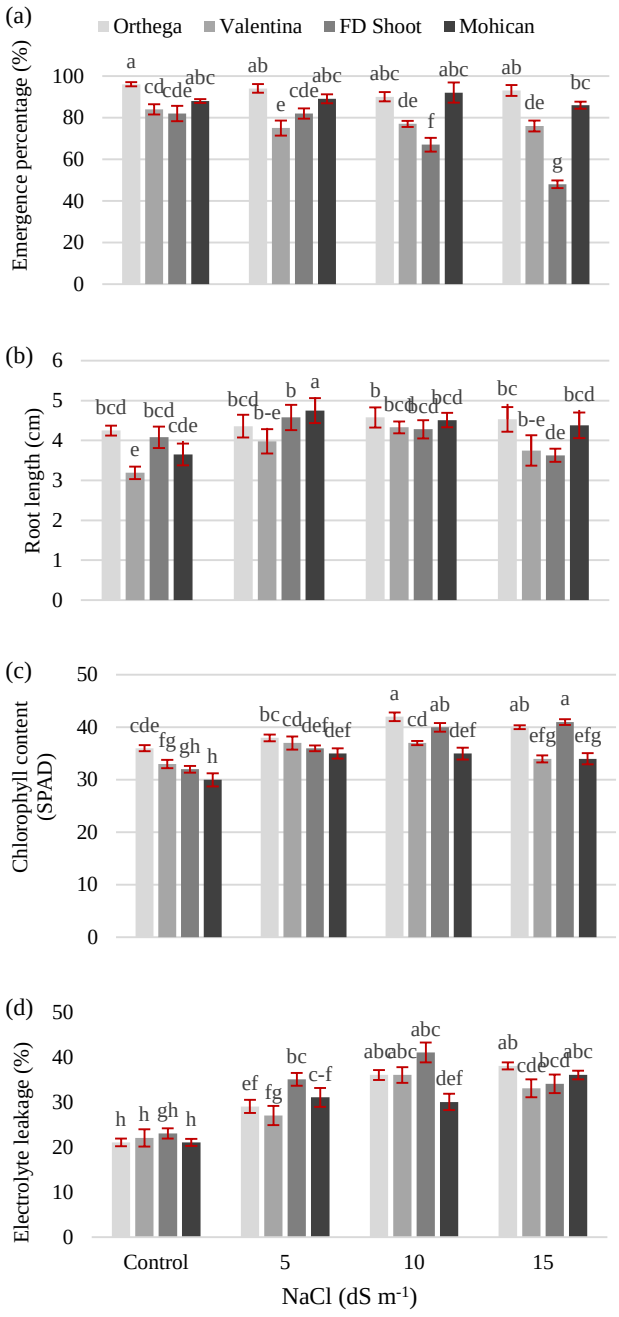

Fig. 2. Interaction of cultivar x NaCl level for a) emergence percentage, b) root length, c) relative chlorophyll content, d) electrolyte leakage of sugar beet in the pod experiment. The means ± SD of four replicates were given. Different letters denote statistically significant differences by Duncan's Multiple Range test ($p<0.05$) among all treatments respectively.

Similar results were obtained from the other sugar beet cultivars and the minimum level of NaCl promoted the seedling growth. Seedling fresh weight evidently increased at NaCl levels of 5 dS m^{-1}; that is why low doses of salts act as plant nutrition during short periods at early development stage. A remarkable reduction in SFW occurred at 15 dS m^{-1} along with significant changes among cultivars. Seedling fresh weight of Orthega did not change from control to 15 dS m^{-1}, but FD Shoot was clearly depressed (Fig. 1d).

In the pod experiments, main factors and interaction effects of the investigated characters of sugar beet cultivars subjected to different NaCl levels were given in Table 2. A two-way interaction was significant for emergence percentage, root length, relative chlorophyll content and electrolyte leakage, and the interactions were displayed in Fig. 2. Orthega had the highest emergence percentage of 92.8%, while FD Shoot had the lowest emergence with 69.3%. Increasing NaCl levels resulted in decreased emergence percentage from 87.0% in control to 75.5% at 15 dS m^{-1}. FD Shoot was the most severely affected by NaCl and its emergence percentage was dramatically decreased at 10 dS m^{-1} and above (Fig 2a). MET was adversely affected by increasing NaCl and the shortest time to emergence was recorded in Orthega. Among the cultivars, Mohican had the longest root length with 4.57 cm, followed by Orthega with 4.43 cm. Under all NaCl levels, sugar beet seedlings produced longer root length than control. Shorter root length at 15 dS m^{-1} than control was attained in FD Shoot and the other cultivars produced the longest root length (Fig 2b).

Shoot length varied between 2.73 cm and 3.27 cm, Orthega and Valentina had the higher values compared to FD Shoot and Mohican. Shoot length was severely decreased when NaCl levels increased. On the other hand, NaCl dose of 5 dS m^{-1} showed a promoter effect on fresh plant weight, significant reductions were observed at 10 and 15 dS m^{-1}.

Physiological parameters were apparently changed by sugar beet cultivars and NaCl levels. Orthega had the highest Chl, while the maximum RWC and electrolyte leakage was obtained from FD Shoot. Increasing salinity levels led to an increase in Chl and electrolyte leakage, and the highest values were detected at 10 dS m^{-1} and dropped at 15 dS m^{-1}. An apparent increase in Chl content of Orthega and FD Shoot was observed under NaCl, but this increase was at minimal level in Mohican and Valentina (Fig. 2c). Considerable variations were found for RWC and electrolyte leakage. RWC reduced by increasing salinity and decreased from 76.7% to 64.9%. FD Shoot exhibited the highest RWC with 72.3%. Salinity induced significant decrease in RWC at higher salinity levels compared to the control. Salt treatment caused a highly significant decrease in RWC of the investigated cultivars. RWC decreased with the increase of salt concentration and less effect was recorded in FD Shoot. Electrolyte leakage reached the maximum level at 15 dS m^{-1} except for Valentina and FD Shoot at 10 dS m^{-1}, whose electrolyte leakage values declined at 15 dS m^{-1}.

Comparison of electrical conductivity values of the growing medium at the end of the pod experiment was illustrated in Fig. 3. At control and 5 dS m^{-1}, no significant changes in EC values of growing medium were observed among sugar beet cultivars. The medium of Orthega and FD Shoot possessed lower EC values at 10 dS m^{-1}, while they were higher at 15 dS m^{-1} than that of Mohican and Valentina.

Table 2. Analysis of variance and main effects of sugar beet cultivars and NaCl levels for emergence percentage (EP), mean emergence time (MET), root length, shoot length, fresh plant weight (FPW), relative chlorophyll content (Chl), relative water content (RWC) and electrolyte leakage (EL) of 28-day old sugar beet plants in the pod experiment. The means ± SD of four replicates were given. Different letters denote statistically significant differences by Duncan's Multiple Range test ($p<0.05$) among all treatments respectively.

Factors	EP (%)	MET (day)	Root length (cm)	Shoot length (cm)	FPW (mg plant^{-1})	Chl (SPAD)	RWC (%)	EL (%)
Cultivars								
Orthega	92.8^{a}±2.56	6.02^{c}±0.72	4.43^{ab}±0.15	3.27^{a}±0.72	1036^{a}±165	39.0^{a}±2.62	69.4^{ab}±4.51	30.9^{b}†±7.98
Valentina	77.6^{c}±4.01	6.29^{c}±0.79	3.81^{c}±0.48	3.16^{a}±0.84	820^{b}±221	35.1^{c}±2.09	66.2^{b}±5.28	29.2^{b}±6.15
FD Shoot	69.3^{d}±15.9	7.04^{a}±1.04	4.14^{bc}±0.40	2.77^{b}±0.65	1131^{a}±336	37.0^{b}±4.27	72.3^{a}±5.99	33.2^{a}±7.40
Mohican	88.5^{b}±2.74	6.65^{b}±0.76	4.57^{a}±0.87	2.73^{b}±0.45	1032^{a}±229	33.5^{d}±2.13	67.7^{ab}±6.90	29.6^{b}±6.15
NaCl (dS m^{-1})								
Control	87.0^{a}±6.19	5.81^{c}±0.33	3.79^{c}±0.47	3.77^{a}±0.42	1125^{b}±178	32.7^{c}±2.26	76.7^{a}±3.32	21.6^{c}±1.01
5	84.7^{ab}±8.55	5.97^{c}±0.43	4.67^{a}±0.76	3.06^{b}±0.50	1238^{a}±156	36.3^{b}±1.53	67.6^{b}±2.11	30.6^{b}±3.54
10	81.1^{b}±11.8	6.61^{b}±0.54	4.42^{ab}±0.14	2.86^{b}±0.22	960^{c}±147	38.5^{a}±3.00	66.4^{b}±4.57	35.6^{a}±4.30
15	75.5^{c}±19.5	7.60^{a}±0.61	4.07^{bc}±0.44	2.23^{c}±0.21	696^{d}±106	37.2^{b}±3.99	64.9^{b}±2.96	35.2^{a}±2.37
Analysis of Variance								
D $_{\text{Cultivars (A)}}$	0.000	0.000	0.001	0.001	0.000	0.000	0.050	0.004
D $_{\text{NaCl (B)}}$	0.000	0.000	0.000	0.000	0.000	0.000	0.000	0.000
D $_{\text{A×B}}$	0.000	0.312	0.010	0.160	0.252	0.000	0.332	0.004

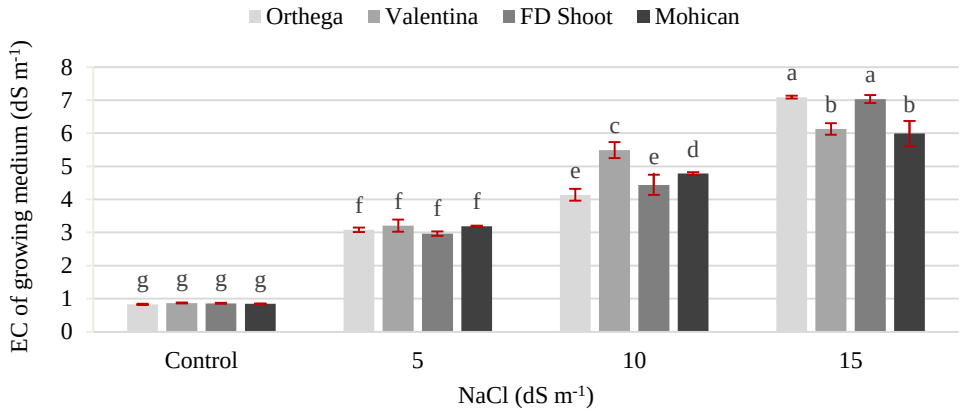

Fig. 3. Electrical conductivity values (1:10) of growing medium after the pod experiment according to NaCl levels and sugar beet cultivars. The means ± SD of four replicates were given. Different letters denote statistically significant differences by Duncan's Multiple Range test ($p<0.05$) among all treatments respectively.

Discussion

The primary effect of salinity stress in plants is restriction of water uptake, ion imbalance and toxicity. Sugar beet is often exposed to salinity by means of irrigation water or naturally saline soils in arid and semiarid regions in Turkey. For this reason, it is necessary to improve salt tolerant sugar beet cultivars or to select the tolerant cultivars. Our results showed that germination performance was reduced and delayed due to increasing NaCl levels with significant variation among sugar beet cultivars. The inhibitory effect of salinity on germination was not determined in Mohican, but MGT was delayed. The results are in agreement with Mostafavi (2012), Khayamim *et al*. (2014) and Pinheiro *et al*. (2018) who observed that sugar beet cultivars were adversely affected by high salt doses and their MGT was prolonged. Kandil *et al*. (2014) found that increasing salinity levels significantly decreased germination percentage, while the shortest MGT was recorded in control. They confirmed that there was genotypic variation among sugar beet cultivars in terms of germination rate and MGT under salinity. Early seedling development was not inhibited up to NaCl level of 15 dS m^{-1}, while sugar beet cultivars showed different responses to salinity. FD Shoot was the most adversely influenced with respect to seedling length and seedling fresh weight. On the other hand, Mohican and Orthega exhibited better performance as NaCl levels increased. Our results confirmed the findings of Mostafavi (2012), Jamil & Rha (2004) and Khorshid *et al*. (2018). They determined a significant reduction in root, shoot length and seedling fresh weight due to increasing salinity. Similar results were obtained from several plants such as soybean (Amirjani 2010) and nine vegetables (Shannon *et al*. 2000). Decreased emergence percentage and retarded MET were determined under NaCl stresses. Mahmoud & Hill (1981) indicated that higher salt levels resulted in reduced and delayed emergence compared to control. Generally, emergence performance was confirmed by germination percentage and MGT. However, germination percentage was observed lower than the emergence percentage in our study. That is why sugar beet seeds have germination inhibitors (Salimi & Boelt 2019) and pleated papers are advised for

germination test. On the other hand, flat papers were employed in this study in order to prevent the leakage of salt ions from germination medium and lower germination rate were achieved than emergence rate.

Root length is considered as an important clue to the response of plants to salt stress, so that they are in contact with soil and absorb water and nutrients from the soil (Kaya *et al*. 2003). Taghizadegan *et al*. (2019) reported that the root length increased by salinity compared to control. Root length showed differences among sugar beet cultivars. Orthega and Mohican were the least affected cultivars by NaCl. Jafarzadeh & Aliasgharzad (2007) recorded a decrease in root length at 16 dS m^{-1} and no considerable change was observed up to 14 dS m^{-1}. Shoot length was the most sensitive character and it was gradually decreased with increasing NaCl. Orthega and Valentina produced longer shoot than the others. Jamil & Rha (2004) reported that salinity significantly reduced shoot length of sugar beet, and shoot length was more sensitive than root length (AboKassem 2007). Depending on the decrease in root and shoot length, FPW was reduced by NaCl levels. The findings of Mostafavi (2012), Jamil *et al*. (2012) and Khayamim *et al*. (2014) confirmed these results. Chl under increasing salinity was changed by sugar beet cultivars. FD Shoot showed linear increases up to 15 dS m^{-1}, while Valentina gradually increased at 10 dS m^{-1} and decreased at 15 dS m^{-1}. Contrarily, Wang *et al*. (2017) stated a clear reduction in Chl in sugar beet as NaCl increased. Skorupa *et al*. (2019) determined that no change was recorded in Chl under saline conditions. The difference in Chl could be resulted from genotypic variation or their tolerance levels and duration of exposure to salinity. RWC diminished when the salinity level increased. Mensah *et al*. (2006) found that the RWC of the pea cultivars under salt stress decreased. Similarly, Ghoulam *et al*. (2002), Wang *et al*. (2017), Skorupa *et al*. (2019), Taghizadegan *et al*. (2019), Tahjib-Ul-Arif *et al*. (2019) and Wang *et al*. (2019) reported that increasing salinity resulted in a decrease in RWC in sugar beet. The decline in RWC stated a loss of turgor leading to limited available water for the cell extension process (Ghoulam *et al*. 2002); consequently, inhibition of growth in FD Shoot might be linked to a decline in RWC caused by salinity stress. Our results showed that salinity induced electrolyte leakage from the leaves of all sugar beet cultivars. This finding was supported by Ghoulam *et al*. (2002), Dadkhah (2011) and Romano *et al.* (2019), who reported that the electrolyte leakage was raised with higher salinities. Excessive accumulation of Na^+ and Cl^- ions in plant tissue causes ion imbalance and deformation, even resulted in killing the cells, which led to improve the ionic leakage from leaves; therefore, higher electrolyte leakage was observed in lower salt tolerant plants. It is used to measure the stability of the cellular membranes against any stress factors. In previous studies, enhanced salinity levels caused by cell membrane injury and electrolyte leakage were supported by Dadkhah (2011) in sugar beet and Dkhil & Denden (2012) in okra.

Conclusion

Sugar beet is considered to be a salinity tolerant plant; however, its tolerance level depends on two main factors, the cultivar and the plant development stage. The seeds of sugar beet are firstly exposed to salinity when they are sown into soils contaminated by salinity or irrigated with water with low quality for emergence. Improvement of salt tolerant cultivars is necessary and/or tolerant cultivars should be selected for successful production in saline soils. In this study, four sugar beet cultivars were imposed to germinate under saline conditions and allowed to grow seedlings. Among the investigated cultivars, Mohican and Orthega were found to be more salt tolerant than the others and the most sensitive cultivar was FD Shoot. Similar trends between germination results and the findings of the emergence experiment were identified. The results of relative chlorophyll content and electrolyte leakage were prominently changed according to salt-tolerant and sensitive cultivars, and consequently, they should be considered for suitable selection criteria for salinity in sugar beet. However, further research should be conducted with more sugar beet cultivars in order to explain precisely the relationship between the germination and physiological properties, and to determine their responses to salinity at successive development stages under field conditions.

Ethics Committee Approval: Since the article does not contain any studies with human or animal subject, its approval to the ethics committee was not required.

Author Contributions: Concept: A.A., M.D.K., Desing: A.A., M.D.K., Execution: A.A., E.G.K., Material supplying: A.A., M.D.K., Data acquisition: M.D.K., N.E., E.G.K., Data analysis/interpretation: M.D.K., N.E., E.G.K., Writing: M.D.K., N.E., E.G.K., Critical review: M.D.K.

Conflict of Interest: The authors have no conflicts of interest to declare.

Funding: The authors declared that this study has received no financial support.

References

1. Abo-Kassem, E.ED.M. 2007. Effects of Salinity: Calcium interaction on growth and nucleic acid metabolism in five spices of *Chenopodiaceae*. *Turkish Journal of Botany*, 31: 125-134.

2. Almansouri, M., Kinet, J.M. & Lutts, S. 2001. Effect of salt and osmotic stresses on germination in durum wheat (*Triticum durum* Desf.). *Plant Soil*, 231: 243-254.

3. Amirjani, M.R. 2010. Effect of salinity stress on growth, mineral composition, proline content, antioxidant enzymes of soybean. *American Journal of Plant Physiology*, 5(6): 350-360.

4. Anonymous, 2003. *International Rules for Seed Testing*. The International Seed Testing Association (ISTA), Edition 2003/1, Bassersdorf, CH-Switzerland.

5. Ashraf, M. 2004. Some important physiological selection criteria for salt tolerance in plants. *Flora-Morphology, Distribution, Functional Ecology of Plants*, 199(5): 361-376.

6. Dadkhah, A. 2011. Effect of salinity on growth and leaf photosynthesis of two sugar beet (*Beta vulgaris* L.) cultivars. *Journal of Agricultural Science and Technology*, 13(7): 1001-1012.

7. Dkhil, B.B. & Denden, M. 2012. Effect of salt stress on growth, anthocyanins, membrane permeability and chlorophyll fluorescence of okra (*Abelmoschus esculentus* L.) seedlings. *American Journal of Plant Physiology*, 7(4): 174-183.

8. Farooq, S. & Azam, F. 2006. The use of cell membrane stability (CMS) technique to screen for salt tolerant wheat varieties. *Journal of Plant Physiology*, 163: 629-637.

9. Ghoulam, C. & Fares, K. 2001. Effect of salinity on seed germination and early seedling growth of sugar beet (*Beta vulgaris* L.). *Seed Science and Technology*, 29: 357-364.

10. Ghoulam, C., Foursy, A. & Fares, K. 2002. Effects of salt stress on growth, inorganic ions and proline accumulation in relation to osmotic adjustment in five sugar beet cultivars. *Environmental and Experimental Botany*, 47(1): 39-50.

11. Hampson C.R. & Simpson, G.M. 1990. Effects of temperature, salt and osmotic pressure on early growth of wheat (*Triticum aestivum* L.). 1. Germination. *Canadian Journal of Botany*, 68: 524-528.

12. Higazy, M.A., Shehata, M.M. & Allam, A.I. 1995. Free proline relation to salinity tolerance of three sugar beet varieties. *Egyptian Journal of Agricultural Research*, 13(1): 175-190.

13. Jafarzadeh, A. & Aliasgharzad, N. 2007. Salinity and salt composition effects on seed germination and root length of four sugar beet cultivars. *Biologia*, 62(5): 562-564.

14. Jamali, S.S., Borzouei, A., Aghamirzaei, M., Khosronejad, H.R. & Fathi, M. 2015. Cell membrane stability and biochemical response of seven wheat cultivars under salinity stress. *Brazilian Journal of Botany*, 38(1): 63-69.

15. Jamil, M. & Rha, E.S. 2004. The effect of salinity (NaCl) on the germination and seedling of sugar beet (*Beta vulgaris* L.) and cabbage (*Brassica oleracea* L.). *Plant Resources*, 7(3): 226-232.

16. Jamil, M., Ashraf, M., Rehman, S., Ahmad, M. & Rha, E.S. 2012. Salinity induced changes in cell membrane stability, protein and RNA contents. *African Journal of Biotechnology*, 11(24): 6476-6483.

17. Kandil, A.A., Sharief, A.E., Abido, W.A.E. & Awed, A.M. 2014. Effect of gibberellic acid on germination behaviour of sugar beet cultivars under salt stress conditions of Egypt. *Sugar Tech*, 16(2): 211-221.

18. Katerji, N., Van Hoorn, J.W., Hamdy, A. & Mastrorilli, M. 2000. Salt tolerance classification of crops according to soil salinity and to water stress day index. *Agricultural Water Management*, 43(1): 99-109.

19. Kaya, M.D., Ipek, A. & Ozturk, A. 2003. Effects of different soil salinity levels on germination and seedling growth of safflower (*Carthamus tinctorius* L.). *Turkish Journal of Agriculture and Forestry*, 27(4): 221-227.

20. Khayamim, S., Tavkol Afshari, R., Sadeghian, S.Y., Poustini, K., Roozbeh, F. & Abbasi, Z. 2014. Seed germination, plant establishment, and yield of sugar beet genotypes under salinity stress. *Journal of Agricultural Science and Technology*, 16(4): 779-790.

21. Khorshid, A.M., Moghadam, F.A., Bernousi, I., Khayamim, S. & Rajabi, A. 2018. Comparison of some physiological responses to salinity and normal conditions in Sugar Beet. *Indian Journal of Agricultural Research*, 52(4): 362-367.

22. Mahmoud, E.A. & Hill, M.J. 1981. Salt tolerance of sugar beet at various temperatures. *New Zealand Journal of Agricultural Research*, 24(1): 67-71.

23. Mekki, B.B. & EL-Gazzar, M.M. 1999. Response of root yield and quality of sugar beet (*Beta vulgaris* L.) to irrigation with saline water and follar potassium fertilization. *Annals of Agricultural Sciences*, 44(1): 213-225.

24. Mensah, J.K., Akomeah, P.A., Ikhajiagbe, B. & Ekpekurede, E.O. 2006. Effects of salinity on germination, growth and yield of five groundnut genotypes. *African Journal of Biotechnology*, 5(20): 1973-1979.

25. Mostafavi, K. 2012. Effect of salt stress on germination and early seedling growth stage of sugar beet cultivars. *American-Eurasian Journal of Sustainable Agriculture*, 6: 120-125.

26. Neumann, P.M. 1995. Inhabitation of content of germinating content root growth by salinity stress: Toxicity or an adaptive biophysical response. Pp. 299-304. In: Baluska, F., Ciamporova, M., Gasparikova, O. & Barlow, P.W. (eds). *Structure and Function of Roots*. The Netherlands: Kluwer Academic Publishers, 354 pp.

27. Pinheiro, C., Ribeiro, I.C., Reisinger, V., Planchon, S., Veloso, M.M., Renaut, J., Eichacker, L. & Ricardo, C.P. 2018. Salinity effect on germination, seedling growth and cotyledon membrane complexes of a Portuguese salt marsh wild beet ecotype. *Theoretical and Experimental Plant Physiology*, 30(2): 113-127.

28. Romano, A., Stevanato, P., Sorgona, A., Cacco, G. & Abenavoli, M.R. 2019. Dynamic response of key germination traits to NaCl stress in sugar beet seeds. *Sugar Tech*, 21(4): 661-671.

29. Salimi, Z. & Boelt, B. 2019. Optimization of germination inhibitors eliminating from sugar beet (*Beta vulgaris* L.) seeds of different maturity classes. *Agronomy*, 9(11): 763.

30. Shannon, M.C., Grieve, C.M., Lesch, S.M. & Draper, J.H. 2000. Analysis of salt tolerance in nine leafy vegetables irrigated with saline drainage water. *Journal of the American Society for Horticultural Science*, 125(5): 658-664.

31. Skorupa, M., Gołębiewski, M., Kurnik, K., Niedojadło, J., Kęsy, J., Klamkowski, K., Wójcik, K., Treder, W., Tretyn, A. & Tyburski, J. 2019. Salt stress vs. salt shock-the case of sugar beet and its halophytic ancestor. *BMC Plant Biology*, 19(1): 1-18.

32. Taghizadegan, M., Toorchi, M., Vahed, M.M. & Khayamim, S. 2019. Evaluation of sugar beet breeding

populations based morpho-physiological characters under salinity stress. *Pakistan Journal of Botany*, 51(1): 11-17.

33. Tahjib-UI-Arif, M., Sohag, A.A.M., Afrin, S., Bashar, K.K., Afrin, T., Mahamud, A.G.M., Polash, M.A.S., Hossain, M.T., Sohel, M.A.T., Brestic, M. & Murata, Y. 2019. Differential response of sugar beet to long-term mild to severe salinity in a soil–pot culture. *Agriculture*, 9(10): 223.

34. Wang, Y., Stevanato, P., Yu, L., Zhao, H., Sun, X., Sun, F., Li, J. & Geng, G. 2017. The physiological and metabolic changes in sugar beet seedlings under different levels of salt stress. *Journal of Plant Research*, 130(6): 1079-1093.

35. Wang, Y., Stevanato, P., Lv, C., Li, R. & Geng, G. 2019. Comparative physiological and proteomic analysis of two sugar beet genotypes with contrasting salt tolerance. *Journal of Agricultural and Food Chemistry*, 67(21): 6056-6073.

36. Willenborg, C.J., Gulden, R.H., Johnson, E.N. & Shirtliffe, S.J. 2004. Germination characteristics of polymer-coated canola (*Brassica napus* L.) seeds subjected to moisture stress at different temperatures. *Agronomy Journal*, 96: 786-791.

37. Yadav, N.S., Shukla, P.S., Jha, A., Agarwal, P.K. & Jha, B. 2012. The SbS0S1 gene from the extreme halophyte *Salicornia brachiata* enhances Na+ loading in xylem and confers salt tolerance in transgenic tobacco. *BMC Plant Biology*, 12: 188.

38. Yang, L., Ma, C., Wang, L., Chen, S. & Li, H. 2012. Salt stress induced proteome and transcriptome changes in sugar beet monosomic addition line M14. *Journal of Plant Physiology*, 169: 839-850.

http://dergipark.org.tr/trkjnat
Trakya University Journal of Natural Sciences, 22(2): 263-274, 2021
ISSN 2147-0294, e-ISSN 2528-9691
DOI: 10.23902/trkjnat.969982

Research Article

SENSITIVE DETERMINATION OF 3,4-DIHYDROXY-L-PHENYLALANINE BY A CLOUD FUNNEL MUSHROOM (*Clitocybe nebularis* (Batsch), P. Kumm.) HOMOGENATE-BASED AMPEROMETRIC BIOSENSOR

Engin ASAV

Kırklareli Univesity, Faculty of Health Sciences, Nutrition and Dietetics Department, Kırklareli, TURKEY
engin.asav@klu.edu.tr ORCID: 0000-0002-6232-3388

Cite this article as:

Asav E. 2021. Sensitive determination of 3,4-dihydroxy-l-phenylalanine by a cloud funnel mushroom (*Clitocybe nebularis* (Batsch), P. Kumm.) homogenate-based amperometric biosensor. *Trakya Univ J Nat Sci*, 22(2): 263-274, DOI: 10.23902/trkjnat.969982

Received: 12 July 2021, Accepted: 08 October 2021, Published: 15 October 2021

Abstract: 3,4-dihydroxy-L-phenylalanine (L-DOPA) is one of the precursor molecules for the biosynthesis of neurotransmitters in the brain. Monitoring of L-DOPA levels as a drug or biomolecule in biological fluids is crucial for the treatment of patients suffering from Parkinson's Disease. This study aimed to construct a cloud funnel mushroom (*Clitocybe nebularis* (Batsch), P. Kumm.) tissue homogenate-based biosensor for precise and sensitive detection of L-DOPA in artificial plasma and urine. For this purpose, in the fabrication of the biosensor, tissue homogenate of *C. nebularis* was immobilized into a carbon paste electrode by using graphite, mineral oil, gelatine and glutaraldehyde. The amperometric signals corresponding to 600 s were recorded as response current for each L-DOPA concentration. All amperometric measurements were carried out at -700 mV (versus Ag|AgCl). The present biosensor successfully detected L-DOPA with a linear dynamic range at 2.5-100 µM and Limit of Detection (LOD) value as 0.76 µM, as well as standard deviation as ±0.41 µM and coefficient of variation as 0.82% (n=16). Additionally, the determination of L-DOPA spiked in artificial plasma and urine was carried out successfully. The present work would be the first study that utilized *C. nebularis* tissue as a biosensor component.

Özet: 3,4-dihidroksifenilalanin (L-DOPA), beyinde nörotransmitter sentezi için öncül moleküllerden biridir. Biyolojik sıvılarda, ilaç veya biyomolekül olarak L-DOPA düzeylerinin izlenmesi, Parkinson hastalığına sahip kişilerin tedavi süreci için önemlidir. Bu çalışmanın amacı, sentetik plazma ve idrar örneklerinde L-DOPA molekülünün doğru ve duyarlı bir tayinine yönelik, bulutlu huni mantarı (*Clitocybe nebularis* (Batsch), P. Kumm.) doku homejenatı temelli bir biyosensör sistemi geliştirmektir. Bu bağlamda, biyosensör yapımında, *C. nebularis* doku homojenatı; grafit, mineral yağ, jelatin ve glutaraldehit kullanılarak karbon pasta elektrot içine immobilize edilmişlerdir. 600. saniyeye karşılık gelen amperometrik sinyaller her L-DOPA konsantrasyonu için yanıt akımı olarak kaydedilmiştir. Tüm amperometrik ölçümler -700 mV (vs Ag|AgCl) potansiyelinde gerçekleştirilmiştir. Geliştirilen biyosensör, L-DOPA molekülünü 2,5-100 µM tayin aralığında ve 0,76 µM tayin limitinin yanı sıra ±0,41 µM standart sapma (n= 16). ve %0,82 varyasyon katsayısı ile saptayabilmiştir. Ayrıca sentetik plazma ve idrar içerisine eklenmiş L-DOPA miktarının da tayini başarı ile gerçekleştirilmiştir. Bu çalışma *C. nebularis* dokusunun ilk kez bir biyosensör bileşeni olarak kullanıldığı çalışmadır.

Edited by:
Özkan Danış

Key words:
Clitocybe nebularis
L-DOPA
Carbon-paste electrode
Tissue homogenate
Electrochemistry

Introduction

In the last two decades, the field of electrochemical biosensors has evolved rapidly by means of various types of transducers including amperometric (Ozcan & Aydin 2016), potentiometric (Rasmussen *et al.* 2007), and voltammetric (Li *et al.* 2015) along with bio-components such as tissues (Ozcan & Sagiroglu 2014), enzymes (Davletshina *et al.* 2020), antibodies (Sayikli Şimşek *et al.* 2015), microorganisms (Gao *et al.* 2017) and DNA (Faria & Zucolotto 2019). Electrochemical biosensors offer various advantages over conventional analytical techniques including sensitivity, precision, low cost and portability as well as simplicity of the instrumentation and fast response time (da Silva *et al.* 2017). Hence, biosensor systems are widely used for the detection of several target molecules in the fields of medical diagnosis (Sun *et al.* 2014), bioprocess control (Pontius *et al.* 2020),

environmental analyses (Nomngongo *et al.* 2011), food quality control (Sagiroglu *et al.* 2011) and pharmaceutical analyses (Camargo *et al.* 2020).

In the construction of tissue-based electrochemical biosensors, tissue homogenates from various living organisms such as pigs (Thoppe Rajendran *et al.* 2020), mushrooms (Sezgintürk & Dinçkaya 2012) and plant tissues including banana (Ozcan & Sagiroglu 2010), artichoke (Odaci *et al.* 2004), Myrtle (Ayna & Akyilmaz 2018) are employed for detection of toxins (Sanders *et al.* 2001), drugs (Thoppe Rajendran *et al.* 2020), herbicides (Breton *et al.* 2006) and phenolic compounds such as rutin (Zwirtes de Oliveira *et al.* 2006), epinephrine (Felix *et al.* 2006), caffeic acid (Fernandes *et al.* 2007), catechol (Ozcan & Sagiroglu 2010) and dopamine (Ori *et al.* 2014).

Clitocybe nebularis (Batsch), P. Kumm. known as clouded agaric or cloud funnel mushroom is a well-studied fungus, thanks to the neuroprotective, antioxidant, antimicrobial and cytotoxic properties of its constituents (Kosanić *et al.* 2020). Although *C. nebularis* was reported to have laccase gene (Luis *et al.* 2004), neither determination of laccase activity nor utilization in biosensor construction have not been studied so far.

3,4-dihydroxy-L-phenylalanine (L-DOPA) has great importance for neurobiochemical reactions in the brain since it is a precursor for catecholamines including dopamine, epinephrine and norepinephrine. Due to the ability to pass the blood-brain barrier, L-DOPA specimens are effective drugs for the treatment of Parkinson's Disease (Hormozi-Nezhad *et al.* 2017). In the last two decades, several analytical methods such as HPLC (Kumarathasan & Vincent 2003), LC/MS (César *et al.* 2011), spectrophotometric (Tashkhourian *et al.* 2011), electrochemical (Brunetti *et al.* 2014), colorimetric (Chou *et al.* 2019) were developed for the detection of L-DOPA, owing to the pharmacological importance of L-DOPA. Amperometry is one of the widely used electrochemical methods in tissue-based biosensors as well as in determination of L-DOPA, since it is easy to apply, inexpensive and allows simultaneous monitoring of responses (Brunetti *et al.* 2014, Sandeep *et al.* 2018, Timur *et al.* 2004).

The aim of our study was the development of a simply constructed *C. nebularis* tissue homogenate-based biosensor, which could detect accurately and sensitively L-DOPA in artificial plasma and urine. Therewithal, the determination of laccase activity of *C. nebularis* by using the ABTS method would be accomplished for the first time.

Materials and Methods

Materials and Reagents

Graphite, mineral oil, 3,4-dihydroxy-L-phenylalanine (L-DOPA), 2,2′-azinobis[3-ethylbenzothiazoline-6-sulfonic acid], diammonium salt (ABTS), bovine serum albumin (BSA) and all other chemicals were purchased from Sigma-Aldrich (St. Louis, MO, USA). In all experiments, measurements and preparation of the solutions, except ABTS prepared in 100 mM citrate buffer at pH 4.0, were carried out in 50 mM phosphate buffer at pH 7.0. The cloud funnel mushroom was collected from Istranca Mountains (Kırklareli-Turkey) in November 2019 and stored at -80°C until use. The commercial drug specimens of L-DOPA named Madopar® containing 100 mg L-DOPA and Dopalevo® containing 100 mg L-DOPA were purchased from a local pharmacy. The artificial serum solution was prepared in a 50 mM phosphate buffer system at pH 7.5 by adding 2.5 mM urea, 0.1% human serum albumin and 4.7 mM (D +)-glucose as well as serum electrolytes including 4.5 mM KCl, 5 mM $CaCl_2$, 145 mM NaCl. The artificial serum solution was used without any dilution. Artificial human urine was prepared in a 50 mM phosphate buffer system at pH 6.5 by addition of 1.49 mM uric acid, 2.45 mM sodium citrate, 7.79 mM creatinine, 249.75 mM urea, 0.19 mM potassium oxalate, 23.67 mM ammonium chloride along with 11.97 mM Na_2SO_4, 4.39 mM $MgSO_4$, 1.66 mM $CaCl_2$, 30.95 mM KCl and 30.05 mM NaCl. This method was described in detail by Sarigul *et al.* (2019).

Apparatus

All electrodes of the three-electrode system including a carbon-paste working electrode, Pt wire as counter electrode and Ag/AgCl as reference electrode were purchased from BASi® Corporate (Indiana, USA). Ag/AgCl reference electrode was stored in 3 M KCl solution for saturation until usage. A PC-controlled potentiostat, PalmSens3®, along with PSTrace® software, which was used in all electrochemical experiments were purchased from PalmSens BV (Utrecht, Netherlands). A Potter-Elvehjem homogenizer purchased from İnterlab (İstanbul, Turkey) was used for homogenization of the mushrooms. A spectrophotometer purchased from ThermoFisher Scientific (Renfrewshire, UK) was used for protein and activity assays. A circulating thermostat named BM302 employed for thermostable conditions in all experiments was purchased from Nüve (Ankara, Turkey).

Determination of Biochemical Properties of Clitocybe nebularis

The isolation of laccase from *C. nebularis* was carried out by the modification of the method described before (Zhang *et al.* 2010, Tuncay & Yagar 2020). For this purpose, washed and dried mushrooms were homogenized by using a Potter-Elvehjem homogenizer containing 0.15 M NaCl. Then, the homogenate was centrifuged at 8000 rpm for 15 min. The resultant supernatant was used as the enzyme source for spectrophotometric measurements.

Protein assays via BSA and Coomassie Brilliant Blue G-250 were carried out according to the Standard Bradford method (Bradford 1976) for determination of the protein amounts of *C. nebularis* tissue homogenates.

A modified version of the ABTS method described by Shin & Lee (2000) was used for determination of laccase activity of tissue homogenates. The absorbance values at 420 nm and 25°C of the assay mixture containing tissue homogenates (0.1 mL) and ABTS (0.9 mL) were

monitored for 3 minutes. The data from the measurements that occurred at time intervals of 0, 30, 60, 90, 120, 180 and 240 s were recorded for calculation of activity. One unit of enzyme activity was defined as the amount of enzyme required to oxidize 1 µmol of ABTS per min. The laccase activity of *C. nebularis* tissue homogenates was calculated according to the equitation of the study of Baltierra-Trejo *et al.* (2015). The laccase activity equitation was given below where,

ΔA: Final absorbance - initial absorbance

Vt: total volume (mL)

Vs: volume of tissue homogenates (mL)

ε: coefficient of molar extinction of ABTS (36,000 L mol^{-1} cm^{-1} at 420 nm)

$$Laccase\ activity\ (U\ L^{-1}) = \frac{\Delta A \times Vt\ (mL) \times 10^6}{\varepsilon \times Vs\ (mL) \times t\ (\text{min.})} \qquad (1)$$

The Biosensor Construction

Prior to use, the carbon paste electrode was sonicated in absolute ethanol to remove physically absorbed particles in the cavity of the electrode. The construction of the biosensor was carried out by the modification of the method described before (Kozan *et al*. 2007). For this purpose, 120 mg of graphite powder and 140 µL (60 mg) of mineral oil were mixed for 10 minutes to obtain a homogenous carbon paste. Subsequently, 30 µL aliquot of *C. nebularis* tissue homogenate, which was obtained by using a Potter-Elvehjem homogenizer containing 0.15 M NaCl, were strewed thoroughly into carbon paste by mixing the slurry. Then, the tissue homogenate modified carbon paste was carefully and firmly packed into the cavity of the electrode. After the electrode surface was smoothed with a weighing paper, 25 µL of gelatine at 2.5 mg/mL concentration was dropped and dispersed onto the modified electrode as a protective layer. After the incubation of the gelatine-modified electrode at +4°C for 30 minutes, the electrode was dipped in the 2.5% glutaraldehyde solution as a cross-linker prepared in 0.1 M PBS at pH 7.5. Finally, for a well-built cross-linking, the electrode was allowed to incubate for 15 minutes in this solution. Then, the biosensor was rinsed carefully with distilled water. The construction of the *C. nebularis* tissue homogenate-based biosensor was schematically shown in Fig. 1.

The Principle of the Measurements

The principle of the measurements was based on monitoring the amperometric responses of the biosensor for the oxidation of L-DOPA to dopaquinone by *C. nebularis* tissue. The amperometric signals were measured by using the three-electrode system at a constant temperature (35°C) and in 20 mL of 50.0 mM PBS at pH 7.5 under the operating potential of -700 mV (versus Ag|AgCl), which was the reduction potential of oxygen (Ozcan & Sagiroglu 2014). For each measurement, the electrode was allowed to equilibrate for 100 s to the signal to reach a steady-state that was recorded as the baseline current.

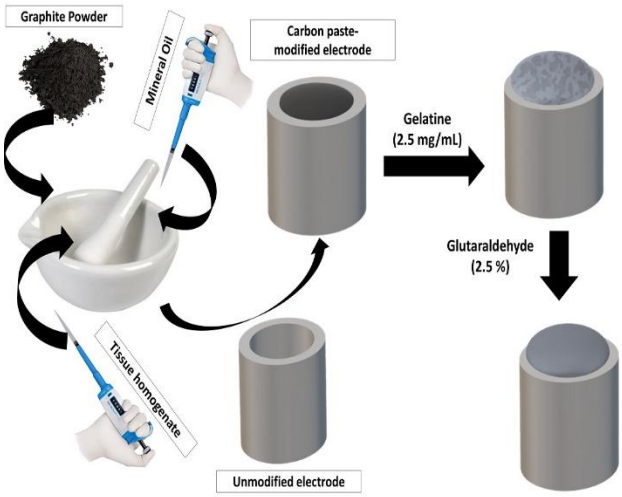

Fig. 1. Schematic presentation of construction of tissue homogenate-based biosensor.

The amperometric signals corresponding to 600 s were recorded as response current for each L-DOPA concentration, which was added separately in a freshened electrolyte solution. The differences between the baseline current values and response current values were calculated and denoted as ΔI. After each measurement, the electrode was allowed to regenerate in PBS for 3 min.

Analyses in Artificial Plasma and Urine

Artificial plasma and urine were prepared as described above. Both of these solutions were used as an electrolyte solution instead of PBS in the measurement cell. Moreover, L-DOPA and commercial drugs named Madopar® and Dopalevo® were spiked in these solutions separately for evaluations of the analytical performance of the proposed biosensor. Tablets of each commercial drug were dissolved in 10 mL PBS at pH 7.5 by incubating in a sonicating bath for 30 min. Then, the drug samples were filtered and centrifuged at 6000 rpm for 10 min to obtain a bright and homogenous drug solution. The spectrophotometric method for the detection of L-DOPA was based on the measurement of absorbance levels at 280 nm (Karpińska *et al.* 2005). An L-DOPA calibration curve with a dynamic range of 10-200 µM was plotted for each reaction medium including PBS, artificial plasma and urine. In case the absorbance was higher than the detection range, a dilution was applied to drug solutions. Furthermore, for drug analyses, another L-DOPA calibration curve with a linear range of 10-200 µM was plotted by using the present tissue homogenate-based biosensor. Concentrations of the drug solutions were not properly calculated, owing to the dissociation problem of the drug tablets. Thus, a spectrophotometric method was employed to determine the exact concentration of the drug solutions. Hence, in biosensor experiments, drug solutions were diluted with PBS, artificial plasma or urine by evaluating the concentrations detected via spectrophotometry. Then, the L-DOPA levels of drug solutions were determined for comparison with the present biosensor.

Statistical Analysis

The Limit of Detection (LOD) representing the lowest detected quantity of L-DOPA biosensor was determined via the equation of $3.3 \times Sd/m$. *Sd* and *m* which represent the standard deviation of the intercepts and slope of the calibration curve, respectively, were calculated by using the regression module of Microsoft Excel® software. For evaluation of the repeatability of the parameters, ΔI values measured for 16 separate addition of L-DOPA at 50.0 µM were replaced as "y" in the equation of calibration curve.

The mean values, standard deviations and coefficients of variation of the biosensor were calculated by using Microsoft Excel® software.

Results

Biochemical Properties of Clitocybe nebularis

In total protein assay via the standard method of Bradford, the protein concentration of *C. nebularis* was determined as 0.421 mg/mL. The laccase activity determined via the ABTS method was calculated as 144.54 U/L according to the equation given above.

Optimization of the Biosensor Fabrication

Optimization experiments of the immobilization steps had great importance to evaluate effective detection characteristics for the biosensor constructed. For this purpose, parameters including the amount of gelatine, the amount of mushroom tissue and the volume of homogenate as well as pH and temperature were optimized.

The concentration of gelatin directly affected the signal rate, since gelatine acted as a slight barrier for oxygen and L-DOPA transport. However, the protection and stability of the electrode surface were provided by the gelatine layer. Thus, the optimization of the concentration of gelatine was one of the crucial steps for biosensor construction. For the determination of optimum gelatine amount, four different electrodes were fabricated by using gelatine at different concentrations as 1.0 mg/mL, 2.5 mg/mL, 5 mg/mL and 10 mg/mL. Calibration curves shown in Fig. 2 for each concentration of gelatine were plotted between ΔI values and L-DOPA concentrations.

The amount of mushroom tissue for the preparation of tissue homogenate was an important parameter for the catalytic reaction of L-DOPA and indirectly the signal rate. Hence, tissue homogenates coalesced with carbon paste were prepared by using different amounts of *C. nebularis* tissue including 50 mg, 100 mg, 200 mg and 400 mg. Calibration curves for each amount of *C. nebularis* tissue plotted between ΔI values and L-DOPA concentrations were shown in Fig. 3.

Determination of the optimum volume of tissue homogenate coalescing to carbon paste is a critical step to obtain a homogenous dispersion of tissue in the carbon paste stuffing the electrode cavity. For this purpose, three different carbon pastes consisted of tissue homogenate at different volumes including 15 µL, 30 µL and 60 µL were prepared and used for biosensor construction. Calibration curves obtained from these biosensors are shown in Fig. 4.

For the determination of optimum pH of the tissue homogenate-based biosensor, different buffer systems including citrate buffer for pH values between 4.5 and 5.5 along with phosphate buffer for pH values between 6.0 and 8.0 were prepared and used in the reaction cell. The measurements and regenerations were carried out separately in these seven buffer systems by using the same biosensor. In the optimum pH experiments, signal levels corresponding to L-DOPA at 5 µM concentrations for each buffer system were monitored and recorded. Relative activity calculated by using biosensor responses at different pH levels is shown in Fig. 5.

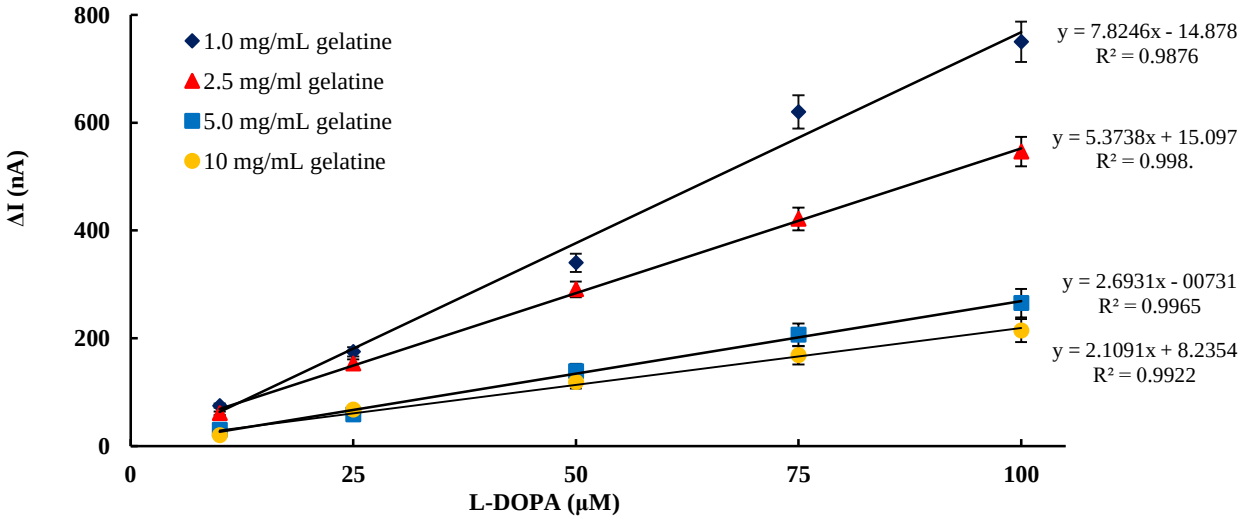

Fig. 2. Calibration curves obtained from the biosensors contained different concentrations of gelatine dissolved in PBS.

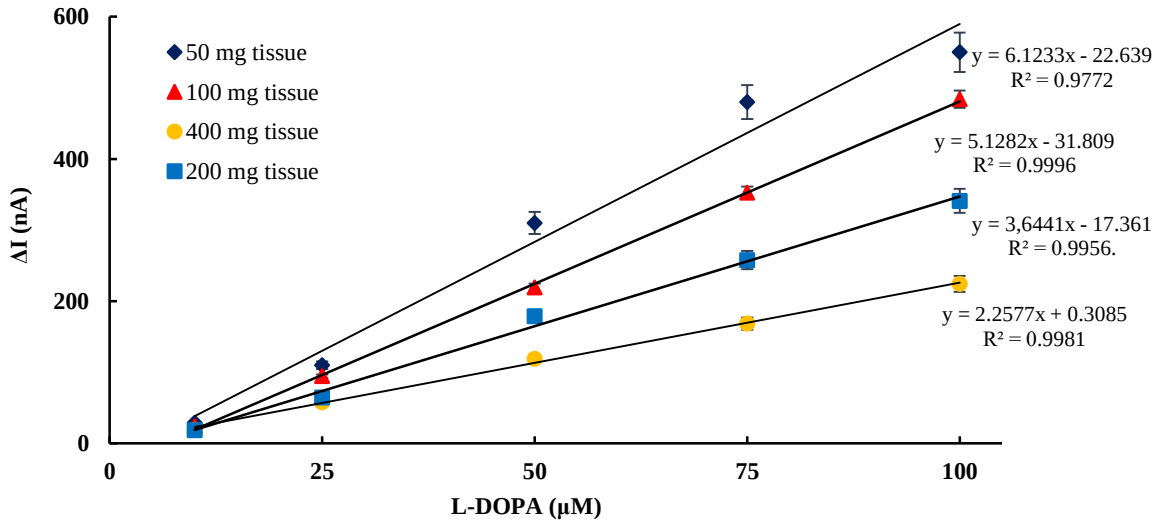

Fig. 3. Calibration curves were obtained from the biosensors prepared with different amounts of *C. nebularis* tissue.

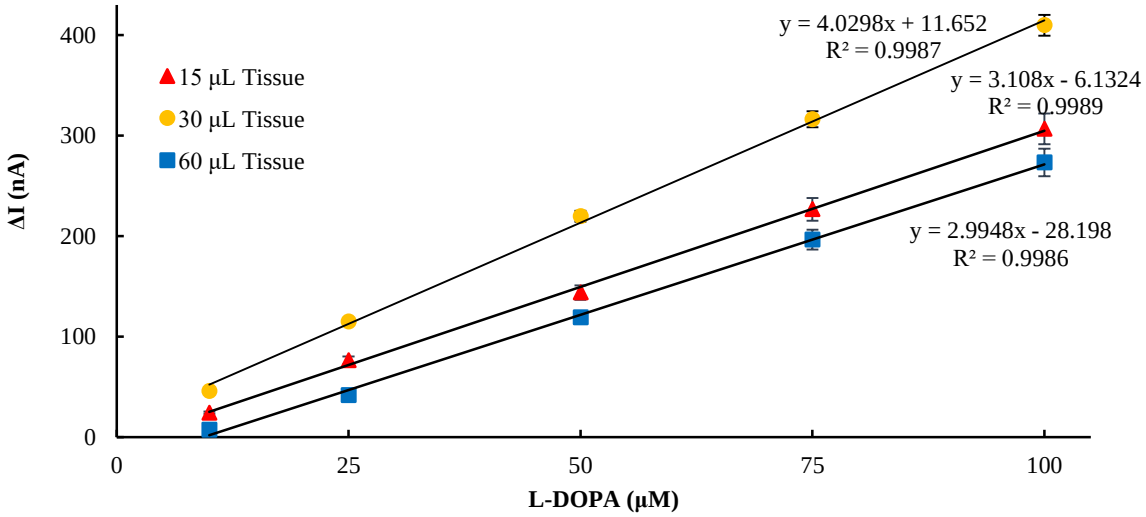

Fig. 4. Calibration curves obtained from the biosensors contained different volumes of tissue homogenate.

For the determination of optimum temperature, the measurements and regenerations were carried out in different temperature conditions including 15°C, 20°C, 25°C, 30°C, 35°C, 40°C and 45°C. In the optimum temperature experiments, biosensor responses corresponding to L-DOPA at 5 µM concentrations for each degree were monitored and recorded. Relative activity calculated by using biosensor responses at different temperatures is shown in Fig. 6.

Linear range

For the determination of linear range, the limit of detection (LOD) and sensitivity of the present biosensor, a biosensor was fabricated by using optimum conditions determined before. Then, a calibration curve shown in Fig. 7 was plotted between ΔI values and L-DOPA concentrations at 2.5 µM, 5.0 µM, 10 µM, 25 µM, 50 µM, 75 µM and 100 µM.

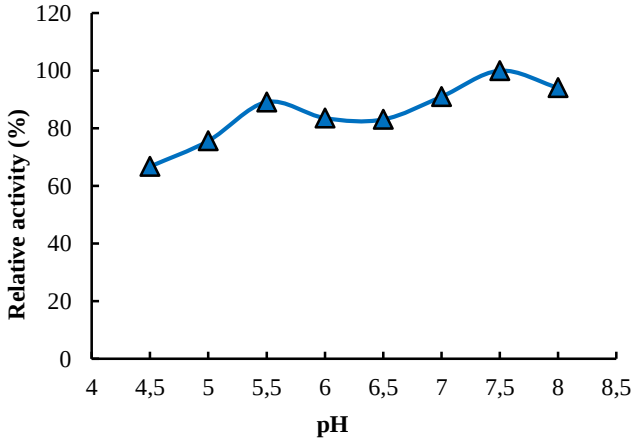

Fig. 5. The effect of pH on biosensor responses.

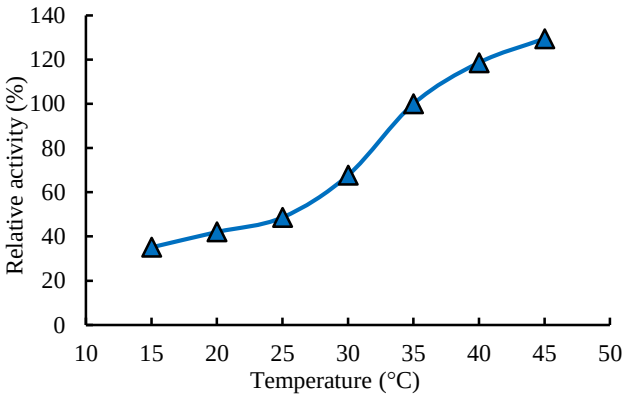

Fig. 6. The effect of temperature on the biosensor responses.

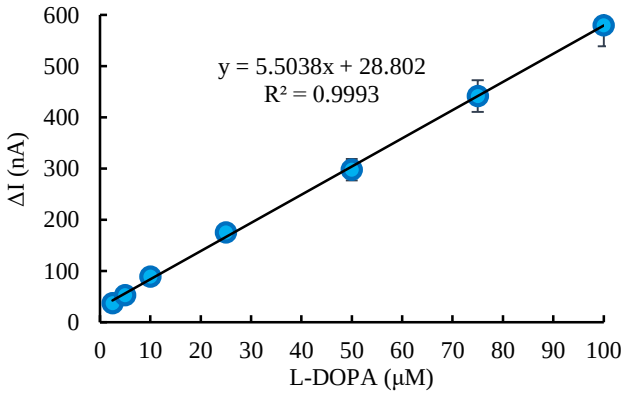

Fig. 7. The calibration curve of *C. nebularis* tissue homogenate-based biosensor.

The LOD value of the proposed biosensor obtained from data of the calibration curve was determined as 0.76 μM for L-DOPA. Moreover, the slope of the calibration curve representing the sensitivity of the L-DOPA biosensor was also determined as 5.5038 $nA\mu M^{-1}$.

Correlations between L-DOPA concentrations and total charge values were also investigated. For this purpose, a calibration curve was plotted by using total charge value measured at 800 s by changing L-DOPA concentrations using 25 μM, 50 μM, 75 μM and 100 μM. The LOD value was also calculated for this detection method by using the calibration curve shown in Fig. 8.

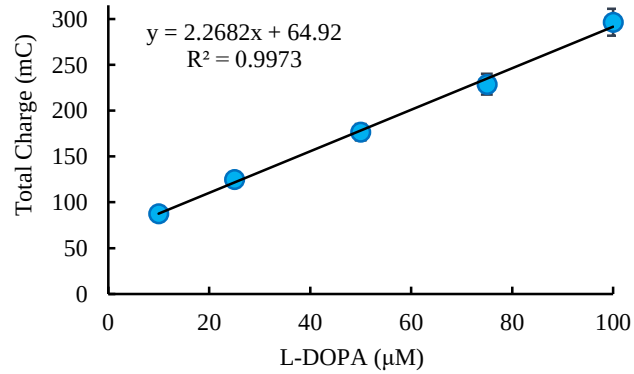

Fig. 8. Calibration curve of the present biosensor for L-DOPA plotted by using total charge values.

Analytical performance of the tissue homogenate-based biosensor, for consecutive additions of L-DOPA, was also examined. The biosensor responses corresponding to different L-DOPA concentrations as 10 μM, 25 μM, 50 μM, 75 μM, 100 μM, 150 μM and 200 μM were shown in Fig. 9. By using these responses, a calibration curve shown in Fig. 10 was plotted between L-DOPA concentrations and cumulative ΔI values, which were calculated by using the differences between the baseline current value at 100 s and the current value (I) measured every 600 s after each L-DOPA addition.

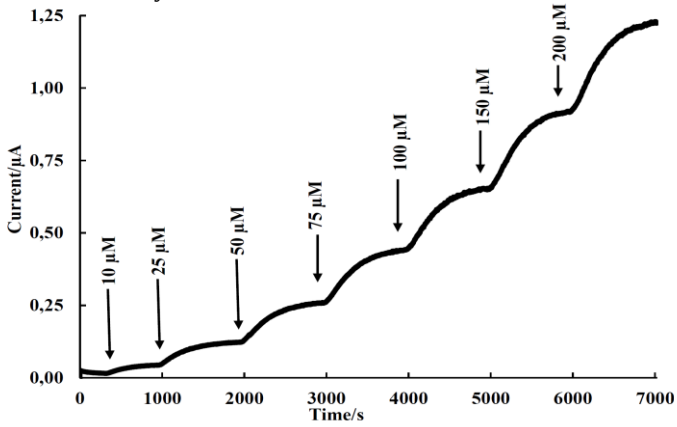

Fig. 9. Biosensor responses for consecutive addition of L-DOPA at different concentrations.

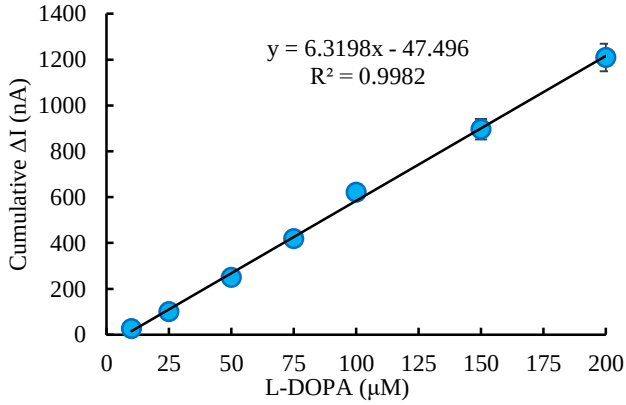

Fig. 10. Calibration curve of the present biosensor plotted by evaluating data from Fig. 9.

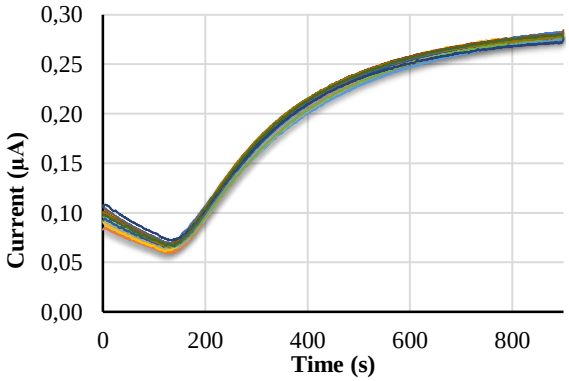

Fig. 11. Biosensor responses for 12 multiple separate measurements for 50.0 μM L-DOPA.

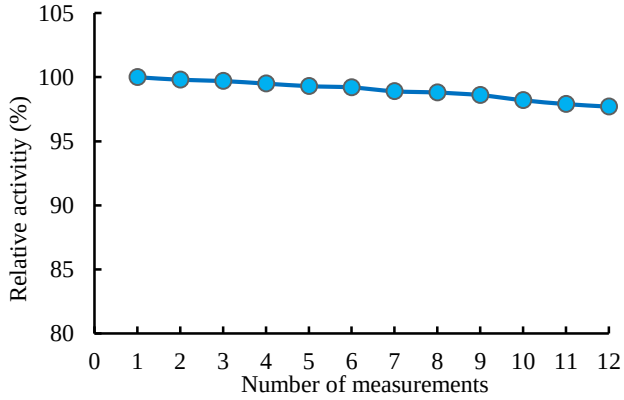

Fig. 12. Operational stability of the biosensor.

Repeatability and operational stability of the biosensor

Repeatability referring to accuracy, precision and standard error is a crucial parameter for biosensor systems. For evaluation of the repeatability parameters, ΔI values measured for 16 separate addition of L-DOPA at 50.0 µM, were replaced as "y" in the equation of calibration curve. The mean value, standard deviation and coefficient of variation of the biosensor were determined as 50.01 µM, ±0.41 µM and 0.82% (n = 16), respectively.

Operational stability that represents the durability of the biosensor to multiple measurements were also studied. For this purpose, 12 separate measurements without regeneration for 50.0 µM L-DOPA were carried out. The biosensor responses and calculated relative activity values for each measurement were shown in Figs 11 and 12, respectively. As can be seen in the figures, the tissue homogenate-based biosensor had good stability for multiple measurements with reasonable precision.

Application to artificial human plasma and urine samples

The monitoring of L-DOPA drugs in urine and plasma has reasonable importance for patients with Parkinson's disease, who are treated with L-DOPA drugs. Evaluation of the analytical performance of the tissue homogenate-based biosensor in physiological fluids is a crucial parameter representing the potential utility of the biosensor in clinical diagnosis. Thus, the analytical performance of the present biosensor was tested in artificial plasma and urine samples. Moreover, the proposed biosensor was examined for the detection of L-DOPA amounts in commercial drugs named Dopalevo® and Madopar®. The dissolving of L-DOPA and drugs as well as all of the measurements were carried out by using artificial plasma and urine instead of PBS. By using the reagent L-DOPA, calibration curves with a detection range between 10-200 µM were plotted for each electrolyte solution including PBS, artificial plasma and urine. R^2 value and LOD values of these calibration curves were calculated as 0.9990, 0.9984, 0.9986 and 2.05 µM, 2.63 µM, 2.46 µM, respectively. In order to determine the concentrations of commercial drugs by using the proposed biosensor, 500 µL of drug solutions were spiked into the reaction cell containing artificial plasma or urine. Concentrations of drug solutions were not curvaceously calculated, owing to the dissociation issue of drug tablets. Thus, a spectrophotometric method was employed to determine the exact concentration of the drug solutions. Hence, drug solutions were diluted with PBS, artificial plasma or urine by evaluating the concentrations detected via spectrophotometry. The biosensor responses and spectrophotometric analyzes were compared in Table 1.

Table 1. The analytical performance of the tissue homogenate-based biosensor in artificial plasma and urine (n=3).

Spiked Samples	L-DOPA measured by spectrophotometer (µM)	L-DOPA measured by present biosensor (µM) (n=3)	Recovery (%)	Bias (%)
L-DOPA in artificial plasma	65.11	65.91 ± 0.53	101.22	1.22
L-DOPA in artificial urine	65.25	67.02 ± 0.51	102.71	2.71
Dopalevo® in artificial plasma	92.91	95.23 ± 0.86	102.50	2.50
Dopalevo® in artificial urine	141.56	146.37 ± 1.39	103.41	3.41
Dopalevo® in PBS	30.09	30.38 ± 0.28	100.98	0.98
Madopar® in artificial plasma	91.43	94.04 ± 0.75	102.86	2.86
Madopar® in artificial urine	144.32	149.70 ± 1.45	103.73	3.73
Madopar® in PBS	56.15	56.73 ± 0.46	101.03	1.03

Discussion

It was reported that some other mushrooms such as *Agaricus bisporus* (J.E. Lange) Imbach, *Coprinus comatus* (O.F. Müller) Persoon, *Ganoderma tsugae* (Murrill), *Lentinellus ursinus* (Fries) Kühner, *Russula delica* (Fries) and *Trametes versicolor* (L Linnaeus) Lloyd have protein concentrations as 0.509 mg/mL, 0.456 mg/mL, 0.316 mg/mL, 0.409 mg/mL, 0.456 mg/mL and 0.409 mg/mL, respectively (Pandey & Budhathoki 2007) similar to *Clitocybe nebularis*, which was used in the present study. Baltierra-Trejo *et al.* (2015) explained in detail and emphasized that there were a lot of identified inconsistencies in values, units and calculation formulas of the laccase activity in the literature. Hence, proper comparisons of laccase activities determined by the ABTS method could not be accomplished.

It is clearly seen in Fig. 2 that, since the concentration of the gelatine could affect the transfer of oxygen and transportation of L-DOPA to the electrode surface, biosensor signals were decreased by increasing gelatine concentrations. Even though the biosensor containing 1.0 mg/mL gelatine had the highest signals, the linearity of this biosensor was worse than the biosensor that contained 2.5 mg/mL gelatine. It was observed that rigidity and thickness of the gelatine layer could not be stable in the case of 1.0 mg/mL gelatine concentration. Hence, probable desertion of tissue from electrode surface to reaction media could occur. Since the biosensor containing 2.5 mg/mL gelatine had the best linearity and stability, 2.5 mg/mL was selected as the optimum concentration for gelatine.

Increased *C. nebularis* tissue was expected to cause more L-DOPA conversion that increased responses of the biosensor. However, as it is seen in Fig. 3, the highest signals for L-DOPA detection were obtained from the biosensor prepared by using 50 mg tissue. This could be a result of the homogenization process applied since homogenization by utilizing a Potter-Elvehjem homogenizer consisted of a small volume and short time process, an increase in tissue amount brought about the problems including dispersion, squeezing and adhesion of tissue in the homogenizer. It was observed that in the case of tissue homogenates containing 200 mg and 400 mg tissue could not be properly smashed, dispersed and squeezed in the homogenizer. Hence, the yield of tissue homogenization, as well as tissue amount coalescing with carbon paste was decreased. Although the biosensor prepared with 50 mg of tissue had the highest signals, it had the lowest R^2 value responding to the linearity of the calibration curve. Thus, considering all results in terms of linearity and biosensor response, 100 mg tissue was selected as the optimum tissue amount for homogenization.

Since carbon paste had a hydrophobic composition without tissue homogenate, an increase in the volume of tissue homogenate could cause a problem for homogenous dispersion of mushroom tissue into the depth of the carbon paste. Hence, the lowest biosensor responses could be obtained from the biosensor fabricated by using 60 μL of tissue homogenate, although its linearity was higher than the other two biosensors. Additionally, in the preparation of carbon paste, when mushroom tissue homogenate volume was higher than 30 μL, aggregate formation on the plate was observed. In case that the volume of tissue homogenate was 15 μL, although a well-built coalescing between tissue and carbon paste occurred, the enzymatic conversion of L-DOPA was inadequate for higher signals. As seen in Fig. 4, the biosensor fabricated by using 30 μL of tissue homogenate had better linearity and higher signal rate than the other biosensors. Thus, the optimum volume of *C. nebularis* tissue homogenate was determined as 30 μL for L-DOPA detection.

In tissue homogenate, many types of enzymes such as laccase, tyrosinase or polyphenol oxidase could convert L-DOPA to dopaquinone. Thus, as seen in Fig. 5, the proposed tissue homogenate-based biosensor worked well by the activity up to 80% and reached to optimum value at pH 7.5. These results were expected results for a tissue homogenate-based biosensor since similar plots were obtained by other tissue-based biosensors (Leite *et al.* 2003a, Sezgintürk *et al.* 2005, Felix *et al.* 2006, Liu *et al.* 2010, Narang *et al.* 2011, Rahimi-Mohseni *et al.* 2018, Sandeep *et al.* 2018). Moreover, the optimum pH depended on both the presence of the catalyzing enzymes and the solubility of the substrate at these pH values. In this case, the solubility of L-DOPA increased slowly at around neutral pH, owing to its charged groups (Ali *et al.* 2014). Furthermore, these properly-working pH scales of the proposed biosensor facilitated the detection of L-DOPA in human samples at different pH values such as plasma at pH 7.4 and urine at pH 6.0. Finally, since the isoelectric point of L-DOPA is 5.2, biosensor responses at pH 5.0 and pH 5.5 might be decreased.

In optimum temperature experiments, although a tendency of increase in the activity was observed at higher degrees, 35°C was selected as the optimum temperature due to the low stability of gelatine at temperatures higher than 35°C (Odaci *et al.* 2004, Topçu *et al.* 2004, Sezgintürk & Dinçkaya 2005, Ozcan & Sagiroglu 2010).

As seen in Fig. 7, the calibration curve had good R^2 representing linearity and a wide detection range, from 2.5 μM to 100 μM, which includes the concentrations of L-DOPA levels in plasma and urine for both healthy and people using L-DOPA drugs determined before (Baranowska & Plonka 2008).

Since an increase in the current caused enhancing the migration of electrons to the electrode surface, the signal was in a tendency of increasing by the addition of L-DOPA. The LOD value of this method evaluated by using the same calculation method discussed above was determined as 2.73 μM. The linearity as R^2 value and the sensitivity of this curve along with LOD value showed that total charge could be promisingly utilized for the quantification of target molecules.

Table 2. Comparison of the L-DOPA biosensors on literature.

Biocomponent	Analytical Method	Detection Range (µM)	Linearity (R^2)	LOD (µM)	Ref.
Isolated laccase from *Pleurotus ostreatus*	Differential Pulse Voltammetry	6.7-70	N/A	0.24	(Leite *et al.* 2003b)
Extracted tyrosinase from *Amorphophallus campanulatus*	Optical	10-1000	0.99	3.0	(Saini *et al.* 2014)
Isolated laccase from *Trametes versicolor*	Amperometry	2.0-20	0.9898	N/A	(Timur *et al.* 2004)
Commercial laccase from *Cerrena unicolor*	Amperometry	1-40	0.999	0.49	(Jarosz-Wilkołazka *et al.* 2005)
Purified laccase from *Trametes versicolor*	Amperometry	1-20	0.9996	0.65	(Haghighi *et al.* 2003)
Commercial tyrosinase from mushroom	Amperometry	0.8-22	0.9907	2.5	(Brunetti *et al.* 2014)
Extracted polyphenol oxidase from *Manilkara Zapota*	Differential Pulse Voltammetry	2-140	0.933	1.85	(Sandeep *et al.* 2018)
Extracted polyphenol oxidase from banana fruit	Amperometry	0.2-400	0.994	0.2	(Narang *et al.* 2011)
Tissue homogenate of *Clitocybe nebularis*	Amperometry	2.5-100	0.9993	0.76	Present study

In Table 2, the present *C. nebularis* tissue-based biosensor was compared to other biosensors for L-DOPA detection in parameters including linear range, LOD and linearity.

Although the biosensors (Haghighi *et al.* 2003, Leite *et al.* 2003b, Jarosz-Wilkołazka *et al.* 2005) have lower LOD values than the proposed biosensor with similar linearity, the detection ranges of these biosensors were narrower than our biosensor had. Even though the biosensors (Saini *et al.* 2014, Sandeep *et al.* 2018) could detect L-DOPA with a wide range, the present biosensor showed a better correlation and had a lower LOD value. Moreover, the linearity, LOD value and detection range of the present biosensor were reasonably preferable to the biosensors (Timur *et al.* 2004, Brunetti *et al.* 2014). The biosensor of Narang *et al.* (2011) has better results than our work, however, it had a more complicated construction process and more expensive materials for the fabrication of the biosensor. Since the transition of L-DOPA and oxygen was a usual challenge for tissue homogenate-based biosensors, all of these L-DOPA biosensors having purified, commercial or extracted enzymes had better response time than the present work. However, the response time of the present biosensor as 600 s was similar to other tissue homogenate-based biosensors in the literature (Sezgintürk & Dinçkaya 2003, 2004, Silva *et al.* 2014). Furthermore, as seen in Table 2, although other biosensors employed different forms of enzymes such as isolated, purified, commercial or extracted enzymes, their analytical performances were not much better than our simply-constructed tissue homogenate-based biosensor. By the use of tissue homogenate-based biosensors, time-consuming and complex processes such as enzyme extraction, isolation and purification are not required. Finally, proposed *C. nebularis* tissue homogenate-based biosensor not only detected L-DOPA molecule consistently, sensitively and accurately but also offered an easy-to-apply and inexpensive alternative to those reported in literature.

The calibration curve shown in Fig. 10 facilitated the monitoring of higher L-DOPA levels with good linearity and sensitivity. Furthermore, the performance of the proposed biosensor in consecutive L-DOPA additions showed that it could work properly with flow-injection systems.

It can be deduced from the results of repeatability experiments that the present biosensor which had better values than the other biosensors (Timur *et al.* 2004, Chawla *et al.* 2010), could detect L-DOPA precisely and reliably.

It is obviously seen in Table 1 that the proposed biosensor had a good performance at analyses of spiked L-DOPA and commercial drugs in all of the measurement media. Since the artificial urine containing uric acid and sulfates might interfere with the signal, a little increase in biosensor responses caused a tiny deviation for L-DOPA detection in artificial urine. Moreover, some constituents of commercial L-DOPA drugs could interfere with the signal.

Conclusion

A simply constructed and inexpensive *C. nebularis* tissue homogenate-based amperometric biosensor was developed for accurate and sensitive detection of L-DOPA. The proposed biosensor would be the first biosensor, which contained a mushroom of *Clitocybe sp.* in the literature. In the fabrication of the biosensor, 30 µL of tissue homogenate was immobilized into the cavity of the carbon-paste electrode by using 120 mg of graphite powder, 140 µL (60 mg) of mineral oil, 2.5 mg/mL of gelatine and 2.5% of glutaraldehyde. The present biosensor detected L-DOPA with a linear dynamic range at 2.5-100 µM and LOD value as 0.76 µM, as well as standard deviation as ±0.41 µM and coefficient of variation as 0.82% (n = 16). It can be noticed from the results that the proposed biosensor showed good performance in terms of the means of precision, linearity and sensitivity for L-DOPA in PBS. Moreover, the determination of L-DOPA spiked as both drug and chemical into artificial biological fluids was accomplished with a decent recovery rate. These results indicate that the biosensor could be utilized for monitoring of L-DOPA levels of patients suffering from Parkinson's disease. Finally, the laccase activity of *C. nebularis* was observed for the first time by using the spectrophotometric ABTS method.

Ethics Committee Approval: Since the article does not contain any studies with human or animal subject, its approval to the ethics committee was not required.

Conflict of Interest: The author have no conflicts of interest to declare.

Funding: The author declared that this study has received no financial support.

References

1. Ali, M., Barman, K., Jasimuddin, S. & Ghosh, S.K. 2014. Fluid interface-mediated nanoparticle membrane as an electrochemical sensor. *RSC Advances*, 4(106): 61404-61408. https://doi.org/10.1039/c4ra12149j

2. Ayna, A. & Akyilmaz, E. 2018. Development of a biosensor based on myrtle (*Myrtus communis* L.) tissue homogenate for voltammetric determination of epinephrine. *Hacettepe Journal of Biology and Chemistry*, 46(3): 321-328. https://doi.org/10.15671/HJBC.2018.240

3. Baltierra-Trejo, E., Márquez-Benavides, L. & Sánchez-Yáñez, J.M. 2015. Inconsistencies and ambiguities in calculating enzyme activity: The case of laccase. *Journal of Microbiological Methods*, 119: 126-131. https://doi.org/10.1016/j.mimet.2015.10.007

4. Baranowska, I. & Plonka, J. 2008. Determination of levodopa and biogenic amines in urine samples using high-performance liquid chromatography. *Journal of Chromatographic Science*, 46(1): 30-34. https://doi.org/10.1093/chromsci/46.1.30

5. Bradford, M.M. 1976. A rapid and sensitive method for the quantitation of microgram quantities of protein utilizing the principle of protein-dye binding. *Analytical Biochemistry*, 72(1-2): 248-254. https://doi.org/10.1016/0003-2697(76)90527-3

6. Breton, F., Euzet, P., Piletsky, S.A., Giardi, M.T. & Rouillon, R. 2006. Integration of photosynthetic biosensor with molecularly imprinted polymer-based solid phase extraction cartridge. *Analytica Chimica Acta*, 569(12): 50-57. https://doi.org/10.1016/j.aca.2006.03.086

7. Brunetti, B., Valdés-Ramírez, G., Litvan, I. & Wang, J. 2014. A disposable electrochemical biosensor for L-DOPA determination in undiluted human serum. *Electrochemistry Communications*, 48: 28-31. https://doi.org/10.1016/j.elecom.2014.08.007

8. Camargo, J.R., Andreotti, I.A.A., Kalinke, C., Henrique, J.M., Bonacin, J.A. & Janegitz, B.C. 2020. Waterproof paper as a new substrate to construct a disposable sensor for the electrochemical determination of paracetamol and melatonin. *Talanta*, 208: 120458. https://doi.org/10.1016/j.talanta.2019.120458

9. César, I.C., Byrro, R.M.D., Santana e Silva Cardoso, F.F., Mundim, I.M., Souza Teixeira, L., Gomes, S.A., Bonfim, R.R. & Pianetti, G.A. 2011. Development and validation of a high-performance liquid chromatography-electrospray ionization-MS/MS method for the simultaneous quantitation of levodopa and carbidopa in human plasma. *Journal of Mass Spectrometry*, 46(9): 943-948. https://doi.org/10.1002/jms.1973

10. Chawla, S., Narang, J. & Pundir, C.S. 2010. An amperometric polyphenol biosensor based on polyvinyl chloride membrane. *Analytical Methods*, 2(8): 1106-1111. https://doi.org/10.1039/c0ay00165a

11. Chou, Y.C., Shih, C.I., Chiang, C.C., Hsu, C.H. & Yeh, Y.C. 2019. Reagent-free DOPA-dioxygenase colorimetric biosensor for selective detection of L-DOPA. *Sensors and Actuators, B: Chemical*, 297: 126717. https://doi.org/10.1016/j.snb.2019.126717

12. da Silva, E.T.S.G., Souto, D.E.P., Barragan, J.T.C., de F. Giarola, J., de Moraes, A.C.M. & Kubota, L.T. 2017. Electrochemical biosensors in point-of-care devices: recent advances and future trends. *ChemElectroChem*, 4(4): 778-794. https://doi.org/10.1002/CELC.201600758

13. Davletshina, R., Ivanov, A., Shamagsumova, R., Evtugyn, V. & Evtugyn, G. 2020. Electrochemical biosensor based on polyelectrolyte complexes with dendrimer for the determination of reversible inhibitors of acetylcholinesterase. *Analytical Letters*, 1-20. https://doi.org/10.1080/00032719.2020.1821700

14. Faria, H.A.M. & Zucolotto, V. 2019. Label-free electrochemical DNA biosensor for zika virus identification. *Biosensors and Bioelectronics*, 131: 149-155. https://doi.org/10.1016/j.bios.2019.02.018

15. Felix, F.S., Yamashita, M. & Angnes, L. 2006. Epinephrine quantification in pharmaceutical formulations utilizing plant tissue biosensors. *Biosensors and Bioelectronics*, 21(12): 2283-2289. https://doi.org/10.1016/j.bios.2005.10.025

16. Fernandes, S.C., de Oliveira, I.R.W.Z. & Vieira, I.C. 2007. A green bean homogenate immobilized on chemically crosslinked chitin for determination of caffeic acid in white

wine. *Enzyme and Microbial Technology*, 40(4): 661-668. https://doi.org/10.1016/j.enzmictec.2006.05.023

17. Gao, G., Fang, D., Yu, Y., Wu, L., Wang, Y. & Zhi, J. 2017. A double-mediator based whole cell electrochemical biosensor for acute biotoxicity assessment of wastewater. *Talanta*, 167: 208-216. https://doi.org/10.1016/j.talanta.2017.01.081

18. Haghighi, B., Gorton, L., Ruzgas, T. & Jönsson, L.J. 2003. Characterization of graphite electrodes modified with laccase from *Trametes versicolor* and their use for bioelectrochemical monitoring of phenolic compounds in flow injection analysis. *Analytica Chimica Acta*, 487(1): 3-14. https://doi.org/10.1016/S0003-2670(03)00077-1

19. Hormozi-Nezhad, M.R., Moslehipour, A. & Bigdeli, A. 2017. Simple and rapid detection of L-dopa based on in situ formation of polylevodopa nanoparticles. *Sensors and Actuators, B: Chemical*, 243: 715-720. https://doi.org/10.1016/j.snb.2016.12.059

20. Jarosz-Wilkołazka, A., Ruzgas, T. & Gorton, L. 2005. Amperometric detection of mono- and diphenols at *Cerrena unicolor* laccase-modified graphite electrode: Correlation between sensitivity and substrate structure. *Talanta*, 66(5): 1219-1224. https://doi.org/10.1016/j.talanta.2005.01.026

21. Karpińska, J., Smyk, J. & Wołyniec, E. 2005. A spectroscopic study on applicability of spectral analysis for simultaneous quantification of l-dopa, benserazide and ascorbic acid in batch and flow systems. *Spectrochimica Acta - Part A: Molecular and Biomolecular Spectroscopy*, 62(1-3): 213-220. https://doi.org/10.1016/j.saa.2004.12.029

22. Kosanić, M., Petrović, N. & Stanojković, T. 2020. Bioactive properties of *Clitocybe geotropa* and *Clitocybe nebularis*. *Journal of Food Measurement and Characterization*, 14(2): 1046-1053. https://doi.org/10.1007/s11694-019-00354-7

23. Kozan, J.V.B., Silva, R.P., Serrano, S.H.P., Lima, A.W.O. & Angnes, L. 2007. Biosensing hydrogen peroxide utilizing carbon paste electrodes containing peroxidases naturally immobilized on coconut (*Cocus nucifera* L.) fibers. *Analytica Chimica Acta*, 591(2): 200-207. https://doi.org/10.1016/j.aca.2007.03.058

24. Kumarathasan, P. & Vincent, R. 2003. New approach to the simultaneous analysis of catecholamines and tyrosines in biological fluids. *Journal of Chromatography A*, 987(1-2): 349-358. https://doi.org/10.1016/S0021-9673(02)01598-4

25. Leite, O.D., Lupetti, K.O., Fatibello-Filho, O., Vieira, I.C. & Barbosa, A. de M. 2003a. Synergic effect studies of the bi-enzymatic system laccaseperoxidase in a voltammetric biosensor for catecholamines. *Talanta*, 59(5): 889-896. https://doi.org/10.1016/S0039-9140(02)00650-1

26. Leite, O.D., Fatibello-Filho, O. & Barbosa, A.D.M. 2003b. Determination of catecholamines in pharmaceutical formulations using a biosensor modified with a crude extract of fungi laccase (*Pleurotus ostreatus*). *Journal of the Brazilian Chemical Society*, 14(2): 297-303. https://doi.org/10.1590/S0103-50532003000200018

27. Li, Y., Han, J., Jiang, L., Li, F., Li, K. & Dong, Y. 2015. A glucose biosensor based on ımmobilization of glucose oxidase on platinum nanoparticle doped santa barbara amorphous material-15. *Analytical Letters*, 48(7): 1139-1149. https://doi.org/10.1080/00032719.2014.974056

28. Liu, Q., Ye, W., Yu, H., Hu, N., Du, L., Wang, P. & Yang, M. 2010. Olfactory mucosa tissue-based biosensor: A bioelectronic nose with receptor cells in intact olfactory epithelium. *Sensors and Actuators, B: Chemical*, 146(2): 527-533. https://doi.org/10.1016/j.snb.2009.12.032

29. Luis, P., Walther, G., Kellner, H., Martin, F. & Buscot, F. 2004. Diversity of laccase genes from basidiomycetes in a forest soil. *Soil Biology and Biochemistry*, 36(7): 1025-1036. https://doi.org/10.1016/j.soilbio.2004.02.017

30. Narang, J., Chauhan, N., Singh, A. & Pundir, C.S. 2011. A nylon membrane based amperometric biosensor for polyphenol determination. *Journal of Molecular Catalysis B: Enzymatic*, 72(3-4): 276-281. https://doi.org/10.1016/j.molcatb.2011.06.016

31. Nomngongo, P.N., Ngila, J.C., Nyamori, V.O., Songa, E.A. & Iwuoha, E.I. 2011. Determination of Selected Heavy Metals Using Amperometric Horseradish Peroxidase (HRP) Inhibition Biosensor. *Analytical Letters*, 44(11): 2031-2046. https://doi.org/10.1080/00032719.2010.539738

32. Odaci, D., Tımur, S. & Telefoncu, A. 2004. Immobilized jerusalem artichoke (*Helianthus tuberosus*) tissue electrode for phenol detection. *Artificial Cells, Blood Substitutes, and Biotechnology*, 32(2): 315-323. https://doi.org/10.1081/BIO-120037836

33. Ori, Z., Kiss, A., Ciucu, A.A., Mihailciuc, C., Stefanescu, C.D., Nagy, L. & Nagy, G. 2014. Sensitivity enhancement of a "bananatrode" biosensor for dopamine based on SECM studies inside its reaction layer. *Sensors and Actuators, B: Chemical*, 190: 149-156. https://doi.org/10.1016/j.snb.2013.08.063

34. Ozcan, H.M. & Aydin, T. 2016. A new PANI biosensor based on catalase for cyanide determination. *Artificial Cells, Nanomedicine and Biotechnology*, 44(2): 664-671. https://doi.org/10.3109/21691401.2014.978979

35. Ozcan, H.M. & Sagiroglu, A. 2010. A novel amperometric biosensor based on banana peel (*Musa cavendish*) tissue homogenate for determination of phenolic compounds. *Artificial Cells, Blood Substitutes, and Biotechnology*, 38(4): 208-214. https://doi.org/10.3109/10731191003776744

36. Ozcan, H.M. & Sagiroglu, A. 2014. Fresh broad (*Vicia faba*) tissue homogenate-based biosensor for determination of phenolic compounds. *Artificial Cells, Nanomedicine and Biotechnology*, 42(4): 256-261. https://doi.org/10.3109/21691401.2013.764313

37. Pandey, N. & Budhathoki, U. 2007. Protein determination through bradford's method of nepalese mushroom. *Scientific World*, 5(5): 85-88. https://doi.org/10.3126/sw.v5i5.2662

38. Pontius, K., Semenova, D., Silina, Y.E., Gernaey, K. V. & Junicke, H. 2020. Automated electrochemical glucose biosensor platform as an efficient tool toward on-line fermentation monitoring: novel application approaches and ınsights. *Frontiers in Bioengineering and Biotechnology*, 8: 436. https://doi.org/10.3389/fbioe.2020.00436

39. Rahimi-Mohseni, M., Raoof, J.B., Ojani, R., Aghajanzadeh, T.A. & Bagheri Hashkavayi, A. 2018. Development of a new paper based nano-biosensor using the co-catalytic effect of tyrosinase from banana peel tissue

(*Musa cavendish*) and functionalized silica nanoparticles for voltammetric determination of L-tyrosine. *International Journal of Biological Macromolecules*, 113: 648-654. https://doi.org/10.1016/j.ijbiomac.2018.02.060

40. Rasmussen, C.D., Andersen, J.E.T. & Zachau-Christiansen, B. 2007. Improved performance of the potentiometric biosensor for the determination of creatinine. *Analytical Letters*, 40(1): 39-52. https://doi.org/10.1080/00032710600952341

41. Sagiroglu, A., Paluzar, H., Ozcan, H.M., Okten, S. & Sen, B. 2011. A novel biosensor based on lactobacillus acidophilus for determination of phenolic compounds in milk products and wastewater. *Preparative Biochemistry and Biotechnology*, 41(4): 321-336. https://doi.org/10.1080/10826068.2010.540607

42. Saini, A.S., Kumar, J. & Melo, J.S. 2014. Microplate based optical biosensor for l-Dopa using tyrosinase from *Amorphophallus campanulatus*. *Analytica Chimica Acta*, 849: 50-56. https://doi.org/10.1016/j.aca.2014.08.016

43. Sandeep, S., Santhosh, A.S., Swamy, N.K., Suresh, G.S., Melo, J.S. & Nithin, K.S. 2018. Electrochemical detection of L-dopa using crude polyphenol oxidase enzyme immobilized on electrochemically reduced RGO-Ag nanocomposite modified graphite electrode. *Materials Science and Engineering B: Solid-State Materials for Advanced Technology*, 232-235: 15-21. https://doi.org/10.1016/j.mseb.2018.10.014

44. Sanders, C.A., Rodriguez, M. & Greenbaum, E. 2001. Stand-off tissue-based biosensors for the detection of chemical warfare agents using photosynthetic fluorescence induction. *Biosensors and Bioelectronics*, 16(7-8): 439-446. https://doi.org/10.1016/S0956-5663(01)00158-0

45. Sarigul, N., Korkmaz, F. & Kurultak, İ. 2019. A new artificial urine protocol to better imitate human urine. *Scientific Reports*, 9: 20159. https://doi.org/10.1038/s41598-019-56693-4

46. Sayikli Şimşek, Ç., Nur Sonuç Karaboğa, M. & Sezgintürk, M.K. 2015. A new immobilization procedure for development of an electrochemical immunosensor for parathyroid hormone detection based on gold electrodes modified with 6-mercaptohexanol and silane. *Talanta*, 144: 210-218. https://doi.org/10.1016/j.talanta.2015.06.010

47. Sezgintürk, M.K. & Dinçkaya, E. 2003. A novel amperometric biosensor based on spinach (*Spinacia oleracea*) tissue homogenate for urinary oxalate determination. *Talanta*, 59(3): 545-551. https://doi.org/10.1016/S0039-9140(02)00539-8

48. Sezgintürk, M.K. & Dinçkaya, E. 2004. An amperometric inhibitor biosensor for the determination of reduced glutathione (GSH) without any derivatization in some plants. *Biosensors and Bioelectronics*, 19(8): 835-841. https://doi.org/10.1016/j.bios.2003.08.012

49. Sezgintürk, M.K. & Dinçkaya, E. 2005. Direct determination of sulfite in food samples by a biosensor based on plant tissue homogenate. *Talanta*, 65(4): 998-1002. https://doi.org/10.1016/j.talanta.2004.08.037

50. Sezgintürk, M.K. & Dinçkaya, E. 2012. Sulfite determination by an inhibitor biosensor-based mushroom (*Agaricus bisporus*) tissue homogenate. *Artificial Cells, Blood Substitutes, and Biotechnology*, 40(1-2): 38-43. https://doi.org/10.3109/10731199.2011.585614

51. Sezgintürk, M.K., Göktug, T. & Dinçkaya, E. 2005. Detection of benzoic acid by an amperometric inhibitor biosensor based on mushroom tissue homogenate. *Food Technology and Biotechnology*, 43(4): 329-334.

52. Shin, K.S. & Lee, Y.J. 2000. Purification and characterization of a new member of the laccase family from the white-rot basidiomycete *Coriolus hirsutus*. *Archives of Biochemistry and Biophysics*, 384(1): 109-115. https://doi.org/10.1006/abbi.2000.2083

53. Silva, L.M.C., De Mello, A.C.C. & Salgado, A.M. 2014. Phenol determination by an amperométrico biosensor based on lyophilized mushroom (*Agaricus bisporus*) tissue. *Environmental Technology (United Kingdom)*, 35(8): 1012-1017. https://doi.org/10.1080/09593330.2013.858755

54. Sun, A., Wambach, T., Venkatesh, A.G. & Hall, D.A. 2014. A low-cost smartphone-based electrochemical biosensor for point-of-care diagnostics. *IEEE 2014 Biomedical Circuits and Systems Conference, BioCAS 2014 - Proceedings*, 312-315. https://doi.org/10.1109/BioCAS.2014.6981725

55. Tashkhourian, J., Hormozi-Nezhad, M.R. & Khodaveisi, J. 2011. Application of silver nanoparticles and principal component-artificial neural network models for simultaneous determination of levodopa and benserazide hydrochloride by a kinetic spectrophotometric method. *Spectrochimica Acta - Part A: Molecular and Biomolecular Spectroscopy*, 82(1): 25-30. https://doi.org/10.1016/j.saa.2011.06.014

56. Thoppe Rajendran, S., Huszno, K., Dębowski, G., Sotres, J., Ruzgas, T., Boisen, A. & Zór, K. 2020. Tissue-based biosensor for monitoring the antioxidant effect of orally administered drugs in the intestine. *Bioelectrochemistry*, 138: 107720. https://doi.org/10.1016/j.bioelechem.2020.107720

57. Timur, S., Pazarloğlu, N., Pilloton, R. & Telefoncu, A. 2004. Thick film sensors based on laccases from different sources immobilized in polyaniline matrix. *Sensors and Actuators, B: Chemical*, 97(1): 132-136. https://doi.org/10.1016/j.snb.2003.07.018

58. Topçu, S., Sezgintürk, M.K. & Dinçkaya, E. 2004. Evaluation of a new biosensor-based mushroom (*Agaricus bisporus*) tissue homogenate: Investigation of certain phenolic compounds and some inhibitor effects. *Biosensors and Bioelectronics*, 20(3): 592-597. https://doi.org/10.1016/j.bios.2004.03.011

59. Tuncay, D. & Yagar, H. 2020. Decolorization of Reactive Blue-19 textile dye by B*oletus edulis* laccase immobilized onto rice husks. *International Journal of Environmental Science and Technology*, 17(6): 3177-3188. https://doi.org/10.1007/s13762-020-02641-z

60. Zhang, G.Q., Wang, Y.F., Zhang, X.Q., Ng, T.B. & Wang, H.X. 2010. Purification and characterization of a novel laccase from the edible mushroom *Clitocybe maxima*. *Process Biochemistry*, 45(5): 627-633. https://doi.org/10.1016/j.procbio.2009.12.010

61. Zwirtes de Oliveira, I.R.W., Fernandes, S.C. & Vieira, I.C. 2006. Development of a biosensor based on gilo peroxidase immobilized on chitosan chemically crosslinked with epichlorohydrin for determination of rutin. *Journal of Pharmaceutical and Biomedical Analysis*, 41(2): 366-372. https://doi.org/10.1016/j.jpba.2005.12.019

Trakya University Journal of Natural Sciences (TUJNS)

Copyright Release Form

Trakya University
Institute of Natural Sciences
Balkan Campus, Institutions Building
22030 EDİRNE, TURKEY

Telephone : 0 284 2358230
Fax : 0 284 2358237
e-mail : tujns@trakya.edu.tr

I, the undersigned, declare that I transfer the copyright and all related financial rights of the article with the title given below to Trakya University, granting Trakya University for rights of publishing and accepting University Publishing Regulations and Trakya University Publication Application Instructions for printing process.

Article Name:

Author(s):

Name, Surname :
Title :
Signature :
Date :

Name, Surname :
Title :
Signature :
Date :

Name, Surname :
Title :
Signature :
Date :

Name, Surname :
Title :
Signature :
Date :

Name, Surname :
Title :
Signature :
Date :

Additional page(s) can be used if the author number exceeds 5. All co-authors of the study are required to sign this form.

Yazım Kuralları

Trakya University Journal of Natural Sciences

(Trakya Univ J Nat Sci)

Trakya University Journal of Natural Sciences, her yıl Nisan ve Ekim aylarında olmak üzere yılda iki sayı olarak çıkar ve **Biyoloji, Biyoteknoloji, Çevre Bilimleri, Biyokimya, Biyofizik, Su Ürünleri, Ziraat, Veterinerlik, Ormancılık, Hayvancılık, Genetik, Gıda, Temel Tıp Bilimleri** alanlarındaki teorik ve deneysel yazıları yayınlar. Dergide yazılar İngilizce olarak yayınlanır. Ancak, yazıda Türkçe özet olmalıdır. Yabancı yazarlar için Türkçe özet desteği verilecektir. Özet kısmında kısaca giriş, materyal ve metot, sonuçlar ve tartışma başlıkları yer almalıdır. Dergide orijinal çalışma, araştırma notu, derleme, teknik not, editöre mektup, kitap tanıtımı yayınlanabilir. Değerlendirilmek üzere dergiye gönderilen yazıların yazımında ulusal ve uluslararası geçerli etik kurallara Committee on Publication Ethics (COPE) uyularak araştırma ve yayın etiğine dikkat edilmesi gerekmektedir. Yazılara konu olarak seçilen deney hayvanları için etik kurul onayı alınmış olmalı ve yazının sunumu esnasında dergi sistemine ek dosya olarak eklenerek belgelendirilmelidir. Basılacak yazıların daha önce hiçbir yerde yayınlanmamış ve yayın haklarının verilmemiş olması gerekir. Dergide yayınlanacak yazıların her türlü sorumluluğu yazar(lar)ına aittir.

Yazıların sunulması

Yazılar http://dergipark.gov.tr/trkjnat web adresi üzerinden gönderilmelidir. Dergiye yazı gönderimi mutlaka online olarak yapılmalıdır.

Yazı gönderiminde daha önce Dergi Park sistemine giriş yapmış olan kullanıcılar, üye girişinden kullanıcı adı ve şifreleri ile giriş yapabilirler.

Yazı gönderiminde sisteme ilk kez giriş yapacak ve yazı gönderecek yazarlar **"GİRİŞ"** bölümünden "**KAYDOL**" butonunu kullanacaklardır.

Yazarlar dergipark sistemine kaydolduktan sonra **"YAZAR"** bölümünden girecek ve yazıyı sisteme, yönergelere uygun olarak yükleyeceklerdir.

Yazı hazırlama ilkeleri

Yazılar, Yayın Komisyonu'na **MS Word** kelime işlemcisiyle **12 punto** büyüklüğündeki **Times New Roman** tipi yazı karakteriyle ve 1,5 aralıklı yazılmış olarak gönderilmelidir. İletişim bilgileri yazının ilk sayfasında tek başına yazılmalı, daha sonraki sayfada yazar isimleri ve iletişim bilgileri bulunmamalıdır. Tüm yazı her sayfası kendi arasında **satır numaraları** içerecek şekilde numaralandırılmalıdır. Yazar adları yazılırken herhangi bir akademik unvan belirtilmemelidir. Çalışma herhangi bir kurumun desteği ile yapılmış ise, teşekkür kısmında kurumun; kişilerin desteğini almış ise kişilerin bu çalışmayı desteklediği yazılmalıdır.

Yazı aşağıdaki sıraya göre düzenlenmelidir:

Yazarlar: Yazının ilk sayfasında sadece yazar isimleri ve adresleri bulunmalıdır. Adlar kısaltmasız, soyadlar büyük harfle ve ortalanarak yazılmalıdır. Adres(ler) tam yazılmalı, kısaltma kullanılmamalıdır. Birden fazla yazarlı çalışmalarda, yazışmaların hangi yazarla yapılacağı yazar ismi altı çizilerek belirtilmeli (sorumlu yazar) ve **yazışma yapılacak yazarın adres ve e-posta adresi yazar isimlerinin hemen altına yazılmalıdır. Bu sayfaya yazı ile ilgili başka bir bilgi yazılmamalıdır. Yazı, takip eden sayfada bulunmalı ve yazar-iletişim bilgisi içermemelidir.**

Başlık: İngilizce olarak Kısa ve açıklayıcı olmalı, büyük harfle ve ortalanarak yazılmalıdır.

Özet ve Anahtar kelimeler: Türkçe ve İngilizce özet 250 kelimeyi geçmemelidir. Özetin altına küçük harflerle anahtar kelimeler ibaresi yazılmalı ve yanına anahtar kelimeler virgül konularak sıralanmalıdır. Anahtar kelimeler, zorunlu olmadıkça başlıktakilerin tekrarı olmamalıdır. İngilizce özet koyu harflerle "Abstract" sözcüğü ile başlamalı ve başlık, İngilizce özetin üstüne büyük harflerle ortalanarak yazılmalıdır. Yazıdaki ana başlıklar ve varsa alt başlıklara **numara verilmemelidir.**

Giriş: Çalışmanın amacı ve geçmişte yapılan çalışmalar bu kısımda belirtilmelidir. Yazıda SI (Systeme International) birimleri ve kısaltmaları kullanılmalıdır. Diğer kısaltmalar kullanıldığında, metinde ilk geçtiği yerde 1 kez açıklanmalıdır. Kısaltma yapılmış birimlerin sonuna nokta konmamalıdır (45 m mesafe tespit edilmiştir). Kısaltma cümle sonunda ise nokta konmalıdır (… tespit edilen mesafe 45 m. Dolayısıyla…).

Materyal ve Metod: Eğer çalışma deneysel ise kullanılan deneysel yöntemler detaylı ve açıklayıcı bir biçimde verilmelidir. Yazıda kullanılan metod/metodlar, başkaları tarafından tekrarlanabilecek şekilde açıklayıcı olmalıdır. Fakat kullanılan deneysel yöntem herkes tarafından bilinen bir yöntem ise ayrıntılı açıklamaya gerek olmayıp sadece yöntemin adı verilmeli veya yöntemin ilk kullanıldığı çalışmaya atıf yapılmalıdır.

Sonuçlar: Bu bölümde elde edilen sonuçlar verilmeli, yorum yapılmamalıdır**.** Sonuçlar gerekirse tablo, şekil ve grafiklerle de desteklenerek açıklanabilir.

Tartışma: Sonuçlar mutlaka tartışılmalı fakat gereksiz tekrarlardan kaçınılmalıdır. Bu kısımda, literatür bilgileri vermekten çok, çalışmanın sonuçlarına yoğunlaşmalı, sonuçların daha önce yapılmış araştırmalarla benzerlik ve farklılıkları verilmeli, bunların muhtemel nedenleri tartışılmalıdır. Bu bölümde, elde edilen sonuçların bilime katkısı ve önemine de mümkün olduğu kadar yer verilmelidir.

Teşekkür: Mümkün olduğunca kısa olmalıdır. Teşekkür, genellikle çalışmaya maddi destek sağlayan kurumlara, kişilere veya yazı yayına gönderilmeden önce inceleyip önerilerde bulunan uzmanlara yapılır. Teşekkür bölümü kaynaklardan önce ve ayrı bir başlık altında yapılır.

Kaynaklar: Yayınlanmamış bilgiler kaynak olarak verilmemelidir (*Yayınlanmamış kaynaklara örnekler: Hazırlanmakta olan veya yayına gönderilen yazılar, yayınlanmamış bilgiler veya gözlemler, kişilerle görüşülerek elde edilen bilgiler, raporlar, ders notları, seminerler gibi*). Ancak, tamamlanmış ve jüriden geçmiş tezler ve DOI numarası olan yazılar kaynak olarak verilebilir. Kaynaklar, yazı sonunda alfabetik sırada (yazarların soyadlarına göre) sıra numarası ile belirtilerek verilmelidir.

Kaynak yazım şekli:

Kaynak yazım şekli için Endnote stilini indirebilirsiniz.

Veya aşağıdaki yönergeyi kullanabilirsiniz.

Yazıların ve kitapların referans olarak veriliş şekilleri aşağıdaki gibidir:

Makale: Yazarın soyadı, adının baş harfi, basıldığı yıl. Makalenin başlığı, *derginin adı*, cilt numarası, sayı, sayfa numarası. Dergi adı italik yazılır.

Örnek:

Tek yazarlı Makale için

Soyadı, A. Yıl. Makalenin adı. (Sözcüklerin ilk harfi küçük). *Yayınlandığı derginin açık ve tam adı*, Cilt(Sayı)**:** Sayfa aralığı.

Kıvan, M. 1998. *Eurygaster integriceps* Put. (Heteroptera: Scuteleridae)'nin yumurta parazitoiti *Trissolcus semistriatus* Nees (Hymenoptera: Scelionidae)'un biyolojisi üzerinde araştırmalar*. Türkiye Entomoloji Dergisi*, 22(4): 243-257.

İki ya da daha çok yazarlı makale için

Soyadı1, A1. & Soyadı2**,** A2. Yıl. Makalenin adı**.** (Sözcüklerin ilk harfi küçük). *Yayınlandığı derginin tam adı*, Cilt(Sayı): Sayfa aralığı.

Lodos, N. & Önder, F. 1979. Controbution to the study on the Turkish Pentatomoidea (Heteroptera) IV. Family: Acanthasomatidae Stal 1864. *Türkiye Bitki Koruma Dergisi*, 3(3): 139-160.

Soyadı1, A1., Soyadı2, A2. & Soyadı3, A3**.** Yıl. Makalenin adı**.** (Sözcüklerin ilk harfi küçük). *Yayınlandığı derginin tam adı*, Cilt (Sayı): Sayfa aralığı.

Önder, F., Ünal, A. & Ünal, E. 1981. Heteroptera fauna collected by light traps in some districts of Northwestern part of Anatolia. *Türkiye Bitki Koruma Dergisi***,** 5(3): 151-169.

Kitap: Yazarın soyadı, adının baş harfi, basıldığı yıl. Kitabın adı (varsa derleyen veya çeviren ya da editör), cilt numarası, baskı numarası, basımevi, basıldığı şehir,toplam sayfa sayısı.

Örnek:

Soyadı, A., Yıl. *Kitabın adı*. (Sözcüklerin ilk harfi büyük, italik). Basımevi, basıldığı şehir, toplam sayfa sayısı s./pp.

Önder F., Karsavuran, Y., Tezcan, S. & Fent, M. 2006. *Türkiye Heteroptera (Insecta) Kataloğu*. Meta Basım Matbaacılık, İzmir, 164 s.

Lodos, N., Önder, F., Pehlivan, E., Atalay, R., Erkin, E., Karsavuran, Y., Tezcan, S. & Aksoy, S. 1999. Faunistic *Studies on Lygaeidae (Heteroptera) of Western Black Sea, Central Anatolia and Mediterranean Regions of Turkey.* Ege University, İzmir, ix + 58 pp.

Kitapta Bölüm: Yazarın soyadı, adının baş harfi basıldığı yıl. Bölüm adı, sayfa numaraları. Parantez içinde: Kitabın editörü/editörleri, *kitabın adı*, yayınlayan şirket veya kurum, yayınlandığı yer, toplam sayfa sayısı.

Örnek:

Soyadı, A., Yıl. Bölüm adı, sayfa aralığı. In: (editör/editörler). *Kitabın adı*. (Sözcüklerin ilk harfi büyük, italik). Basımevi, basıldığı şehir, toplam sayfa sayısı s./pp.

Jansson, A. 1995. Family Corixidae Leach, 1815—The water boatmen. Pp. 26–56. In: Aukema, B. & Rieger, C.H. (eds). *Catalogue of the Heteroptera of the Palaearctic Region.* Vol. 1. Enicocephalomorpha, Dipsocoromorpha, Nepomorpha, Gerromorpha and Leptopodomorpha. The Netherlands Entomological Society, Amsterdam, xxvi + 222 pp.

Kongre, Sempozyum: Yazarlar, Yıl. "Bildirinin adı (Sözcüklerin ilk harfi küçük), sayfa aralığı". Kongre/Sempozyum Adı, Tarihi (gün aralığı ve ay), Yayınlayan Kurum, Yayınlanma Yeri.

Örnek:

Bracko, G., Kiran, K., & Karaman, C. 2015. The ant fauna of Greek Thrace, 33-34. Paper presented at the 6th Central European Workshop of Myrmecology, 24-27 July, Debrecen-Hungary.

Internet: Eğer bir bilgi herhangi bir internet sayfasından alınmış ise (*internetten alınan ve dergilerde yayınlanan yazılar hariç*), kaynaklar bölümüne internet sitesinin ismi tam olarak yazılmalı, siteye erişim tarihi verilmelidir.

Soyadı**,** A. Yıl. Çalışmanın adı. (Sözcüklerin ilk harfi küçük) http://www..... (Date accessed: 12.08.2009).

Hatch, S., 2001. Studentsperception of online education. Multimedia CBT Systems. http://www.scu.edu.au/schools/sawd/moconf/papers2001/hatch.pdf (Date accessed: 12.08.2009).

Kaynaklara metin içinde numara verilmemeli ve aşağıdaki örneklerde olduğu gibi belirtilmelidir.

Örnekler:
... x maddesi atmosferde kirliliğe neden olmaktadır (Landen 2002). Landen (2002) x maddesinin atmosferde kirliliğe neden olduğunu belirtmiştir. İki yazarlı bir çalışma kaynak olarak verilecekse, (Landen & Bruce 2002) veya Landen & Bruce (2002)'ye göre. ... şeklinde olmuştur; diye verilmelidir. Üç veya daha fazla yazar söz konusu ise, (Landen *et al.* 2002) veya Landen *et al.* (2002)'ye göre .... olduğu gösterilmiştir; diye yazılmalıdır.

Şekil ve Tablolar: Tablo dışında kalan fotoğraf, resim, çizim ve grafik gibi göstermeler "Fig." olarak verilmelidir. Resim, şekil ve grafikler, net ve ofset baskı tekniğine uygun olmalıdır. Her tablo ve şeklin metin içindeki yerlerine konmalıdır. Tüm tablo ve şekiller yazı boyunca sırayla numaralandırılmalı (Table 1, Fig. 1, Figs 3, 4), başlık ve açıklamalar içermelidir. Şekillerin sıra numaraları ve başlıkları, alta, tabloların ki ise üstlerine yazılır.

Şekiller (tablo dışında kalan fotoğraf, resim, çizim ve grafik gibi) tek tek dosyalar halinde en az **300 dpi** çözünürlükte ve **tif** dosyası olarak şekil numaraları dosya isminde belirtilmiş şekilde ayrıca sisteme ek dosya olarak yüklenmelidir.

Sunulan yazılar, öncelikle Dergi Yayın Kurulu tarafından ön incelemeye tabii tutulur. **Dergi Yayın Kurulu, yayınlanabilecek nitelikte bulmadığı veya yazım kurallarına uygun hazırlanmayan yazıları hakemlere göndermeden red kararı verme hakkına sahiptir.** Değerlendirmeye alınabilecek olan yazılar, incelenmek üzere iki ayrı hakeme gönderilir. Dergi Yayın Kurulu, hakem raporlarını dikkate alarak yazıların yayınlanmak üzere kabul edilip edilmemesine karar verir.

SUİSTİMAL İNCELEMELERİ VE ŞİKAYETLER

Dergide yayınlanmış veya yayınlanma sürecine girmiş her türlü yazı hakkındaki suistimal şüphesi ve suistimal şüphesiyle yapılan şikayetler dergi Yayın Kurulu tarafından değerlendirilir. Yayın kurulu suistimal şüphesini veya şikayeti değerlendirirken COPE (Committee on Publication Ethics)'un yönergelerine bağlı kalır. Şüphe veya şikayet sürecinde şikayet taraflarıyla hiçbir bağlantısı olmayan bir ombudsman belirlenerek karar verilir. Şikayetler baş editöre tujns@trakya.edu.tr adresi kullanılarak yapılabilir.

TELIF HAKKI

Telif hakkı, makalenin yayınlandığı andan itibaren (Erken Görünüm dahil) herhangi bir kısıtlama olmaksızın makalenin yazarına / yazarlarına devredilir.

YAYIN SONRASI DEĞİŞİKLİK VE GERİÇEKME İSTEĞİ

Dergide yazının yayınlanması sonrası yazar sırasında değişiklik, yazar ismi çıkarma, ekleme ya da yazının geriçekilmesi tujns@trakya.edu.tr adresine yapılacak bir başvuru ile gerçekleştirilebilir. Gönderilecek e-postada mutlaka gerekçe ve kanıtlar sunulmalıdır. Sunulan gerekçe ve kanıtlar Yayın Kurulu tarafından görüşülüp karara bağlanır. Yukarıda belirtilen değişiklik ve geri çekme istekleri oluştuğunda tüm yazarların dergiye gönderecekleri yazılar işlem süresi içerisinde otomatik olarak reddedilir.

ÜYELİK/AYRI BASKI/ERİŞİM

Dergi üyelik gerektirmeyip Açık Erişime sahiptir. Dergide yazısı basılan tüm sorumlu yazarlara 15 ayrı baskı ve yazının çıktığı 1 dergi ücretsiz gönderilmektedir. Dergide yayınlanan tüm yazılara erişim ücretsiz olup full-text pdf dosyaları CC-BY 4.0 uluslararası lisansı kapsamında kullanılabilir.

REKLAM VERME

Dergiye reklam vermek üzere tujns@trakya.edu.tr adresine yapılacak başvurular dergi sahibi tarafından değerlendirilecektir.

Baş Editör **:** Prof. Dr. Kadri KIRAN

Trakya Üniversitesi
Fen Bilimleri Enstitüsü
Balkan Yerleşkesi
22030 - EDİRNE

Tel : 0284 235 82 30
Fax : 0284 235 82 37
e-mail : tujns@trakya.edu.tr

Trakya University Journal of Natural Sciences
(Trakya Univ J Nat Sci)

Trakya University Journal of Natural Sciences, is published twice a year in April and in October and includes theoretical and experimental articles in the fields of **Biology, Biotechnology, Environmental Sciences, Biochemistry, Biophysics, Fisheries Sciences, Agriculture, Veterinary and Animal Sciences, Forestry, Genetics, Food Sciences** and **Basic Medicine Sciences**. Original studies, research notes, reviews, technical notes, letters to the Editor and book reviews can be published in the journal. The publishing language for all articles in the journal is **English**. On the other hand, authors are required to provide a Turkish abstract also. The Turkish version of the abstract will be supply by the journal for foreign authors. Abstracts should include introduction, material and methods, results and discussion sections in summary. The authors should pay attention to research and publication ethics Committee on Publication Ethics (COPE) in preparation of their manuscripts before submission by considering national and international valid ethics. An approval of Ethics and Animal Welfare Committee is mandatory for submissions based on experimental animals and this approval should be provided during submission of the manuscripts. Articles which have not been published elsewhere previously and whose copyright has not been given to anywhere else should be submitted. All responsibilities related to published articles in Trakya University Journal of Natural Sciences belong to the authors.

Submitting articles

Articles should be submitted on the web through http://dergipark.gov.tr/trkjnat and all submissions should be performed online.

Authors, who are already a member of the DergiPark system, can enter in the login section using their "user name" and "password" to submit their articles.

Authors entering the DergiPark system for the first time to submit an article will enter in the "**REGISTER**" section to submit their articles.

Article preparation rules

Articles should be submitted to the Journal using **MS Word** preparing **12 points Times New Roman** font and 1.5 raw spacing. Author names and contact info must be in first page, article must continue in second page without author names and contact info. Whole article should have numbered with **line number** restarting each page. The author's name must not be specified any academic titles. If studies supported by a foundation, this support should have been written in the acknowledgement section.

Articles should be arranged as below:

Authors: The name(s) of the author(s) should not be abbreviated and must be written under the title one by one, with surnames in capital letters. Address(es) should be written in full. Corresponding authors in multiple authored submissions should be indicated, and the address and e-mail of the corresponding author should be written just under the author(s) list. **No other information about the manuscript should be included in this page. The main manuscript text should start with the following new page and should not include any author-contact information.**

Title: Should be short and explanatory and written in capital letters and centered.

Abstract and keywords: Turkish and English abstracts should not exceed 250 words. "Keywords" should be written under the abstract in small letters and all keywords should be written using a comma after all. Keywords should not be replica of the title words, if it is not obligatory. Abstract should begin "Abstract" word from the left side of the page. The main and sub headers (if present) should not be numbered.

Introduction: The aim of the submitted and history of the previous studies should be indicated in this section. SI (Systeme International) system and abbreviation should be used in the article. Other abbreviations- should be explained once in their first appearance in the text. No "." sign should be used after abbreviations except those used at the end of a sentence (…the determined distance is 45 m. Therefore, …).

Material and Method: If the submitted study is experimental, methods of the experiments should be given in detail. The method(s) used in the article should be descriptive for others to repeat. If a widely known experimental method is used, the method does not need to be explained in detail. In this situation, indicating only the name of the experimental method or citing the study who used the method for the first time will be enough.

Results: Obtained results should be given in this section without any comment. Results can be explained with tables, figures or graphics, if necessary.

Discussion: Results must be discussed, but unnecessary duplications should be avoided. In this section, rather than giving literature data, authors should focus on their results considering similarities and differences with and between previously conducted researches, and should discuss possible reasons of similarities and differences. The contribution to science and importance of the obtained results should also be mentioned as much as possible in this section.

Acknowledgements: Should be as short as possible. Thanks are usually made to institutions or individuals who support the study or to experts who reviewed the article before submitting to the journal. Acknowledgement section should be given before the references section in a separate header.

References: Unpublished information should not be given as a reference (examples of unpublished references: articles in preparation or submitted somewhere, unpublished data or observations, data obtained based on interviews with individuals, reports, lecture notes, seminars, etc.). However, thesis completed and signed by a jury and articles with DOI numbers given can be used as reference. References should be given at the end of the text, sorted alphabetically by author's surname and should be given with numbering.

Reference style:

You can download the Endnote style of TUJNS from http://www.researchsoftware.com.

Or you can follow the instruction below.

Articles: Surname of author, first letter of author's first name, publication year, article title, the *name of the journal,* volume, issue, page numbers. Journal name is written in italics.

Example:

Articles with single author

Surname, N. Year. Article title (First letter of all words small). *Whole name of journal*, Volume (Issue)**:** page range.

Aybeke, M. 2016. The detection of appropriate organic fertilizer and mycorrhizal method enhancing salt stress tolerance in rice (*Oryza sativa* L.) under field conditions. *Trakya University Journal of Natural Sciences,* 17(1): 17-27.

Articles with two or more authors

Surname1, N1. & Surname2**,** N2. Year. Article title (First letter of all words small). *Whole name of journal*, Volume (Issue)**:** page range.

Dursun, A. & Fent, M. 2016. Contributions to The Cicadomorpha and Fulgoromorpha (Hemiptera) fauna of Turkish Thrace region. *Trakya University Journal of Natural Sciences,* 17(2): 123-128.

Surname1, N1., Surname2**,** N2. & Surname3, N. Year. Article title (First letter of words small). *Whole name of journal*, Volume (Issue)**:** page range.

Becenen, N., Uluçam, G. & Altun, Ö. 2017. Synthesis and antimicrobial activity of iron cyclohexanedicarboxylic acid and examination of pH effect on extraction in water and organic phases.*Trakya University Journal of Natural Sciences,* 18(1): 1-7.

Book: Surname of author, first letter of author's first name, Year. *Book title* (name of translator or book editor if present), volume, edition number, press, city, page number.

Example:

Surname, N. Year. *Book Title* (First letter of words small and italic), volume, edition number, press, city, page number.

Czechowski, W., Radchenko, A., Czechowska, W. & Vepsäläinen, K. 2012. *The ants of Poland with reference to the myrmecofauna of Europe*. Museum and Institute of Zoology PAS, Warsaw, 496 pp.

Book Section: Surname of author, first letter of the author's first name, Year. Section name, page range. In: (Editor(s) of Book, *Book title,* press, city, page number).

Example:

Surname, N. Year. Section name, page range. In: (Editor of Book, *Book title* (First letter of words small and italic), press, city, page number)

Jansson, A. 1995. Family Corixidae Leach, 1815—The water boatmen. pp. 26-56. In: Aukema, B. & Rieger, C.H. (eds). *Catalogue of the Heteroptera of the Palaearctic Region.* Vol. 1. Enicocephalomorpha, Dipsocoromorpha, Nepomorpha, Gerromorphaand Leptopodomorpha. The Netherlands Entomological Society, Amsterdam, xxvi + 222 pp.

Congress, Symposium: Surname, N. Year. Presentation title (first letters of all words small), page range. Name of Congress/Symposium, Date (day range and month), place.

Example:

Bracko, G., Kiran, K., & Karaman, C. 2015. The ant fauna of Greek Thrace, 33-34. Paper presented at the 6th Central European Workshop of Myrmecology, 24-27 July, Debrecen-Hungary.

Internet: If any information is taken from an internet source (articles published in journals and taken from internet excluded), internet address should be written in full in references section and access date should be indicated.

Surname**,** N. Year. Name of study (First letter of words small). http://www..... (Date accessed: 12.08.2009).

Hatch, S. 2001. Student sperception of online education. Multimedia CBT Systems. http://www.scu.edu.au/schools/sawd/moconf/papers2001/hatch.pdf (Date accessed: 12.08.2009).

References within the text should not be numbered and indicated as in the following examples.

Examples:

... atmospheric pollution is causing by x matter (Landen 2002). If an article has two authors, it should be indicated in the text as (Landen & Bruce 2002) or ... according to Landen & Bruce (2002) .... If there are three or more authors, references should be indicated as (Landen *et al.* 2002) or according to Landen *et al.* 2002 ...

Graphics and tables: All photos, pictures, drawings and graphics except tables should be indicated as Figures. Pictures, figures and graphics should be clear and ready to print with offset technique. The places of all tables and figures should be indicated in the text. All tables and figures should be numbered within the text respectively (Table 1, Fig. 1, Figs 3, 4). Figure numbers and legends are written below the figures, table numbers and legends are written above the tables.

All figures (all pictures, drawings and graphics except table) should also be uploaded to the system separately with 300dpi resolution at least as .tif file using the figure numbers in the files name.

Submitted articles are subjected to prior review by the Editorial Board. Editorial Board has the right to reject the articles which are considered of low quality for publish or those which are insufficiently prepared according to the author guidelines. The articles accepted for consideration for evaluation will be sent to two different referees. Editorial Board decides to accept or reject the submissions for publication by taking into account the reports of referees.

COPYRIGHT

LICENSE

EXPLOITATION ENQUIRY AND COMPLAINTS

All kinds of exploitation doubts and complaints about manuscripts, either published or in publication process, are evaluated by the Editorial Board. The Editorial Board strictly follows the directives of COPE (Committee on Publication Ethics) during the evaluations. An ombudsman who has no connection with the parts in any stage of the complaint is appointed and a decision is made. Complaints can be sent to the editor in chief by sending an e-mail to tujns@trakya.edu.tr.

POST-PUBLICATION CHANGE AND WITHDRAWAL OF A MANUSCRIPT

Changes in author ordering, removal or addition of a new author in and withdrawal of a published manuscript can be realized by sending an application to tujns@trakya.edu.tr. The application e-mail should include the reason of the requested change with the evidences. The reasons and the evidences are discussed and finalized by the Editorial Board. Further submissions of authors of a formerly accepted manuscript undergoing a change process are automatically sent back to the authors until the final decision of the manuscript in process.

ADVERTISING

Advertising applications send to tujns@trakya.edu.tr will be evaluated by the journal owner.

Editor-in-Chief **:** Prof. Dr. Kadri KIRAN

Trakya Üniversitesi
Fen Bilimleri Enstitüsü
Balkan Yerleşkesi
22030 - EDİRNE-TURKEY

Phone : +90 284 235 82 30
Fax : +90 284 235 82 37
e-mail : tujns@trakya.edu.tr